GeoFocus volume 31

Eva MATZENAUER

Tectonics of the Préalpes Klippen and the Subalpine Molasse (Canton Fribourg, Switzerland)

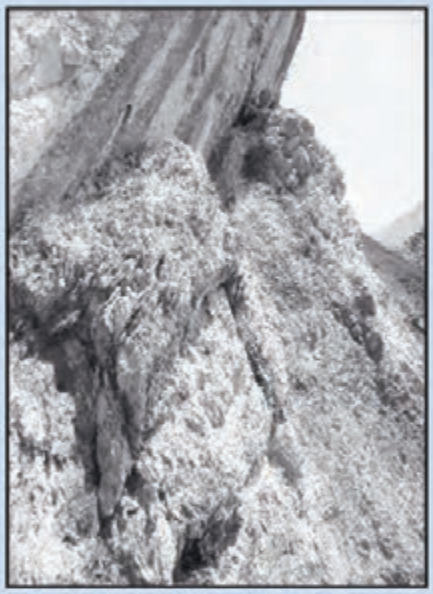

Département de Géosciences, Sciences de la Terre, Université de Fribourg (Suisse)

Departement de Geosciences – Earth Sciences
University of Fribourg (Switzerland)

Tectonics of the Préalpes Klippen and the Subalpine Molasse (Canton Fribourg, Switzerland)

Thesis

presented to the Faculty of Sciences of the University of Fribourg (Switzerland) in consideration for the award of the academic grade of *Doctor rerum naturalium*

by

Eva MATZENAUER

from Neckertal (SG), Switzerland

Thesis No: 1737

Multiprint, Fribourg, 2012

Accepted by the Faculty of Science of the University of Fribourg (Switzerland) upon the recommendation of:

Prof. Jon MOSAR	University of Fribourg (Switzerland)	Thesis supervisor
Prof. Jean-Pierre BERGER	University of Fribourg (Switzerland)	Examiner
Dr. Damien DELVAUX	Royal Museum for Central Africa (Belgium)	Examiner
Prof. Olivier LACOMBE	Université Pierre et Marie Curie (France)	Examiner
Prof. Neil MANCKTELOW	ETH Zürich (Switzerland)	Examiner
Prof. Martin HOELZLE	University of Fribourg (Switzerland)	President of the Jury

Fribourg, 1st of Decembre 2011

Thesis supervisor: Dean:

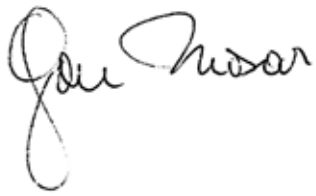

Prof. Jon MOSAR Prof. Rolf INGOLD

TABLE OF CONTENTS

*****

ABSTRACT

This thesis deals with a structural analysis of the préalpine nappe stack with major focus on the frontal part of the Préalpes Romandes and the Subalpine Molasse. The préalpine nappes underwent a complex paleo- and Alpine tectonic deformation history to attain the present-day position to the NW of the Helvetic nappes and to the SE of the Western Molasse basin. In contrast to most of the previous studies, the emphasis lays in the structural and geodynamical aspect, rather than in surface geology and stratigraphy. Diverse structural features of different scales, ranging large-scale fault-related faults, faults, and fault zones to small-scale fractures, secondary faults, veins, stylolites, and brittle shear bands witness an eventful history of the Préalpes Klippen. These tectonic features were carefully analysed and investigated in order to unravel the tectonic history of the Préalpes Romandes - mainly of the Préalpes Médianes nappe - and to attribute the observed structures to a corresponding deformational event pre-, syn-, or post-dating the préalpine nappe emplacement (30Ma - present-day).

Extensive field work in the Préalpes Médianes and its adjacent structural units allowed measuring and interpreting characteristic structural features, mostly fracture planes with fault-slip indicators, but also veins, stylolites and brittle shear bands. These observations were complemented with analyses of aerial photographs, digital elevation models, and already existing geological maps to define the extent of the large-scale structures.

The observed local fracture pattern is mainly related to the fold-and-thrust development during the nappe emplacement. The majority of the folds are fault-propagation folds verging towards NW. However, some hinterland verging backthrusts were identified associated probably to the eastward prolongation of the Ultrahelvetic lens of the Massif de Montsalvens underneath the Préalpes Médianes. In the Schopfenspitz area an important backthrust, the Maischüpfen thrust exposes a large fault zone with brittle shear bands indicating an unambiguous thrusting movement towards SE. Probably associated to the folding, normal faults develop both parallel and perpendicular to the fold axis leading to a strong segmentation of the fold limbs. However, the reactivation of these fault planes as strike-slip faults attests an on-going deformational evolution post-dating the nappe emplacement. As an example for these common structural elements, a closer look is given at the Dent de Broc and the Tzintre area, where the complexity of the structures due to reactivation is clearly visible.

The emplacement of the préalpine nappes onto the Alpine foreland announced a final period of thrusting. Uplift rates, earthquakes, and out-of-sequence thrusts witness an on-going deformation of the Alpine wedge trying to readjust its instable wedge geometry by interplay of erosion and the formation of crustal imbricates. Within the Préalpes Médianes, several thrusts hint out-of sequence thrusts, especially along important paleofaults, cutting through the whole préalpine nappe pile. The Schopfenspitz thrust - interpreted as an out-of-sequence fault - corresponds to the Rianda-Stockhorn paleofault outcropping in the Jaun valley and thrusting the Schopfenspitz mountaintop. Post-emplacement thrusting is also affecting the Gurnigel nappe by a late thrusting of the Préalpes Médianes nappe on top of the initially superimposing nappe. As well as Ultrahelvetic lenses, outcropping within the Gurnigel nappe are indicating a late stage of thrusting.

Additionally, an ubiquitous strike-slip facture pattern consisting mostly of two fault directions - a N-S oriented sinistral and a WNW-ESE oriented dextral fracture set - prove another a neotectonic to on-going deformation. Acting together as conjugated fault zones, the préalpine fault system coincides on a larger scale with conjugated fault systems common in the Jura mountains and the Molasse basin.

Moreover, fault kinematic analyses and paleostress reconstructions allow a better insight into the evolution of the stress field of the frontal part of the Préalpes

Romandes. Fault slip data collected at more than 50 measurement sites, mostly in the Préalpes Médianes, but also in the Gurnigel nappe and the Subalpine Molasse expose a heterogeneous dataset influenced by local tectonic structures, but also by reactivation of inherited structures. Overprinting relationships of fault-striation with opposed slip directions indicate the influence of several stress regimes belonging to different tectonic events. Careful data separation allowed the reconstruction of homogeneous subsystems. Hereby, the results show two different deformation phases. The first one seems to be related to the folding and the thrusting of the préalpine nappe displaying mostly a fold axis parallel extension. While the second one, a strike-slip stress regime, is prevailing throughout the entire investigation area characterised by N-S trending sinistral and WNW-ESE oriented dextral strike-slip faults. Within different structural entities ranging from the Préalpes Médianes towards the Molasse basin, indications for both a strike-slip and a compressional stress regime related to the out-of-sequence thrusting were observed. Even if the origin of these two stress regimes differs, a mutual interaction between them is possible. Maintaining the identical orientation of the compressional stress axis, a permutation of the extensional and intermediate stress axes defines the one or the other stress regime.

Furthermore, a 3D modelling approach allowed representing the complex structures of the allochthonous nappe stack of the Préalpes Romandes, as well as the fold-and-thrust structures of the Préalpes Médianes. These models give a better insight into the spatial continuation of the geology at depth than common 2D cross-sections. Additionally, the 3D models help to validate the existing geological maps, cross-sections, and our interpretations, as well as to prove the consistency amongst these different data inputs. Taking into account available data and personal interpretations, the established 3D models do not intend to give a precise reproduction at depth, but rather a suggestion of a possible solution.

*****

ZUSAMMENFASSUNG

Die vorliegende Dissertation befasst sich mit der Strukturanalyse des präalpinen Deckenstapels mit Augenmerk gerichtet auf den vorderen Bereich der Préalpes Romandes und die Subalpine Molasse. Die präalpinen Decken machten eine komplexe Deformationsgeschichte durch, um ihre heutige Lage NW der helvetischen Decken und SE des Westlichen Molasse Beckens einzunehmen. Im Gegensatz zu vielen vorangegangenen Untersuchungen liegt der Schwerpunkt dieser Arbeit vielmehr im strukturellen und geodynamischen Bereich als in der Erforschung der Oberflächengeologie und Stratigraphie. Verschiedene strukturelle Elemente unterschiedlicher Grösse bezeugen eine abwechslungsreiche Vergangenheit der präalpinen Decken von grossräumigen, überschiebungsbezogenen Falten, Verwerfungen und tektonische Störungszonen bis hin zu kleinräumigen Klüften, Brüchen, Adern, Styloliten und spröden Scherbändern. Es wurde eine sorgfältige Untersuchung der tektonischen Strukturen durchgeführt, um die geodynamische Geschichte der Préalpes Romandes - vor allem diejenige der Préalpes Médianes Decke - zu entwirren und einem entsprechenden Deformationsvorgang vor-, während- oder nach der Überschiebung der präalpinen Decken auf das alpine Vorland (30 Ma bis heute) zuzuordnen.

Umfangreiche Feldarbeit in der Préalpes Médianes Decke und in angrenzenden strukturellen Einheiten ermöglichen das Erfassen und Interpretieren von charakteristischen Strukturen, vor allem von Kluftflächen mit Schersinnindikatoren, aber auch von Adern, Styloliten und spröde Scherbänder. Diese Beobachtungen wurden vervollständigt durch die Analyse von Luftbildern, digitale Höhenmodelle und bereits bestehende geologische Karten, um das Ausmass der gross-räumigen Strukturen erkennen.

Das beobachtete Kluftnetz lässt sich vorwiegend im Zusammenhang mit der Entstehung des Falten- und Überschiebungsgürtels erklären. Die Mehrheit der Falten sind nach NW geneigte, frontale Knickfalten (fault-propagation folds). Es wurden jedoch auch Richtung Hinterland geneigte Falten erkannt, welche durch Rücküberschiebungen entstanden waren und möglicherweise durch eine östliche Erweiterung der ultrahelvetischen Linse des Montsalvens Massivs unterhalb der Préalpes Médianes hervorgerufen wurde. Im Gebiet des Schopfenspitzs bringt eine mächtige Rücküberschiebung, die Maischüpfen-Überschiebung, eine breite Bruchzone - geprägt von spröden Scherbändern - zum Vorschein, die eine eindeutige Überschiebungsrichtung gegen SE aufzeigt.

Verbunden mit der Faltung entstanden sowohl parallel, als auch senkrecht zur Faltenachsen verlaufende Abschiebungen, welche zu einer starken Segmentierung der Falten führen. Hingegen die Reaktivierung der Bruchflächen weist auf eine andauernde Deformation der präalpinen Decken nach der Überschiebung auf das alpine Vorland hin. Als Beispiel für dieses weitverbreitete Strukturelement werden das Dent de Broc Gebiet und die Steinbrüche von Tzintre und Le Brésil genauer betrachtet, wobei eine vielschichtige Deformation aufgrund der Reaktivierung eindeutig sichtbar wird.

Die Überschiebung der präalpinen Decken auf das alpine Vorland kündigt eine letzte Phase der Überschiebung an. Hebungsraten, Erdbeben und durchbrechende Überschiebungen (out-of-sequence thrusts) weisen auf eine andauernde Deformation des alpinen Keils hin, um die instabile Keilgeometrie durch ein Zusammenspiel von Erosion und der Bildung von Krustenimbrikationen wieder anzupassen. Innerhalb der Préalpes Médianes deuten mehrere Überschiebungen - hauptsächlich entlang von wichtigen Paläostörungen - auf durchbrechende Überschiebungen hin, welche den gesamten Deckenstapel durchschneiden. Die Schopfenspitz Überschiebung wird als durchbrechende Überschiebung interpretiert, die mit der Rianda-Stockhornstörung zusammenfällt, im Jauntal aufschliesst und die Spitze des Schopfenspitzs überschiebt. Durchbrechende Überschiebungen beeinträchtigen auch die Gurnigeldecke, indem sich in einem letzten Überschiebungsvorstoss

die Préalpes Médianes auf die ursprünglich tektonisch höherliegende Gurnigeldecke schiebt. Zudem weisen aufschliessende ultrahelvetische Linsen im Innern der Gurnigeldecke auf eine späte Überschiebungsphase hin, die von darunterliegenden ultrahelvetischen Linsen abgeschert wurden. Des Weiteren herrscht ein Kluftnetz hauptsächlich bestehend aus N-S ausgerichteten linkssinnigen und WNW-ESE orientierten Blattverschiebungen vor, dies als weiteren Beweis für eine neotektonische bis heutzutage andauernde Deformation. Die beiden Bruchsysteme wirken zusammen als konjugierte Verwerfungen und stimmen im grösseren Massstab mit den konjugierten Verwerfungen des Juras und des Molassebeckens überein.

Zusätzlich ermöglichten störungskinematische Analysen und Paläospannungsanalysen einen besseren Einblick in die Weiterentwicklung des Spannungsfelds im frontalen Bereich der Préalpes Romandes. Verwerfungsebenen mit Schersinnindikatoren wurden systematisch an mehr als 50 Messorten erfasst - hauptsächlich in den Préalpes Médianes, aber auch in der Gurnigeldecke und Subalpinen Molasse. Die Messungen zeigen einen heterogenen Datensatz auf, der sich zum einen auf das Vorhandensein von lokalen Strukturen, zum andern auf die Reaktivierung von vererbten Strukturen zurückführen lässt. Überprägungen von gegengesetzte Rutschharnischen auf einer Verwerfungsebene machen den Einfluss von mehreren Verwerfungsphasen sichtbar. Sorgfältige Trennung der heterogenen Datensätze ermöglicht eine Unterteilung in verschiedene homogene Verwerfungspopulationen. Die Resultate zeigen Stresssysteme unterschiedlicher Deformationsphasen. Das erstere, ein Extensionsregime mit Dehnungsachse parallel zu den Faltenachsen hängt mit der Faltung und Überschiebung der präalpinen Decken zusammen. Das zweite Stresssystem, ein Blattverschiebungsregime, herrscht im gesamten Untersuchungsgebiet vor und zeichnet sich durch N-S verlaufende linkssinnige und WNW-ESE ausgerichtete rechtssinnige Blattverschiebungen aus. Die unterschiedlichen Struktureinheiten von Préalpes Médianes bis zum Molassebecken zeigen gleichzeitig Anzeichen für Kompressionsregime als auch Blattverschiebungsregime auf. Obwohl deren Ursprung dieser zwei Spannungsregime sehr unterschiedlich ist, kann trotzdem eine abwechslungsweise Interaktion zwischen den beiden stattgefundene haben. Da die kompressive Spannungsachse bei beiden Spannungsregimen gleich ausgerichtet ist, bestimmt eine Vertauschung der extensiven und intermediären Spannungsachse das eine oder das andere Spannungsregime.

Anhand eines 3D Modellierungsansatz wurde die Veranschaulichung der komplexen Strukturen des präalpinen Deckenstapels, sowie der Strukturen des Falten- und Überschiebungsgürtels der Préalpes Médianes Decke ermöglicht. Diese Modelle geben einen besseren Einblick in den räumlichen Fortverlauf der geologischen Strukturen in der Tiefe als geläufige 2D Profile. Ausserdem helfen die 3D Modelle bereits bestehende geologische Karten, Profile und unsere Interpretationen zu werten, als auch die geometrische Folgerichtigkeit der einzelnen Dateneingaben zu prüfen. Im Anbetracht der zur Verfügung stehenden Daten und unseren Interpretationen zielen diese Modelle nicht darauf ab eine möglichst genaue Wiedergabe der Geologie im Untergrund zu geben, sondern vielmehr einen möglichen Lösungsvorschlag aufzuzeigen.

*****

ACKNOWLEDGEMENTS

As my work on the dissertation of the Tectonics in the Préalpes Klippen at the Fribourg Uni is ending, I would like to thank many colleagues, friends, and family for their support, company, and simply good times together. Without them, the realisation of this thesis would not have been possible, or a lot harder.

First, I would like to thank my "Doktorvater", Jon Mosar, for offering a possibility to continue the investigation of the structural geology of the Canton of Fribourg. Hereby, I could discover the wonderful landscape of the Préalpes, a region that was completely unknown to me coming from Eastern Switzerland. Jon's support in the fieldwork, as well as for the analysis and interpretation of my data was essential; his "anti-authoritarian" approach in guiding PhD and other students leaves lots of freedom in trying out new methods and making up theories, but he is always there to help get back on track when the theories get too crazy, as well as keep the spirits high in difficult times. Merci, Jon!

I am sincerely grateful to the KGV (cantonal building insurance) of the Canton Fribourg for their interest in the geology of the Préalpes and their financial contribution of this thesis.

Special thanks go to Jean-Pierre Berger, who stepped in as "last-minute expert" of my thesis. I am deeply touched by his sudden death and sad that his unique laughter became silent in the geological institute.

I am especially grateful to Damien Delvaux (Royal Museum for Central Africa, Belgium), Olivier Lacombe (Université Pierre et Marie Curie, France) and Neil Mancktelow (ETH Zurich) for their agreement to be experts and Jury members for my dissertation and that they took time to evaluate this thesis. Big thanks go to Neil, who willingly accepted to exchange field experiences by visiting my investigation area in the Préalpes and in return showing me the Rawil area, Luca Cardello's study area. Despite the unfortunate weather conditions (with a day trapped in a little hut because of heavy snowfall), the excursion with Neil and Luca was enriching for the continuation of my thesis, especially the focus on the characteristics of veins in the Helvetic in comparison to the ones in the Préalpes.

I would like to thank Luc Braillard, who has a huge experience and knowledge of my investigated area. His recent and current work (the development of the geological map of Boltigen of the Geological Atlas of Switzerland) overlaps my terrain between Boltigen, Schwarzsee, and the Gastlosen. His critical remarks and perceptive interpretative approaches often let me pause to reconsider my own interpretations. Moreover, Luc gave me the opportunity to assist at the elaboration of the "Sentier géologique des Gastlosen" and to help out with the guided tours in German. I also like to thank Luc for many great moments we spent together: the Buskers evening, Guarda, numerous parties in the Pavillon vert that is in fact red….

A big „merci" goes to Christian Caron, former director of the institute, who was with his enthusiasm for geological maps, cross-sections and the Préalpes indirectly responsible of my choice to write a thesis in structural geology.

I am also indebted to Martin Bochud, my former office neighbour, for mutual encouragement during the tougher periods of our theses. I would like to thank him for his help with ArcGIS, for his local knowledge of my study area, for motivating me in the final phase of my thesis. But it was also Martin, who was responsible for several, sometimes more (drinking coffee, watching speleo photographs, going for a beer), sometimes less pleasant work interruptions (kromocs, annoying me by any means, taking him to hospital…). Thank you very much Martin!

Big thanks go to all the other members of the struc-

tural geology group in Fribourg, with whom it was always a great pleasure to discuss 3D modelling, GIS, and structural geology questions. Thank you Martinus, Naomi, Meinrad, Tobi.

I also would like to thank all the Master students working in the Préalpes and Molasse basin for many discussions in the field and at the university about interpreting the “complexe mess” of the préalpine structures and about the methods of evaluating the fault-slip data. Merci Claudio, François-Xavier, Marius, Michi, Stéphanie, Sylvain, Tina, Thierry and Yannick.

Many thanks go to my other colleagues at University: Bastien, Bertrand, Claudius, Christoph, Daniel, Daniela, David, Florent, Giordana, Juanita, Katja, Laureline, Maëlle, Mario, Monica, Noémie, Raphaëlle, Roy, Stephan, and Thibault for lots of “Friday beers”, apéros, coffee breaks, skiing trips and other great recreational and professional activities

Many thanks go to my friends who supported me during this period: Sarah, for the countless times we were having lunch together and mutual encouragement during these times of ups and downs. Thank you, Annick, for your effort to help me leave the office from time to time to change ideas (climbing, windsurfing, sailing). I also want to thank Domi and Bruno, Reto and Tina for many unforgettable weekend trips in Switzerland and abroad.

I thank my family: my parents, Christina and Max and my sister, Wera, for their material and immaterial support during all my studies and their interest in my work.

Last, but certainly not least, I thank you, Peter, for all your support, not only by helping me with the 3D modelling, PC problems, English corrections, field work assistance, but also by encouraging me day by day to move on. Simply your presence gives me the power to move mountains.

*****

1 - Introduction

The Préalpes Klippen belt has attracted attention of several generations of geologists, because of its allochthonous position on top of the Subalpine Molasse in front of the Helvetic nappes. Earliest documents on the préalpine geology date back to the beginning of the eighteenth century (LOPRIENO et al., 2011). An important boost in geological investigation of the Préalpes took place at the turn of the twentieth century, including new aspects, such as nappe tectonics (JEANNET, 1922; SCHARDT, 1893b) and was enriched by the pioneer work of Lugeon (1902), Argand (1911), Gagnebin (1941), Favre (1887), Masson (1976), Peterhans (1923), Lemoine (1988) and finally Trümpy (1957), who firmly established the Briançonnais origin of the Préalpes Médianes (BERNOULLI and SENGÖR, 2011). The interest in the Préalpes Klippen steadily increased until 1990, mainly supported by the Lausanne and Fribourg Universities by a large number of doctoral and diploma thesis. In this sense, this thesis maintains the Fribourg tradition of regional geology.

While most of the previous studies deal with surface geology, especially with focus on stratigraphy and mapping, this dissertation treats in a first step the structural and geodynamical aspects of the Préalpes Klippen. Diverse structural features of different scales, ranging from large-scale fault-related folds, faults, and fault zones to small-scale fractures, secondary folds, veins, stylolites and brittle shear zones, witness the eventful history of the Préalpes Klippen. Generally, within this study, three major deformational phases were distinguished: the pre-emplacement phase, generating structures related to the rifting of the Alpine Tethys, the syn-emplacement phase, referring to structures associated to the nappe transport and the post-emplacement phase, developing structures after the emplacement of the préalpine nappes. The attribution of the observed structures to a corresponding deformational event, as well as their possible reactivation in a later stage, were carefully analysed and investigated.

Within a second step, a fault kinematic approach providing a better insight into the recent geodynamic evolution of the Préalpes Médianes and its adjacent structural units, the Gurnigel and the Subalpine Molasse was developed. Analyses are mainly based on fault-slip data and are combined with field observations, remote sensing analysis, the comparison with recent earthquake data, as well as 3D modelling. Hereby, the expression of the stress field within different structural entities are compared, to define the influence of pre-existing structures (Préalpes Médianes and Gurnigel), as well as to identify most recent stress systems affecting every unit in the same way. Regional stress fields of the Molasse Basin and the Jura mountains were also compared to obtain a more complete image of the structural behaviour on a larger scale.

In a third step, the complex structures of the préalpine nappe stack of the Préalpes Romandes, as well as the fold-and-thrust structures of the Préalpes Médianes were computed into five 3D-models with different resolutions to obtain a better understanding of the spatial continuation of the geology at depth and to validate our and previous interpretations.

1 Objectives

1.1 Problem Statement

During a multifaceted structural history of the Préalpes Klippen - ranging from paleotectonics to Alpine tectonics to more recent tectonics after the emplacement of the préalpine nappes - various structural features developed. Several of these structures were reactivated under different stress regimes after their generation. For this reason, it appeared to be important to establish a classification of the structures with reference to their original development. Fracture analysis in the field and subsequent paleostress reconstructions represent mostly a hetero-

geneous arrangement of faults and fault-slip. Only by combining field observations with a careful separation of the fault-slip data set, it was possible to gain an overview of the fracture patterns.

An interesting aspect is not only to what extent local structures are influencing the resulting stress regime, but how far the general stress regime are affecting an entire region. Another important aspect insufficiently analysed in previous studies is the comparison of the fracture pattern of different structural units. The Préalpes Médianes bear fractures accumulated over several deformational phases, which therefore result in complex structural arrangements. The fracture arrangement in the Gurnigel nappe is mostly the result of turbidites and thrusting structures related to the nappe transport, whereas the Subalpine Molasse features only the latest deformation phases. Similarities amongst the different structural entities would indicate a coincidence within the most recent stress system, while differences could be ascribed to their diverse structural background, as well as to a differing stress regime.

The interest in structural and fault kinematics analyses of the frontal part of the Préalpes Romandes is based on the direct vicinity to the Molasse basin, which is subject of on-going structural and (nano-) seismic studies (IBELE, 2011; MOSAR et al., 2011; MOSAR et al., 2010). Whereas the investigation of the Molasse basin is mostly driven by economical and actuarial interests (nuclear power plants, building insurance companies) because of its densely populated areas, the research in the Préalpes Klippen is mainly based on scientific interests because of its complex structural context.

1.2 Aims

One aim of this thesis is to gain an overview of the various structures developed during different deformational phases of the Préalpes Médianes, the Gurnigel Nappe, and the Subalpine Molasse. Detailed observation in the field, but also on maps, aerial photographs, and DTMs allow the definition as well as the attribution to deformational events.

A second aim is the reconstruction of the stress field based on the evaluation of fault orientation and their kinematic indicators. The resulting stress regimes are attributed to the previously defined structures allowing the reconstruction of the deformational history.

The compilation of already existing maps and profiles, as well as the mapped and measured structures of the Préalpes Romandes are compiled in a GIS-based database. Complemented with structural interpretations, this groundwork allows the computation and visualisation of the préalpine nappe stack and four discussed areas in detailed interactive 3D models.

The final challenge of this work is the integration of the interpreted préalpine structures into the context of the Alpine orogenic wedge.

1.3 Methology and Organisation of the Thesis

Intensive fieldwork within the Préalpes Médianes and its adjacent structural units allowed measuring and interpreting characteristic structural features, mainly fracture planes with slickensides, but also veins, fold axes, slickensides, stylolites, as well as brittle shear zones.

Subsequent analyses were focused on the interpretation of large-scale structures detected on orthophotographs and DTMs, as well as on already existing geological maps and cross-sections. The field data, the remote sensing interpretations, as well as the compilation of previous maps and cross-sections are maintained by a GIS-database created in ArcGIS10® software produced by ESRI (2011).

Fault kinematic analyses gives a quantification of brittle deformation commonly determining the reduced stress tensor consisting of the directions of the three principal stress axes ($\sigma1>\sigma2>\sigma3$) and the stress ratio R. The calculation of the stress tensors were realised using the TectonicsFP program (REITER and ACS, 1996 - 2002) to gain a first overview of the orientation of the different kind of data. Subsequently, the WinTensor program (DELVAUX, 2006) was applied to treat the heterogeneous fault-slip dataset to subdivide them into subordinate stress regimes developed during different deformation events.

Finally, the interpreted structures were visualised by constructing and computing five 3D models by the use of 3DGeoModeller Editeur Géologique©, a modelling software developed by the BRGM (Bureau de Recherches Géologiques et Minières, France) and the Australian company Intrepid Geophysics.

This thesis is subdivided into five parts, starting with an introductory part to define the context, as well as the investigation area to its tectonic and stratigraphic context. The second chapter is dedicated to the analysis of the different structures within the Préalpes Médianes; whereas in the third chapter the focus is directed towards the dynamic aspect of the previously

discussed structures. The forth chapter deals with the 3D reproduction of the préalpine nappes and four areas of major structural interest. The integration of the structural interpretations of the previous chapters into the more global context of the Alpine orogenic wedge is the topic of the fifth chapter, whereas in the last chapter a brief conclusion of the entire work is presented.

The chapters of this thesis are structured in a "paper-style". Therefore, they are independent of the other chapters allowing an individual "out of context" study of every chapter. The disadvantage of this structure is redundancies, especially in the introductory parts of each chapter. Therefore, the courageous reader of the entire manuscript is requested to turn a blind eye to a figure or paragraph, seeming to be already known.

2 General Context

2.1 Study Area

The Préalpes Klippen belt is situated along the Alpine boundary from the Mythen in the NE to the Annes (Central Switzerland) klippe to the SW (France, South of the Lake Geneva). The Préalpes klippen belt is subdivided into two major lobes, the Préalpes du Chablais southwest and the Préalpes Romandes northeast of the Rhône valley. Originating mostly in the Briançonnais sedimentation realm (TRÜMPY, 1957), the préalpine nappes were detached and transported 60 - 100km towards NW (SCHARDT, 1893b), where they overthrust the Molasse basin for about 30km. Erosion, related to the uplift of the External Crystalline Massifs led to the isolation of the Préalpes to the NW of the Helvetic nappes (Fig. 1.1).

The different structural units of the préalpine nappe stack present diverse paleogeographic origins, based on that, four different nappes are defined (Fig. 1.1) (from the top to the bottom):

- the Nappe Supérieure containing another four subordinate nappes: the Gurnigel, Dranse, Simmen and Gets Nappe (CARON, 1972; TRÜMPY, 1980);
- the Breccia Nappe (DALL'AGNOLO, 2000; LUGEON, 1896, 1949; STEFFEN et al., 1993);
- the Préalpes Médianes Nappe (BAUD, 1972; BIERI, 1925; GENGE, 1957; ISENSCHMID, 1979; JEANNET, 1922; METTRAUX, 1989; MOSAR, 1991; MOSAR and BOREL, 1992; MOSAR et al., 1996; PLANCHEREL, 1979; WISSING and PFIFFNER, 2002) and
- the Niesen Nappe (ACKERMANN, 1986; BERNOULLI et al., 1979; CARON, 1972, 1973; HOMEWOOD et al., 1984; MATTER et al., 1980).

The "Zone Submédiane" (Weidmann et al., 1976) and the Ultrahelvetics (BADOUX, 1963; HOMEWOOD, 1977) are considered as a tectonic mélange zone developed during the transport of the préalpine nappes and are therefore located underneath the nappe pile. Within this study, the major focus lies on the frontal part of the préalpine nappes, namely on the Préalpes Médianes and the Gurnigel nappe.

The Préalpes Médianes is the most important and best-exposed nappe, it is subdivided into two parts: the Préalpes Médianes Plastiques (PMP), mainly governed by large-scale fault-related folds, and the Préalpes Médianes Rigides (PMR), dominated by imbricated thrust slices dipping to the N/NW (LUGEON and GAGNEBIN, 1941).

The Gurnigel Nappe corresponds to the most external digitation of the Nappe Supérieure that remained isolated in between the Subalpine Molasse and the Préalpes Médianes. Originally transported on top of the Préalpes Médianes, the Gurnigel Nappe was finally overthrust by the Préalpes Médianes.

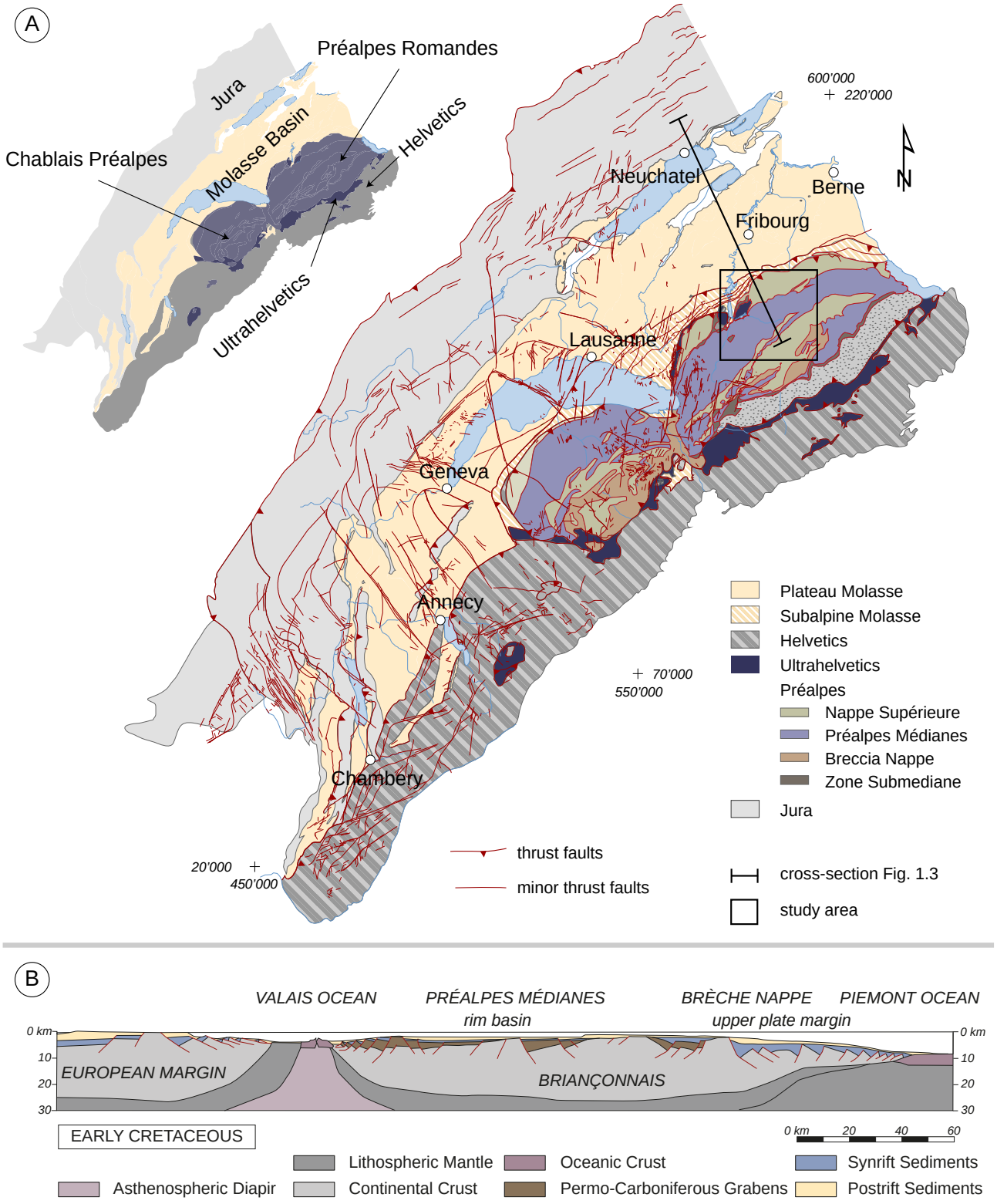

Fig. 1.1: A) Structural map of the Préalpes, the Western Molasse Basin, and its adjacent structural units; the Jura mountains and the Helvetic nappes. The black section line corresponds to the present-day cross-section of Fig. 1.3. The black square represents the investigation area of this study. B) Cross-section showing the localisation of the Briançonnais micro-continent in between the Pyrenean and Piemont ocean at the Early Cretaceous times (modified after STAMPFLI et al., 2002).

In addition, particular attention is given to the Subalpine Molasse located below and NW of the frontal boundary of the Préalpes Klippen. The Subalpine Molasse is characterised by a narrow band of thrust slices spreading along the former northern Alpine front.

2.2 Regional Structures

The majority of the large-scale structures characterising the Préalpes Médianes developed during the nappe transport. Thin-skinned tectonics led to the typical fold-and thrust belt evolution of the Préalpes Médianes. Generally, foreland-propagating thrusts are branching off the basal décollement horizon of the préalpine nappes leading to the development of large-scale arc-shaped folds striking from the Western to the Eastern part of the Préalpes Romandes.

Differences in the general structural style within the Préalpes Médianes are mainly related to changes in lithology associated to paleostructures. For this reason, the Préalpes Médianes are roughly subdivided into two parts: the PMP to the NW and the PMR to the SE. The PMP are deposited in a basin environment and shows a nearly complete stratigraphic series from the Triassic to the Cretaceous and the Tertiary. The sedimentation realm of the PMR however, corresponds to a platform and lagoonal environment with a stratigraphic record marked by stratigraphic gaps. These stratigraphic differences result within the PMP in a more plastic deformation, expressed by large-scale fault related folds, whereas the deformation style of the PMR occurs in a "rigid" way, forming steeply dipping thrust slices.

Furthermore, the Préalpes Médianes expose an omnipresent arrangement of faults, on the one hand related to the fold development, on the other hand post-dating the nappe emplacement, and crosscutting the existing folds. Throughout the entire Préalpes Médianes strike-slip faults can be identified mostly oriented N-S with a sinistral, and WNW-ESE with a dextral displacement. One interpretation of this strike-slip fault system is the activity of faults rooting in the basement affecting both the overlying and underlying structural units. Strike-slip movements along these fault planes influence the Préalpes Médianes above by provoking its characteristic fold-and thrust structure (PLANCHEREL, 1976, 1979). According to this interpretative approach, the faulting, as well as the contemporaneous folding-and-thrusting took place after the emplacement of the préalpine nappe. Another interpretation associates the folding-and thrusting to the transport of the préalpine nappes, where thrusts are branching off the major décollement. The strike-slip faults are on the one hand related to tear faults

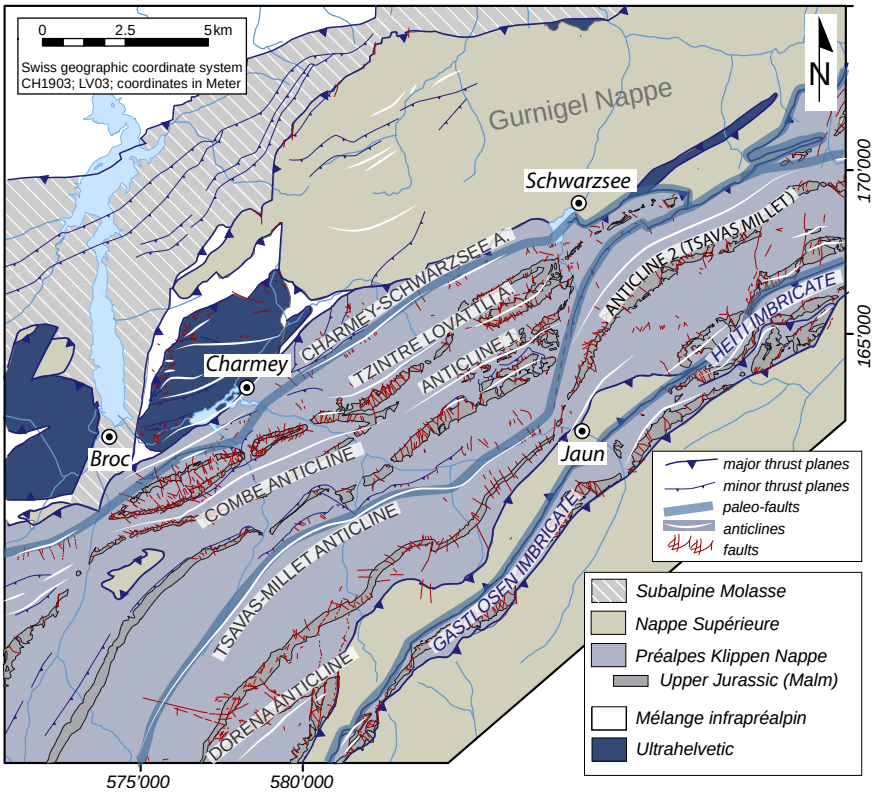

Fig. 1.2: Structural map illustrating the large-scale structures of the investigation area, especially of the Préalpes Médianes: fault-related anticlines, as well as paleofaults. Synclines were omitted for reasons of simplification.

(MOSAR, 1997) provoked by a differential advancing of the fold-generating thrust planes mostly guided by pre-existing paleostructures. On the other hand, the folding of the Préalpes Médianes provoked the generation of normal faults oriented favourably for a strike-slip reactivation after the emplacement of the préalpine nappes.

2.3 Stratigraphy

Because of important changes in the sedimentation realm, the lithologies of the different structural units vary considerably, reaching from sandstone deposits of the Subalpine Molasse, to flysch deposits in the Gurnigel nappe, to limestone, shale, and marl deposits in the Préalpes Médianes. In the Préalpes Médianes, the stratigraphic series ranges from Triassic to Upper Cretaceous to Tertiary flysch deposits, whereas since the Early Jurassic two distinct sedimentation realm developed leading to a nearly complete stratigraphic series to the NW, because of a large basin (Préalpes Médianes Plastiques). To the SE, a platform, lagoonal paleoenvironment marked the stratigraphic record with important stratigraphic gaps (Préalpes Médianes Rigides). The Nappe Supérieure with its frontal sub-nappe, the Gurnigel nappe, consists mainly of flysch deposits ranging from Maastrichtian (Upper Cretaceous) to Bartonian (Middle Eocene) age. The youngest sediments are found in the Subalpine Molasse reaching from the Rupelian (Lower Oligocene) belonging to the UMM (Lower Marine Molasse) to the Chattian (Upper Oligocene) of the USM (Lower Freshwater Molasse). Within this chapter, a brief overview over the stratigraphy of the discussed structural units is presented.

2.3.1 Préalpes Médianes

Triassic

During Triassic times, the future distinctive sedimentation realm of the Préalpes Médianes and the Préalpes Rigides represents a rather uniform shallow marine or lagoonal depositional environment. These platform carbonates are deposited in a steadily subsiding, stable water environment, which may result from the opening of the Hallstatt-Meliata ocean (MOSAR et al., 1996) (detailed subsidence history in Borel (1995)).

In the Préalpes Médianes Rigides, the Triassic sedimentation begins in the Middle Triassic (Anisian) with 600 - 700m of littoral to lagoonal carbonate series. The majority of the Triassic sediments are composed of a rather monotonous succession of dark limestones with grey alteration surfaces and lighter coloured dolomites (BAUD, 1972).

The stratigraphic series in the Préalpes Médianes, starts in the Upper Triassic with chaotic crushed layers of gypsum and cornieules. Jeanbourquin (1988) convincingly demonstrated that the cornieules are chemical or collapsed breccia formations related to a telogenetic Quaternary process of dissolution. These transformations prove the high amount of circulating fluids in these sheared Triassic sequences. These evaporitic layers constitute the basal detachment of the Préalpes Médianes (BAUD, 1972). Well stratified dolomite rock and dolomitic limestones dominate the main part of the Upper Triassic sediments (Norian; Baud (1972)).

Morphological appearance

Triassic rocks appear mostly in the core of eroded anticlines or in frontal thrust slices of the nappe (PASQUIER, 2005). Intense fracturing of the evaporitic rocks facilitates their alteration and erosion and leads to the formation of large depressions filled with Quaternary deposits (PLANCHEREL, 1979). However, Middle Triassic layers of the Préalpes Médianes Rigides form steep cliffs and mountains (e.g. Wiriehorn, Mont d'Or, St-Triphon).

Lower Jurassic (Lias)

After the Early Liassic rifting event of the Alpine Tethys, the Briançonnais rim basin became divided into distinct facies domains by synsedimentary faulting. Sediments of different depositional environments were accommodated - from very shallow to intermediate depth (METTRAUX and MOHR, 1989). Fast differential subsidence starts in the southern Préalpes Médianes, developing different small basins that are separated by structural highs, as the most important Château d'Oche-Corbeyrier high (SEPTFONTAINE, 1983). South of this structure, the Heiti basin developed filled up with Lower and Middle Jurassic sediments. Even farther SW, a platform is located giving rise to the sedimentation realm of the Préalpes Médianes Rigides (Fig. 1.4). During this period emersion of certain parts leads to intensive erosion of Liassic and Upper Triassic sediments and even formation of karst (MOSAR et al., 1996; SARRET and MOSAR, 2010). As a result, Liassic sediments are not preserved in the Préalpes Médianes Rigides. There, the transgressive contact to the middle Jurassic sediments makes an angular unconformity with the underlying Triassic of 10° (BAUD and SEPTFONTAINE, 1980) (Fig. 1.4). Consequently, considerable lateral thickness and facies variations are characteristic of the Liassic deposits. An average thickness of 200m can be assumed (PLANCHEREL, 1979).

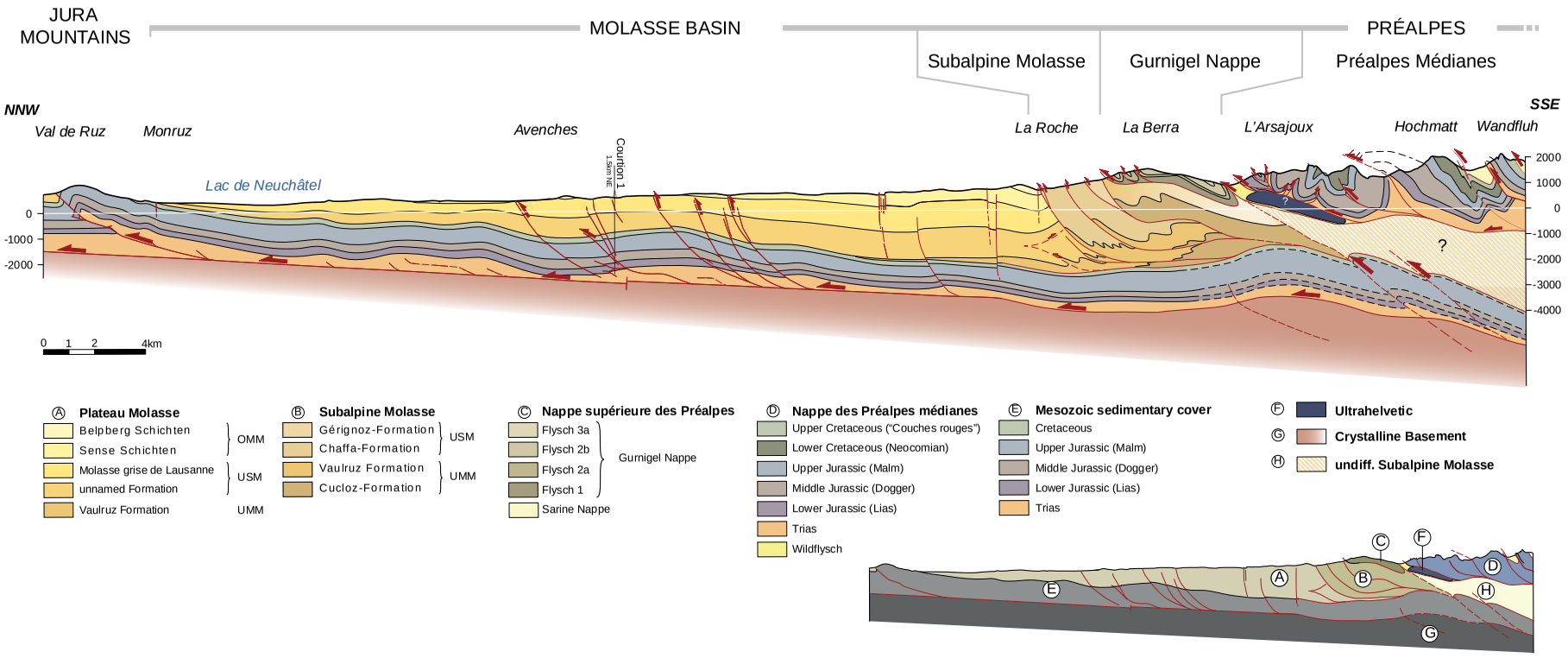

Fig. 1.3: Detailed cross-section showing the transition from the Préalpes Médianes, the Gurnigel nappe, the Subalpine Molasse to the Western Molasse basin and the Jura mountains and the relationship among these different structural units. The cross-section is based on surface investigations and on a compilation of already existing literature (BAUD and SEPTFONTAINE, 1980; BRAILLARD, 1998; MANDIA, 1984; PASQUIER, 2005; PYTHON et al., 1998; TERCIER, 1928; WEIDMANN, 2005). The localisation of this profile is indicated on Fig. 1.1.

Morphological appearance

Despite the major spatial and temporal discrepancies in sedimentation, the Liassic deposits have at least one common aspect: the predominance of spathic, oolitic or siliceous limestone. This determines its specific structural behaviour by forming pronounced reliefs, as the Liassic limestones are surrounded by the less competent levels of the underlying Triassic and overlying Middle Jurassic (Dogger) levels. Furthermore, the structural behaviour of the Liassic limestones is similar to the one of the competent Upper Jurassic (Malm) level which give rise to brittle deformation (PLANCHEREL, 1979).

Middle Jurassic (Dogger)

In the Early Dogger, only one large basin remains to the N of the Château d'Oche-Corbeyrier structural high, separated by a sedimentary ramp from a lagoon and platform to the south. This domain has constantly suffered from erosion and non-deposition. This is indicative for the rift shoulder in the south (S of Médianes Rigides domain. South of this rift shoulder the Breccia nappe sedimentation is dominated by breccia deposits (MOSAR et al., 1996). In the Préalpes Médianes, two different sedimentation realms develop (BOREL, 1995): the Staldengraben formation to the north with important thickness variation between 500m - 600m in the frontal part and 800m-1500m in the Hochmatt region. Its lithology is marked by its calcareo-argillaceous properties and its yellow-brownish tint provoked by alteration (PASQUIER, 2005). In the south, on the emerged Briançonnais platform, about 100m of lagoonal, coal bearing Mytilus Dogger was deposited, its thickness decreasing to the south (SEPTFONTAINE, 1995).

Morphological appearance

The monotonous slopes between the resistant lithologies of the Upper and the Lower Jurassic are the most obvious morphological characteristic of the Middle Jurassic layers. While the whole Dogger behaves in a "plastic" way, the numerous calcareous layers act as brittle levels (PLANCHEREL, 1979). The alternating limestone and marls layers control the tectonic style of the Middle Jurassic formation.

Upper Jurassic (Malm)

At the beginning of the Upper Jurassic series, a transgression changes the sedimentation realm drastically: flooding of the platform (Médianes Rigides) brings the platform boundary of the Dogger into deeper water depth. Not until the end of Upper Jurassic a high-energy barrier forms at the outer platform margin protecting the internal lagoon (HEINZ and ISENSCHMID, 1988). Throughout the Préalpes Médianes, the sedimentation in the Upper Jurassic was exclusively calcareous and appears as the most constant and characteristic formation of this nappe (PLANCHEREL, 1979). In general, the very light grey and massive, micritic Malm limestones form the morphological and structural skeleton of the Préalpes Médianes Plastiques. Late Jurassic sediments are normally about 300 - 400m thick, but in the slope area between northern and southern facies realms, thicknesses are generally reduced to 120m or less (ISENSCHMID, 1979).

In the external part of the nappe, the Malm formation starts with the typical facies of the "nodular limestones": alternating marls, limestones and nodular shales, rather thick in the frontal part they are thinning out towards south. The subsequent Kimmeridgian formation is marked by macroscopic homogeneous limestones, massive or with thick strata, generally without marly interbeds (PLANCHEREL, 1979).

Morphological appearance

In the Préalpes Médianes Plastiques, the Upper Jurassic - due to its less resistant neighbouring formations (Dogger and Neocomian) - builds the rigid skeleton of the nappe and provides gentle folding in a "plastic" way. Where these surrounding layers are absent, for non-depositional or erosional reasons, the Malm behaves under deformation in a brittle way ("Préalpes Médianes Rigides"). Nevertheless, these different deformational styles are only valuable to the large-scale structures, and allow the existence of numerous brittle faults in the Préalpes Médianes Plastiques (PLANCHEREL, 1979). The Upper Jurassic limestones accommodate a large number of fault planes that are mostly karstified, which makes the identification of fault-kinematic indicators difficult.

Lower Cretaceous (Neocomian)

The transition occurred gradually between the massive Upper Jurassic limestones and the pelagic, thin-bedded limestones ("Calcaires Plaquetés") of the Lower Cretaceous (Neocomian). Concerning the lithology, the Neocomian limestones are characterised by remarkable thin layering, even more pronounced by marly interlayers. Due to this stratification, the Lower Cretaceous formation is intensively folded (chevron-type folds), which makes the estimation of the exact thickness difficult (between 70m - 150m). Towards S the thickness diminish continuously until non deposition in the domain of the Tour d'Aï, Heiti and Gastlosen (BOLLER, 1963). The Préalpes Médianes Rigides were probably exposed, explaining the absence of the Neocomian deposits (PLANCHEREL, 1979).

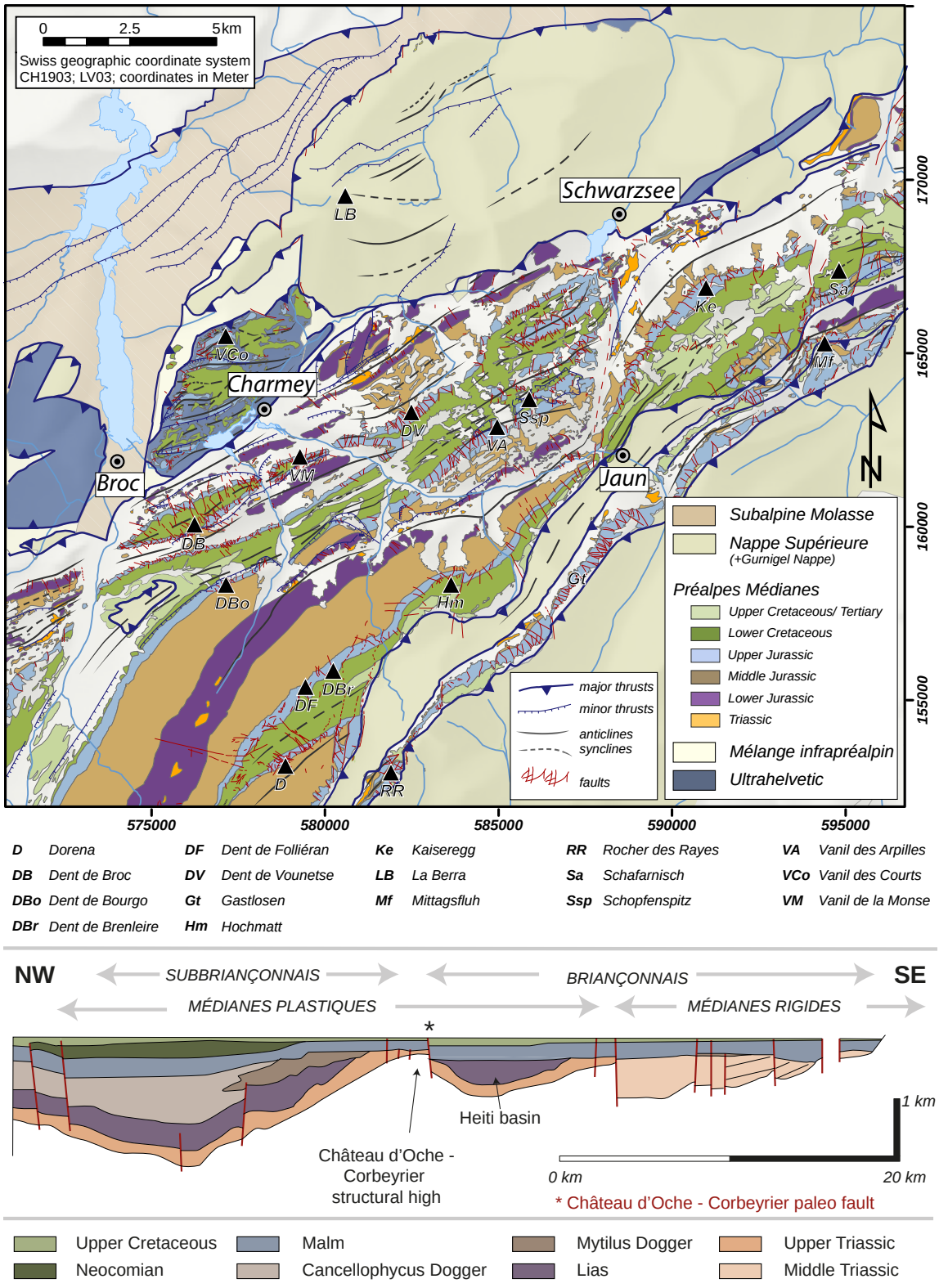

Fig. 1.4: Above: Geological map of the investigated Préalpes Médianes completed with a simplified structural map of the adjacent structural units, based on geological maps (ANDREY, 1974; BIERI, 1925; BOREL, 1991; BOVET, 1990; GISIGER, 1967; PAGE, 1969; PASQUIER, 2005; PLANCHEREL, 1979; SPICHER, 2005; THALMANN, 1990), but also on field observations. This map is an extract of the GIS data bank and is therefore very detailed. Below: palinspasti ectonic reconstruction model for the Préalpes Médianes highlighting the strong influence of paleofaults affecting the sediment deposition. The horizontal line corresponds to the deposition of the Eocene Flyschs (modified after BAUD and SEPTFONTAINE, 1980; BOREL and MOSAR, 2000).

Morphological appearance

The Neocomian rocks are situated on the flanks of the synclines as a transition between the massif limestone cliffs and the overlying gentler shapes of the Couches Rouges and the Flyschs without marking a clear contact. Easy weathering of this formation provides vegetation growth even in the steepest slopes (Plancherel 1979). Faults deriving from the Upper Jurassic limestones are often immediately absorbed within the „Calcaires Plaquetés“. The shortening of the Neocomian layers is mostly compensated by small-scale folding.

Middle Cretaceous and Upper Cretaceous/ Eocene (Couches Rouges)

In a complete lithological series, as in cores of synclines, the Neocomian limestones are successively overlain by an interplay of limestones and dark argillaceous shales of the “Complexe schisteux” (Middle Cretaceous) and the limestones and marls of the Couches Rouges formation (Upper Cretaceous/ Eocene). The sometimes red, but more often grey or green marly limestones occur throughout the entire Préalpes Médianes and the adjacent Breccia nappe (Guillaume, 1986) and reach thicknesses between 100m- 200m (Plancherel, 1979). In early Late Cretaceous a change in sedimentary conditions occurred, that gives rise to important stratigraphic hiatuses. Detailed stratigraphic descriptions are found in CARON and DUPASQUIER (1989), GUILLAUME (1986), HABLE (1997)

Morphological appearance

The “Complexe schisteux” and the Couches Rouges follow the underlying structures: to the north - where Neocomian limestones exist - they fill the core of the synclines with their numerous small-scale folds, and to the south the Couches Rouges are closely associated with their Late Jurassic (Malm) substratum (PLANCHEREL, 1979).

Structural evolution of the Préalpes Médianes during sedimentation

The paleotectonic history of the Préalpes Médianes, before incorporation of the Briançonnais terrane and nappe emplacement, is characterised by the evolution of its sedimentation realm. In a rim basin context, the Préalpes Médianes were located to the N-NW of the Briançonnais upper rift shoulder and north of the passive margin (MOSAR et al., 1996; STAMPFLI and MARTHALER, 1990). The sedimentary rocks of the Préalpes Médianes, consisting of limestones, dolomites, marls and shales of Triassic to Eocene age (BADOUX and MERCANTON, 1962; BAUD et al., 1989; BAUD and SEPTFONTAINE, 1980; BOREL, 1995; 1990; TRÜMPY, 1980), recorded some major structural events of the pre-emplacement phase.

Although, most of the préalpine structures developed during the transport of the préalpine nappes, paleofaults generated during sedimentation largely predefine zones of weakness. Pre-emplacement structures are rarely visible, mostly they are expressed as indirect structural features, such as important thickness variations or horizons caused by erosion. The detailed description of the paleostructures in the field was beyond the scope of this thesis; therefore, a short compilation of already documented tectonic events is illustrated in the below.

2.3.2 Gurnigel Nappe

The Gurnigel Nappe consists entirely of turbiditic Flysch sediments deposited during Maastrichtian and Eocene in an abyssal to bathyal environment of the Piemont Ocean (VAN STUIJVENBERG 1979). Generally, the outcrops within this structural unit are of mediocre quality and additionally, the lateral facies changes and the local structures appear to be quite complex (WEIDMANN, 2005). For this reason, the different stratigraphic units of the Gurnigel nappe are discussed here with fewer details (for more precise descriptions see CARON (1976), TERCIER (1928), VAN STUIJVENBERG ET AL. (1976), WEIDMANN (2005), WINKLER (1984))

The oldest flysch deposit of the Gurnigel nappe is of Maastrichtian age - known as Hellstätt series (TERCIER, 1928) - consists of shales, diverse marls, polygenic conglomerates, and particularly of limestones with a characteristic pale grey tint. Their layers are often chaotically arranged due to intensive fracturing and refolding (thickness: 100 - 300m). The only location in Switzerland, where the Cretaceous-Tertiary boundary was recognised was in the Gurnigel nappe (DE KAENEL et al., 1989).

The subsequent layers of Danian age are marked by dark shales and sandstones rich in glauconite. Outcropping Danian layers are rarely visible and their thickness is estimated being less than 100m (VAN STUIJVENBERG et al., 1976; WEIDMANN, 2005).

The Thanetian deposits show a remarkable occurrence of sandstones forming contrasting changes in morphology by protruding slopes, escarpments, and crests (thickness: 100-150m). Outcrops consisting of Thanetian flysch are relatively frequent, for example in the Tatüre quarry.

In contrast, the following Ilerdian and Cuisian strata are essentially marly with characteristic alterna-

Series	Structural evolution of the Préalpes Médianes		Tectonic event	Literature
Eocene/ Oligocene	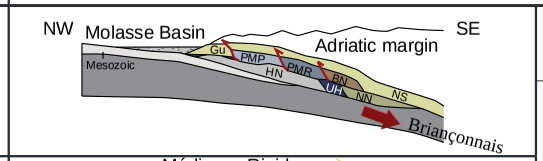	Nappe transport	Oceanic closure, detachment of the Briançonnais and incorporation as terrain into the accretionary wedge of the Alpine Tethys	
Upper Cretaceous	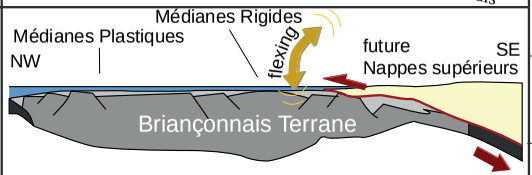	Incorporation of the Briançonnais into accretion prism provokes flexural uplift, which is represented by phases of sediment starvation (hardground) and emersion. Start of decollement and structuring of the Nappe supérieure (83 Ma), indicated by first Flysch deposits. Basin closure, extension towards NNE-SSW	Uncoupling of the Briançonnais from the Iberian plate and pre-collisional flexure	Borel (1995), Caron (1966, 1972), Stampfli & Marthaler (1990), Stampfli et al. (2002)
Upper Jurassic - Lower Cretaceous	subsidence	Lower Cretaceous: pelagic sedimentation in the North, non-deposition in the South Retarded subsidence due to the opening of the Valais ocean. Sedimentation of the massive upper Jurassic limestones	Uncoupling of the Iberian plate from the European plate, rifting of the Valais Domain, the Briançonnais on the southern margine	Borel (1995), Hable (1997)
Middle Jurassic	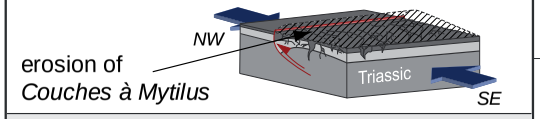	Compressional movements cause a strong uplift exposing and eroding the Mytilus formation. Thermal subsidence: important thickness changes due to small en-echelon synsedimentary normal faults.	Seafloor spreading of the alpine Tethys, Briançonnais turn into a rim basin of this ocean (ophiolithes ~155 Ma)	Septfontaine (1995), Borel (1995), Bill (1997)
Lower - Middle Jurassic	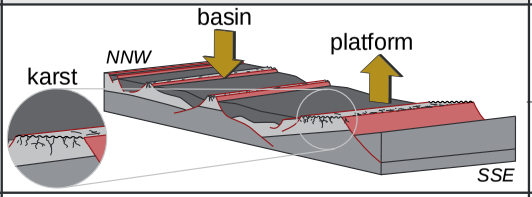	First local compressional phase is triggering the inversion of paleofaults leading to erosion of the Heiti formation and karst formation. Extensional movement causes tilting of the basin of the Médianes: subsidence to the N and emersion to the S of the NW zone.	Rifting of the alpine Tethys, the Briançonnais is on the northern margin	Baud & Septfontaine (1989), Borel (1995), Mettraux & Mosar (1989)
Triassic - Lower Jurassic	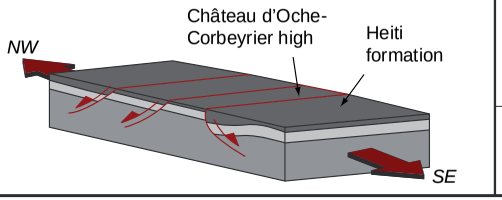	Lower Jurassic: maximum extension, marine basin structure is controlled by three important NE-SW oriented paleofaults revealing important thickness variations, but also N-S oriented fractures. Intensified extensional fracturing expressed by thickness changes in Norian and Rhetian series and Breccia horizons in the Upper Triassic.	Fracturing of the European plate	Borel & Mosar (2000), Borel (1997), Septfontaine (1995) Baud (1987), Borel (1997) Genge (1957) Hürlimann et al. (1996)

Fig. 1.5: Overview of the tectonic evolution of the Briançonnais domain from the Triassic until the Eocene/ Oligocene. Abbreviations of the Eocene/ Oligocene scheme: H = Helvetic; UH = Ultrahelvetic; NN = Niesen Nappe; PMP = Préalpes Médianes Plastiques; PMR = Préalpes Médianes Rigides) BN = Breccia Nappe; Gu = Gurnigel Nappe; NS = Nappe Supérieure).

tions of sandstones and marls and pelites. At the base, the content of coarse sandstones is relatively high, that is cropping out at Fall and the Zollhaus quarry. The Ilerdian layers are often strongly folded; therefore the estimation of the thickness suffers from uncertainties and varies between 50 and 500m.

The turbidite deposits of the Lutetian are thin, marly, and always calcareous with a frequent abundance of nanoflora. The thickness of the Lutetian layers is again difficult to estimate due to intensive folding (thickness > 1000m).

2.3.3 Subalpine and Plateau Molasse

The Molasse basin consists essentially of detrital sediments derived mainly from the rising Alps. Generally, four lithostratigraphic groups are distinguished: the Lower Marine Molasse (UMM (German abbreviations)), the Lower Freshwater Molasse (USM), the Upper Marine Molasse (OMM), and the Upper Freshwater Molasse (OSM). They correspond to two major sedimentation sequences linked to the evolution of the raising Alps and are influenced by connections to the Paratethys, to the Rhine graben to the north and the Rhône river system to the south. Within the investigation area, the Upper Freshwater Molasse is missing and is not further discussed.

Lower Marine Molasse (UMM) ~ Middle Oligocene

The Lower Marine Molasse is only outcropping in the Subalpine Molasse. Within the Western Molasse basin the UMM consists of two formations: the Cucloz Formation and the Vaulruz formation. The base of the Cucloz formation consists of shales with fine sandstone interlayers corresponding to thick, often incomplete turbidite sequences. Subsequently, a deltaic sedimentation realm leads to the deposition of coarse, polygenic sandstones, either as classic turbidites or as channel infill.

An important thrust marks the contact of the Cucloz and the Vaulruz formation. The base of the Vaulruz formation consists of laminated, greyish marls corresponding to a protected paleoenvironment, such as a lagoon or a platform (estimated thickness 100-300m). The top of the Vaulruz formation is indicated by fine grained calcareous sandstone deposits of 30-50m thickness expressing a high wave activity.

Lower Freshwater Molasse (USM) ~ Upper Oligocene and early Lower Miocene

This stage is characterised by the retreat of the sea from the Molasse depression and the strong rising of the Alps, at rise of almost 1mm/year. The Plateau Molasse landscape at late Oligocene times is dominated by at least seven gravel fans, at the northern margin of the Alps (TRÜMPY, 1980). The Subalpine Molasse of the Western Molasse basin, the USM are subdivided into the Chaffa and the Gérignoz formation (MORNOD, 1945). The Chaffa formation is characterised by fluviatile and floodplain deposits: coarse grains, multicoloured conglomerates, thinly laminated sandstones (crevasse splays) and claystones. Due to intensive folding, the apparent thickness of the Chaffa formation varies between 700m and 1000m (WEIDMANN et al., 1982). The Gérignoz formation consists primarily of multicoloured marls with some sandstone and freshwater limestone interlayers that are attributed to a sedimentation realm corresponding to vast floodplains with meandering rivers (WEIDMANN, 2005).

Upper Marine Molasse (OMM) ~ Late Lower Miocene

A marine transgression marked the “Burdigalian” and “Helvetian” stages, linking the Rhône Basin with the Vienna Basin. The northern shoreline arrived within the present Jura mountains. To the south, the shallow and at times brackish sea covered most of the present-day folded Molasse, while the Subalpine Molasse belt was standing out (Trümpy, 1980). In the Burdigalian, feldspathic and often glauconitic sandstones were prevailing with siliceous and calcareous grains with some thin marl interlayers. The top of the Upper Marine Molasse is formed by the Belpberg formation by its characteristic conglomeratic deposits, whose pebbles were analysed regarding its pressure-solution marks. The composition of the pebbles varies in terms of their geographic and stratigraphic situation from quartzite, radiolarite, siliceous limestones, to flysch sandstones (Weidmann, 2005).

*****

2 - Thrusting and Faulting in the Préalpes Médianes

Abstract

Detailed study of deformational structures of the Préalpes Médianes nappe - belonging to the préalpine nappe stack to the NW of the Helvetic nappes and the External Crystalline Massifs - indicates different structural elements developed during pre-, syn- and post-emplacement of the préalpine nappes. Extensive fieldwork, completed with the study of aerial photographs and digital terrain models, allowed the compilation of data on a large number of faults planes mostly bearing slickensides, fault arrangements, lineaments, vein systems, stylolites, brittle shear bands, as well as large- and small-scale folds. Two cross-sections help understand the complex composite arrangement of the various encountered structural features accumulated and partly reactivated throughout different deformation events. Structural elements related to pre-emplacement phase are characterised by the synsedimentary extensional faults related to the Alpine rifting, mainly expressed by sedimentary thickness changes, forming weakness zones pre-defining subsequent deformation phases. During the syn-emplacement phase, most of the structures of the Préalpes Médianes were acquired, such as fault-related folds, imbrications, tear faults related to differential advancing of the thrust planes, as well as normal faults associated with fold axis parallel extension. The post-emplacement phase is marked by the presence of out-of-sequence thrusts cutting through the préalpine nappe pile, following mainly pre-existing weakness zones, such as paleofaults or nappe contacts. Presumably, they can be linked to the development of crustal imbricates. Moreover, an ubiquitous conjugate strike-slip fault system developed within the Préalpes Médianes, where mostly pre-existing fault planes were reactivated. However, the N-S oriented sinistral and NW-SE oriented dextral strike-slip faults, clearly offsetting previous structures, can be found as well in the adjacent préalpine nappes, in the Subalpine Molasse, Plateau Molasse and in the Jura mountains.

1 Introduction

The Préalpes klippen extend along the Alpine front of the French and the Swiss Alps, bordered to the NW by the Western Molasse basin and towards the hinterland by the Helvetic nappes and the External Crystalline Massifs. The Préalpes originate in the Briançonnais and Sub-Briançonnais area (TRÜMPY, 1960, 1980), where they were detached in the course of the Alpine collision and its subsequent incorporation of the Briançonnais micro-continent into the accretionary wedge (STAMPFLI et al., 1998). Subsequently, the préalpine nappes were transported to the N/NW and emplaced onto the Alpine foreland. Erosion linked to the uplift of the crystalline massifs and the development of the Helvetic nappes provoked a subsequent isolation of the Préalpes klippen (Fig. 2.1) (BONNET et al., 2007).

Different structural features, such as faults and fractures, are important witnesses providing significant insights into the complex structural history of the Préalpes klippen belt, which is subdivided here in three different deformational phases: pre-, syn- and post-emplacement of the préalpine nappes. The observed local fracture pattern is mainly related to the fold-and-thrust development due to the nappe transport. However, the reactivation of these fault planes as strike-slip faults, as well as more recently formed N-S oriented sinistral and WNW-ESE oriented dextral faults, cutting through previous stvructures, attest to an on-going deformational evolution postdating nappe emplacement.

Within this chapter, the focus lies on the different structures characterising the Préalpes Médianes and the aim is to attribute them to a particular structural event pre-, syn-, or post-emplacement. First an overview

of the structural trends of folds and faults respecting their distribution and orientation is given, as well as a detailed description of small-scale structural features measured in the field such as fault associations and slickenside bearing fault planes and veins. Subsequently, based on field data and complemented by a compilation of already existing geological maps, two cross-sections are presented, highlighting particular structures.

The cross-sections allow a better understanding of the complex composite arrangement of the various structural features accumulated and partly reactivated throughout different deformation events.

Within the Préalpes klippen belt, two major lobes have been distinguished: to the south-west of the Rhône valley the Chablais Préalpes and towards NE the Préalpes Romandes. The Préalpes klippen consist of a pile of structural nappes with the following succession (from top to bottom):

- Nappe Supérieure containing another four subordinate nappes: the Gurnigel, Dranse, Simmen and Gets Nappe (CARON, 1972; TRÜMPY, 1980),
- Breccia Nappe (DALL'AGNOLO, 2000; LUGEON, 1896, 1949; STEFFEN et al., 1993),

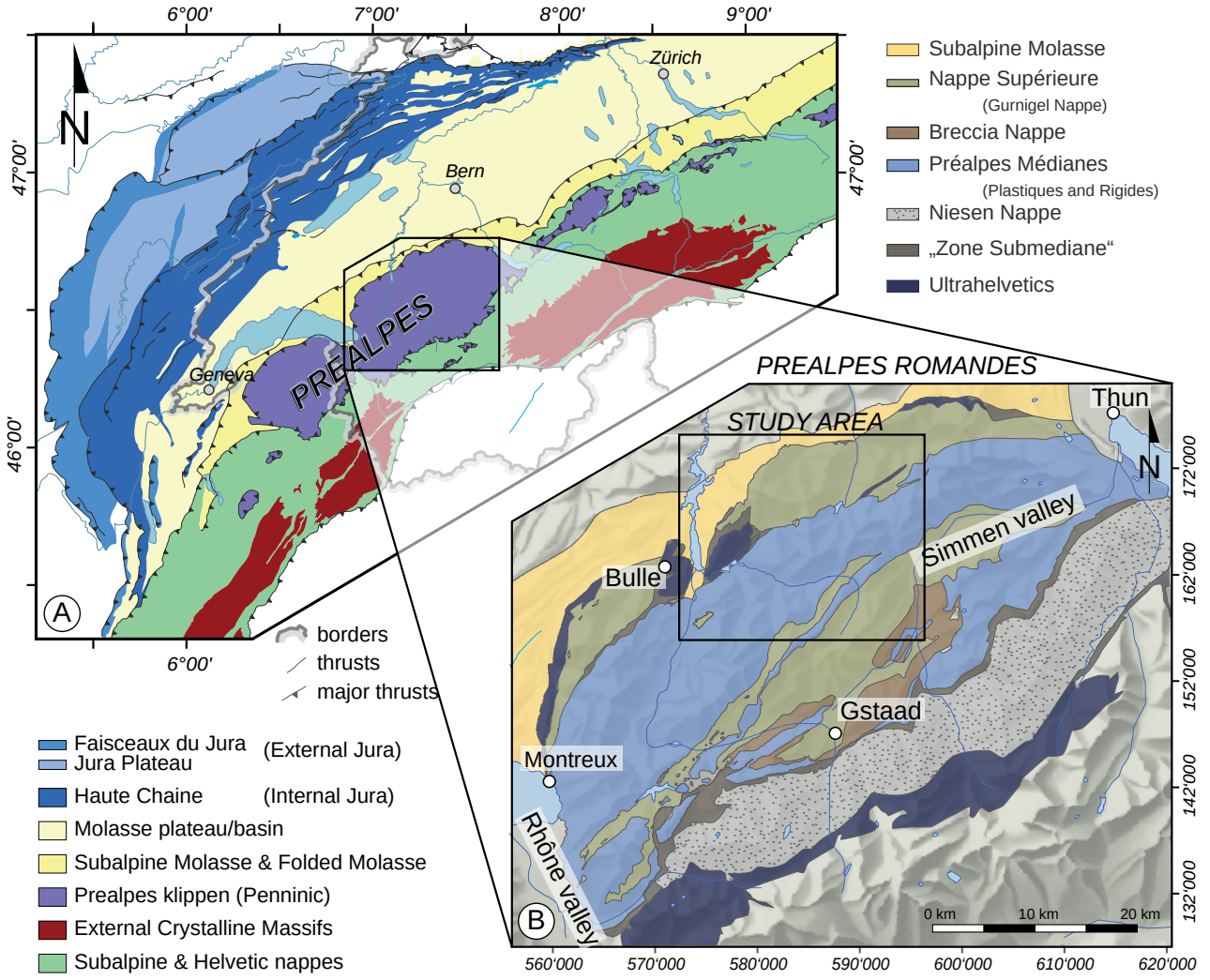

Fig. 2.1: Location of the Préalpes klippen belt in the context of the Western Alpine orogen. A) simplified tectonic map of the Western Alps highlighting the large-scale structural units including the Préalpes klippen belt located along the northern front of the Swiss and the French Alps and NW of the Helvetic nappes and the External Crystalline Massifs (modified after SCHLUNEGGER and MOSAR, 2010). The Préalpes klippen belt is characterised by two large lobes: the Préalpes du Chablais SW and the Préalpes Romandes NE of the Rhône valley. B) Structural map of the Préalpes Romandes modified after Caron (1973). The allochthonous préalpine nappes are piled up in the following order (from top to bottom): a) Nappe Supérieure, b) Breccia Nappe, c) Préalpes Médianes and d) Niesen Nappe (existing only in the Préalpes Romandes) and two mélange zones developed during the nappe transport: the Zone Submédiane and the Ultrahelvetics.

- Préalpes Médianes Nappe (BAUD, 1972; BIERI, 1925; GENGE, 1957; ISENSCHMID, 1979; JEANNET, 1922; METTRAUX, 1989; MOSAR, 1991; MOSAR and BOREL, 1992; MOSAR et al., 1996; PLANCHEREL, 1979; WISSING and PFIFFNER, 2002) and

- Niesen Nappe (ACKERMANN, 1986; BERNOULLI et al., 1979; CARON, 1972, 1973; HOMEWOOD et al., 1984; MATTER et al., 1980).

During the nappe transport a mélange zone developed, the "Zone Submédiane" (Weidmann et al., 1976), which can be found together with tectonically emplaced lenses of Ultrahelvetics (BADOUX, 1963; HOMEWOOD, 1977 in the frontal part of the Préalpes, below the Préalpes Médianes and in the most internal regions (TRÜMPY, 1980).

In the Préalpes Romandes, the Préalpes Médianes Nappe is the most important and best-exposed préalpine nappe, originating in a rim basin context located to the N-NW of the Briançonnais rift shoulder of the Tethyan rift margin (MOSAR, 1997; MOSAR et al., 1996; STAMPFLI and MARTHALER, 1990). Extensional synsedimentary faults influenced the sediment distribution considerably, leading to the development of several different facies realms perpendicular to strike (BAUD and SEPTFONTAINE, 1980) (Fig. 2.2). As a result the Préalpes Médianes are subdivided into two different units; the Préalpes Médianes Plastiques (PMP) situated in the frontal part of the nappe and the Préalpes Médianes Rigides (PMR) in the rear part (LUGEON and GAGNEBIN, 1941).

The Préalpes Médianes Plastiques (PMP) located to the NW of the nappe complex stack, show a nearly complete stratigraphic series from the Upper Triassic to the Upper Cretaceous and ends with tertiary flysch deposits. In the Préalpes Médianes Rigides (PMR) on the contrary, the stratigraphic series starts in Middle Triassic and terminates with Tertiary flysch deposits, but it is characterised by significant stratigraphic gaps in the Lower Jurassic, Middle Jurassic, and Lower Cretaceous (Fig. 2.2). Since the Lower Jurassic, paleofaults are separating several smaller basins (Fig. 2.2B) leading to the formation of an intermediate zone between the PMP and the PMR, the future Heiti and Gastlosen imbricate.

In the N-NW, where the PMP are deposited, a large basin enables the deposition of nearly the entire stratigraphic series from the Upper Triassic to the Tertiary

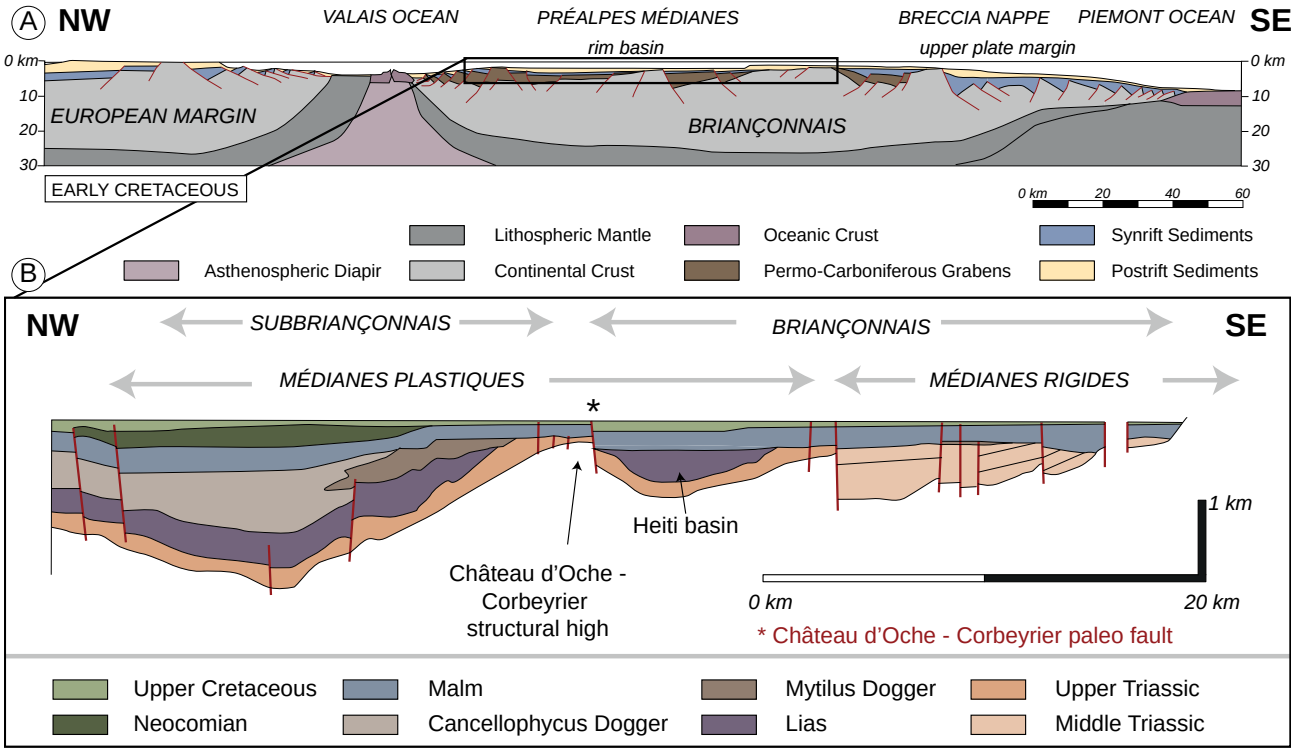

Fig. 2.2: Above, cross-section showing the localisation of the Briançonnais micro-continent in between the Pyrenean and Piemont ocean at the Early Cretaceous times (modified after STAMPFLI et al., 2002). Below, palinspastic and tectonic reconstruction model for the Préalpes Médianes highlighting the influence of paleofaults affecting the sediment deposition. The horizontal line corresponds to the deposition of the Eocene Flyschs (modified after BAUD and SEPTFONTAINE, 1980; BOREL and MOSAR, 2000).

with important stratigraphic gaps in the Upper Cretaceous (Couches rouges) (Fig. 2.2) containing exclusively limestones, dolomites, shales, and marls (BADOUX and MERCANTON, 1962; BAUD et al., 1989; BAUD and SEPTFONTAINE, 1980; BOREL, 1995; PLANCHEREL, 1979; TRÜMPY, 1960, 1980). To the south in the sedimentation realm of the PMR a platform and lagoon environment prevailed, associated to a continuously active structural high (MOSAR, 1997).

The PMP with their more varied lithology of alternating marly beds with thick stiff limestones allow the development of large-scale fault-related folds trending from E-W in the eastern part of the nappe to the N-S in the western part of the fold-and-thrust belt (BADOUX

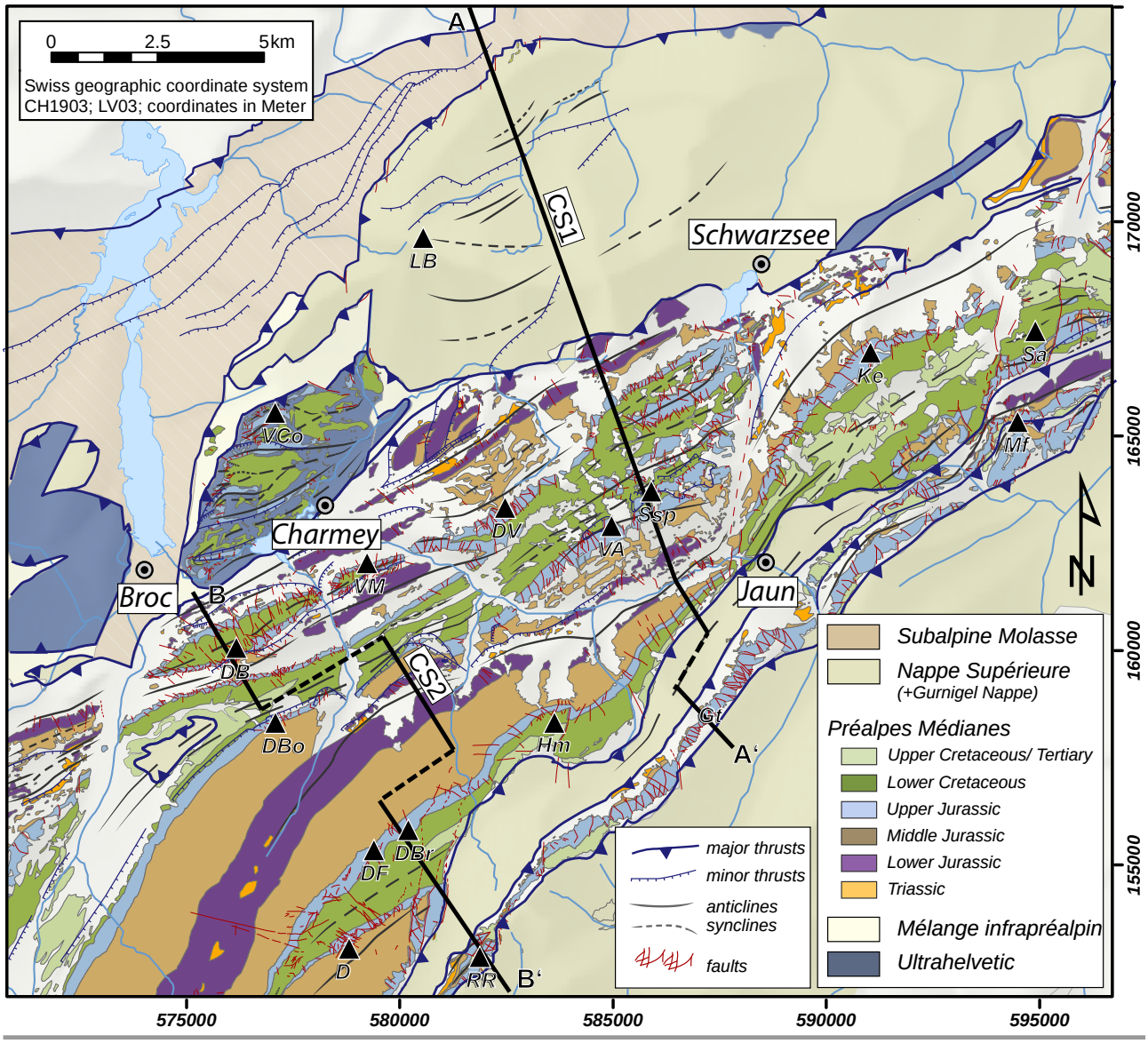

D	*Dorena*	**DV**	*Dent de Vounetse*	**LB**	*La Berra*	**Ssp**	*Schopfenspitz*
DB	*Dent de Broc*	**Gt**	*Gastlosen*	**Mf**	*Mittagsfluh*	**VA**	*Vanil des Arpilles*
DBo	*Dent de Bourgo*	**Hm**	*Hochmatt*	**RR**	*Rocher des Rayes*	**VCo**	*Vanil des Courts*
DBr	*Dent de Brenleire*	**Ke**	*Kaiseregg*	**Sa**	*Schafarnisch*	**VM**	*Vanil de la Monse*
DF	*Dent de Folliéran*						

Fig. 2.3: Geological map of the investigated Préalpes Médianes completed with a simplified structural map of the adjacent structural units. Section traces of cross-section A and B (Fig. 2.15) are indicated by two dark lines. The geological map of the Préalpes Médianes is based on geological maps (ANDREY, 1974; BIERI, 1925; BOREL, 1991; BOVET, 1990; BUGNON, 1995; CAMPANA, 1941; GISIGER, 1967; PAGE, 1969; PASQUIER, 2005; PLANCHEREL, 1979; SPICHER, 2005; THALMANN, 1990), but also on field observations.

et al., 1960; BADOUX and MERCANTON, 1962; BONNET, 2007; BOREL and MOSAR, 1993; GAGNEBIN, 1922; JEANNET, 1922; METTRAUX, 1989; MOSAR, 1988a, b, 1989; MOSAR, 1991; MOSAR, 1994, 1997; MOSAR and BOREL, 1992; MOSAR et al., 1996; MÜLLER and PLANCHEREL, 1982; PLANCHEREL, 1979). In contrast, the PMR, where more "ductile" layers are missing, formed one major and in some places two minor, imbricated thrust slices dipping to the N/NW (MOSAR, 1997).

The various formations of the Préalpes Médianes were described and discussed by several authors:

Triassic:	Baud (1972), Jeanbourquin (1988), Masson (1972)
Early Jurassic:	Mettraux (1989), Mettraux and Mosar (1989), Thury (1973), Favre (1859), Peterhans (1926)
Middle Jurassic:	Septfontaine (1995), Furrer (1979), Furrer and Septfontaine (1977)
Late Jurassic:	Weiss (1949), Heinz (1980), Heinz and Isenschmid (1988), Isenschmid (1983)
Lower Cretaceous:	Boller (1963)
Middle Cretaceous:	Caron and Dupasquier (1989), Python-Dupasquier (1990)
Upper Cretaceous	Guillaume (1986), Hable (1997a)
Tertiary Flysch:	Bugnon (1995)

The pre-emplacement phase is characterised by a passive margin period, starting in the Triassic, but is mainly active during the Jurassic and is expressed by normal faults, subsidence induced basins above extensional faults. The sedimentation realm of the Préalpes Médianes evolved as a rim basin behind the northern rift shoulder of the Piemont Ocean. Therefore, it is strongly influenced by typical extensional structural features, such as synsedimentary growth faults, but also partially by inversion structures leading to important stratigraphic variation.

The syn-emplacement period occurred during Middle and Upper Eocene (Lutetian-Bartonian), and is marked by an active margin phases. The continental collision during Eocene until present gave rise to the development of the main structures of the fold and thrust belt. After detachment, the Préalpes Médianes underwent thin-skinned tectonics, frequently marked by break-through and back thrusts.

The post-emplacement phase started with the arrival of the Préalpes klippen on the Ultrahelvetic and Helvetic domain, more precisely, on top of the Subalpine Molasse during Late Eocene/ Lower Oligocene indicated by the deposition of conglomerates of the Mont Pélérin in the Chattian, derived from the Nappe Supérieure. Especially, the PMR was reacting with renewed large-scale deformation expressed by the present day steeply inclined or overturned imbricates. In a final thrusting period, related to the external crystalline massif of the Alps, out-of-sequence thrust developed cutting though the Préalpine nappe structure and presumably through the underlying Subalpine Molasse. (MOSAR et al., 1996).

2 Structural Trends and Interpretations

During nappe transport, the Préalpes Médianes underwent thin-skinned tectonics and evolved as a typical foreland fold-and-thrust belt with generally foreland propagating thrusts branching off the basal décollement horizon at the base of the Triassic evaporite layers. These thrusts resulted in large-scale folds extending arc-shaped from the western to the eastern part of the Préalpes Romandes from SSW-NNE to W-E, and markedly influence the morphology of the Préalpes Médianes considerably. Indirectly, these structures were influenced by the presence of pre-existing extensional structures and related lateral variations in stratigraphic thicknesses that result in a different subsequent deformational behaviour. Furthermore, the Préalpes Médianes expose an omnipresent arrangement of faults, on the one hand related to the fold development, on the other hand post-dating the nappe emplacement, and cross-cutting the existing fold. In following subchapters, the distinguishing characteristics of folds, thrusts, and faults of the Préalpes Médianes are discussed to obtain a better insight of the observed structures and their kinematic links.

2.1 Structural Trends

2.1.1 Fold and thrust

The PMP consists of a succession of large-scale fault-generated folds bending between Montreux and Thun from SSW-NNE to W-E (BIERI, 1925; JEANNET, 1922; MÜLLER and PLANCHEREL, 1982; PLANCHEREL, 1976, 1979; PLANCHEREL and WEIDMANN, 1972; SCHARDT, 1884).

The thrusts responsible for the folding are not continuous throughout the entire Préalpes Médianes. On the contrary, they die out laterally, forcing the folds to terminate as periclinal closures (METTRAUX, 1989; MOSAR and BOREL, 1992; MOSAR et al., 1996). For this reason, fold axes are seldom consistently horizontal, but rather plunge in both directions along strike. In between two disappearing folds, relay zones develop accommodating the accumulated

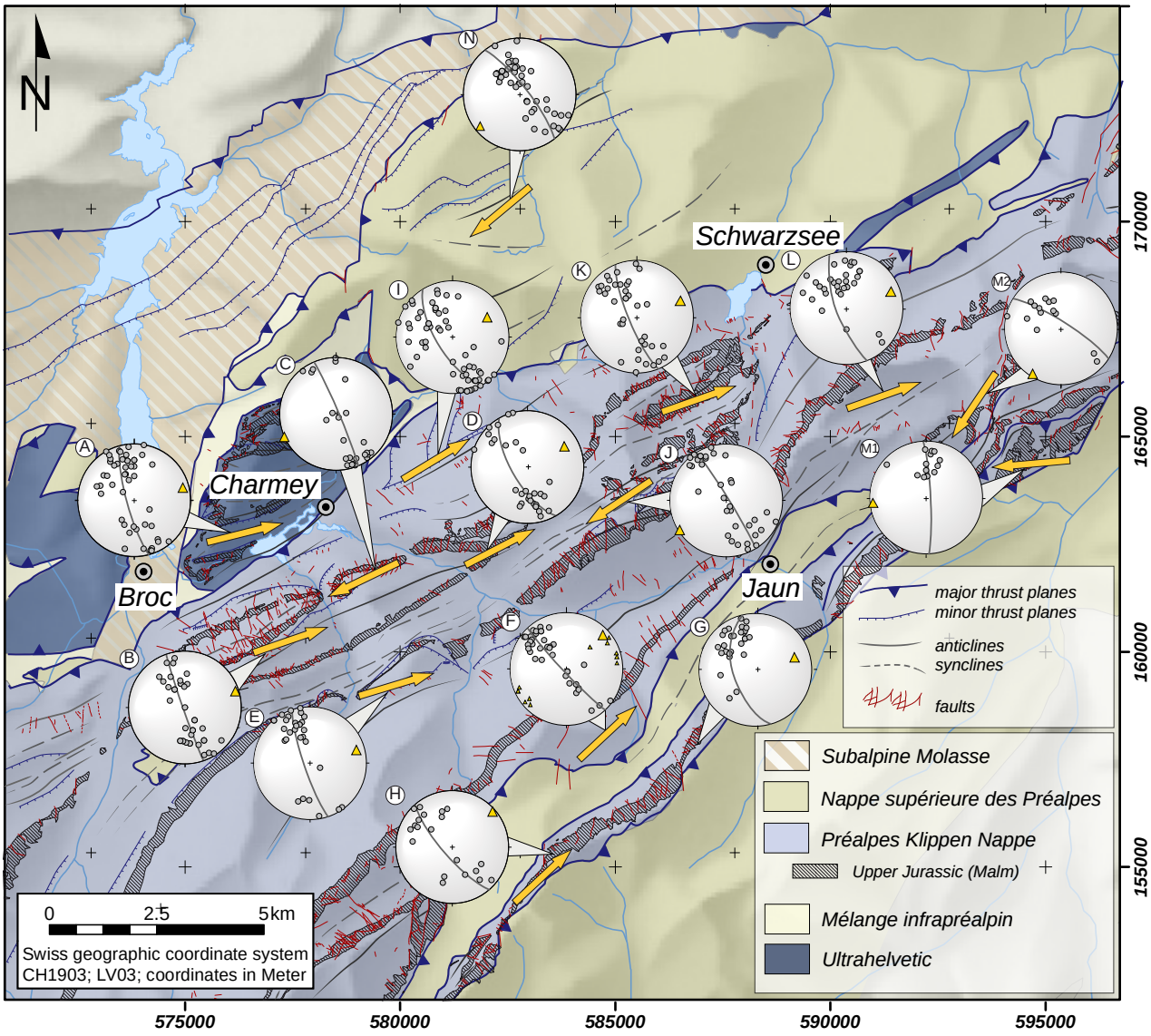

	Area	N	Fold Axis
A	Montsalvens	48	075/11
B	Dent de Broc	38	071/03
C	Vanil de la Monse	24	245/03
D	Les Vanils	30	060/23
E	Gros Haut Crêt	30	071/09

	Area	N	Fold Axis
F	Petit Mont	39	047/05
G	Gastlosen	28	075/34
H	Rocher des Rayes	20	049/14
I	Arsajoux - Vounetse	59	058/23
J	Schopfenspitz	34	071/03

	Area	N	Fold Axis
K	Breccaschlund	37	238/04
L	Kaiseregg - Walop	31	071/18
M1	Mittagsfluh	14	267/07
M2	Holzerhorn	14	212/10
N	Plasselbschlund	46	232/12

Fig. 2.4: Structural map of the study area situated in the Préalpes Médianes Plastiques romandes indicating the distribution of the bedding orientation by means of 15 stereographic pole to bedding projections on the lower hemisphere (equal area projection). The fold axes and best fit great circles were calculated by the TectonicsFP program (REITER and ACS, 1996 - 2002). The yellow arrows indicating the plunge direction of the fold axis show a general NE-SW trend; exact values of fold axes and the amount of data are given in the table above.

strain by a lateral offset, described as tear faults. Tear faults occur per definition in allochthonous structural units generated by differential displacement among the transported masses (BIDDLE and CHRISTIE-BLICK, 1985). The extent of fold-generating thrusts is most probably linked to the pre-existing extensional paleostructures, which were - after their reactivation under compressional forces - guiding the fold development during the nappe emplacement.

Folds in the PMP generally appear as foreland verging folds with a steeper, sometimes overturned north-western fold limb and a more gentle dipping south-eastern fold limb. Anticlines are often thrusting the south-eastern limb of the leading syncline, leaving only the anticlinal backlimb exposed. Folds often show a narrow fold hinge zone. Fold axes trends and their plunging orientation show in the study area a general NE-SW orientation with moderate plunges of maximum 34° towards SW and NE (Fig. 2.4.).

In the Préalpes Médianes three major fault-related fold types related to a ramp and flat geometry occur: fault-propagation folds, fault bend folds, and detachment folds.

Fault-propagation folds developing at the tip of a continuously developing thrust (SUPPE, 1985) are widely distributed in the PMP and are characterised by their asymmetric fold shape, with one steep or overturned frontal limb. As long as the propagating thrust is not breaking through the topography (breakthrough), the fault slip is consumed by folding of the overlying strata. In the Préalpes Médianes, this fold type prevails wherever the lithology is interbedded by marls, shales and limestones. Most of these fold-generating thrust planes are steeply dipping towards SE and, unless erosion interacts, they remain hidden as blind thrust. The Combe anticline in the Dent de Broc area and the Tsavas-Millets anticline in the Gros Haut Crêt/ Schopfenspitz area are typical examples of this fold type (Fig. 2.5). These fault-propagation faults break through the surface and are therefore accessible in the field. Additionally, at the Combe anticline the

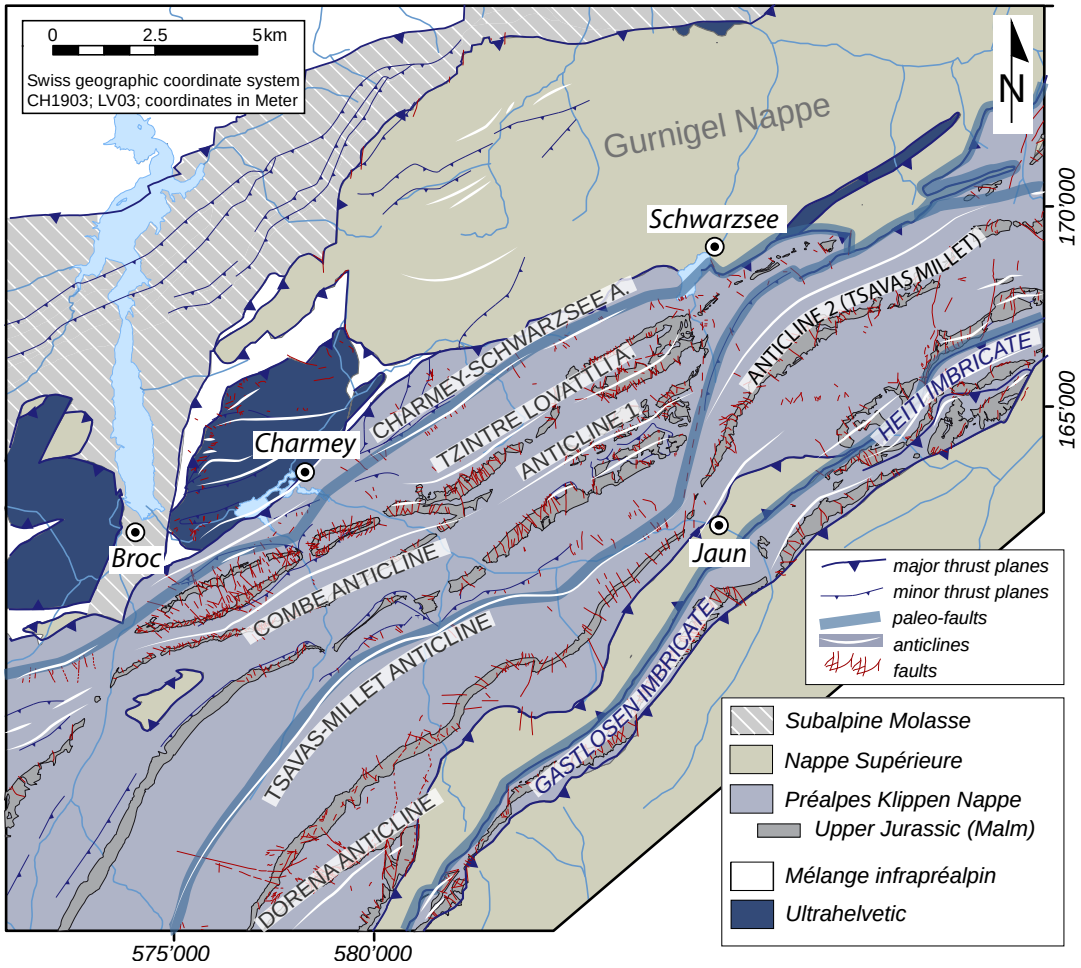

Fig. 2.5: Structural map illustrating the large-scale structures of the investigation area, especially of the Préalpes Médianes: fault-related anticlines, as well as paleofaults. Synclines were omitted for reasons of simplification.

erosion uncovered a lateral insight into the prolongation of the thrust plane at depth. The Dent de Broc fault-propagation fold is thought to have evolved from an initial box fold shaped detachment fold (CHATTON, 1974) - a special type of fault-propagation fold with a vertical ramp fault - into a fault-propagation fold. The transition of a detachment fold into a fault-propagation fold seems to be function of thrust propagation kinematics, the fault steepness, and the different amount of displacement along any thrust surface (MITRA, 2003; MOSAR et al., 1996). In the area between Charmey and Schwarzsee, several blind fault-propagation folds are suspected, showing, with a steeply inclined southern limb of the anticlines, an opposite fold shape in comparison to the previously described ones, which can possibly be associated to backward verging fault-propagation folds.

Fault bend folds occur mainly in the PMR where thick, massif limestones of the Triassic and the Upper Jurassic dominate (MOSAR, 1991). The development of fault bend faults is associated to the presence of a ramp-flat structure, which forces the hanging wall strata to bend by passing this irregular fault surface (SUPPE, 1983). In the PMP, the fault-bend folds are typical for the frontal imbricates near Montreux (MOSAR, 1997), whereas in the intermediate zone they are known in the Gastlosen area.

Detachment folds are relatively rare in the Préalpes Médianes, but are linked to box-fold shaped structures (MOSAR, 1997). This fold type developed symmetrically or asymmetrically over the termination of a detachment or a bedding parallel thrust fault. This folding is independent of a ramp structure. As already mentioned above, under on-going compression, they can transform into fault-propagation folds (JAMISON, 1987; MITRA, 1992).

2.1.2 Faults

Besides the thrust and fold related faults/thrusts, the Préalpes Médianes expose a complex fracture arrangement ranging from small-scale, outcrop-sized fractures up to large-scale faults influencing the morphology of the Préalpes Médianes considerably. Throughout different deformational phases linked to the préalpine pre-, syn- and post-emplacement history, fractures were generated and subsequently reactivated during successive deformational stages.

Measured fault planes bearing fault-slip indicators show a prevailing occurrence of strike-slip faults of both sinistral and dextral sense of movement. Sinistral strike-slip faults are above all oriented in direction N-S, whereas dextral strike-slip faults expose a preferred orientation towards NW-SE. Measured normal fault planes reveal no obvious directional tendency, reverse faults however correspond with the orientation of the NE-SW directed fold axis (Fig. 2.6C). The range of fault types, based on dip and striation are summarised in Fig. 2.6. Many fault planes consist, regardless their type, of steeply inclined fault planes. Fault planes vary from a purely strike-slip to a steeply oblique normal or reverse fault movement. The variable relationship between fault plane dip and fault lineation dip is thought to reflect multiple reactivations of fault planes during different deformation phases.

The observed fracture array allowed a subdivision into thrusts responsible for the folding, faults related to the fold bending, and strike-slip faults that are clearly crosscutting already existing structures. Fractures pre-dating the nappe emplacement are difficult to distinguish in the field as many of these faults were presumably reactivated during Alpine deformation. Therefore, major interest in this subchapter is given to the faults related to folding and strike-slip movements.

Associated to folding in the PMP, a large amount of faults, either parallel or perpendicular to the fold axes, is generated. Normal faults perpendicular to the fold axis lead to a segmentation of the folds that may enhance the plunge of the fold axis as in the Dent de Broc area. The Upper Jurassic limestones standing out in morphology mostly as the highest mountain ranges expose a clear segmentation by normal faults, which were assumed to be reactivated in a later stage as strike-slip faults, as proved by overprinting slickenfibres in the Tzintre quarry, near Charmey. Fold axis parallel faults occur less frequently, due to the outcrop orientation lying mostly parallel to these structures, but also because of their orientation in direction SSW-NNE to W-E, which makes them less favourable to a strike-slip reactivation under a NW-SE oriented compression.

Strike-slip faults, both dextral and sinistral, are clearly prevailing in the Préalpes Médianes (Fig. 2.6). Two main directions are dominating: sinistral N-S to NNE-SSW oriented strike-slip faults, already extensively discussed by Plancherel (1976; 1979) and dextral W-E to NW-SE oriented strike-slip faults. These strike-slip faults are clearly crosscutting the folding structure, as for example in the Weissenburg area (BIERI, 1925; MOSAR and BOREL, 1992; PLANCHEREL, 1979). Furthermore, overprinting relationship among fault slickenfibres prove a latest fault movement in strike-slip component. Faults perpendicular to the fold axis, generated under a fold axis parallel extensional regime, can easily have been reactivated under a strike-slip stress regime with a NW-SE directed compressional stress axis.

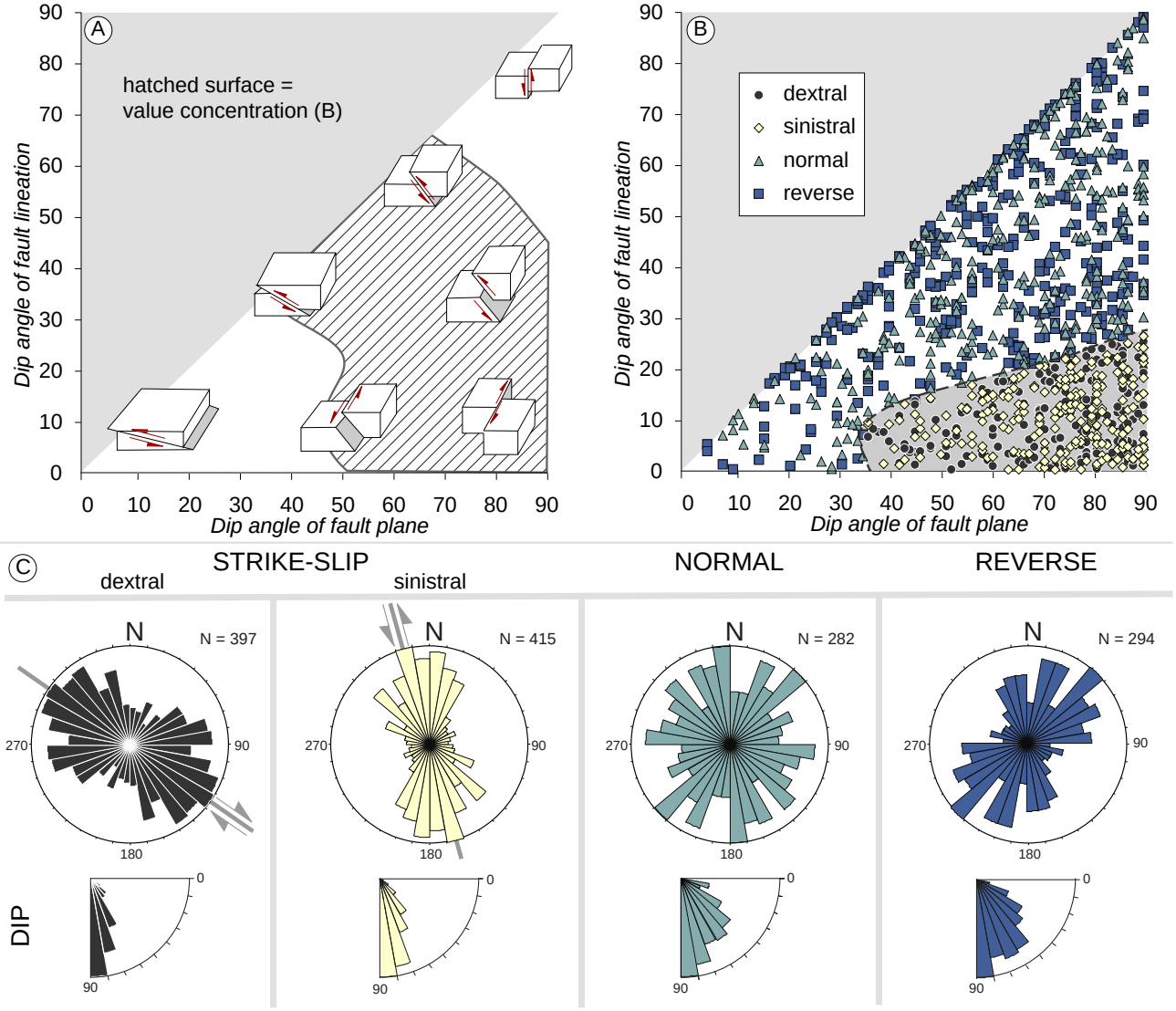

Fig. 2.6: Diagram illustrating the relationship between the dip angle of every measured fault plane and the dip of their lineation. A) shows schematically how different faults and their movement are oriented: from a low to a high angle fault plane and from a thrust to an strike-slip regime. B) The fault plane dip vs. fault lineation dip ratio of 1388 fault measurements shows a randomly distribution with a concentration of steeply dipping strike-slip towards oblique fault planes, indicated as hatched surface in A. C) Four rose diagram representing the fault direction referring to their fault movement.

Lineaments

Lineaments are the surface expression of zones of weakness or structural displacement in the crust of the earth (Hobbs, 1912). They can be straight river and valley segments, aligned surface sags, and depressions (dolines), soil tonal changes indicating soil moisture variations, alignment in the vegetation, or topographic changes. All of these phenomena might be the result of a structural accident such as faults, joint sets, folds, cracks, and fractures. The analysis of the lineaments guarantees a rapid localisation of the different geological structures (KIM et al., 2004). The interpretability of these lineaments depends strongly on the dip of the underlying structures. The higher the dip the more clearly the lineaments appear. At different spatial resolution, certain structures, for example anastomosing shear zone patterns, appear as linear features (CHANDRASIRI EKNELIGODA and HENKEL, 2010).

For this study, lineaments were analysed mostly in the Préalpes Médianes, but also in the Gurnigel nappe, the Ultrahelvetics and in the Subalpine Molasse. These different structural units expose different outcrop conditions, forcing an adjustment of the observational scale. For instance the Gurnigel nappe, as well as the Subalpine Molasse expose only few outcrops, the majority of the structures are hidden below vegetation. At a regional observation scale, structural alignments following valleys and creeks, show a similar lineament pattern than in the neighbouring Préalpes Médianes. In the Préalpes Médianes, the average length of all linea-

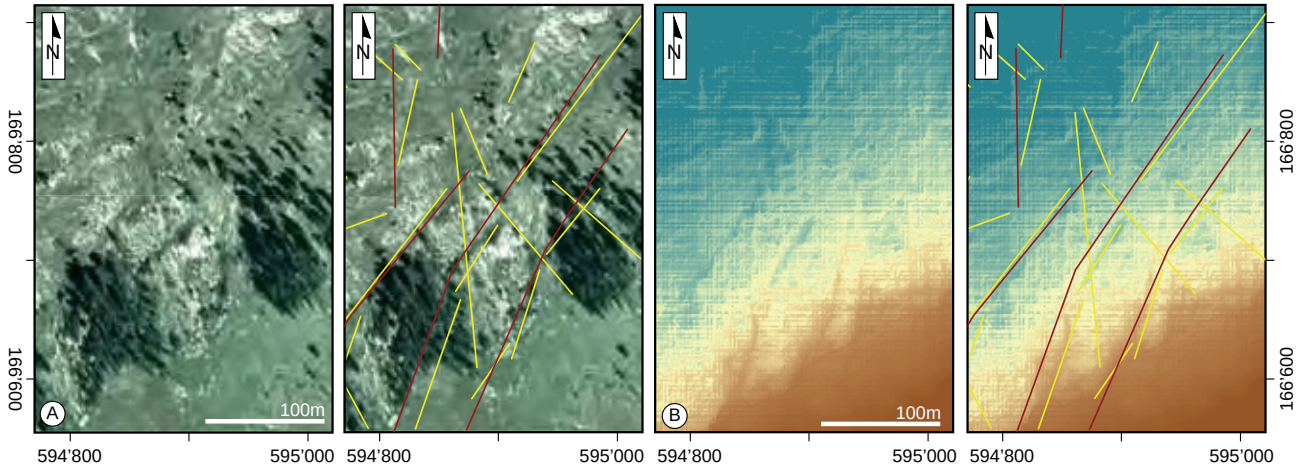

Fig. 2.7: Faults (red) and Lineaments (yellow) plotted on an orthophotograph (A) and a DTM grid (B) in the Schafarnisch area; the four images correspond to the same extract allowing a comparison between the two different representations of the topography. Small-scale parallel offsets between lineaments and mapped faults are most probably related to cartographic inaccuracies.

ments was around 200m, in the Gurnigel Nappe 300m, and in the Subalpine Molasse about 120m.

The lineament investigation is based on the analysis of orthophotographs ("swissimage, © 1998"), Digital Height Models ("DOM, 2000/2001 swisstopo") and Digital Terrains Models ("DTM-AV, 2000/2001 swisstopo", with resolutions higher than 1m. In order to guarantee the existence of the detected lineaments, orthophotographs, DTMs as well as topographic maps were alternately examined to complete the observations and to verify their presence on different documents and identify them as tectonic faults (Fig. 2.8).

After constructing the lineaments in the ArcGis database, these were exported and evaluated in a specially developed Excel program to visualise their spatial distribution in rose diagrams weighted by their length (Fig. 2.8). In this way, longer lineaments were more respected than smaller, less important ones. The lineament analysis focuses on zones of special interest (indicated by frames (Fig. 2.8)) where the structural context is well known, and comparison between measured fractures was possible (discussions found in subsequent chapters).

The rose diagram representing all lineaments displays two major directions (Fig. 2.8), a NNW-SSE and WNW-ESE orientation and a subordinated third peak oriented towards N-S, corresponding to the predominating orientation of the faults collected from maps. The general orientation of mapped faults and lineaments coincides well, except that different prevailing directions occur: the lineaments show an overall NW-SE trend, whereas the compilation of mapped faults exposes a N-S tendency. These differences are probably linked to interpretative mapping. The five regional lineament analyses reveal the importance of the local structural context, as for instance the influence of extensional faults in the Dent de Broc and conjugated strike-slip shear zones in the Weissenburg area.

2.2 Deformational Structures

The multiple deformation history of the Préalpes Médianes is not only represented by large-scale structures, as described in the previous chapter, but also in small-scale structures, such as slickensides bearing fractures of outcrop-scale, veins, shear bands and subordinate small-scale folds. At this point, we provide a more detailed discussion of every element measured or structural feature used for later kinematic interpretation.

2.2.1 Slickensides bearing fault planes

By the systematic compilation of fault orientation data throughout the entire investigation area particular attention was paid to fault kinematic indicators, especially to slickenside allowing shear-sense reconstruction. Based on morphological and geometrical appearance several different slickenside groups can be distinguished (DOBLAS, 1998; PETIT, 1987). Thereof the most important subgroups are slickenfibres, developed by precipitation of elongated fibres during fault movement characterised by their typically stepped appearance and slickenlines, ridges or grooves arising by mechanical abrasion due to asperities, or linear aggregates of cataclased material in lenses or behind obstacles (PASSCHIER and TROUW, 2005).

Due to irregularities on fault surfaces, the majority of the faults initially contain striae, but depending on

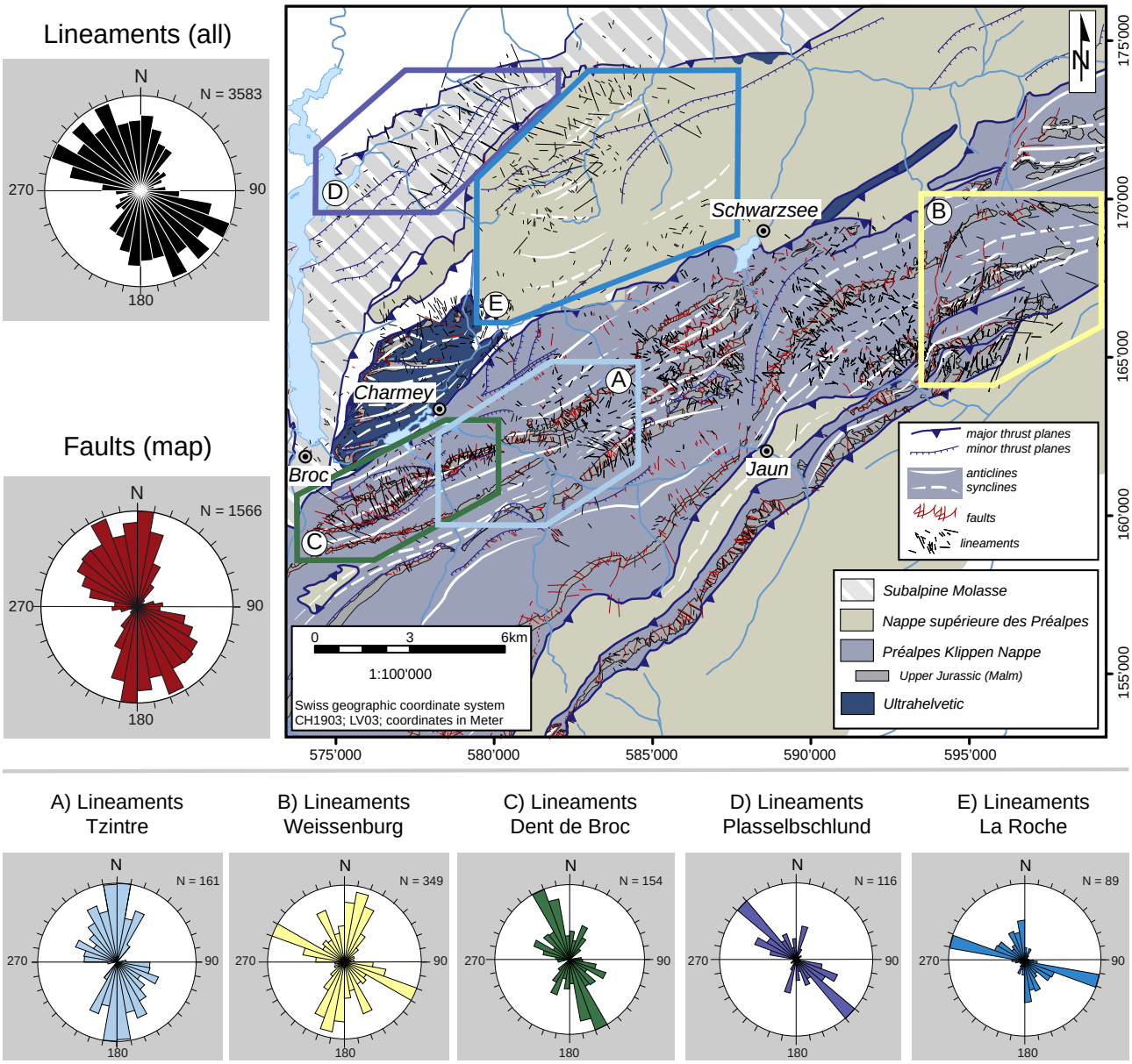

Fig. 2.8: Structural map exposing the lineament pattern in the Préalpes Médianes, the Gurnigel Nappe, the Ultrahelvetic, and the Molasse Subalpine in the investigation area. This map section was chosen at this scale to represent the different area where lineament analyses were made. The purple rose diagram above indicates the arrangement of every lineament weighted by their length, whereas the red rose diagram below corresponds to the orientation of every fault collected from geological maps. The five smaller rose diagrams represent lineament analyses of specific areas, further discussed and compared with measured fractures in subsequent chapters.

the lithology, the slickensides are more or less sensitive to weathering. Even though Upper Jurassic limestones are generally indicative for good outcrop conditions, their fault planes are often karstified, so that slickensides are missing.

Different movement phases on the same fault plane lead to a superposition of several slickenside generations overprinting the previously developed ones. Although, a reactivation of fault planes during different deformational stages is assumed, the presence of overprinting slickensides is scarce. The picture of a fault plane in the Tzintre quarry (Fig. 2.13A) indicates two generations of slickensides, where the horizontal one is overprinting the oblique one.

2.2.2 Fault associations

Evident shear sense indicators are hardly found on fault planes, so it is important to consider their fracture arrangement. Fractures rarely occur as one single fault plane, more often they are arranged in fault families or arrays of fractures. Often fractures are arranged as conjugate faults with an initial major fault plane and a conjugated plane separated by an angle of approximately 60°, as proved by laboratory experiments.

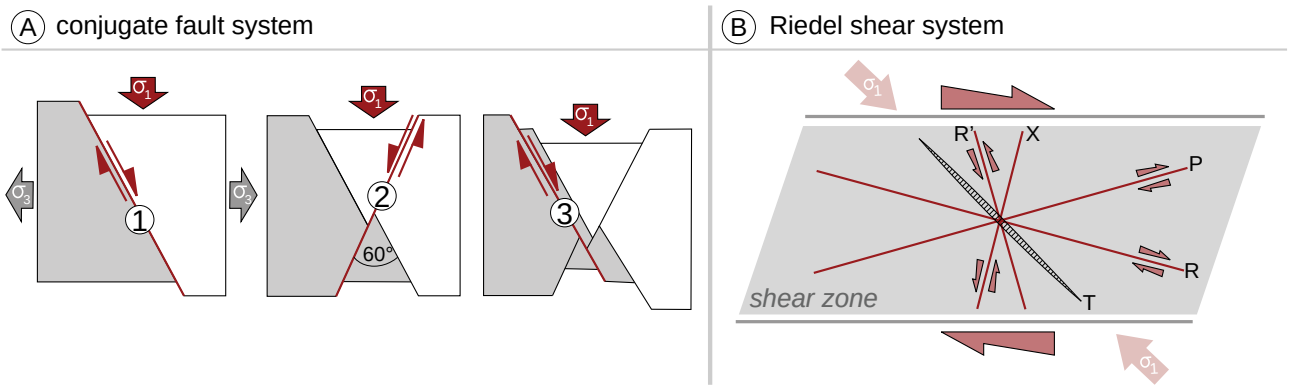

Fig. 2.9: Individual inclined fault planes show a three-step sequential development in conjugate fault systems. As fault 1 stabilises, the conjugated fault 2 becomes active and transects the former fault 1. Then fault 2 becomes inactive and fault 3, parallel to fault 1, cuts through the previous faults and displaces them. (modified after Ramsay and Huber (1987)). B) Dextral Riedel system with orientation of major fault subset, stress orientation, and veins. The chronology generally observed is a growth of tension gashes T, followed by the propagation of 2nd order faults (R and R' and then of P and X (modified after Nicolas (1987) and Tchalenko (1970)).

In a reverse approach, while examining a freshly developed conjugate fault system, the compressional stress axis is situated at the bisecting angle of 30° between these two planes. The conjugated plane is a zone of weakness, which can easily be activated as a fault plane. Hence, it's not surprising, that a conjugate fracture system develops by a three-step sequential movement along the fault planes (Fig. 2.9 (RAMSAY and HUBER, 1987)).

In the Préalpes Médianes, similar conjugate fault systems were observed, for example near the Oberbergpass in the Gastlosen mountain range (see Fig. 2.13B). The interplay of the two conjugate fault planes is clearly visible, so that the orientation of the principle stress axes for this particular outcrop can easily be deduced. Slickensides covering the outcrop surface exposing a dextral strike-slip movement reveal a superposed strike-slip stress system corresponding to the latest deformational stage.

Another fault arrangement worth discussing is fractures developed within a shear system, oriented in a distinct pattern, the so-called Riedel shear faults (NAYLOR, 1986; RIEDEL, 1929; TCHALENKO, 1970; WILCOX, 1973). During shearing, antithetic and synthetic fractures develop, which are initially characterised by a conjugate angle of 60°. The synthetic strike-slip faults are Riedel shears (R), and are typically oriented at a small, acute angle (about 15°) to the trace of the main shear zone. The antithetic strike-slip zones are conjugated Riedel shears (R'), and are oriented at a very high angle (about 75°) to the main zone (WILCOX, 1973). The orientation angle of the Riedel faults is dependent on the coefficient of friction (Φ), which varies between different rocks. The direction of the greatest principle stress (σ1) bisects the angle between R and R' (DAVIS, 1996). If the deformation after the conjugate fracturing proceeds, a combination of strike-slip faulting and plastic distortion occurs (WILCOX, 1973). Two coexisting mechanism dominate this deformation: discrete, abrupt faulting in the form of conjugated deformation bands and continuous grain flow subparallel to the R-deformation bands. This generates simple shear of the entire Riedel structure and rotation of its R' deformation bands (KATZ and WEINBERGER, 2005). Thus, the acute angle between the two faults grows (>90°) as the two faults rotate away from each

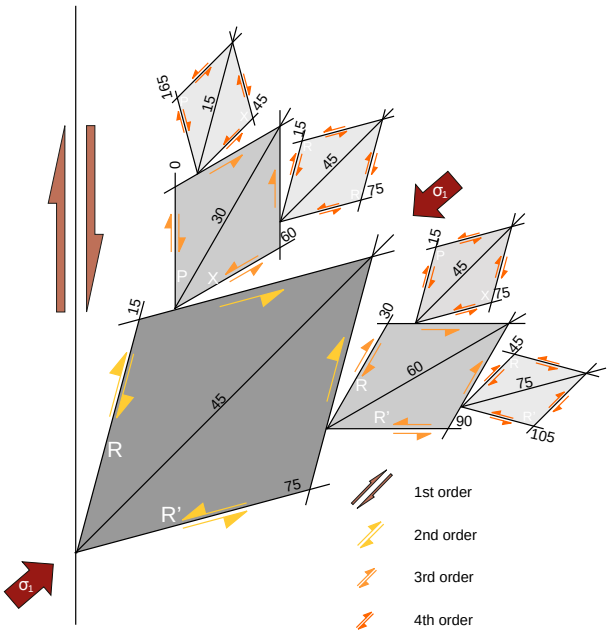

Fig. 2.10: : Four successive orders of shear zones linked to a N-S dextral strike-slip considered as first order. The angles between major shear zone and Riedel shear faults of different hierarchies are indicated, the red arrows represent the principle stress (σ1) (modified after Vialon (1976)).

other (WILCOX, 1973). Once the R' faults are nearly perpendicular to the main shear zone, they undergo distortion and rotation to become less steep. New strike-slip faults (P and X faults) develop, which are symmetric to R respectively to R' in relation to the main shear.

In the Préalpes Médianes, Riedel shear zones are difficult to recognise at outcrop-scale, since shear zones are formed by reactivation of already existing structures, no typical Riedel shear fault pattern developed. However, Riedel shears can be documented in areas of regional shear zones, as for instance in the Weissenburg-Schafarnisch area. There, two shear zones prevail: a WNW-ESE striking dextral and a NNE-SSW oriented sinistral fault direction. Nevertheless, at outcrop level the measured fractures slightly deviate from the regional fault trend. It is assumed that the regional strike-slip zones correspond to a large-scale Riedel shear zone; the measured fractures correspond to subordinated Riedel shear fault. Then each elementary shear R, R', P and X may represent a principal displacement zone on its own, wherein one can find smaller subsets of faults organised in the same Riedel pattern. Such subsystems define different orders of faults organised in a complex pattern (VIALON, 1976).

2.2.3 Vein systems

Extension fractures are generated under a maximum tension perpendicular to their walls and are filled with precipitated minerals sealing the fracture (RAMSAY, 1967). Elongated growth fibres of these minerals indicate the maximum extension direction and therefore allow the determination of one of the three principle stress axes. Crosscutting relationship among different vein sets help unravel a polyphase deformational history.

In the Préalpes Médianes, veins occur frequently, but display mostly a chaotic pattern with vein sets cutting non-systematically through other vein sets implying a contemporaneous formation. The vein filling material is almost exclusively calcitic in nature and is therefore supposed to derive from their host rock.

Within the veins, mineral fibres are rarely visible. The veins filling mostly appear as blocky crystals or as nearly homogeneous, strongly weathered fracture filling. Without other indications (oblique mineral fibres), under normal conditions, veins develop perpendicular to σ_3. Therefore, most of the observed veins were estimated to be orientated perpendicular to extensional stress axis. En-echelon vein arrays indicating shear movement are scarce (Fig. 2.13/D).

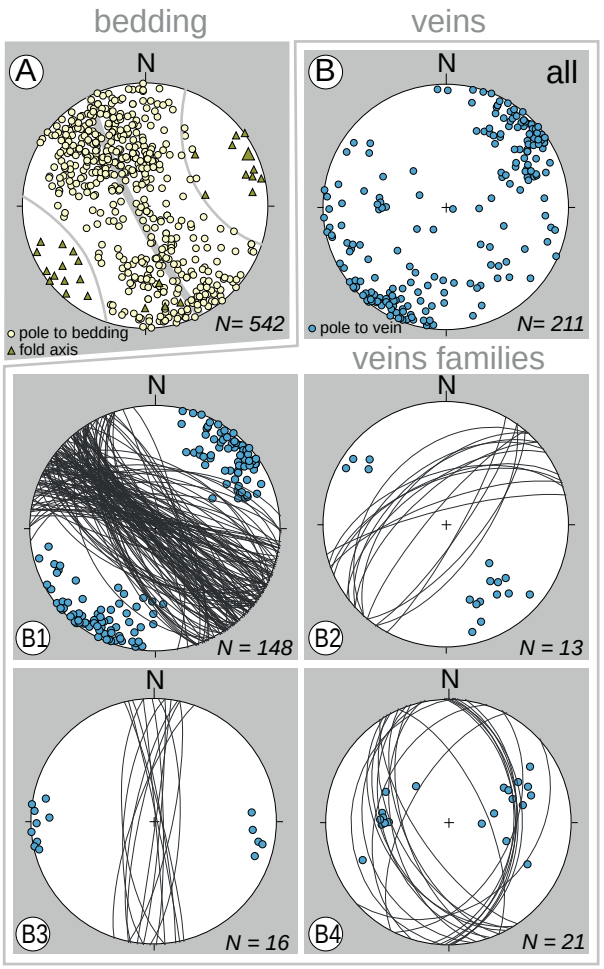

Fig. 2.11: A) showing the stereographic pole projection of every bedding measurement (lower hemisphere, equal area projection,), the calculated fold axis (taller triangle) and measured fold axis reveals clearly a NE-SW oriented folding trend. B) represents the pole projection of every measured vein and is subdivided into four vein families, whereas vein set B1 is clearly overrepresented. B2, B3 and B4 are assumed to be related to the folding of the Préalpes Médianes.

Despite their heterogeneous appearance, the measured vein directions expose a predominant NW-SE orientation perpendicular to the fold axis representing a fold axis parallel extension. Veins parallel to the fold axis and others with a N-S orientation can be observed, but are less frequent (Fig. 2.11).

2.2.4 Stylolites

Pressure-solution is responsible for the formation of stylolites expressed as irregular suture zones characterised by a highly indented surface with interlocking teeth from both wall rocks. Stylolites differ from the host rock, generally a limestone, by its enrichment of insoluble material. Bedding parallel stylolites are commonly considered to be diagenetic (PASSCHIER and TROUW, 2005). In stylolites, teeth (stylolite peaks)

and the inferred shortening direction are oriented normal to the plane. For this reason, stylolites can be used as an indicator for the principle compressional stress axis.

In the Brésil quarry, optimal outcrop quality allows the observation of different intersecting stylolites and vein families: bedding parallel stylolite seams induced by compaction during digenesis (Fig. 2.13E, (1)) are clearly intersected by a second stylolite family (2), forming a weakness zone that re-opened under an extensional stress by forming veins (3).

2.2.5 Brittle shear bands

Shear bands are minor shear zones that develop under higher grade of deformation within a shear zone. They consist of two components: a shear planes C (cisaillement) and at an acute angle, in between the shear planes, a foliations S (schistosité) (BERTHÉ et al., 1979). C-type and a C'-type shear band can be distinguished. Whereas the first one is oriented parallel, the second one lies obliquely, at an angle between 15°-35° to the shear zone boundaries (PASSCHIER and TROUW, 2005). The C'-type shear band cleavages develop mainly in a strongly foliated mylonitic context. However, similar structures can be observed locally in foliated cataclasites within high strain zones, as in the Préalpes Médianes, where a brittle environment prevails. Foliated cataclasites resemble low-temperature mylonites in many aspects. Although deformation in brittle fault rocks is by sliding on microfaults, fracturing and pressure solution, a coarse penetrative flow develops, showing similar effects on the formation of asymmetric structures as ductile flow by dislocation creep and recrystallisation (PASSCHIER and TROUW, 2005).

In the Préalpes Médianes, brittle shear bands exist in the vicinity of important thrusts such as in the Maischüpfen area (Fig. 2.18) or in the Rocher de Rayes area. Frequently, they show an angular deviation from the major thrust plane and correspond thus mostly to the C'-type shear band showing a striking similarity with the Riedel fault systems displaying the same inclination as C' to the shear zone boundary than the Riedel fault R.

The brittle shear band of the Rocher de Rayes area exposes shear planes with a spacing of 30cm, centimetric foliation, and veins (Fig. 2.13G) belonging to a distinct shear zone with the principle compressional axes oriented parallel to the vein plane, provoking a top to the NW movement of the shear band.

2.2.6 Small-scale folds

Especially, the Lower Cretaceous marly limestone layers are marked by tight, metric folds. Not only their sensitivity to folding due to the lithology and the closely spaced layering, but also their position within the narrow synclines forces the layers to fold,

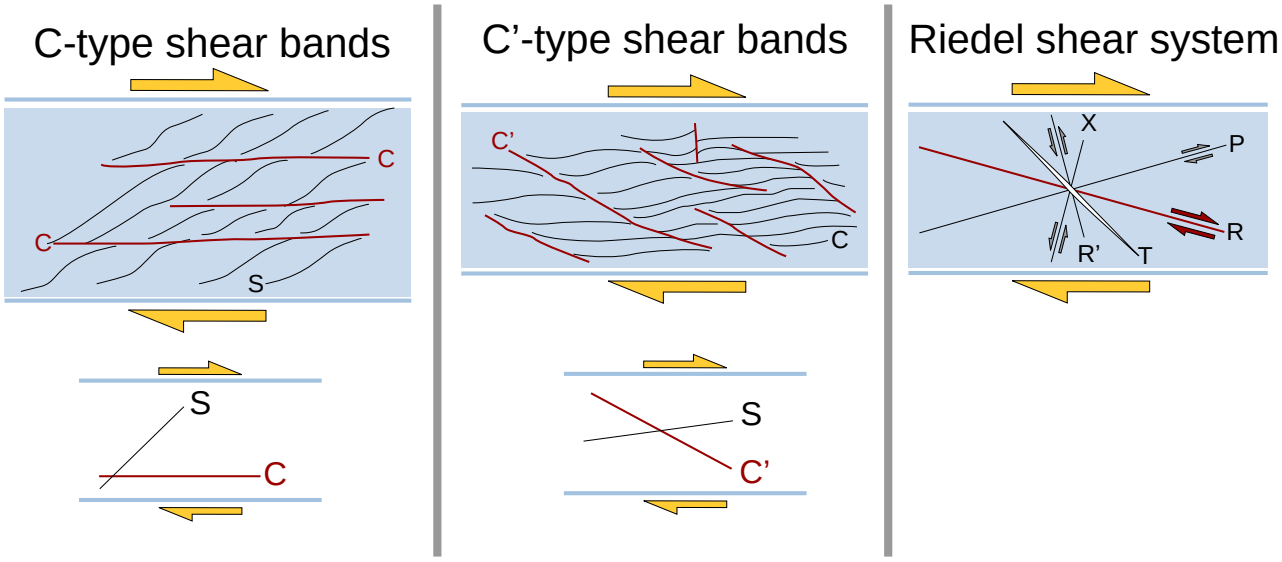

Fig. 2.12: Different types of shear bands compared to the Riedel shear system. C-type or C'-type shear bands describe the orientation of the C-S structure (c = cisaillement, s = schistosité). In C-type shear bands C is parallel to the shear zone boundary while in C'-type shear bands are inclined at an angle of 35° (PASSCHIER and TROUW, 1996). Within a Riedel shear system the Riedel shear R shows a similar orientation to the shear zone boundary than the C' shear faults (modified after Nicolas (1987) and Tchalenko (1970)).

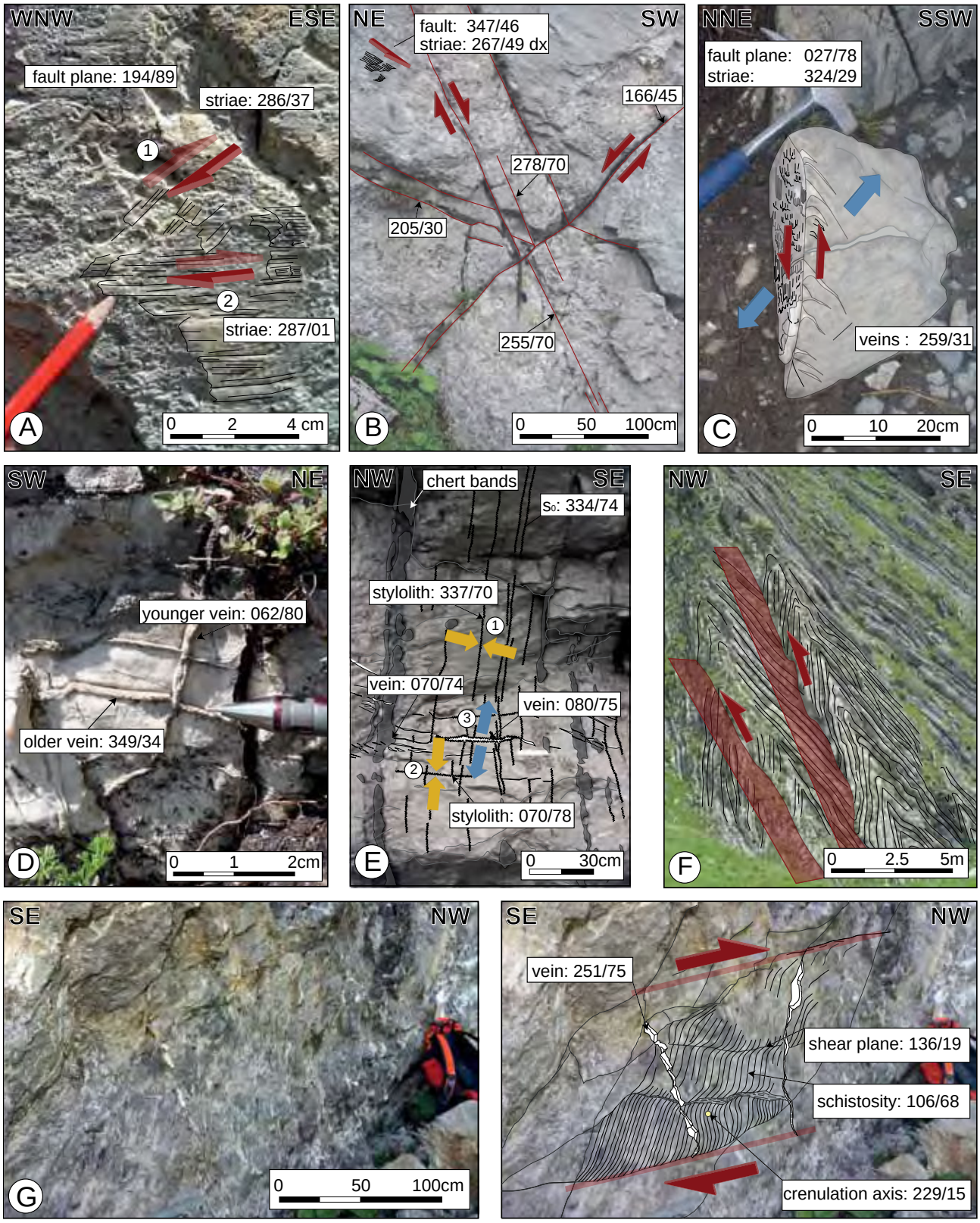

Fig. 2.13: Compilation of different structural features observed in the limestones of the Préalpes Médianes: A) overprinted slickenfibres with the older (1) and the younger (2) shear sense (Middle Jurassic, Tzintre quarry, 580'555/ 162'170); B) conjugated fault array (Upper Jurassic, Oberbergpass, 587'672/ 158'949); C) en echelon veins and slickenfibres (Kaiseregg, Middle Jurassic, 590'468/ 167'000); D) Crosscutting veins (Upper Jurassic, Dent de Broc area, 575'905/ 159'625); E) stylolites and veins (1) oldest phase: stylolites parallel to bedding, (2) middle phase: stylolites perpendicular to first ones, F) mesoscopic folds offset by thrusts (Maischüpfen, Lower Cretaceous, 585'164/ 163'492); G) brittle shear band with vein (Rocher des Rayes, Middle Jurassic , 582'189/ 153'140); f) vein array (Sattelspitzen, Upper Jurassic 586'796/ 158'084 (3) youngest phase: extensional veins (Le Brésil quarry, Upper Jurassic, 582'813/ 161'034).

often they are accompanied by small-scale thrusts taking on the narrowing. As second-order folds, their limbs are following the general trend of the superordinate syncline; however, they tend to have steeper, sometimes overturned "hinterland" limbs (Fig. 2.13F), forming characteristic chevron folds. In the PMP, the fold axes orientation changes progressively from ENE-WSW near Montreux to NE-SW near Thun (see Fig. 2.1). Regionally the fold axes plunge in both directions: towards NE and SW, and can reach a plunging up to 40° (Fig. 2.4) (MOSAR, 1991).

3 Cross-Sections

Two structural profiles based on a compilation of already existing geological maps completed with field measurements help to localise the various structural styles observed in the investigation area. For constructing the cross sections (Fig. 2.15) several geological maps were consulted (ANDREY, 1974; BRAILLARD, 1998; CAMPANA, 1941; FAVRE, 1984; FUCHS, 2003; MANDIA, 1984; PASQUIER, 2005; SPICHER, 1980) and refined by more recent interpretations on the deeper structure (BOREL and MOSAR, 2000; MOSAR, 1991; WISSING and PFIFFNER, 2002). The two schematic cross-sections were established to situate the most characteristic structural elements in their large scale tectonic context, and therefore, the line of section is shifted several times.

Since seismic lines and deep borehole data are scarce in the Préalpes Médianes, the construction of the cross-section relies on projections of the surface data to depth by respecting the geometrical consistency. Therefore, with a balancing approach, the structures hidden underneath the surface may be reconstructed. This method proceeds on the assumption that post-depositional deformation, such as the folding and thrusting of the préalpine nappes, produces no significant changes in the rock volume. In the PMP, this supposition is supported by the observation that rocks have suffered little or no internal deformation under very low grade metamorphic to diagenetic conditions (MOSAR, 1988b, 1989)

The surface area of a bed and its length should remain constant.

Considering the width of the different sectors to be identical in reference cross-sections (Tab. 2.1), this constant width can be used to reconstruct original length along new sections. Within the following subchapters, the paleogeographically induced thickness changes in the Préalpes Médianes will be discussed, as well as the length comparison amongst different cross-sections and the associated interpretative approach.

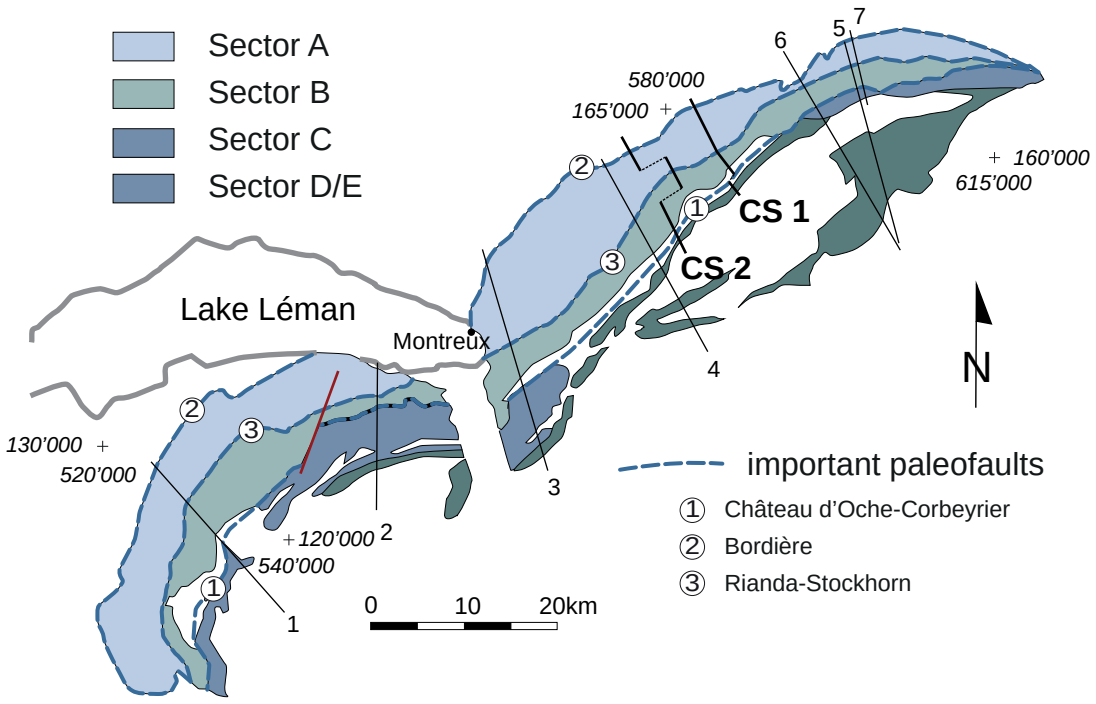

Fig. 2.14: Schematic map of the Préalpes Médianes indicating the 5 paleogeographic sectors (A-E) delimited by important paleofaults (blue dashed lines) that can be followed throughout the entire Préalpes. Black lines correspond to section lines with restored sector length (1-7) (Tab. 2.1), and CS1, CS2 to the cross-section in Fig. 2.15 (modified after BOREL and MOSAR, 2000).

3.1 Paleofaults and Paleosectors

Thicknesses of different stratigraphic units along the cross-section in the PMP display important variations from SSE towards NNW. These changes are ascribed to the paleogeographic history of the Préalpes Médianes in the Sub-/Briançonnais sedimentation realm on top of the NW rift shoulder of the Alpine Tethys. Especially, since the Lower Jurassic, the sedimentation realm of the Préalpes Médianes is influenced by large-scale synsedimentary faults leading to half-graben-like basin causing important thickness changes. Three major paleofaults were traced throughout the entire Préalpes Klippen allowing a subdivision into five sectors (sector A-E) delimited by major paleofaults, as suggested by Borel (2000) and Wissing (2002), and based on previous paleogeographic studies.

A short overview of the main particularities of the different paleogeographic sectors will help understand these relevance in the present day geometry and hence in the development of the folds and thrusts.

Sector A is situated in the frontal part of the Préalpes Médianes and most of the measured sites are located within this sector. As the most external fault of the Préalpes Médianes has been eroded, the outermost (s. str.) thrust of sector A - the reactivated Bordière paleofault - does not correspond to the external limit of this nappe. In the two cross-sections (Fig. 2.15), sector A comprises the frontal segment with the Dent de Broc syncline, the Combe Anticline/ Anticline 1 and the Grand Forcla/ Sarine Syncline. Towards SSE, the thickness of the Dogger increases rapidly.

Delimited by the inverted Château d'Oche-Corbeyrier and Rianda-Stockhorn paleofaults, sector B appears between the Gros Haut Crêt and the Combifluh, where it thrusts the top of the Schopfenspitz-Combifluh and remains as tectonic klippe on the mountaintops. Its south-eastern delimitation is mostly hidden underneath the Nappe Supérieure, on the external part of the Gastlosen mountain range. The Lower and Middle Jurassic sequences become thinner towards the SW.

Sector C does not occur continuously in the Préalpes klippen belt. In the Tour d'Aï area, this sector displays an important thickness of Lower Jurassic sediments, whereas the Middle Jurassic and the Lower Cretaceous sequence are completely missing. Assuming this sector is plunging in direction NE, it can still exist in the Rocher des Rayes area (CS2 in Fig. 2.15) without appearing at the surface. Further to the NE, near Boltigen, sector C occurs again as the Heiti imbricate.

The sector D represents the Gastlosen imbricates, which is characterised by its transitional nature between the Préalpes Médianes Plastiques and Rigides. In this sector, Lower Jurassic and Lower Cretaceous sediments are missing, whereas Middle Jurassic sequences still occur, unlike in the Préalpes Médianes Rigides, which represents the southernmost sector E, where they are non-existent.

3.2 Length Reconstruction

For each segment, the sector width was restored by measuring layer length parallel to the bedding along five profiles by Borel et al. (2000) and Wissing (2000) as listed in Tab. 2.1.

The already reconstructed sector lengths were most helpful for the creation of CS1 and CS2, particularly in the south-eastern part of CS2, where only a few outcrops exist. Without the projection of sector C in between sector B and D, the stratigraphic sequences remain too shallow and leave an undefined volume underneath the Rocher des Rayes (Fig. 2.15; Fig. 2.16). Thanks to the given length of sector C, a possible reconstruction of this part could be found.

To validate the structural consistency, the obtained sector lengths of CS1 and CS2 were compared to the existing ones Tab. 2.1. In general, the measured sector length of CS1 and CS2 are shorter than the ones observed in the south-western part of the Préalpes Médianes. One explanation is a general narrower occurrence of the sectors due to paleogeographic reasons; another one could be associated to the existence of sector segments lying on top of each other, similar to the structure in the Rocher des Rayes (Fig. 2.15).

Profiles		Sector A	Sector B	Sector C	Sector D
1	Monts d'Hermoine-Roc d'Enfer	15km	8.5km	9km	non-existent
2	Locum-Cornettes de Bise	10km	2.5km	10km	6km
3	Caux-Tour d'Ai	15km	10km	10km	-
4	Moléson-Gummfluh	15km	6km	-	7km
5	Hohmad-Turnen	12km	5km	2km	-
6	P1	-	-	7km	5.5km
7	P2	6km	7km	-	-
	CS 1	7km	4.5km	-	1.6km
	CS 2	6km	6km	3km	2km

Tab. 2.1 Restored length of the sectors A-D based on cross-sections throughout the entire Préalpes Médianes Nappe in comparison with the sector length of CS1 and CS2. The top five profiles were established by Borel et al. (2002) and P1 and P2 by Wissing (2000).

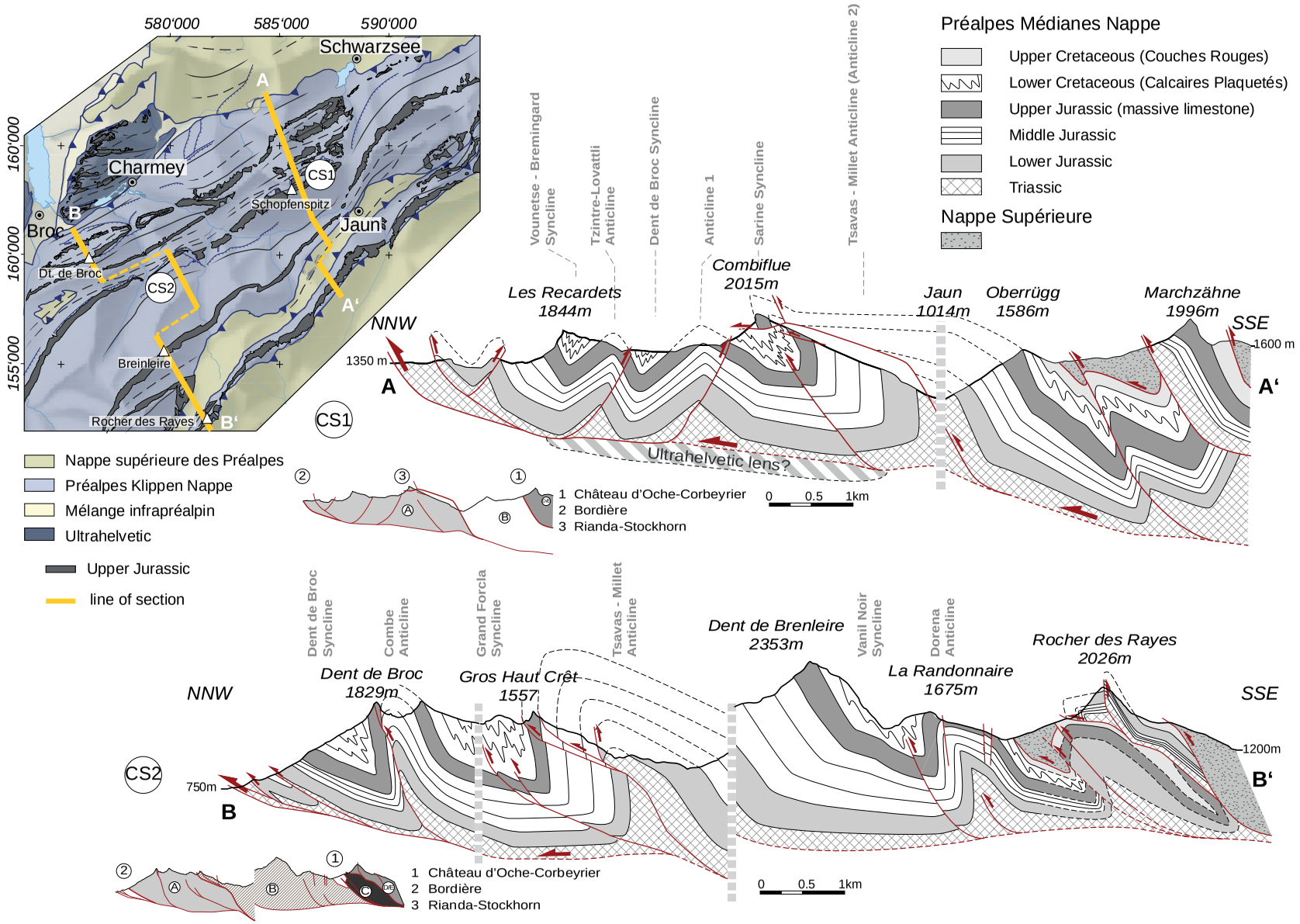

Fig. 2.15: Two cross-sections throughout the Préalpes Médianes Rigides and Plastiques exposing the most important structural styles of the investigation area. The structural map indicates the line of section of CS1 and CS2, which is shifted several times to include the characteristic structural elements into the profile.

However, these two cross-sections remain speculative, since the continuation of the structures at depth has not been proven by seismic data. Nevertheless, by lateral projection of structures into section and comparison of the sector length, plus by respecting the geometrical consistency of the structures and their layer thickness, rather accurate results can be obtained.

3.2.1 Discussion

As only few information about the structures at depth are available, several segments of the cross-sections are based on interpretations worth further discussion, as for instance the Rocher des Rayes Structure in CS2, and the Charmey area highlighting significant differences between CS1 and CS2.

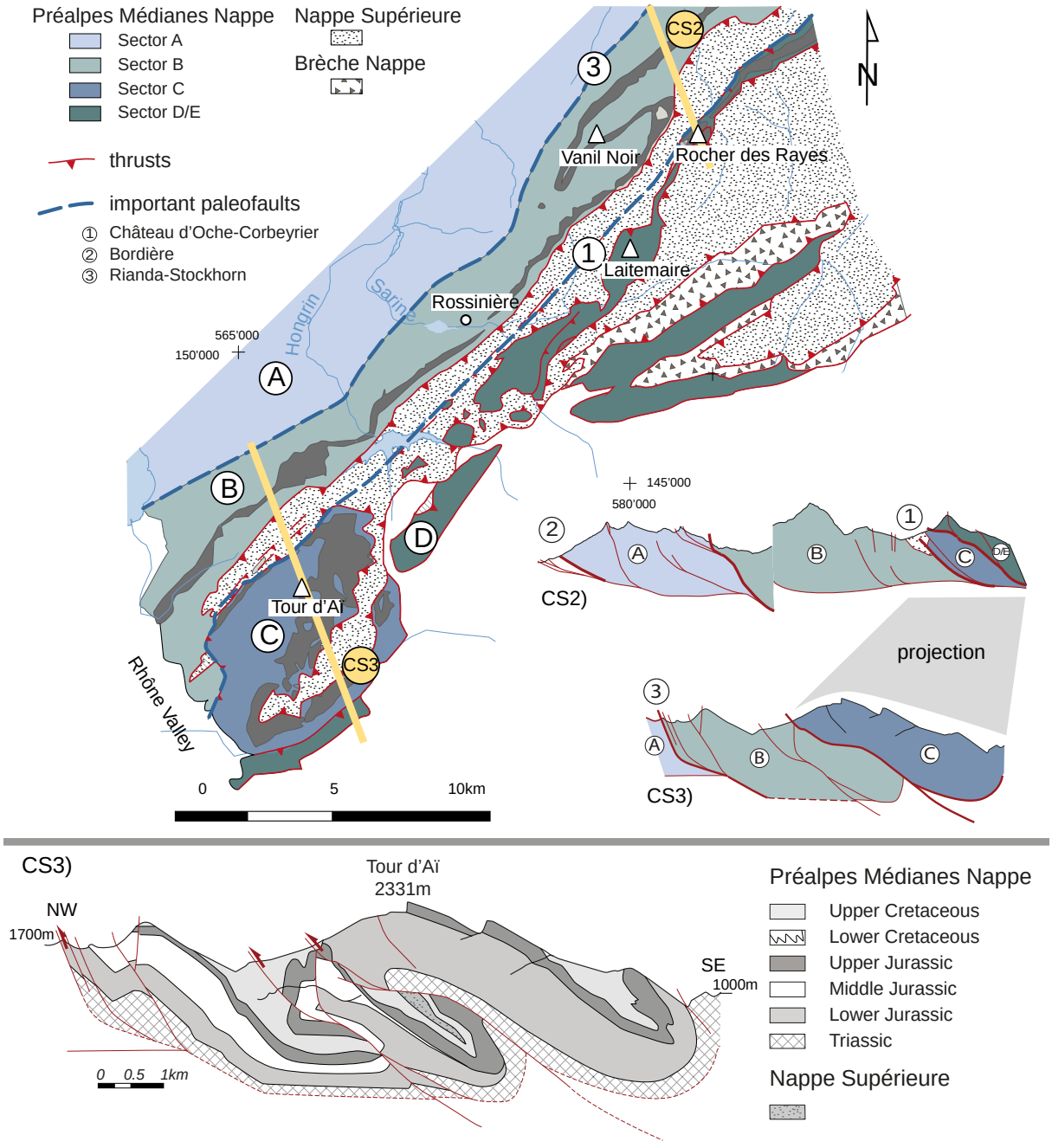

Fig. 2.16: Structural map revealing the structural continuation towards SW showing the connection between CS2 and the Tour d'Aï cross-section (CS3) (modified after BOREL and MOSAR, 2000; METTRAUX and MOSAR, 1989). Schemes with focus on the different sectors showing a projection of sector C, the Tour d'Aï structure, underneath the Gastlosen imbricate (sector D) in the Rocher des Rayes area. Hereby, the most credible solution to resolve the space problem is given.

3.2.2 Rocher des Rayes

The construction of CS2 in the Rocher des Rayes is restrained by the lack of controlling outcrops and prompts questions concerning the structures underneath the Rocher des Rayes/ Dents des Combettes. The out-cropping structures belong to the prolongation of the Gastlosen range and therefore to sector D, whose strata are less inclined than in CS1 leading to a space problem underneath. A possible solution to this space problem is demonstrated in CS2 by projecting the structures of sector C in the Tour d'Aï area (CS3, reconstructed after Badoux (1965), Trümpy (1960), Mettraux and Mosar (1989) and Borel and Mosar (2000) onto CS2. Based on geometry and the existing sector length, a projection of the Tour d'Aï anticline - characterised by its important Lower Jurassic layers fading out towards SSE - into the CS2 was established (Fig. 2.16). The Tour d'Aï anticline is clearly plunging towards NE leading to the disappearance of sector C at the surface, but its prolongation below the topography can be assumed, since some smaller imbricates that can be attributed to the Tour d'Aï structure are visible in isolated outcrops (MOSAR et al., 1996). Further to the NE of CS2, sector C is missing until the Boltigen area, where it reappears as the Heiti imbricate.

3.2.3 Charmey area

The two cross-sections expose different fold orientation in their frontal part, concerning mainly the Dent de Broc syncline, and the Combe anticline, further NE known as anticline 1, which are southwest of the Jaun valley verging towards the hinterland and NE of the Jaun valley towards the foreland. The latter are possibly related to the prolongation of the Montsalvens massif at depth, a large ultrahelvetic lens outcropping in front of the Préalpes Médianes near Charmey, forcing a thrusting towards the SE.

4 Structural Elements

Field measurements, remote sensing analyses, as well as the interpretation of already existing data revealed several characteristic structural elements generated under different structural conditions related to the three major deformational phases: the pre-, syn-, and post-emplacement. Several regions show evidence of these different structural events, but they are often not evenly pronounced throughout the entire investigation area. Within this chapter, a chronological overview of the typical structural elements acquired during these three phases is given.

4.1 Pre-Emplacement Structures

Prior to the detachment of the préalpine nappes from their mostly Briançonnais homeland, they underwent a major rifting phase corresponding to the opening of the Alpine Tethys during Liassic times (BAUD and MASSON, 1975; BOREL, 1997). The Préalpes Médianes developed in a rim basin context to the NNW of the Briançonnais upper rift shoulder (MOSAR et al., 1996; STAMPFLI and MARTHALER, 1990), where their sedimentation was particularly controlled by the development of three major basin parallel paleofaults (BOREL and MOSAR, 2000), as well as N-S trending faults (METTRAUX and MOSAR, 1989). These extensional synsedimentary faults especially influenced the sediment distribution perpendicular to strike. The differences in facies, bedding, and thickness led to greatly differing overall rheologies yielding different tectonic styles. Already discussed in the previous section these paleofaults delimit five different sectors with distinct deformational characteristics.

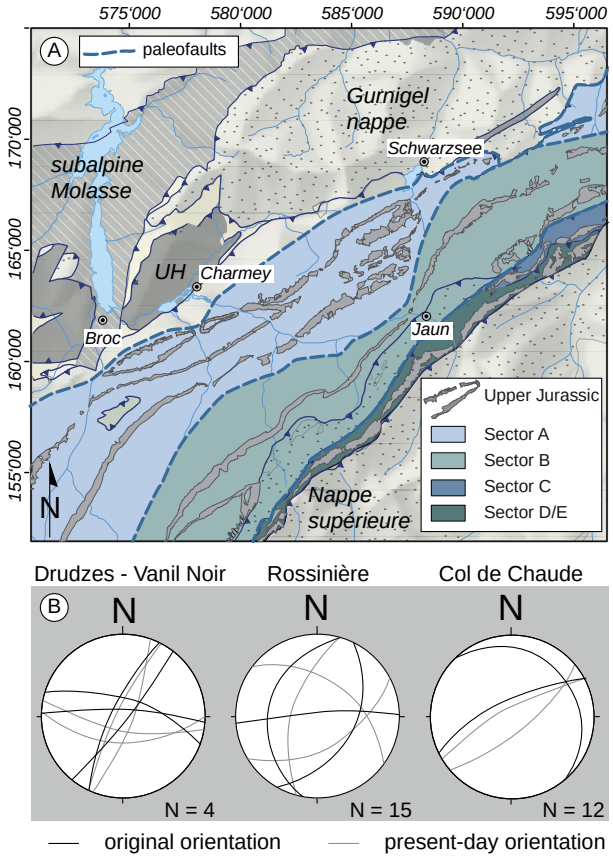

Fig. 2.17: A) Major paleofaults influencing the sedimentation and therefore the structural evolution of the Préalpes Médianes during and after nappe emplacement are indicated by blue dashed lines. The different paleogeographic sectors of the Préalpes Médianes delimited by these paleofaults correspond to the ones defined by Borel (2000) and Wissing (2002), see Fig. 2.14. B) Stereographic projection of paleofaults in its present-day and in its original orientation after rotating back into their orientation before the Alpine deformation (lower hemisphere, equal area projection) (modified after METTRAUX and MOSAR, 1989).

Apart from sedimentological thickness variations among different sectors, these paleofaults are hardly visible in the field. Analysing the fault-slip data collected within the frame of this study though, the assumption was made that a large amount of measured fault planes are inherited and were reactivated during and after nappe emplacement.

Mettraux and Mosar (1989) analysed the orientation of faults of both the Alpine and the rifting deformation phase. The latter, defined as paleofaults, are associated with polyphase breccia and synsedimentary fracture filling related to an original extension. Back-rotation of these paleofaults into their pre-folding position exposes a NE-SW and a WNW-ESE oriented fault family. Although the amount of data to demonstrate this fact is small, field evidence, such as associated breccias and paleokarstifications demonstrate their significance.

A second example for pre-emplacement structures is given by the St-Triphon quarries well known for their extensional deformation during the lower Jurassic rifting phase (BAUD and MASSON, 1975). Recent paleostress analysis carried out by Sarret and Mosar (2010) allow the distinction of two different stress regimes predating the alpine deformation: an NW-SE oriented extensional phase related to the development of the rift during the Lower Jurassic, and a strike-slip stress regime with a NE-SW oriented compressional component interpreted as transitional phase between the rifting and the alpine deformational event.

Detailed analyses of pre-emplacement structures, however, go beyond the scope of this study. Nevertheless, it is crucial to bear in mind the presence of fractures predating the nappe emplacement, which can easily be reactivated by on-going deformation.

4.2 Syn-Emplacement Structures

During the Bartonian/Priabonian (Upper Eocene), the Préalpes Médianes detached from their Briançonnais homeland and were transported towards the foreland (MOSAR et al., 1996). During its transport, the Préalpes Médianes nappe acquired most of its present-day structural features like fault-related folds in the PMP, and imbrications in the PMR. Fault-bend folds and fault-propagation folds occur frequently in the PMP; however, the thrust plane responsible for the folding often remains hidden below the surface. Generally, the thrust planes are disappearing laterally relaying different faults by tear faults. Although most of the faults are dipping to the hinterland, there exist a number of thrusts dipping backward, towards the foreland. In the PMR, backthrusts are more common in the south-eastern part, while the frontal part of the PMR is mainly dominated by thrust imbrications.

Additionally, the fold development during nappe emplacement provokes the development of normal faults, both perpendicular and parallel to the fold axis.

In the following chapter, detailed explanations discuss the different syn-emplacement structures as fault-propagation folds, both hinterland and foreland verging with examples of the Dent de Broc and the Maischüpfen area, as well as normal faults perpendicular (Dent de Broc area) and parallel to fold axes (Rocher des Rayes).

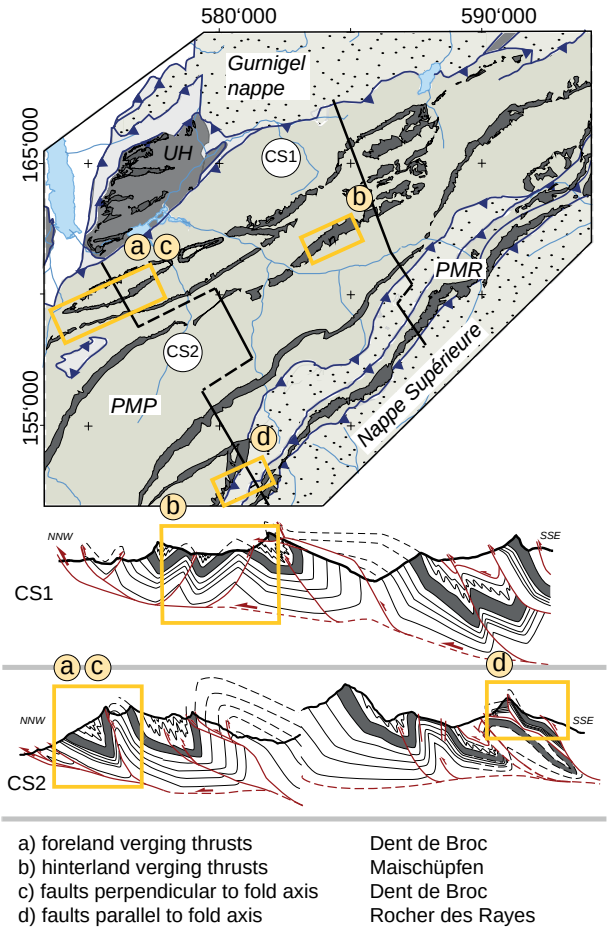

Fig. 2.18: Simplified map and crossection to localise the different syn-emplacement structures observed in the Préalpes Médianes and Gurnigel nappe (more detailed cross-sections see Fig. 2.15).

4.2.1 Fault-related folds

The folds characterising the Préalpes Médianes are mostly related to thrusts rooting at the detachment horizon, which were - while the thrusting progressed - forcing the overlying strata to bend. These fault-propagation folds are most common in areas where the lithology is alternating between marls, shales and limestones (MOSAR, 1997; PLANCHEREL,

1979). The important thrust planes mostly lie hidden below anticlines and only rarely break through to the topographic surface, mostly due to erosion exposing deeper geological levels. The thrust planes are not continuous throughout the entire Préalpes Médianes; instead, they are dying out laterally initiating periclinal closures of folds and are forming lateral relay structures. Their general movement direction is top to the NW, however, as observed in the Schopfenspitz area, important backthrusts with top to the SE orientation exist.

Foreland verging thrusts

Generally, foreland verging thrusts dominate in the Préalpes Médianes Plastiques, where - except for a rather small part in the centre of the investigated area - most faults involve thrusting top to the NW thrusting. The following figure (Fig. 2.19) illustrates the fold-thrust relationship in the frontal part of the PMP, in the Dent de Broc area.

Hinterland verging thrusts, backthrusts

In the area between Charmey and Schwarzsee (Fig. 2.20) thrusts generating folds of an unusual geometry with a steep backlimb and a gently dipping forelimb were suspected to be related to backthrusting towards SE. An outcropping backthrust can be observed in the Maischüpfen area. As already described by Mosar (1997), backthrusts are well-known structural features in the Préalpes Médianes, occurring mainly in the PMR. The origin of these backthrusts is either related to a reactivation of inherited structures or associated with ramp structures, which is most likely for this area. A possible explanation for this delimited area affected by backthrusts is found related to their position in the vicinity of a large-scale, tectonically emplaced Ultrahelvetic lens, better known as the Montsalvens massif. This Ultrahelvetic lens may play the role of a structural ramp that induces backthrust in the overlying nappe. Fold trends in the Montsalvens area are slightly oblique to the PMP and support the hypothesis of an eastward continuation under the PMP where backthrusts are developed in a causal link with this Ultrahelvetic tectonic sliver. Additionally, oblique ramps can be observed (Arsajoux) caused by the lateral ramp geometry of the Montsalvens. This clearly indicates the importance of underlying features in the structural development of the overlying frontal PMP.

Example: Maischüpfen backthrust

Situated at the south-eastern limb of the anticline 1, the Maischüpfen thrust exposes an important fault plane on the hanging wall side, consisting of massive Upper Jurassic limestone overlain by Lower Cretaceous layers (Fig. 2.22A). The less competent Lower

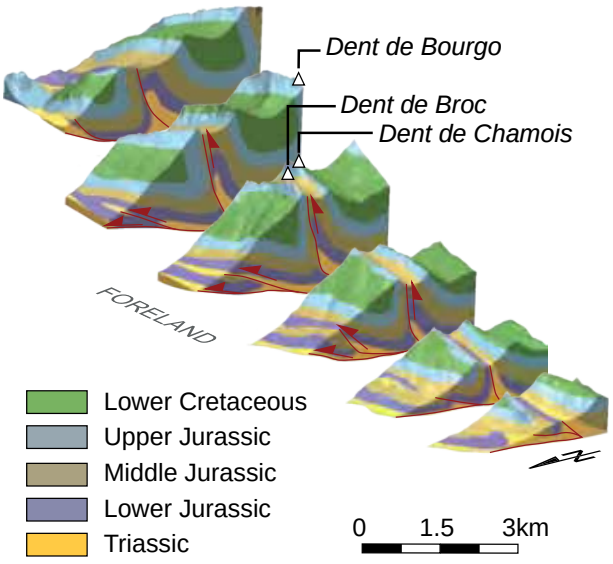

Fig. 2.19: 3D representation of the Dent de Broc area showing foreland verging thrusts.

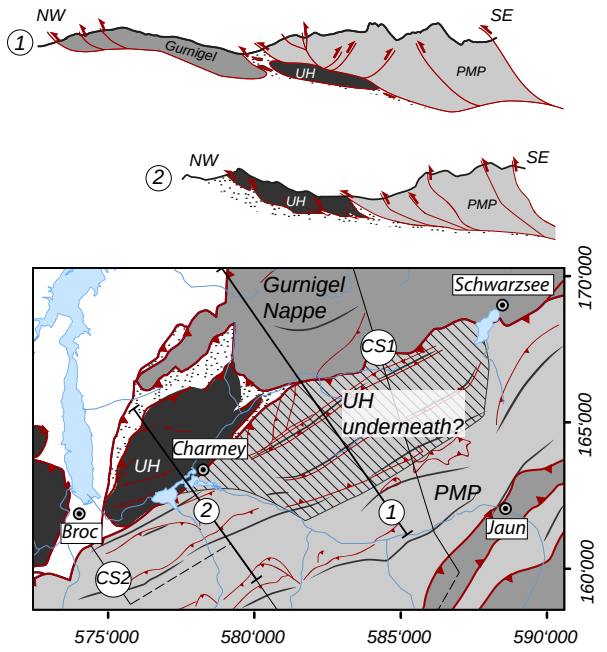

Fig. 2.20: Scheme explaining the occurrence of backthrusts in the area between Charmey and Schwarzsee. The Ultrahelvetic lens most probably extends below the Préalpes Médianes Plastiques (hatched zone), forming a structural ramp, which leads to the development of backthrusts, illustrated in profile 1. The two profiles above (1 and 2) are situated in between the previously discussed cross-sections CS1 and CS2 (Fig. 2.15).

Cretaceous layers accommodated the shortening by a small-scale folding of its thinly layered marly limestones, though the continuation of this fault disappears and reappears farther to the ENE (Fig. 2.22B). The Maischüpfen fault is not only characterised by its large-scale fault plane dipping towards NW, but also by its important fault core of up to 6m of width with its typical asymmetric succession of a sharp boundary fault, a gouge zone and breccia zone (BILLI, 2005). A sharp fault plane delimits the fault zone to the NW, followed by a zone of cemented fault gouge of 30cm width, and a breccia zone corresponding in this case to a foliated cataclastic zone distinct by the presence of brittle shear bands. The north-western damage zone affects up to several meters of Upper Jurassic limestones, whereas the south-eastern part has disappeared due by erosion.

The fault gouge consists of fine grained, light yellowish material deriving from milled limestones of the Upper Jurassic and forming a nearly homogeneous layer separating the fault plane and the foliated cataclastics. The preservation of a fault zone of such an important width is relatively rare, since foliated fault breccia provide a weakness zone facilitating its alteration. The fault breccia of the Maischüpfen fault is characterised by a cataclastic zone consisting of brittle shear bands with shear planes separated by bands with steeply inclined foliations (Fig. 2.21), confirming a top to the SE movement of the Maischüpfen backthrust. Further to the NE, a lateral view on the prolongation of the Maischüpfen thrust exposes a similar foliated cataclastic zone with shear bands with an identical azimuth and dip for shear planes and foliation (Fig. 2.22B). Additionally, a lateral view on the fault plane proves the prolongation of the fault dip towards NW and highlights the relationship between the faulting and the folding, indicated by the generation of the anticline 1 on top of the Maischüpfen thrust.

A closer look at the foliated cataclasites zone exposes brittle shear bands with a different degree of deformation. Close to the Maischüpfen fault, a gouge zone accommodates most of the deformation, immediately adjacent, the foliated cataclasites zone generates C'-type brittle shear bands at an angle of 20° to the Maischüpfen boundary fault (Fig. 2.21). Even further away (<2.5m), brittle shear bands act as C-type shear bands exposing a shear zone C parallel to the major fault orientation.

The Maischüpfen boundary fault (Fig. 2.21). Even further away (<2.5m), brittle shear bands act as C-type shear bands exposing a shear zone C parallel to the major fault orientation.

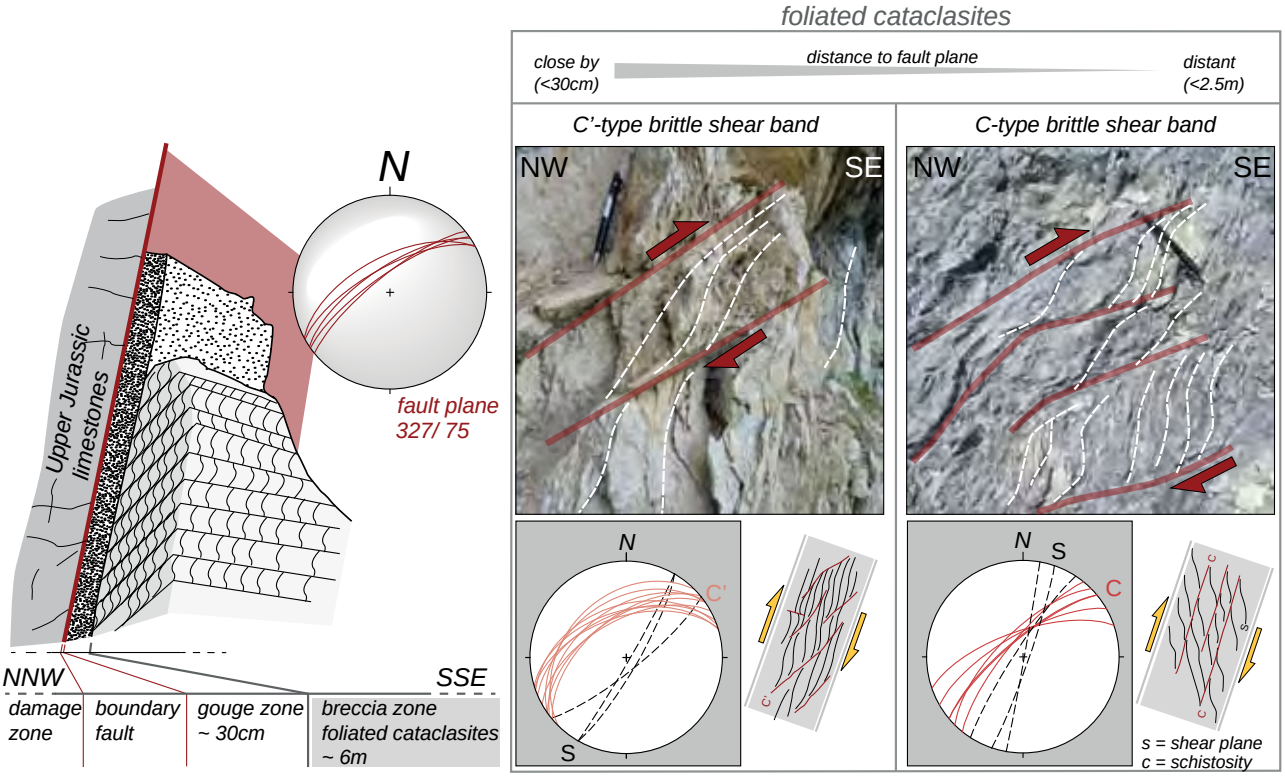

Fig. 2.21: The asymmetric fault zone of the Maischüpfen fault displaying a distinct boundary fault and a fine-grained gouge zone taking up the majority of the displacement. The adjacent breccia zone characterised by foliated cataclasites exposes a zonation ranging from higher deformation next to the gouge zone to less deformation further away, expressed by the presence of C'-type and C-type shear bands. C'-type shear bands reveal shear planes inclined 20° to the Maischüpfen fault, whereas C-type shear bands remain parallel, as represented on the stereographic projections of the fault planes and shear bands.

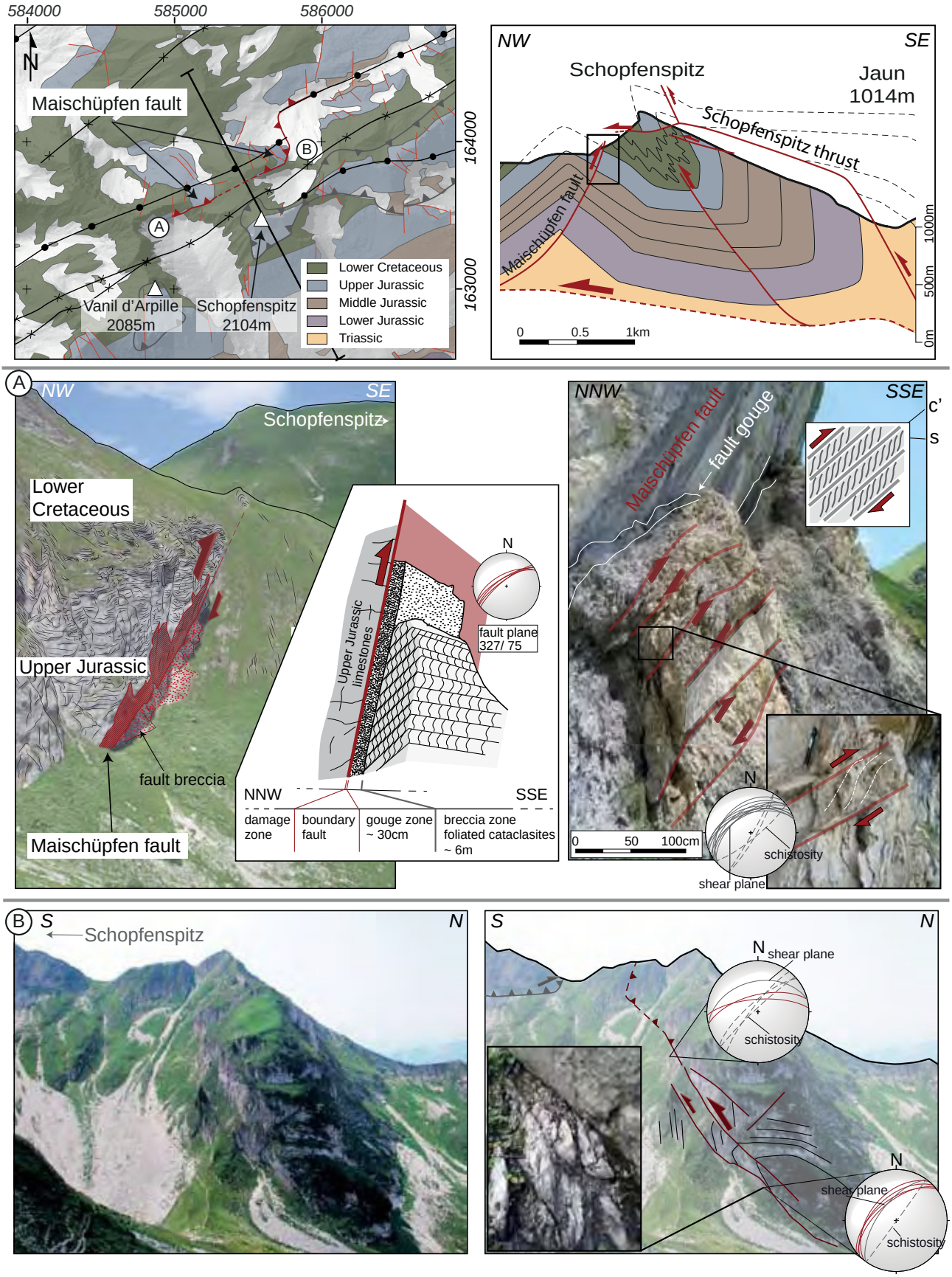

Fig. 2.22: Localisation of the Maischüpfen back thrust with its western part (A) and eastern part (B) is provided on a structural map on the left and the corresponding cross-section on the right. A) Overview of the western Maischüpfen fault plane and its significant fault zone characterised by a gouge zone and a breccia zone consisting of foliated cataclasites. Zoom into fault zone exposes remarkable brittle shear bands indicating a top to the SE movement. B) Eastern fault prolongation revealing a similar shear band bearing fault zone.

The Maischüpfen fault zone dispays unambiguously the gradual deformation of an asymmetric fault zone that is characterised by a straight boundary fault, which takes up most of the displacment, followed by a gouge zone and a zone of foliated cataclasites ranging from highly deformed C'-type to C-type brittle shear bands towards the external part.

Childs et al. (2009) displayed a significant correlation of the fault zone thickness with fault displacement, postulating the larger a fault zone the higher the displacement. For fault zones they obtained a displacement thickness ratio (D:T ratio) of 2.5 Applying this D:T ratio to the at least 6 m wide fault zone the Maischüpfen fault results in an offset up to 15m. As the exact thickness of the fault zone is unknown and this ratio decrease, for large fault zones decreases, the assumed offset can only be considered hypothetical.

4.2.2 Fold related normal faults

In the Préalpes Médianes, a large number of faults can be associated with the development of folds occurring both parallel and perpendicular to the fold axes. Fold-axes-parallel faults are generated by the folding and appear as conjugated normal faults. Faults developing perpendicular to the fold axes are mostly related to a periclinal closure of the fold dividing large-scale folds into segments, which can accentuate the axial plunging of a fold. In the Préalpes Médianes, fold-axes-parallel faulting appears more frequently in the intermediate zone between the PMP and PMR (Gastlosen range) than in the PMP, but this most probably depends on outcrop orientation, as outcrops perpendicular to the folding are rare in the PMP, but relatively frequent in the intermediate zone.

Faulting parallel to fold axes

The NW-SE oriented rock face of the Dent de Combette in the Rocher des Rayes area exposes a large amount of fold-axes-parallel normal faults related to extension provoked by the flexing of the Gastlosen imbricate, perpendicular to the fold axes. Conjugate normal faults mainly affect the competent Upper Jurassic limestones layers and disappear in less competent Middle Jurassic layers.

Wherever a lateral view on the structure is provided, similar conjugate faults can be observed along the Gastlosen and the Heiti imbricate, further to the NE. Only few fault slip indicators were measured, which reveal mostly a reactivation of these faults in a later stage of deformation.

Faulting perpendicular to fold axes

Several faults are oriented transverse or even perpendicular to the fold-axis and therefore induce a segmentation of the large folds. The succession

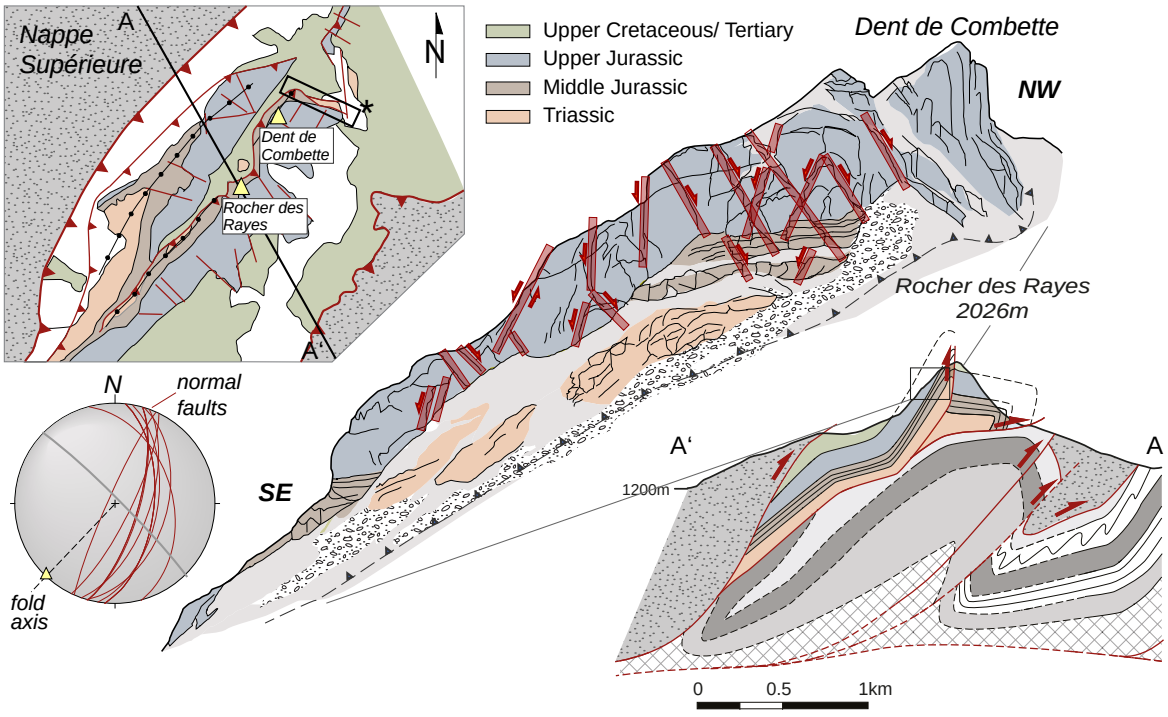

Fig. 2.23: Overview on the fold-axes-parallel normal faults in the Rocher des Rayes area. Schematic map to situate the Dent de Combette rock face and the discussed sector (A-A') of the second cross-section Fig. 2.15 within their structural context. Stereographic projection (lower hemisphere) shows a NNW-SSE orientation for the normal faults.

of several normal faults lead to more pronounced plunging of the fold axis. Slickenside and vein data as well as the morphological observations expose axial parallel extension in the Dent de Broc region (PMP).

Example: Dent de Broc

The Dent de Broc area shows a complex interplay of the different structural elements already mentioned in the previous section. On the one hand, the morphology of the landscape with steep, elongated calcareous cliffs and their periclinal closures indicate large-scale NE-SW fault-related folds. Three structural parts can be distinguished: a frontal zone governed by several imbricates, the Dent de Broc syncline and the Combes anticline thrusting the southern limb of the Dent de Broc syncline (Fig. 2.25D). Large normal faults perpendicular to the fold axis cut the Dent de Broc syncline in discrete segments, which further accentuates the plunging of the fold axis. We assume these faults have developed during the folding event and were reactivated later on as strike-slip faults.

A compilation of faults, indicated on already existing geological maps (CHATTON, 1974; FAVRE, 1984; PASQUIER, 2005) and observed on the digital elevation model and orthophotos, point out three major fault directions. The NNW-SSE (N160°) is the best-represented fault family (fault family 1 in Fig. 2.24A), whereas the other two fault families are equally distributed - the one in direction WNW-ESE (N110°), the other in direction NNE-SSW (N30°), (2 and 3 in Fig. 2.25A).

These regional faults extend over several hundreds of meters and are most likely related to the folding process. The dominating NNW-SSE fault direction corresponds to extensional faults oriented perpendicular to the fold axis (Fig. 2.25E), the orientation of mode I veins represent the same tendency (Fig. 2.25C), the pole projection indicates a fold axis parallel extension. The second regional fault family (Fig. 2.25A) oriented WNW-ESE is more abundant in the western part of the Dent de Broc area, where they show a dextral slip direction. In the north-eastern part of the Préalpes Médianes prevails the third family, with a NNE-SSW orientation with a sinistral sense of shear.

The rose diagram illustrating the orientation of the measured fault planes exposes a similar fault pattern than the observation on geological map and DEMs. The dominating fault family, oriented NNW-SSE corresponds to the normal faults generated by the folding process. A minor fault direction (NE-SW) is also provoked by the folding, but is oriented parallel to fold axis. Considering the slip direction of these faults, by contrast, strike-slip movements are clearly prevailing, whereas normal faults are almost missing. Sinistral and dextral strike-slip faults occur both in NNE-SSW as well as in NW-SE direction. One interpretation suggests the existence of two opposing strike-slip stress regimes with compressional stress axes oriented either NNW-SSE or NE-SW. Another one, favoured here, assumes that the normal faults developed during thrusting and folding of the Préalpes Médianes generated important fault zones, which can easily be reactivated under a subsequent stress system.

Paleostress reconstruction (Fig. 2.25B) reveals a continuous NE-SW trend for the extensional stress axes belonging to an either extensional or strike-slip stress regime with a compressional, respectively intermediate stress component oriented NW-SE. The investigation on extension vein orientation attests the same overall extension trend, represented as pole to vein plane projections Fig. 2.25C). However, the NE-SW oriented extension axis can be attributed to both, an extensional or a strike-slip stress regime. Fault-slip analysis exposed a heterogeneous dataset requiring a subdivision into different subsets, reducing the amount of data, but bringing light into the complex fracturing history. The secondary stress regimes of Petit Liençon (B2) and Dent de Broc (B1) displays two strike-slip stress regimes with compressional axes oriented NE-SW, resulting in opposite fault movement; a dextral movement for fault planes oriented N-S and a sinistral for NW-SE oriented fault planes.

As an explanation for this particular stress state, we suggest the reactivation of inherited normal fault structures complicating the determination of the orientation of the stress axes, so that a relatively low angle between the fault plane and the maximum compressional axis can be assumed.

4.2.3 Gastlosen and Heiti imbricates

With the arrival of the préalpine nappes on top of the Ultrahelvetic and Helvetic domains in the Late Eocene/ Lower Oligocene, a renewed large-scale deformation

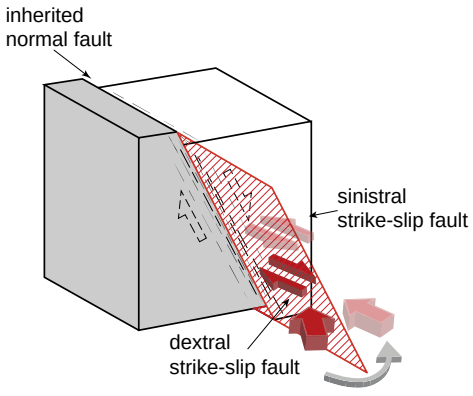

Fig. 2.24: Reactivation of an inherited normal fault structure as strike-slip faults exposing an opposite slip direction.

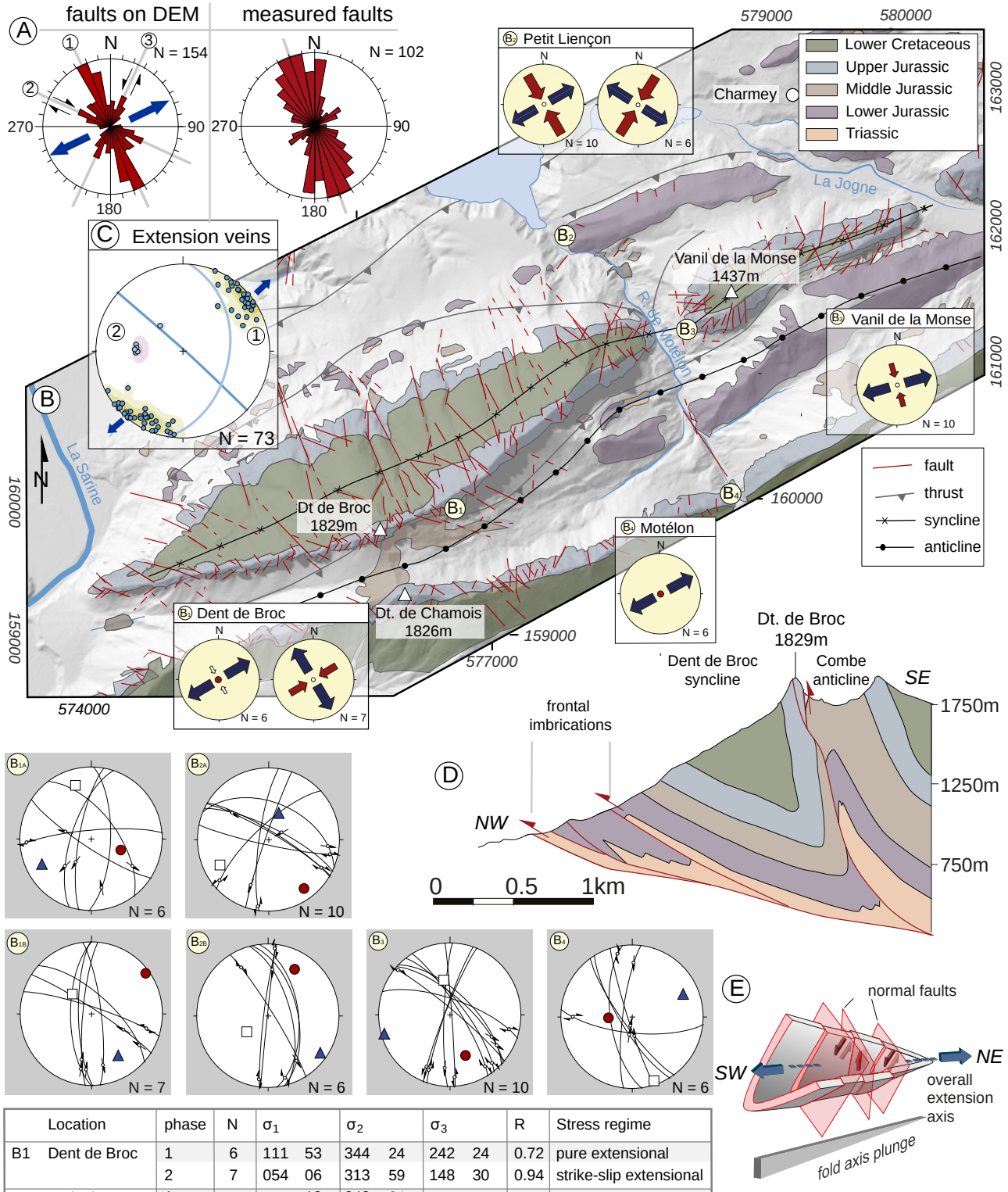

	Location	phase	N	σ_1		σ_2		σ_3		R	Stress regime
B1	Dent de Broc	1	6	111	53	344	24	242	24	0.72	pure extensional
		2	7	054	06	313	59	148	30	0.94	strike-slip extensional
B2	Petit Liençon	1	10	144	18	243	24	021	58	0.19	strike-slip compressive
		2	6	029	27	235	60	125	13	0.47	pure strike-slip
B3	Vanil d.l. Monse	1	10	159	39	351	50	254	05	1.1	strike-slip extensional
B4	Motélon	1	6	267	63	161	07	068	24	0.5	pure extensional

Fig. 2.25: Compilation of the structures in the Dent de Broc area. A) Rose diagrams: the first one shows the orientation of faults collected from maps and observed as lineaments on DEMs, the major fault families are indicated by numbers, whereas the second one points out the directions of the measured fault planes. B) Structural map of the Dent de Broc area localising the stress tensors obtained by paleostress analysis, details are represented by the stereographic projection of the sorted fault planes and a table listing the results of the paleostress analysis. C) Extension veins illustrating by a pole to vein plane projection the general extensional trend (1) towards NE-SW. D) Cross-section of the Dent de Broc area exposing the thrust planes below. E) Schema pointing out the segmentation of the syncline by fold axis parallel extension resulting in an increased axial plunging of the fold.

affected especially the PMR, so they achieve their present-day position as steeply inclined monoclinal imbricates dipping towards SE (MOSAR et al., 1996). The two imbricates, the Gastlosen and the Heiti/ Tour d'Aï imbricate, correspond to an intermediate zone in between the Préalpes Médianes Plastiques and the Préalpes Médianes Rigides (JACCARD, 1908; LUGEON, 1943; PLANCHEREL, 1979). As a consequence of differences in paleogeography, these imbricates show a different stratigraphic series, corresponding to the sector C and D of the previously mentioned paleo sectors. To the north as well as to the south both the Gastlosen/Heiti imbricates are almost always bordered by the Nappe Supérieure units (BUGNON, 1995; MOSAR et al., 1996; MÜLLER and PLANCHEREL, 1982; PAGE, 1969)

Unlike the Gastlosen imbricate, the Tour d'Aï/ Heiti imbricate is marked by an important amount of Lower Jurassic strata containing a particular dark limestone formation interlayered with black shales known as "Heitischichten". Heiti layers reach a maximal thickness up to 500m, 200m in the Tour d'Aï area, allowing a more gentle deformation expressed by the important Tour d'Aï anticline and the adjacent syncline. The Heiti imbricate appears in the south-western part of the Préalpes Romandes in the Tour d'Aï area, is missing in the central part and reappears to the north-west of Jaun until Oberwil (Fig. 2.26). The construction of the cross-section suggests a further prolongation of the Tour d'Aï structure underneath at least the Rocher des Rayes (Fig. 2.26; Fig. 2.16).

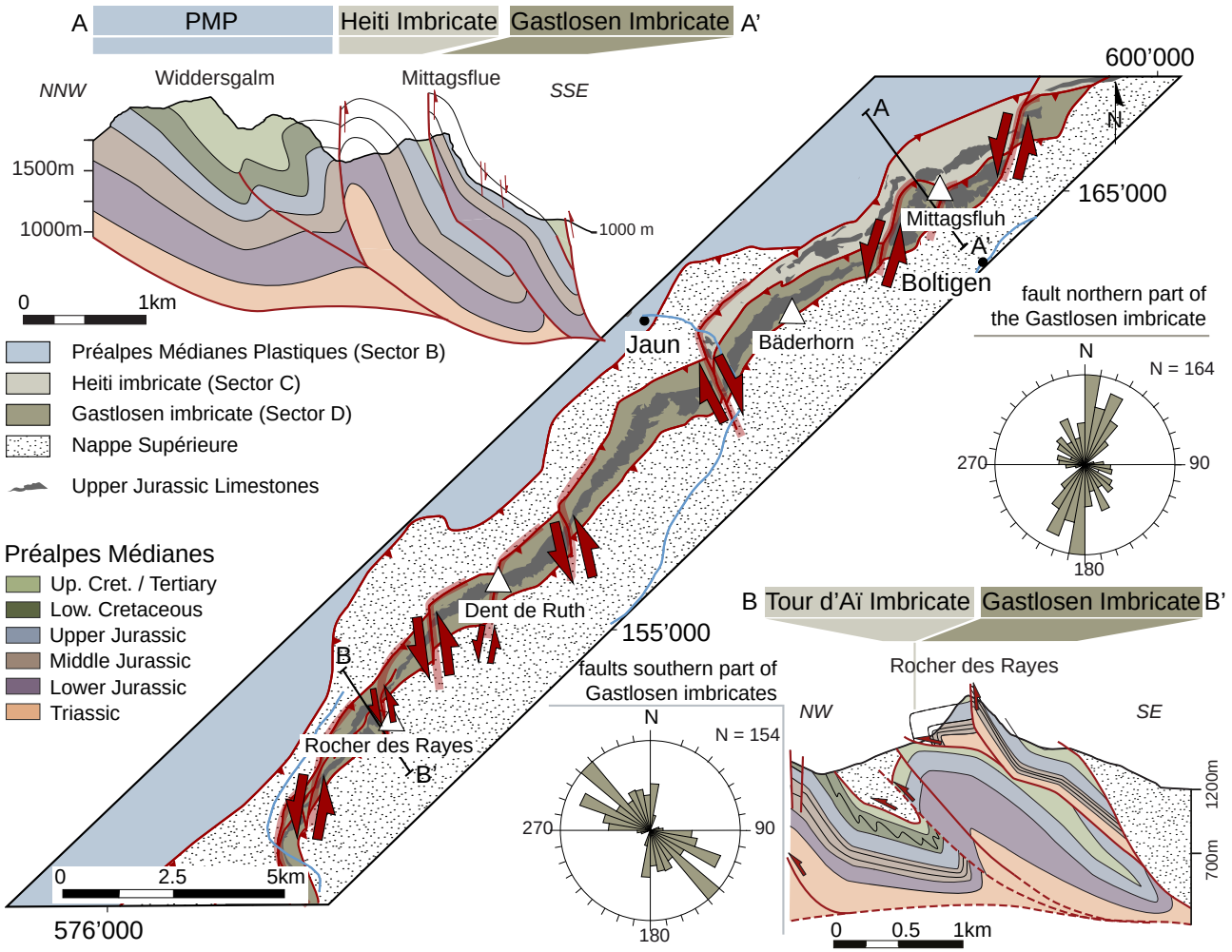

Fig. 2.26: Structural map showing the extent of the central and the northern part of the Gastlosen and Heiti imbricate between Château d'Oex and Boltigen, highlighting the segmentation of the Gastlosen range into sinistral offsetting units. Two schematic cross-sections explain the differences between the north-eastern part (A-A') and the south-western part (B-B') of these imbricates. Rose diagrams expose the fracture orientation both of the northern and the southern part of the Gastlosen and Heiti imbricate.

South-east of the Heiti imbricate, the Gastlosen imbricate extends from the Tour d'Aï area until Boltigen, where it disappears completely and possibly continues underneath the frontal part of the principal imbricate of the PMR (MOSAR, 1991). Structural differences along the Gastlosen imbricate are remarkable, ranging from a structural style related to a fault related fold in the Laitemaire-Dent de Ruth area - sometimes with thrust splays in the outer part forming a doubly folded frontal structure, as in the Rocher des Rayes area (Fig. 2.26) - towards a monoclinal imbricate in the Gastlosen - Boltigen area. The Gastlosen imbricate does not appear as a continuous mountain range, but as displaced segments, exposing mostly an advancing north-eastern part, as can be seen in the figure below. These sinistral displacements can either be explained as related to the large-scale N-S oriented sinistral strike-slip zones described by Plancherel (1979), or interpreted as tear faults related to a differential advancing of the thrust planes. A change in orientation of these segmenting strike-slip faults is observed from a N-S orientation in the Rocher des Rayes area towards a NNE-SSW orientation in the Boltigen area. Faults in the southern part of the Gastlosen imbricates expose a dominant NW-SE fracture orientation, whereas in the northern part a N-S fracture orientation prevails.

4.3 Post-Emplacement Structures

The arrival of the préalpine nappes on the foreland basin is recorded by the deposition of Mont Pélerin conglomerates resulting from the erosion of the Nappe Supérieure during the Chattian (MOSAR, 1999; TRÜMPY and BERSIER, 1954). The emplacement onto the Alpine foreland announced a final period of thrusting, affecting the entire préalpine nappe stack. Uplift rates, earthquakes and out-of-sequence thrusts witness an on-going deformation of the alpine wedge trying to readjust its instability by an interplay of erosion and the development of crustal imbricates (BONNET, 2007; MOSAR, 1999). Within the Préalpes Médianes, several thrusts are out-of-sequence thrusts, especially along important paleofaults (Fig. 2.17.), cutting through the whole préalpine nappe pile as well as the underlying Ultrahelvetics (JEANBOURQUIN et al., 1992; MOSAR, 1999). One out-of-sequence thrust is supposed to coincide with the PMP and PMR transition, often hidden underneath the Nappe Supérieure, another one is probably related to the Rianda-Stockhorn paleofault outcropping in the Jaun valley and thrusting the Schopfenspitz mountaintop. Post-emplacement thrusting is also affecting the

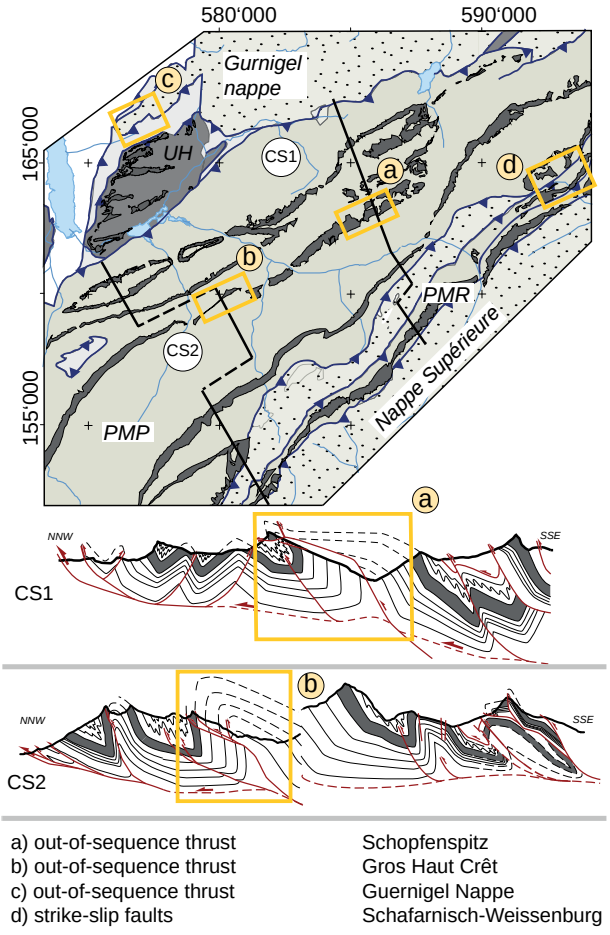

Fig. 2.27: Simplified map and crossection to localise the different post-emplacement structures observed in the Préalpes Médianes and Gurnigel nappe (more detailed cross-sections see Fig. 2.15).

Gurnigel nappe by a late thrusting of the PMP on top of the Gurnigel Nappe. Additionally, Ultrahelvetic lenses outcropping within the Gurnigel nappe are indicating a late stage of thrusting, bringing them from underneath the préalpine Nappe towards the surface (MOSAR et al., 1996).

Furthermore, in a final stage of deformation a ubiquitous strike-slip fracture pattern develops throughout the Préalpes Médianes, reactivating already existing faults or creating new small-scale fractures with a significant N-S orientation for sinistral and WNW-ESE orientation for dextral strike-slip faults. Acting together as conjugated fault zones, the préalpine fault system coincides with conjugated fault systems common in the Jura mountains and the Molasse basin (DELACOU et al., 2004; KASTRUP et al., 2007; KASTRUP et al., 2004; MOSAR and BOREL, 1992).

4.3.1 Out-of-sequence thrusts

Within the Préalpes Médianes, several thrusts hint at late post-emplacement movements, mainly in the Western part of the Préalpes Romandes, in the Tour d'Aï region, but also at the contact of structural units as for instance at the contact of the Préalpes Médianes Rigides with the underlying Niesen Nappe, as well as to the East of Montreux. These thrusts were described in detail by Mosar et al. (1996). With the following examples, out-of sequence thrusts situated in the central part of the Préalpes Médianes are discussed.

Example: Schopfenspitz thrust

The area of the Combifluh-Schopfenspitz (Gros Brun) and Maischüpfenspitz (Vanil d'Arpille) attracts attention because of thrusts offsetting the Upper Jurassic limestones of the southern limb of the Sarine syncline by several meters. Above all, the largest offset exposes the Schopfenspitz thrust, which completely decoupled the mountaintops mentioned above. Nowadays they remain as klippen, separated by a clearly visible thrust plane that was subject of several previous investigations (ANDREY, 1974; FUCHS, 2003; PLANCHEREL, 1976).

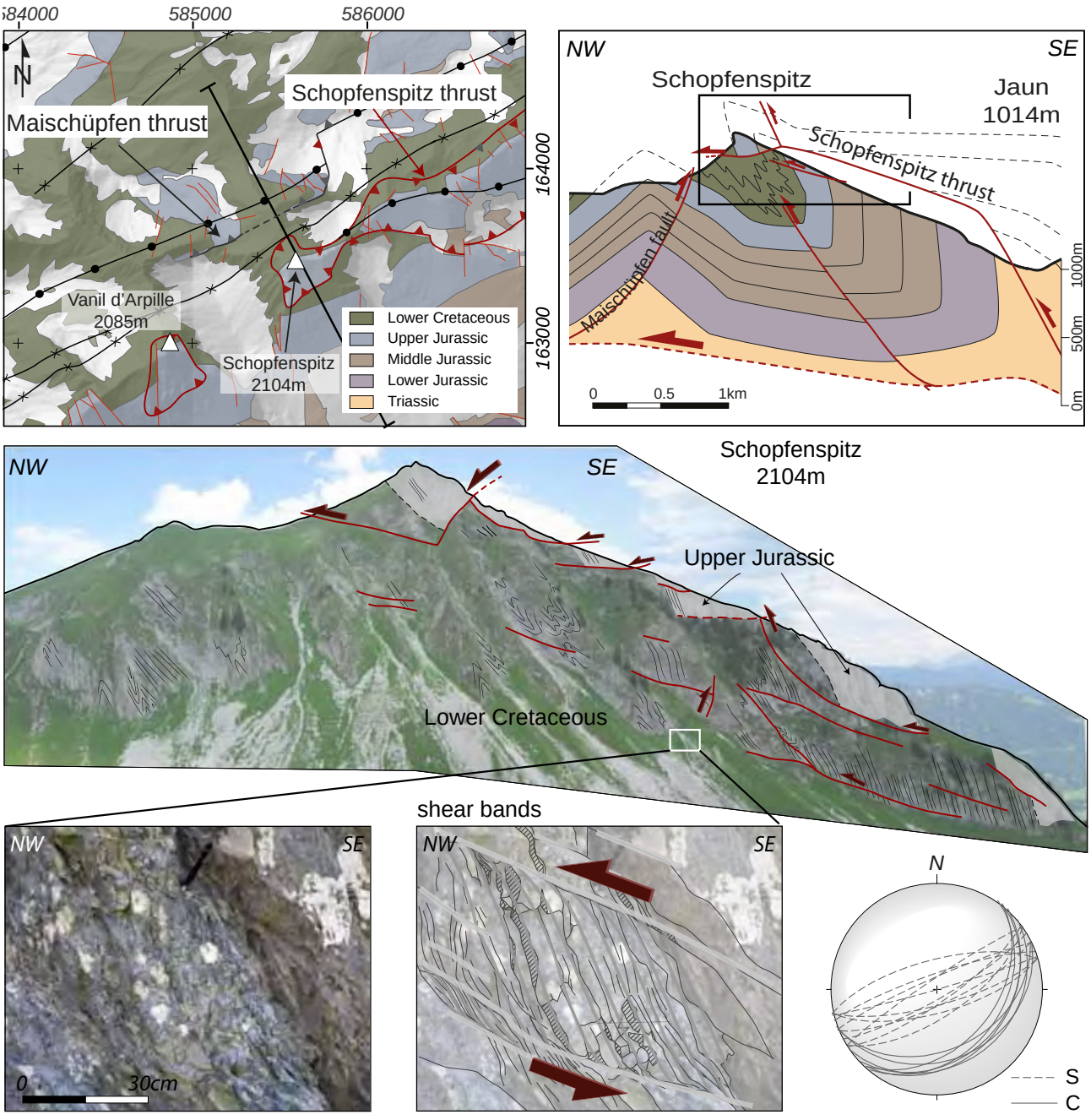

Fig. 2.28: Schopfenspitz thrust schematically indicated on a structural map and cross-section (above). The Panoramic view of the Schopfenspitz shows the displaced Upper Jurassic limestone layers and the prolongation of their thrust planes towards the Lower Cretaceous layers offsetting small-scale folds. The stereographic projection (lower hemisphere, equal area projection,) indicates a NE-SW oriented thrust plane with a top to the NW movement (measured at the base of the Schopfenspitz rock face). Fault zone shows characteristic brittle shear bands of 30 to 50cm width.

The orientation of the minor thrust planes at the base of the western Schopfenspitz rock face, indicate a NW-SE orientation of the thrust plane dipping generally about 30° towards SE. Assuming a similar orientation for the Schopfenspitz thrust, the main thrust plane should continue in the Jaun valley, as indicated on the cross-section on Fig. 2.28. Locally known as Schopfenspitz thrust, the important fault coincides with the inherited paleofault Rianda-Stockhorn developed during the Pliensbachian. Slumps discovered in the Middle Jurassic limestones show a northwards verging movement direction and suggest a fault activity until that time (FUCHS, 2003). The Middle Jurassic layers show highly variable thicknesses, reaching from about 300m at the NW until nearly 900m to the SE on the north-western part of the Rianda-Stockhorn fault, clearly related to a synsedimentary fault growth.

Similar to the Maischüpfen fault zone, the minor thrusts parallel to the Schopfenspitz frequently expose brittle shear band, indicating a top to the NW movement. However, the shear band zone, measuring a width of 30-50cm, is considerably narrower than the Maischüpfen one.

Crosscutting already existing small-scale folds of the Lower Cretaceous, the thrusts are clearly postdating the main folding phase. Relatively rare throughout the Préalpes Médianes, the same situation exists along the south-western limb of the Sarine syncline. As a possible explanation for the development of these minor thrust planes parallel to the important Schopfenspitz thrust, we suggest the following scenario (Fig. 2.29):

- The development of the Rianda-Stockhorn paleofault generated by the main rifting phase of the Alpine Tethys provoked not only one major normal fault, but rather a suite of several minor normal faults accumulating together a significant normal offset.

- During nappe emplacement, large-scale fault related folds established and led - in the todays Schopfenspitz area - to the development of the Sarine Syncline and the Tsavas-Millet anticline. As a result, the former normal fault zone turned into an overturned position dipping towards SE.

- In a more recent deformation phase, the inherited normal faults were dislocated and thrust towards NW, whereas one of them, the Schopfenspitz thrust, took up the largest displacement and thrust completely the Sarine syncline.

Nevertheless, it remains speculative to attribute an age to this last event, since it remains uncertain if the thrust movement is a continuous consequence of the folding or if a temporal gap prevailed in between these two phases.

Paleostress analyses carried out in this area reveal a predominant NW-SE oriented compressional stress regime, with only minor occurrence of the usually prevailing strike-slip stress regime (for data see Appendices). This implies a further evidence for a relatively late thrust activity in the Schopfenspitz area, independently from the thrusting event related to the folding of the Préalpes Médianes, because compressional stress regimes are scarce throughout the Préalpes Médianes and occur mostly in vicinity of areas where a post-emplacement thrust movement was suspected.

According to Plancherel (1976), the Schopfenspitz thrust is generated under influence of the nearby sinistral strike-slip fault zone of the Euschelspass that is supposed to pre-date the structures separated

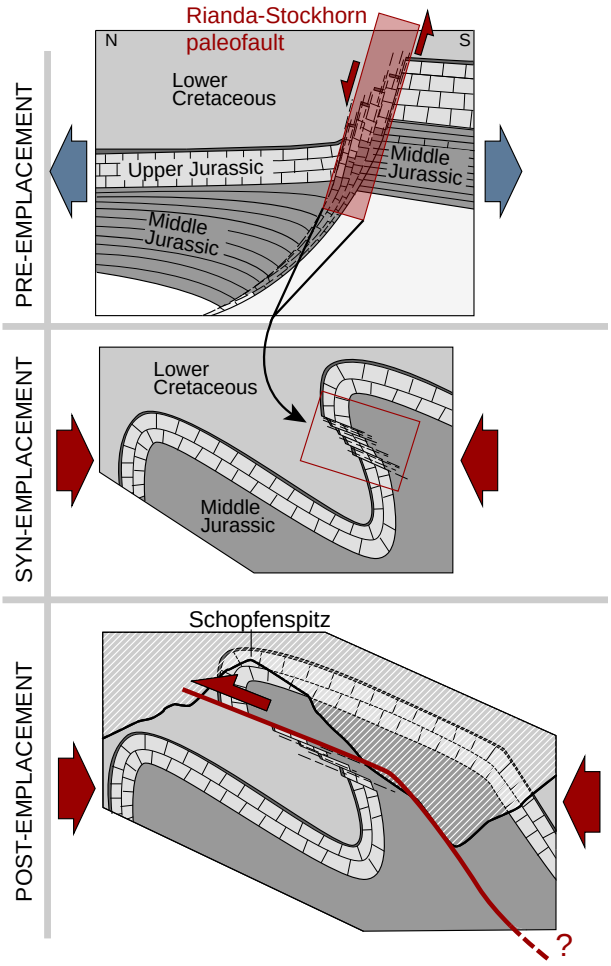

Fig. 2.29: Schematic evolution of the Schopfenspitz thrust by three different stages. Pre-emplacement; the development of a composite normal fault zone instead of one single paleofault. Syn-emplacement; folding and overturning of the inherited normal fault zone. Post-emplacement; reactivation of these former normal faults as thrusts, whereas the Schopfenspitz thrusts takes up the largest displacement.

by this wrench zone. This explains the independent structural style on both sides of the Euschel wrench zone. Another interpretation suggests the already mentioned Rianda-Stockhorn paleofault coinciding with the localisation of the Euschel fault zone and therefore delimiting two completely different paleogeographic sedimentation realms (see Fig. 2.17, sector A and sector B). A reactivation of this ancient normal fault zone led to the development of the Schopfenspitz thrust. Along the Rianda-Stockhorn paleofault zone, other indications for a more recent reactivation of this inherited normal fault can be found, for example in the Gros Haut Crêt area.

Example: Gros Haut Crêt

The Gros Haut Crêt structure attracts attention by an advancing thrust structure showing a significant offset of the Upper Jurassic massive limestones for about 200m. Displacing the already existing fold structures, as well as aligned in the direct prolongation of the Schopfenspitz fault, we attribute the Gros Haut Crêt thrusting to the same post-emplacement structure. The Gros Haut Crêt thrust is further affected by two thrust splays leading to an on-going compression of the Tsavas-Millet anticline. The main thrust plane is plunging obliquely towards SW leading to the disappearance of this forward thrusting part of the ancient Rianda-Stockhorn paleofault. Paleostress analyses witness mainly an extensional stress regime perpendicular to the fold axis, which can be linked to an intensified bending of the Tsavas-Millet anticline.

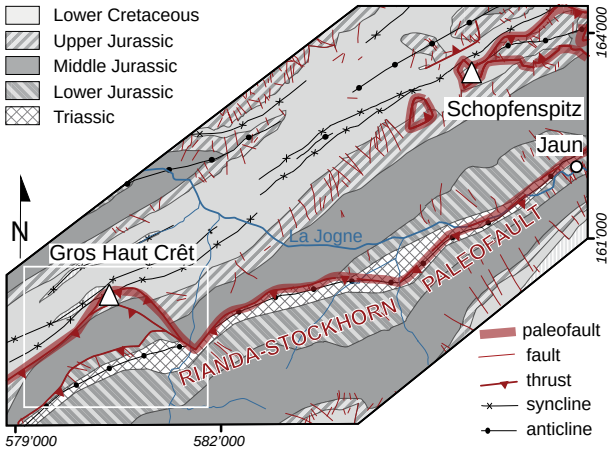

Fig. 2.30: Schematic structural map indicating the trace of the Rianda-Stockhorn paleofault and highlighting the spatial and temporal relationship between the Schopfenspitz and the Gros Haut Crêt thrust.

Example: Subalpine Molasse and Gurnigel nappe

The Subalpine Molasse is characterised by an intensively deformed stack of imbricated thrust sheets at the Alpine boundary. Further to the east, in eastern Switzerland, Bavaria (GER), and Austria, this zone is marked by an important blind back thrust, delimiting a triangular sector, known as the "triangle zone" (Berge and Veal, 2005; Pfiffner et al., 1988; Vollmayr and Wendt, 1987). Similar structures are developed in analogue models of the alpine foreland basin (Bonnet, 2007) and their occurrence is therefore also not improbable in the Western part of the Molasse basin. Further to the east in the Emmental, Subalpine Flysch and the Helvetic nappes intersect the Subalpine Molasse. Elsewhere, the triangular zone is thrust by a newly developed thrust, related to the backstepping of the Alpine deformation front into the Subalpine Molasse (Schlunegger and Mosar, 2010). Apatite fission track analysis carried out by Cederbom (2011) recorded the latest thrusting in the Subalpine Molasse at, or since the major erosion event, during Plio-Pleistocene times.

The contact of the Gurnigel Nappe and the PMP exposes an overturned position of the Gurnigel layer which can be related to the late reactivation of an out-of-sequence thrust between these two nappes thrusting the PMP nappe on top of the internal part of the Gurnigel nappe (De Kaenel et al., 1989).

Interpretation

Earthquakes, uplift rates, and out-of-sequence thrusts witness a still persisting orogenic evolution of the alpine accretionary wedge related to a readjustment of the critical wedge. Its geometry is supposed to be in a supercritical state (Mosar, 1999) after the northwestward shift of the Alpine deformation front into the Plateau Jura during Pliocene times forming a long thinned out wedge. Therefore, recent backstepping thrusting activity towards the Subalpine Molasse or even further back into the Préalpes klippen belt can be expected.

Analogue tapered wedge models established by Bonnet et al. (2007, 2008) show similar tendencies. Additionally, they point out the important link between tectonic evolution, basin sedimentation, and erosion for the evolution of the foreland basin coupled with tectonic underplating of basement nappes.

In order to restore internal stability of the wedge, the tectonic underplating of sedimentary and/or crustal material from the lower plate into the upper plate thickens the accretionary wedge. Below the Helvetic domain, the development of two new crustal imbricates were postulated by the interpretation of seismic data (Escher and Beaumont, 1997). In the Préalpes, this process is represented by a basement high in the in the Lake Geneva area, as well as by the described out-of-sequence thrusts expressing the

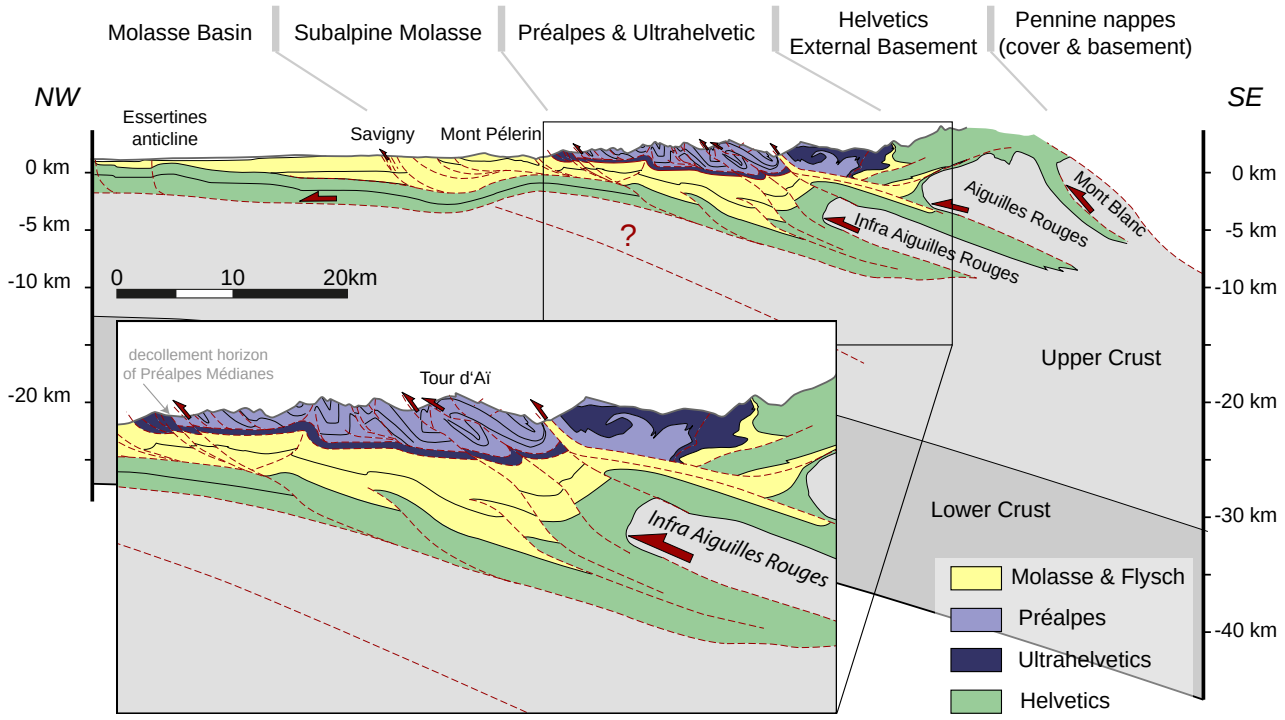

Fig. 2.31: Simplified cross-section across the Alps and the foreland basin (modified after MOSAR et al., 1996; SCHLUNEGGER and MOSAR, 2010; SOMMARUGA, 1997).Highlighting a possible connection between the developing crustal imbrications and the out-of-sequence thrust cropping out in the préalpine klippen. Visible on the zoom, the out-of-sequence thrusts coincide with important weakness zones in between nappe boundaries or provoked by reactivated paleofaults. Additionally, this cross-section points out the important amount of Subalpine Molasse lying underneath the Préalpes klippen belt.

recent stacking below. Presumably, these thrusts are linked with the ones generated by the basal imbricates and are therefore crosscutting throughout the entire Subalpine Molasse deposits in between. Generally, the out-of-sequence thrusts in the Préalpes klippen belt are supposed to reactivate already existing weakness zones as for instance nappe contacts (Gurnigel Nappe-PMP or PMP-PMR) or inherited paleofaults (Rianda-Stockhorn fault, Château d'Oche-Corbeyrier or Bordière fault).On the Fig. 2.31, it is clearly visible that not only the Préalpes Médianes are affected by the development of out-of-sequence thrusts, but also the Gurnigel nappe and the Subalpine Molasse in front of the Préalpes Médianes.

4.3.2 Strike-slip faults

In the Préalpes Médianes, as well as in the adjacent Gurnigel Nappe and Subalpine Molasse, detailed fracture measurements revealed a predominating occurrence of strike-slip faults showing two major directions: N-S to NNE-SSW oriented sinistral strike-slip faults (detailed descriptions were carried out by Plancherel (1979)) and W-E to NW-SE oriented dextral strike-slip faults (BOREL, 1991; MOSAR, 1991) acting together as conjugated shear zones. These ubiquitous strike-slip faults clearly offsetting already existing folding structure as well as overprinted slickensides on fracture planes prove a most recent strike-slip movement.

These strike-slip faults are represented either as small-scale fractures, measured and analysed for paleostress reconstruction, or as large-scale lineaments visible on DTMs, orthophotographs and maps, as for instance in the Weissenburg-Schafarnisch area (Fig. 2.32A/E). As illustrated on Fig. 2.32, the measured strike-slip faults and the detected lineaments show similar principal orientations with respect to the bending of the Préalpes leading to a radial fanning of the two principal directions and for this reason to a broader spectrum of the peak directions within a rose diagram. Within the rose diagram of the measured fault (Fig. 2.32C), the dextral faults show a broader distribution, pointing generally towards the NW-SE, whereas the orientation of the sinistral faults is mainly in a N-S direction. This widespread range of the orientation of dextral faults is probably related to the reactivation of former normal faults perpendicular to fold axis bending throughout the investigation area. The lineaments (Fig. 2.32D) point out three principal

directions: two major directions, the NNW-SSE and WNW-ESE orientated faults, attributed to dextral strike-slip faults and a N-S directions corresponding to sinistral strike-slip faults.

Structural investigations in the Schafarnisch-Weissenburg area exposed minor deviations among the lineaments directions (15-30°) and the measured fractures related to two important shear zones with a fault pattern developed as Riedel shears within this shear zones. These deviations are only visible at a limited zone of investigation (for example the Schafarnisch-Weissenburg area), where the principal orientations of lineaments and faults are less scattered and

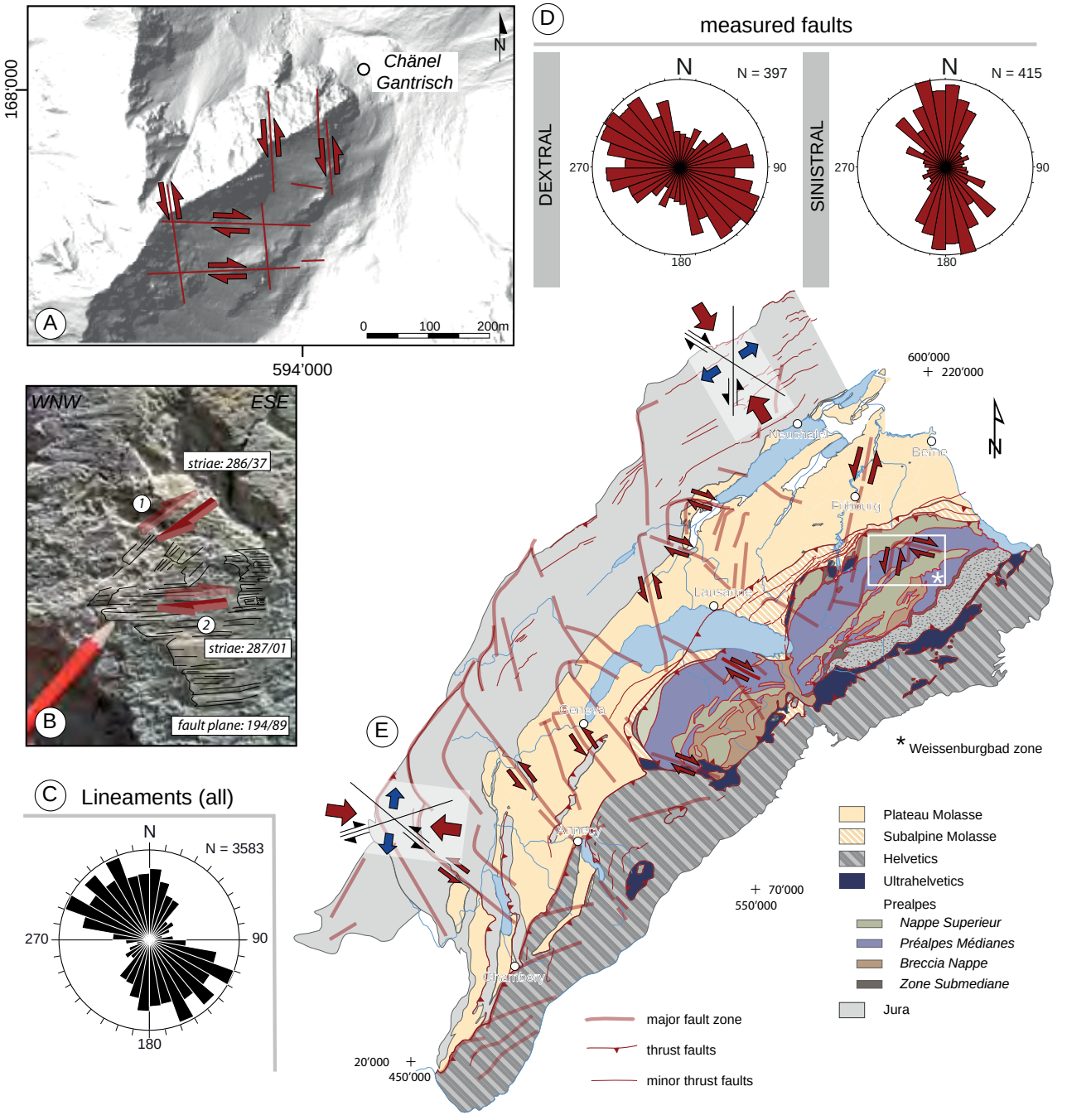

Fig. 2.32: Overview of strike-slip faults occurring in the Préalpes klippen belt. A) Lineaments detected on DTMs show an obvious sinistral offset for N-S oriented and a dextral offset for E-W oriented strike-slip faults in the Schafarnisch area. B) Overprinted slickensides expose a more recent dextral strike-slip movement on a normal fault plane in the Tzintre area. C) Rose Diagram exposing the resulting direction of lineament analysis exposing a two principal directions towards NW-SE and WNW-ESE, assumed to be dextral strike-slip faults, and a third principal direction oriented N-S considered as sinistral strike-slip faults. D) Rose diagrams representing both the sinistral and the dextral strike-slip faults that are dominating in the Préalpes klippen belt: a NW-SE orientation for the dextral strike-slip faults and a N-S orientation for the sinistral strike-slip faults. E) Simplified structural map, including the Jura mountains, the Western Molasse Basin, and the Préalpes klippen belt highlighting major fault zones that show a similar conjugate fault pattern, similar to the one observed in the Préalpes Médianes.

not influenced by the general bending of the préalpine structures. Taking the entire fault and lineament dataset into account, no distinct deviations can be observed due to the broad data scattering related to the rotation of the general structures.

Extensive paleostress analysis, further discussed in the following chapter, confirms an overall prevailing strike-slip stress regime with a generally NW-SE orientation for the compressional and a NW-SE orientation for the extensional stress axes, which is clearly dominating the stress regimes related to the folding and thrusting of the Préalpes klippen. This strike-slip stress system matches the observed sinistral and dextral strike-slip faults.

The regional stress field, including the Western Molasse Basin and the Jura mountains, reveals a similar pattern of conjugate strike-slip fault zones rotating from East to West, remaining in perpendicular position to the Alpine arc (Fig. 2.32E).

5 Discussion and Conclusion

Characterising the Préalpes Médianes and their adjacent préalpine nappe units, structural key-elements were accumulated during a complex deformational history. Rather than to attribute an absolute chronology to the different structural elements observed in the Préalpes Médianes, the aim is to understand the circumstances of their formation, to associate them to an event during the préalpine history and to infer hereby a relative chronology. The table below gives an overview over the different structural elements, and how they developed during the préalpine history.

Paleostress analyses, discussed in the following chapter, reveals the predominating strike-slip stress system and subordinate stress-systems related to the folding and the thrusting of the préalpine nappes, as for instance a fold axis parallel extension. Additionally, the results of the paleostress analyses demonstrate that most of the inherited structures, be it the syn-emplacement structures, were reactivated in a later stage of deformational history.

	Time	Event	Structural elements	Examples
Pre-emplacement	Triassic until Upper Jurassic/ Lower Cretaceous, but primarily Lower Jurassic	Extension leading to the formation of the Tethys Ocean	Paleofaults, pre-structuring of the sedimentation realm leading to sediment thickness variations	Château d'Oche-Corbeyrier, Bordière, and Rianda-Stockhorn paleofault
Syn-emplacement	Eocene (Bartonian) until Oligocene (Chattian)	Alpine collision provoking the detachment of the préalpine nappes and their transport towards NW	Fault-related folds; mainly fault-propagation folds verging towards NW, but also some hinterland verging backthrusts	most of the folds in the Préalpes Médianes, e.g. Dent de Broc area (foreland-verging thrust), Maischüpfen fault (hinterland verging thrust)
			Imbrication; arrival on top of the Ultrahelvetic/ Helvetic in the Late Eocene/ Lower Oligocene provoked an upright position of the Gastlosen and Heiti imbricates	Gastlosen and Heiti imbricates
			Fold related normal faults; the non-cylindrical bending of the préalpine folds results in extension parallel and perpendicular to the fold axis	normal faults perpendicular to the fold axis: Dent de Broc normal faults parallel to the fold axis: e.g. Rocher des Rayes
Post-emplacement	Chattian until present-day	Readjustment of wedge instabilities after the arrival on the Alpine foreland and resetting of a new stress system	Out-of-sequence thrusts cutting through the préalpine nappe pile and probably also through the Subalpine Molasse below; presumably they are linked to the development of crustal imbricates. Basement involvement.	Reactivation of important paleofaults as the Rianda-Stockhorn faults; e.g. the Schopfenspitz thrust.
			Predominant N-S oriented sinistral and NW-SE oriented dextral strike-slip faults acting together as conjugated shear zones and clearly offsetting the previously developed folding structure	Predominating fault-slip movement throughout the Préalpes Médianes, e.g. Schafarnisch - Weissenburg strike-slip zone

Tab 2.2: Overview of the structural elements acquired throughout the deformational history of the préalpine klippen.

3 - Fault Kinematics and Paleostress Analysis

Abstract

Based on fault kinematic analyses and paleostress reconstructions, we attempt to gain a better insight into the evolution of the stress field of the frontal part of the Préalpes Romandes, with focus on the Préalpes Médianes, but also the Nappe Supérieure (Gurnigel Nappe) and the Subalpine Molasse, beyond the Préalpes klippen belt. Fault-slip data collected at more than 50 measurement sites expose heterogeneous datasets influenced by local tectonic structures. Data processing with the WinTensor program (DELVAUX, 2006) allowed the separation of these datasets into subsets of homogeneous stress states at nearly every measurement site, indicating multiple deformation events. The observations of slip indicators on fault planes with overprinting slickenfibres and of intersecting extension veins confirm this assumption. Hereby, two different deformation phases can be distinguished. The first one seems to be related to the folding and thrusting process displaying mostly extensional stress regimes either parallel or perpendicular to the fold axes trend (NE-SW) and compressional stress regimes oriented in NNW-SSE direction. The second one, a strike-slip stress regime characterised by N-S trending sinistral and WNW-ESE striking dextral faults, prevails throughout the entire investigation area. Additionally, the observation of fault lineations on Digital Elevation Models (DEM) exposes large-scale conjugate fault zones oriented NNW-SSE for the sinistral and WNW-ESE for the dextral fault zones. The measured strike-slip fractures presumably act as subordinate Riedel-type fractures within these fault zones, similar to those found at several sites in the Western Molasse basin and in the Jura mountains.

Keywords: Préalpes Médianes, paleostress reconstruction, polyphase, fault reactivation, strike-slip

1 Introduction

The Préalpes klippen, built up of a pile of tectonic nappes, underwent a complex history of structural deformation before, during, and after the nappe transport. The majority of the many studies realised in the Préalpes klippen belt focussed on the surface geology and surface structures and only few analyses interpret the kinematic evolution in the préalpine nappe stack (e.g. Bonnet, 2007; Borel and Mosar, 2000; Guyomard et al., 2009; Mettraux and Mosar, 1989; Mosar, 1999; Mosar and Borel, 1992). Faults and fractures are important witnesses that give a significant insight into the kinematic history of the Préalpes klippen belt. The observed local fracture pattern is mainly related to the fold-and-thrust development due to the nappe transport. However, the reactivation of these fault planes as strike-slip faults, as well as more recently formed N-S oriented sinistral and WNW-ESE oriented dextral faults cutting through previous structures attest to an on-going deformational evolution postdating nappe emplacement.

In this study, fault kinematic analysis focuses on the frontal part of the Préalpes Romandes, mainly on the Préalpes Médianes, but also the Gurnigel Nappe, the Ultrahelvetics and the Subalpine Molasse (Fig. 3.2). The zone between the surroundings of Charmey and Jaun to Schwarzsee and Boltigen was analysed with more detail, based on a large data set of new fault-slip measurements.

An important issue of this study is to clarify the paleostress evolution, mainly related to the syn- to post-emplacement phase of the préalpine nappes. Detailed fault-slip data processing allowed the separation of the mostly heterogeneous dataset into homogeneous subsets pertaining to different stress regimes. For this investigation, kinematic fault analysis were primarily realised in the Préalpes Médianes nappe. However, in

order to obtain a better insight into how the stress field reacts in adjacent structural units (Gurnigel nappe, Ultrahelvetics and Subalpine Molasse) the study area extends towards the foreland basin. In this way, we attempt to distinguish the fracture arrangement related to previous, fold-related structures from those postdating the nappe emplacement and to find a possible link between the structural units towards the Molasse basin.

1.1 Geological and Structural Setting

The Préalpes klippen belt is formed by a series of nappes detached from their mostly Briançonnais homeland during its incorporation into the orogenic wedge (Caron, 1972; Caron and Dupasquier, 1989). Subsequently, the préalpine klippen were transported to the N/NW and emplaced onto the foreland, where they remain isolated by erosion as several tectonic klippen along the northern front of the Swiss and French Alps and to the NW of the Helvetic nappes. The Préalpes klippen belt is subdivided in two major lobes, the Préalpes du Chablais southwest and the Préalpes Romandes northeast of the Rhône valley.

In the préalpine nappe pile, the following four structural units (Fig. 3.2) are commonly differentiated (from top to bottom):

- the **Nappe Supérieure** containing another four subordinate nappes: the Gurnigel, Dranse, Simmen and Gets Nappe (Caron, 1972; Trümpy, 1980),
- the **Breccia Nappe** (Dall'Agnolo, 2000; Lugeon, 1896, 1949; Steffen et al., 1993),
- the **Préalpes Médianes Nappe** (Baud, 1972; Bieri, 1925; Genge, 1957; Isenschmid, 1979; Jeannet, 1922; Mettraux, 1989; Mosar, 1991; Mosar and Borel, 1992; Mosar et al., 1996; Plancherel, 1979; Wissing and Pfiffner, 2002) and
- the **Niesen Nappe** (Ackermann, 1986; Bernoulli et al., 1979; Caron, 1972, 1973; Homewood et al., 1984; Matter et al., 1980)

and two mélange zones created during nappe transport: the "Zone Submédiane" (Weidmann et al., 1976) and the Ultrahelvetics (Badoux, 1963;

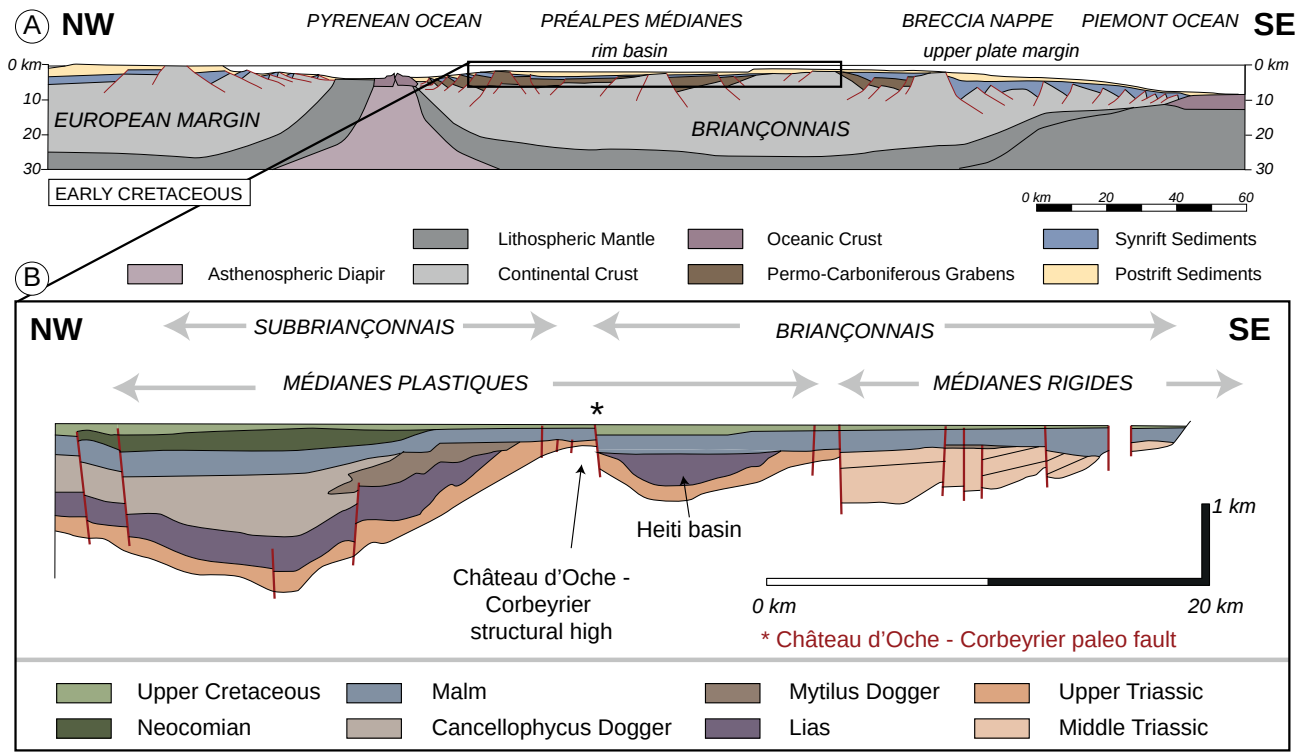

Fig. 3.1: A) Cross-section showing the localisation of the Briançonnais micro-continent in between the Pyrenean and Piemont ocean at the Early Cretaceous times (modified after STAMPFLI et al., 2002). B) Palinspastic and tectonic reconstruction model for the Préalpes Médianes highlighting the strong influence of paleofaults affecting the sediment deposition. The horizontal line corresponds to the deposition of the Eocene Flyschs (modified after BAUD and SEPTFONTAINE, 1980; BOREL and MOSAR, 2000).

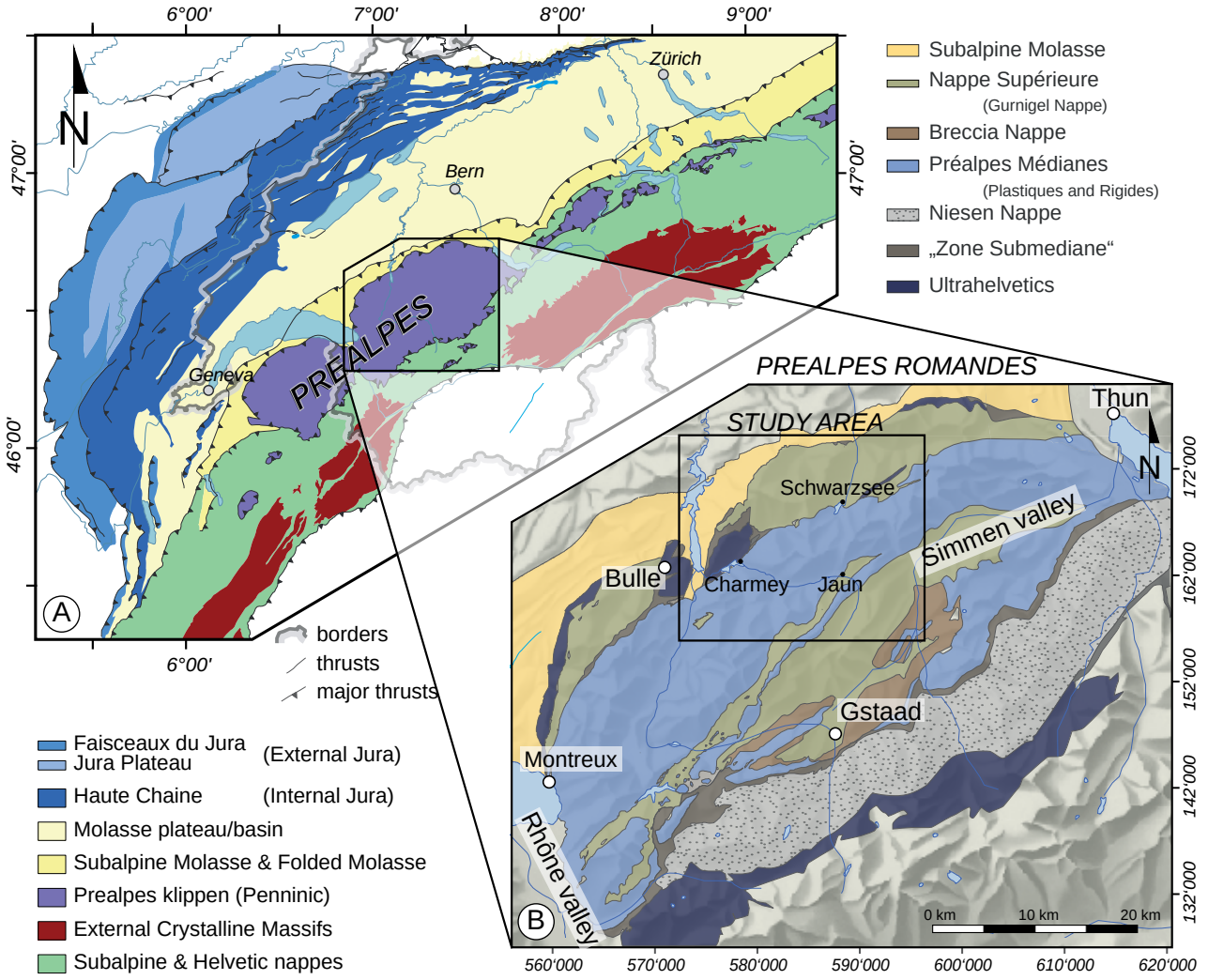

Fig. 3.2: Location of the Préalpes klippen belt in the context of the Western Alpine orogen. A) Simplified tectonic map of the Western Alps highlights the large-scale structural units including the Préalpes klippen belt located along the northern front of the Swiss and the French Alps and NW of the Helvetic nappes and the External crystalline massifs (modified after SCHLUNEGGER and MOSAR, 2010). The Préalpes klippen belt is characterised by two large lobes: the Préalpes du Chablais SW and the Préalpes Romandes NE of the Rhône valley. B) Structural map of the Préalpes Romandes modified after Caron (1973). The allochthonous préalpine nappes are piled up in the following order (from the top to bottom): a) Nappe Supérieure, b) Breccia Nappe, c) Préalpes Médianes and d) Niesen Nappe (existing only in the Préalpes Romandes) and two mélange zones developed during the nappe transport: the Ultrahelvetics and the "Zone Submédiane".

Homewood, 1977), which can also be found in the frontal part of the Préalpes, below the Préalpes Médianes and in the most internal regions (Trümpy, 1980).

1.1.1 *Préalpes Médianes*

The most important and best-exposed nappe, the Préalpes Médianes, is subdivided into two parts: the Préalpes Médianes Plastiques mainly governed by large-scale fault-related folds, and the Préalpes Médianes Rigides, dominated by imbricated thrust slices dipping to the N/NW showing a ramp-flat structure. On an evaporitic basal décollement, situated at the base of Middle and Late Triassic (Baud, 1972; Baud and Septfontaine, 1980), the Préalpes Médianes were detached from their homeland and transported more than 100km (Schardt, 1893b). The Préalpes Médianes are composed of limestones, dolomites, marls, and shales, deposited from the Triassic until the Tertiary. Their sedimentation realm has been interpreted in terms of rim basin located in the Sub-Briançonnais to the N-NW of the Briançonnais upper plate rift shoulder of the Tethyan rift margin (Mosar, 1997; Mosar et al., 1996; Stampfli and Marthaler, 1990) (Fig. 3.1). Extensional synsedimentary faults influenced the sediment distribution considerably, which led to the development of several different facies realms perpendicular to strike (Baud and Septfontaine, 1980). Two major sedimentation realms clearly differentiate since Early Jurassic: the Préalpes Médianes Plastiques to the N-NW, characterised by an important

sediment thickness and the Préalpes Médianes Rigides to the south, marked by several stratigraphic gaps associated with a continuously structural high giving way to a platform and lagoonal environment (Baud and Septfontaine, 1980; Borel, 1995; Mosar, 1994, 1997; Mosar et al., 1996). An intermediate domain is situated in between the Préalpes Médianes Plastiques and the Préalpes Médianes Rigides showing intermediate characteristics leading to the formation of the future Heiti and Gastlosen imbricate (Baud, 1972; Lugeon and Gagnebin, 1941; Mosar et al., 1996; Plancherel, 1979).

1.1.2 Gurnigel Nappe

The Gurnigel Nappe consists entirely of turbiditic Flysch sediments deposited during Maastrichtian and Eocene in an abyssal to bathyal environment of the Piemont ocean (Van Stuijvenberg 1979). Its internal structure shows metric folds probably formed during the turbiditic transport (slumps) before lithification.

Originally, the Gurnigel nappe is associated with the lowermost unit of the Nappe Supérieure (Caron, 1972, 1976; Lemoine, 1984; Van Stuijvenberg 1979; Winkler, 1984), which thrust to the north in an early stage of nappe transport and remains as a digitation at the northern alpine front, on top of the Subalpine Molasse. Subsequently, in late deformational stage the Gurnigel nappe was thrust by the Préalpes Médianes and the Ultrahelvetics during Middle-Late Oligocene.

The general structural style of the Gurnigel nappe is characterised by several imbricated thrust sheets and duplexes with a lateral extension of several kilometres (De Kaenel et al., 1989). This deformational phase is associated with a subduction/accretion regime during an early stage of orogeny (Paleocene - Lutetian) (Weidmann, 2005).

Towards the contact with the Préalpes Médianes in the south, the internal slice of the Gurnigel nappe is overturned, which may be a consequence of a late reactivation of a thrust plane forming an “out of sequence thrust” bringing the Préalpes Médianes over the internal part of the Gurnigel nappe. (De Kaenel et al., 1989).

1.1.3 Subalpine Molasse

As a part of the Molasse basin, the Subalpine Molasse spreads along the northern boundary of the former northern Alpine front and forms a narrow deformed zone. It is characterised by a succession of isoclinal imbricates dipping towards SE and whose thrust planes can sometimes be followed over long distance. The thrust stack exposes Lower Marine Molasse (Rupelian), but mainly Lower Freshwater Molasse (Chattian) sediments (Homewood et al., 1986). In the eastern and central part of the Subalpine Molasse, backthrusts are common, forming characteristic triangular structures with a basal blind thrust and a subsurface stacking (Berge and Veal, 2005; Müller et al., 1988; Vollmayr and Wendt, 1987). Locally, these structures were detected in the Western Molasse basin as well (Vollmayr and Wendt, 1987).

The precise timing of faulting and thrusting of the Subalpine Molasse is difficult to determine. The youngest folded sediments within the Molasse basin are latest Middle Miocene (OSM) (Schmid, 1970). Sedimentary records between this time and the Pleistocene glacial and interglacial deposits are missing (Burkhard, 1990), thus precluding the detailed timing.

At several localities, the triangular zone is thrust by newly developed thrust, related to the backstepping of the Alpine deformation front into the Subalpine Molasse (Schlunegger and Mosar, 2010). Apatite fission track analysis carried out by Cederbom (2011) recorded the latest thrusting in the Subalpine Molasse at, or since the major erosion event, during Plio-Pleistocene times.

1.2 Paleotectonics and Structural Evolution

In order to gain a better understanding of the paleostress field in the Préalpes Médianes it is important to bear in mind their structural evolution before, during, and after the nappe emplacement.

1.2.1 Pre-emplacement

The paleotectonic history of the Préalpes Médianes before incorporation of the Briançonnais terrane and nappe emplacement is characterised by the evolution of its sedimentation realm. In a rim basin context, the Préalpes Médianes were located to the N-NW of the Briançonnais upper rift shoulder and north of the passive margin (Mosar et al., 1996; Stampfli and Marthaler, 1990). During the Triassic, intensified extensional fracturing started mainly with NE-SW, but also with a N-S orientation. This led to a main rifting phase of the Alpine Tethys during Liassic times (Baud and Masson, 1975; Borel, 1997). Three major paleofaults (Borel and Mosar, 2000), are controlling the paleogeography and result in important thickness variations in sedimentation (Borel, 1997). In Lower and Middle Jurassic, on-going extension caused an overall regional tilting of the sedimentary basin of the Préalpes Médianes with subsidence in the northern and emersion in the southern part leading to

erosion and karstification (Baud and Septfontaine, 1980; Mettraux and Mosar, 1989) and a probable outcropping of the basement in the S (Sartori, 1987). From Middle Jurassic to Lower Cretaceous thermal subsidence took place, but is interrupted by a compressional phase that triggered the inversion of paleofaults and provoked the erosion of the Mytilus formation (Middle Jurassic) (Baud and Septfontaine, 1980; Borel, 1995; Septfontaine, 1995). The period of Upper Cretaceous - Eocene is characterised by phases of sediment starvation and emersion related to the uncoupling of the Briançonnais terrane from the Iberian plate and to flexural uplift caused by the incorporation into the accretionary wedge (Borel, 1995).

1.2.2 Syn-emplacement

The evolution of the tectonic nappes is important for comprehension of the present positions of the different units. A chronological overview of the nappe emplacement starts with:

- An initial segmentation of the Nappe Supérieure, which was originally located in the Piemont ocean domain, and its subsequent incorporation into the accretionary prism started in the Santonian (83 Ma) (Wicht, 1984)/ Maastrichtian (70 Ma) (Caron, 1972; Caron et al., 1980a; Stampfli and Marthaler, 1990).

- In an early stage of nappe transport, the Nappe Supérieure together with its external digitation, the Gurnigel nappe, thrust the Breccia and the Préalpes Médianes Nappe (42 Ma).

- The Breccia Nappe loaded with the Nappe Supérieure then moved onto the Préalpes Médianes while the frontal part of the Nappe was still advancing (40-41 Ma). Probably, the Breccia nappe was moving in a different direction to the Préalpes Médianes underneath (to see at local scale in the Diemtigtal (Mosar, 1988a)).

- Subsequently, the thrusting of the Breccia nappe stopped, while the backmost part of the Préalpes Médianes Rigides detached from its substratum and thrust backwards during a movement over ramps.

- Then the Gastlosen thrust slice developed, inducing a refolding of the Nappe Supérieure. From the internal towards the external part of the Préalpes Médianes Plastiques, several fault-related folds developed (40-39 Ma) (1991).

- The Préalpes Médianes were transported passively over the crystalline massifs on top of the Helvetic nappes from the Priabonian (39Ma) to the Burdigalian (± 18Ma), until today.

1.2.3 Post-emplacement

The arrival of the préalpine nappes onto the Alpine foreland announced by the erosion and deposition of the Mont Pélérin conglomerates (around the Chattian (30Ma) originating from the Nappe Supérieure (Lateltin, 1988; Trümpy and Bersier, 1954). This period is characterised by a final phase of thrusting, affecting the entire préalpine nappe stack. Uplift rates, earthquakes and out-of-sequence thrusts witness an on-going deformation of the alpine wedge trying to readjust its instability by an interplay of erosion and the development of crustal imbricates (Bonnet, 2007; Mosar, 1999). Within the Préalpes Médianes, preferentially along already existing weakness zones, such as inherited normal faults or nappe contacts, out-of sequence faults are located cutting through the whole préalpine nappe pile as well as the underlying Ultrahelvetics (Jeanbourquin et al., 1992; Mosar, 1999). The out-of-sequence thrusts, but also the structural relief in the western Préalpes Romandes and eastern Chablais Préalpes can probably be related to a possible inversion of a Permo-Carboniferous graben (Burkhard and Sommaruga, 1998; Sommaruga, 1997, 1999) due to the development of a new thrust in the European basement below the frontal Préalpes klippen belt (Mosar, 1999; Mosar et al., 1996).

Additionally, during a final deformation event an ubiquitous strike-slip fracture pattern develops throughout the Préalpes Médianes, reactivating already existing faults or creating new small-scale fractures with a significant N-S orientation for sinistral and WNW-ESE orientation for dextral strike-slip faults.

	Time	Event	Structural elements	Examples
Pre-emplacement	Triassic until Upper Jurassic/ Lower Cretaceous, but primarily Lower Jurassic	Extension leading to the formation of the Tethys Ocean	Paleofaults, pre-structuring of the sedimentation realm leading to sediment thickness variations	Château d'Oche-Corbeyrier, Bordière, and Rianda-Stockhorn paleofault
Syn-emplacement	Eocene (Bartonian) until Oligocene (Chattian)	Alpine collision provoking the detachment of the préalpine nappes and their transport towards NW	Fault-related folds; mainly fault-propagation folds verging towards NW, but also some hinterland verging backthrusts	most of the folds in the Préalpes Médianes, e.g. Dent de Broc area (foreland-verging thrust), Maischüpfen fault (hinterland verging thrust)
			Imbrication; arrival on top of the Ultrahelvetic/ Helvetic in the Late Eocene/ Lower Oligocene provoked an upright position of the Gastlosen and Heiti imbricates	Gastlosen and Heiti imbricates
			Fold related normal faults; the non-cylindrical bending of the préalpine folds results in extension parallel and perpendicular to the fold axis	normal faults perpendicular to the fold axis: Dent de Broc normal faults parallel to the fold axis: e.g. Rocher des Rayes
Post-emplacement	Chattian until present-day	Readjustment of wedge instabilities after the arrival on the Alpine foreland and resetting of a new stress system	Out-of-sequence thrusts cutting through the préalpine nappe pile and probably also through the Subalpine Molasse below; presumably they are linked to the development of crustal imbricates. Basement involvement.	Reactivation of important paleofaults as the Rianda-Stockhorn faults; e.g. the Schopfenspitz thrust.
			Predominant N-S oriented sinistral and NW-SE oriented dextral strike-slip faults acting together as conjugated shear zones and clearly offsetting the previously developed folding structure	Predominating fault-slip movement throughout the Préalpes Médianes, e.g. Schafarnisch - Weissenburg strike-slip zone

Tab. 3.1: Overview of the structural elements acquired throughout the deformational history of the préalpine klippen.

1.2.4 Structural elements

Most of the structures were acquired during the folding and thrusting, but they were often guided by the influence of synsedimentary structures or reactivated in a later stage after the nappe emplacement. A brief overview of the characteristic structures determined in the field and on maps or digital terrain models is presented with the following table (Tab. 3.1).

2 Data

Brittle deformation is mainly expressed by the formation of faults and fractures and can be quantified using kinematic analysis methods. Measurements of meso-scale faults and their related slip indicators allow the reconstruction of their kinematic history. For that reason, a large number of fractures with corresponding fault-slip indicators was measured. However, an analysis purely based on the arrangement of fractures and their movement of slip allows the determination of the directions of the principle stress axes, but it aquires an interpretation respecting the structural context of an area. For that reason, not only faults and fractures were measured, but also many bedding measurements, as well as extension veins, shear bands and stylolites to gain a better understanding of the results of the stress and kinematic analyses.

Faults and Fractures

In total, 1388 meso-scale fault orientations and their corresponding slip indicators - mainly slickenfibres - were collected at 51 locations of different lithologies distributed over the entire investigation area. In the Préalpes Médianes Nappe, the Gurnigel Nappe, as well as in the Subalpine Molasse, the slickenfibres consist mainly of calcite, which precipitated as elongated fibres during the fault movement showing a typical stepped appearance.

Since the local structural context changes rapidly, measurement sites were defined in a rather restrictive way. Their extent does not exceed more than a hundred meters of diameter and lie within a known structural context. Furthermore, attention was paid not to overestimate a dominant fault direction due to outcrop condi-

tions and to take into account all possible fault orientations to obtain fault planes as various as possible.

Best outcrops were found in quarries (as in the Tzintre or Tatüre quarry) where recently exposed insights into the complex interaction of the different fault systems are given. Otherwise, fresh outcrops were preferably found along streets and mountain paths; elsewhere fault surfaces were mostly weathered with scarce fault slip indicators. At each locality a general number of 20 - 40 fault striae data was collected, but during data processing the final data amount decreased.

Overprinting relationships of fault-striations and directly opposed slip directions indicate that most of the observed fault sets were influenced by several stress regimes corresponding to different tectonic events and are therefore referred as being heterogeneous with homogeneous subsystems. Overprinting and crosscutting slickenfibres, as well as vein orientations can help attribute a chronology to the observed subsets.

The quality of measurements was taken into account as far as they differ significantly from the average measurement quality.

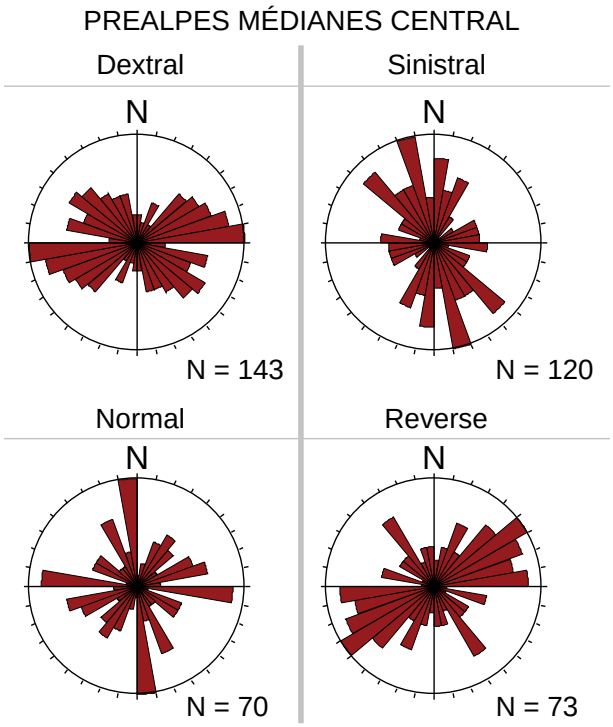

Fig. 3.3: Rose diagrams expressing the directions of the fault planes in the Préalpes Médianes Central region (see map in Fig. 3.5), separated into four groups depending on their movement direction. Only faults with known slip direction are considered, the data amount (N = x) is therefore smaller than in the rose diagram representing all faults of this region (see: Fig. 3.5.).

In Fig. 3.4, six rose diagrams outline the orientation of the measured fault planes respecting their regional distribution, and are therefore roughly subdivided into six zones: the Préalpes Médianes NE, Central, SW, as well as the Subalpine Molasse, the Gurnigel Nappe and the Ultrahelvetics. The general trend of the fault planes shows a predominant NNW-SSE (N160-180°), except in the Ultrahelvetic where a WNW-ESE direction prevails. The rose diagram of the Préalpes Médianes in the NW and SE expose a similar fault distribution, whereas in the Préalpes Médianes Central, between Charmey and Schwarzsee the orientations of the fault planes is less pronounced, showing a wide-ranging distribution. In fact, the Préalpes Médianes Central rose diagram consists of several components (see Fig. 3.3), with the dominant NE-SW / ENE-WSW direction corresponding to reverse, and dextral faults.

A clear dominance of strike-slip faults prevails; both dextral and sinistral fault planes are evenly represented (812 fault planes). Faults with a NW-SE (N120-140°) are dextral faults, whereas these with a N-S (N160-190°) strike are sinistral. Reverse faults trend mainly in NE-SW direction a (N40-60°) and coincide with the NE-SW striking fold orientation. Except the major fault direction, trending NNW-SSE (N160-180°), the other secondary orientations are less constrained, but nevertheless, they show two secondary orientations, one in NE-SW (N20-60°) and the other in NW-SE (N110-120°) direction, which are either parallel or perpendicular to the fold axis.

Folds

Measurements of the orientation and the dipping of the strata were consistently compiled within different lithology throughout the entire investigation area. The poles to bedding projections illustrated in Fig. 3.4, indicate a general NE-SW oriented folding trend in the Préalpes Médianes and the Gurnigel Nappe. The Subalpine Molasse and the Ultrahelvetics however, show a ENE-WSW folding trend. A more detailed observation of the fold axes demonstrates a mutual plunging of the fold axes related to a fading influence of thrust plane lying underneath the folds.

Veins and Stylolites

In the Préalpes Médianes, veins often show a chaotic arrangement. For that reason they were only taken into account when showing certain regularity and exposing a chronology by intersecting each other. The presented stereographic plots in Fig. 3.4 are obviously depending on the bedding orientation, but generally, the extension veins show a dominating NW-SE direction.

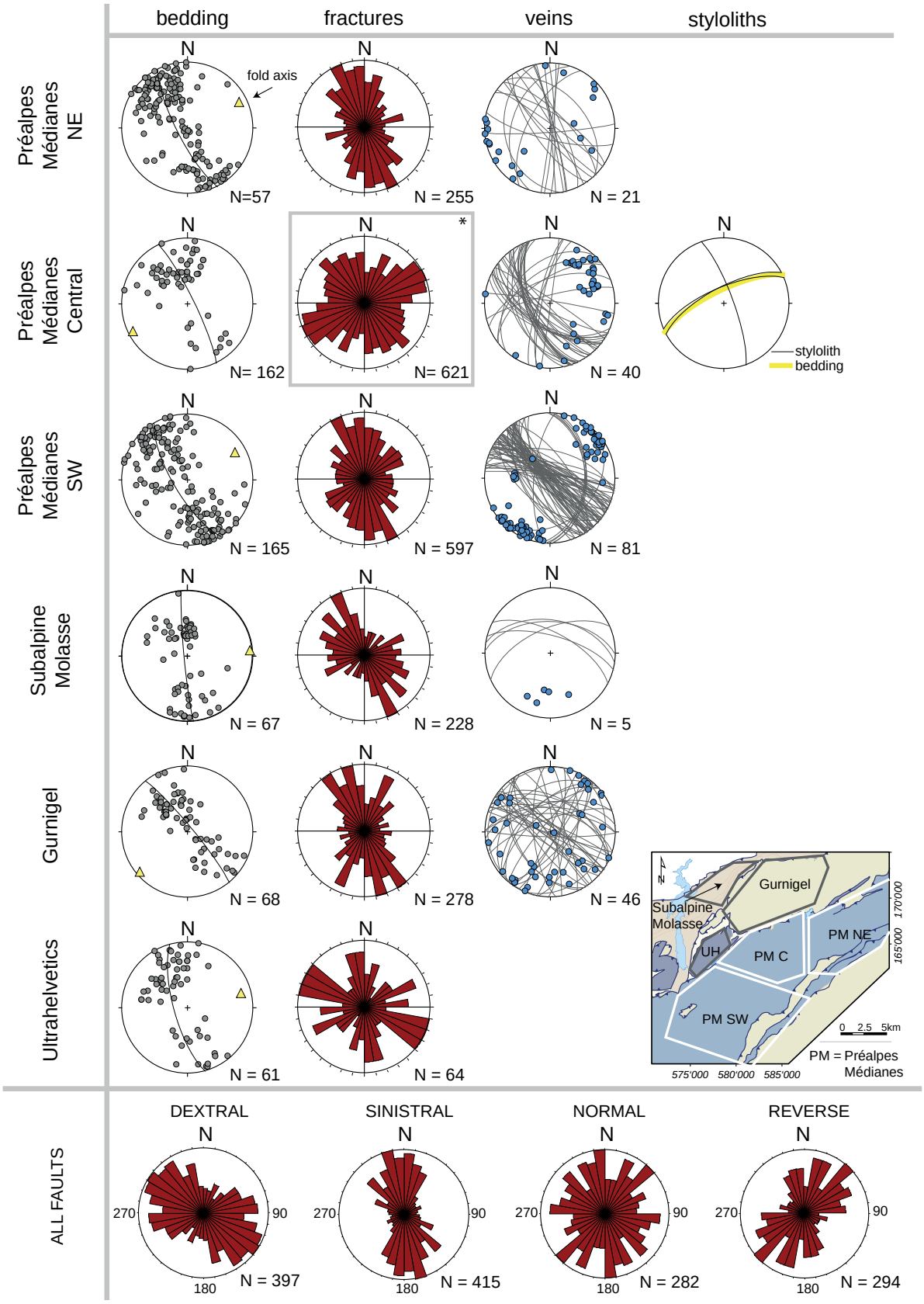

Fig. 3.4: Above: overview over the collected data in the investigation area, which is subdivided into six regional sectors. The bedding measurements are represented with a stereographic pole to bedding projection on the lower hemisphere (equal area projection). All measured faults and fractures are plotted as rose diagrams revealing the major fault direction. The orientation of rose diagram of the fractures of the Préalpes Médianes Central (*) is explained with more detail in Fig. 2.4. Vein and stylolite measurements are indicated by Great Circles and their corresponding poles. Below: subdivision of all fault-slip data in terms of their sense of slip.

Like the veins, intersecting stylolites help to unravel the chronology of different deformational phases. Stylolites occur ubiquitously, but only at one outcrop at the Brésil quarry, could a clear succession of deformational events be defined.

3 Method of Investigation

Processing of the collected fault-slip data aims to reconstruct the paleostress of the different measurement sites. Several different methods were developed for calculating the paleostress tensor: the direct inversion method (Angelier, 1979), the numerical dynamical analysis (Spang, 1972), the analysis of the pressure and tension axes the P-T-method) (Marrett and Allmendinger, 1990) and the right dihedra method (Angelier and Mechler, 1977). The stress tensor calculations were realised in a first step by the TectonicsFP program (Reiter and Acs, 1996 - 2002) to gain an overview of the measured fault-slip data and their stress axes (and to recognise if different stress regimes are prevailing (see appendices). In a second step, with the WinTensor computer program (Delvaux, 2006) a more detailed analysis of the fault-slip data led to the subdivision into several subsets, whose stress tensors are calculated independently. Additionally, the WinTensor program allowed the calculation of the stress ratio R ($R = (\sigma_2 - \sigma_3)/(\sigma_1 - \sigma_3)$), plus a validation of the quality of the obtained stress tensor.

3.1 Paleostress Analysis

One of the aims of this study is to relate the observed structures to the causative tectonic forces, responsible for the formation of the structures. Based on slickensides bearing fault planes, the paleostress state of a defined area can be characterised by three principal stress axes ($\sigma_{1 \geq} \sigma_{2 \geq} \sigma_{3)}$. Modern methods for determining paleostress axes are based on the Wallace-Bott hypothesis (Bott, 1959; Wallace, 1951), stating that the shear traction applied on a given fault plane causes a slip in the direction and orientation of that shear traction, irrespective of the faults created in an

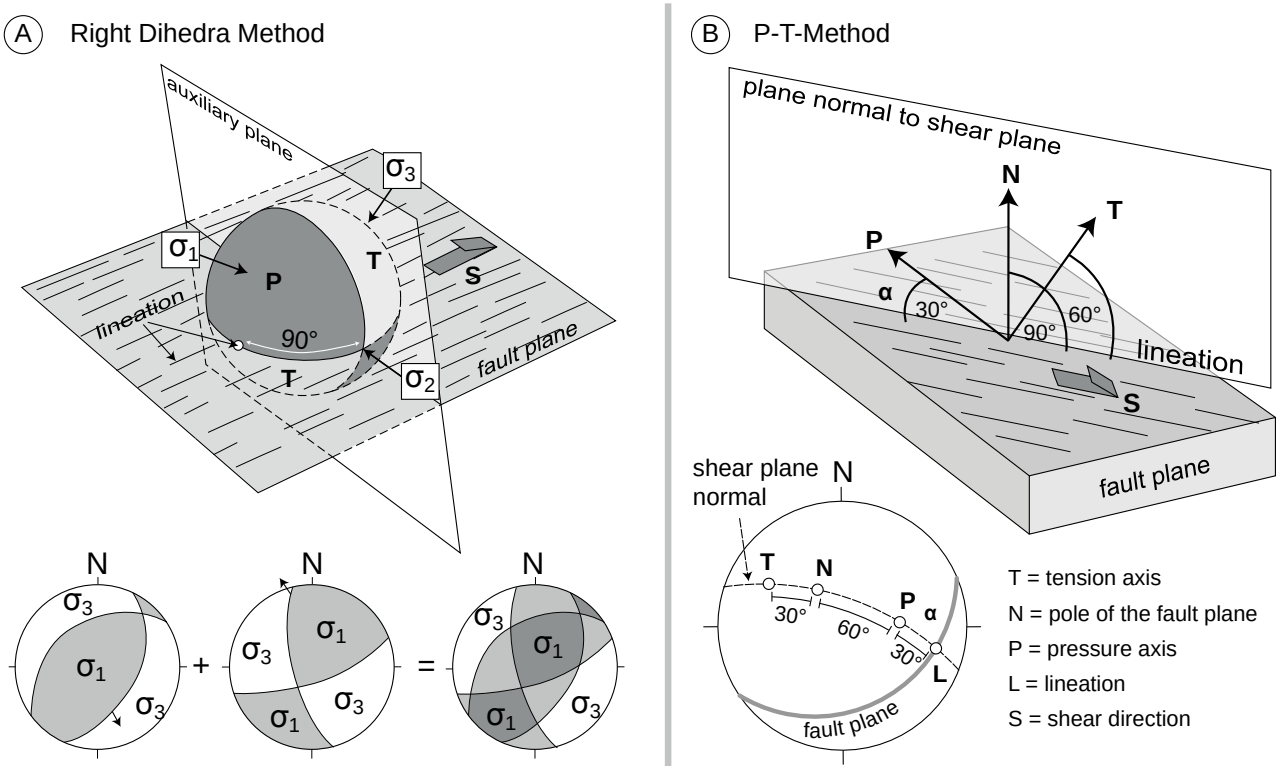

Fig. 3.5: A) Stereographic representation of the right dihedra method. The fault plane and its auxiliary plane delimit two compressional dihedra P (grey) and two extensional dihedra T (white). S indicates the direction of shear (modified after LISLE and LEYSHON, 2004). The three right dihedra plots below show, how the superposition of different right dihedra plots more and more restricts the probable orientation of the stress axes. B) P-T method represented by a block-diagram and a stereographic projection. The P- and the T-axis are situated on an auxiliary plane constructed by the intersection of the lineation plane with the fault normal N.

intact rock or along a pre-existing fracture. However, experiments prove (POLLARD et al., 1993) violations of the Wallace-Bott assumption caused by fault interactions with angular discrepancies between shear stress and fault slip direction.This means that the movement on one fault plane accommodates the stress state and causes a change in regional stress orientation in the vicinity of that fault, so influences the movement on another fault.

Within this study, the right dihedra method (ANGELIER and MECHLER, 1977) and the P-T method - both based on the geometric relationship of fault planes and lineation - were applied to calculate the paleostress axes. In the following subchapters, the different approaches of the two methods as well as the relationship between the different stress axes are discussed.

3.1.1 Right dihedra method

In between each fault plane and its perpendicular oriented auxiliary plane, two compressional, respectively extensional dihedra are determined. The right dihedra method does not provide the exact position of σ_1 and σ_3 of each fault plane. By superimposing the dihedra of every considered fault plane, the zones of possible orientations of the stress axes get more restricted (see Fig. 3.5 A). σ_2 concurs with the intersection line between the fault plane and the auxiliary plane.

The right dihedra method assumes that the different faults were generated under the same stress regime. Furthermore, this method implies a parallel orientation of the slip on a fault plane and the acting shear (RAMSAY and LISLE, 2000)

The accuracy of the results is largely dependent on the variety of the geometrical orientations of the fault-slip data: the more diversified the fault-slip orientations, the tighter constrained the stress axes will be.

3.1.2 P-T-method

The P-T method calculates, for every fault plane, a compressional (P-axis) and an extensional axis (T-axis), which are both lying in the plane given by the shear plane normal and the slip line. Respecting the perpen-dicular orientation of the three axes, the intermediate stress axis (B-axis) lies within the fault plane, perpen-dicular to the slip direction (the lineation). The angle α between the P-axis and the fault plane depends on the angle of friction (ϕ) of the rock material ($\alpha = 45° - \phi/2$). Experimental values for α for newly formed fault planes cluster around 30° (Fig. 3.6). The compressional axis P, inclined 30° on average to the fault plane, as well as the extensional axis T inclined 60° are plotted along the great circle of the plane normal to the shear plane in lineation direction (Fig. 3.6 B) bottom).

The P-T method assumes a homogeneous rock mass, newly formed faults, and that the P- and T-axes are lying in the movement plane, which is rarely achieved in nature. The interest in this method lies in its clear representation of the individual results for every fault plane allowing the detection of a heterogeneous dataset. This further leads to a simplification of the data separation process.

3.1.3 Stress ratio R, stress regime and stress index R'

The relationship between the three stress directions σ_1, σ_2 and σ_3 is represented by the stress ellipsoid and can be described by the stress ratio R ranging from 0 to 1 (ANGELIER, 1994).

$$R = (\sigma_2 - \sigma_3)/(\sigma_1 - \sigma_3)$$

Uniaxial compression ($\sigma_2 = \sigma_3$) with a R ratio = 0 and uniaxial extension ($\sigma_1 = \sigma_2$) with a R ratio = 1 are relatively rare, normally the R ratio lies in between 0.2 and 0.8 (see Tab. 3.2).

The stress ellipsoid graphically displays the relationship between the three principal stress axes for three different cases (Fig. 3.6). The shape of the stress ellipsoid is mainly defined by the intermediate stress axis σ_2, relative to the extreme stress axis σ_1 and σ_3. The uniaxial compressional stress ellipsoid is represented by a cigar-shaped ellipsoid around the σ_1 axis, whereas in the case of an uniaxial extensional stress, the ellipsoid is pie-shaped.

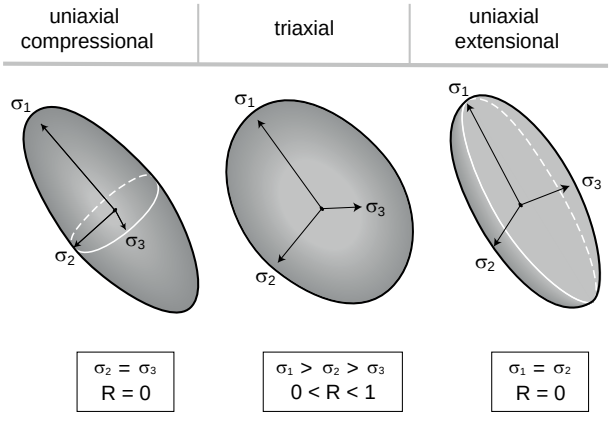

Fig. 3.6: three stress ellipsoids representing graphically the ratio between the three principle stress axes. The uniaxial compressional and the uniaxial extensional stress ellipsoids express the rare case where two stress axes are equal and form therefore either a cigar- or a pie-shaped stress ellipsoid (modified after ANGELIER, 1994)

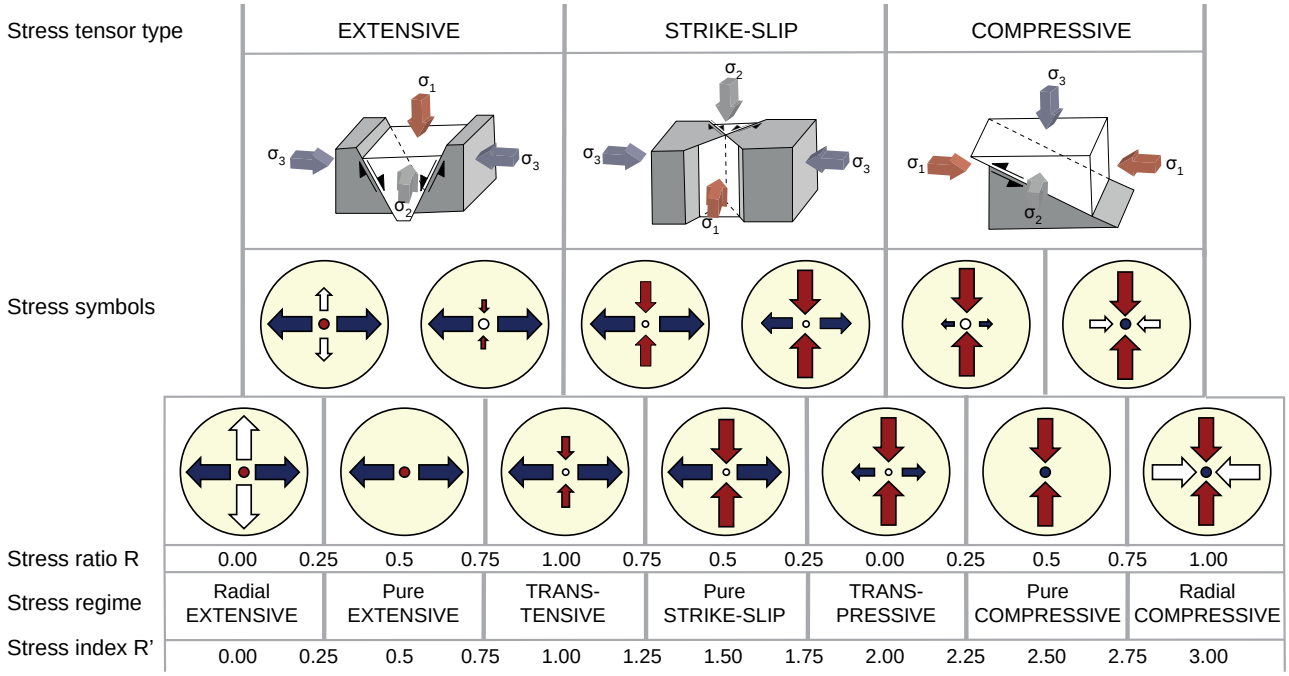

Fig. 3.7: Illustration showing the different stress regimes defined by stress index R' composed of stress ratio R and the orientation of the principle axes of the stress ellipsoid. Their length and colour symbolise the horizontal deviatoric stress magnitude (blue outward arrows: extensional deviatoric stress; red inward arrows: compressional deviatoric stress; white arrow: intermediate deviatoric stress) (DELVAUX et al., 1997).

Generally, the main stress regimes are a function of the shape of the stress ellipsoid and the nature of the vertical stress axis:

σ_1 = vertical → extensional stress regime
σ_2 = vertical → strike-slip stress regime
σ_3 = vertical → compressional stress regime

For a stress ratio R close to 0.5, the stress regimes are stated as "pure" extensional/ strike-slip/ compressional. Fig. 3.7 confronts the stress ratio R with the different types of stress regimes and reveals repeated R values for different stress regimes, for example an extensional stress regime with R = 1 is equivalent to a strike-slip stress regime with R=1. For reasons of simplification, Delvaux et al. (1997) defined a stress regime index R' to gain a better representation of the range of the different stress regimes. R' expresses numerically the stress regime in the following way (Fig. 3.7) (DELVAUX and SPERNER, 2003):

R' = R when σ_1 is vertical (extension regime)
R' = 2 - R when σ_2 is vertical (strike-slip regime)
R' = 2 + R when σ_3 is vertical (compressional regime).

3.2 PROGRAMS

Paleostress analysis were realised by the use of the TectonicsFP (REITER and ACS, 1996 - 2002) and the WinTensor (DELVAUX, 2006) software. Both tools have several advantages and disadvantages and were therefore applied complementary. Additionally the application of two nearly similar tools allowed a cross-check of the results, reducing the risk of manipulation errors.

3.2.1 TectonicsFP

With TectonicsFP, a first overview of the entire data set can be easily obtained. For every measured location the Angelier plot - representing the orientation of the fault plane and its corresponding slip direction, the P-T plot and the Right dihedra plot were calculated with the unseparated data set (see appendices). The P-T plot illustrates the p-, b-, and t-axes for every fault plane and allows therefore a first detection of different deformational events. This first evaluation of the data demonstrates the need for a separation of nearly every data set. The TectonicsFP program offers a manual data separation application, which is useful for an early subdivision of the data set. For complex data sets, the more sophisticated data separation method of the WinTensor program was favoured.

An advantage TectonicsFP is the simplicity to create a data file and to export the data plots as digitised

graphics. For this reason, most of the stereographic projections (great circles, Pi-plots, rose diagrams) were generated in TectonicsFP.

3.2.2 WinTensor

The WinTensor program proved to be very efficient when processing heterogeneous datasets. The preliminary data evaluation by TectonicsFP demonstrated that most of the measured fault-slip data belong to different deformation events. The data separation of WinTensor takes into account a larger spectrum of faults acting within the same stress regime, than subsets created by purely visual criterion, which are mostly focussed on the detection of conjugated fault sets.

Other advantages of the WinTensor program are the calculation of the stress ratio R and the quality ranking of the obtained stress tensors. In the subsequent subchapters, the data separation method and the calculation of the tensor, as well as the quality ranking realised by the WinTensor program are discussed more precisely.

Improved Right Dihedra method and Data separation

An improved version of the Right Dihedra method - originally developed by Angélier et Mechler (1977) - determines not only the paleostress tensor ($\sigma_1>\sigma_2>\sigma_3$), but also its stress ratio R (Delvaux and Sperner, 2003). Additionally this method allows a first filtering of compatible fault-slip data and excludes misfitting fault-slip data completely or attributes them to another subset. For an appropriate constraint on a stress tensor, data subsets should be composed of more than two families of data. Therefore, the larger amount of families of different type and orientation, the better constrained the stress tensor in a data subset (Delvaux and Sperner, 2003).

It is an advantage of the WinTensor program that the data separation is not completely automatic, but rather a stepwise approach to define the ideal subsets. During this process, an interaction by the user is helping to control every parameter. In the WinTensor program by applying the improved Right Dihedra method, preliminary tensors are obtained, which serve as starting point in the following subsequent rotational optimisation procedure (Delvaux and Barth, 2010).

Sub-quality	Number of data	Percentage of data	Confidence number (slip-sense determ.)	Fluctuation [°] (average misfit)	Data type
A	≥25	≥60	≥0.70	≤9	≥0.9
B	≥15	≥45	≥0.55	≤12	≥0.75
C	≥10	≥30	≥0.40	≤15	≥0.5
D	≥6	≥15	≥0.25	≤18	≥0.25
E	<6	<15	<0.25	>18	<0.25

Tab. 3.1: Quality ranking scheme for fault-slip data (SPERNER et al., 2003)

Rotational optimisation

An optimisation of the resulting tensor is realised by

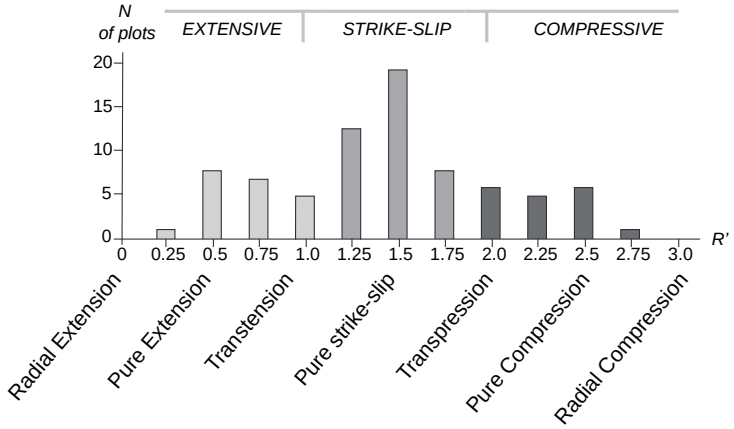

Stress regime	R'	N of plots	N of faults
pure extension:	(0.25< R' >0.74)	13	109
transtension:	(0.75< R' >1.24)	12	102
pure strike-slip:	(1.25< R' >1.74)	32	349
transpression:	(1.75< R' >2.24)	15	106
pure compression:	(2.25< R' >2.74)	8	97

Fig. 3.8: Overview of the calculated stress regimes in the investigation area based on R', showing an accumulation around R' = 1.5, which corresponds to a pure strike-slip stress regime. Extensional and compressional stress regimes also exist, but occur less frequently. The table expresses the number of plots representing a stress regime, as well as the amount of faults corresponding to this stress regime.

a progressive rotation of the tested tensors around each of its axes to minimise the misfitting angle α between the observed and resolved slip vectors on the plane, and by testing different values of R. Additionally, the resolved shear stress magnitude is maximised, whereas the resolved normal stress magnitude is minimised in order to favour slip on the plane (Delvaux and Barth, 2010). During this process, the tensor is getting more restricted and obtains its stabilised final value.

The resulting subsets were validated by the comparison with the P-T plots calculated by the TectonicsFP program and additionally verified with geological context of the outcrop site.

Quality ranking

In cooperation with the World Stress Map (WSM) project (Zoback, 1992) a quality ranking scheme was developed, which allows qualifying and comparing the results obtained throughout the data processing. The quality is indicated from A to E (A = best quality and E = worst).

The quality ranking developed by the WSM differs slightly from the one established by the WinTensor program, but they coincide within our data evaluation.

The results from the Préalpes dataset are mostly classified as "C" and "D" in the quality ranking, which indicates a rather low quality. The reason can be found in the restricted amount of data available per locality. Grouping several measurement sites together, the data amount increases but shows mostly a lower quality ranking due to large influences of local structural circumstances. The heterogeneity of the data set proves a complex deformational history of the Préalpes Médianes, but has a negative influence on the quality of the data set. This is because tensors from sites with polyphase fault datasets have, for the same amount of data, generally lower ranks than single-phase sites (Delvaux et al., 1997).

Despite the rather low rating by the WinTensor program, the fault-slip data are of good quality control. The quality ranking also helps comparing different data sets among each other and gives a confidence index for our stress results.

4 Results of Paleostress analysis

The paleostress analysis based on 1388 fault-slip data result in 80 stress tensors corresponding to 51 sites, mainly in the Préalpes Médianes nappe (57 plots), but also in the Gurnigel nappe (10 plots), the Subalpine Molasse (7 plots) and in the Ultrahelvetics (6 plots) (Fig. 3.10/ Tab. 3.2).

Almost every site exposes a heterogeneous data set developed under different stress regimes, which therefore require a subdivision into two, and rarely into three subsets, each one being consistent with one specific stress regime. An overview of the resulting stress regimes reveals a predominant occurrence of strike-slip stress regimes (Fig. 3.9), but also extensional and compressional stress regimes, whereas the former is more common than the latter.

An overview of the resulting stress tensors, separated into the three main stress regimes - the extensional, the compressional and strike-slip stress regimes - is presented in the first part of this subchapter. Subsequently, four key-regions were discussed in more detail to provide an insight into the heterogeneity of the datasets, the interaction of the different stress regimes and the influence of local structures. In the appendices, the results of the paleostress analysis of every outcrop are listed, as well as a short description of the outcrop conditions and a brief interpretation of the results.

4.1 Overview

The obtained stress tensors are projected on the structural map to gain an overview of their spatial distribution in terms of the four prevailing stress regimes. The stress tensors are represented on four different maps, subdivided into an extensional, a compressional, and two strike-slip stress regimes (Fig. 3.12). The latter differ in the orientation of the σ_1 and σ_3, exposing a NW-SE orientation of σ_1 for the strike-slip regime I and a NE-SW orientation for the strike-slip regime II.

The strike-slip I stress regime prevails throughout the Préalpes Médianes nappe, the Gurnigel nappe, Subalpine Molasse, as well as in the Ultrahelvetics. The extensional stress regime is evenly distributed

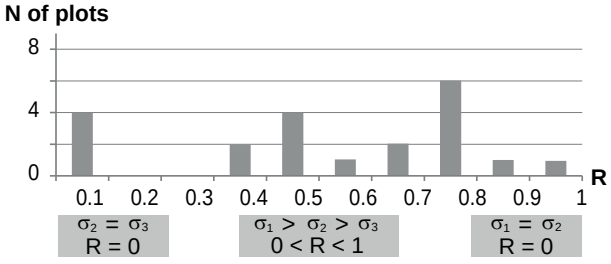

Fig. 3.9: Diagram representing the stress ratio R of all extensional stress regimes. The most of the R-values are ranging from 0.4-0.8 whereas a concentration around 0.8 is visible, representing a relatively strong σ_3 stress axis.

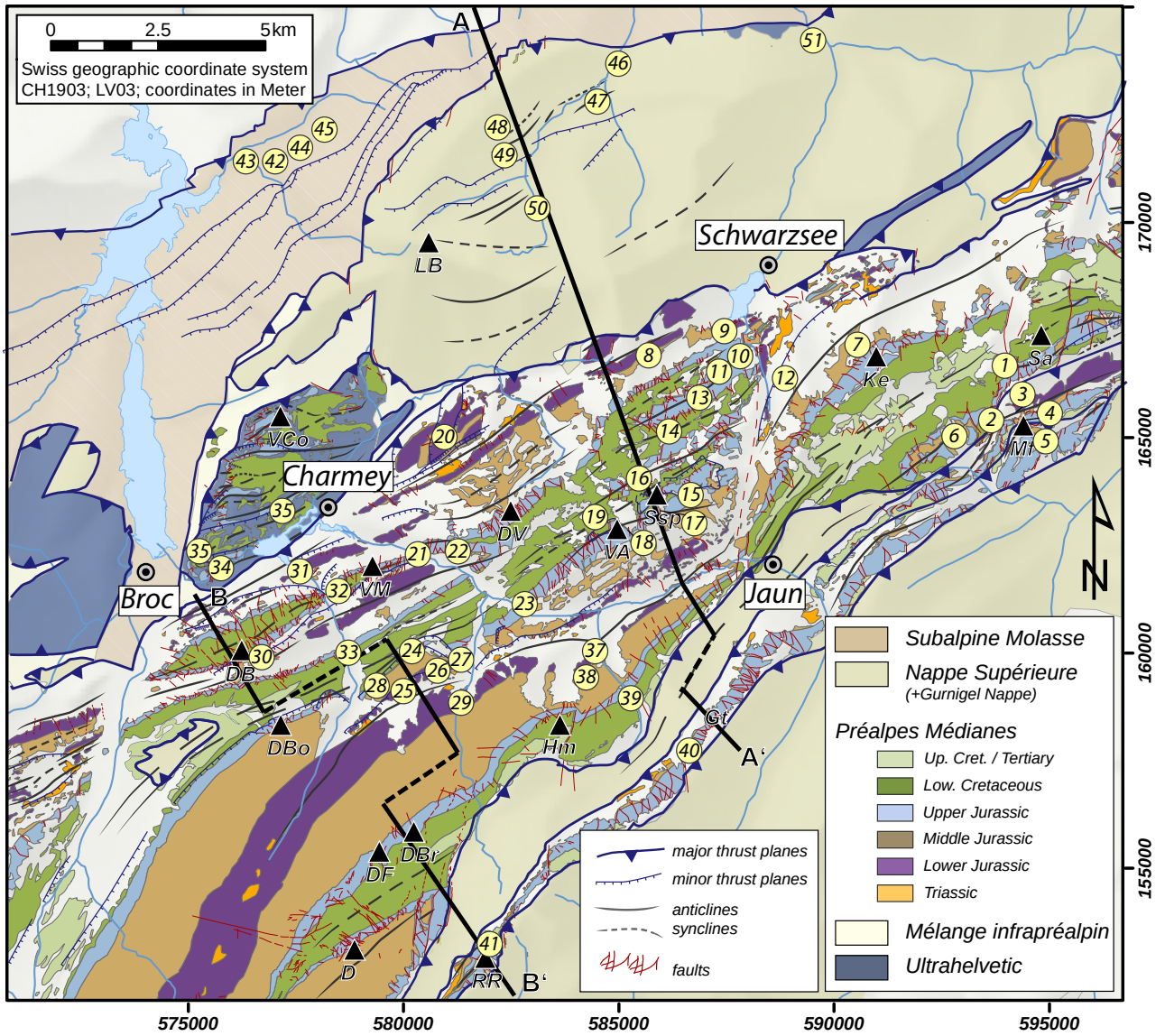

	Site
1	Schafarnisch
2	Trimlegabel
3	Erbetlaub
4	Holzerhorn
5	Mittagsfluh Egg
6	Walop
7	Kaiseregg
8	Unter Recardet
9	Hubel Rippa
10	Welschi Rippa

	Site
11	Underi Rippa
12	Mitzlere
13	Brecca
14	Cerniets Combi
15	Combi Alpligen
16	Schopfenspitz
17	Jansegg
18	Maischüpfen
19	Arpille
20	Arsajoux

	Site
21	Tzintre quarry
22	Les Vanils
23	Brésil quarry
24	Gros Haut Crêt
25	Long Sia
26	Le Contin
27	Rochua dessous
28	La Morarda
29	Rouvenens devant
30	Dent de Broc

	Site
31	Petit Liençon
32	Vanil de la Monse
33	Motélon
34	Gorge de la Jogne
35	Châtel sur Montsalvens
36	Cerniat
37	Petit Mont Weidli
38	Petit Mont Ratzewald
39	Petit Mont Schänis
40	Gastlosen

	Site
41	Rocher des Rayes
42	La Roche sur le Bey
43	Ruisseau du Stoutz
44	Ruisseau du Bey
45	Ruisseau du Hap
46	Fall quarry
47	Tatüre quarry
48	Wüsterbach
49	Paradiesbach
50	Gérine Italienera
51	Zollhaus

mountain tops

D	Dorena
DB	Dent de Broc
DBo	Dent de Bourgo
DBr	Dent de Brenleire
DF	Dent de Folliéran
DV	Dent de Vounetse
Gt	Gastlosen
Hm	Hochmatt
Ke	Kaiseregg
LB	La Berra
Mf	Mittagsfluh
RR	Rocher des Rayes
Sa	Schafarnisch
Ssp	Schopfenspitz
VA	Vanil des Arpilles
VCo	Vanil des Courts
VM	Vanil de la Monse

Fig. 3.10: Localisation of fault-slip measurements collected mainly in the Préalpes Médianes nappe, but also in the nappe Supérieure, the Ultrahelvetics and the Subalpine Molasse. The geological map of the Préalpes Médianes is based on existing geological maps (ANDREY, 1974; BIERI, 1925; BOREL, 1991; BOVET, 1990; GISIGER, 1967; PAGE, 1969; PASQUIER, 2005; PLANCHEREL, 1979; SPICHER, 2005; THALMANN, 1990), but also on fievld observations. To simplify comprehension the Subalpine Molasse and the Nappe Supérieure are represented as structural units without any subdivision. The black lines indicate the line of section of the two cross-sections A-A' and B-B' in Fig. 3.37.

No	Site		X	Y	Z	n	n/nT	σ1az	σ1pl	σ2az	σ2pl	σ3az	σ3pl	R	α	Q	R'	F5	Stress regime
1	Schafarnisch	1	593869	166818	1700	8	0.38	126	8	284	81	35	3	0.73	9.38	D	1.3	4.41	extensional strike-slip
		2				7	0.33	254	07	006	69	161	18	0.41	11.8	D	1.59	6.27	pure strike-slip
2	Trimlegabel	1	593829	165271	1800	6	0.46	134	14	253	63	38	22	0.17	3.55	D	1.8	1.08	compressional strike-slip
3	Erbetlaub		594264	165383	1800	7	0.47	070	73	209	12	302	10	0.84	11.6	D	0.85	11.6	strike-slip extensional
4	Holzerhorn		594337	165264	1810	6	0.55	298	10	50	61	203	25	0.64	4.47	D	1.4	1.98	pure strike-slip
5	Mittagflue Egg		594680	164905	1480	8	0.57	102	18	276	70	12	2	0.75	15.77	D	1.3	15.77	extensional strike-slip
6	Walop	1	592977	164960	1430	13	0.46	324	2	228	69	55	20	0.37	14.12	C	1.6	10.35	pure strike-slip
		2				6	0.21	12	19	177	69	281	4	1.74	7.20	D	1.7	2.33	compressional strike-slip
7	Kaiseregg	1	590482	166485	2010	11	0.34	267	37	42	42	156	24	0.36	11.66	C	0.36	11.66	pure extensional
		2				7	0.22	129	22	274	62	33	14	.14	17.86	D	1.86	11.97	pure compressive
8	Unter Recardet		586708	167540	1200	9	0.82	188	27	43	58	286	15	0.7	8.27	D	1.3	9.01	extensional strike-slip
9	Hubel Rippa		587435	167436	1130	8	0.62	145	8	28	71	238	16	0.4	13.33	D	1.6	6.78	pure strike-slip
10	Welschi Rippa	1	587623	167180	1210	9	0.45	20	45	197	44	288	1	0.78	16.58	D	0.8	16.43	strike-slip extensional
		2				6	0.3	094	17	201	44	349	40	0.18	9.48	D	1.82	9.48	pure compression
11	Underi Rippa		587256	166659	1366	9	0.47	339	38	123	45	234	19	0.74	12.77	D	1.3	7.03	extensional strike-slip
12	Mitzlere	1	578922	166637	1300	10	0.78	163	4	60	71	254	18	0.29	14.11	D	1.2	7.78	extensional strike-slip
		2				12	0.34	298	6	186	73	30	15	0.31	9.12	C	1.7	3.31	compressional strike-slip
13	Brecca	1	587013	165933	1320	9	0.35	174	19	281	39	63	44	0.33	17.43	D	2.3	12.42	pure compressive
		2				7	0.27	52	82	250	6	160	2	0.78	8.64	D	0.8	4.19	strike-slip extensional
14	Cerniets Combi		586095	164996	1490	10	0.6	218	66	43	23	312	1	0.31	12.38	C	0.3	10.40	pure extensive
15	Combi Alpligen		586701	163568	1630	7	0.54	283	13	39	61	186	24	0.01	9.06	D	1.9	4.75	compressional strike-slip
16	Schopfenspitz		585482	163639	2012	7	0.44	104	15	209	42	359	43	0.26	12.61	D	2.3	8.51	pure compressive
17	Jansegg		585973	163252	1750	7	0.58	195	23	311	45	086	34	0.45	13.21	D	1.55	11.21	pure strike-slip
18	Maischüpfen		585325	162630	1750	10	0.5	305	2	35	3	182	86	0.56	9.95	C	2.6	6.37	pure compressive
19	Arpille	1	584504	163378	1750	10	0.37	220	26	48	63	312	3	0.35	12.08	C	1.7	6.06	compressional strike-slip
		2				8	0.3	315	21	108	65	221	9	0.51	8.86	D	1.5	4.35	pure strike-slip
20	Arsajoux	1	580878	164714	1350	13	0.62	141	45	302	42	41	9	0.74	11.98	C	0.7	6.01	pure extensional
		2				6	0.29	64	15	186	63	327	21	0.12	7.47	D	1.9	4.43	compressional strike-slip
21	Carrière Tzintre	1	580552	162203	880	29	0.32	110	7	211	55	15	33	0.6	14.58	C	1.4	8.60	pure strike-slip
		2				17	0.18	328	42	151	47	59	1	0.46	16.85	D	0.4	11.54	pure extensional
22	Les Vanils	1	581072	162311	1030	10	0.56	356	8	177	81	86	0	0.03	15.87	C	2	11.34	compressional strike-slip
		2				6	0.33	120	0	211	46	29	43	0.74	13.10	D	1.3	1.26	extensional strike-slip
23	Carrière Le Brésil	1	582773	161049	900	9	0.27	217	23	110	33	335	47	0.6	9.74	D	2.6	8.34	pure compressive
		2				9	0.27	128	9	257	75	36	11	0.35	12.47	D	1.7	12.47	compressional strike-slip
24	Gros Haut Crêt	1	580084	159863	1560	9	0.45	68	40	197	36	311	29	0.64	14.61	D	0.6	10.54	pure extensional
		2				8	0.4	324	16	110	70	231	10	0.38	15.57	D	1.6	13.45	pure strike-slip
25	Long Sia		579841	158955	1390	9	0.69	21	72	229	15	137	7	0.79	14.83	D	0.8	14.00	strike-slip extensional
26	Le Contin	1	580719	159382	1250	11	0.42	18	63	266	10	171	25	0.7	13.45	C	0.7	6.95	pure extensional
		2				6	0.25	337	26	85	31	216	46	0.38	9.80	D	2.4	9.50	pure compressive
27	Rochua dessous		580988	159747	1140	9	0.56	341	4	245	61	73	28	0.44	13.66	C	1.6	8.68	pure strike-slip
28	La Morarda	1	579453	159034	1300	10	0.43	301	10	200	46	40	42	0.87	14.33	C	1.1	11.40	strike-slip extensional
		2				6	0.26	29	57	211	32	120	1	0.42	7.45	D	0.4	4.42	pure extensional
29	Rouvenens devant	1	581354	158734	1000	7	0.44	138	11	236	32	32	54	0.14	13.11	D	1.6	8.03	pure strike-slip
		2				6	0.38	297	67	67	14	161	16	0.61	15.16	D	0.6	12.07	pure extensional
30	Dent de Broc	1	576280	159734	1710	6	0.28	111	53	344	24	242	24	0.72	5.85	D	0.7	3.19	pure extensional
		2				7	0.28	54	6	313	59	148	30	0.94	6.86	D	1.1	5.91	strike-slip extensional
31	Petit Liençon	1	576339	159797	900	10	0.45	144	18	243	24	021	58	0.19	13.58	C	2.19	13.58	strike-slip compressive
		2				6	0.27	29	27	235	60	125	10	0.47	15.72	D	1.5	1.53	pure strike-slip
32	Vanil d.l. Monse		578190	161175	880	10	0.53	159	39	351	50	254	5	0.95	1.05	C	1.1	1.91	strike-slip extensional
33	Motélon		578783	159983	980	6	0.75	267	63	161	7	68	24	0.5	11.93	D	0.5	0.49	pure extensional
34	Gorge de la Jogne	1	575498	161854	830	11	0.31	330	47	156	42	63	2	0.38	9.96	C	0.4	6.38	pure extensional
		2				9	0.26	185	0	93	68	275	21	0.8	16.18	D	1.2	16.18	strike-slip extensional
35	Chatel sur Montsalvans	1	575418	162067	860	11	0.52	150	10	339	79	241	1	0.7	14.87	C	1.3	10.36	extensional strike-slip
		2				8	0.38	52	3	317	56	144	33	1	8.79	D	1	8.59	strike-slip extensional
36	Cerniat	1	577913	163858	1020	8	0.44	191	27	319	49	86	26	0.91	13.50	D	1.1	8.69	strike-slip extensional
		2				7	0.39	73	60	180	9	275	27	0.43	15.14	D	0.4	13.54	pure extensive
37	Pt. Mont Weidli		584609	160199	950	10	0.45	119	24	16	26	244	53	0.5	11.88	C	2.5	8.23	pure compressive
38	Petit Mont Ratzewald	1	584799	159330	1120	10	0.31	316	12	177	74	049	10	0.03	16.69	D	1.97	10.57	compressional strike-slip
		2				9	0.28	137	61	232	02	323	28	0.27	5.2	D	0.27	5.2	pure extensional
39	Petit Mont Schänis	1	585379	159037	1330	16	0.44	208	21	349	62	112	15	0.62	14.89	C	1.4	10.79	pure strike-slip
		2				8	0.22	106	13	214	53	7	33	0.57	10.51	D	1.4	8.74	pure strike-slip
40	Gastlosen		586810	158120	1820	14	0.67	335	25	104	53	233	24	0.16	11.8	C	1.84	11.8	compressional strike-slip
41	Rocher des Rayes	1	582099	153180	1910	7	0.35	320	9	185	77	52	8	0.18	12.56	D	1.8	9.04	compressional strike-slip
		2				8	0.4	45	23	150	32	286	48	0.16	10.36	D	2.2	5.67	strike-slip compressive

No	Site		X	Y	Z	n	n/nT	σ1az	σ1pl	σ2az	σ2pl	σ3az	σ3pl	R	α	Q	R'	F5	Stress regime
42	La Roche Sur le Bey	1	576900	171215	820	12	0.41	316	33	161	54	54	111	0	11.42	C	2	4.74	compressional strike-slip
		2				7	0.24	324	66	221	12	127	19	0.43	16.00	D	0.4	12.00	pure extensional
43	Ruisseau du Stoutz	1	576727	171140	760	11	0.37	323	12	221	41	66	45	0.19	12.53	C	2.2	8.23	strike-slip compressive
		2				7	0.23	284	39	118	49	20	7	0.31	13.11	D	1.7	6.54	compressional strike-slip
44	Ruisseau du Bey	1	577355	171618	780	10	0.37	319	1	49	1	170	87	0.47	13.90	C	2.5	13.90	pure compressive
		2				8	0.3	125	57	225	6	319	31	0.96	16.49	D	1	13.02	extensional strike-slip
45	Ruisseau du Hap		578246	172364	820	9	0.64	309	8	176	77	40	9	0.6	11.53	D	1.4	5.47	pure strike-slip
46	Carrière Fall	1	585030	173753	880	15	0.48	151	9	259	62	56	25	0.28	14.53	C	1.7	12.27	compressional strike-slip
		2				9	0.29	258	14	17	61	161	23	0.61	16.02	D	1.4	13.79	pure strike-slip
47	Carrière Tatüre	1	584328	172805	1030	23	0.38	301	32	122	57	31	0	0.44	14.23	C	1.6	8.90	pure strike-slip
		2				16	0.26	16	3	117	73	285	16	0.72	16.01	D	1.3	8.74	extensional strike-slip
48	Wüsterbach		582285	171946	1200	9	0.62	148	12	33	61	244	25	0.24	12.99	D	1.8	6.32	compressional strike-slip
49	Paradiesbach		582001	171563	1250	8	0.44	252	23	106	62	348	13	0.51	10.03	D	1.5	7.40	pure strike-slip
50	Gérine Italienera	1	583227	170207	1100	23	0.31	266	23	175	1	81	65	0.55	9.63	C	2.6	4.59	pure compressive
		2				12	0.16	298	16	53	55	198	29	0.74	9.98	D	1.3	5.29	extensional strike-slip
		3				13	0.18	147	0	56	64	237	25	0.1	13.55	D	1.9	7.70	compressional strike-slip
51	Zollhaus		589895	173959	880	7	0.41	112	31	271	56	16	9	0.56	6.26	D	1.4	3.59	pure strike-slip

Tab 3.2: Paleostress tensors obtained at 51 measured sites: No = outcrop number; Site = outcrop locality (name cited in text); X, Y, Z = coordinates based on the Swiss coordinate system; n = number of measurements; n/nT = number of measurements in relation to the total number of fault data measured; σ1,2,3 az = azimuth of the principal stress axes and σ1,2,3 pl = plunge of the principal stress axes.; R = stress ratio (σ2- σ3)/(σ1 - σ3); α = mean slip deviation (°); Q = quality ranking; R' = stress index, highlighted by colour shading: blue = extensional, white = strike-slip and red = compressional; F5 = rotational optimisation (°); stress regime = based on R'.

throughout the investigation area and is not restricted to a limited area, but rather related to regional structures, most probably to the folding and thrusting of the Préalpes Médianes. However, the compressional stress regime appears more limited, especially to the region between Charmey and Schwarzsee.

Detailed consideration of the individual sites allows theattribution of the calculated stress tensors to a specific structural feature lying in direct vicinity; in this way, the preponderance of a specific stress regime over another can be explained by the influence of a more important geological structure close by.

Important synsedimentary structures caused important lateral sedimentary thickness variations, which define zones with a potential liability to failure (Baud and Septfontaine, 1980; Borel and Mosar, 2000; Mettraux and Mosar, 1989). But, how far the observed stress regimes are influenced by the existence of inherited pre-emplacement structures is difficult to access.

An overall relative age relationship between the different fault sets could not be obtained, but considering vein intersections and overprinted slickenfibres several possible kinematic sequences at some restricted localities can be proposed.

4.1.1 Extensional stress regime

Extensional regimes are common throughout the entire Préalpes Médianes (Fig. 3.12A), but frequently they occur subordinate to the predominating strike-slip stress regime. The extensional stress axes are oriented either parallel or perpendicular to the overall fold axes direction. In the study area, the folds are bending from a general trend of SW-NE to the W towards WSW-ENE to the E. Regarding the extensional stress axes similar observations can be made.

In the Gurnigel nappe, however, no clear evidence for an extensional stress regime could be recognised at any measuring site, and in the Subalpine Molasse, only at one locality an extensional stress regime was documented representing most probably a former compressional stress regime that turned into an extensional tress regime due to the tilting of the subalpine thrust slices. Within the Préalpes Médianes, SW of the Jogne valley, extensional stress regimes occur abundantly, whereas in the frontal part in the Dent de Broc area mostly a fold axis parallel extension and in the rear part an extension perpendicular to the fold axis prevail. A possible reason could be the accentuated bending of the general folding trend leading to a stretching of the frontal and a buckling of the back part.

Another reflection may be that the orogen parallel extensional stress axes can be related to the orogen parallel stretching, which is rather ubiquitous throughout the Alps since the last 20Ma (Champagnac et al., 2004; Delacou et al., 2004; Sue and Tricart, 2002). (Delacou et al., 2004; Dietrich, 1989; Ramsay, 1989). This implies an extensional stress regime after the nappe emplacement. It remains uncertain if observed normal faults striking perpendicular to the fold axis developed under the same stress regime or were formed earlier during the nappe emplacement and reactivated after 20Ma.

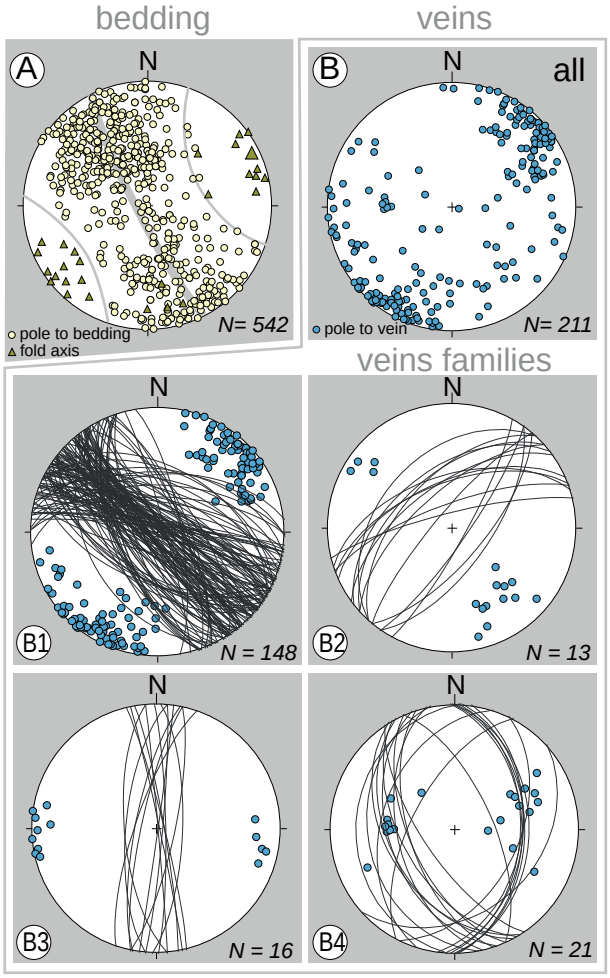

Fig. 3.11: A) showing the pole projection of every bedding measurement. The calculated (large triangle) and measured (small triangles) fold axis clearly reveal a NE-SW oriented folding trend. B) represents the pole projection of every measured vein and is subdivided into four vein families, whereas vein set B1 is clearly overrepresented. B1, B2 B3 and B4 are assumed to be related to the folding of the Préalpes Médianes.

A closer consideration of the stress ratio R reveals a trend towards an oblate stress ellipsoid. R-values are ranging from 0.4 to 0.8 with an accumulation around 0.8, signifying a pronounced extensional stress axis,

Extension veins measured in the entire investigation area display predominant NW-SE orientation (Fig. 3.11B). Their extension direction - supposed to be oriented perpendicular to the vein plane - agrees with the overall NE-SW extension direction parallel to the fold axis trend (see pole projection of the stratigraphy (Fig. 3.11A). The formation of vein family B1 and B2 can clearly be associated to an extension related to the folding. By a majority, the veins of the vein set B2 are crosscut by veins of B1. Nevertheless, as both of them are genetically linked to the folding event, an initial contemporaneous development is assumed, where veins of B1 were probably active for a longer period. The N-S trending veins of family B3 can also be associated to the fold development by considering them as veins evolving diagonally to the fold axis. In that case, it has to be assumed that the extension of the vein does not occur perpendicular to the vein plane, but rather parallel to the fold axis. The vein family B4 consists of two conjugate vein sets and is most probably related to an E-W oriented extension.

4.1.2 Compressional stress regime

Compressional stress regimes were observed in fewer localities than extensional regimes and are more limited to particular zones in vicinity to an important thrusting structure, as in the Schopfenspitz area or near La Roche in the Subalpine Molasse (Fig. 3.12B). Except at one measurement location, the compressional deviatoric stress is oriented in NW-SE direction and fits into the structural environment dominated by NE-SW trending thrust system associated to the inversion of a normal fault. Hidden mostly below anticlines, thrusts generating these folds hardly ever crop out at the surface. This could be an explanation for the lower and often subordinated occurrence of compressional stress regime localities. The observation of the spatial distribution of recorded compressional stress regimes shows a concentration in the central part of the investigation area, in between the Jogne valley and Schwarzsee. More specifically, most of them are distributed within the range of influence of an important out-of-sequence fault, for example, the Schopfenspitz fault being active after the emplacement of the préalpine nappe. Therefore, another reason for the underrepresentation of the compressional stress regime could be that slickensides clearly representing a compressional stress regime associated to the fold-and-thrusting of the Préalpes Médianes are strongly overprinted or non-existent anymore. Probably, only relatively young thrusting activity, such as the out-of-sequence thrusting, is documented by slickensides. This is further supported by the observation that thrusts related to “early” fold-and-thrust development are associated with the formation of shear zones.

4.1.3 Strike-slip stress regime

Strike-slip stress regimes are unambiguously the most represented stress regime throughout the entire study area, in the Préalpes Médianes, the Gurnigel Nappe, as well as in the Subalpine Molasse. Nearly every outcrop location is influenced by a strike-slip stress regime either as dominant or as subordinate stress state. The strike-slip regimes are distinguished based on the orientation of the compressional deviatoric stress trending either NW-SE (strike-slip regime I) or NE-SW (strike-slip regime II), the latter occurring less frequently.

The fault sets associated with the dominant strike-

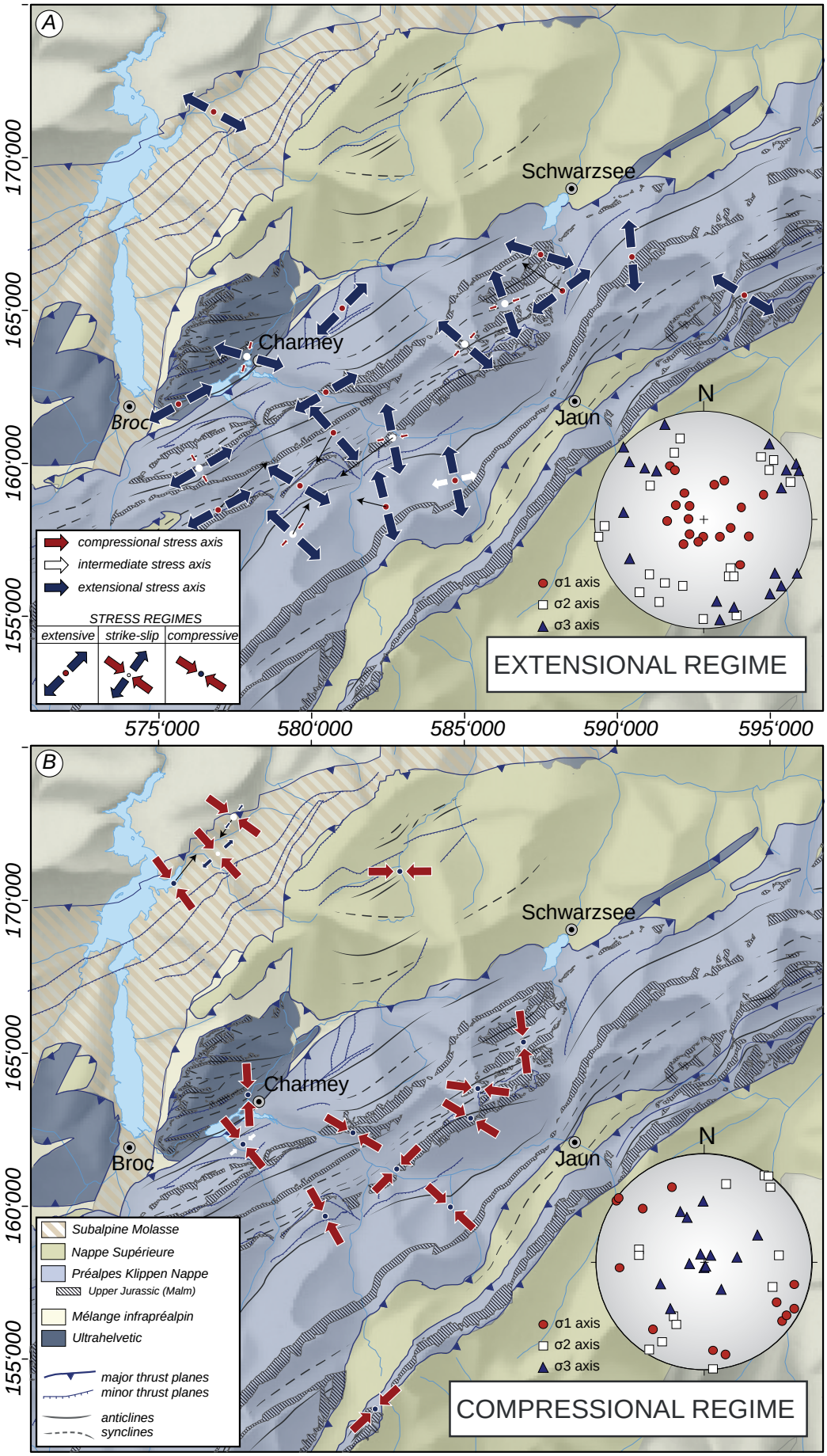
A
Schwarzsee
Charmey
Broc
Jaun
N
compressional stress axis
intermediate stress axis
extensional stress axis
STRESS REGIMES
extensive
strike-slip
compressive
σ1 axis
σ2 axis
σ3 axis
EXTENSIONAL REGIME
170'000
165'000
160'000
155'000
575'000
580'000
585'000
590'000
595'000
B
Schwarzsee
Charmey
Broc
Jaun
N
Subalpine Molasse
Nappe Supérieure
Préalpes Klippen Nappe
Upper Jurassic (Malm)
Mélange infrapréalpin
Ultrahelvetic
major thrust planes
minor thrust planes
anticlines
synclines
σ1 axis
σ2 axis
σ3 axis
COMPRESSIONAL REGIME
170'000
165'000
160'000
155'000

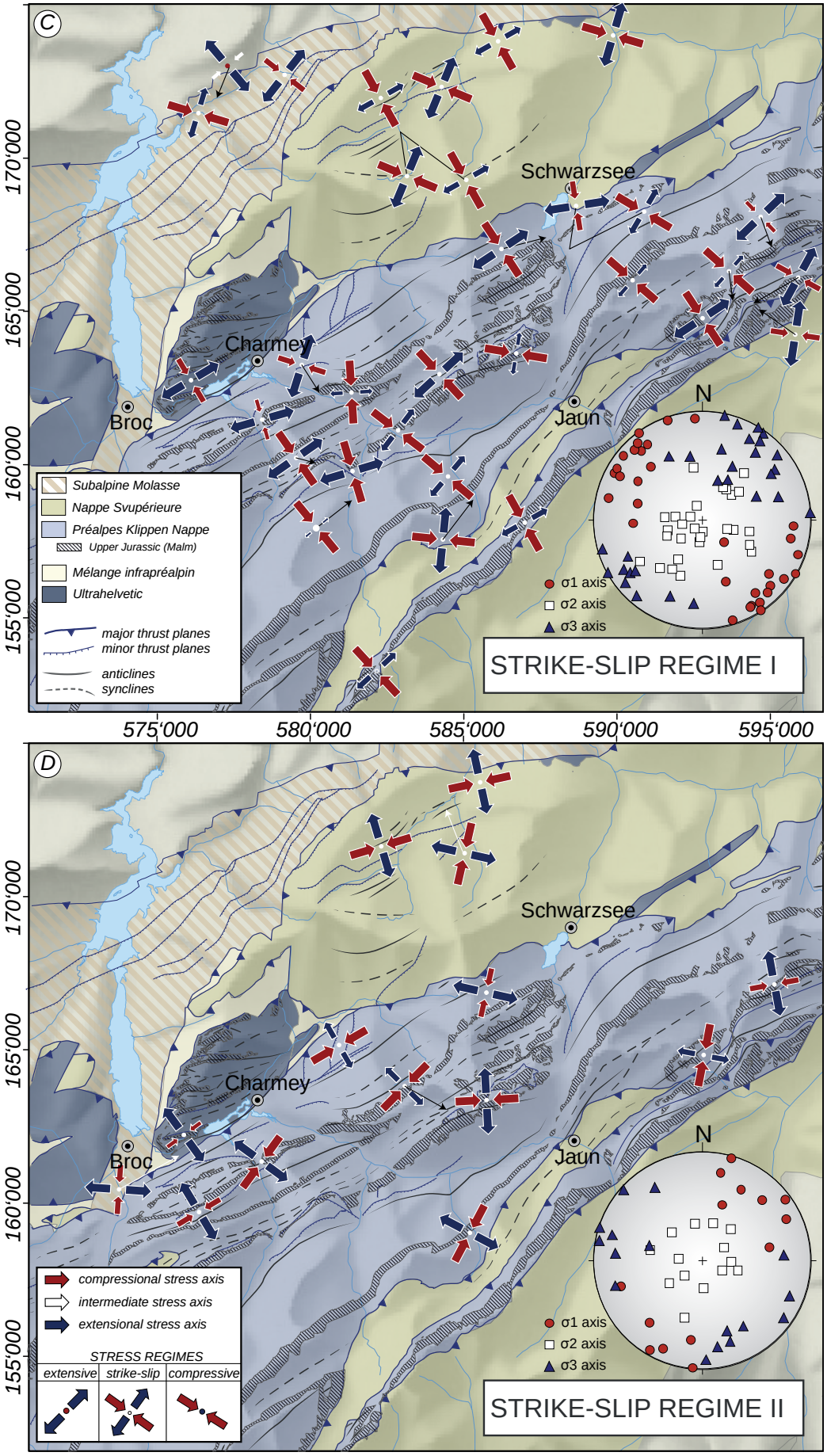
C
Schwarzsee
Charmey
Broc
Jaun
N
Subalpine Molasse
Nappe Svupérieure
Préalpes Klippen Nappe
Upper Jurassic (Malm)
Mélange infrapréalpin
Ultrahelvetic
major thrust planes
minor thrust planes
anticlines
synclines
σ1 axis
σ2 axis
σ3 axis
STRIKE-SLIP REGIME I
170'000
165'000
160'000
155'000
575'000
580'000
585'000
590'000
595'000
D
Schwarzsee
Charmey
Broc
Jaun
N
compressional stress axis
intermediate stress axis
extensional stress axis
STRESS REGIMES
extensive
strike-slip
compressive
σ1 axis
σ2 axis
σ3 axis
STRIKE-SLIP REGIME II
170'000
165'000
160'000
155'000

Fig. 3.12: Structural maps of the study area representing the stress regimes obtained by the analysis of 1388 fault-slip measurements at 51 different locations. Most of the heterogeneous raw data plots were divided into subsets because of different stress regimes. Depending on the stress regime, the resulting stress orientations were plotted on the corresponding map. A) Most extensional stress regimes show a preferred orientation for the extensional stress axis towards NW-SE or NE-SW; either perpendicular or parallel to the fold axes. B) The compressional stress regimes show a NW-SE trending orientation. C/D) The strike-slip regimes were subdivided into two groups depending on the orientation of the compressional stress axes: the majority is oriented in NW-SE direction (strike-slip regime I) and only few compressional stress directions are trending towards NE-SW (strike-slip regime II)

slip direction highlight two different main shear directions: NNE-SSW to NNW-SSE sinistral or WNW-ESE dextral. Nevertheless these fault-slip data correspond generally to rather small, outcrop-scale fault planes being part of broader shear zones. Strike-slip fractures are not only highly abundant, but they are also overprinting slickensides associated with previous deformations. Frequently, normal faults generated by fold axis parallel extension are reactivated with a strike-slip movement. For this reason the strike-slip stress regime are not always fulfilling the ideal conditions of strike-slip faults with nearly vertical fault planes, they are acting mostly on already existing structures.

The secondary strike-slip stress regime with a compressional stress axis oriented NW-SE is most probably related to inversion structures of the former normal faults or to local structural circumstances.

4.2 Detailed Stress Field Examples

In order to give a better insight into the stress field associated with the late and recent tectonics of the Préalpes Médianes and its adjacent units, four areas from different tectonic settings are described in more detail.

Two areas are situated within the Préalpes Médianes nappe, the Tzintre - le Brésil area (1) and the Schafarnisch-Mittagflue area (2), whereas the latter is located at the transition of the Préalpes Médianes Plastiques towards the intermediate zone. The Plasselbschlund area (3) represents the structural features related to the Flysch deposits of the Gurnigel Nappe. The La Roche area (4) is located in the Subalpine Molasse and is therefore not affected by the deformation related to the nappe transport.

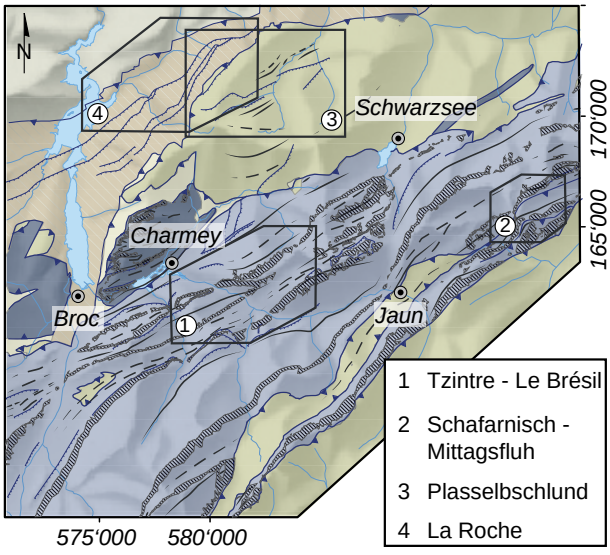

Fig. 3.13: Localisation of the four areas discussed in detail.

4.2.1 The Tzintre - Le Brésil area

Two active quarries between Charmey and Im Fang expose many structural features and fault kinematic indicators that give a better insight in the complexity of the heterogeneous fault sets. The combination of overprinted and curved slickenfibres, the orientation of crosscutting extensional veins and crosscutting stylolites makes it possible to define a relative chronology of different stress states.

In the north-eastern part of the Jaun valley, the Tzintre-Le Brésil area is affected by folds related to backthrust plunging towards NW, whereas the thrusts south of the Jaun valley are dipping in the general SE direction. The folding process provoked the formation of normal faults perpendicular, diagonal, or parallel to the fold axis. Digital elevation models (DEM), geological maps and even the morphologic appearance of the massive Upper Jurassic limestone reveal sets of normal faults striking oblique in conjugate sets to fold axis.

Fault orientation

The first rose diagram Fig. 3.14C represents fault directions compiled from geological maps (Chatton, 1974; Pasquier, 2005; Spicher, 1966), DEMs and orthophotographs. Four major directions stand out:

1) N-S (N170-190°),

2) NNW-SSE (N159-160°)

3) NE-SW (N30-40°) and

4)WNW-ESE (N110-120°).

The dominating fault direction (1) - oriented N-S - segments the mountain ranges consisting of massive Upper Jurassic limestones with generally sinistral offsets, whereas its conjugated counterpart (4) - oriented WNW-ESE - shows a dextral displacement.

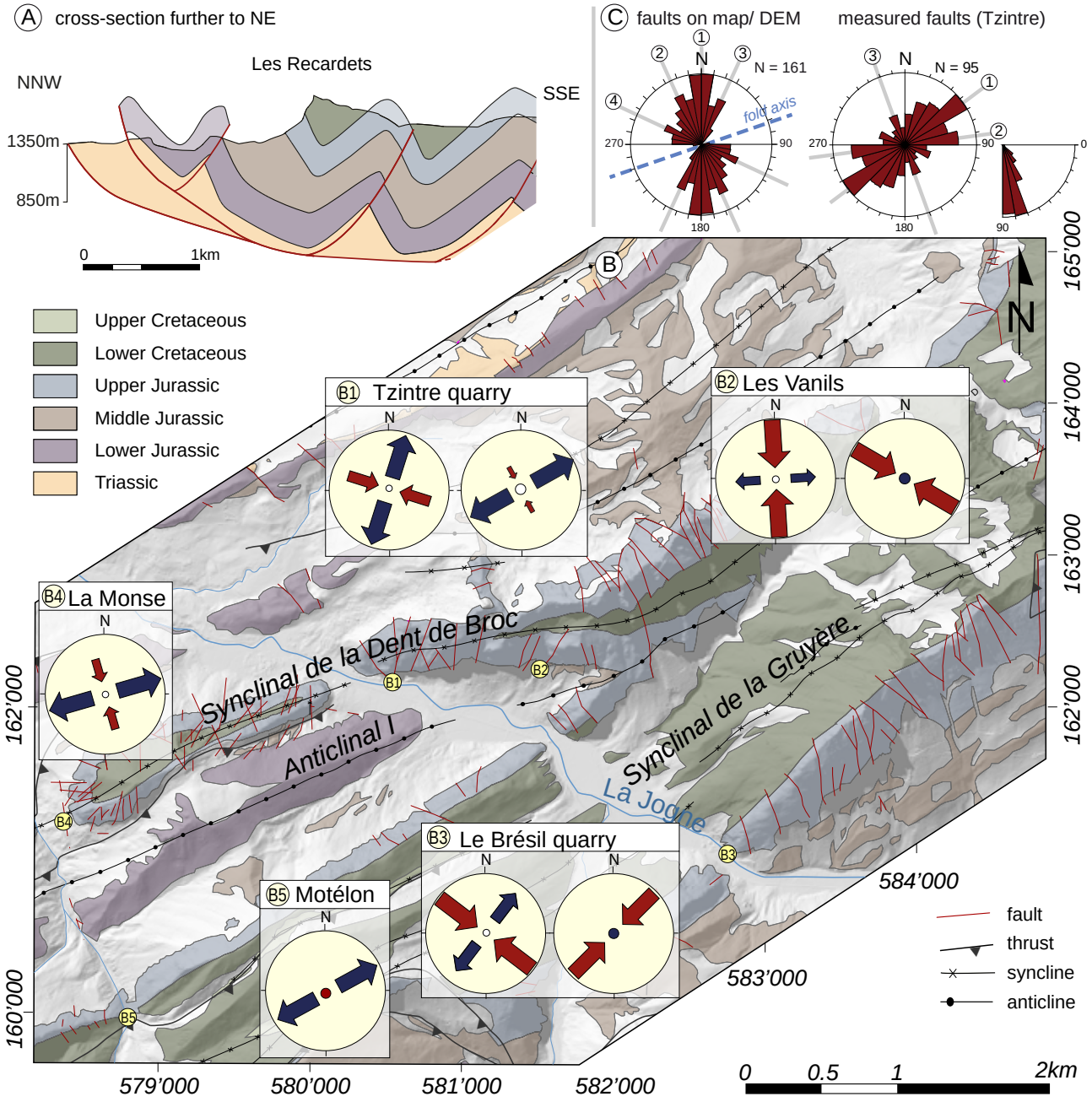

Fig. 3.14: Results of the paleostress analysis in the area of the two active quarries Tzintre and Le Brésil. A) Schematic cross-section located further to the NW (part of the cross-section illustrated in Fig. 3.37/ transect indicated in Fig. 3.10). B) Structural map representing the different stress regimes. The heterogeneous data plot nearly always requires a subdivision into two subsets. A strike-slip stress state with an important extensional component towards NE-SW is dominating. C) Two rose diagrams showing the distribution of faults extracted on maps and DEMs and the distribution of the measured fault planes in the Tzintre quarry.

The second fault direction is oriented perpendicular to the observed fold axis and corresponds to normal faults that developed under a fold axes parallel extensional stress regime.

The second rose diagram (Fig. 3.14C) illustrates the orientation of the measured fault planes at the Tzintre quarry. The dominant fault directions are strikingly different compared to the previous rose diagram.

Three main fault families can be distinguished:

1) NE-SW (N 40-60°),

2) E-W (N80-90°) and

3) NNW-SSE.

The predominant fault family (1) is not at all represented on DEM and maps (first rose diagram), which can possibly be related to the scale of the fault planes.

The scale of fault indicated on maps ranges over several hundreds of meters, whereas the measured fractures remain of metric scale. Additionally, the NE-SW oriented faults (1) lie parallel to the fold axes and for this reason, to the best-exposed Upper Jurassic limestones too. Consequently, these faults are less visible on maps and orthophotos. The third fault direction corresponds to the normal faults oriented perpendicular to the fold axis, like the second fault family in the first rose diagram.

Paleostress analysis

The resulting stress regimes show a dominating strike-slip regime with the compressional axes oriented NW-SE and an important extensional component trending to the NE-SW (Fig. 3.15B/ Fig. 3.16). An extensional stress regime appears in the Tzintre quarry (B1) and the Motélon site (B5), both related to the fold axis parallel extension. At the measurement sites Les Vanils (B2) and Le Brésil quarry (B3), a purely compressional stress field occurs as a subordinate stress state that might be related to the local influence of a thrust fault.

site	PRESENT ORIENTATION bedding	stress axes		fault planes	rotational axes/ rotation angle	BACK-TILTED ORIENTATION stress axes		fault planes
B1 Tzintre quarry 1	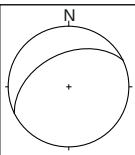	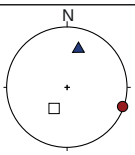	● 110/ 07 □ 211/ 55 ▲ 015/ 33	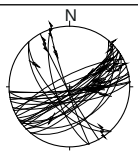	axis: 238/ 04 angle: -44°	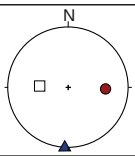	● 093/ 38 □ 273/ 51 ▲ 183/ 01	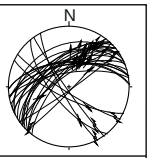
Tzintre quarry 2	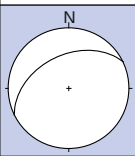	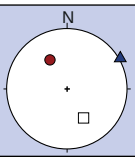	● 328/ 42 □ 151/ 47 ▲ 059/ 01	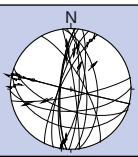	axis: 238/ 04 angle: -44°	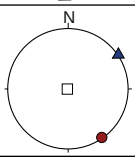	● 145/ 02 □ 280/ 89 ▲ 055/ 00	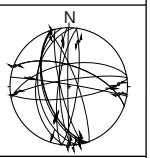
B2 Les Vanils 1	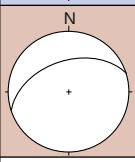	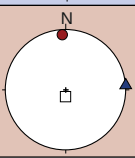	● 356/ 08 □ 177/ 81 ▲ 086/ 01	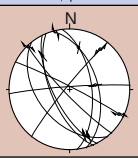	axis: 238/ 04 angle: -47°	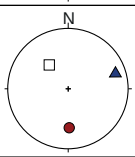	● 177/ 34 □ 320/ 51 ▲ 074/ 20	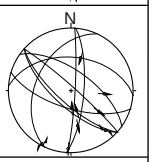
Les Vanils 2	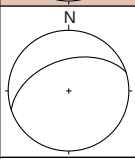	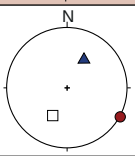	● 120/ 00 □ 211/ 46 ▲ 029/ 43	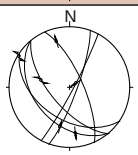	axis: 238/ 04 angle: -47°	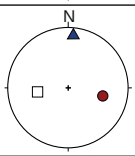	● 106/ 40 □ 262/ 47 ▲ 006/ 11	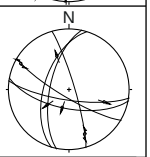
B3 Le Brésil 1	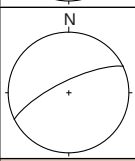	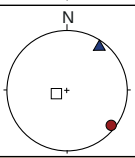	● 128/ 09 □ 257/ 75 ▲ 036/ 11	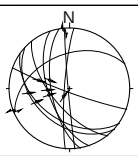	axis: 238/ 04 angle: -74°	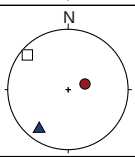	● 070/ 66 □ 310/ 12 ▲ 214/ 20	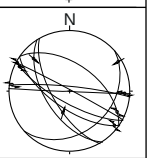
Le Brésil 2	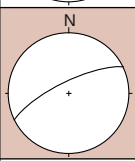	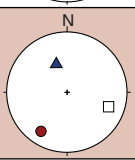	● 215/ 24 □ 109/ 31 ▲ 336/ 48	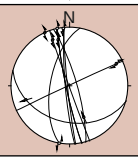	axis: 238/ 04 angle: -74°	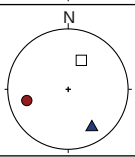	● 254/ 30 □ 026/ 49 ▲ 149/ 26	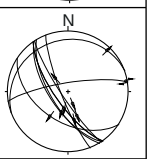
B4 La Monse	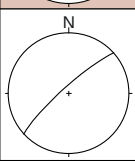	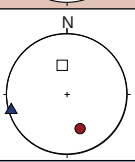	● 159/ 39 □ 351/ 05 ▲ 254/ 05	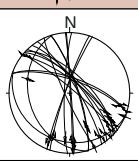	axis: 245/ 03 angle: -81°	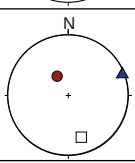	● 330/ 60 □ 126/ 30 ▲ 068/ 06	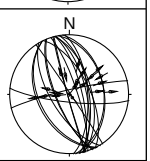
B5 Motélon	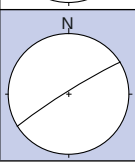	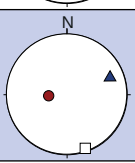	● 267/ 65 □ 161/ 07 ▲ 068/ 24	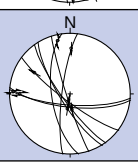	axis: 238/ 00 angle: -86°	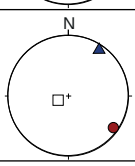	● 126/ 08 □ 252/ 77 ▲ 034/ 10	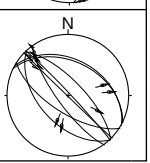

Fig. 3.15: Results of the paleostress analysis showing the orientation of the average bedding, the stress axes obtained using the right dihedra method, the orientation of the fault planes and the results of the back tilting. The colour coding represents the stress regime: white = strike-slip, blue = extensional and red = compressional. The location of the measure sites B1-B5 are indicated in the previous figure (Fig. 3.15).

An overview over the detailed paleostress result of every measuring site is listed in Fig. 3.15. Additionally, calculated paleostress axes, as well as the present fault plane orientations were tilted backwards into its pre-folding position. It remains debatable, if slickensides that developed before the folding phase are still preserved. For this reason, mainly the fault plane orientation was taken into consideration. The orientation of the fractures of the Tzintre quarry 1 (Fig. 3.15B1), for example, the dextral NE-SW oriented faults, correspond in their pre-/ early-folding position to NW dipping back-thrusts, reactivated in a later stage as dextral strike-slip fault.

Tzintre quarry

On the northern limb of the backward inclined Anticline I (Fig. 3.14) at the contact between the Middle and the Upper Jurassic, the Tzintre quarry shows a whole suite of faults and joints. The influence of important normal faults (striking NNE-SSW and NW-SE) seems obvious (Fig. 3.16A). However, detailed observation reveals a more complex fracturing system, as several of these ancient normal faults are reactivated. Fault-slip data show a predominance of NE-SW striking dextral strike-slip faults. Together with its corresponding NNW-SSE trending sinistral fault set, they define the most prominent stress field

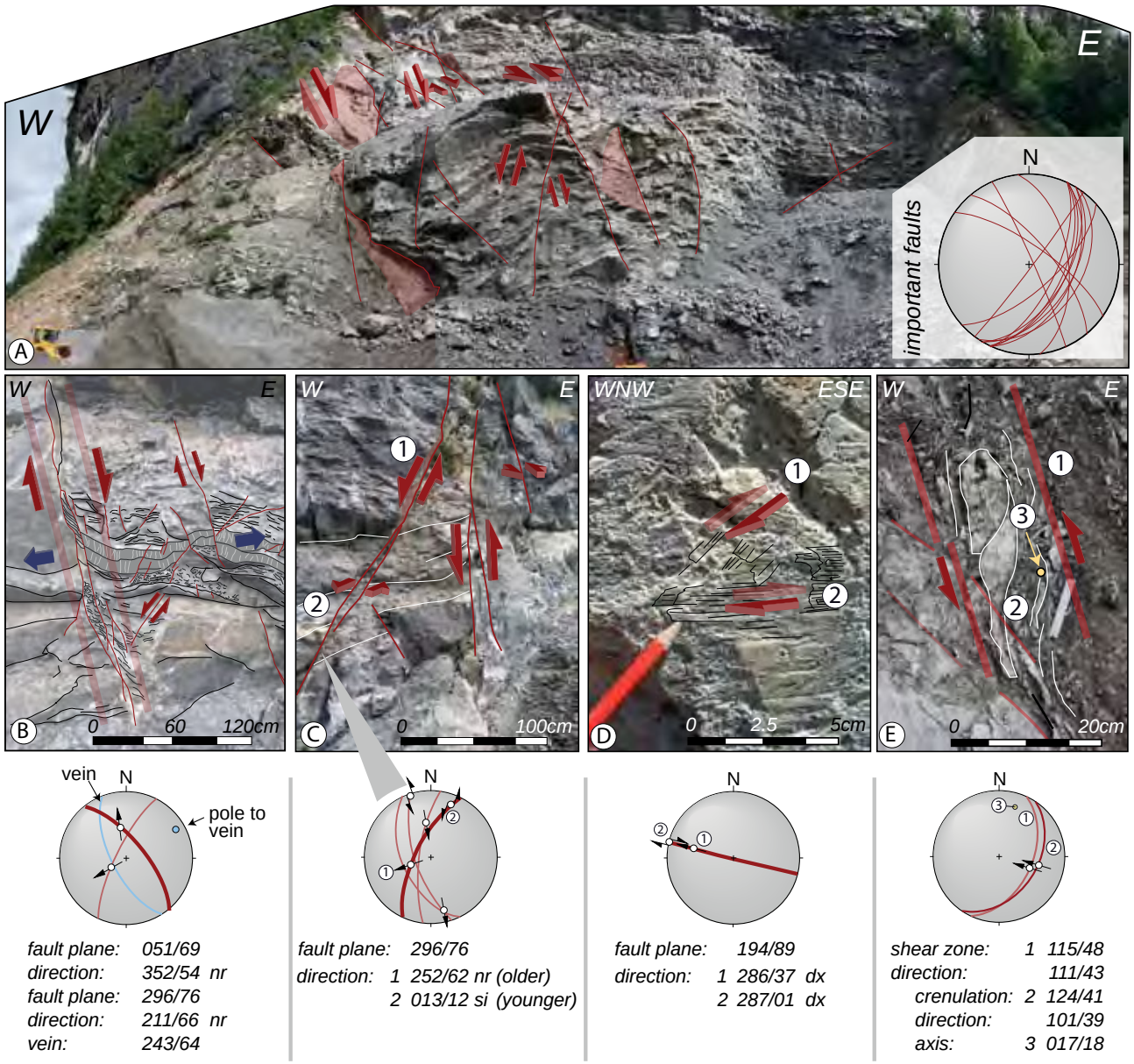

Fig. 3.16: Overview of the structural style of the Tzintre quarry highlighting the features, which contribute to the development of a possible stress field chronology. A) Panoramic view of the Tzintre outcrop showing the influence of large-scale normal faults. B) Detail of a small-scale graben structure with a normal shear band and extension veins segmenting chert bands. C) Normal faults that bear slickenfibres indicating a strike-slip sense of shear. D) Overprinted slickenfibres support the transition of oblique slip towards strike-slip. E) Shear bands attesting also reverse reactivation of a normal fault plane.

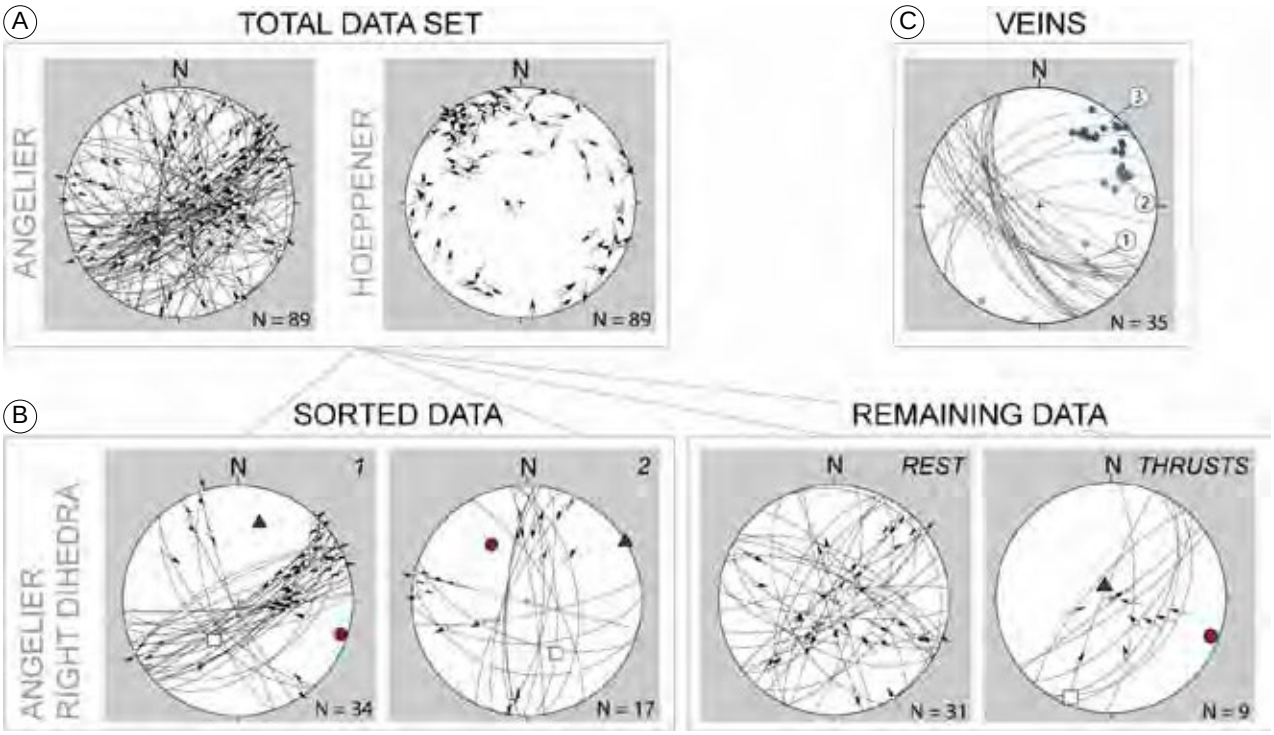

Fig. 3.17: Stereographic projections (lower hemisphere equal area projection) of the fault-slip analysis at the Tzintre outcrop. A) Total data set of 89 fault-slip data represented both by an Angelier plot and a Hoeppener plot by the use of TectonicsFP (REITER and ACS, 1996 - 2002). B) The data separation realised with the WINTENSOR program (DELVAUX, 2006) exposes two major stress regimes: a dominant strike-slip regime and an extensional regime with an oblique strike-slip component. Within the remaining data set, the reverse faults were sorted out. C) A stereographic projection of vein planes and their poles show a chronology corresponding to their intersecting relationships: (1) the oldest - (3) the youngest veins.

of this outcrop; the strike-slip stress regime with its compressional axes oriented NW-SE (Fig. 3.17). By the process of data separation, a secondary more oblique strike-slip stress regime with a dominating extensional component directed NE-SW was also identified.

With the remaining non-separated data, the thrusting fault planes oriented in NE-SW direction were sorted out manually. The orientation of the thrusts planes parallels the orientation of the fold axes, for this reasons they can be interpreted as thrusts that were generating the anticline above (Fig. 3.14). On these reverse fault planes, shear band features exposing a top to the NW movement can be recognised (Fig. 3.16E).

Frequently, the faults developed during the folding process - both thrust and normal faults - were reactivated with a recent strike-slip movement, as indicated on Fig. 3.16C and D. Normal faults, that are clearly offsetting the stratigraphic layers, bear shear sense indicators attesting a strike-slip movement (Fig. 3.16C), or show an overprint of slickenfibres turning from a normal to a strike-slip movement (Fig. 3.16D). The two dominating stress regimes both seem to benefit from prevailing normal fault and thrusting structures. For example, the dominant strike-slip stress regime reactivates ancient NE-SW oriented thrust faults with a dextral strike slip movement, as well as ancient NNW-SSE oriented normal faults with a sinistral strike-slip movement. Within the second stress regime, similar observations concerning the reactivation of former fault planes can be made (Fig. 3.17).

Occasionally, chert bands are segmented by extensional veins oriented in NNW-SSE direction supporting together with extensional faults an ENE-WSW oriented extension direction (Fig. 3.16B). The analysis of intersecting extension veins exposes three different vein families (Fig. 3.17C). The oldest veins (1) intersected by every other vein family are striking towards NE-SW and show an extensional trend towards NW-SE. These veins are most probably related to a pre-emplacement extensional phase. The NNW-SSE oriented intermediate veins (2) are cutting the oldest veins, but are interrupted by the youngest veins (3) oriented towards NW-SE with an overall extension axis towards NNE-SSW.

Apart from thrusts, normal faults perpendicular to the folding trend are assumed the oldest structures affecting the Tzintre outcrop. They were generated

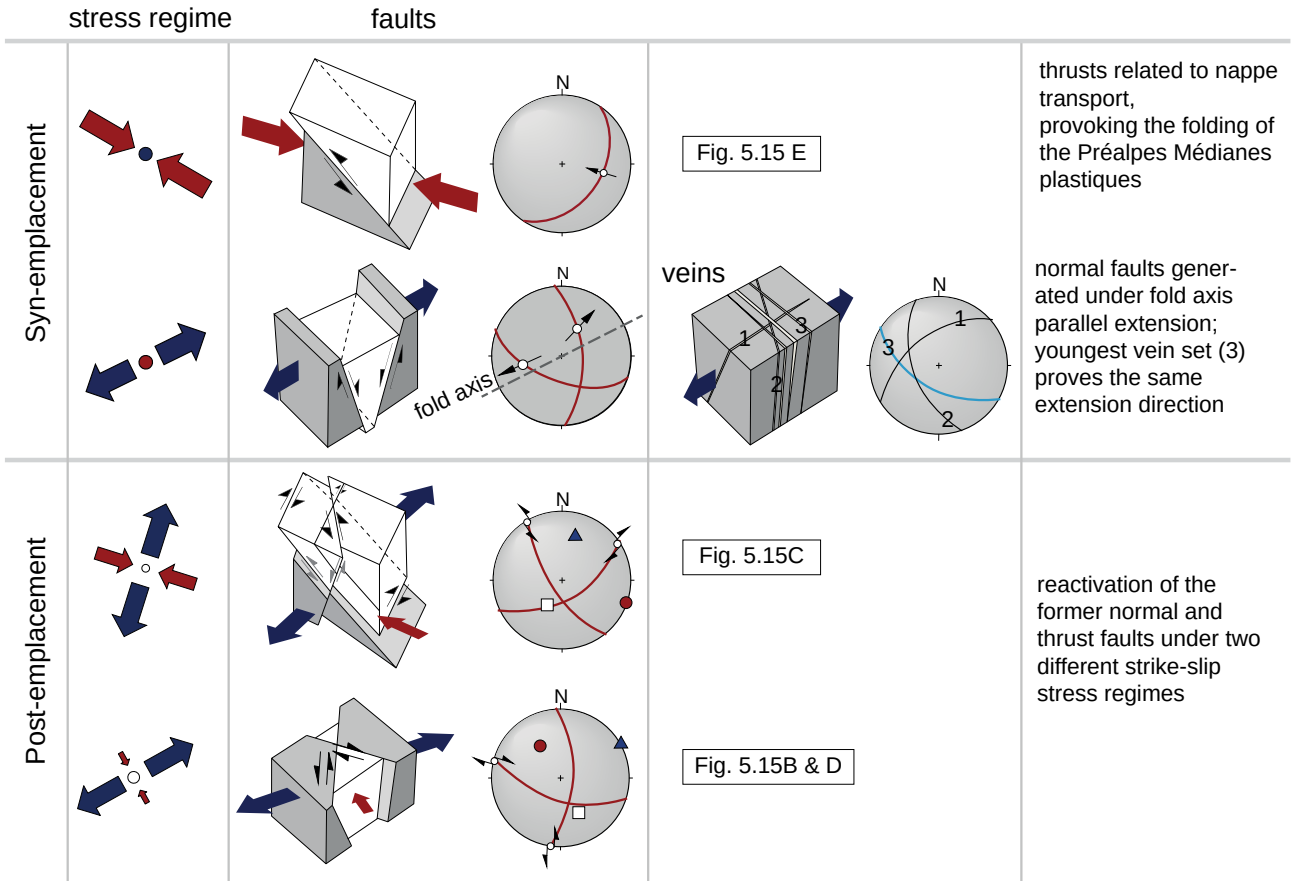

Fig. 3.18: Overview of the chronological order of the stress regimes and their corresponding structural features by a schema and a simplified stereographic plot. The graphic shows that after the emplacement, thrusting and normal faults structures were reactivated by strike-slip faults.

under an extensional stress regime parallel to the fold axis, related to the folding process of the Préalpes Médianes Plastiques. Only few slickenfibres were found to prove the normal movement on the fault planes, since a strike-slip reactivation of these faults overprinted or removed the majority of the predating fault-slip indicators.

Overprinting relationships between different kinds of slickenfibres expose a reactivation of the former normal faults by a more recent strike-slip movement (see Fig. 3.16D and E) agreeing with the dominating strike-slip stress regime.

An overview of the chronological order of the structures of the Tzintre outcrop is given in the following illustration (Fig. 3.18).

Le Brésil quarry

Situated on the SE limb of the Gruyères syncline, the Brésil quarry exposes massive Upper Jurassic limestones, which are less fractured in contrast to the Tzintre outcrop, apart from two important large-scale fault planes bearing a large fault zone in between (Fig. 3.19A). The predominant fault direction is N-S with a sinistral sense of shear. The heterogeneous fault-slip data set witnesses an influence of several deformational phases. After careful data separation, two major stress regimes were detected: A strike-slip stress regime with a NW-SE oriented compressional stress axis and a purely compressional stress regime oriented towards NE-SW. The remaining data set is composed of several subsets, but due to the sparse amount of data, they are not representative.

The two important large-scale faults trending in N-S direction show a rather chaotic arrangement of several superimposed slickenfibres attesting a repeated reactivation of the same fault plane (Fig. 3.19A.

The evolution of different stress phases was studied by analysing the relationship of crosscutting veins and stylolites (Fig. 3.19 B&C). Stylolites parallel to the bedding plane are a proof of compression during the compaction of the sediments (Fig. 3.20A). These stylolites are cut by NNW-SSE oriented stylolites indicating a compression in NE-SW direction (B). By rotating these stylolites into their pre-folding position, they attain a vertical position. Subsequently,

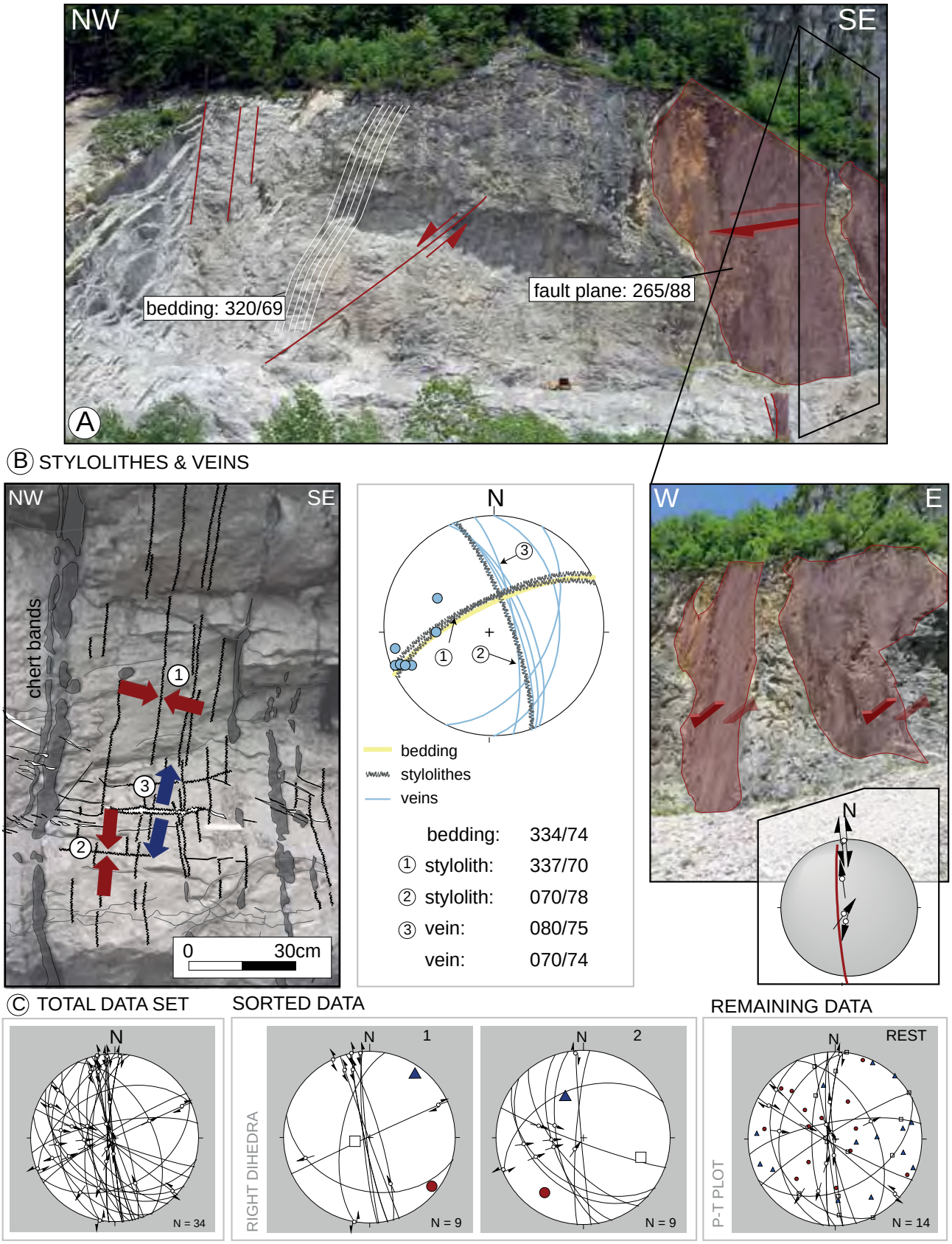

Fig. 3.19: A) Panoramic view of the Le Brésil quarry showing two major fault planes with an important fault zone. Slickenside arrangement in different directions witnesses multiple reactivations of the same faults, recognisable on the stereographic plot of the fault plane. B) Detail of the relationship between stylolites and veins allowing reconstruction of a succession of tectonic events (see Fig. 3.21): 1) stylolites parallel to the stratification, 2) stylolites perpendicular to the stratification, 3) opening of veins perpendicular to the stratification. C) Stereographic projections (lower hemisphere equal area projection) of the fault-slip analysis at the Le Brésil outcrop. Data processing generates two stress fields: a strike-slip stress regime with a NE-SW oriented compressional axis and a purely compressional stress towards NE-SW.

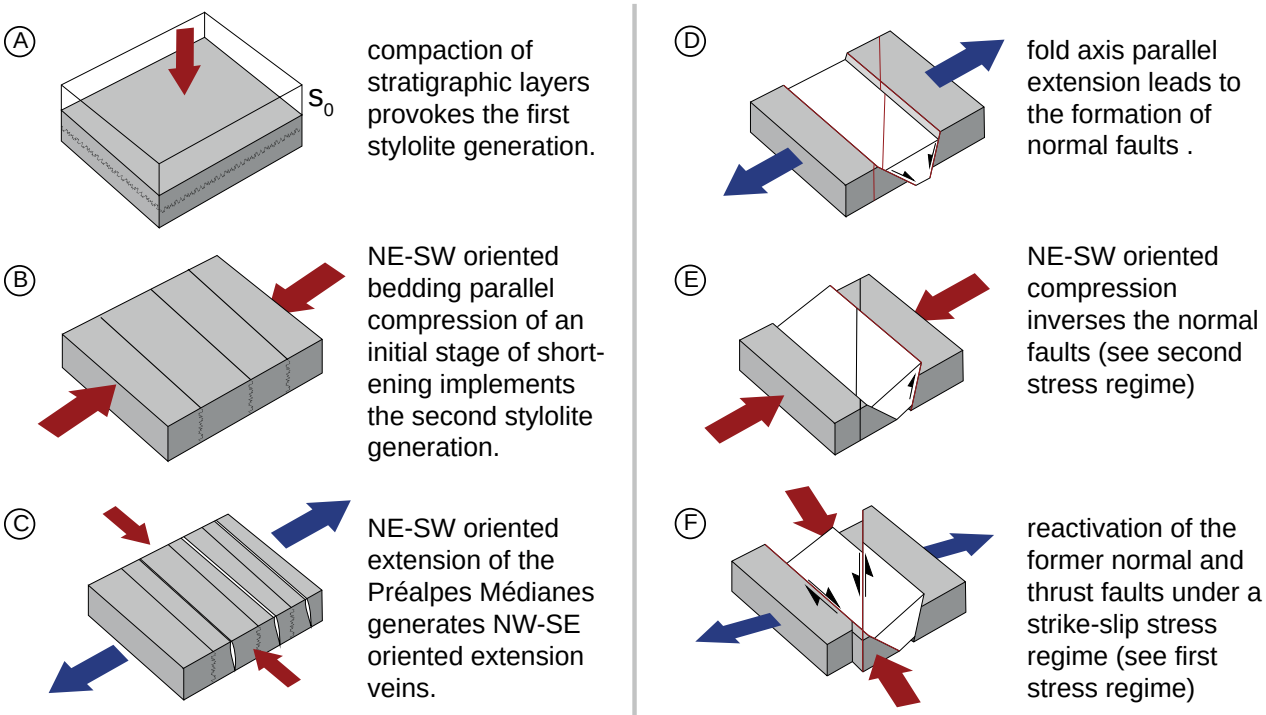

Fig. 3.20: Schema presenting a possible chronology of the different events affecting the Brésil quarry

during the folding and thrusting process, these planes of weakness - formed by the stylolites - were opened as extension veins perpendicular to the fold axes (C). Simultaneously, like in the Tzintre outcrop (Fig. 3.16) NW-SE striking normal faults developed (Fig. 3.20D), which were in a later stage inverted (E) as thrusts. This compressive stress regime agrees with the second paleostress regime, presented in the previous figure (Fig. 3.19C). Finally, the ancient normal and thrust faults are reactivated under a strike-slip stress regime within the following way: the N-S oriented faults with a sinistral and the NW-SE oriented faults with dextral sense of shear (Fig. 3.20F).

The comparison of the Brésil with the Tzintre quarry reveals many common features, such as the basic structures related to the fold-and thrusting of the Préalpes Médianes. Based on the observation of overprinting slickensides, it can be shown that under the recent strike-slip regime most fractures are reacti-vating already existing structures and only a few are newly developed. For that reason, the fault-slip data are not fulfilling ideal conditions for paleostress analysis, as the slickensides are bound to fault planes dating back to another deformation event.

These two outcrops differ mainly within the degree of fracturing, since the Tzintre quarry exposes a dense fracture network, with partially a chaotic fault arrangement, whereas the Brésil quarry is less affected. A possible reason could be the transition of a foreland verging to a hinterland verging thrust passing from the SW to the NE of the Jogne valley. The folds of the Préalpes Médianes Plastiques between Charmey and Schwarzsee feature an asymmetric shape with a steeper inclined backlimb and a gently dipping forelimb. These folds seem to be generated by backthrusts underneath, whose origin can either be associated to the reacti-vation of inherited structures or to a ramping structure. The vicinity of a large-scale Ultrahelvetic lens to the NW (Massif de Montsalvens) let us infer the presence of another Ultrahelvetic lens underneath the discussed part of the Préalpes Médianes. This probably forced the advancing nappe to pass this ramp, provoking the faults to thrust backward (cross-section B, Fig. 3.21). The Tzintre quarry is situated in between this transition zone, where foreland and hinterland verging thrusts merge into each other. This transfer zone might take up the interfering movement by a dextral strike-slip fault zone (Fig. 3.21).

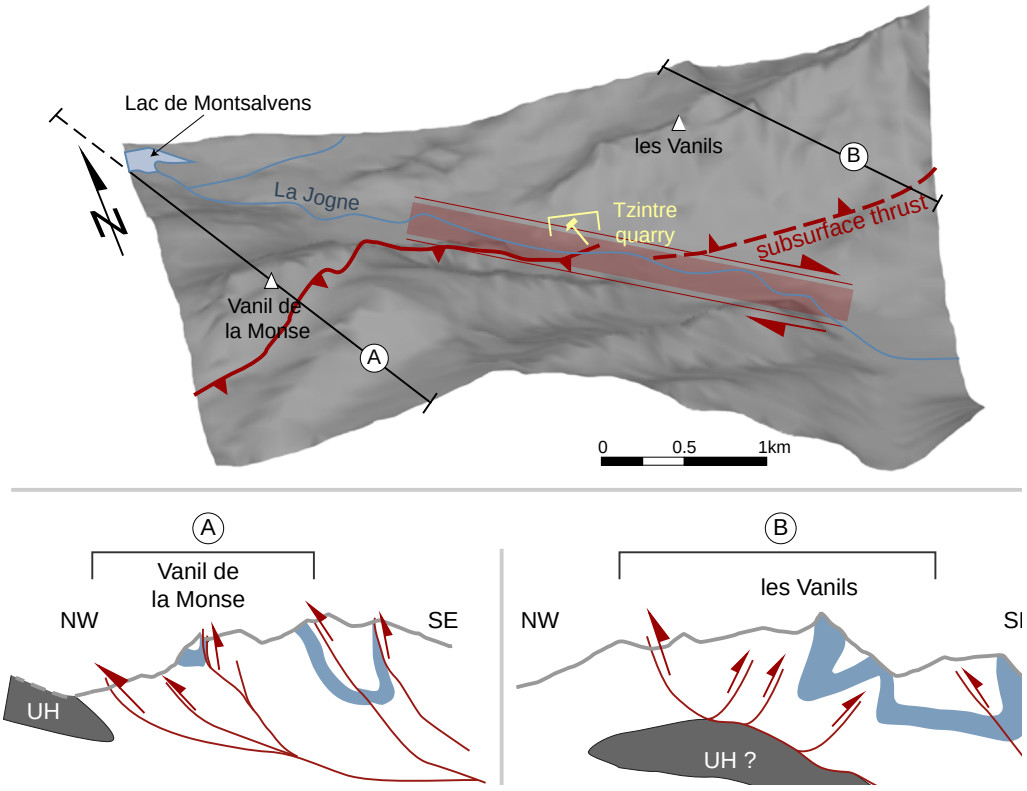

Fig. 3.21: Relief between the Vanil de la Monse and les Vanils situating the Tzintre quarry outcrop within the transition zone between the foreland and hinterland verging thrusts. Cross-section A shows the normal type of fault-related folds, whereas in cross-section B the folds are related to backward thrusting faults that can probably be associated to a ramping over an Ultrahelvetic lens underneath.

4.2.2 Schafarnisch - Mittagflue

A second region of detailed investigation extends from the Schafarnisch to the NW and the Mittagflue area to the SE (Fig. 3.22), mainly at the boundary of the Préalpes Médianes Plastiques and the intermediate zone, marked by the two important imbricates: the Heiti imbricates to the NW and the Gastlosen imbricate to the SE (Lugeon and Gagnebin, 1941), which are thrusting top to the NW. These thrust faults lead back to ancient Liassic paleofaults affecting sediment deposition, which subsequently have been inverted during alpine deformation, separating sectors with different tectonic style and different lithostratigraphic contents (sector B, C and D in Fig. 3.22B), as proposed by Borel and Mosar (2000). Sector B, belonging to the Préalpes Médianes Plastiques, is characterised by strike-slip and thrust faults cutting through the major fold structure (Wissing and Pfiffner, 2002). Sector C corresponds to the Heiti, and sector D to the Gastlosen imbricate, both of which are affected by sedimentary gaps that influence their structural behaviour marked, as by the presence of important thrusts.

The observation of DTMs, orthophotographs and the morphology of the landscape exposes large-scale N-S to NNE-SSW oriented sinistral (fault set 1 and 2) and WNW-ESE oriented dextral faults (fault set 3), as can be identified on the rose diagram in Fig. 3.22A. These strike-slip faults are clearly offsetting existing anticlinal and synclinal fold structures for about 700 Meters. In a larger extent they might act as a counterpart to the important right lateral strike-slip zone in vicinity to Weissenburgbad, northeast of Boltigen (Fig. 3.29) (Bieri, 1925; Borel, 1991; Mosar and Borel, 1992; Plancherel, 1979).

The heterogeneous fault-slip data consists of multiple superimposed stress regimes. However, the secondary stress regime was often not clearly defined due to the limited amount of data at each measurement site, thus, frequently only the main stress field could be significantly identified. Generally, a strike-slip stress regime with a NW-SE oriented compressional component is prevailing, which agrees with the movement of the large-scale sinistral and dextral strike-slip faults (Fig. 3.22B). The extensional component striking in NE-SW direction is more pronounced, than the compressional. A particular extensional stress regime oriented NW-SE is displayed at the Erbetlaub area (Fig. 3.22B3 & Fig. 3.23B3), located between the Holzerhorn and the Trimlehorn summits related to a horst-like structure.

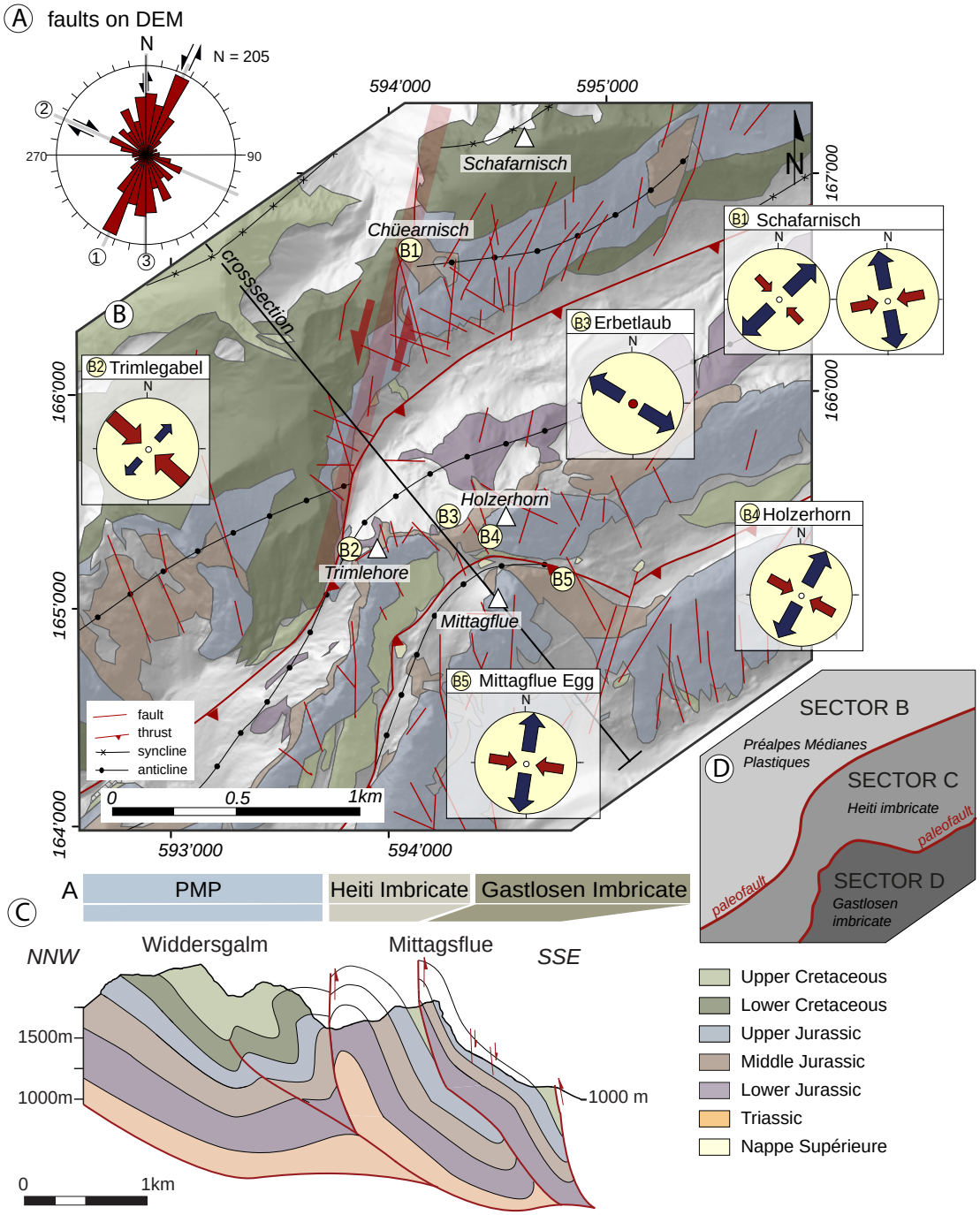

Fig. 3.22: Overview of the structures and results of the Schafarnisch-Mittagflue area. A) Rose diagram indicating the spatial distribution of faults observed on maps, orthophotos and DEMs; three major fault directions are visible: (1) a NNE-SSW oriented sinistral, a WNW-ESE oriented dextral fault family and a N-S oriented fault family B) Structural map showing the result of paleostress analysis: most of the heterogeneous data set show a strike-slip stress regime (compressional axis oriented NW-SE), C) Simplified cross-section highlighting the structural units: Préalpes Médianes, Heiti and Gastlosen imbricate (location see B), D) Outline of the important paleofaults and the three sectors occurring in this area.

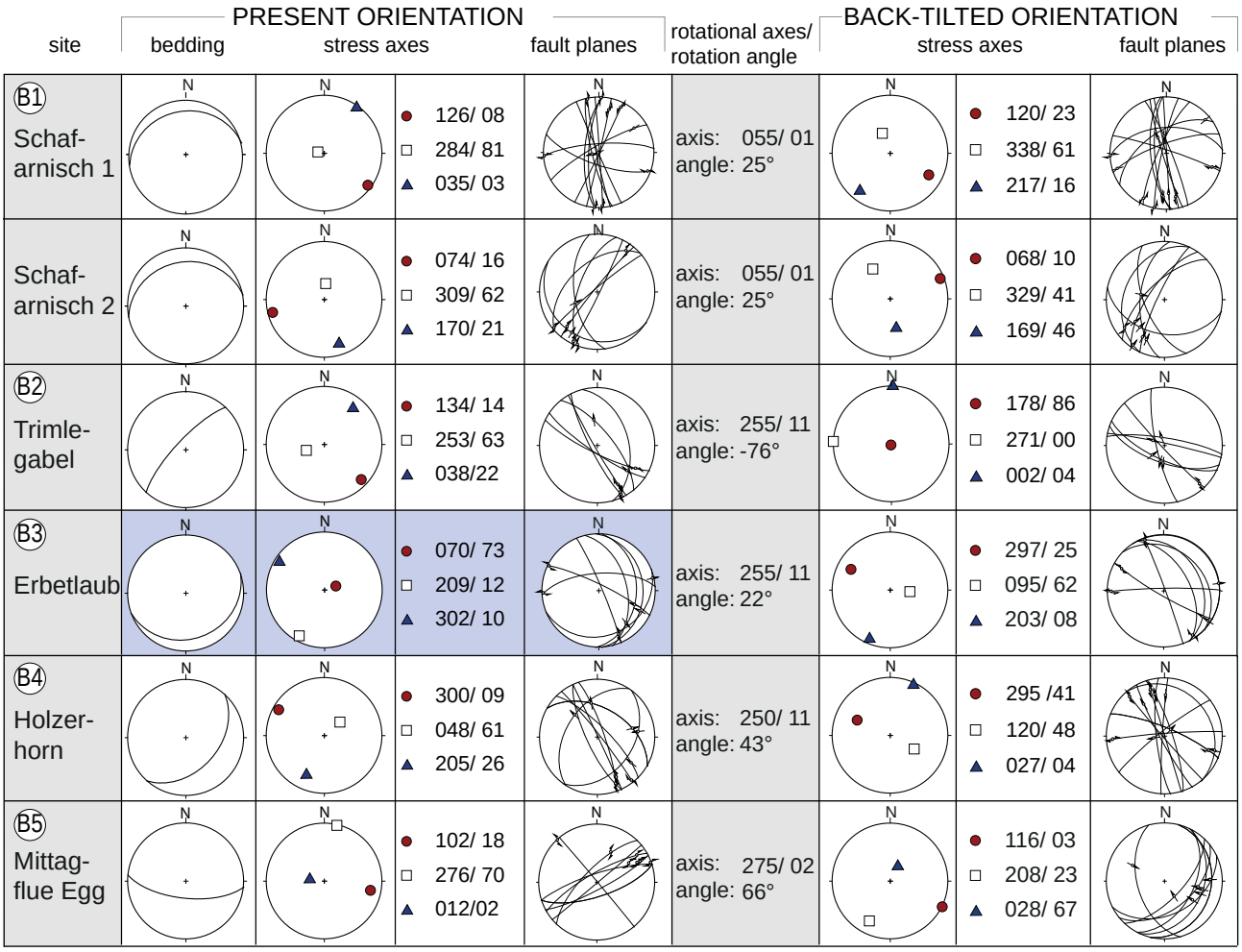

Fig. 3.23: Results of the paleostress analysis showing a stereographic projection of the average bedding orientation for every measurement locality; the projection of the principal stress axes obtained by applying the Right Dihedra method, the orientation of the fault planes and the results of the back tilting procedure. The colour coding represents the stress regime: white = strike-slip, blue = extensional and red = compressional. The location of the measurment sites B1-B5 are indicated in the previous figure (Fig. 3.23).

Schafarnisch

Fault-slip measurements were gathered in an area influenced by a large-scale sinistral strike-slip fault zone displacing several smaller anticlinal segments for hundreds of meters (Chüearnisch, Fig. 3.22). Lower Cretaceous small-scale folds mask the continuation of the fault zone until outcropping Upper Jurassic limestones (farther north) show another important displacement (Chänelgantrisch, Fig. 3.29).

Fault kinematic analysis results in two stress regimes, both strike-slip states with dominating extensional components. The prevailing stress state agrees with a N-S oriented fault zone with a NW-SE oriented compressional stress axis. The secondary stress regime is mostly affected by NW-SE oriented dextral faults and works therefore under a strike-slip system with a NE-SW oriented compressional stress axis.

Intersecting extension veins indicate the following chronology (Fig. 3.24): NNW-SSE trending veins are younger and crosscut the older, NW-SE oriented veins. Stylolites striking in direction NE-SW developed under NW-SE oriented compression possibly related to an early stage of the folding process.

Pole-to-plane projection of the older veins demonstrates a fold-axis parallel extension suggesting a formation during the fold development. The NNW-SSE orientation of the younger vein set coincides with the orientation of the major sinistral strike-slip faults. However, the pole-to-plane projection of the younger veins shows a WSW-ENE extension that does not completely agree with the extensional axes of the dominating strike-slip stress regime (Fig. 3.23).

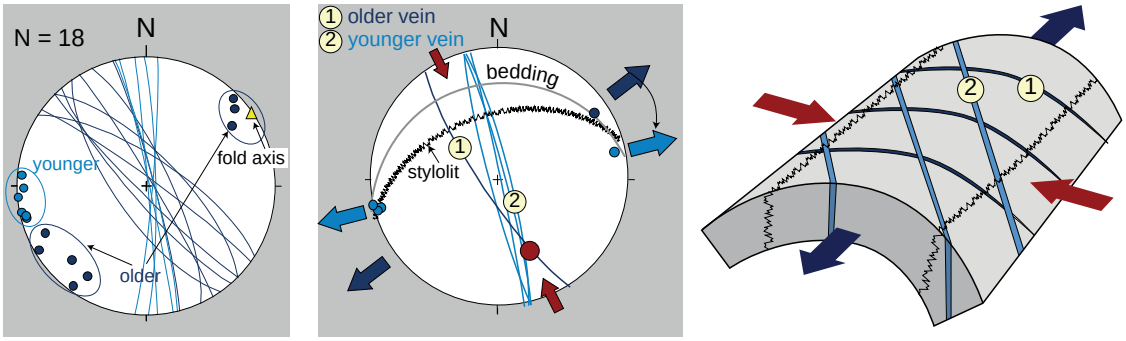

Fig. 3.24: Crosscutting vein and stylolites relationship. The first stereographic plot shows the orientation of every vein measured and the second refers to an observed example where NW-SE oriented veins are intersected by NNW-SSE oriented veins. The schema explains a probable relationship among the veins and stylolites, which can mostly be associated to the formation of fold, whereas the youngest vein set reactivated under the strike-slip stress regime.

Erbetlaub

Large-scale normal faults expose Middle Jurassic rocks in a horst-like structure between the Holzerhorn and the Trimlehorn, both consisting of Upper Jurassic massive limestones (Fig. 3.25). The NW-SE orientation of these normal faults suggests an initial fold axis parallel extension towards NE-SW (see block diagram A in Fig. 3.25). However, fault kinematic analyses attest an extensional stress regime with a NW-SE oriented extensional stress axis. This is probably related to their particular localisation in between the influence of thrust of the Gastlosen imbricate and the important strike-slip fault of the Schafarnisch. The Erbetlaub normal faults were reactivated as oblique normal faults with a dextral strike-slip component (block diagram B in Fig. 3.25). The NW-SE orientation of the normal faults favours a dextral strike-slip reactivation associated to the conjugate counterpart of the large-scale sinistral fault zone, similar to the Weissenburg dextral fault zone (Fig. 3.25), except that

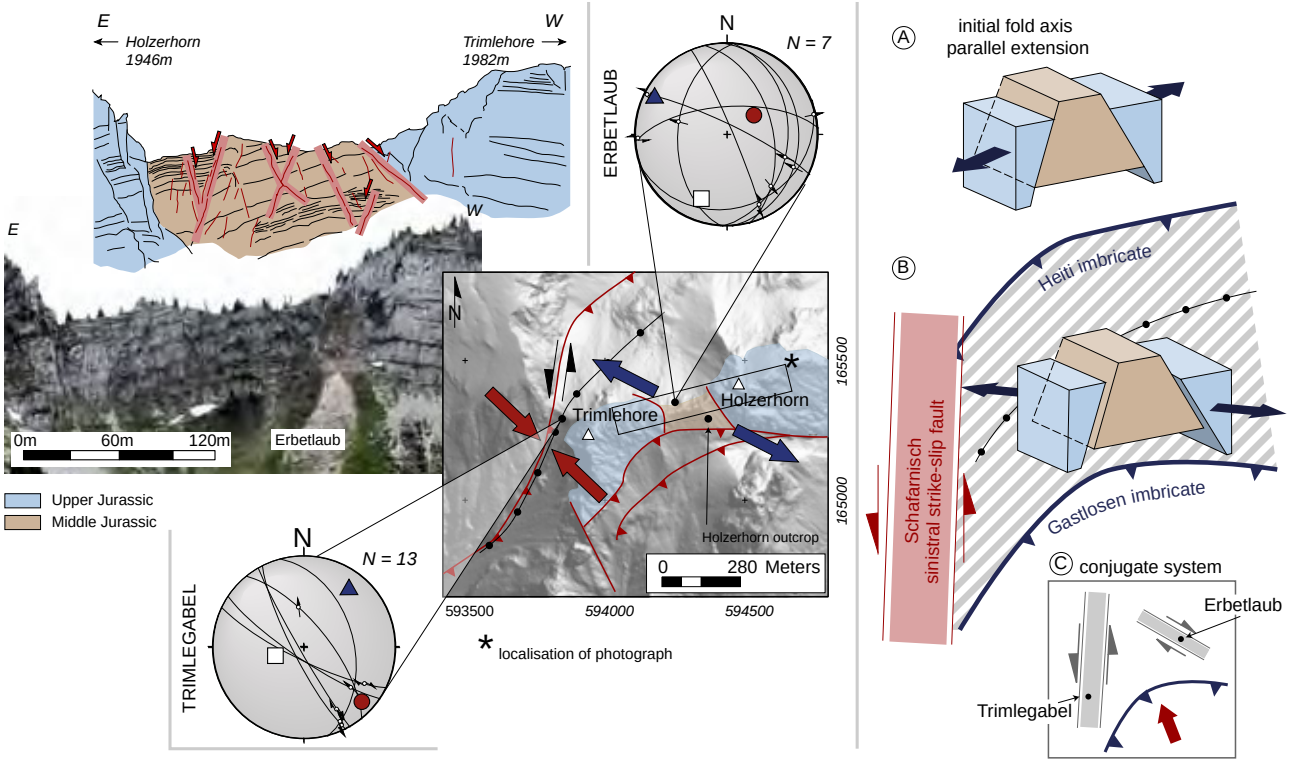

Fig. 3.25: Photograph and sketch of the Erbetlaub area show Middle Jurassic layers in a horst-like structure between Holzerhorn and Trimlehorn. The map shows a schematic structural overview of the Erbetlaub area and localisation of the stereographic projection of the Trimlehorn and Erbetlaub fault plane and their corresponding stress axes obtained by the Right Dihedra method. A scheme of this area explains the initial fold-axis parallel extension creating normal faults (A), which wtere in a later stage reactivated under the influence of the Schafarnisch strike-slip fault and the thrust of the Gastlosen imbricate (B). (C) shows an interpretation of the reactivation of the Erbetlaub normal faults as dextral fault zone, conjugate to the Schafarnisch sinistral fault zone.

the fault movement is oblique instead of purely strike-slip. Moreover, detailed analysis of the fault-slip data set revealed fault planes with a reverse shear sense proving a reactivation of the former normal faults as thrusts, as well as NNW-SSE trending sinistral strike-slip faults.

The Erbetlaub outcrop is characterised by the influence of diverse, important structures, whose interactions are complex and marked by reactivation of the ancient normal fault planes. A possible interpretation is illustrated in Fig. 3.25, the presence of thrust faults and sinistral strike-slip faults however, points out an even more intricate relationship of the different structures.

Holzerhorn

The Holzerhorn outcrop is located to the southeast of the previous site, between the Holzerhorn and the Trimlehorn and is still part of the Heiti imbricate (sector C in Fig. 3.22D). The NNW-SSE oriented Upper Jurassic rock face of the Holzerhorn exposes major normal faults paralleling the fold axis (Fig. 3.28A), suggesting an initial extension perpendicular to the fold, related to the bending of the anticline. One key-outcrop along this rock face displayed a normal fault plane striking NW-SE, corresponding to the faults discussed at the Erbetlaub outcrop. A detailed photograph of this outcrop (Fig. 3.28B) features two normal faults clearly offsetting marly layers at the basis of the cliff. Two generations of slickensides indicate two distinct shear directions on this fault plane: an older one normal oblique towards NNW and a more recent one normal oblique towards ENE. The first one was probably active during the folding event under a fold-axis parallel extension, provoking the offset of the clearly visible marly layers. The orientation of the fault plane, as well as its slip direction coincides with the normal faults of the Erbetlaub outcrop. The more recent slip direction normal oblique towards ENE is distinctly represented by slickensides; however, no important offset was observed at outcrop-scale. The reactivation of the normal faults, most probably related to the horst-like structure of the previous outcrop prove an oblique dextral movement, as assumed at the Erbetlaub site (schema Fig. 3.28C).

Nevertheless, the general trend of the collected fault-slip data is a NNW-SSE orientation of sinistral strike-slip faults, similar to the Schafarnisch fault zone. For this reason, the prevailing stress regime at the Holzerhorn outcrop results in a strike-slip stress regime with a NW-SE oriented compressional stress axis. Additionally, extension veins with oblique fibres directed NNE-SSW confirm a NNE-SSW extension. The initial orientation of the veins can most probably be associated to a fold-axis parallel extension during the folding.

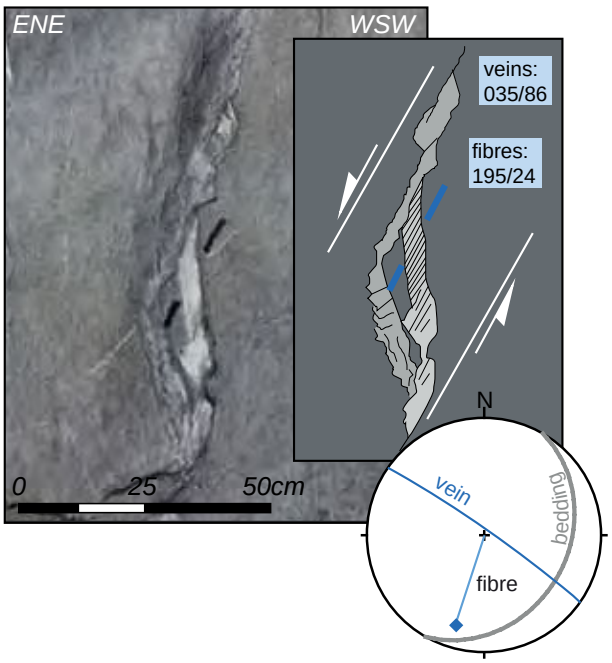

Fig. 3.26: Extension vein of the Holzerhorn site with oblique crystal fibres indicating a NNE-SSW oriented extension, whereas the initial orientation of the vein suggests a fold axis parallel extension.

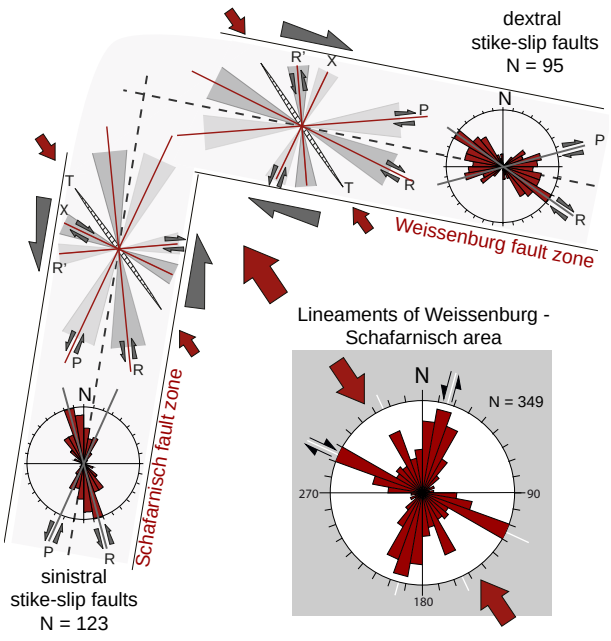

Fig. 3.27: The result of the lineament analysis exposes two major fault directions (rose diagram B), similar to the orientation of the Schafarnisch and Weissenburg fault zone. Measured faults are oriented as subordinate Riedel faults within a larger fault zone.

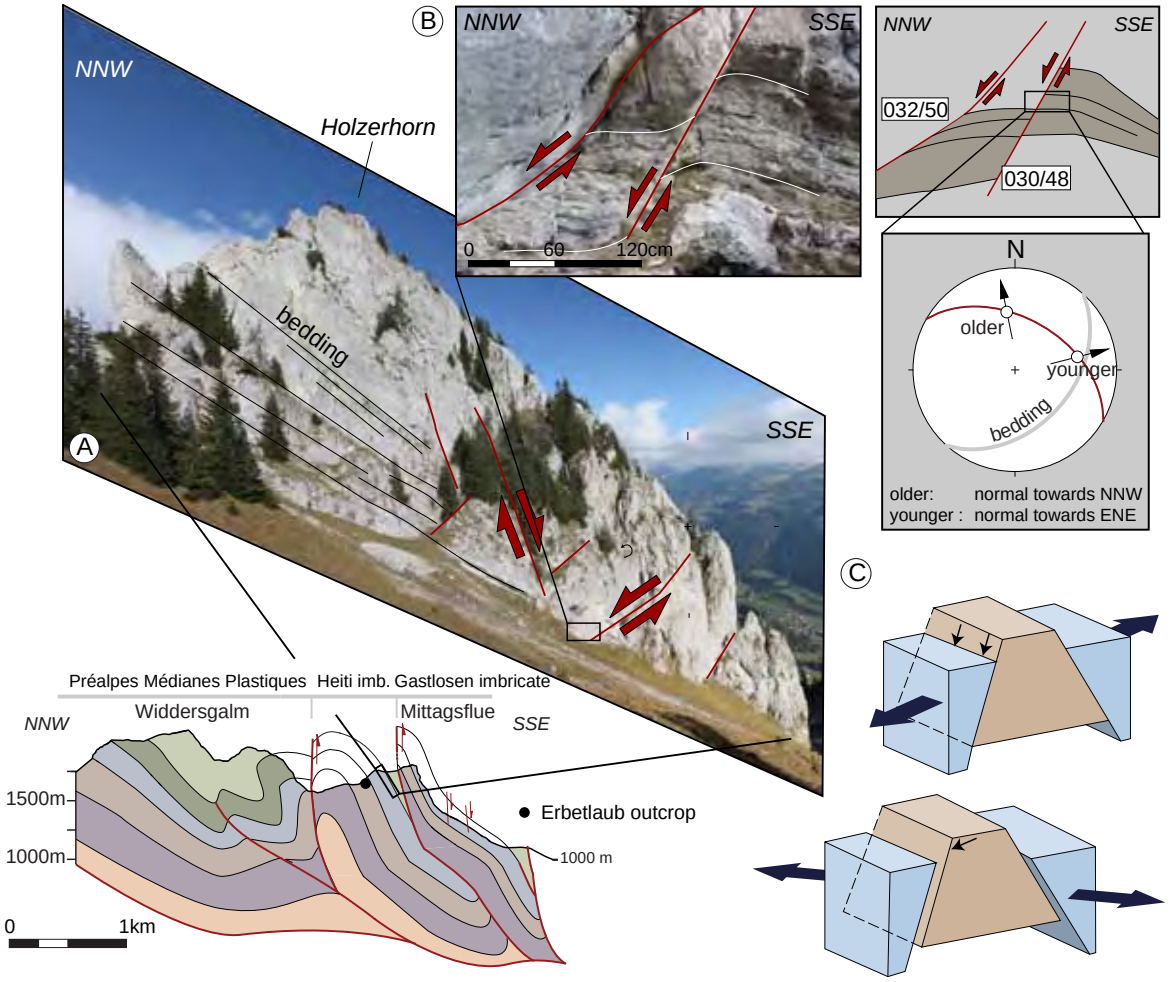

Fig. 3.28: A) NE-SW oriented normal faults characterise the Holzerhorn rock face. However, fault-slip measurements most often show a sinistral NNW-SSE oriented strike-slip movement. B) Normal faults clearly offsetting the stratigraphic layers, overprinting slickensides expose an older NNW directed oblique normal and a more recent ENE directed oblique normal fault movement. The movement on this fault plane coincides with the one observed at the Erbetlaub outcrop, illustrated by two block diagrams (C).

Weissenburg strike-slip zone

In contrast to the Schafarnisch-Mittagflue area, which is mostly dominated by sinistral N-S oriented fault zones, the Weissenburg area farther to the NE is affected by WNW-ESE oriented dextral strike slip faults. Near Weissenburgbad in the Simmen valley, an important fault zone extends over 6km in direction NW-SE (N 120°) and dips 75-80° towards SW. This fault zone is clearly offsetting existing anticlines and synclines by 500-800m (Fig. 3.29) and is for this reason distinctively visible in morphology. Detailed descriptions were carried out by Bieri (1925) and Plancherel (1979), as well as more detailed investigations focussed on fault kinematic of this fault (Borel, 1991; Mosar and Borel, 1992). Paleostress analysis in vicinity of the Weissenburg fault zone reveals a strike-slip stress regime similar to the one observed in the Schafarnisch-Mittagflue area. Fault-slip data were analysed with respect to the different lithologies and demonstrate well-defined directions for the resulting compression and extension, despite the important differences of lithology among the Upper Cretaceous-Eocene, the Lower Cretaceous, the Upper and the Middle Jurassic.

Fault lineament analysis based on DEMs, orthophotographs and already mapped faults in the region between the Weissenburg fault zone and the Mittagflue area expose two predominant fault families (rose diagram Fig. 3.27): a WNW-ESE striking dextral and a NNE-SSW oriented sinistral fault direction. Towards the Weissenburg fault zone, the dextral transversal faults dominate, whereas in our investigation area the sinistral fault family is mainly represented. Bieri (1925) observed in the near Chänelgantrisch (see Fig. 3.29) an oblique thrusting top-to-the-NW superimposing an anterior sinistral strike-slip movement, which corresponds to the prolongation of the sinistral strike-slip fault zone of the Schafarnisch area. The thrusting component corresponds exactly to the right lateral displacement direction of the nearby-situated Scheibe fault.

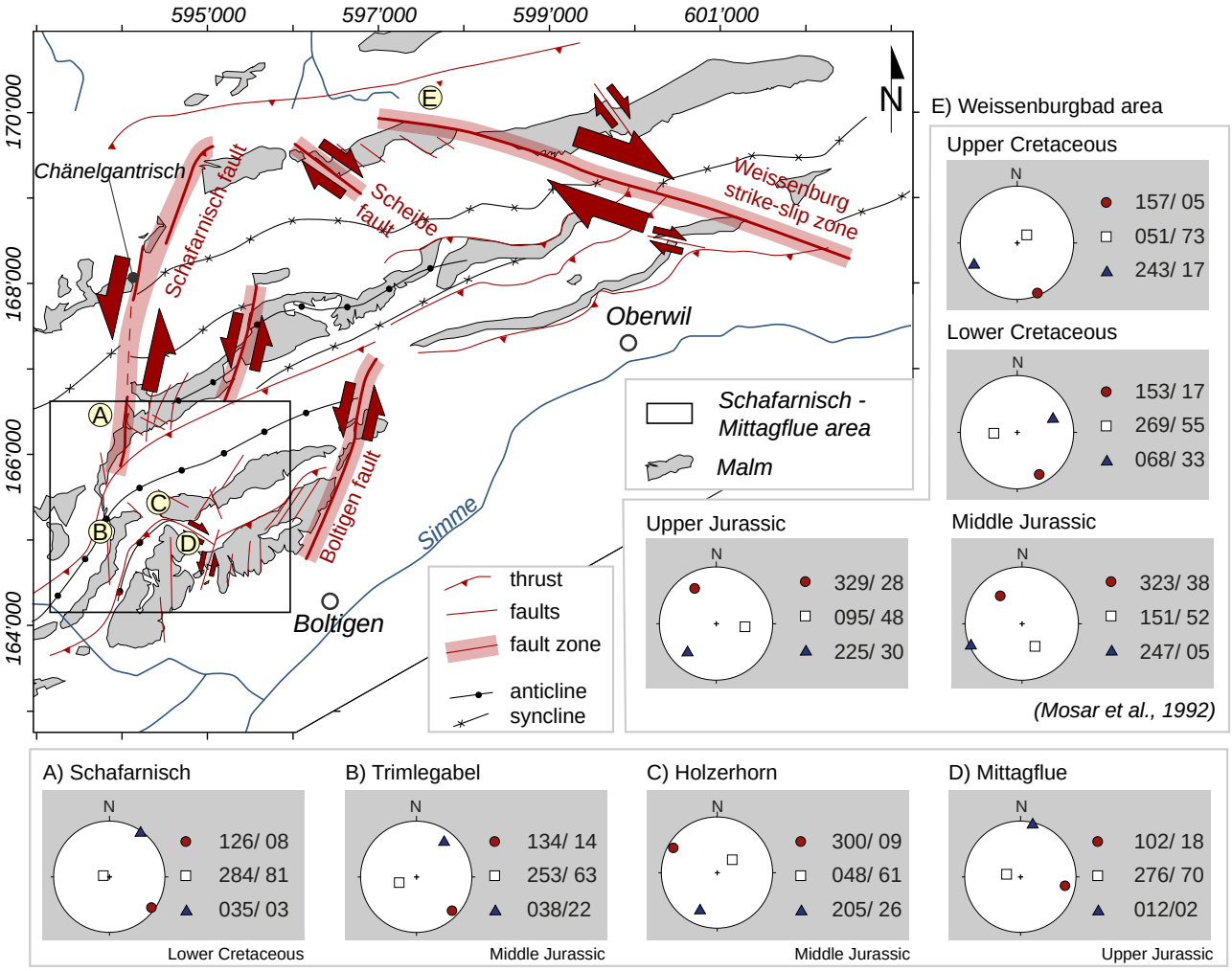

Fig. 3.29: Regional overview highlighting the structural connection between the Weissenburg WNW-ESE oriented dextral strike-slip fault zone and the Schafarnisch-Mittagflue area influenced by a sinistral NNW-SSE oriented strike-slip fault zone) Compilation of the stress tensors resulting from the fault kinematic analysis of the Schafarnisch-Mittagflue area (A-D) and complemented by stress tensors of the Weissenburg area realised by Mosar and Borel (1992).

The regional aspect of the strike-slip environment between Mittagflue-Weissenburg areas shows a close link between two large vertical fault zones that can be considered as conjugated fault zones with an either sinistral or dextral movement (Fig. 3.27). Measured faults within the Schafarnisch area, present a similar trend than the lineaments, but with a slight deviation of a few degrees (15-30°). It seems obvious, that the large-scale fault zones observed in the morphology are not representing one single fault plane, but rather an arrangement of smaller faults interacting with each other within a broad fault zone. The array of measured small-scale faults matches with the Riedel shear model, where most of the measured faults correspond to the Riedel shear R (see Fig. 3.27) within a superordinate fault zone displaying an angle of 15-30° with respect to each other (Fig. 3.27). Measured fractures with a purely sinistral sense of shear (slip inclination <10°) are attributed to the Schafarnisch fault zone, whereas fractures with a purely dextral sense of shear to the Weissenburg fault zone. Comparing their arrangement with the Riedel shear model, the majority of sinistral and dextral faults correspond to Riedel shear R and P (Fig. 3.27).

The presence of the two conjugated fault zones with a NNW-SSE oriented sinistral and a WNW-ESE oriented dextral part is well-known in the entire Préalpes Médianes, as demonstrated by the extensive analysis of fault-slip data. However, in the area Boltigen and Weissenburg, both components of the conjugate system are very pronounced and distinctively visible in the morphology. This can probably be associated to important paleostructures predefining already important weakness zones and to an accentuated bending of the préalpine structures leading to an increasing compression of this region, which is compensated by the development of an advancing triangular structure provoking the formation of tear faults at its boundary.

4.2.3 Gurnigel Nappe - Plasselbschlund

Towards the NW of the Préalpes Médianes, the Gurnigel Nappe extends along the external boundary of the Préalpes klippen belt. Initially, the Gurnigel nappe is associated to the Nappe Supérieure representing the southernmost of the préalpine nappes. Thrusting the Préalpes Médianes and the Breccia nappe during an early stage of nappe transport the Gurnigel part was brought into its present-day position at the front of the Préalpes klippen belt. In contrast to the limestones and marls of the Préalpes Médianes nappes, the Gurnigel nappe consists entirely of turbiditic Flysch sediments. This is one reason, for the interest in a fault kinematic analysis in the Gurnigel nappe; another is the non-existent inherited paleo structures and the presence of slump structures.

The Gurnigel Nappe, but also the more restricted Plasselbschlund area is influenced by some large-scale imbricate thrust planes and duplex structures trending in NE-SW direction, as well as associated NE-SW striking, large-scale synclines and anticlines. Outcrops of the Plasselbschlund area are patchy and therefore complicate the understanding of the continuation of geology and structures. Despite a generally mediocre outcrop quality of the Gurnigel Flysch, the Gérine River, its feeding rivers, as well as some active and abandoned quarries expose a large amount of fractures with nicely developed slip indicators.

Unlike previous studies (PLANCHEREL, 1979) emphasising Mio-Pliocene age of N-S oriented sinistral strike-slip faults, our investigation based on

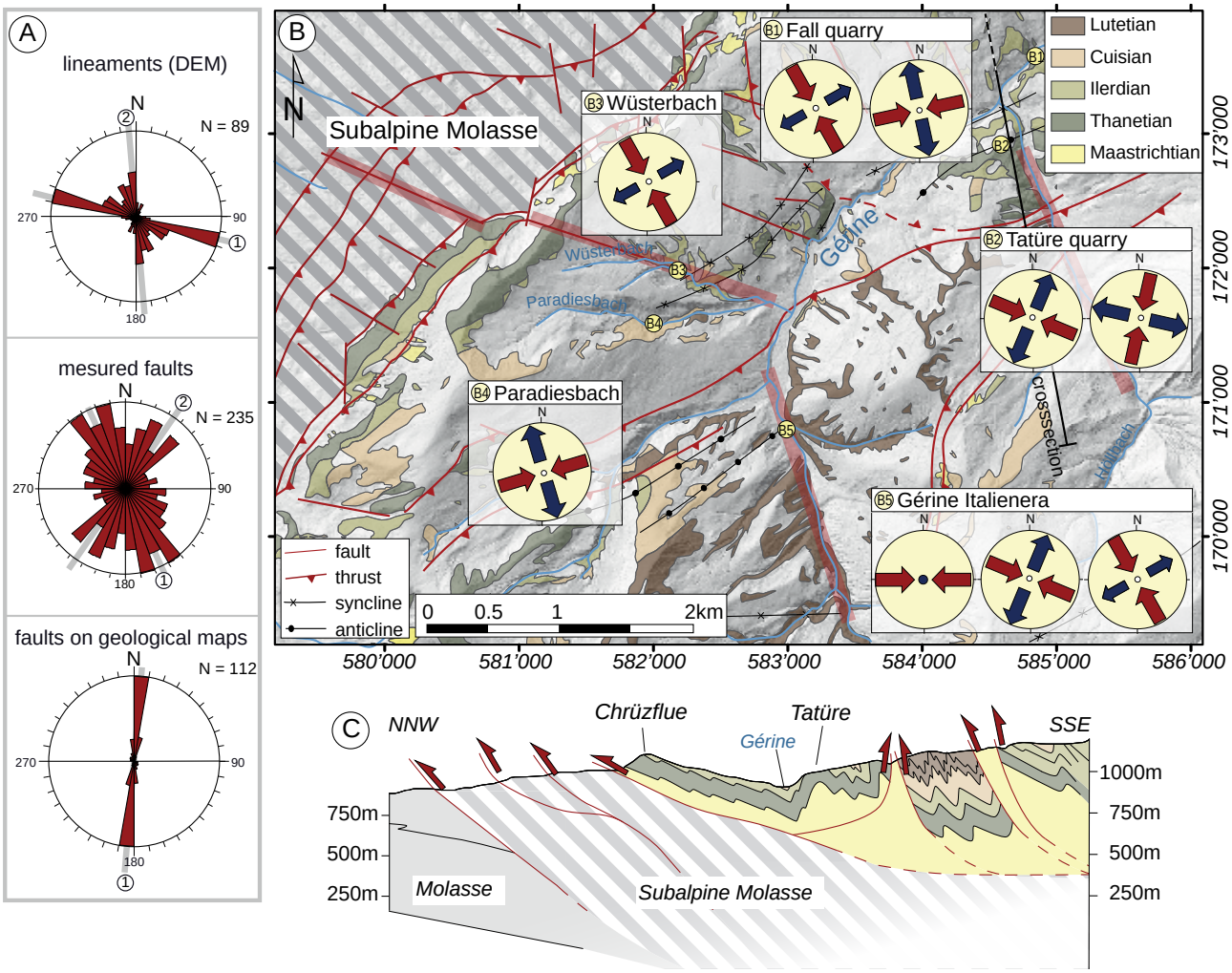

Fig. 3.30: Overview of the Plasselbschlund investigation area. A) Three rose diagrams showing the orientation of lineaments observed on DEMs (top), the trend of the measured fracture planes (centre) and the direction of faults indicated on the geological map (WEIDMANN, 2005). Numbers indicate the main fault sets. B) Structural map of the Plasselbschlund highlighting the major fault zones (thick red lines) and the distribution of the results of paleostress analysis. C) A schematic cross-section oriented in NNW-SSE direction highlights the main structural components of the Gurnigel nappe in the Plasselbschlund area.

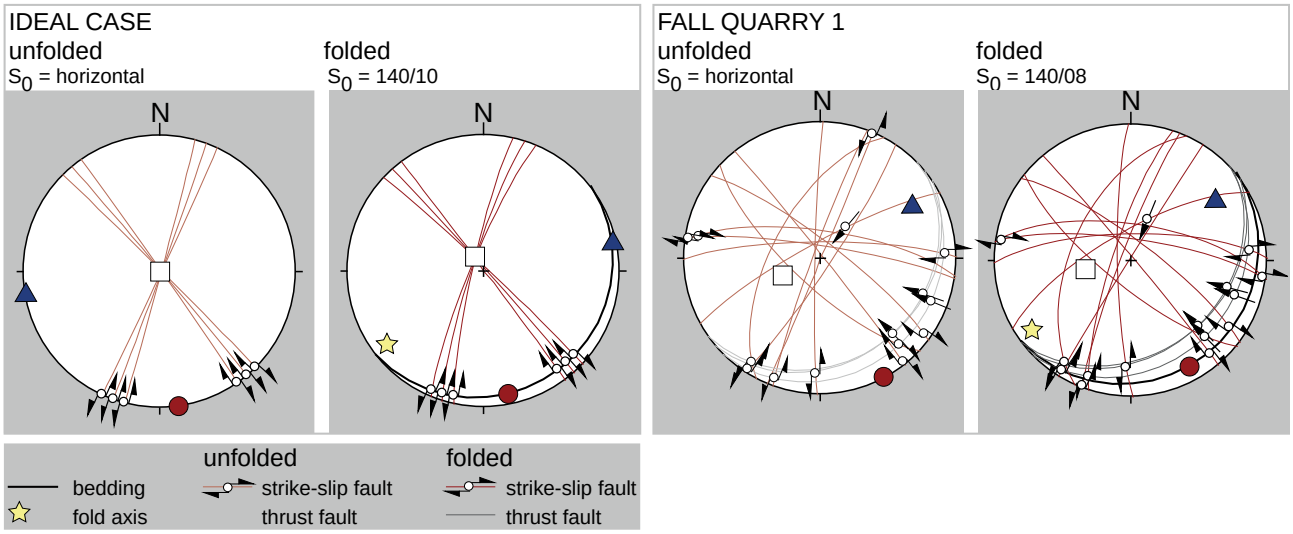

Fig. 3.31: Stereographic projections of an ideal case and the Fall quarry 1 plot explaining the rotation of an original horizontal strike-slip stress regime around the fold axis in the course of a folding of the strata.

an exhaustive analysis of DEMs reveals a predominant WNW-ESE fault orientation and a subordinate N-S fault direction, as indicated on the rose diagrams (Fig. 3.30A). Measured fractures expose a NW-SE and a NE-SW orientation tendency, while every other fault direction is represented in a subordinate way. The discrepancies between the orientation of the measured fractures and the fault lineaments based on DEM analysis are probably related to the scale of observation biased towards a model of N-S oriented sinistral strike-slip faults, as suggested by Plancherel (1979).

Fault-slip measurements were collected at different locations and were finally gathered in five groups (Fig. 3.30B). The heterogeneous dataset required data separation into appropriate subsets to calculate the corresponding stress state.

Fault kinematic analysis show different stress systems mostly linked to a direct influence of an important structural feature in vicinity. As we can see in the Italienera outcrop (Fig. 3.32), the first stress tensor obtained is purely compressional, which can be associated to a thrusting structure nearby. Nevertheless, at every outcrop location a strike-slip stress regime was detected with a dominating compressional stress axis in NW-SE direction.

The stress tensors in the Plasselbschlund area appear less heterogeneous than the one calculated in the Préalpes Médianes, which could possibly be ascribed to the more recent tectonic history of the Gurnigel Flysch deposits (Paleocene/ Eocene) and therefore the absence of ancient extensional paleo structures, as well as to the generally more homogeneous lithology.

Rotating the calculated stress axes and fault planes back into their pre-folding position reveals at least two plots (Fall and Tatüre quarry 1) displaying today a tilted stress regime. The plot of the Fall quarry 1 exposes, in a unfolded position, horizontal striations on strike-slip faults, as well as a subhorizontal compressional and extensional stress axes (Fig. 3.31). The figure 3.31

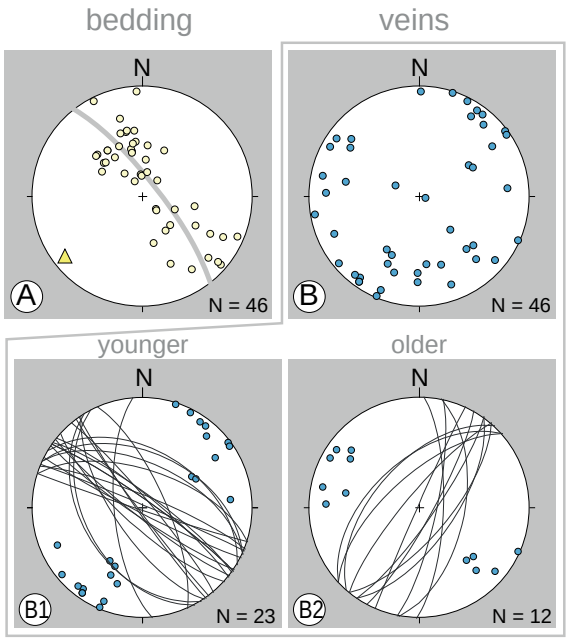

Fig. 3.32: A) Pole projection of the bedding measurements of the Plasselbschlund shows a NW-SE oriented fold orientation (triangle = fold axis). B) Pole projection of the vein measurements in the Plasselbschlund allows a subdivision into two vein sets: the younger vein set B1 oriented perpendicular and B2 oriented parallel to the fold axis.

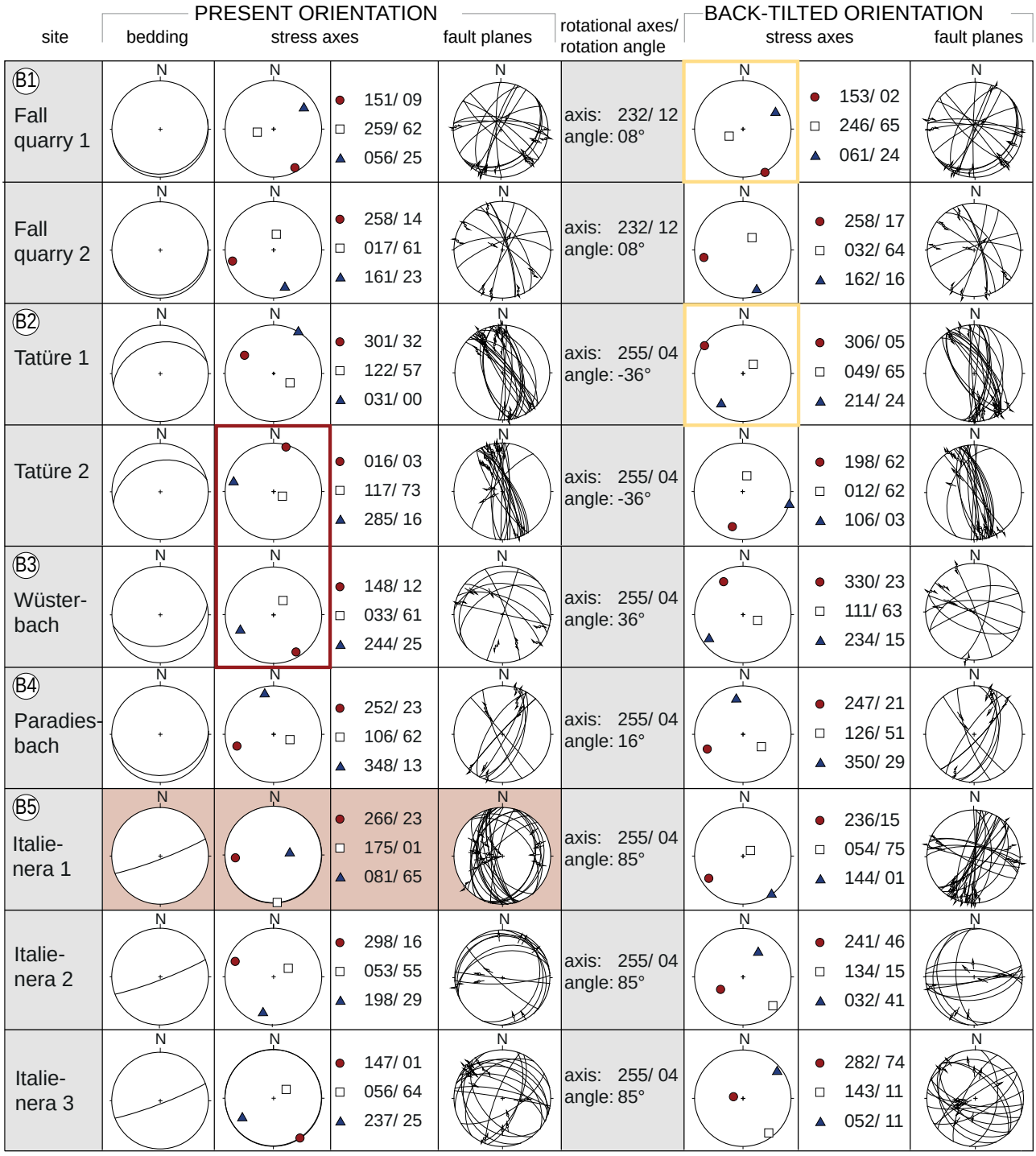

Fig. 3.33: Results of the fault kinematic analysis in the Plasselbschlund area shows a stereographic projection of the average bedding orientation for every measurement site; the projection of the principle stress axes obtained by applying the Right Dihedra method, the orientation of the fault planes and the results of the back tilting procedure. Yellow frames indicate stress regime signify a tilted stress regime after the folding, whereas red frames indicate a late strike-slip stress regime after the folding. The colour coding represents the stress regime: white = strike-slip, blue = extensional and red = compressional. The location of the measure sites B1-B5 are indicated in the previous figure (Fig. 3.31).

displays the ideal case of a set of conjugate strike-slip faults in their original horizontal orientation and their tilted position after a rotation of 10° around the fold axis. The comparison of the ideal case with the Fall quarry 1 plot demonstrates a comparable tilting of the strike-slip striation, as well as the compressional stress axes around the fold axis. Similar observations can be made in the Tatüre quarry 1 plot.

In contrast, two plots indicate a strike-slip stress regime that is clearly post-dating the folding (Tatüre quarry 2 and Wüsterbach; Fig. 3.32). Here, the striation

on strike-slip faults and the compressional stress axes are horizontal in the folded position and become tilted by unfolding the strata. Considering the remaining plots, a gradual tilting of the mostly strike-slip stress regime could be observed, suggesting a strike-slip stress regime acting simultaneously with the folding.

Veins are numerous in the Gurnigel flysch sediments and are at first appearance randomly distributed (Fig. 3.32B). A closer look reveals a prevailing NW-SE vein orientation corresponding to an orientation perpendicular to the general NE-SW fold axes trend (Fig. 3.32B1). Additionally, veins oriented parallel to the fold axes occur frequently (Fig. 3.32B2) corresponding to an extension perpendicular to the folds. Crosscutting relationships among the different veins assign the veins striking NW-SE to the most recent veins. However, based on the common origin, the two fold-related veins B1 and B2 can be considered as developed simultaneously, where vein set B1 could have remained active over a longer time span, since the overall extension direction towards NE-SW coincides with the extensional stress axes of the more recent strike-slip stress system.

4.2.4 Subalpine Molasse - La Roche

Belonging to the Molasse foreland basin, the Subalpine Molasse spreads as a closely spaced, strongly deformed zone along the geographical Alpine front, characterised by imbricated thrust slices dipping towards SE. Within the area of the Préalpes klippen

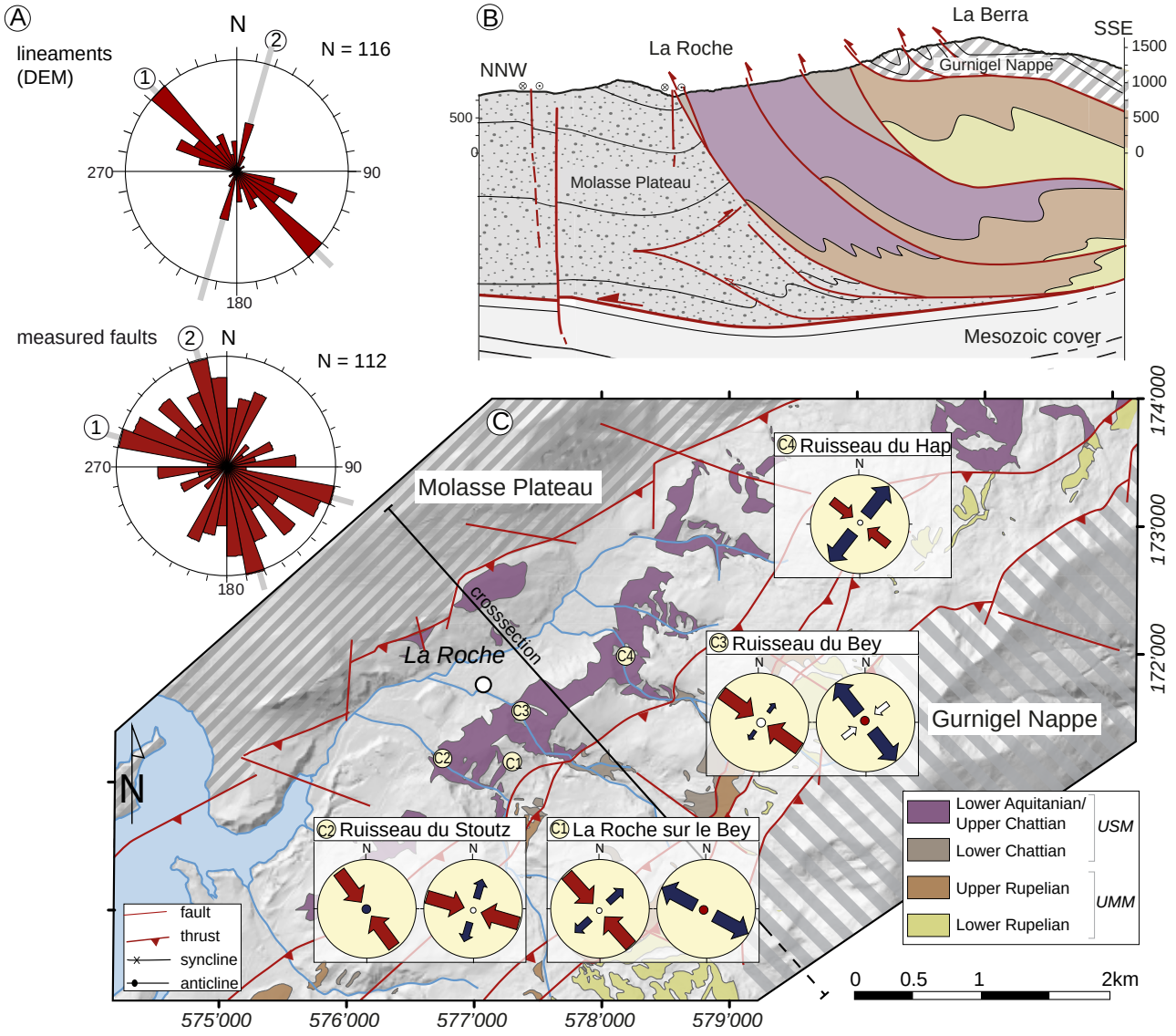

Fig. 3.34: Overview of the structures and results of the fault kinematic analysis in the Subalpine Molasse near La Roche. A) Rose diagrams highlighting the orientation of faults observed on DEMs (above) and the orientation of the measured fractures (below), numbers are indicating the major fault families. B) Cross-section showing the thrust slices of the Subalpine Molasse and their propagation below the préalpine nappe stack (modified after WEIDMANN, 2005) C) Structural map pointing out the main tectonic elements helps to situate the results of the fault kinematic analysis.

belt, the majority of the Subalpine Molasse is overlain by the préalpine nappes.

The Subalpine Molasse in the area of la Roche is affected by three main imbricates and some thrusting digitations at the surface. The majority of the measured fractures belongs to strike-slip faults oriented WNW-ESE (1) with a right lateral and NNW-SSE (2) with a left lateral displacement (Fig. 3.34A, second diagram). Furthermore, steeply inclined reverse faults oriented NNE-SSW thrusting top to the SSE were frequently measured. Only few reverse faults were measured coinciding with the general thrust trend of the Subalpine Molasse.

The regional fault distribution observed on the DEM shows an obvious NW-SE trend and a minor peak in NNE-SSW direction (Fig. 3.34A). The differences between these two diagrams are probably due to different hierarchies of transverse fault zones; so that the measured fractures belong to a subordinate fault system acting under the same stress regime.

Near La Roche, the fault-slip datasets in the Subalpine Molasse expose a heterogeneous array of faults requiring a separation into subsets. The predominant stress regime obtained, corresponds to a strike-slip to oblique compressional stress regime with a NW-SE directed compressional axis. Reverse faults are mainly oriented NE-SW dipping either

site	PRESENT ORIENTATION bedding	stress axes		fault planes	rotational axes/ rotation angle	BACK-TILTED ORIENTATION stress axes		fault planes
C1 Sur le Bey 1			316/ 33 161/ 54 054/ 11		axis: 211/ 19 angle: 54°		030/ 70 158/ 12 251/ 17	
Sur le Bey 2			342/ 66 221/ 12 127/ 19		axis: 211/ 19 angle: 54°		101/ 51 223/ 23 327/ 30	
C2 R. du Stoutz 1			323/ 12 221/ 41 066/ 45		axis: 211/ 19 angle: 54°		005/ 51 194/ 38 099/ 04	
R. du Stoutz 2			284/ 39 118/ 49 020/ 07		axis: 211/ 19 angle: 54°		220/ 84 325/ 02 045/ 06	
C3 R. du Bey 1			316/ 33 161/ 54 054/ 11		axis: 211/ 19 angle: 35°		346/ 62 155/ 27 247/ 06	
R. du Bey 2			125/ 57 225/ 06 319/ 31		axis: 211/ 19 angle: 35°		133/ 24 230/ 16 350/ 59	
C4 R. du Hap			309/ 08 176/ 77 040/ 09		axis: 211/ 19 angle: 51°		338/ 53 144/ 35 239/ 07	

Fig. 3.35: Results of the fault kinematic analysis in the La Roche area shows a stereographic projection of the average bedding orientation for every measurement site; the projection of the principle stress axes obtained by applying the Right Dihedra method, the orientation of the fault planes and the results of the back tilting procedure. Yellow frames indicate stress regime signify a tilted stress regime after the folding, whereas red frames indicate a late strike-slip stress regime after the folding. The colour coding represents the stress regime: white = strike-slip, blue = extensional and red = compressional. The location of the measure sites B1-B4 are indicated in the previous figure (Fig. 3.34.

towards SE or towards NW whereas strike-slip faults, both sinistral and dextral, trend N-S, respectively WNW-ESE (see plots in Fig. 3.34B). Analysis of fault distribution on DEMs and already existing geological maps (WEIDMANN, 2005), as well as field observations indicate a recent strike-slip movement, agreeing with the results of the paleostress analysis. Subordinate stress regimes express mainly an extensional stress regime. Tilting the secondary stress state of the Ruisseau de Bey site backwards, shows how an initial NW-SE oriented compression rotates into an apparent extensional regime due to the tilting of the Molasse Subalpine. This observation suggests that initially, during the formation of the subalpine thrust slices, a compressional NW-SE oriented stress regime was prevailing. Under a more recent strike-slip stress regime, several of these thrust planes were reactivated both with a strike-slip and a compressional movement, as documented by overprinting slickensides.

5 DISCUSSION

Fault-slip analysis in the Préalpes Médianes and the adjacent structural units allow the determination of various fault kinematic stress regimes that are strongly influenced by local tectonic structures. On this account, the mostly heterogeneous data sets yield a dominant stress system related to a local tectonic structure in vicinity, although stress states of regional importance most probably occur but appear in a subordinate way.

The general stress pattern is related to the fold-and-thrust development as revealed by extensional and compressional stress systems, oriented either parallel to the general fold axes trend (extensional) or perpendicular (extensional and compressional) (Fig. 3.12A and B). Additionally, field observations expose a high number of faults related to strike-slip stress regimes with the compressional axes trending NW-SE, as can be seen in Fig. 3.12C.

5.1 POLY- OR SINGLE-PHASE DEFORMATION?

Considering the complex array of fractures, as well as the superimposition of distinct generations of striae on the same fault plane, as well as intersecting and offsetting veins, a poly-phase deformation must be assumed. Structures clearly related to fold development, such as normal faults perpendicular to fold axis (Dent de Broc area), are often reactivated in subsequent stages of deformation (Tzintre quarry outcrop), mostly as strike-slip faults.

It can be shown that some of the subordinate stress regimes were in a tilted position with the result that the calculated stress axes do not correspond to their initial orientation. Rotating the resulting stress state into its pre-folding position generates - only at a few locations - evident indications for a rotated stress regime (Tzintre quarry 2, La Monse, Ruisseau du Bey 2). One reason could be the presence of ancient paleo structures guiding the fold-and-thrust structures and therefore influencing the determination of the prevailing stress system considerably.

From our observations and interpretations, we conclude that at least two deformational phases prevail, one related to the folding and thrusting of the préalpine nappes - expressed mainly by a fold axis parallel or perpendicular extensional stress regimes - and a more recent strike-slip stress regime superimposing the already existing structures developed during the previous deformation phase. Most probably, between these two phases, around 20Ma, another NE-SW oriented extensional phase could have occured, provoked either by a slab-roll back or result from vertical indentation above an uprising tectonic wedge pushed at the front of the front of the Adriatic indenter (SUE and TRICART, 2002).

5.2 CHRONOLOGY OF DEFORMATIONAL PHASES

As reactivation of extensional faults acting before the folding and faulting of the Préalpes erased every useful slip indication for paleostress reconstruction, these ancient deformation phases were not considered here. Fault kinematic analysis and field observation expose two different phases of deformation: one is related to the fold development and the more recent one is related to a strike-slip stress regime with two main shear zones: a N-S oriented sinistral and a WNW-ESE oriented dextral strike-slip zone.

Some of the strike-slip movement is attributed to the fold and thrust development, where they act as tear fault to compensate the displacement caused by lateral termination of fold related thrusts (MOSAR and BOREL, 1992). Their origin is possibly related to structures in the paleogeographic realm (MOSAR et al., 1996). These strike-slip faults are particularly visible in morphology, where they form a broad fault zone with fractures arranged in a Riedel shear pattern.

The more common structural feature corresponding to this deformational phase are normal faults parallel or perpendicular to the fold axes leading to a segmentation of the fold structure as well as thrust planes that are mostly hidden below the anticlines, but crop out in

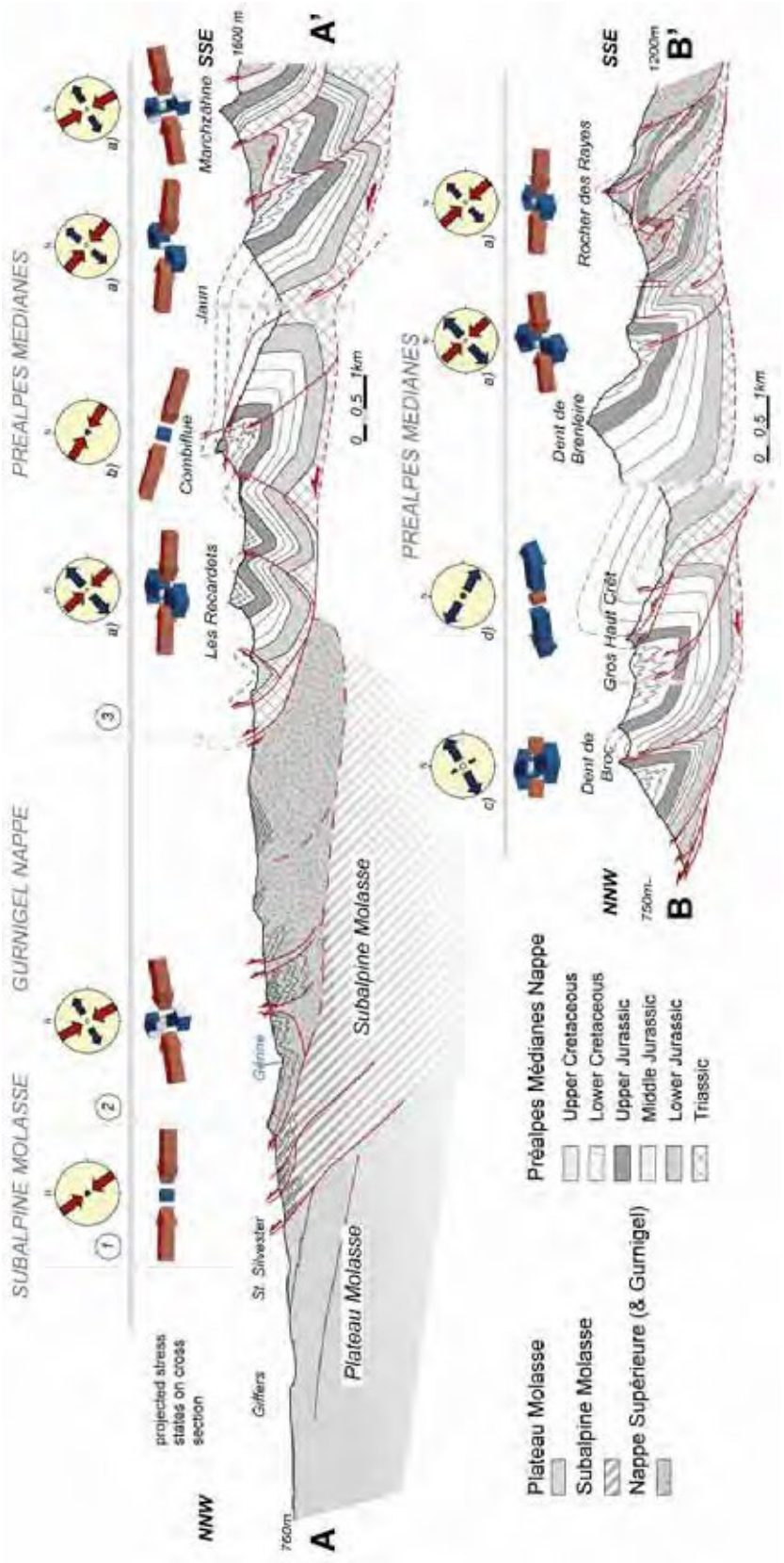

Fig. 3.36: Cross-sections across the Préalpes Médianes and the Gurnigel nappe towards Molasse basin (section line see Fig. 3.10) indicating the characteristic stress regimes along the profile. The plots explaining the orientation and relationship of the different stress axes obtained by the right dihedra method are displayed above, whereas the plots below are projected into the cross-section and rotated if the stress axes are not located in a horizontal plane. 1) Molasse Subalpine: predominant NW-SE oriented compressional or strike-slip compressional regime. 2) Gurnigel nappe: frequent occurrence of strike-slip stress regime with NW-SE trending compressional axes. 3) Préalpes Médianes: ubiquitous appearance of strike-slip stress regime (a), but also compressional (b) and extensional stress regimes (c/d) related to the folding and thrusting of the Préalpes Médianes.

the Schopfenspitz area.

Reactivation of faults developed under the first deformational phase with a strike-slip movement is frequent, as show overprinted slickenfibres (Tzintre quarry). Additionally, dominating occurrence of strike-slip stress regimes throughout the entire investigation area leads us to the assumption that this deformation phase belongs to a more recent structural event. Morphologically, the strike-slip faulting is represented by rather small-scale faults with only minor offsets and is most probably subordinate to two major strike-slip zones in N-S and WNW-ESE direction acting as conjugated regional fault zones under a strike-slip stress system with a NW-SE oriented compression and a NE-SW oriented extension.

The NE-SW trending extensional stress axes of all stress regimes seem to be the most consistent ones throughout the entire investigation area, a permutation of the NW-SE intermediate and the compressional stress axes lead to a change from a extensional to a strike-slip stress regime with a NW-SE directed compressional axis. Permutations of these two stress axes probably occur frequently depending on local movements and structural features (Mosar and Borel, 1992). The relationship among the three stress axes is represented by the stress ratio R and ranging mainly from R = 0.4 to 0.8 (Tab. 3.2), considering a relatively robust σ_3 stress axis, so that a permutation of σ_1 and σ_2 stress axes is favoured.

5.3 Different Behaviour under Stress Exposure among Distinct Structural Units

As the origin and the evolution of the discussed structural units of the Préalpes klippen belt differ considerably, they do not generate identical fracture patterns under the same stress exposure (Fig. 3.36). The Préalpes Médianes are characterised by the existence of inherited normal fault structures related to the rifting of the alpine Tethys. This ancient fault system and the associated variations in sedimentation have mainly influenced their folding and thrusting behaviour during the emplacement. Reactivation of the paleofaults as well as the creation of a fault system related to the fold and thrust development are the characteristic features during the nappe transport and emplacement. Within the Préalpes Médianes, the influence of the paleo structures is expressed differently. The Lower Cretaceous layers that are less affected by paleofaults react differently than the Jurassic layers, whose fracture pattern is more influenced by the presence of inherited normal faults (Fig. 3.25). The more recent strike-slip stress regime - occurring also in the Gurnigel nappe and the Subalpine Molasse - is typically imposed on the structural heritage of the previous deformational phases related to the rifting and to the préalpine nappe transport. For this reason, the resulting stress tensors are most likely affected by the presence of already existing fault planes. Additionally, the influence of local structures associated to the structural heritage should not be neglected.

The structural background of the Gurnigel nappe is mostly related to the turbiditic nature of the sediments and their transport on top of the Préalpes Médianes. Observations in the Gurnigel nappe showed an influence of large-scale fold and thrust structure (Tatüre quarry), but generally a strike-slip stress system prevails with a large amount of probably newly formed NNW-SSE oriented fractures. Furthermore, during a younger deformation phase, the Préalpes Médianes thrust the Gurnigel nappe, in such a way that the Gurnigel deposits were dragged into an overturned position (De Kaenel et al., 1989). It was however impossible to detect this kind of rotation in the observed fracture pattern, presumably because the faulting postdates the overturning.

The Subalpine Molasse, as the youngest of the discussed structural units, exposes a less multiphase fracture pattern that is mostly linked to the thrusting of the Subalpine imbricates and again to the recent strike-slip stress regime. Fractures are mainly NE-SW oriented thrust planes or NNW-SSE and WNW-ESE oriented strike-slip faults.

Furthermore, after nappe emplacement the entire nappe pile (Mosar et al., 1996) as well as the underlying Ultrahelvetics (Jeanbourquin et al., 1992) were affected by out-of-sequence thrusts which can most probably be linked to the development of imbricates in the autochthonous basement (Mosar, 1999). The analysed stress system does not clearly reflect the out-of-sequence thrusting (except in vicinity of the Schopfenspitz fault), which can probably be associated to the restricted occurrence of these thrust faults along important paleogeographic weakness zones, as for instance the limit of the Préalpes Médianes Plastiques and Rigides (Borel and Mosar, 2000).

5.4 Seismicity and Recent Stress Field

The distribution of seismic activity in the canton of Fribourg shows a conspicuous N-S oriented alignment in the east of Fribourg, where focal mechanisms expose a left lateral strike-slip movement (Fig. 3.37). Whether this zone, known as the Fribourg zone, is related to one single left-lateral strike-slip fault (Kastrup, 2002; Kastrup et al., 2007) or to an extended fault zone

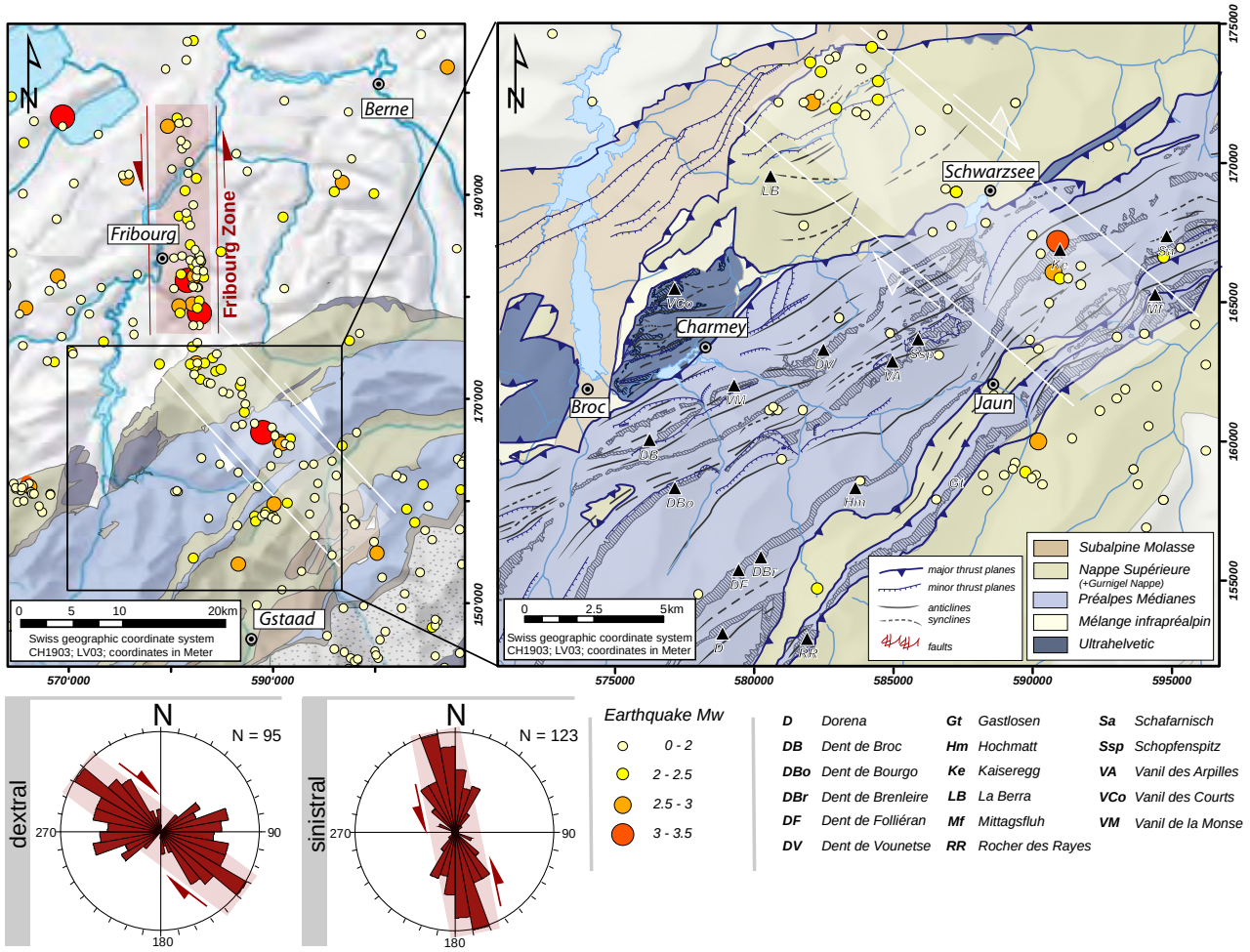

Fig. 3.37: Maps of seismicity showing on the left an overview of the distribution of instrumentally measured earthquakes since 1975 including the N-S alignment, known as Fribourg zone. On the right hand side, a more detailed map situates the earthquakes into their structural context among the préalpine nappes: Earthquakes are clustered at the external boundary of the Gurnigel Nappe, but also in the area of the Kaiseregg and near Jaunpass. A NW-SE alignment of seismic events can be observed from Plasselb via Kaiseregg towards Boltigen, which agrees with the NW-SE oriented dextral strike-slip faults of the most recent deformation phase. Rose diagrams indicate the spatial distribution of every dextral and sinistral strike-slip faults of the latest strike-slip regime of the study area. The earthquakes are based on the ECOS database of the Swiss Seismological Survey and are situated mostly in the crystalline basement.

hosting several small-scale faults (Mosar, 2006) is still subject of discussion and is beyond the scope of this study. In the Préalpes, the recorded earthquakes of minor importance are even more concentrated in certain zones. At the frontal thrust of the Gurnigel nappe, an accumulation of seismic activity can be observed, especially in the area near Plasselb, but also in vicinity to Bulle. Fewer earthquakes were registered near Jaunpass at the boundary of the Nappe Supérieure and the Préalpes Médianes Nappe, whereas another accumulation of earthquakes can be observed in the Kaiseregg area.

Similar to the Fribourg zone, another alignment of earthquakes in NW-SE direction can be recognised, touching the Gurnigel Nappe as well as the Préalpes Médianes Plastiques and Rigides. It remains elusive to establish a connection to a major structural feature generating these earthquakes, however, a conspicuous consistency to the prevailing NW-SE oriented right-lateral strike-slips can be observed (see first rose diagram on Fig. 3.37).

5.5 Integration into the Regional Stress Field

The style of faulting and the orientation of the stress field vary considerably along and across the Alps. The Northern Alpine Foreland shows predominant strike-slip mechanisms with normal faulting component and some shallow thrust mechanism reflecting a large-scale convergence of Africa and continental Europe, with a maximum horizontal stress axis that rotates from east to west and remains perpendicular to the Alpine arc (Kastrup et al., 2004). Conjugate strike-slip

fault zones are common in the Jura mountains and the Molasse basin (Delacou et al., 2004; Kastrup et al., 2007; Kastrup et al., 2004; Mosar and Borel, 1992) with sinistral faults oriented N-S in the northern part (Fribourg zone) rotating towards a NW-SE fault zone in the western part of the Northern Alpine Foreland (Vuache fault zone). Their corresponding dextral strike-slip faults occur less frequent but turn in the same anticlockwise direction from north to south from a WNW-ESE (La Lance fault) to NE-SW orientation. This pattern of conjugated faults can be detected in the Préalpes klippen belt as well (Delacou et al., 2004; Mosar and Borel, 1992). Both, fault-slip analyses, carried out within the scope of this study, and the interpretation of large-scale faults identified on DEMs, expose conjugate fault systems related to a more recent deformation phase. They expose a similar WNW-ESE orientation for the dextral and a N-S orientation for the sinistral fault zones. In the Préalpes Médianes, in the Weissenburg area (Fig. 3.38), already existing weakness zones were reactivated forming a broad fault zone. Measured fractures show a slight angular

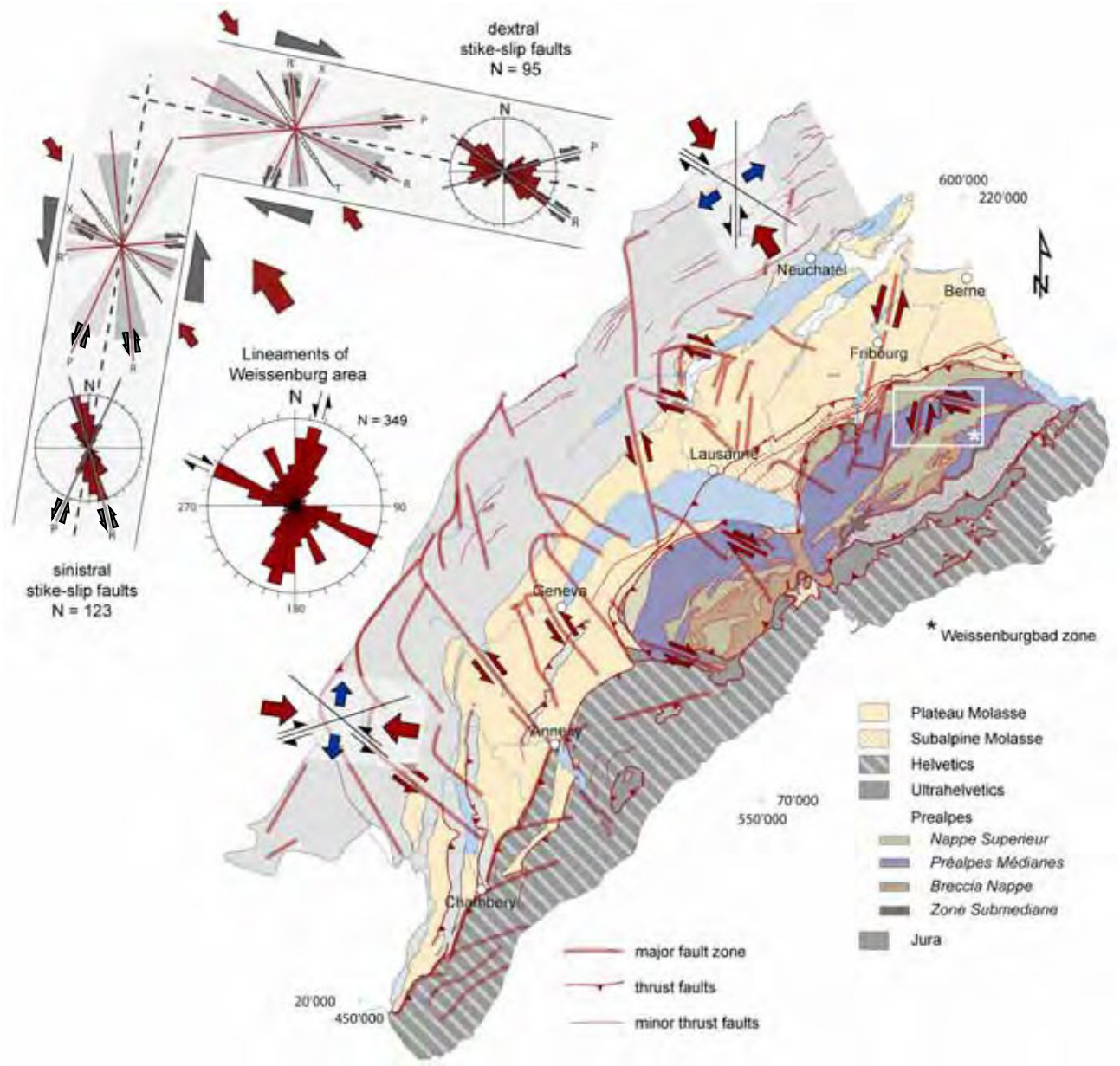

Fig. 3.38: Simplified tectonic map of the Western Alpine foreland, including the Jura mountains, the Molasse basin, and the Préalpes. Major fault zones are highlighted with the broad, thicker red lines, and where known, the sense of movement of the fault zone is indicated. The fault zones are arranged in a conspicuous conjugate pattern, rotating along strike of the Alpine arc, so that the compressional axes remain perpendicular to latter. In the Préalpes the same pattern of conjugated fault zones was detected, as for instance in the Weissenburg area (see rose diagram of the orientation of lineaments recorded in the Weissenburg area). Measured transcurrent fractures of a recent strike-slip stress regime that are most probably subordinate to the general WNW-ESE and NNE-SSW oriented fault zones where they are arranged as Riedel shear faults.

deviation (15-30°) to the general trend of the préalpine fault zones (Fig. 3.38). In an attempted explanation, the recent strike-slip faults are considered to belong to a subordinate fault system in the two major conjugated fault zones of the Weissenburg area. The fracture orientation agrees with a Riedel type fault arrangement, corresponding to the R and P fault direction, whereas the P-shears normally develops in a later stage of the shear zone evolution. As sinistral strike-slip faults are prevailing in a sinistral fault zone, these fractures were attributed to the sinistral Riedel system; the same applies for dextral fractures in dextral shear zone. The faults and lineaments localised on DEMs correspond to the main shear zones, as they coincide accurately with the WNW-ESE and NNE-SSW oriented conjugated shear zones (Fig. 3.38).

This conjugated strike-slip system is considered as relatively recent, post-dating the Jura folding and most possibly still active today indicated by earthquake focal mechanisms. However, as no accurate age could be attributed to the fault-slip data measured in the field a comparison with seismicity has to be handled with care.

6 Conclusion

Fault kinematic analysis and paleostress reconstruction show a polyphase deformation history characterised by fault and fracture patterns originating before, during and after the emplacement of the préalpine nappes onto the alpine foreland. The study of overprinted slickenfibres as well as of intersecting veins shows that reactivation of fault planes occur frequently. This explains the heterogeneous datasets generated by mostly two or three different stress regimes. Structures pre-dating the alpine collision are mainly expressed by large-scale normal faults provoking thickness changes in sedimentation, which thereby influence the structural style during nappe transport. As slip indicators of this period are hardly recognisable, paleostress reconstruction focuses on the deformation during and after the emplacement of the préalpine Nappe. Several stress regimes are related to the fold development, as for example extensional stress regimes, either perpendicular or parallel to the fold axes, or compressional stress regimes with a maximum compressional axis oriented NW-SE. The discussed outcrops in the Tzintre-Le Brésil area are affected by the presence of different fault families generated during the thrusting and folding of the Préalpes Médianes: normal faults parallel, perpendicular, or diagonal to the fold axis, as well as thrust faults responsible for the folding (Fig. 3.39-1). In the Schafarnisch-Mittagsfluh area, at the Erbetlaub/ Holzerhorn outcrop, a similar fold axis parallel extension provoked the development of a horst-like structure in between the Holzerhorn and the Trimlegabel (Fig. 3.39-2). Fold-related faulting strongly affects the Préalpes Médianes as revealed by the important segmentation of the mountain chains built up of massive Upper Jurassic limestones.

However, a detailed study of fault kinematic indicators shows a strike-slip reactivation of the fold-related fault planes. In the Tzintre quarry outcrop, ancient thrust faults were overprinted by a dextral strike-slip movement, whereas normal faults perpendicular to the fold axis were reactivated with a sinistral sense of shear. Similar observations were made in other analysed sites.

Within the entire investigation area, the majority of the observed stress regimes are strike-slip stress regimes with a NW-SE oriented compressional and a NE-SW oriented extensional stress axis. Their fracture pattern is mostly represented as N-S oriented sinistral and NW-SE oriented dextral strike-slip faults, whereby in the Préalpes Médianes, these faults are rarely newly developed, but rather reusing already existing weakness zones.

In the Schafarnisch-Mittagsfluh area, sinistral and dextral strike-slip faults are more pronounced. This is related to two important conjugate fault zones, the NNW-SSE oriented sinistral Schafarnisch strike-slip fault zone, and the dextral Weissenburg strike-slip fault zone. It is proposed that these fault zones are originally related to tear faults resulting of a differential advancing of thrust planes during the nappe transport, with two important fault zones developing. Within these morphologically clearly distinct fault zones, fractures develop acting as Riedel shears, mainly R and R' and in a later stage also P shears. The kinematic analysis of these fractures proves a recent strike-slip stress regime (Fig. 3.39-2).

In the Gurnigel nappe, the influence of the structural inheritance is less pronounced. However, strike-slip faults, both in the unfolded and folded position, indicate a persistent stress regime since the folding of the Gurnigel nappe (Fig. 3.39-3).

The fault-kinematic analysis in the Subalpine Molasse results in a compressional strike-slip stress regime exposing both a thrusting and a strike-slip component (Fig. 3.39-4).

The ubiquitous prevailing strike-slip stress regime fits into the regional stress field, which is characterised by developing conjugate fault zones oriented WNW-ESE for dextral and NNE-SSW for sinistral fault zones.

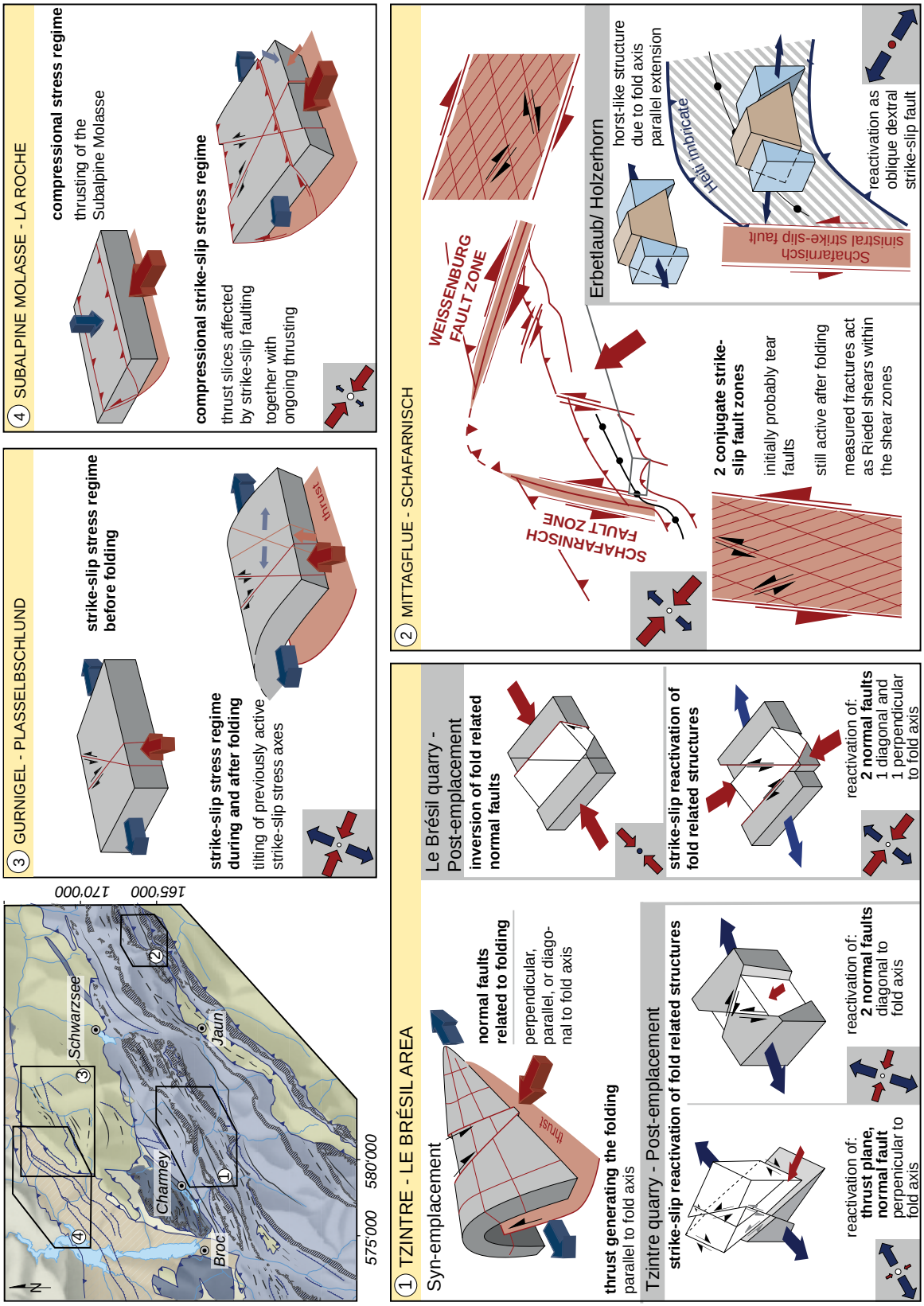

Fig. 3.39: Overview of the results of the paleostress analysis in the zones of major interests. 1) The Tzintre - Le Brésil area is highly influenced by the presence of fold related structures that were reactivated under a strike-slip stress regime. 2) The stress system of the Schafarnisch-Mittagsfluh area is dominated by the presence of two important conjugate strike-slip fault zones: the sinistral Schafarnisch and the dextral Weissenburg fault zone wherein the measured fractures act as Riedel shear faults. A horst-like structure in the Erbetlaub-Holzerhorn area proves a fold axis parallel extension that turned into a dextral oblique extension due to the influence of the nearby imbricates and the Schafarnisch fault zone. 3) The Gurnigel nappe in the Plasselbschlund area is strongly affected by a strike-slip stress system, whereas 4) the Subalpine Molasse in the La Roche area shows the influence of a compressional strike-slip stress system resulting in thrusts and strike-slip faults.

4 - 3D Modelling of the Préalpes

ABSTRACT

The complex structure of the allochthonous nappe stack of the Préalpes Romandes, as well as the fold-and-thrust structures of the Préalpes Médianes were represented as five 3D models generated by the 3D GeoModeller Editeur Géologique© program, developed by the BRGM (Bureau de Recherches Géologiques et Minières, France) and the Australian company Intrepid Geophysics. Within the general 3D model of the préalpine nappes, a compilation of existing cross-sections and seismic lines, as well as the crystalline basement topography help to constrain the model, but still leave much room for interpretation. Therefore, the presented 3D visualisation is not a reproduction of unknown structures at depth, but rather gives a suggestion of a possible solution taking into account available data. The detailed 3D models of the Dent de Broc, the Gros Haut Crêt, the Schopfenspitz and the Schafarnisch-Mittagflue region intend to represent the characteristic structures of these areas, such as fault-related folds, normal faults perpendicular to the fold axis, out-of-sequence faults and thrust sheets of the Heiti and Gastlosen imbricates.

1 Introduction

3D visualisations of complex geological structures gain more and more in importance today, since they allow a better insight into the spatial continuation of the geology at depth than common 2D cross-sections. With the aid of a 3D model, even a complicated structural context can be explained most plausibly to a non-geologist; for this reason, 3D models serve as basis within different domains, such as civil engineering, risk management of natural disasters, as well as the organisation of energy and natural resources. The aim of the generated 3D models in the Préalpes Romandes is the representation of the complex préalpine nappe structure, as well as the detailed visualisation of areas of major structural interest. With the 3D modelling, it became possible to constrain vertical structures by interpolating surface data, as well as data from geological cross-sections applying basic rules of conservation of volume (non-eroded stratigraphic layers have a constant thickness throughout their appearance), because information of structures at depth are scarce. Additionally, the 3D models were highly useful as validation of the existing geological maps, cross-sections, our interpretations as well as validation of the consistency amongst these different data inputs. However, the established 3D models do not intend to give a precise reproduction of unknown structures at depth, but rather give a suggestion of a possible solution taking into account available data and personal interpretations.

Using the 3D GeoModeller Editeur Géologique© program, developed by the BRGM (Bureau de Recherches Géologiques et Minières, France) and the Australian company Intrepid Geophysics, five 3D models were constructed; one explaining the general nappe structure of the Préalpes Romandes and the four others outlining the detailed structures of areas of major interest. It is beyond the scope of this study to construct analytical models to unfold the préalpine nappe structure and their geological layers; especially because the structures at depth as well as the original basin width are still poorly constrained by existing observational data. For that reason, the focus of these 3D models lies mainly in the representation of the interpreted structures serving for a better understanding of the complex structures, but also as base volume for hydrogeological analysis.

The Préalpes klippen, built up by a series of tectonic nappes detached from their Briançonnais origin are situated along the northern front of the Swiss and the

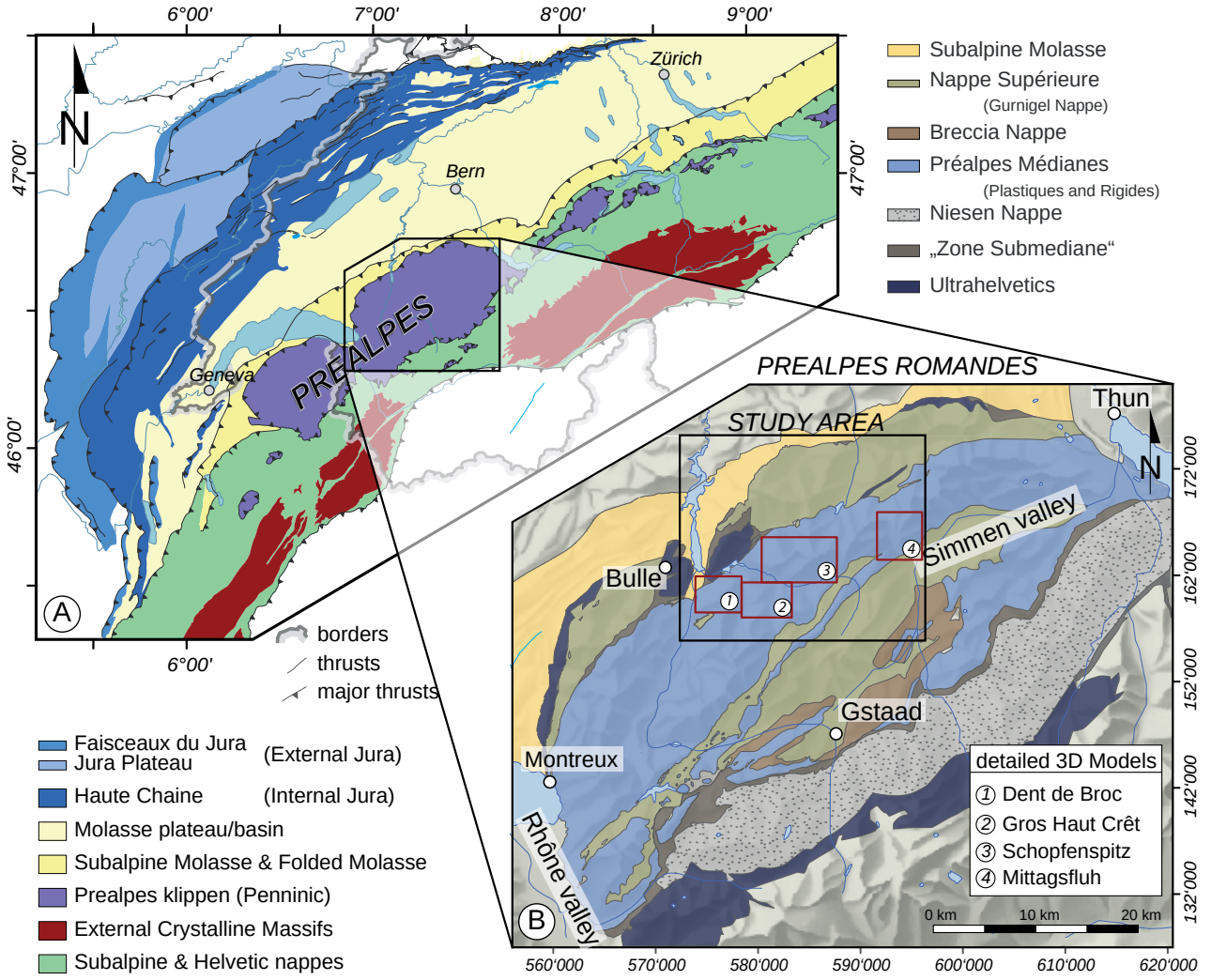

Fig. 4.1: Location of the Préalpes klippen in the context of the Western Alpine orogen. A) simplified tectonic map of the Western Alps highlighting the large-scale structural units including the Préalpes klippen located along the northern front of the Swiss and the French Alps and NW of the Helvetic nappes and the External Crystalline Massifs (modified after SCHLUNEGGER and MOSAR, 2010). The Préalpes klippen are characterised by two large lobes: the Préalpes du Chablais SW and the Préalpes Romandes NE of the Rhône valley. B) Structural map of the Préalpes Romandes modified after Caron (1973). The allochthonous préalpine nappes are piled up in the following order (from the top to bottom): a) Nappe Supérieure, b) Breccia Nappe, c) Préalpes Médianes and d) Niesen Nappe (existing only in the Préalpes Romandes) and two mélange zones developed during the nappe transport: the Ultrahelvetics and the "Zone Submédiane". The position of the four detailed 3D models is indicated by red rectangles. The less detailed 3D model covering the entire préalpine nappe structure corresponds to the limits of the Préalpes Romandes.

French Alps, in the NW of the Helvetic nappes and the External Crystalline Massifs (Fig. 4.1).

Previous studies of the Préalpes klippen focussed mainly on geology and structures at the surface, only a few, more recent studies involve interpretations of the structures at depth. Therefore, the general 3D model of the Préalpes Romandes is only constrained by few investigations (BOREL and MOSAR, 2000; CARON, 1973; ERARD, 1999; MOSAR, 1991; MOSAR, 1994; PFIFFNER et al., 1997b; WISSING and PFIFFNER, 2002). Detailed geological maps and cross-sections, which were consulted to reconstruct the four detailed 3D models, are: Andrey (1974), Bovet (1990), Favre (1984), Fuchs (2003), Mandia (1984), Spicher (1980), Pasquier (2005), Wissing and Pfiffner (2002).

2 METHODS

The five 3D models generated within this study were calculated with 3D GeoModeller Editeur Géologique©, which proves to be highly suitable for modelling the complex structures of the Préalpes klippen. Unlike most common 3D modelling programs designed for the requirements of the Oil industry (mostly disposing of cost intensive seismic analyses or multiple deep boreholes), 3D GeoModeller enables the construction of volumetric coherent geological models based on more available common geological data, such as maps, digital terrain model (DTM), cross-sections, orientation data, and boreholes. Additionally, it is possible to introduce the geologists' interpretation to optimise the calculated 3D output (CHILÈS et al., 2004).

Merely by taking contact points of delimitation of the boundaries of geological units and orientation data (bedding measurements), a simple, but coherent 3D model can be constructed by creating a potential field to interpolate the structural trend in between known contact points (CALCAGNO et al., 2008). The potential field method defines geological interfaces as an iso-surface of a scalar field represented in 3D. A unique solution for the 3D geometry of the interfaces between formations is obtained by assuming that contact points of each geological delimitation lie on a potential field surface and that orientation data are orthogonal to a local tangential plane to the potential field (Fig. 4.2) (CHILÈS et al., 2004; MCINERNEY et al., 2005). Since, in the field, geological orientation data hardly coincides exactly with geological contacts, the potential field method is of considerable interest for geologists having no access to seismic lines or borehole data.

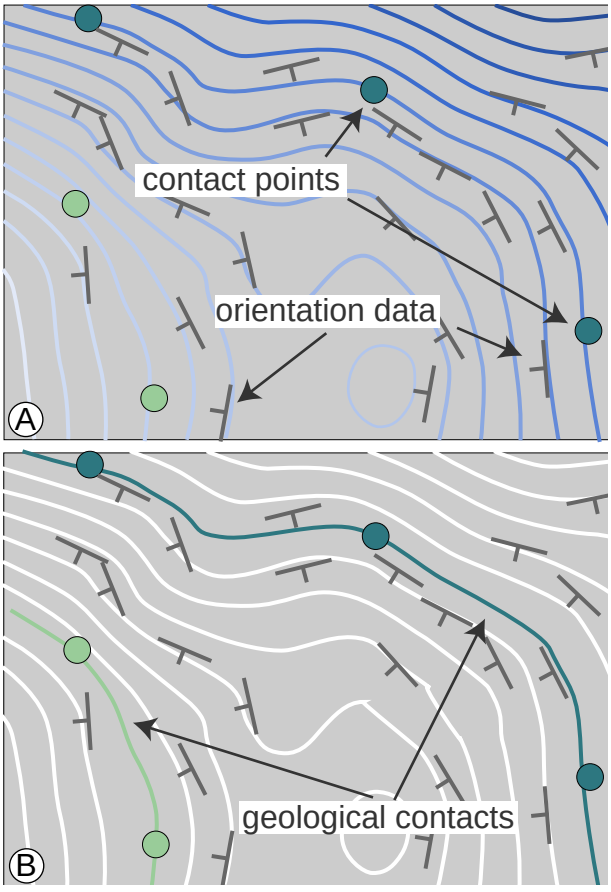

Fig. 4.2: A) map showing known geological contacts (dark green and light green dots) belonging to a single structural series as well as orientation data. The potential field has been computed by taking into account all orientation data. B) Two iso-potentials are plotted, so that they pass through the two sets of geological contact points. The interpolator has proposed a geologic model which honours the contact data point and takes full account of the orientation data, both above and below the geological contacts (MCINERNEY et al.).

This method is actually very close to classical geological thinking, since both attempt to reproduce a geological drawing by taking into account the given field data, geological contacts, dip measurement and the topography. The situation created by the potential field interpolation method is frequently attained by many geological situations, thus iso-potential lines/ surfaces follow geological structures as for example the stratigraphic horizons in sedimentary rocks, the internal structures of igneous rocks or foliations in metamorphic terrains (MCINERNEY et al.).

Furthermore, the potential field approach of the 3D GeoModeller program supports the detection of uncertainties or errors on already existing maps and points out where structural discontinuities must be affecting the geological strata.

3 3D Modelling of the Préalpine Nappes

3.1 Introduction

The aim of this 3D-modelling approach is to bring light into the complex structure of the préalpine nappe stack, situated as klippen along the northern front of the Swiss and the French Alps between the Mythen near Lucerne (Switzerland) to the Klippe des Annes near Annecy (France). The modelling area is limited to the Préalpes Romandes - one of the two major prealpine lobes - extending from the east of the Rhône valley to the Lake Thun (Xmin: 556’000 / Xmax: 620’500 and Ymin: 127’000 / Ymax: 180’000; Swiss geographic coordinate system, CH1903).

A 3D-modelling approach allows not only the generation of the préalpine nappes in 3D, but also the validation of different data available of this area: DEM, geological maps, cross-sections and seismic profiles. As no deep borehole data exists and only few seismic lines transect the Préalpes Romandes, most geological cross-sections are based on surface interpretations and geometrical consistencies of the known stratigraphic layers. For that reason, as far as interpretations of the deeper structures of the préalpine nappes are concerned, they are highly influenced by interpretative concepts leading to strongly differing cross-sections throughout the Préalpes klippen (Fig. 4.3). Within a 3D model based on these geological cross-sections, different interpretation approaches can be easily localised and discussed in context of the general trend of the 3D model. Even respecting the scarce restricting data: the top of crystalline basement heights (MOSAR, 1991; PFIFFNER et al., 1997c), seismic

lines (MOSAR et al., 1996; PFIFFNER et al., 1997b; STECK et al., 1997), and the superficial geological cross-sections, wide-ranging interpretational liberties are given. Hence the 3D model presented here corresponds to a possible conceptual solution amongst other plausible interpretations.

Although the present day position of the préalpine nappes is in the NW of the Helvetics, their paleogeographic origin is located in the Sub-Briançonnais and Briançonnais sedimentation realm. During the nappe transport, the préalpine nappe obtained their imbricate structure by thrusting and decoupling of each other in such way that originally adjacent nappes were separated and emplaced far apart from each other (Fig. 4.4). Therefore, the knowledge of the nappe structure and their origin is inevitable; and a short introduction to the different characteristics and their origin is given in the following chapter.

3.1.1 Geological and structural setting

The nappe transport from its Briançonnais homeland until its present-day position at the northern-western front of the Alps occurred during the Alpine orogeny and led to the thrusting of the préalpine klippen on top of the Autochthonous and Subalpine Molasse to the NW and on the Helvetic nappes to the SE (Fig. 4.3). A brief description of every nappe unit is given below, following their present day position from the top nappe to the bottom.

Originating in the Piemont domain, the Nappe Supérieure subdivided into four subunits, the Simmen, Gets, Dranse and Gurnigel nappe, is the southernmost nappe of the préalpine nappes. Early Flysch deposits of Santonian age (83 Ma) (WICHT, 1984)/ Maastrichtian (70Ma) (CARON, 1972, 1976; CARON et al., 1980a) indicate an initial structuring of the Nappe Supérieure, as well as the beginning of the décollement (STAMPFLI and MARTHALER, 1990). The Nappe Supérieure thrusts the Breccia and Préalpes Médianes Nappes around 42 Ma (CARON, 1966, 1972; CARON et al., 1980a) (Fig. 4.4A), and continues moving above the Préalpes Médianes Plastiques until the external front of the Préalpes klippen, where they thrust the Subalpine Molasse. In a final deformational stage, the external part of the Nappe Supérieure - the Gurnigel Nappe - is thrust by the Préalpes Médianes Plastiques probably due to reactivation of normal or reverse faults (Fig. 4.4F).

The paleogeographic origin of the Breccia nappe lies at the boundary of the southern briançonnais passive margin, representing the transition of the continental crust of the micro-continent and the Piemont ocean (DALL'AGNOLO, 2000). The Breccia nappe loaded with the Nappe Supérieure thrusts the rear part of Préalpes Médianes at the Bartonian (41-40 Ma) and is transported passively together with the Préalpes Médianes (MOSAR, 1991). In the Chablais Préalpes, the Breccia Nappe is widely distributed, whereas in the Préalpes Romandes they remain only as three isolated synclines plunging to the NW (Fig. 4.4B/C). The contact between the Breccia nappe and the underlying Préalpes Médianes is disharmonically folded, explaining an independent folding at the beginning of the folding events (JEANNET, 1922).

The paleogeographic origin of the Préalpes Médianes was in the Briançonnais and Sub-Briançonnais sedimentation realm (CARON, 1972, 1973; TRÜMPY, 1960, 1980). In the Préalpes Romandes, the Préalpes Médianes Nappe is the largest and best exposed of all the préalpine nappes. Related to the changing structural style due to paleogeographic differences, the Préalpes Médianes are subdivided into the Préalpes Médianes Plastiques in the external part characterised by a fold-dominated structural style and into the Préalpes Médianes Rigides marked by important imbricate structures in the trailing part (LUGEON and GAGNEBIN, 1941). The Gastlosen range is situated in between the Préalpes Médianes Plastiques and Préalpes Médianes Rigides, consisting therefore of intermediate characteristics. (BAUD, 1972; LUGEON and GAGNEBIN, 1941; MOSAR et al., 1996; PLANCHEREL, 1979).

The Préalpes Médianes Nappe was transported over a distance exceeding 100km (SCHARDT, 1893b) on a basal décollement of evaporites located at the base of middle and Late Triassic. The transport over the crystalline massifs took place rather passively on top of the Helvetic nappes from the Priabonien (39 Ma) to the Burdigalian (± 18 Ma), until today (MOSAR, 1991). The Préalpes Médianes reach the outer front of the Helvetic estimated by the conglomerates of the Mont Pélérin (around the Chattian (30Ma) originating from the Nappe Supérieure (LATELTIN, 1988; TRÜMPY and BERSIER, 1954) (Fig. 4.4D). During this final stage of deformation, the external part of the Préalpes Médianes thrust the Gurnigel Nappe. It cannot be excluded that these last deformational movements are due to thrusting or movements of the basement reactivating some thrusts as reverse or normal faults (Fig. 4.4F).

The paleogeographic origin of the Niesen Nappe is attributed to the north Penninic domain directly south of the Ultrahelvetic sedimentation realm. The Niesen Nappe exists only in the Préalpes Romandes and forms today the southernmost structural unit of the préalpine nappes The Niesen Nappe contains upper Cretaceous and Tertiary flysch-type sediments from the Valais

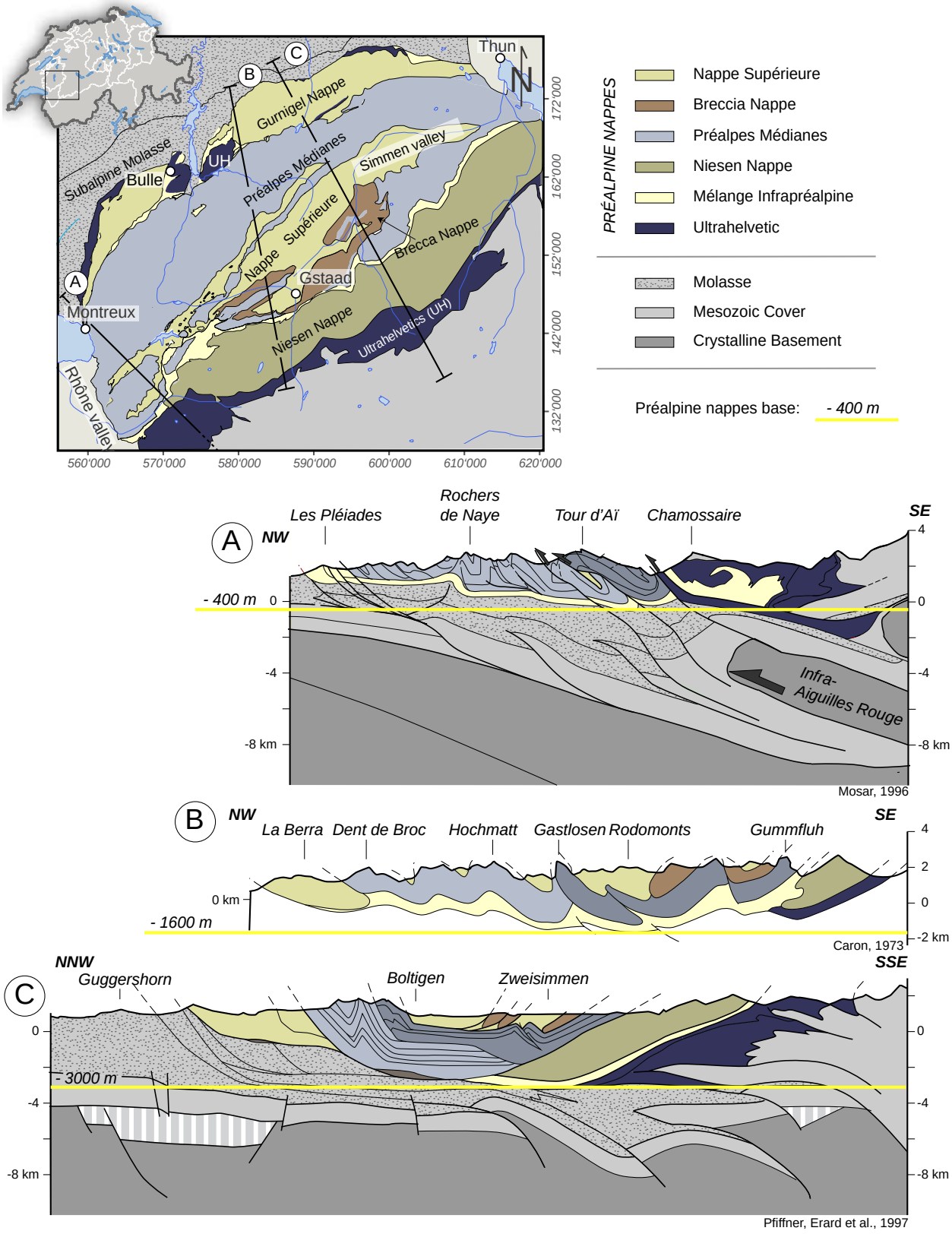

Fig. 4.3: Extent of the 3D model of the Préalpes Romandes including several tectonic nappes - the Nappe Supérieure and its frontal part, the Gurnigel Nappe, the Préalpes Médianes, the Breccia Nappe and the Niesen Nappe -, "the Zone Submédiane" and the Ultrahelvetic, the Subalpine Molasse, the Mesozoic basement cover and the basement. Three cross-sections revealing the stacking of the préalpine Nappes and interpretations of the structures below the Préalpes klippen mostly based on seismic lines. Cross-section A) in the south-western part of the Préalpes Romandes (MOSAR et al., 1996), B) the schematic cross-section throughout the Préalpes Romandes established by Caron (1973) and to the NE a cross-section carried out by Pfiffner et al. (1997b) based on analysis of the NRP20. The yellow line indicates the base of the préalpine Nappes varying considerably throughout the different cross-section, which is both related to the local situation and to the interpretation approach.

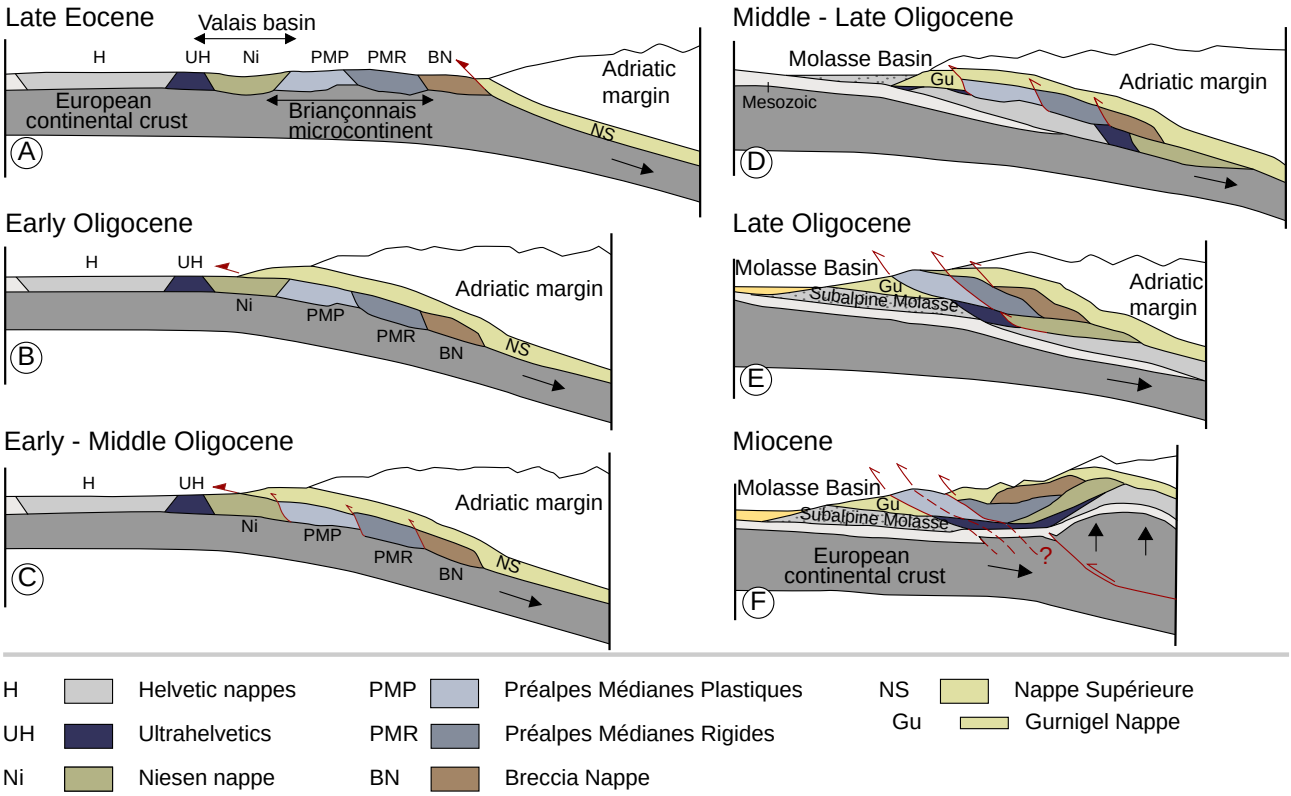

Fig. 4.4: Schema illustrating the chronological order of the nappe emplacement (modified after WISSING and PFIFFNER, 2002)

trough (TRÜMPY, 1960).

At the base of the Préalpes Médianes we find the "Zone Submédiane" structural unit, which separates them from the Niesen Nappe (WEIDMANN et al., 1976). Elsewhere, the base of the Préalpes klippen is in contact with the underlying units (Subalpine Molasse and Flysch to the north and Helvetic nappes to the south) often in a zone of tectonic mélange (BADOUX, 1963; HOMEWOOD, 1977; JEANBOURQUIN, 1991; JEANBOURQUIN and GOY-EGGENBERGER, 1991; JEANNET, 1922; LEMPICKA MÜNCH and MASSON, 1993; MOSAR et al., 1996).

3.2 PROCEDURE

The first step of this 3D modelling approach was the definition of the modelling extent (horizontally and vertically) and the import of the DTM of this area giving the topography its morphological shape. Subsequently, the stratigraphic pile was defined indicating the succession of the tectonic units and the relationship amongst each other (onlap or erosive). Then, several geological maps and cross-sections were imported allowing the setting of contact points and orientation data required for the definition of the 3D geometry. Additional, interpretational cross-sections were constructed to correct the model. In order to obtain a 3D volume, the given data was computed according to the defined resolution. Due to program limitations the final resolution of the 3D shape of the nappe structure was a compromise between maximal model size (memory issues) and geometrical appearance (more detail causes greater model size, and longer simulation time, while less detail provokes geometrical errors in the topography but is faster and more stable to calculate).

3.2.1 Digital terrain model (DTM)

The DTM gives the 3D model its morphological shape, which plays an important role concerning the intersection of geological contacts and the topography. Depending on model size, different DTM resolutions can be applied. In our case (64.5 x 53km area!), the given DTM with 25m resolution had to be simplified to 75m to avoid memory issues in the program. Moreover, the elevation data from the DTM raster also required transformation of the data set before importing into GeoModeller (see appendices).

3.2.2 Stratigraphic pile

The definition of the stratigraphic pile is one of the major issues of 3D modelling. Since the stratigraphic

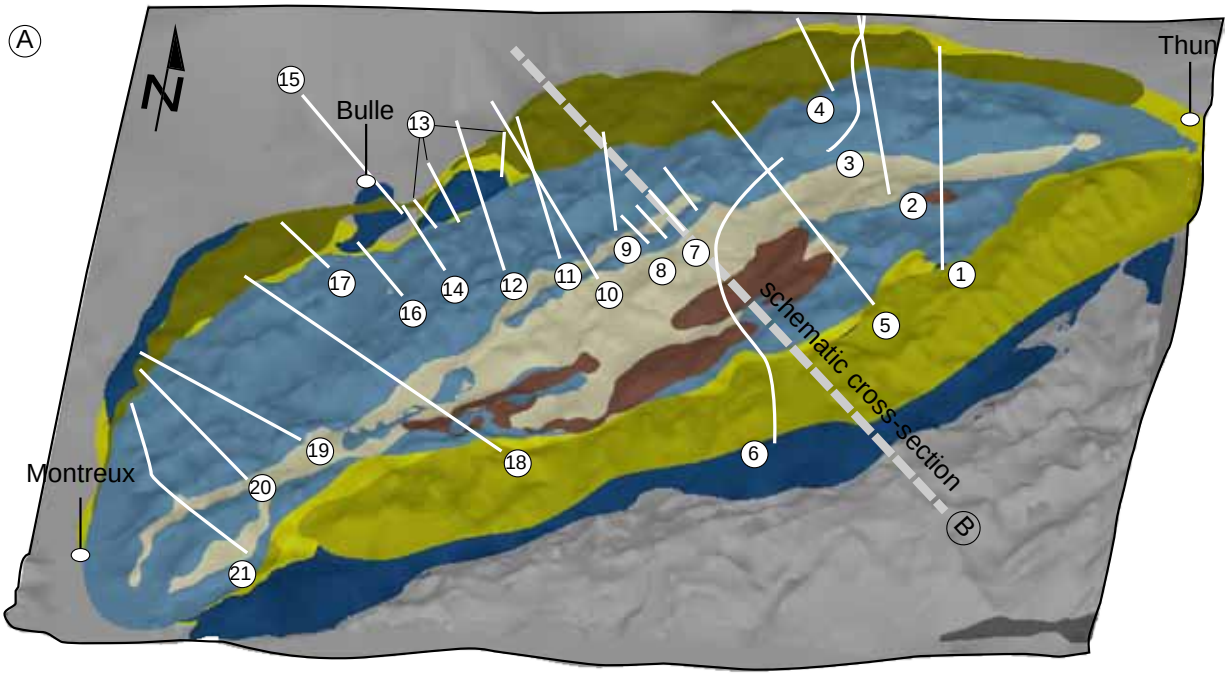

1	Hohmad - Twierihorn	(Mosar, 1991)
2	Gantrisch - Weissenburg	(Wissing and Pfiffner, 2002)
3	W792	(Erard, 1999)
4	Gurnigel Area	(Van Stuijvenberg, 1979)
5	Kaiseregg - Chalberhorn	(Wissing and Pfiffner, 2002)
6	BS12_92	(Erard, 1999)
7	Chällihorn - Bäderhorn	(Bossy, 1998)
8	Jaun - Gastlosen	(Braillard, 1998)
9	Schopfenspitz	(Fuchs, 2003)
10	La Berra - Wandfluh	
11	La Berra - Hochmatt	(Pasquier, 2005)
12	Vanil des Cours - Le Folliu	(Pasquier, 2005)
13	Massif de Montsalvens	(Guillaume, 1986)
14	Dent de Broc	(Pasquier, 2005)
15	Gibloux - Broc	(Pasquier, 2005)
16	Albeuve - Sarine	(Pasquier, 2005)
17	Les Joncs - Albeuve	(Pasquier, 2005)
18	Moléson Gumfluh	(Mosar 1991)
19	Molard - Planachaux	(Mosar 1997)
20	Le Folly - Pte. d'Aveneyre	(Mosar, 1997)
21	Cubly - Leysin	(Mettraux - Mosar, 1989)

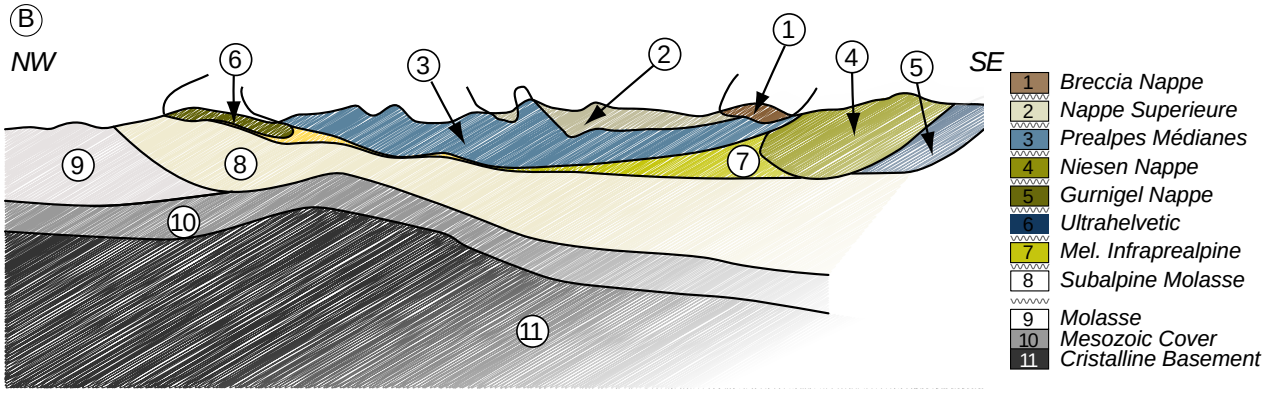

Fig. 4.5: A) Projection of the modelled structures on the topography to indicate the cross-sections used for constructing the 3D model of the Préalpes. B) A schematic cross-section of the modelling area allows the determination of the stratigraphic pile. The different layers of the substratum are differentiated in the stratigraphic pile, but for the representation of the model, they were taken together, as too many uncertainties prevail regarding their structural behaviour.

pile used for constructing a 3D model corresponds to the tectonic succession of different stratigraphic units, it is not per se stratigraphically correct. The Gurnigel nappe, for example, originally situated on top of the Préalpes Médianes, is thrust in a later stage of deformation by the Préalpes Médianes (Fig. 4.4). Defining the stratigraphic pile of the present position of the Gurnigel nappe leads to a placement below the Préalpes Médianes. Additionally, the contact between different stratigraphic series needs to be defined either as erosional or as onlapping. In the Préalpes Romandes model, the contact lines are determined by the bottom line, so the most contact lines coincide with the thrust planes of the tectonic nappes. Therefore, except for

the Molasse and the Mesozoic cover, all tectonic units were defined as erosive contacts.

3.2.3 Maps and cross-sections

For the 3D construction of the Préalpine nappes, maps and cross-sections are an essential support to place the contact and orientation data at the right position in order to correctly guide the computation of the model. Setting the contact points at the topography was possible due to the tectonic map based on tectonic sketches (Fig. 4.3) and the Swiss Tectonic map (Spicher, 2005). Fig. 4.5 illustrates the position of the 22 cross-sections used in the model. However, it is worth mentioning that numerous additional cross-sections exist in this area, which were however not considered because they do not reach the nappe base.

The appearance of the crystalline basement is defined by the isolines gathered from the results of the NRP20 (Pfiffner et al., 1997a) clearly showing the structural high related to the External Crystalline Massifs as well as a second, more smoother structural elevation, which is most probably related to the formation of a new crustal imbricate underneath the Préalpes (Burkhard and Sommaruga, 1998; Gorin et al., 1993).

To help 3D GeoModeller combine and calculate a correct interpretation of the given data, several additional cross-sections had to be constructed and inserted into the model database.

3.2.4 Export of 3D model and visualisation

The 3D representation of the structure only makes sense if a visual or conceptual advantage can be achieved compared to traditional 2D schemas. Therefore, an appropriate resolution of the calculated grid has to be defined. The internal structure of the 3D model of the préalpine nappe structure remains broadly defined, as only scarce data to constrain the model are available. However, a high resolution of the modelling grid is necessary to obtain a diagnostically conclusive representation of the topography (considering that the 700-1500m wide Gastlosen need to be visible in the final model). Consequently, the choice of the resolution is a compromise solution between the maximal memory capacities of the program and the precision desired for the visualisation of the surface structure (topography). A convergence analysis (stepwise approach of simulation models with shape resolution as factor) allowed the definition of the ideal resolution for modelling. For a model with complex topography (see detailed 3D models in chapter 4.2; 4.3; 4.3; 4.5), at around 1'500'000 shapes, or a resolution of 30m, the calculation of the 3D model starts causing difficulties. However, if the resolution of the topography is reduced, as is the case with the simplified model of the entire préalpine nappe structure, the 3DGeoModeller program can generate a higher amount of shapes. In the case of the 3D model of the Préalpes Romandes, the final accuracy obtained was 220m (4'166'200 shapes). Due to the high resolution combined with the maximal computable model size, the 3D Viewer of GeoModeller was unfortunately hopelessly overcharged when visualising the entire model (despite an Intel i5 2x2.53Ghz with 512Mb graphic card). An export of the model into a more powerful 3D tool via an ASCI file format was therefore necessary. Exporting the data as tsurf file (originally a parametric surface format for mathematical programs), preserved exclusively the contact surfaces instead of the entire volume between the contacts - the 3Dmodel becomes "lighter" and therefore easier to handle. One disadvantage of this export method is that, interfering contact surfaces at out-thinning layers provoke errors such as vacant and redundant facets in the triangular mesh. For that reason, the mesh of the exported model surfaces requires a cleaning of the model impurities by the use of MeshLab (Cignoni, 2011). The visualisation and the creation of relevant cross-sections throughout the 3D models were carried out in NX Unigraphics 7.5, a powerful 3D engineering program (Siemens, 2011). Detailed information about these different model development steps, as well as a list of advantages and disadvantages of 3DGeoModeller and solutions how to deal with them are presented in the appendices.

3.3 Results: 3D model

The result of the model of the 3D structures of the préalpine nappes are represented as five slices cutting through the entire 3D model. In the 3D model of the Préalpes Romandes, the major focus was directed towards the internal structure of the préalpine nappes and their distribution (Fig. 4.6). Therefore, a distinction of the different units lying underneath the préalpine basal thrust was neglected, so the Subalpine Molasse, the Plateau Molasse, the Mesozoic cover, and the Helvetic nappes were joined together.

The 3D model clearly shows that the Préalpes Médianes represent the largest nappe of the Préalpes Romandes, but also the Niesen nappe in the rear part is of significant importance. The nappe Supérieure with its frontal part the Gurnigel nappe and the Breccia nappe appear as superficial nappes of minor thickness. The Zone Submédiane (Mélange Infrapréalpine) developed as a structural Mélange zone at the base of the préalpine nappe is interpreted as a rather thin structural unit containing most probably some Ultrahelvetic lenses, as the one in front of the Préalpes Médianes in

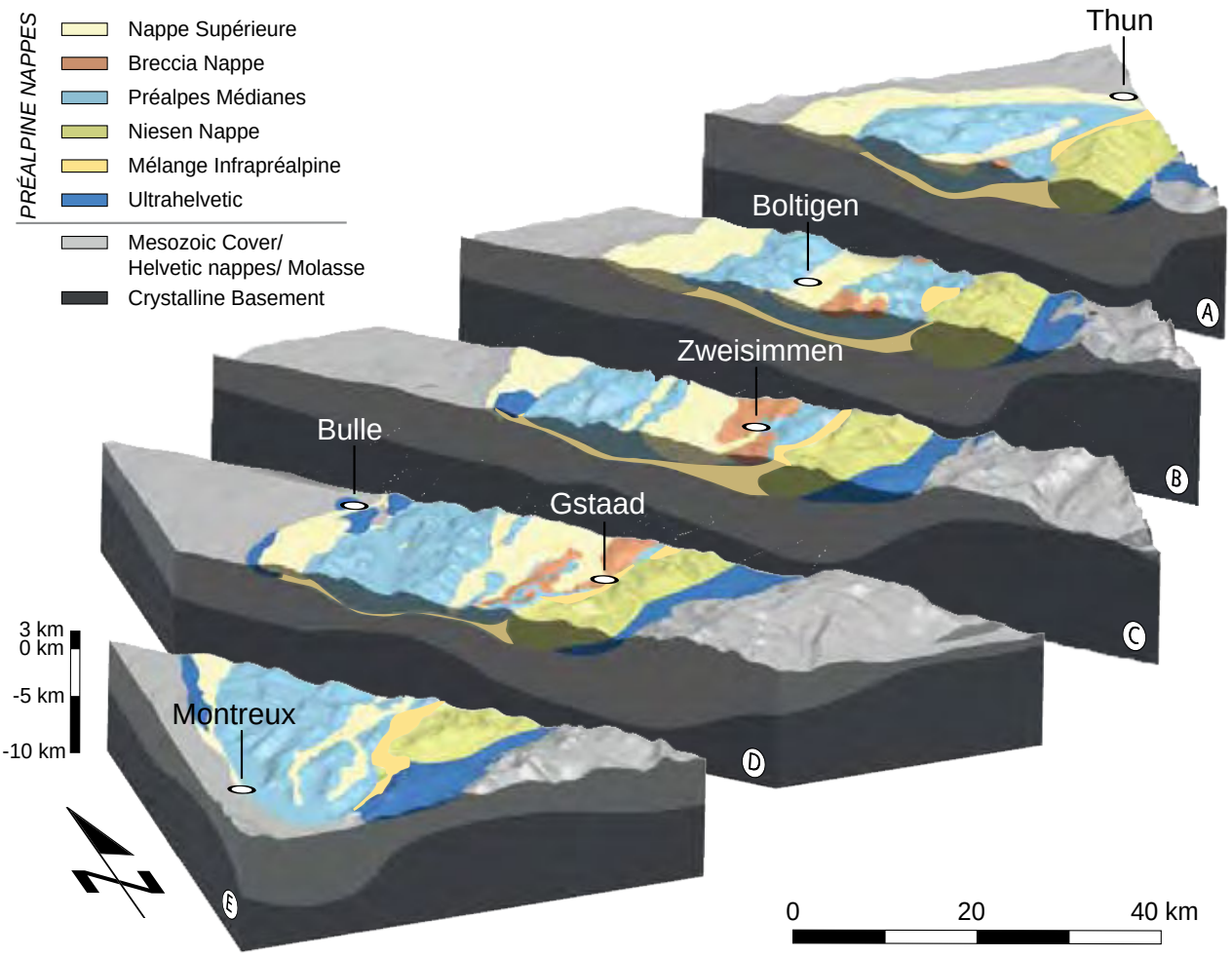

Fig. 4.6: 3D model illustrating the nappe stack of the Préalpes Romandes mostly based on superficial geological cross-sections indicating the dipping of the nappe contact at the surface, but also some cross-sections based on seismic data completed with schematic cross-sections based on our interpretations. Sources for the 3D model construction are defined in Fig. 4.3. The model shows the shallow depth of the basal décollement of the préalpine nappes and the large volume in between the nappe base and the top of the crystalline basement. As no approved information of this intermediate volume was available, the Mesozoic basement, the Helvetic nappes, the Molasse including the Subalpine Molasse were not differentiated here.

the Charmey/Gruyères region. However, a clear localisation of these lenses remains impossible, so they were taken together with the Zone Submédiane.

In the digital form of the appendices, a 3-dimensional pdf-file allows a more individual insight into the 3D model with the possibility to rotate, zoom, and cut through the models.

3.4 Discussion and Conclusion

The 3D model points out the shallow depth of the Penninic basal thrust changing along strike of the general fold trend from -1km in the eastern part to 1km in the western part of the Préalpes Romandes in the Lake Geneva area (Fig. 4.3) (Mosar, 1999). The arrangement of the nappe stack still strongly reflects their transport history (see Fig. 4.4), although some more recent structural developments can be observed in the model, as for instance the thrusting of the Préalpes Médianes on top of the Gurnigel nappe (Fig. 4.6, section B). Moreover, on Fig. 4.7 representing the top of the crystalline basement based on the structure contour map of top of the crystalline basement (Pfiffner et al., 1997a), a structural high of about 2500m appears directly underneath the Western Préalpes Romandes. Deep seismic investigation with reflectors between 20 and 40km attributed by Steck et al. (1997) to the lower crust, are reinterpreted by Mosar (1999) as a tectonic imbricate of the lower crust. Similar investigations carried out by Escher and Beaumont (1997) and Steck (1997) defined two new basement nappes under the Aiguilles Rouges-Helvetics-Préalpes (Infra-Rouges 1 and Infra Rouges 2 nappes). Similar basement imbricates are described

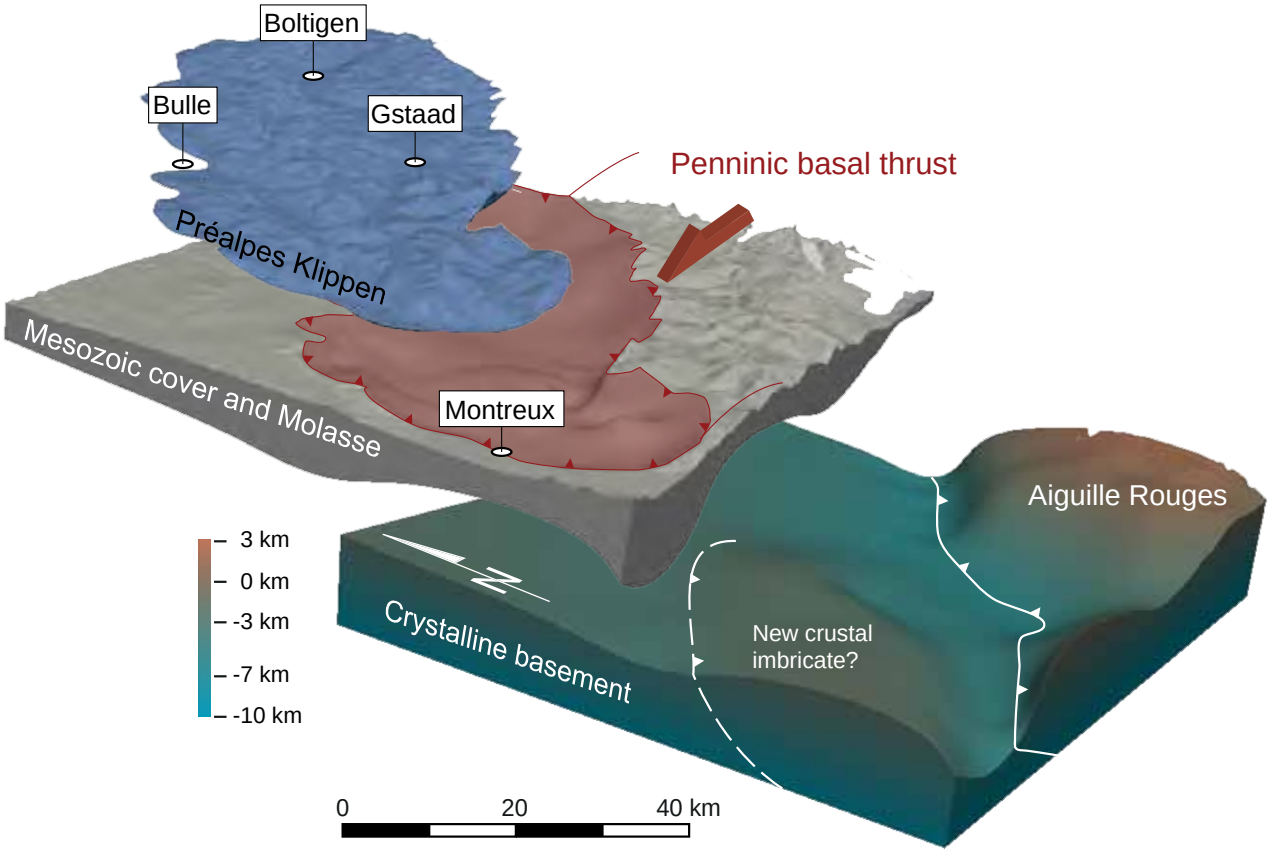

Fig. 4.7: Top crystalline basement based on the structure contour map (PFIFFNER et al., 1997a). Structural high underneath the Préalpes klippen possibly related to the formation of new crustal imbricates, which are influencing the structures of the Préalpes klippen above and is thus post-Oligocene (post-emplacement) (MOSAR, 1999). The 3D model points out the important volume in between the Préalpes klippen and the basement consisting of the Mesozoic cover and the Subalpine Molasse.

in the Alpine foreland SE of the Chablais Préalpes beneath the Annes and Sulens klippen (GUELLEC et al., 1990).

When looking at the earthquake distribution within the extent of the Préalpes Romandes model, the highest earthquake concentration is found in the south-east of the modelling area, corresponding to the Helvetic domain and the External Crystalline Massifs (GIARDINI et al., 2004). Another less important accumulation of earthquakes is located in the western part of the Préalpes Romandes towards the Lake Geneva coinciding approximately with the supposed basement imbricate (Fig. 4.8). Focal mechanisms of the earthquake within the Helvetic nappes and external massifs north of the Rhône valley are characterised by strike-slip focal mechanisms with a maximum compression axis plunging 30° towards NW and a horizontal maximum extensional axis oriented in NE-SW direction (MAURER et al., 1997).

Uplift rates of the same area display a high uplift towards the Helvetic nappes and the External Crystalline Massifs where they exceed 1 mm/year (KAHLE et al., 1997; MOSAR, 1999). In the Préalpes klippen, the uplift ranges from 0.2 - 0.6 mm/year. In the Rhône Valley near the Lake Geneva, the uplift curves slightly deviate from their normal course indicating a minor uplift increase, whereas between Gstaad and Zweisimmen the uplift is attenuated. This is probably related to the lateral disappearance of the basement high of the Préalpes Romandes.

The uplift rates and the earthquake array hint at an on-going deformation of the Alpine wedge trying to readjust its instability by an interplay of erosion and the development of crustal imbricates, which certainly also influence the Mesozoic cover, the Subalpine Molasse and also the overlying préalpine nappes.

Despite the relatively good understanding of the préalpine nappe transport until its emplacement onto the Alpine foreland in Oligocene times, a clear comprehension of the structural evolution post-dating the nappe emplacement was not yet given by any of the reviewed authors treating the area. The three dimensional reconstruction of the préalpine nappes of the Préalpes Romandes provides an idea of their

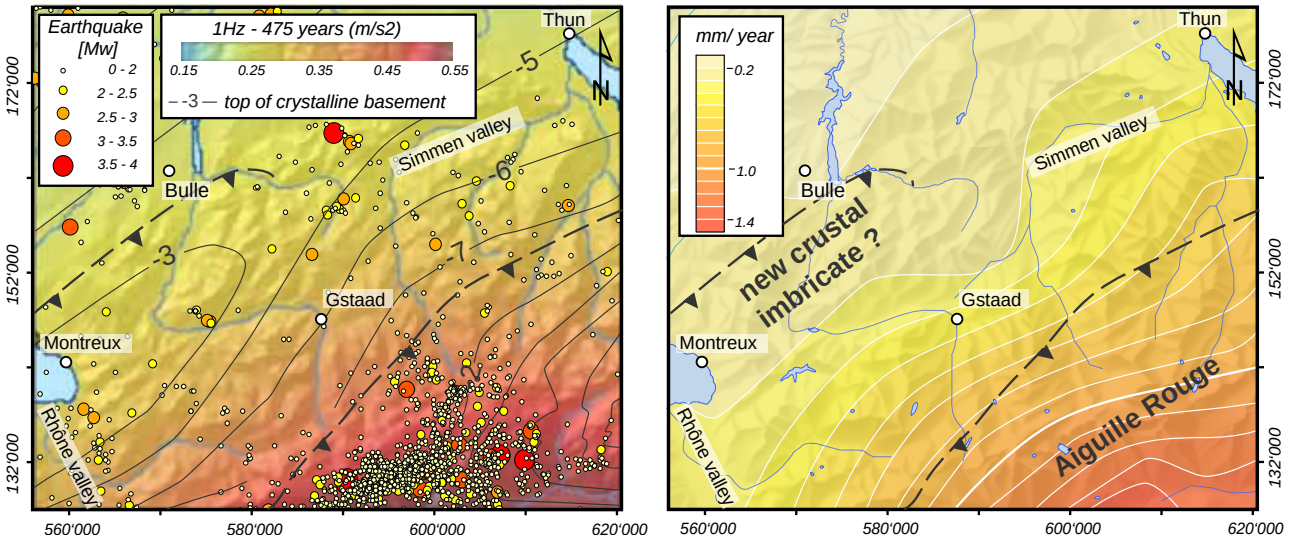

Fig. 4.8: Seismic hazard map of the Préalpes Romandes depicts the level of horizontal ground motion expected to be reached in a period of 475 years (GIARDINI et al., 2004) with registered earthquakes since 1975 extracted from the earthquake catalogue of Switzerland (ECOS02). Towards the Helvetic nappes and the External Crystalline Massifs, a remarkable concentration exists whereas near the eastern part of the Lake Geneva another, less marked accumulation prevails The grey lines represent the topography of the top of the crystalline basement (numbers correspond to the elevations [km]) (PFIFFNER et al., 1997a). On both maps the thrust front of the Aiguille Rouge massif and the presumed crustal imbricate are indicated by grey dashed lines. Uplift rates (mm/year) show an increasing uplift towards the south-east, exceeding 1 mm/year (KAHLE et al., 1997).

spatial arrangement, but also an idea of the volume in between the préalpine detachment horizon and the crystalline basement accommodating possible out-of sequence thrusts.

4 Detailed 3D Models

Whereas the previous 3D model of the entire Préalpes Romandes provides a raw insight into the general nappe structure, the following 3D models are aimed to unravel the more detailed structures of four areas of particular structural interest: the Dent de Broc, the Gros Haut Crêt, the Schopfenspitz, and the Holzerhorn-Schafarnisch area. These models were developed generally by means of geological maps and cross-sections. Moreover, extensive fieldwork in these areas, mainly aiming to improve the understanding of the tectonic structures and their kinematics, allow constraining the model with observed bedding measurements. At last, as the geological structures are not entirely known throughout the entire three-dimensional block, a large amount of geological interpretation was implemented.

Located in the Préalpes Médianes, the structural elements of these four modelling areas are mainly related to fold and thrust tectonics due to alpine compression. Remains of extensional events taking place before the alpine deformation, as well as most of the more recent strike-slip faulting structures could not be represented in these models. Stratigraphically following units were distinguished throughout every model: Triassic, Lower, Middle and Upper Jurassic, as well as Lower and Upper Cretaceous.

The 3D GeoModeller program is highly suitable for constructing geological structures as onlapping and eroding layers, folded and faulted structures, but less suitable for modelling structures related to thrusting. As the computing algorithm in 3D GeoModeller always attempts to retain the same layer dip and to link the two sides of a fault, it is nearly impossible to develop a model that represents a thrust volume that is transported over a larger distance. To resolve this inconvenience, several independent packages of the same stratigraphic successions were built separated by erosive layers representing the thrust planes. Detailed information about the succession of these stratigraphic packages is given in the appendices.

4.1 Geological Setting of the Préalpes Médianes

The established 3D models are for the most part situated in the Préalpes Médianes Plastiques (PMP), only the Schafarnisch-Holzerhorn model contains a part of the intermediate imbricates in between the Préalpes Médianes Rigides (PMR) and the Plastiques. In the Préalpes Médianes, these two major domains were distinguished referring to their paleogeographic sedimentation realm. Both originate in the Sub-Briançonnais and Briançonnais sedimentation realm (Caron, 1972, 1973; Trümpy, 1960), whereas the PMP

were deposited in a deeper basin allowing a nearly complete stratigraphic series from the Upper Triassic to the Upper Cretaceous and the Tertiary Flysch, the PMR however have its origin in shallower water and are therefore characterised by important stratigraphic gaps. The different sedimentation realms of the PMP and the PMR influence their structural behaviour under deformation: the PMP tend to form large-scale fault-related folds striking in NE-SW direction (Badoux et al., 1960; Badoux and Mercanton, 1962; Bonnet, 2007; Borel and Mosar, 1993; Gagnebin, 1922; Jeannet, 1922; Mettraux, 1989; Mosar, 1988a, b, 1989; Mosar, 1991; Mosar, 1994, 1997; Mosar and Borel, 1992; Mosar et al., 1996; Müller and Plancherel, 1982; Plancherel, 1979). The PMR however, form one or two major imbricated thrust slices dipping towards the N/NW (Mosar, 1997). In between the PMP and the PMR, an intermediate zone can be situated corresponding to a basin of middle depth, showing characteristics of both structural parts; this intermediate zone can be attributed to the Gastlosen/ Heiti zone (Jaccard, 1908; Lugeon, 1943; Plancherel, 1979). For generation of the 3D models a stratigraphic subdivision is used based on a structural classification depending on the relative competence of the series (Jaccard, 1908; Lugeon, 1943; Mosar, 1997; Plancherel, 1979). Since the competent layers appear as cliffs and the more erodible lithologies as depressions, this subdivision is consequently morphologic and does not respect a strict chronostratigraphic scale. The different units are named after the corresponding geological stage or system: Triassic, Lower, Middle and Upper Jurassic, Lower and Upper Cretaceous.

4.2 3D Model Dent de Broc

The major interest in constructing a 3D model of Dent de Broc was on the one hand to represent the folding and thrusting structure clearly influencing the morphology of the landscape of this area and on the other hand to include nearly vertical normal faults affecting particularly the Upper Jurassic and Lower Cretaceous layers of the Dent de Broc syncline. As three major thrusts extend throughout the entire Dent de Broc model, three different parts of on-lapping layers have to be defined limiting the upper and the lower part of the thrust. The thrust plane itself is defined as an erosive Triassic layer. The package DDB1 together with the erosive Triassic1 layer (Fig. 4.10) is thrusting DDB2 and Triassic2, which in turn thrust DDB3 and Triassic3. The stratigraphic pile of this 3D model only has a limited stratigraphic chronology, as it represents mostly the succession of thrust packages in order to their thrusting hierarchy.

Whereas the internal part of the different packages are composed of successive stratigraphic layers, DDB1, DDB2 and DDB3 are defined as onlapping contacts. That signifies that they are abutting upon the lower series and not cross-cutting them, in contrast to the erosive Triassic layers, which remove every earlier geological unit above the defined erosive surface. Several sub-vertical fault planes were defined affecting

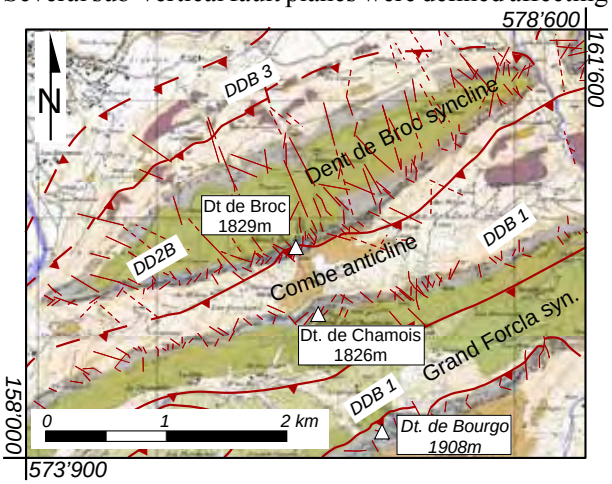

Fig. 4.9: Geological map of the Dent de Brocmodelling area. DDB 1, DDB 2, and DDB3 signify the three different modelling packages.

the layers in the Dent de Broc syncline, whereas by far not every fault plane was respected. Their extent was limited by the thrust planes (base of the Triassic layers), and does not exceed 1200 m horizontally and 800 m vertically.

4.2.1 Geological and structural setting

The Dent de Broc area is located in the frontal part of the Préalpes Médianes characterised by two to three external thrust slices (Jeannet, 1922; Mosar, 1997; Schardt, 1893a). (For a simplification of the 3D model, this zone of frontal imbrications was taken together as one thrust slice (DDB3). Farther to the SE, the Dent de Broc syncline (DDB2) (Fig. 4.9) attracts attention by its overturned backlimb, especially by its Upper Jurassic limestone layers shaping the remarkable crest of the Dent de Broc range, which is highly affected by normal faults leading to a segmentation of the entire fold structure. Finally, the largest structural part is occupied by the Combe anticline thrusting the top of the Dent de Broc and the Grand Forcla syncline (Fig. 4.9; Fig. 4.11). In general, in the Préalpes Médianes, the morphology of the landscape reveals the structural trend underneath, as for instance the massive limestones of the Upper Jurassic, which form the mountain ranges of highest elevation.

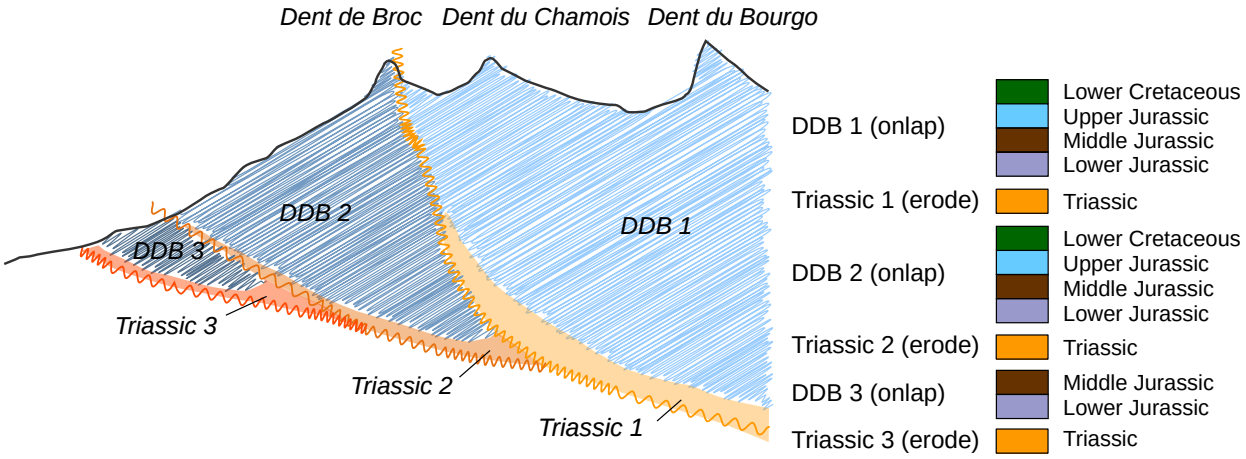

Fig. 4.10: Sketch explaining the order of the stratigraphic pile. For constructing reasons (modelling of thrust planes), the modelling area was separated into three main packages separated by erosive horizons (base of Triassic layers) to keep the thrusting character of the entire structure.

4.2.2 Results

The complex 3D structure of the DDB area required a high resolution for computation of a useful 3D representation. Only in this way was the relationship between the topography and the geological structures visible. Additionally, a relatively high resolution of the topography supports the spatial orientation within the model. The ideal resolution for this model was determined at 30m allowing on the one hand, a clear recognition of topographic features such as the steep Upper Jurassic cliffs with its important faults; on the other hand, the size of the modelling grid was still calculable and manageable (1'540'800 shapes). The disadvantage of this high resolution is the long calculation time and the errors created in the facet grid by the export requiring an exhaustive post-treatment.

To gain an overview of the 3D representation of the Dent de Broc model a segmented view with a subdivision into six sectors was chosen giving insight into

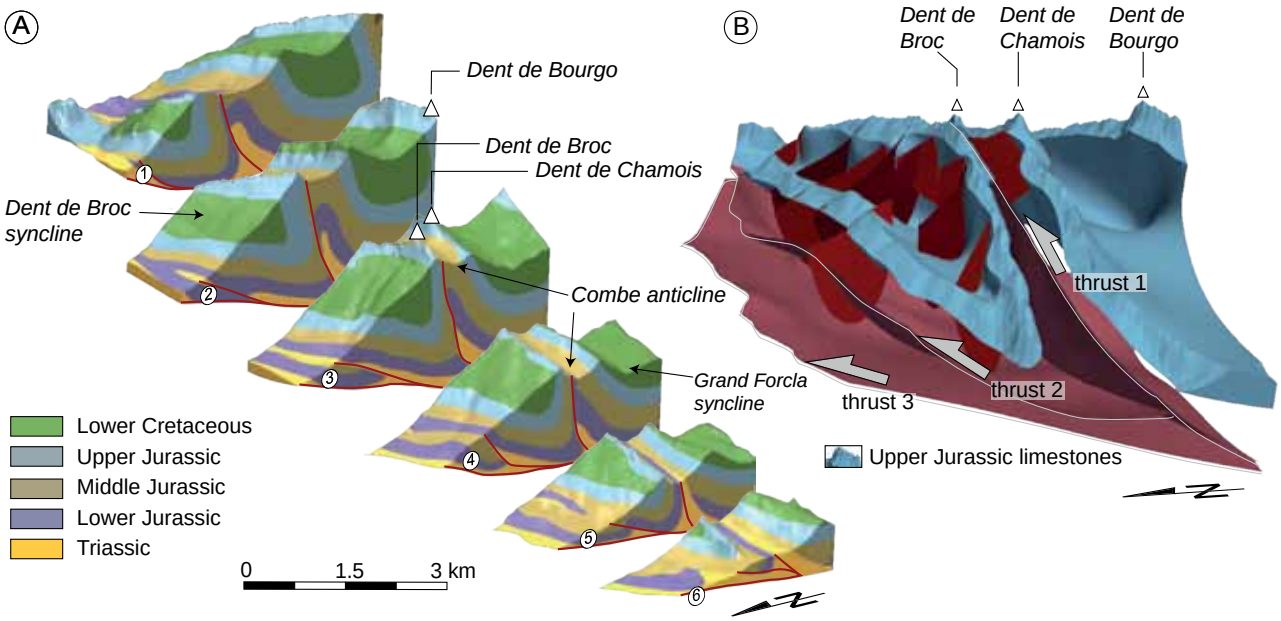

Fig. 4.11: Two 3D representations of the Dent de Broc area generated by 3DGeoModeller. On the left, a view of different sections is exposing the internal structures, and on the right an illustration of the three thrust planes and the normal faults with most influence in this area.

the internal structure of the Dent de Broc area (Fig. 4.11). The three major thrust planes are calculated by three erosive Triassic layers highlighted by the red lines, which were drawn in afterwards. For the calculation of the model, several important faults affecting the Dent de Broc area were taken into account, which are illustrated on the structural figure to the right (red fault planes).

4.2.3 Discussion and conclusion

The general structures of the Dent de Broc area are well represented by the 3D model. However, some uncertainties remain, especially in the frontal part, where only a few patchy outcrops show the frontal imbricated thrust slices. For simplification reasons, the frontal part was joined together as one imbrication and for that reason it only represents the general trend of this thrust slice respecting the information of the largest outcrops. The generated fault planes are vaguely defined, as their extent is not exactly known. On orthophotographs and on DTMs fault lineaments were identified crosscutting the Sarine syncline, clearly visible between the two Upper Jurassic fold limbs. Paleostress measurements carried out in this area result in a mainly extensional or strike-slip stress regime both with extensional stress axes oriented parallel to the fold axes. On that account, it is speculated that the faults, generated under an extensional stress regime and afterwards reactivated under a strike-slip regime, are cutting through the thrusting structure (Fig. 4.11).

4.3 3D Model Gros Haut Crêt

In the region of the Gros Haut Crêt and the Gros Mont valley, a large amount of structural data was collected allowing firstly to reconstruct the paleostress of this area (see appendices) and secondly to define the folding and the thrusting structure. An important thrust fault and its secondary fault splays initially responsible for the forming of the Tsavas-Millet anticline (Fig. 4.12) are breaking through topography and are further off-setting the folding structure. The oblique dipping of the thrust plane results in a triangular structure in the Gros Haut Crêt area. Lying in the structural prolongation of the Schopfenspitz thrust fault a link to this out-of-sequence fault is very probable (chapter 4.2.4).

Based on this structural background and the large amount of structural data, the 3D representation of this area was quite straightforward. The extent of the 3D model ranges from 578’000/157’500 to 583’000/161’000 Swiss coordinates system (CH1903) including both sides of the Gros Mont valley, the eastern, and the western part with its triangular thrust structure.

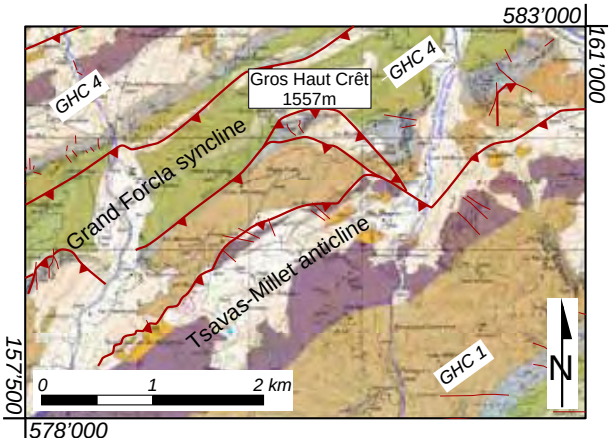

Fig. 4.12: Geological map of the Gros Haut Crêt modelling area. GHC1 and GHC 4 signify the two different modelling packages.

Similar as in the previous section, the definition of the stratigraphic pile depends on the thrust hierarchy; more details to the stratigraphic pile of this model can be found in the appendices.

4.3.1 Geological and structural setting

The Gros Haut Crêt 3D model is situated to the east of the Dent de Broc and to the south-west of the Schopfenspitz modelling area and is mainly dominated by the presence of the Grand Forcla syncline and the Tsavas-Millet anticline generated by an important thrust fault (Fig. 4.12; Fig. 4.13) (Mandia, 1984; Pasquier, 2005). On-going deformation leads to a further advancing of the thrust plane and the formation of fault splays resulting in a significant offset of the Upper Jurassic limestones of about 200m. Paleostress analyses (see chapter 4, 4.2.4) displayed a prevailing extensional stress regime, oriented mostly perpendicular to the fold axis, indicating a recent bending of the fold. Coinciding with the location of the inherited normal fault, known as the Rianda-Stockhorn fault (Borel and Mosar, 2000), the Gros Haut Crêt thrust is supposed to be an out-of-sequence thrust, which was or is still active after the emplacement of the préalpine nappes. The major thrust plane is oriented obliquely leading towards the SE to the disappearing of the forward thrusting part of the former Rianda-Stockhorn fault, whereas towards the NW the thrust together with its frontal splays are exposed.

4.3.2 Results

The topographical circumstances of the Gros Haut Crêt modelling extent with a valley in between of two

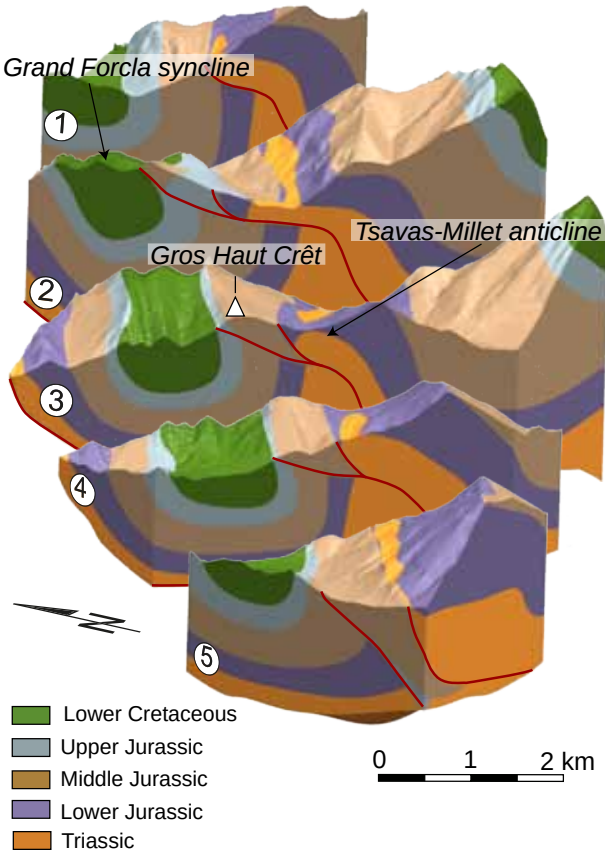

Fig. 4.13: 3D model of the Gros Haut Crêt/ Gros Mont Valley

mountain faces makes it difficult to obtain an overview of the 3D model represented in 2D. For that reason, the Gros-Mont valley is often not visible in a lateral-oblique view. The section view of the Gros Haut Crêt model below (Fig. 4.13) clearly shows the thrusting of the Tsavas-Millet anticline towards NW on top of the Grand Forcla syncline. Furthermore, the thickness variations of the Lower, but especially of the Middle Jurassic layers are nicely represented in the 3D model below. The stratigraphic differences between these two parts are related to the Rianda-Stockhorn paleo-fault, a former synsedimentary normal fault.

The resolution of the model was kept as high as possible amounting 30m, which corresponds to a modelling grid of 2‘930‘900 shapes.

4.3.3 Discussion and conclusion

Generally, the 3D model of the Gros Haut Crêt area nicely represents the thrusting structure also observed in the field. Sometimes, thickness variations along strike occur - particularly in vicinity of the model boundaries, which can, in this particular case, be attributed to errors in the modelling algorithm of the GeoModeller program.

4.4 3D Model Schopfenspitz

The Schopfenspitz area attracts major attention because of the Schopfenspitz thrust fault characterised by the isolation of the Schopfenspitz mountaintop as tectonic klippe. Moreover, the region between the Jaunbach valley and the Schwarzsee is affected by fault-related folds thrusting backwards, which are dying out laterally forming a relay zone between them. As these thrusts are discontinuous throughout the whole modelling area, they have to be defined as faults with a certain extent in the model. Different structural packages only make sense when a thrust plane is defining a distinct limit transecting the modelling area, such as the Schopfenspitz fault. Whereas the other faults are affecting the stratigraphic layers locally and diminish laterally. The modelling extent was determined to range from 580’000/ 161’000 to 588’000/ 165’500, covering the most important backthrust and the Schopfenspitz thrust.

4.4.1 Geological and structural setting

A succession of asymmetric anticlines and synclines are influencing the Schopfenspitz region; ranging NW to SE from the Vounetse-Bremingard syncline, the Tzintre-Lovattli anticline, the Dent de Broc syncline, the Anticline 1, the Sarine syncline and finally, the Tsavas-Millet anticline (Fig. 4.14). These folds are related to backthrusts, mostly hidden underneath, developed during the transport of the Préalpes Médianes nappe. The interpretation of these faults as backthrusts is in contrast to previous studies from this area (Andrey, 1974; Fuchs, 2003; Pasquier, 2005; Spicher, 1966). The interpretation presented here is mainly based on the asymmetric fold morphology with a steeper inclined back limb, based on field measurements and the interpretation of geological maps. Additionally, this assumption is supported by the presence of an important backthrust outcropping in the Maischüpfen area, as well as by kinematic indicators showing a top to the S movement. Thicknesses of the stratigraphic layers show an important increase towards SE, especially in the Middle Jurassic layers, where an increase of about 500m to 1000m is recorded.

The mountaintops of the Vanil d’Arpille, the Schopfenspitz and the Combifluh are completely dislocated from their surrounding structures, as they are remains of an important thrust outcropping in the Jaun valley and its prolongation towards the Euschelspass that is thrusting the summits of the highest mountains. This thrust is attributed to a former synsedimentary paleo-fault, the Rianda-Stockhorn fault (Borel and Mosar, 2000), delimiting the stratigraphic series to the SE.

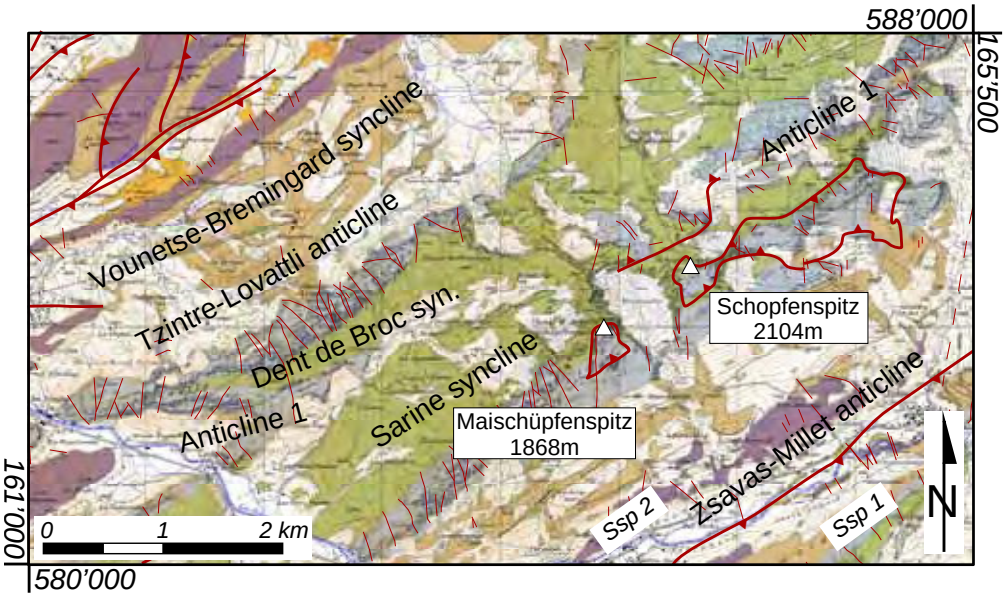

Fig. 4.14: Geological map of the Schopfenspitz modelling area. Ssp 1 and Ssp 2 signify the two different modelling packages.

The tectonic klippen show remnants of the Tsavas-Millet anticline that is completely over thrusting the Sarine syncline below.

4.4.2 Results

The resulting 3D visualisation of the Schopfenspitz area precisely represents the fold-and thrust structure of this region. The section view (Fig. 4.15) displays the relationship between the backthrusts and the generated folds. Furthermore, the link between the south-eastern face of the Jaunbach valley and the Schopfenspitz klippe is nicely pointed out in Fig. 4.15 on the right. The resolution of this 3D model reaches 29m, corresponding to a grid of 5'540'000 shapes.

4.4.3 Discussion and conclusion

The major challenge of the Schopfenspitz was the interpolation of the backthrusts, as faults and their

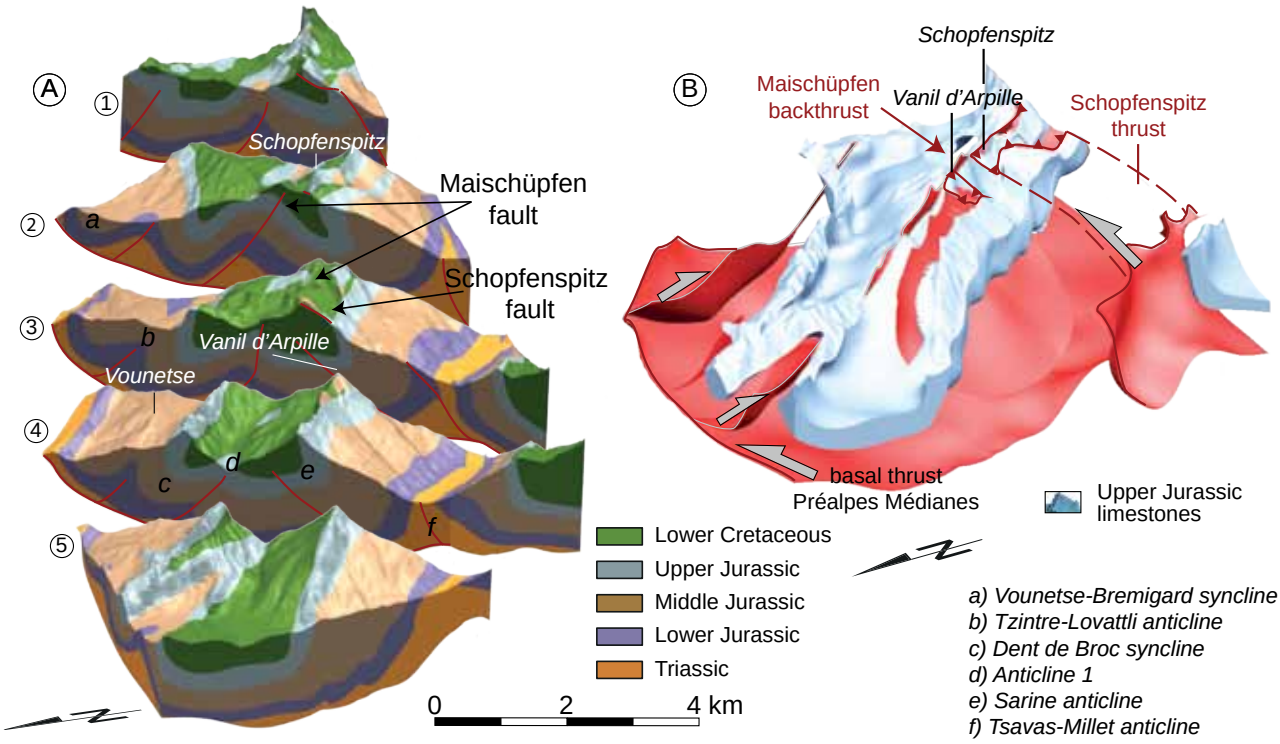

Fig. 4.15: 3D model of the Schopfenspitz area. A) Section view of the major geological structures B) Most important thrusts of this area, the backthrusts and the Schopfenspitz thrust, as well as the Upper Jurassic limestone layers as reference.

offsetting geological strata corresponding to a weak point of the 3DGeoModeller program. In the previous models, it was possible to define different independent stratigraphic parts to reconstruct important thrust faults. Within the Schopfenspitz model however, as the thrusts do not always reach the surface and are laterally not consistent, the determination of independent stratigraphic units was only possible for the Schopfenspitz thrust part. For this reason, the offset of the thrusts was not always computed precisely, and thickness differences on both sides of the faults were generated (Fig. 4.15; see the Lower Jurassic in sector 2 and 3). To improve the model quality in vicinity of thrusts, an even denser input of stratigraphic contact data would be necessary; resulting in a "heavier" model and thus preventing computation at higher resolutions (topography detail will suffer).

The doubling of the thickness of Middle Jurassic strata presents an additional difficulty for the 3D modelling algorithm. With the aim to represent the same thickness, the 3DGeoModeller program inserts a layer of Upper Jurassic within the Middle Jurassic layers. Extensive post-treatment of the data in external programs (meshlab and NX Unigraphics) was required to erase the additional erratic structures.

The 3D model of the Schopfenspitz area shows nicely how the computed model remains a product of a compromise between the precision, the capacities of the modelling program and the time available. Despite these critical remarks, the 3D model of the Schopfenspitz area gives a precise overview of this region, especially in the upper part of the model, which also corresponds to the area of reliable data, whereas the structures at depth are still not clearly defined and only based on geometrical consistency.

4.5 3D Model Schafarnisch - Mittagflue

4.5.1 Geological and structural setting

The Préalpes Médianes Plastiques in the north-western part of the 3D model are affected by the Stockhorn-Kaiseregg anticline and the broad Stockhorn-Jaun syncline (Fig. 4.16) (Bieri, 1925). The latter displays a small-scale anticline in between, related to a thrust fault underneath.

The fold axes are displaced by important strike-slip faults of a sinistral shear sense. Fault-slip measurements and subsequent paleostress analyses attest a prevailing strike-slip stress system with a dominating sinistral component. It proposed, that these sinistral strike-slip faults act as conjugated counterpart to the important Weissenburg strike-slip fault with a dextral shear sense.

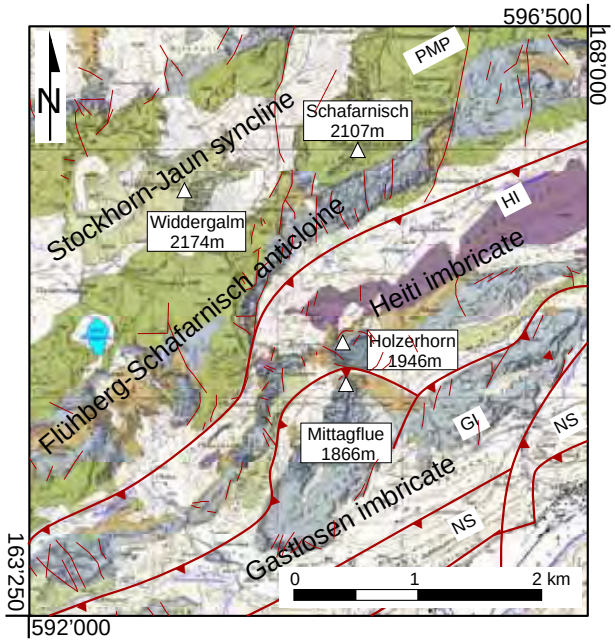

Fig. 4.16: Geological map of the Schafarnisch-Mittagflue modelling area. PMP, HI, GI, and NS signify the four different modelling packages.

The Heiti imbricate farther to SE is represented by an important asymmetric anticline, which is bending in vicinity of the sinistral strike-slip fault of the Schafarnisch in a NW oriented position and is farther to the south-west re-establishing its initial NE-SW oriented position. Influenced by the absence of more ductile layers, the Gastlosen imbricate is mainly superimposing the Heiti imbricate as a rigid plate.

4.5.2 Results

The visualisation of the geological structures in the Schafarnisch-Mittagsfluh 3D model clearly shows the different structural styles of the Préalpes Médianes Plastiques and the two imbricates of the intermediate zone. The geology is represented by a section view giving insight into the internal part of the 3D model, but also exposing the superficial prolongation of the structures (Fig. 4.17A). The structures, mainly the thrust planes delimiting the structural imbricates, but also the strike-slip faults that are dominating the Schafarnisch area, are displayed in a structural model (Fig. 4.17B). Moreover, the limits of three different structural sectors are represented in a segmented view, separating the different sectors from each other (Fig. 4.17C).

The precision of the 3D model corresponds to 30m, as in the previous 3D models and amounts to a grid containing 2'974'400 shapes.

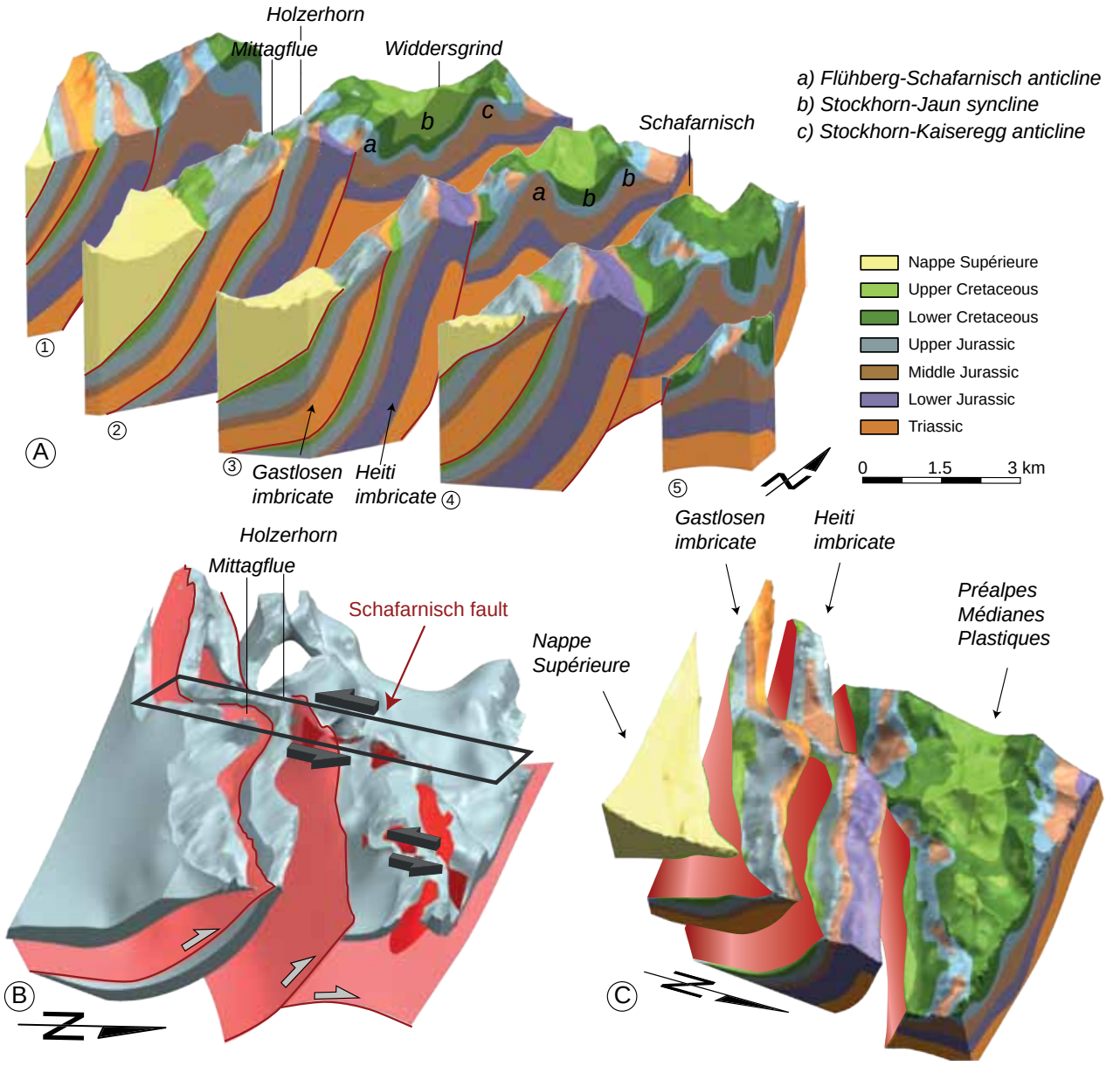

Fig. 4.17: The 3D model of the Schafarnisch-Mittagsfluh area is represented with a section view (A) showing the inside structures of this area that is characterised by three different structural parts: the Préalpes Médianes Plastiques, the Gastlosen and the Heiti imbricate. The thrust planes and the important fault planes are highlighted in B), whereas C) shows in a segmented view three structural components as well as a part of the Nappe Supérieure.

4.5.3 Discussion and conclusion

Reconstructing the 3-dimensional geology of the Schafarnisch and the Holzerhorn area focusses on the reconstruction of the characteristic structures of three different domains. The two imbricates nicely reflect the interpreted structures, since both of them feature distinct, well-defined structures. The fold-and-thrust-structures of the Préalpes Médianes with its sinistral offsetting fold axes represent a major challenge, since the presence of faults strongly disturbs the modelling algorithm. It is therefore mainly the presence of faults, which are having negative effects on the layer thicknesses. Constraining the model by further data input is possible, but would result in a “heavier” 3D model requiring a downgrading of the modelling resolution. Despite these inaccuracies, mostly in the Triassic, Lower and Middle Jurassic layers, the 3D model of the Schafarnisch-Holzerhorn largely fulfil the aim of obtaining an interpretational aid and a structural overview of this area.

5 Discussion and Conclusion

The aim of a visualisation of the geological structures in 3D - both the large-scale structures of the préalpine nappes and the detailed structures of four specific areas - was fully achieved by the reconstruction of the five 3D models generated in the Préalpes Romandes. These models allow a better understanding of the spatial distribution and the continuation of the geological units, layers and the significant discontinuities. The different components, the nappes in the 3D model of the Préalpes, but also the faults and the thrusts, as well as particular stratigraphic layers can be treated isolated from each other, which can be useful for future investigations.

Since only few constraining data at depth are available, the 3D models are largely based on surface data interpolated to depth and completed by interpretational inputs. For that reason, to obtain a higher accuracy of the 3D models, better subsurface data such as seismic lines or borehole data would be required. Additionally, the precision of the 3D reconstructions is limited due to the weakness of the modelling algorithm concerning the layer continuation on both sides of a thrust and along the model boundaries. These inaccuracies, mostly affecting the layer thicknesses, can be removed by increasing the amount of restricting data, but with negative side effects regarding the weight of the reconstruction and the computation time, by reaching the limits of the 3DGeoModeller program. On that account, the presented 3D models show an accurate representation of the suggested geological structures of the various modelling areas. Prospective projects could involve the restoration of the undeformed state based on the already generated 3D models. Thereby, the actual geological structures could be validated by the means of balancing, to refine the 3D model in such a way that the model reaches geometrical and kinematical correctness.

*****

5 - Geodynamic Context of the Préalpes Klippen Belt within the Alpine Evolution

1 Introduction

The préalpine nappes underwent a complex paleo- and Alpine tectonic deformational history to attain their present-day position to the NW of the Helvetic nappes and to the SE of the Western Molasse Basin. The objective of this chapter is to situate the structural and kinematic observations attained in the central part of the Préalpes Médianes Romandes and its adjacent units - the Gurnigel nappe and the Subalpine Molasse - into a larger structural context of an evolving orogenic wedge. Major interest is given to the tectonic evolution after the préalpine nappe emplacement (post-Early Oligocene 30Ma). Despite a large amount of diverse investigations of the Préalpes klippen belt exist, the understanding of the structural processes is still fragmentary. Post-emplacement deformation is mainly expressed by uplift rates, earthquakes, and out-of-sequence thrusts trying to readjust the unstable accretionary wedge geometry by interplay of erosion and the development of crustal imbricates (Bonnet, 2007; Champagnac et al., 2009; Champagnac et al., 2007; Mosar, 1999).

Additionally, an ubiquitous strike-slip fracture pattern consisting of two major fault directions - a N-S oriented sinistral and a WNW-ESE oriented dextral fracture set - witness a recent to on-going deformation. Acting together as conjugated fault zones, the préalpine fault system coincides on a broader scale with conjugated fault systems common in the Jura mountains and the Western Molasse basin (Delacou et al., 2004; Kastrup et al., 2007; Kastrup et al., 2004; Mosar and Borel, 1992).

Within this chapter, a short overview of the Alpine deformation is presented. Subsequently, a focus on the Préalpes Klippen gives an insight into the behaviour of the different nappes during the Alpine deformation, as well as their evolution within the orogenic wedge after the emplacement. The second part of this chapter involves the results and the observations of the investigated folded and Subalpine Molasse, the Gurnigel nappe and the Préalpes Médianes. The focus lies in finding coinciding deformational features within every structural unit.

2 Préalpes Klippen within the Orogenic Wedge

To bring the geodynamic evolution of the préalpine nappes into its larger context of a developing orogenic wedge, the understanding of the deformational history of the Western Alps, as well as of the préalpine nappes is essential. For this reason, a short overview of the major phases of the Alpine deformation and an overview of the different origins and characteristics of the préalpine nappes are presented in the first part of this chapter. The second part deals with the evolution of the préalpine nappes after their emplacement in context of a progressing orogenic wedge.

2.1 Tectonic Evolution of the Western Alps

The tectonic evolution of the Alps has been roughly subdivided into three major periods based on the tectono-metamorphic activity (Dal Piaz et al., 1972; Escher et al., 1997; Handy et al., 2011; Hunziker et al., 1989; Hunziker et al., 1992; Schmid et al., 2004; Trümpy, 1980): the Eoalpine orogenic events, Cretaceous to Early Paleocene (140-60 Ma), the Mesoalpine orogenic events, of Late Eocene to Early Oligocene (45-30 Ma) and the Neoalpine orogenic events, of Late Oligocene and younger (30-0 Ma).

The Eoalpine event is characterised by the south-dipping subduction of the Alpine Tethys and the opening, as well as the subsequent closure of the Valais ocean leading to a progressive closure of the Alpine Tethys (see: Loprieno et al., 2011). Probably in an early stage of subduction, the stacking of the Austroalpine nappes took place to the SE of the

Piemont oceanic crust. (ESCHER et al., 1997; MOSAR et al., 1996; STAMPFLI, 1993; STAMPFLI et al., 1998).

During the Mesoalpine event, the Briançonnais domain, and the internal part of the European continental crust started to deform due to the continental subduction towards SE that resulted in the formation and stacking of basement nappes, as well as in the development of an orogenic wedge. The préalpine nappes escaped the intense ductile deformation by thrusting as cover nappes towards NW. The metamorphism in the Préalpes klippen is of low grade (300°) and syn-deformational (MOSAR, 1988a; MOSAR et al., 1996). It is related to the initial incorporation in to the orogenic wedge and the subsequent nappe transport, but prior to the final emplacement. At a final stage of the Mesoalpine phase, the major Helvetic nappes started to shape, whereby the inversion of inherited normal faults plays a major role. Progressively, from the SE to the NW, the formation of the basement units (Mt Chetif, Gotthard, and Mont Blanc-Aar massifs) took place and their corresponding cover nappes were individualised. At the end of this period, the internal European crustal units were thrust by tectonic underplating below the external Briançonnais units thus arriving into the upper plate (ESCHER et al., 1997).

The Neoalpine event, starting around 30Ma, is characterised by continued frontal accretion, as well as intensive S and SE verging back-folding and thrusting together with strong dextral strike-slip faulting in the more internal part of the Western Alps. The onset of large-scale SE verging movements combined with a continuing NW verging thrusting initiated the present wedge shape of the Western Alps. These opposing movements provoked a strong uplift of the Alpine wedge, accompanied by the erosion and deposition of Molasse-type sediments in peripheral foredeep basins (ESCHER et al., 1997).

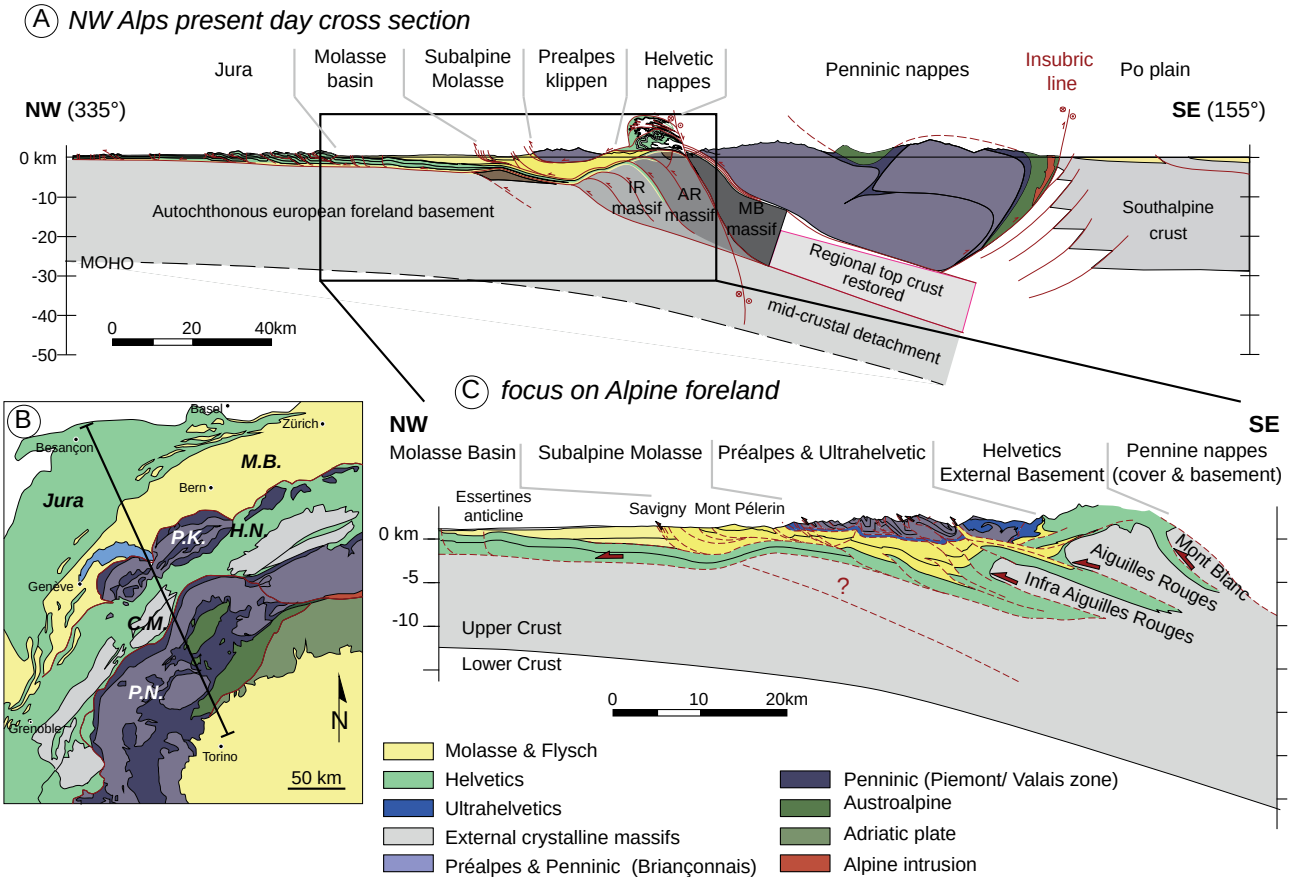

Fig. 5.1: A) Present-day cross-section across the NW Alps (modified after BURKHARD and SOMMARUGA, 1998) showing the converging European plate and its successive basement units (various shades of grey) and their Mesozoic and Tertiary cover (light green and yellow) and the Adriatic upper plate consisting mainly of Penninic nappes (purple), from which the Préalpes were detached. B) Localisation of cross-section (A) on a structural map (modified after SCHMID et al., 2004). C) Focus on the préalpine nappes and the Alpine foreland highlighting a possible connection between the developing crustal imbrications and the out-of-sequence thrusts cropping out in the Préalpes klippen (modified after MOSAR et al., 1996; SCHLUNEGGER and MOSAR, 2010; SOMMARUGA, 1997).

2.2 The Geodynamic Evolution of the Préalpes Klippen Belt

The Préalpes klippen belt is composed of different elements from the European margin at the base (Ultrahelvetic, the Zone Submédiane Niesen nappes) (Stampfli, 1993; Stampfli et al., 2002), from the Briançonnais domain (Préalpes Médianes Plastiques and Rigides and Breccia Nappe) and sediments formerly pertaining to the oceanic accretionary prism of the Alpine Tethys (Nappe Supérieure). For this reason, the préalpine nappes are composed of sediment series with differing lithostratigraphic build and mechanical stratigraphy controlling their behaviour under tectonic deformation.

The Nappe Supérieure - originating in the Piemont domain - is mainly built up by Cretaceous and Paleocene flysch deposits and is generally subdivided in four subunits: the Simmen, Gets, Dranse, and Gurnigel nappe (Caron, 1972, 1976; Van Stuijvenberg 1979; Winkler, 1984). The subduction of the Piemont Ocean induced the formation of these turbiditic nappes. Therefore, the flysch deposits of the préalpine nappes reveal relevant information about the timing of this event considering their depositional age (Bernoulli and Winkler, 1990; Caron et al., 1980a; Caron et al., 1989; Homewood and Lateltin, 1988; Winkler, 1984). The oldest flysch deposits of the Nappe Supérieure are of Turonian to Maastrichtian age, while the youngest ones are found in the Gurnigel nappe, ranging from Maastrichtian to Bartonian age. The Nappe Supérieure thrusts the Breccia and Préalpes Médianes Nappes around 42 Ma (age given by the youngest sediments of the Breccia nappe (Caron, 1966, 1972; Caron et al., 1980b), continues moving above the Préalpes Médianes Plastiques until the external front of the Préalpes klippen belt, where they thrust the Subalpine Molasse. Today, the Nappe Supérieure can often be found within synclines of the Préalpes Médianes. The Gurnigel nappe remains as NW digitation isolated at the outer boundary of the préalpine nappe stack. In a final deformational stage, the external part of the Nappe Supérieure - the Gurnigel Nappe - is thrust by the Préalpes Médianes Plastiques.

The paleogeographic origin of the Breccia nappe is attributed to the south-eastern passive margin of the Briançonnais microcontinent and the Piemont Ocean (Dall'Agnolo, 2000; Lugeon, 1896; Stampfli, 1993; Weissert and Bernoulli, 1985). The Breccia nappe contains Jurassic breccias and shales related to the extensional structures of the passive margin. Thrust by the Nappe Supérieure, the Breccia nappe is emplaced on top of the Préalpes Médianes Rigides. In the Préalpes Romandes, the Breccia nappe is less abundant than in the Chablais Préalpes and is mainly characterised by three isolated synclines plunging towards NW (Arbenz, 1947; Jaccard, 1904).

The Préalpes Médianes consist of limestones and shales ranging from Triassic to Upper Cretaceous to Early Tertiary flysch series deposited on the Briançonnais microcontinent. The sedimentation realm is interpreted as rim basin to the north of the northern alpine Tethyan rift shoulder. South of the Rhône valley, the Siviez-Mischabel and Pontis nappe of the Pennine Alps expose equivalent stratigraphic units, which remained attached to their pre-Triassic basement and were intensively deformed during Alpine deformation(Sartori, 1987; Sartori and Marthaler, 1994; Stampfli et al., 1998). However, the Préalpes Médianes nappes were detached from their basement in Priabonian times (39Ma) and transported over 100km towards NW (Schardt, 1893b) where they reached the outer front of the Helvetic domain around Chattian times (30Ma) (Lateltin, 1988; Trümpy and Bersier, 1954). The transport over the crystalline massifs took place rather passively on a basal décollement of evaporites located at the base of the Middle and Late Triassic. The present-day position as tectonic klippen resulted from the separation of the Préalpes Médianes and their homeland. This separation is due to the uplift of the External Crystalline Massifs and the erosion of the uplifted series.

The Préalpes Médianes is the best-exposed and largest nappe of the Préalpes Romandes and is commonly subdivided into the Préalpes Médianes Plastiques to the NW and the Préalpes Médianes Rigides to the SE, related to the changing structural style due to paleogeographic differences. The Préalpes Médianes Plastiques in the external part is characterised by a fold-dominated structural style, whereas the Préalpes Médianes Rigides are marked by important imbricate structures in the trailing part (Lugeon and Gagnebin, 1941).

The Niesen nappe consists of Upper Cretaceous to Tertiary flysch-type sediments from the Valais trough (Homewood, 1974; Trümpy, 1960). This prealpine structural unit exists only in the Préalpes Romandes and forms today the southernmost structural unit of the préalpine nappes.

During the emplacement of the préalpine nappes towards the Alpine foreland, major structural features were acquired, such as the folding and thrusting of the Préalpes Médianes and the associated fold axis parallel and perpendicular faulting, which were partly reactivated in a later stage of deformation.

The subsequent deformation of the Préalpes Klippen, but also of the adjacent Subalpine Molasse is mainly related to the entire evolution of the orogenic

wedge in the Western Alps.

2.3 Present-day Orogenic Wedge in the Western Alps

The Alpine orogen forms today a tapered, doubly vergent wedge geometry with a pro-wedge towards NW and a retro wedge towards SE (Beaumont et al., 1996; Escher and Beaumont, 1997) (Fig. 5.2A). Earthquakes (Maurer et al., 1997; Pavoni et al., 1997) and uplift-rates (Jouanne et al., 1995; Kahle et al., 1997) imply a still active Alpine orogen. The geometry of the entire Alpine orogenic wedge, including the Molasse basin and the Jura fold-and-thrust belts, in context with the critical taper model, shows an important thickness of the wedge towards S and a basal thrust (27°) leading to a narrow frontal thinning (Fig. 5.2C). The critical taper model (Dahlen, 1984, 1990; Davis et al., 1983) predicts that the geometry of a growing wedge (defined by its surface slope α and its basal slope β) is a function of material strength and basal friction. A facilitated deformation within the wedge - compared to high friction along the basal thrust - leads to a steeper critical taper angle. This process persists until the internal deformation gets more difficult than sliding along the basal décollement. The opposite occurs if the basal décollement deforms more easily, leading to a back stepping of the frontal thrust, likely associated with out-of-sequence thrusting.

Within the Western Alpine orogenic wedge, the overall geometry appears to be unstable, requiring either frontal accretion or tectonic underplating in order to regain stable conditions (Mosar, 1999) (Fig. 5.2C). A closer look at the Neoalpine evolution of the position of the basal thrust through time, gives us a better understanding of the present-day unstable wedge geometry. After the emplacement of the préalpine nappes onto the Alpine foreland, the thrust front seemed to remain in a stable position SE of Lausanne (from 22 - 12 Ma). The thrusting of the Subalpine Molasse must have occurred in the same time interval and was active at least until Middle Miocene (Homewood et al., 1986). In Early Miocene, the exhumation of the External Crystalline Massifs (Aiguille Rouge, Mont Blanc, Aar and Gastern massifs) started, as indicated by fission track analysis (Bogdanoff et al., 2000; Burkhard, 1990; Gebauer et al., 1997; Hurford, 1986; Leloup et al., 2005; Schaer et al., 1975).

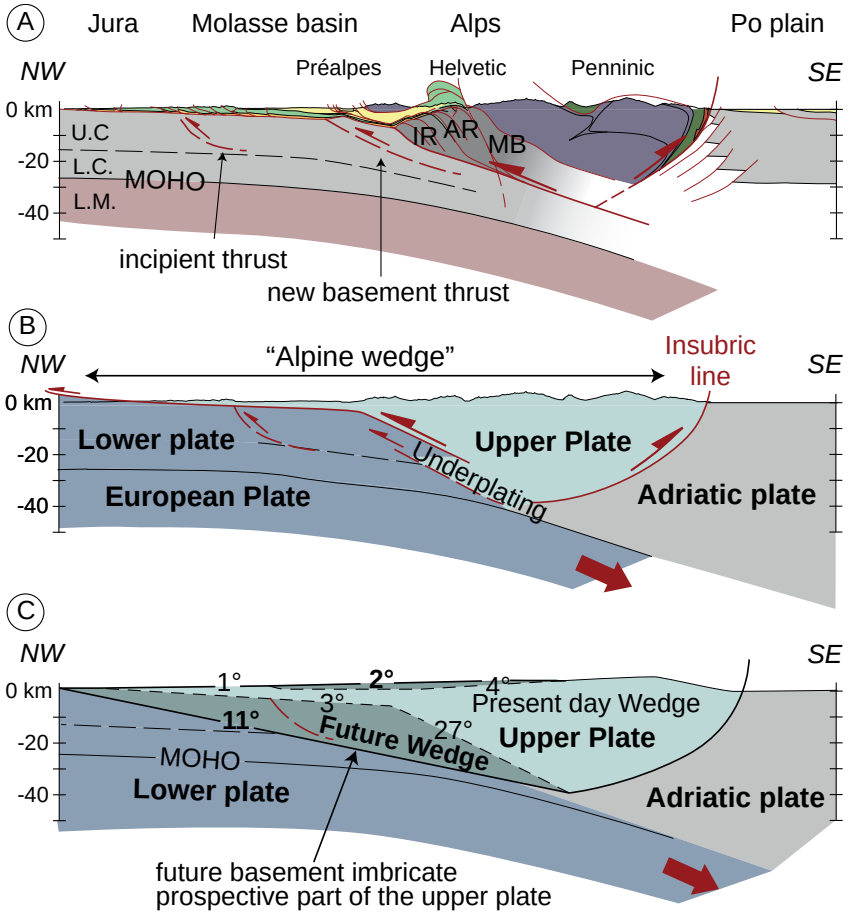

Fig. 5.2: A) Simplified cross-section through the Western Alps (localisation Fig. 5.1) showing the major structural units. B) scheme of the orogenic wedge of the Western Alps with its Lower and Upper Plate attribution. C) Critical taper model adapted to the Western Alpine wedge, proposing a future stable wedge geometry (MOSAR, 1999).

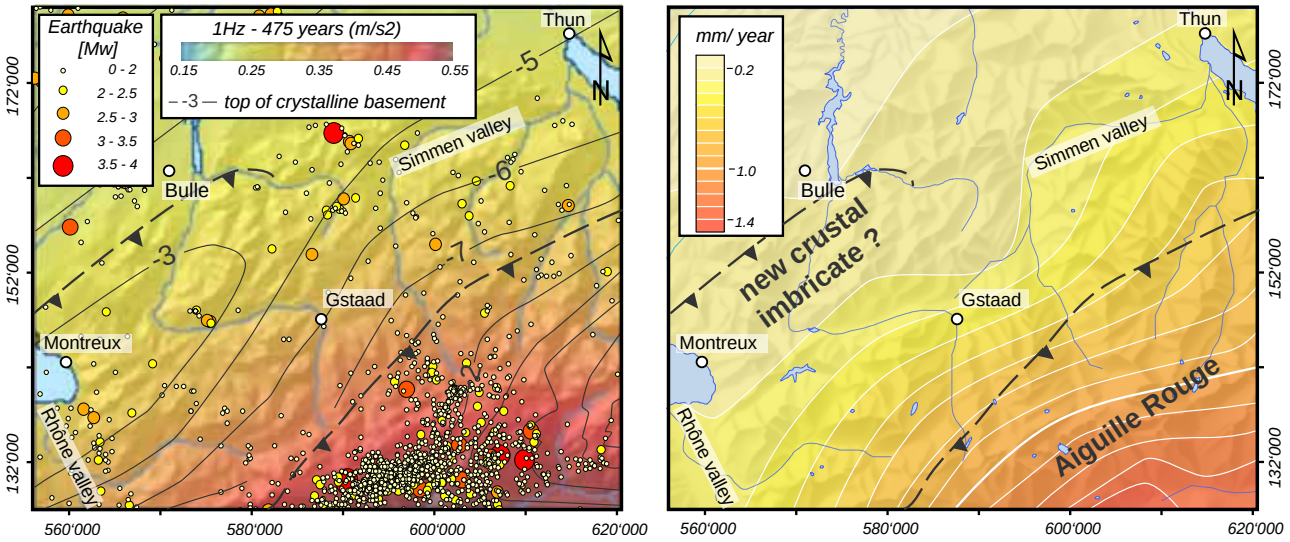

Fig. 5.3: Seismic hazard map of the Préalpes Romandes depicts the level of horizontal ground motion expected to be reached in a period of 475 years (GIARDINI et al., 2004) with registered earthquakes since 1975 extracted from the earthquake catalogue of Switzerland (ECOS02). Towards the Helvetic nappes and the External Crystalline Massifs, a remarkable concentration exists whereas near the eastern part of the Lake Geneva another, less marked accumulation prevails The grey lines represent the topography of the top of the crystalline basement (numbers correspond to the elevations [km]) (PFIFFNER et al., 1997a). On both maps the thrust front of the Aiguille Rouge massif and the presumed new crustal imbricate are indicated by dashed lines. Uplift rates (mm/year) expose an increasing uplift towards the south-east, exceeding 1 mm/year (KAHLE et al., 1997).

The important stacking of the cover nappe and basement uplift provoked a higher topographic relief S of the préalpine nappe stack, which lead to a taper angle greater than the critical angle. Around 11 Ma, a major jump of the basal thrust from S of the Western Molasse basin to the N of the Jura mountains occurred, forming the most external limit of the Alpine orogenic wedge with the youngest fold-and thrust geometry. Recent uplift rates, earthquakes activity, out-of-sequence faulting in the Préalpes klippen (MOSAR, 1999) and Subalpine Molasse (CEDERBOM et al., 2011) as well as the presence of a heightened basement relief underneath the Préalpes Klippen indicates that the orogenic wedge geometry is still not in equilibrium. By tectonic underplating - the accretion of lower plate material to the upper plate - the unstable orogenic wedge thickens, and thus triggers a dynamic response to attain its internal stability (MOSAR, 1999) (Fig. 5.2.B&C).

The distribution of the earthquake occurrences reveals the highest concentration in the Helvetic domain and in the External Crystalline Massifs (GIARDINI et al., 2004) (see Fig. 5.3). A second, less important concentration is situated in the western part of the Préalpes Romandes towards Lake Geneva, corresponding with the developing basement imbricate. The present uplift rates expose a similar pattern with a high uplift towards the Helvetic nappes and the External crystalline massifs where an uplift of 1mm/year is exceeded (KAHLE et al., 1997; MOSAR, 1999). In the Préalpes klippen belt, the uplift range from 0.2 mm/year to 0.6 mm/year. In the Rhône Valley near the Lake Geneva, the uplift curves slightly deviate from their normal course indicating a minor uplift increase, whereas between Gstaad and Zweisimmen the uplift is attenuated. This is probably related to the lateral disappearance of the basement high of the Préalpes Romandes.

3 TRANSITION PRÉALPES MÉDIANES - GURNIGEL NAPPE - SUBALPINE MOLASSE AND MOLASSE BASIN

Structural and fault kinematic analysis in the frontal part of the Préalpes Klippen and in the adjacent Subalpine and Folded Molasse give a better insight of the transition of these different structural units towards the Western Molasse basin. Although presenting different origins, tectonic histories and stratigraphic series, the Préalpes Médianes and Gurnigel nappe, as well as the Molasse Subalpine show a similar post-emplacement deformation. They were on the one hand affected by out-of-sequence thrusts as a reaction to readjust the equilibrium of the Alpine orogenic wedge, on the other hand influenced by more recent strike-slip movements. Within the different structural units, both deformation systems are visible, but they are expressed differently due to the presence of inherited structures (Préalpes Médianes, Gurnigel nappe) and diverse lithologies (limestones, marls, sandstones).

3.1 Folded Molasse - Gouchit Anticline

The Plateau Molasse exposes NNE-SSW to NE-SW striking gentle folds that are thought to represent early stages of buckle folds with Triassic cores filled with well-organised evaporite accumulations and duplexes (Sommaruga, 1997, 1999). The internal deformation and shortening of the Molasse Plateau and its underlying Mesozoic cover is relatively weak (Burkhard, 1990; Jordan, 1992; Pfiffner, 1986). Without a sharp boundary, the folds in the Plateau Molasse increase towards SE, towards the frontal thrust of the Subalpine Molasse. The narrow belt (2-7km wide) - known as Folded Molasse - exposes steeply dipping beds of the Lower Freshwater Molasse, forming synclines and anticlines marked by sub-vertical beds. Generally, this folded zone exists above all in the Lower Freshwater Molasse of eastern Switzerland (Trümpy, 1980).

Near Plaffeien, a well-developed anticline, the Fall anticline, attracted major interest of several generations of geologists (Marescot, 2000; Schmid, 1970). Regarding the morphological expression of this anticline, the elongated Sinnebüel hill, shows that

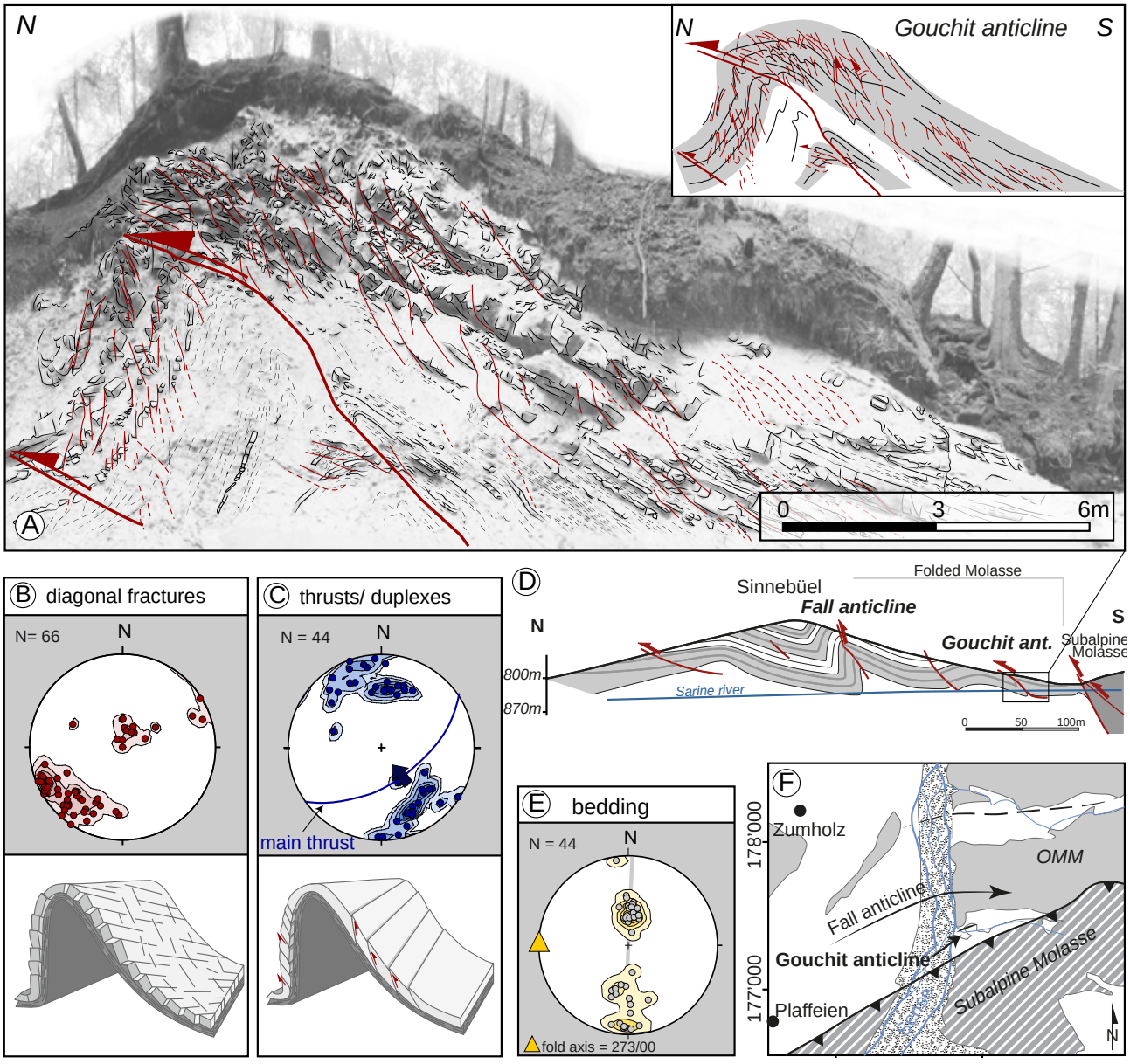

Fig. 5.4: Overview of the structures of the Gouchit anticline situated in the folded part of the Plateau Molasse in direct vicinity to the frontal thrust of the Subalpine Molasse (50m). B and C shows the orientation of different types of fractures measured by stereographic pole projection on the lower hemisphere (equal area projection) and two sketches illustrating the arrangement of: B) the diagonal fractures related to the folding and C) thrusts associated to on-going compressional movements. D) shows the localisation of the Gouchit anticline within the context of the Folded Molasse with the northern Fall anticline and the Subalpine Molasse to the south. E) pole to bedding projection clearly shows the E-W striking orientation of the Gouchit fold. C) schematic map shows Gouchit anticline localisation (589'900/ 177'420) within the folded Upper Marine Molasse (OMM) near the boundary to the Subalpine Molasse.

towards the east the fold dies rapidly out laterally, whereas the extent towards west cannot be followed. The asymmetric inclined anticline with a steep frontal limb displays an alternating stratification of plastic marly and rigid conglomeratic layers allowing an eased folding (Fig. 5.4D). In vicinity to the frontal thrust of the Subalpine Molasse, the small-scale Gouchit fold developed, displaying a similar structure to that of the Fall anticline, but of smaller wavelength (about 30m length). The accessible outcrop allowed the study of its internal structures (Fig. 5.4): the major thrust plane within the fold structure is clearly offsetting the competent layers for several centimetres, both in the core of the anticline and in the external part. The strongly fractured limbs expose tight duplex structures with SSE dipping thrust planes, which are steeper inclined in the northern, than in the southern fold limb (Fig. 5.4C). Especially in the hinge area, the fracturing of the fold increases by forming multiple splay faults developing a chaotically fractured zone. Towards the north, the hinge of the frontal syncline is marked by the presence of an out-of-syncline thrust. Marly layers in between the core and the fold envelope are compensating their deformation. For this reason, the thrust observed in the core can only be traced over a short distance and cannot be connected in between. Diagonal fractures related to the fold bending are segmenting the fold limbs into smaller blocs (Fig. 5.4B).

Temporal constraints to the formation of these folded structures, as well as their further development are difficult to attribute. The duplex structures seem to post-date the folding of the Molasse layers and can probably be related with more recent thrusting movements within the adjacent Subalpine Molasse. Regarding the stereographic projections of the pole of the thrust planes and the bedding clearly exposes that the thrusting occurs oblique to the folding suggesting an independent development of the folds and thrusts. This evidently confirms the assumption of a thrusting post-dating the folding of the Subalpine Molasse.

Due to the lack of slickensides preserved on fault planes, the strike-slip deformation could not be identified in this outcrop. However, detailed paleostress analysis in the Western Molasse basin of the Canton Fribourg, based on fault-slip data revealed an unambiguous strike-slip deformational phase (Ibele, 2011). A clear timing of this deformation was not possible, hence a relatively imprecise time interval from Middle Miocene to present was proposed. Earthquake focal mechanisms within the "Fribourg zone" - a zone characterised by an alignment of weak seismic events - displaying a N-S oriented sinistral movement (Kastrup et al., 2007), suggest a recent deformation system.

3.2 Subalpine Molasse

Farther south of the previous outcrop, an important thrust front marks the transition from the folded Molasse (Upper Marine Molasse - OMM) towards the Subalpine Molasse (Lower Freshwater Molasse - USM). The Subalpine Molasse is characterised by an intensively deformed stack of steeply dipping imbricated thrust sheets at the former Alpine boundary. It is assumed that the thrusting of the subalpine thrust sheets started in internal zones around Middle Oligocene, related to the northward propagation of the thrusting activity (Burkhard, 1990). In eastern Switzerland, Bavaria (GER), and Austria, this zone is marked by an important blind back thrust, delimiting a triangular sector, known as "triangle zone" (Berge and Veal, 2005; Pfiffner et al., 1988; Vollmayr and Wendt, 1987). As similar structures are developing in analogue models of the Alpine foreland basin (Bonnet, 2007), their occurrence is not improbable in the western part of the Molasse basin. Farther to the east in the Emmental, Subalpine Flysch and the Helvetic nappes intersect the Subalpine Molasse. Elsewhere, the triangular zone is thrust by newly developed thrust, related to the backstepping of the Alpine deformation front into the Subalpine Molasse (Schlunegger and Mosar, 2010). Recent apatite fission track analysis (Cederbom et al., 2011) recorded the latest thrusting activity in the Subalpine Molasse at, or since the major erosion event, during Plio-Pleistocene times.

Paleostress analysis within four sites near La Roche exposes a heterogeneous fault-slip dataset revealing the influence of both thrusting and strike-slip movement. The predominant stress regime obtained corresponds to a strike-slip to oblique compressional stress regime with a NW-SE directed compressional axis. Reverse faults are mainly oriented NE-SW and dipping either towards SE or towards NW, whereas strike-slip faults, both sinistral and dextral, trend N-S, or WNW-ESE. Subordinate stress regimes mainly express an extensional stress regime turning into a compressional stress regime by tilting back into their pre-thrusting position. Therefore, an initial NW-SE oriented compressional stress regime is assumed during the formation of the Subalpine Molasse imbricates. Under the more recent strike-slip stress regime, several of these thrust planes were reactivated both with a strike-slip and a compressional movement, as shown by overprinting slickensides.

We suggest that the backstepping of the orogenic front and the associated renewed thrusting activity within the Subalpine Molasse act simultaneously with the strike-slip stress regime. Depending on the proximity to important structures - both, thrust faults, and strike-slip fault zone - the corresponding stress

regime prevails. This assumption remains hypothetical as no clear evidence were provided by the analysis of fractures in the field, as most of the observed fault planes were of relatively small (0.5 - 1.5m) extent without an intersecting relationship between them. However, the ratio between the different stress axes (R) exposes a generally strong compressional component (σ_1) and a varyingly pronounced extensional component (σ_3). Hence, interchanging stress regimes - a compressional or a strike-slip regime - are possible.

3.3 Nappes Supérieure: Gurnigel

Towards the SE of the Subalpine Molasse, the Gurnigel Nappe extends along the external boundary of the Préalpes klippen belt. The Gurnigel Nappe belongs to the Nappe Supérieure, but in the course of the emplacement of the préalpine nappes, the most external part became isolated. In a later stage of deformation, the Gurnigel Nappe was thrust by the Préalpes Médianes Plastiques. This can be related to the late reactivation of an out-of-sequence thrust between these two nappes thrusting the PMP nappe on top of the internal part of the Gurnigel nappe (De Kaenel et al., 1989). The general deformational style of the Gurnigel nappe is characterised by several imbricated thrust sheets and duplexes showing a lateral extension of several kilometres (Weidmann, 2005). In contrast to the limestones and marls of the Préalpes Médianes nappes, the Gurnigel nappe consists entirely of turbiditic Flysch sediments, which are influenced by slump structures and exposes no pre-emplacement structures.

The analysis of large-scale structures (lineaments of 161 - 2500m length) based on analysis of aerial photographs and DTMs revealed a predominant WNW-ESE fault orientation and a subordinate N-S fault direction, unlike the dominance of postulated N-S oriented struc-

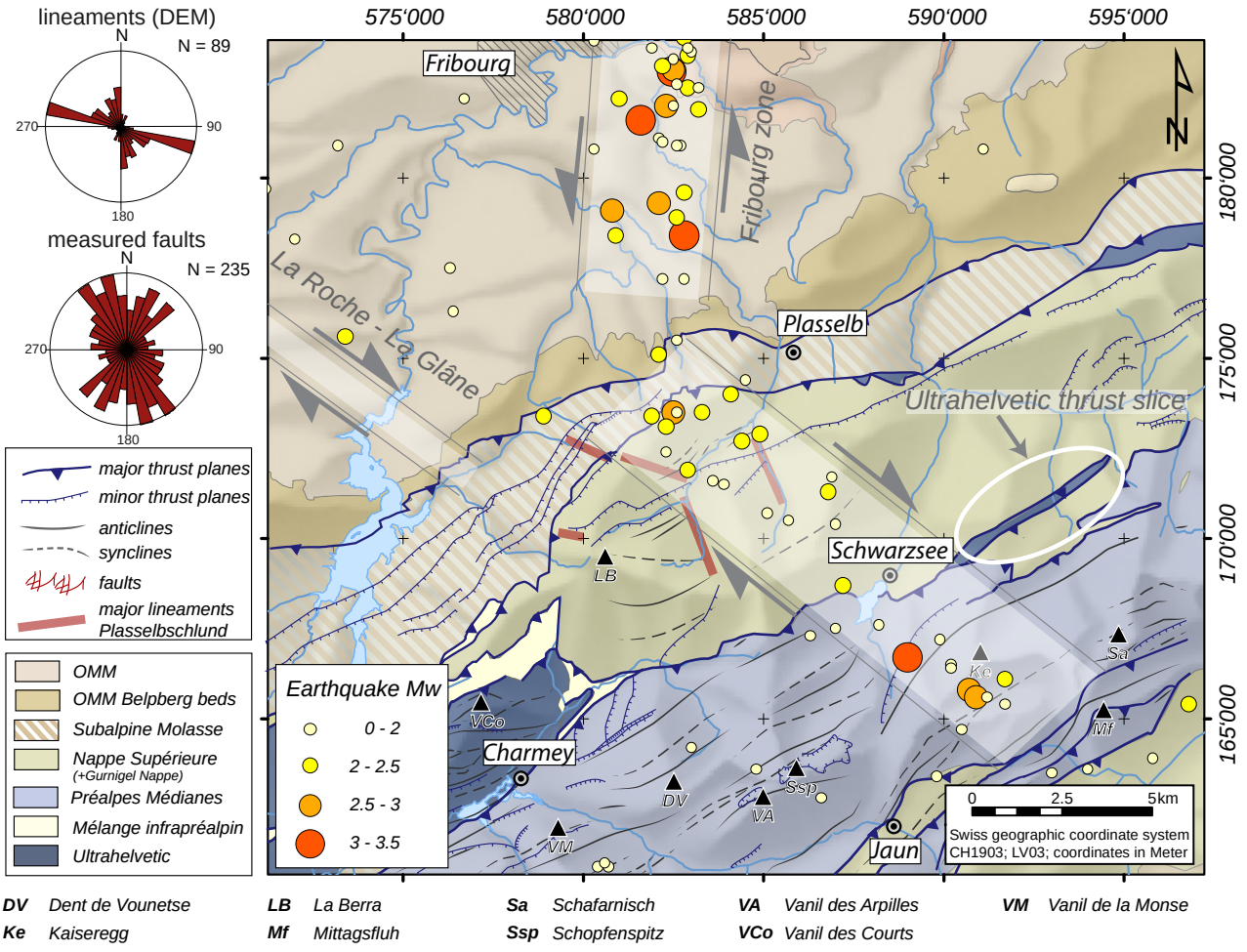

Fig. 5.5: Structural map representing the distribution of the instrumentally measured earthquakes since 1979. Apart from the N-S alignment of the Fribourg zone, a second NW-SE oriented accumulation of earthquakes can be recognised reaching from the Subalpine Molasse, to the Gurnigel nappe to the Préalpes Médianes. The orientation of this presumed NW-SE oriented dextral fault zone parallels the La Roche-Glâne fault zone. Rose diagrams display the orientation of the lineaments and the orientation of the measured fractures in the Plasselbschlund area. To the NE of the earthquake alignment an Ultrahelvetic thrust slice is visible affirming a recent thrusting activity.

tures of previous studies (PLANCHEREL, 1979). Fracture measurements in the field expose a NW-SE and a NE-SW trend generally with a strike-slip movement. Their kinematic analysis of the heterogeneous data set exposes a predominance of strike-slip stress regimes, whereby the stress regime of a NW-SE oriented compression clearly prevails. Back rotating the fault-slip measurements into its pre-folding position confirms the presence of the NW-SE oriented strike-slip regime already before the folding. As the exact age of the large-scale folds of the Gurnigel nappe is not known, we suggest a relatively recent folding related to the formation of out-of-sequence faults.

Evidence for the latest thrusting activity in the Gurnigel nappe can be found on the one hand by thrusting of the Préalpes Médianes on top of the Gurnigel nappe, on the other hand by the Ultrahelvetic thrust slices within the Gurnigel nappe, which are probably sheared off from the Ultrahelvetic layers located below (Fig. 5.5).

A series of recent earthquakes (1972-1992) of low intensity were registered in the area south-west of Plasselb. Their interpretation (FRÖHLICH, 1991; PAVONI, 1992) reveals the existence of a sinistral strike-slip zone oriented towards N-S. However, this fault zone is not clearly visible at the surface or on seismic lines (WEIDMANN, 2005). This observation corresponds with the general trend of N-S oriented sinistral strike-slip faults described by Plancherel (1979). However, investigations of DEMs and orthophotographs record a prevailing occurrence of their conjugated counterparts - dextral WNW-ESE oriented fault zones (see rose diagram of lineaments; Fig. 5.5). The consideration of the earthquake arrangement showss not only an accumulation at the frontal part of the Gurnigel nappe (near Plasselb), but also a NW-SE oriented alignment reaching from the Subalpine Molasse, to the Gurnigel nappe, to the Préalpes Médianes. This alignment of earthquakes is interpreted as fault zone, similar as the La Roche - La Glâne fault zone in the Plateau Molasse exposing a dextral sense of shear (Fig. 5.5).

The analysis of the Plasselbschlund area confirmed the presence of both recent thrusting and a strike-slip stress regime within the Gurnigel nappe. The strike-slip stress regime is mainly expressed by fault kinematics, the arrangement of large-scale lineaments, as well as a dextral fault zone delimited by the arrangement of earthquakes. Thrusting activity is represented by the over-thrusting Préalpes Médianes at the back part of the Gurnigel nappe, and by Ultrahelvetic thrust slices within these nappes.

3.4 PRÉALPES MÉDIANES

The Préalpes Médianes Plastiques to the NW of the Préalpes Médianes consist of a series of fault-related folds, which developed during nappe emplacement. Their axial trends reach from E-W in the eastern part to NNE-SSW in the western part. Structures related to these folds, such as normal faults parallel, diagonal, or perpendicular to the fold axis or thrust faults, constrain the subsequent deformation, which reactivates these important fault planes. Moreover, the Préalpes Médianes are influenced by paleo structures - mostly extensional structures, but also inversion structures - related to the rifting phase of the Alpine Tethys. Important sedimentary thickness changes are witness to this pre-emplacement deformation phase, forming major weakness zones commonly oriented NE-SW (BOREL and MOSAR, 2000).

Kinematic analysis based on fault-slip measurement revealed a heterogeneous data set, probably due to reactivation of already existing structures. Hence, former normal faults, probably generated by fold axis parallel extension, show a superimposed strike-slip movement. In the Préalpes Médianes, as in the previously discussed structural units, a strike-slip stress regime is prevailing with a NW-SE oriented compressional component. Therefore, the orientation of the fracture planes not always corresponds to the ideal conjugated, sub-vertical fault planes N-S orientated sinistral fault planes, respectively NW-SE orientated dextral fault planes. Ancient normal faults perpendicular to the fold axis generally featuring a NW-SE orientation and N-S oriented diagonal faults are oriented advantageously for a reactivation under a strike-slip stress regime.

In the Préalpes Médianes major fault zones, most probably related to ancient paleostructures, exist, namely in the Schafarnisch - Weissenburg area, where an important N-S oriented sinistral and a conjugated WNW-ESE oriented dextral fault zone is offsetting the folding structure (Fig. 5.6). These predefined weakness zones were reactivated under the accentuated bending of the Préalpine arc, leading to an increased compression in this region. By the development of an advancing triangular structure, the compression was compensated. Thereby two important tear faults developed generating Riedel type fractures within these two broad fault zones. We suggest the presence of similar fault zones within the Euschelspass region and in the Sarine valley, which seem to be related to tear faults of differentially advancing thrust components.

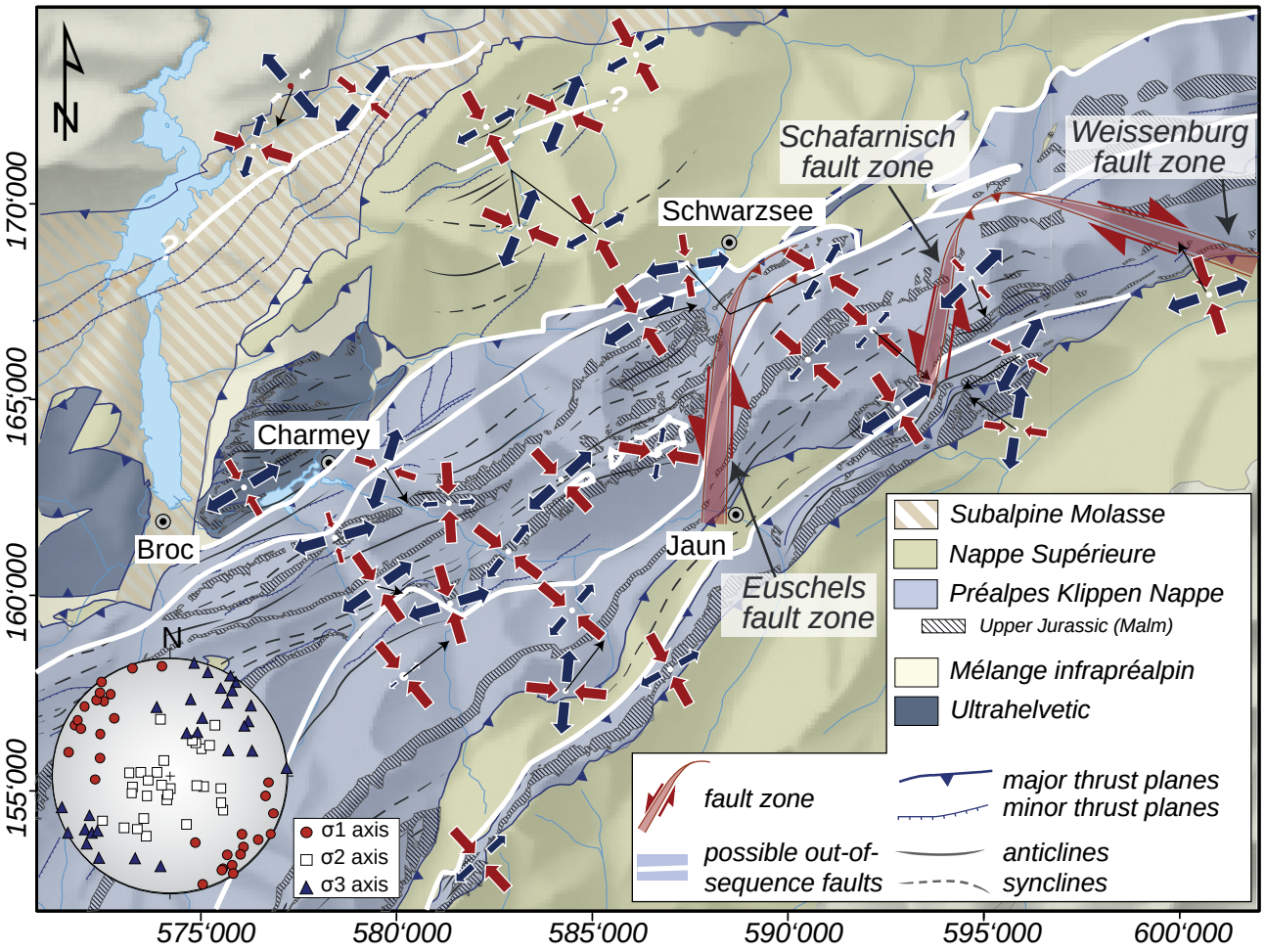

Fig. 5.6: Structural map showing the distribution of the overall prevailing strike-slip stress regime in the Préalpes Médianes, but also in the Gurnigel nappe and the Subalpine Molasse. Conjugated fault zones in the Schafarnisch-Weissenburg area probably related to paleostructures expose fractures arranged as Riedel faults within these zones. The dashed lines indicate the probable trend of out of sequence faults based on zones of structural weakness along nappe boundaries or sedimentary thickness changes.

In the Préalpes Médianes It can be shown that out-of-sequence thrusts are possibly located along important weakness zones, such as along paleofaults developed during the rifting phase or nappe boundaries. In the Schopfenspitz area, as well in its southwestern prolongation in the Gros Haut Crêt area, the presence of an out-of-sequence thrust fault is expected. The Schopfenspitz thrust and its secondary, auxiliary thrusts are crosscutting already existing structures, such as small-scale folds of the Lower Cretaceous that clearly signifies a thrusting activity after the folding phase. Paleostress analyses of fault-slip data in vicinity of the Schopfenspitz thrust fault indicate unambiguously a compressional stress regime with a NW-SE oriented compressional component. In the entire investigation area, only at a few sites compressional stress regimes were recorded, mostly nearby suspected out-of-sequence faults.

4 Discussion

Within the different structural entities ranging from the Préalpes Médianes towards the Molasse Basin, indications for both stress regimes - a compressional, related to out-of-sequence thrusting, and a strike-slip stress regime stress regimes - were observed. However, they expose no evident chronology amongst these two regimes. As focal earthquake mechanisms reveal a prominent strike-slip stress system, it is presumed that this stress regime is still active today, whereas the youngest thrusting movement within the Subalpine Molasse is dated 5 to 4 Ma (Cederbom et al., 2011). Even if the origin of these two stress regimes differs, a mutual interaction between them is possible. Maintaining the identical orientation of the compressional stress axis, a permutation of the extensional and the intermediate stress axis defines the one or the other stress regime. Another proposition tends to consider the general orientation of the faults within

the two stress regimes. Within the compressional stress regime, faults are trending NE-SW and are mostly steeply dipping towards SE, but also towards NW. Under a strike-slip stress-regime, generally two conjugate fault directions develop a N-S oriented sinistral and a WNW-ESE oriented dextral strike-slip faults. All of these three fault directions show an ideal orientation to be activated under a NW-SE orientated compression. The question remains open how the interplay of thrusting and strike-slip within the Alpine foreland took place. Are the out-of-sequence thrusts dominating over the strike-slip movement, or are they locally restricted? Paleostress analysis and seismic activity report an ubiquitous strike-slip stress regime, whereas the thrusting movement are mostly missing. One could suggest that thrusting movements are limited to particular weakness zones that take up the entire thrusting movement, whereas the strike-slip movements are more widespread. Another suggestion could be that the strike-slip stress regime is continuously active and the compressional stress regime occurs more occasionally. That would also explain the tilted and the non-tilted strike-slip stress regime in the Subalpine Molasse. However, without more persisting evidences from the field or seismic measurements, these reflections remain purely hypothetical.

5 Conclusion

The post-emplacement evolution of the different tectonic units ranging from the folded Molasse, the Subalpine Molasse, the Gurnigel, and the Préalpes Médianes Nappe show similar characteristics despite their diverging stratigraphic and tectonic background. These structures appear as out-of-sequence thrusts related to a compressional stress regime and as ubiquitous strike-slip faults, mainly occurring as N-S oriented sinistral and WNW-ESE oriented dextral faults associated to a strike-slip stress regime. However, the recent deformations are still considerably influenced by pre-existing structures, which accommodate the younger stress systems by reactivation of inherited faults of previous deformation phases.

A transect of the frontal accretionary wedge structure (Fig. 5.7), a synoptic view over the post-emplacement structures of the different view is given. In the folded Molasse (Fig. 5.7A), as well as in the Plateau Molasse sub-vertical strike-slip faults are prevailing. However, the Gouchit fold, near Plaffeien, exposes a major thrust plane clearly offsetting the fold structures and additionally, duplex thrusting oblique to the bedding orientation witness a recent thrusting of the entire fold structure. The Molasse Subalpine (Fig. 5.7B), shows a renewed thrusting activity, which is acting together with the strike-slip, faults, showing partly a tilting of an ancient strike-slip stress regime by the thrusting movement. Within the Gurnigel Nappe (Fig. 5.7C) similar observations can be made, except that the influence of the folding structure, as well as the Flysch nature of this structural unit has to be taken into account. Paleostress analyses of the Gurnigel fault-slip measurements show obviously a less heterogeneous result than in the Préalpes Médianes, probably due to less constraining syn-emplacement structures. In the Préalpes Médianes (Fig. 5.7D), mainly strike-slip faults are prevailing that are mostly strongly influenced by the presence of normal faults and thrusts generated during the folding. Out-of sequence faults exists, but are mainly following important weakness zones, such as paleofaults generated during the rifting phase of the Alpine Tethys.

The results of this thesis points out the importance of the relationship between the complex structural features observed today within the frontal part of the Préalpes Romandes and the structural heritage influencing the succeeding deformation phases by forming weakness zones far easier to reactivate. Based on detailed field observations, geological maps, orthophotographs and DEM, as well as thorough paleostress analyses, we achieved to get an overview over the successive events characterising the Préalpes Médianes. In the following, a chronology and a structural interpretation of the deformational evolution of the Préalpes Médianes are presented based on the results of this thesis.

During the Lower Jurassic major paleostructures developed as the rifting of the Alpine Tethys attained its maximum. The marine basin structure is mainly controlled by three important NE-SW striking synsedimentary paleofaults, however also N-S oriented paleofaults occur. These paleofaults result in important thickness variations in sedimentation, which were influencing the structural behaviour of the Préalpes Médianes during, as well as after the nappe emplacement. The Schopfenspitz fault (Rianda-Stockhorn paleofault), the Weissenburg-Schafarnisch fault zone, as well as the Euschels fault zone are prominent examples for the reactivation and the on-going movement along these paleofaults. Subsequently in the Lower and Middle Jurassic, fast differential subsidence led to the development of several small basins separated by structural highs giving way to the development of the three major sedimentation realms corresponding to the future Préalpes Médianes Plastiques to the NW, the intermediate zone (Gastlosen and Heiti zone) and the Préalpes Médianes Rigides in the SE. These structures

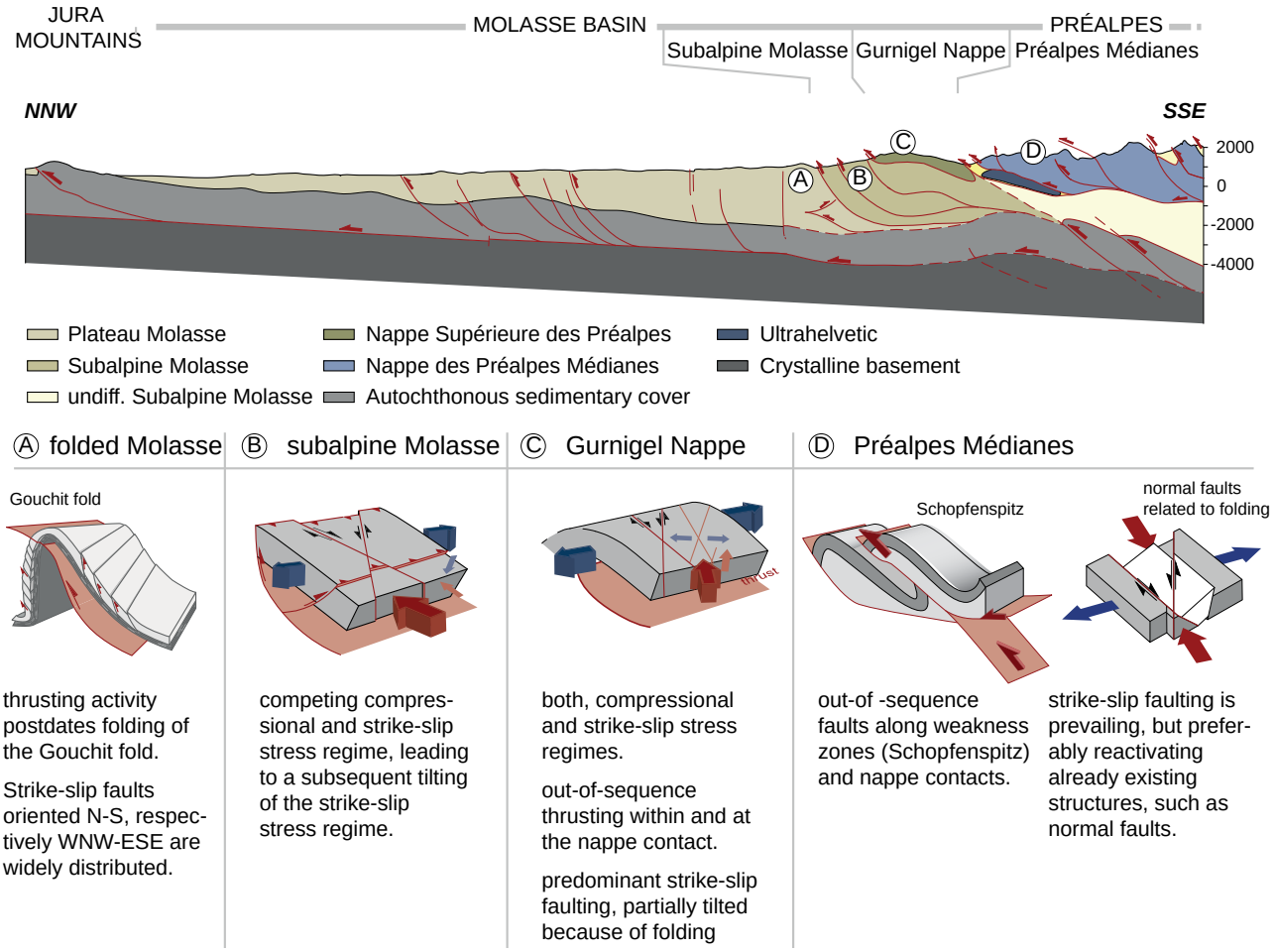

Fig. 5.7: Overview of the post-emplacement structures of the different structural units ranging from the folded Molasse, via the Subalpine Molasse and the Gurnigel Nappe to the Préalpes Médianes Nappes.

Compressional phases occur in the Middle Jurassic, triggering the inversion of paleofaults leading to karst formation and the erosion of the Heiti formation. The interplay of faults, normal or inverted, generates the developing structures in an overall extensional regime of a passive margin.

Since Late Eocene (Bartonian), low-grade metamorphism occurs in the trailing part of the Préalpes Médianes associated to the thrusting of the overlying nappes (Nappe Supérieure and Breccia Nappe) and the subsequent burial related to the incorporation into the accretionary prim. Continental collision from Late Eocene (Priabonian) to present is characterised by the development of the main structural features of the fold-and-thrust belt of the Préalpes Médianes Plastiques. Fault-related folds, mainly fault-propagation folds, are verging towards the foreland, but less frequently, backthrusts are generating folds verging towards the hinterland. Fault zones of these fold-generating thrusts expose an important width containing brittle shear bands, implying an important faulting activity (e.g. Maischüpfen fault). Simultaneously, due to the non-cylindical folding of the Préalpes Médianes, normal faults are generated by a fold axis parallel extension resulting in a segmentation of the folds (e.g. Dent de Broc area, Tzintre quarry). Large-scale strike-slip faults zone developed during the nappe emplacement are interpreted as differentially advancing thrust planes, mostly guided by pre-existing paleostructures (e.g. Schafarnisch, Euschels).

With the arrival of the préalpine Nappes on top of the Ultrahelvetic and Helvetic domains in the Late Eocene/ Lower Oligocene (probably Rupelian), a renewed large-scale deformation affected especially the Préalpes Médianes Rigides, so they achieve their present-day position as steeply inclined monoclinal imbricates dipping towards SE (e.g. Gastlosen and Heiti imbricate). The Mont Pélérin conglomerates - deposited in the Chattian - register the arrival of the préalpine nappes on top of the Molasse basin, as these sediments derive from the eroded Nappe Supérieure.

Since the Upper Oligocene (Chattian) until present, a final period of thrusting occurs, which is probably related to readjustment of the wedge instabilities after the arrival on the Alpine foreland. Out-of-sequence thrust (e.g. Schopfenspitz thrust) are cutting through the préalpine nappe pile and are probably linked to the development of a new crustal imbricates.

Furthermore, recent strike –slip faulting can be observed in several structural units ranging from the frontal préalpine nappes, to the Subalpine and Plateau Molasse, to the Jura mountains. However, depending on their structural background, the strike-slip movement takes place on already existing fault planes or on newly created one.

*****

6 - References

Ackermann, A. 1986. Le flysch de la nappe du Niesen. Eclogae geologicae Helvetiae 79, 641-684.

Andrey, J.D. 1974. Géologie de la partie orientale du Massif des Bruns. PhD, No 592 thesis.

Angelier, J. 1994. Fault Slip Analysis and Palaeostress Reconstruction. In Hancock P.L. ed. Continental Deformation. Pergamon Press. Oxford, New York, Seol, Tokyo.

Angelier, J., Goguel, J. 1979. Sur une méthode simple de détermination des axes principaux des contraintes pour une population de failles. Comptes Rendus de l'Académie des Sciences de Paris, Série D 288, 307-310.

Angelier, J., and Mechler, P. 1977. Sur une méthode graphique de recherche des contraintes principales également utilisable en tectonique et en séismologie: la méthode des dièdres droits. Bulletin de la Société géologique de France 19, 1309-1318.

Arbenz, K. 1947. Geologie des Hornfluhgebietes (Berner Oberland). Matériaux pour la Carte Géologique de la Suisse 89, 1-91.

Argand, E. 1911. Les nappes de recouvrement des Alpes Pennines et leurs prolongements structuraux. Matériaux pour la Carte Géologique de la Suisse 31, 26.

Badoux, H. 1963. Les unités ultrahelvétiques de la Zone des Cols. Eclogae geologicae Helvetiae 56, 1-13.

Badoux, H. 1965. Montreux, Feuille nº47, notice. Atlas Géologique de la Suisse 1:25'000. Basel. Commission géologique Suisse.

Badoux, H., Chessex, R., Jeannet, A., Lugeon, M., and Rivier, F. 1960. Monthey, Feuille nº37, notice. Atlas Géologique de la Suisse 1:25'000. Basel. Commission géologique Suisse.

Badoux, H., and Mercanton, C.H. 1962. Essai sur l'évolution tectonique des Préalpes médianes du Chablais. Eclogae geologicae Helvetiae 55, 135-188.

Baud, A. 1972. Observations et hypothèses sur la géologie de la partie radicale des Préalpes médianes. Eclogae geologicae Helvetiae 65, 43-55.

Baud, A., Heinz, R., and Septfontaine, M. 1989. Compte rendu de l'excursion de la Société Géologique Suisse dans les Préalpes, du 2 au 4 octobre 1988. Eclogae Geologicae Helvetiae 82, 359-377.

Baud, A., and Masson, H. 1975. Preuves d'une tectonique de distension dans le domaine briançonnais: failles conjugées et paléokarst à Saint-Triphon (Préalpes médianes, Suisse). Eclogae geologicae Helvetiae 68, 131-145.

Baud, A., and Septfontaine, M. 1980. Présentation d'un profil palinspastique de la nappe des Préalpes médianes en Suisse occidentale. Eclogae geologicae Helvetiae 73, 651-660.

Beaumont, C., Ellis, S., Hamilton, J., and Fullsack, P. 1996. Mechanical model for subduction-collision tectonics of Alpine-type compressional orogens. Geology 24, 675-678.

Berge, T.B., and Veal, S.L. 2005. Structure of the Alpine foreland. Tectonics 24.

Bernoulli, D., Caron, C., Homewood, P., Kälin, O., and Stuijvenberg, v.J. 1979. Evolution of continental margins of the Alps. Schweizerische Mineralogische und Petrographische Mitteilungen 59, 165-170.

Bernoulli, D., and Sengör, C. 2011. Rudolf Trümpy - Incarnation du géologue alpin. Géochronique 117, 1-4.

Bernoulli, D., and Winkler, W. 1990. Heavy mineral assemblages from Upper Cretaceous South and Austro-alpine flysch sequences (N-Italy and S-Switzerland): source terranes and paleotectonic implications. Eclogae geologicae Helvetiae 83, 287-310.

Berthé, D., Choukroune, P., and Jegouzo, P. 1979. Orthogneiss, mylonite and non coaxial deformation of granites: the example of the South Armorican Shear Zone. Journal of Structural Geology 1, 31-42.

Biddle, K.T., and Christie-Blick, N. 1985. Glossary: Strike-slip deformation, Basin formation and Sedimenation. special publication society economic paleontologists and mineralogists 37.

Bieri, P. 1925. Der Bau der Klippendecke zwischen Gantrisch und Simmental (Berner Oberland). Jahresbericht der philosophischen Fakultät II Universität Bern 5, 89-109.

Billi, A. 2005. Grain size distribution and thickness of breccia and gouge zones from thin (<1 m) strike-slip fault cores in limestone. Journal of Structural Geology 27, 1823-1837.

Bogdanoff, S., Michard, A., Mansour, M., and Poupeau, G. 2000. Apatite fission track analysis in the Argentera massif: evidence of contrasting denudation rates in the External Crystalline Massifs of the Western Alps. Terra Nova 12, 117-125.

Boller, K. 1963. Stratigraphische und Mikropaläontologische Untersuchungen im Neocom der Klippendecke (östlich der Rhône). Eclogae geologicae Helvetiae 56, 15-102.

Bonnet, C. 2007. Interactions between tectonics and surface processes in the Alpine foreland: Insights from analogue model and analysis of recent faulting. Ph.D. thesis thesis: Fribourg.

Bonnet, C., Malavielle, J., and Mosar, J. 2007. Interactions between tectonics, erosion, and sedimentation during the recent evolution of the Alpine orogen: analogue modelling insights. Tectonics 26.

Bonnet, C., Malavielle, J., and Mosar, J. 2008. Surface processes versus kinematics of thurst belts: impact on rates of erosion, sedimentation adn exhumation - Insights from analogue models Bull. Geol. France 179, 297-314.

Borel, G. 1991. Etudes géologiques et minéralogiques de la région du Widdersgrind (Préalpes romandes). Licence thesis.

Borel, G. 1995. Préalpes médianes romandes: courbes de subsidence et implications géodynamiques. Bulletin de la Société vaudoise des Sciences naturelles 83, 293-315.

Borel, G. 1997. Dynamique de l'extension mésozoïque du domaine briançonnais: les Préalpes médianes au Lias. Lausanne.

Borel, G., and Mosar, J. 1993. Une analyse historique et structurale d'un pli au coeur des Préalpes médianes. 11ième Réunion du Groupe Tectonique Suisse. ETH Zürich, 26/27 Février 1993.

Borel, G., and Mosar, J. 2000. Subsurface structures in the Chablais Préalpes: New tectonic interpretations of the Préalpes Médianes nappe based on palinspastic lengths. Eclogae geologicae Helvetiae 93, 307-314.

Bott, M.H.P. 1959. The mechanics of oblique slip faulting. Geological Magazine 96, 109-117.

Bovet, L. 1990. Géologie des Préalpes médianes de l'est du Kaiseregg. Diplôme thesis.

Braillard, L. 1998. Etude géologique de la région entre Jaun et les Gastlosen (Préalpes fribourgeoises).

Bugnon, S. 1995. Les Flyschs à Helminthoïdes des Préalpes franco-suisses. Ph.D n°1084 thesis.

Burkhard, M. 1990. Aspects of the large-scale Miocene deformation in the most external part of the Swiss Alps (Subalpine Molasse to Jura fold belt). Eclogae geol. Helv. 83, 559-583.

Burkhard, M., and Sommaruga, A. 1998. Evolution of the Swiss Molasse basin: structural relations with the Alps and the Jura belt. Geological Society of London, Special Publication 134, 279-298.

Calcagno, P., Chilès, J.P., Courrioux, G., and Guillen, A. 2008. Geological modelling from field data and geological knowledge Part I. Modelling method coupling 3D potential-field interpolation and geological rules. Physics of the Earth and Planetary Interioirs 171, 147-157.

Campana, B. 1941. Faciès et extension de la nappe de la Simme au nord-est de Château d'Oex. Eclogae geologicae Helvetiae 34, 221-227.

Caron, C. 1966. Sédimentation et tectonique dans les Préalpes: flysch à lentilles et autres complexes chaotiques. Eclogae geologicae Helvetiae 59, 950-957.

Caron, C. 1972. La nappe supérieure des Préalpes: subdivisions et principaux caractères du sommet de l'édifice préalpin. Eclogae geologicae Helvetiae 65, 47-73.

Caron, C. 1973. Survol géologique des Alpes occidentales. Bulletin de la Société Fribourgeoise des Sciences Naturelles 62, 73-81.

Caron, C. 1976. La nappe du Gurnigel dans les Préalpes. Eclogae geologicae Helvetiae 69, 297-308.

Caron, C., Homewood, P., Morel, R., and Van Stuijvenberg, J. 1980a. Témoins de la Nappe du Gurnigel sur les Préalpes médianes: une confirmation

de son origine ultrabriançonnaise. Bulletin de la Société Fribourgeoise des Sciences Naturelles 69, 64-79.

Caron, C., Homewood, P., and van Stuijvenberg, J. 1980b. Flysch and Molasse of Western and Central Switzerland. In Trümpy R. ed. Geology of Switzerland, a guide-book, Part B, Geological Excursions. Wepf. and Co. Basel, 274-278.

Caron, C., Homewood, P., and Wildi, W. 1989. The original Swiss Flysch: A reappraisal of the type deposits in the Swiss Prealps. Earth-Science Reviews 26, 1-45.

Caron, M., and Dupasquier, C. 1989. Litho- et biostratigraphie des dépôts du «Crétacé moyen» dans les Préalpes Médianes. Geobios, mémoire spécial 11, 49-58.

Cederbom, C.E., van der Beek, P., Schlunegger, F., Sinclair, H.D., and Oncken, O. 2011. Rapid extensive erosion of the North Alpine foreland basin at 5–4 Ma. Basin Research.

Champagnac, J.-D., Schlunegger, F., Norton, K., von Blanckenburg, F., Abbühl, L.M., and Schwab, M. 2009. Erosion-driven uplift of the modern Central Alps. Tectonophysics 474, 236-249.

Champagnac, J.-D., Sue, C., Delacou, B., and Burkhard, M. 2004. Brittle deformation in the inner NW Alps: from early orogen-parallel extrusion to late orogen-perpendicular collapse. Terra Nova 16, 232-242.

Champagnac, J.D., Molnar, P., Anderson, R.S., Sue, C., and Delacou, B. 2007. Quaternary erosion-induced isostatic rebound in the western Alps. Geology 35, 195-198.

Chandrasiri Ekneligoda, T., and Henkel, H. 2010. Interactive spatial analysis of lineaments. Computers & Geosciences 36, 1081-1090.

Chatton, M. 1974. Géologie des Préalpes médianes entre Gruyères et Charmey. Mémoires de la Société Fribourgeoise des Sciences Naturelles 13, 1-128.

Childs, C., Manzocchi, T., Walsh, J.J., Bonson, C.G., Nicol, A., and Schöpfer, M.P.J. 2009. A geometric model of fault zone and fault rock thickness variation. Journal of Structural Geology 31, 117-127.

Chilès, J.P., Aug, C., Guillen, A., and Lees, T. 2004. Modelling the Geometry of Geological Units and its Uncertainty in 3D From Structural Data - The Potential-Field Method. Workshop Proceedings: Orebody Modelling and Strategic Mine Planning WA. Perth.

Cignoni, P. 2011. MeshLab v1.3.0. in CNR V.C.L.-I.-. ed.

Dahlen, F.A. 1984. Noncohesive critical Coulomb wedges: an exact solution. Journal of Geophysical Research B, solid earth and planets 89, 10125-10133.

Dahlen, F.A. 1990. Critical taper model of fold-and-thrust belts and accretionary wedges. Annual Review of Earth and Planetary Sciences 18, 55-99.

Dal Piaz, G.V., Hunziker, J.C., and Martinotti, G. 1972. La zona Sesia-Lanzo e l'evolutione tettonico-metamorfica delle Alpi nordoccidentali interne. Memorie di scienze geologiche 32, 1-16.

Dall'Agnolo, S. 2000. Le Crétacé de la Nappe de la Brèche (Préalpes franco-suisses). Données nouvelles et essai de synthèse stratigraphique et paléogéographique. Eclogae geologicae Helvetiae 93, 157-174.

Davis, D.M., Suppe, J., and Dahlen, F.A. 1983. Mechanics of Fold-and-Thrust Belts and Accretionary Wedges. Journal of Geophysical Research B, Solid earth and planets 88, 1153-1172.

Davis, G.H., Reynolds, S. J. 1996. Structural geology of rocks and regions. John Wiley & Sons, inc. New York, 776.

De Kaenel, E., Salis Von, K.V., and Lindinger, M. 1989. The Cretaceous/Tertiary boundary in the Gurnigel Flysch (Switzerland). Eclogae geologicae Helvetiae 82, 555-581.

Delacou, B., Sue, C., Champagnac, J.-D., and Burkhard, M. 2004. Present-day geodynamics in the bend of the western and central Alps as constrained by earthquake analysis. Geophysical Journal International 158, 753-774.

Delvaux, D. 2006. WINTENSOR, VERSIO 1.3.75. in Royal Museum for Central Africa T.B.D.G.-M. ed.

Delvaux, D., and Barth, A. 2010. African stress pattern from formal inversion of focal mechanism data. Tectonophysics 482, 105-128.

Delvaux, D., Moeys, R., Stapel, G., Petit, C., Levi, K., Miroshnichenko, A., Ruzhich, V., and San'kov, V. 1997. Paleostress reconstructions and geodynamics of the Baikal region, Central Asia, Part 2. Cenozoic rifting. Tectonophysics 282, 1-38.

Delvaux, D., and Sperner, B. 2003. Stress tensor inversion from fault kinematic indicators and focal mechanism data: the TENSOR program. New Insights into Structural Interpretation and Modelling. 212: Geological Society, London, Special Publications, 75-100.

Dietrich, D. 1989. Fold-axis parallel extension in an arcuate fold- and thrust belt: the case of the Helvetic nappes. Tectonophysics 170, 183-212.

Dietrich, D., and Casey, M.A. 1989. A new tectonic model for the Helvetic nappes. In Coward M.P., Dietrich D., and Park R.G. eds. Alpine tectonics. 45: Geol. Soc. London Spec. Publ., 47-64.

Doblas, M. 1998. Slickenside kinematic indicators. Tectonophysics 295, 187-197.

Erard, P.-F. 1999. Traitement et interprétation de cinq lignes sismique réflexion à travers la Plateau molassique et les Préalpes suisses, de Bienne à Lenk. Thèse de doctorat thesis: Institut de Géophysique.

Escher, A., and Beaumont, C. 1997. Formation, burial and exhumation of basement nappes at crustal scale: a geometric model based on the Western Swiss-Italian Alps. Journal of Structural Geology 19, 955-974.

Escher, A., Hunziker, J., Masson, H., Sartori, M., and Steck, A. 1997. Geologic framework and structural evolution of the western Swiss-Italian Alps. In Pfiffner O.A., Lehner P., Heitzman P.Z., Mueller S., and Steck A. eds. Deep structure of the Swiss Alps - Results from NRP 20. Birkhäuser AG. Basel, 205-222.

ESRI. 2011. Release 10. in Institute. E.S.R. ed. ArcGIS Desktop. Redlands, CA.

Favre, A. 1859. Mémoire sur les terrains liasiques et keuperiens de la Savoie. Mémoire de la société de physique et des sciences naturelles de Genève 15, 1-90.

Favre, D. 1984. Etude géologique des Préalpes médianes entre Dent de Broc et Dent du Bourgo. Diplôme thesis.

Favre, E., and Schardt, H. 1887. Description géologique des Préalpes du canton de Vaud et du Chablais jusqu'à la Dranse et de la chaîne des Dents du Midi formant la partie NW de la feuille XVII. Matériaux pour la Carte Géologique de la Suisse 22, 1-636.

Fröhlich, A. 1991. Seismotektonik der Westschweiz unter Berücksichtigung der Bebenserien von Freiburg (1987), Romont (1988) und Boltigen (1989). Diplomarbeit thesis.

Fuchs, S. 2003. Geologie und Strukturgeologie des Massif des Bruns (Kanton Freiburg). Fribourg.

Furrer, U. 1979. Stratigraphie des Doggers der östlichen Préalpes (Bern). Eclogae geologicae Helvetiae 72, 623-672.

Furrer, U., and Septfontaine, M. 1977. Nouvelles données biostratigraphiques dans le Dogger à faciès briançonnais des Préalpes médianes romandes (Suisse). Eclogae geologicae Helvetiae 70, 717-737.

Gagnebin, E. 1922. Préalpes entre Montreux et le Moléson et du Mont Pélerin, carte spéciale nº99. Matériaux pour la Carte Géologique de la Suisse, 1:25'000. Basel. Commission géologique Suisse.

Gebauer, D., Schertl, H.P., Brix, M., and Schreyer, W. 1997. 35 Ma old ultrahigh-pressure metamorphism and evidence for very rapid exhumation in the Dora Maira Massif, Western Alps. Lithos 41, 5-24.

Genge, E. 1957. Ein Beitrag zur Stratigraphie der S Klippendecke im Gebiet Spillgerten - Seehorn. Eclogae geologicae Helvetiae 51, 151-211.

Giardini, D., Wiemer, S., Fäh, D., and Deichmann, N. 2004. Seismic Hazard Assessment of Switzerland. in Swiss Seismological Service E.Z. ed.

Gisiger, M. 1967. Géologie de la région Lac Noir-Kaiseregg-Schafberg (Préalpes médianes plastiques de Fribourg et Bern). Eclogae geologicae Helvetiae 60, 237-349.

Gorin, G.E., Signer, C., and Amberger, G. 1993. Structural configuration of the western Swiss Molasse Basin as defined by reflection seismic data. Eclogae geologicae Helvetiae 86, 693-716.

Guellec, S., Mugnier, J.L., Tardy, M., and Roure, F. 1990. Neogene evolution of the western Alpine foreland in the light of ECORS data and balanced cross sections. In Roure F., Heitzmann P., and Polino R. eds. Deep structure of the Alps. 1: Mémoires de la Société géologique Suisse. Zürich, 165-184.

Guillaume, M. 1986. Révision stratigraphique des Couches Rouges de la nappe des Préalpes Médianes Romandes. PhD, n° 910 thesis.

Guyomard, A., Josnin, J.-Y., Hippolyte, J.-C., and Fudral, S. 2009. Contemporaneous multi-scale structures in the Montagne des Mémises (Préalpes du Chablais, Haute-Savoie, France). Swiss Jounal of Geosciences 102, 3-14.

Hable, R. 1997. Biostratigraphie, Sedimentologie und paläogeographische Entwicklung der Préalpes Médianes des Chablais (Haute Savoie) von Apt bis Unter-Eozän. Ph.D thesis. Fribourg.

Handy, M.R., Bousquet, R., Kissling, E., and Bernoulli, D. 2011. Reconciling plate tectonic reconstructions of Alpine Tethys with the record of spreading and subduction in the Alps. . Earth Science Reviews.

Heinz, R., and Isenschmid, C. 1988. Mikrofazielle und stratigrafische Untersuchungen im Massifkalk (Malm) der Préalpes Médianes. Eclogae geologicae Helvetiae 81, 1-62.

Heinz, R.A. 1980. Geologie der vorderen Stockhorn-Kette zswischen Nüneneflue und Walalpgrat. Diplôme thesis.

Homewood, P. 1974. Le flysch du Meilleret (Préalpes Romandes) et ses relationsavec les unitées de l'encadrant. Eclogae geologicae Helvetiae 67, 349-401.

Homewood, P. 1977. Ultrahelvetic and North-Penninic flysch of the Prealps: a general account. Eclogae geologicae Helvetiae 70, 627-641.

Homewood, P., Ackermann, T., Antoine, P., and Barbier, R. 1984. Sur l'origine de la nappe du Niesen et la limite entre les zones ultrahelvétiques et valaisanne. Comptes Rendus des Séances de l'Académie des Sciences de Paris, série II 299, 1055-1059.

Homewood, P., Allen, P.A., and Williams, G.D. 1986. Dynamics of the Molasse Basin of western Switzerland, 199-217.

Homewood, P., and Lateltin, O. 1988. Classic swiss clastics (flysch and molasse): The alpine connection. Paris, 1-11.

Hunziker, J.C., Desmond, J., and Martinotti, G. 1989. Apine thermal evolution in the central and western Alps. COWARD et al , ed., Alpine tectonics Geol. Soc. Spec. Publ., 45, 353-367.

Hunziker, J.C., Desmons, J., and Hurford, A.J. 1992. Thirty-two years of geochronological work in the Central and Western Alps: a review on seven maps. Mémories de Géologie (Lausanne) 13, 1-52.

Hurford, A.J. 1986. Cooling and uplift patterns in the Lepontine Alps South Central Switzerland and an age of vertical movement on the Insubric fault line. Contributions to Mineralogy and Petrology 92, 413-427.

Hürlimann, A., Besson-Hürlimann, A., and Masson, H. 1996. Stratigraphie et tectonique de la partie orientale de l'écaille de la Gummfluh (Domaine Briançonnais des Préalpes). Mémoires de Géologie (Lausanne) 28, 132.

Ibele, T. 2011. Tectonics of the Western Swiss Molasse Basin during Cenozoic Times. GeoFocus 27, 166.

Isenschmid, C. 1979. Die Klippendecke zwischen Widdergalm und Märe (Préalpes fribourgeoises). Diplôme thesis.

Isenschmid, C. 1983. Der Malm im Mittelabschnitt der Préalpes médianes zwischen Thuner- und Genfersee. PhD thesis.

Jaccard, F. 1904. La région de la Brèche de la Hornfluh (Préalpes Bernoises). Bulletin des laboratoires de géologie, minéralogie, géophysique et du Musée géologique de l'Université de Lausanne 5, 1-205.

Jaccard, F. 1908. Brachiopodes des calcaires de Saint-Triphon. Bulletin de la Société Vaudoise des Sciences Naturelles 43, 162-164.

Jamison, W.R. 1987. Geometric analysis of fold development in overthrust terranes. Journal of Structural Geology 9, 207-219.

Jeanbourquin, P. 1988. Nouvelles observations sur les cornieules en Suisse occidentale. Eclogae geologicae Helvetiae 81, 511-538.

Jeanbourquin, P. 1991. Ultrahelvétique et mélanges sur le dos des nappes helvétiques des Diablerets et du Wildhorn. Bulletin de la Société Fribourgeoise des Sciences Naturelles 80, 76-104.

Jeanbourquin, P., and Goy-Eggenberger, D. 1991. Mélanges suprahelvétiques: sédimentation et tectonique au front de la nappe de Morcles (Vaud, Suisse). Géologie Alpine 67, 43-62.

Jeanbourquin, P., Kindler, P., and Dall'Agnolo, S. 1992. Les mélanges des Préalpes internes entre Arve et Rhône (Alpes occidentales franco-suisses). Eclogae geologicae Helvetiae 85, 59-83.

Jeannet, A. 1922. Das romanische Deckengebirge, Préalpes und Klippen. In Heim A. ed. Geologie der Schweiz. II/2: Tauschniz. Leibzig, 589-676.

Jordan, P. 1992. Evidence for large scale decoupling in the Triassic evaporites of Northern Switzerland: an overview. Eclogae geologicae Helvetiae 85, 677-69.

Jouanne, F., Ménard, G., and Darmendrail, X. 1995. Present-day vertical displacements in the northwestern Alps and the southern Jura Mountains: Data from leveling comparisons. Tectonics 14, 606-616.

Kahle, H.-G., Geiger, A., Bürki, B., Gubler, E., Marti, U., Wirth, B., Rotbacher, M., Gurtner, G., Beutler, G., Bauersima, I., and Pfiffner, A.O. 1997. Recent crustal movements, geoid and density distribution: Contribution from integrated satellite and terrestrial measurements. In Pfiffner O.A., Lehner P., Heitzman P.Z., Mueller S., and Steck A. eds. Deep structure of the Swiss Alps - Results from NRP 20. Birkhäuser AG. Basel, 251-259.

Kastrup, U. 2002. Seismotectonics and stress field variations in Switzerland. Zurich.

Kastrup, U., Deichmann, N., Fröhlich, A., and Giardini, D. 2007. Evidence for an active fault below the northwestern Alpine foreland of Switzerland. Geophysical Journal International 169, 1273-1288.

Kastrup, U., Zoback, M.L., Deichmann, N., Evans, K.F., Giardini, D., and Michael, A.J. 2004. Stress field variations in the Swiss Alps and the northern Alpine foreland derived from inversion of fault plane solutions. Journal of Geophysical Research 109, 1 - 22.

Katz, Y., and Weinberger, R. 2005. Strian localization in sandstones during embryonic stages of shear-zone evolution. Terra Nova 17, 311-316.

Kim, G.-B., Lee, J.-Y., and Lee, K.-K. 2004. Construction of lineament maps related to groundwater occurence with ArcView and Avenue TM scripts. Computers and Geosciences 30, 1117 - 1126.

Lateltin, O. 1988. Les dépôts turbiditiques oligocènes d'avant-pays entre Annecy (Haute-Savoie) et le Sanetsch (Suisse), Grès de Taveyannaz et du Val d'Illiez. PhD no 949 thesis.

Leloup, P.H., Arnaud, N., Sobel, E.R., and Lacassin, R. 2005. Alpine thermal and structural evolution of the highest external crystalline massif: The Mont Blanc. Tectonics 24, 1-26.

Lemoine, M. 1984. La marge occidentale de la Téthys ligure et les Alpes occidentales. In Boillot G. ed. Les marges continentales actuelles et fossiles autour de la France. Masson. Paris, 155-248.

Lemoine, M. 1988. Des nappes embryonnaires aux blocs basculés: évolution des idées et modèles sur l'histoire mésozoique des Alpes occidentales. Bulletin de la Société géologique de France, 8ième série 4, 787-797.

Lempicka Münch, A., and Masson, H. 1993. Dépôts d'âge tertiaire de la nappe ultrahelvétique du Sex Mort entre la Simme et Adelboden (Préalpes). Bulletin de la Société Vaudoise des Sciences Naturelles 82, 369-389.

Lisle, R.J., and Leyshon, P.R. 2004. Stereographic Projection Techniques for Geologists and Civil Engineers. Cambridge University Press. Cambridge.

Loprieno, A., Bousquet, R., Bucher, S., Ceriani, S., Torre, F.H.D., Fügenschuh, B., and Schmid, S.M. 2011. The Valais units in Savoy (France): a key area for understanding the palaeogeography and the tectonic evolution of the Western Alps. International Journal of Earth Sciences 100, 963-992.

Lugeon, M. 1896. La région de la Brèche du Chablais. Bulletin du service de la carte géologique de France 7, 337-646.

Lugeon, M. 1902. Les grandes nappes de recouvrement des Alpes du Chablais et de la Suisse. Bulletin de la Société géologique de France 4, 723-825.

Lugeon, M. 1943. Observations à la communication de M. Augustin Lombard et âge de la brèche du Hahnenmoos. Eclogae geologicae Helvetiae 35, 124-125.

Lugeon, M. 1949. La brèche de la colline d'Aigremont (Préalpes vaudoises): une erreur et une énigme. Eclogae geologicae Helvetiae 42, 155-175.

Lugeon, M., and Gagnebin, E. 1941. Observations et vues nouvelles sur la géologie des Préalpes romandes. Bulletin du Laboratoire de Géologie de l'Université de Lausanne 72, 1-90.

Mandia, Y. 1984. Etude géologique des Préalpes médianes entre les vallées du Motélon et du Gros Mont. Diplôme thesis.

Marescot, L. 2000. La Molasse de la région de la Sense. Diploma thesis: Fribourg.

Marrett, R., and Allmendinger, R.W. 1990. Kinematic analysis of fault-slip data. Journal of Structural Geology 12, 973-986.

Masson, H. 1972. Sur l'origine de la cornieule par fracturation hydraulique. Eclogae geologicae Helvetiae 65, 27-41.

Masson, H. 1976. Un siècle de géologie dans des Préalpes: de la découverte des nappes à la recherche de leur dynamique. Eclogae geologicae Helvetiae 69, 527-575.

Matter, A., Homewood, P., Caron, C., Rigassi, D., van Stuijvenberg, J., Weidmann, M., and Winkler, W. 1980. Flysch and Molasse of Western and Central Switzerland. In Trümpy R. ed. Geology of Switzerland. PartB: geological excursions, excursion IV: 26th International Geological Congress: Wepf. Basel, 261-293.

Maurer, H.R., Burkhard, M., Deichmann, N., and Green, A.G. 1997. Active tectonism in the central Alps: contrasting stress regimes north and south of the Rhône valley. Terra Nova 9, 91-94.

Maxelon, M. 2004. Reformattor Toolbox. Some Tools for three-dimensional Modelling in Structural Geology and Tectonics.

McInerney, P., Guillen, A., Courrioux, G., Calcagno, P., and Lees, T. 2005. Building 3D Geological Models Directly from the Data? A new approach

applied to Broken Hill, Australia.

METTRAUX, M. 1989. Sédimentologie, paléotectonique et paléoocéanographie des Préalpes Médianes (Suisse Romande) du Rhétien au Toarcien. PhD, n° 947 thesis.

METTRAUX, M., AND MOHR, B. 1989. Stratigraphy of Triassic/Jurassic boundary in the Préalpes médianes nappe: facies and palynology. Eclogae geologicae Helvetiae 82, 743-763.

METTRAUX, M., AND MOSAR, J. 1989. Tectonique alpine et paléotectonique liasique dans les Préalpes Médianes en rive gauche du Rhône. Eclogae geologicae Helvetiae 82, 517-540.

MITRA, S. 1992. Balanced structural interpretations in fold and thrust belts. In Mitra S., and Fisher G.W. eds. Structural geology of fold and thrust belts. Johns Hopkins University press. Baltimore, 53-77.

MITRA, S. 2003. A unified kinematic model for the evolution of detachment folds. Journal of Structural Geology 25, 1659 - 1673.

MONEY, A. 1990. Géologie des Préalpes médianes plastiques dans le secteur Märe - Schibe - Widdersgrind. Diplôme thesis.

MORNOD, L. 1945. Molasse subalpine et bord alpin de la région de Bulle (Basse Gruyère). Eclogae geologicae Helvetiae 38, 441-451.

MOSAR, J. 1988a. Métamorphisme transporté dans les Préalpes. Schweizerische Mineralogische und Petrographische Mitteilungen 68, 77-94.

MOSAR, J. 1988b. Structures, déformation et métamorphisme dans les Préalpes Romandes (Suisse). PhD thesis.

MOSAR, J. 1989. Déformation interne dans les Préalpes Médianes (Suisse). Eclogae geologicae Helvetiae 82, 765-793.

MOSAR, J.. 1991. Géologie structurale dans les Préalpes médianes (Suisse). Eclogae geologicae Helvetiae 84, 689-725.

MOSAR, J.. 1994. Géologie structurale à l'est de Montreux (Préalpes médianes plastiques, Suisse). Eclogae geologicae Helvetiae 87, 11-32.

MOSAR, J. 1997. Folds and thrust in the Préalpes Médianes plastiques romandes. Bulletin de la Société Vaudoise des Sciences naturelles 84, 347-384.

MOSAR, J. 1999. Present-day and future tectonic underplating in the Western SwissAlps: reconciliation of basement/wrench-faulting and décollement folding of the Jura and Molasse Basin in the Alpine foreland. Earth and planetary Science Letters 173, 143-145.

MOSAR, J. 2006. Aléa sismique dans le canton de Fribourg Evaluation de l'état des connaissances scientifiques - Perspectives. Département de Géoscience.

MOSAR, J., ABEDNEGO, M., AND VOUILLAMOZ, N. 2011. Nano-seismology. Resun.

MOSAR, J., ABEDNEGO, M., VOUILLAMOZ, N., AND MATZENAUER, E. 2010. Tectonic Map of the Central Western Molasse Basin. Resun.

MOSAR, J., AND BOREL, G. 1992. Paleostress from the Préalpes médianes (Switzerland). Annales Tectonicae 6, 115-133.

MOSAR, J., STAMPFLI, G.M., AND GIROD, F. 1996. Western Préalpes médianes: timing and structure. A review. Eclogae geologica Helvetiae 89, 389-425.

MÜLLER, I., AND PLANCHEREL, R. 1982. Contribution à l'étude de l'hydrogéologie karstique du massif du Vanil Noir et de la chaîne des Gastlosen (Préalpes fribourgeoises, Suisse). Bulletin de la Société Fribourgeoise des Sciences Naturelles 71, 102-132.

MÜLLER, M., NIEBERDING, F., AND WANNINGER, A. 1988. Tectonic style and pressure distribution at the northern margin of the Alps between Lake Constance and the River Inn. Geologische Rundschau 77, 787-796.

NAYLOR, M.A., MANDL, G., SIJPESTEIJN, C. H. K. 1986. Fault geometries in basement-induced wrench faulting under different initial stress states. Journal of Structural Geology 8, 737-752.

NICOLAS, A. 1987. Principes de Tectonique. Masson. Paris.

PAGE, C. 1969. Observations géologiques sur les Préalpes au NW des Gastlosen orientales. Bulletin de la Société Fribourgeoise des Sciences Naturelles 58, 83-177.

PASQUIER, J.-B. 2005. 1225 Gruyères. Geologischer Atlas der Schweiz 1:25'000. Bundesamt für Wasser und Geologie.

PASSCHIER, C.W., AND TROUW, R.A.J. 2005. Microtectonics. Springer. Berlin Heidelberg.

PAVONI, N. 1992. Seismoactive fault systems in the basement and sedimentary cover of the Swiss Plateau and the Jura Mountains. Eclogae geol. Helv. 85, 781- 784.

PAVONI, N., MAURER, H.R., ROTH, P., AND DEICHMANN, N. 1997. Seismicity and seismotectonics of the Swiss Alps. In Pfiffner O.A., Lehner P., Heitzman P.Z., Mueller S., and Steck A. eds. Deep

structure of the Swiss Alps - Results from NRP 20. Birkhäuser AG. Basel, 241-250.

PETERHANS, E. 1923. Sur la tectonique des Préalpes entre Meillerie et Saint-Gingolph (Haute-Savoie). Bulletin de la Société géologique de France, 4. série 23, 51-56.

PETERHANS, E. 1926. Etude du Lias et des géanticlinaux des Préalpes médianes entre la vallée du Rhône et le lac d'Annecy. Mémoires de la Société Helvétique des Sciences Naturelles 69, 191-344.

PETIT, J.P. 1987. Criteria for the sense of movement on fault surfaces in brittle rocks. Journal of Structural Geology 9, 597-608.

PFIFFNER, A.O., SAHLI, S., AND STÄUBLE, M. 1997a. Structure and evolution of the external basement massifs (Aar, Aiguilles Rouges/Mt. Blanc). In Pfiffner O.A., Lehner P., Heitzman P.Z., Mueller S., and Steck A. eds. Deep structure of the Swiss Alps - Results from NRP 20. Birkhäuser AG. Basel, 139-153.

PFIFFNER, O., FREI, W., FINKH, P., AND VALASEK, P. 1988. Deep seismic reflection profiling in the Swiss Alps: explosion seismology results for line NFP 20-East. Geology 16, 987-990.

PFIFFNER, O.A. 1986. Evolution of the north Alpine foreland basin in the Central Alps. Special Publication of the international Association of sedimentologists 8, 219-228.

PFIFFNER, O.A., ERARD, P.-F., AND STÄUBLE, M. 1997b. Two cross sections through the Swiss Molasse basin (lines E4-E6, W1, W7-W10). In PFIFFNER O.A., LEHNER P., HEITZMAN P.Z., MUELLER S., AND STECK A. eds. Deep structure of the Swiss Alps - Results from NRP 20. Birkhäuser AG. Basel, 64-72.

PFIFFNER, O.A., SAHLI, S., AND STÄUBLE, M. 1997c. Compression and uplift of the external massifs in the Helvetic zone. In PFIFFNER O.A., LEHNER P., HEITZMANN P., MÜLLER S., AND STECK A. eds. Deep structures of the Swiss Alps - Results of NRP 20. Birkhäuser. Basel.

PLANCHEREL, R. 1976. Essai d'interprétation de la dislocation transversale de Bellegarde-Lac Noir (Préalpes médianes Fribourgeoises). Eclogae geologicae Helvetiae 65, 461-469.

PLANCHEREL, R. 1979. Aspects de la déformation en grand dans les Préalpes médianes plastiques entre Rhône et Aar. Eclogae geologicae Helvetiae 72, 145-214.

PLANCHEREL, R. 1990. Les Préalpes du Chablais - Présentation générale. In Charollais J., and Badoux H. eds. Suisse Lémanique pays de Genève et Chablais. Guides Géologiques Régionaux. Masson, 183-190.

PLANCHEREL, R., AND WEIDMANN, M. 1972. Géologie des tunnels de Glion (RN 9). Bulletin de la Société Vaudoise des Sciences Naturelles 71, 1-7.

POLLARD, D.D., SALTZER, S.D., AND RUBIN, A.M. 1993. Stress inversion methods, are they based on faulty assumptions? Journal of Structural Geology 22, 1359-1378.

PYTHON-DUPASQUIER, C. 1990. La formation de l'Intyamon («Crétacé moyen») des Préalpes médianes romandes. Thèse 978 thesis.

PYTHON, C., BERGER, J.-P., AND PLANCHEREL, R. 1998. 1185 Fribourg - Notice explicative. Geologischer Atlas der Schweiz. Landeshydrologie und -geologie.

RAMSAY, J.G. 1967. Folding and Fracturing of Rocks. Mc Graw-Hill. New York, 568.

RAMSAY, J.G. 1989. Fold and fault geometry in the Western Helvetic nappes of Switzerland and France and its implications for the evolution of the arc of the western Alps. In Coward M.P., Dietrich D., and Park R.G. eds. Alpine tectonics. 45: Geological Society of London, Special Publication, 33-46.

RAMSAY, J.G., AND HUBER, I.M. 1987. The techniques of modern structural geology.

RAMSAY, J.G., AND LISLE, R.J. 2000. Application of continuum mechanics in structural geology. Modern Structural Geology Series. 3: Academic Press. London, 785 - 805.

REITER, F., AND ACS, P. 1996 - 2002. TectonicsFP 1.6 Computer Software for Structural Geology. Operating Manual.

RIEDEL, W. 1929. Zur Mechanik geologischer Bruchserscheinungen. Centralblatt für Mineralogie, Geologie und Paläontologie 1929B, 354-368.

SARRET, Y., AND MOSAR, J. 2010. Paléotectonique et tectonique alpine dans l'écaille de St-Triphon. Bulletin de la Société Vaudoise des Sciences Naturelles 92, 1-14.

SARTORI, M. 1987. Blocs basculés briançonnais en relation avec leur socle originel dans la nappe de Siviez-Mischabel (Valais, Suisse). Comptes Rendus de l'Académie des Sciences de Paris, Série II 305, 999-1005.

SARTORI, M., AND MARTHALER, M. 1994. Exemples de relations socle-couverture dans les nappes penniques du Val d'Hérens. Schweizerische Mineralogische und Petrographische Mitteilungen 74, 503-509.

Schaer, J.P., Reimer, G.M., and Wagner, G.A. 1975. Actual and ancient uplift rate in the Gotthard region, Swiss Alps: a comparison between precise levelling and fission track apatite age. Tectonophysics 29, 293-300.

Schardt, H. 1884. Etudes géologiques sur le Pays d'Enhaut vaudois. Bulletin de la Société Vaudoise des Sciences Naturelles 20, 1-183.

Schardt, H. 1893a. Coup d'oeil sur la structure géologique des environs de Montreux. Bulletin de la Société Vaudoise des Sciences Naturelles 29, 241-255.

Schardt, H. 1893b. Sur l'origine des Préalpes romandes. Archives de physique et des sciences naturelles de Genève 3, 570-583.

Schlunegger, F., and Mosar, J. 2010. The last erosional stage of the Molasse Basin and the Alps. International Journal of Earth Sciences, 1-16.

Schmid, G. 1970. Geologie der Gegend von Guggisberg und der angrenzenden subalpinen Molasse. Matériaux pour la Carte Géologique de la Suisse n.s. 139, 1-113.

Schmid, S.M., Fügenschuh, B., Kissling, E., and Schuster, R. 2004. Tectonic map and overall architecture of the Alpine orogen. Eclogae geologicae Helvetiae 97, 93-117.

Septfontaine, M. 1983. Le Dogger des Préalpes médianes suisses et françaises (Stratigraphie, évolution paléogéographique et paléotectonique). Mémoires de la Société Helvétique des Sciences Naturelles 97, 1-121.

Septfontaine, M. 1995. Large scale progressive unconformities in Jurassic strata of the Préalpes S of lake Geneva: interpretation as synsedimentary inversion structures, Paleotectonic implications. Eclogae geologicae Helvetiae 88, 553-576.

Sommaruga, A. 1997. Geology of the Central Jura and the Molasse Basin: new insight into an evaporite-based foreland fold and thrust belt. Mémoire de la société neuchâteloise des sciences naturelles 12, 176.

Sommaruga, A. 1999. Décollement tectonics in the Jura foreland fold-and-thrust belt. Marine and Petroleum Geology 16, 111-134.

Spang, J.H. 1972. Numerical method for dynamic analysis of calcite twin lamella. Geological Society of America Bulletin 83, 467-472.

Sperner, B., Müller, B., Heidbach, O., Delvaux, D., Reinecker, J., and Fuchs, K. 2003. Tectonic stress in the Earth's crust: advances in the World Stress Map project. Geological Society, London, Special Publications 212.

Spicher, A. 1980. Tektonische Karte der Schweiz. Schweizerische Geologische Kommission.

Spicher, A. 2005. Carte tectonique de la Suisse. Wabern. Office fédéral des eaux et de la géologie.

Spicher, J.P. 1966. Géologie des Préalpes médianes dans le Massif des Bruns, partie occidentale. Eclogae geologicae Helvetiae 58, 591-742.

Stampfli, G., and Marthaler, M. 1990. Divergent and convergent margins in the North-Western alps. Confrontation to actualistic models. Geodinamica Acta 4, 159-184.

Stampfli, G.M. 1993. Le Briançonnais, terrain exotique dans les Alpes? Eclogae geologicae Helvetiae 86, 1-45.

Stampfli, G.M., Borel, G.D., Marchant, R., and Mosar, J. 2002. Western Alps geological constraints on western Tethyan reconstructions. The Virtual Explorer 8, 75-104.

Stampfli, G.M., Mosar, J., Marchant, R., Marquer, D., Baudin, T., and Borel, G. 1998. Subduction and obduction processes in the Swiss Alps. Tectonophysics 296, 159-204.

Steck, A., Epard, J.L., Escher, A., Lehner, P., Marchant, R.H., and Masson, H. 1997. Geological interpretation of the seismic profiles through Western Switzerland: Rawil (W1), Val d'Anniviers (W2), Mattertal (W3), Zmutt-Zermatt-Findelen (W4) and Val de Bagnes (W5). In Pfiffner O.A., Lehner P., Heitzman P.Z., Mueller S., and Steck A. eds. Deep structure of the Swiss Alps - Results from NRP 20. Birkhäuser AG. Basel, 123-138.

Steffen, D., Jaques, C., Nydegger, T., Petroons, D., and Wildi, W. 1993. La Brèche du Chablais à son extremité occidentale (Haute-Savoie, France): sédimentologie, éléments stratigraphiques et interprétation paléogéographique. Eclogae geologicae Helvetiae 86, 543-568.

Sue, C., and Tricart, P. 2002. Widespread post-nappe normal faulting in the Internal Western Alps: a new constraint on arc dynamics. Journal of the Geological Society London 159, 61-70.

Suppe, J. 1983. Geometry and kinematics of fault bend folding. American Journal of Science 282, 648-721.

Suppe, J. 1985. Principles of structural Geology. Prentice-Hall. New-Jersey, 1-537.

Tchalenko, J.S. 1970. Similarities between Shear Zones of Different Magnitudes. Geological Society of America Bulletin 81, 1625-1640.

TERCIER, L. 1928. Géologie de la Berra. Matériaux pour la Carte Géologique de la Suisse n.s. 60, 1-111.

THALMANN, M. 1990. Geologie der Voralpen N von Boltigen (Simmental). Diplôme thesis.

THURY, M. 1973. Der Lias der östlichen Préalpes médianes zwischen Boltigen und Spiez. PhD thesis.

TRÜMPY, R. 1957. Quelques problèmes de paléogéographie alpine. Bulletin de la Société Géologique de France 6, 443-461.

TRÜMPY, R. 1960. Paleotectonic evolution of the Central and Western Alps. Geological Society of America Bulletin 71, 843-908.

TRÜMPY, R. 1980. Geology of Switzerland: a guide-book. Wepf. and Co.

TRÜMPY, R., AND BERSIER, A. 1954. Les éléments des conglomérats oligocènes du Mont-Pélerin. Pétrographie, statistique, origine. Eclogae geologicae Helvetiae 47, 119-166.

VAN STUIJVENBERG , J. 1979. Geology of the Gurnigel area. Matériaux pour la Carte Géologique de la Suisse n.s. 151, 1-111.

VAN STUIJVENBERG, J., MOREL, R., AND JAN DU CHÊNE, R. 1976. Contribution à l'étude du flysch de la région des Fayaux (Préalpes externes vaudoises). Eclogae geologicae Helvetiae 69, 309-326.

VIALON, P., RUHLAND, M., GROLIER, J. 1976. Eléments de tectonique analytique. Masson. Paris, 118.

VOLLMAYR, T., AND WENDT, A. 1987. Die Erdgasbohrung Entlebuch 1, ein Tiefenaufschluss am Alpennordrand. Bulletin der Vereinigung Schweizerischen Petroleum-Geologen und -Ingenieure 53, 67-79.

WALLACE, R.E. 1951. Geometry of shearing stress and relation to faulting. Journal of Geology 59.

WEIDMANN, M. 2005. 1205 Rossens - Notice explicative. Bundesamt für Wasser und Geologie.

WEIDMANN, M., HOMEWOOD, P., CARON, C., AND BAUD, A. 1976. Réhabilitation de la "Zone Submédiane" des Préalpes. Eclogae geologicae Helvetiae 69, 265-277.

WEIDMANN, M., HOMEWOOD, P., AND FASEL, J.M. 1982. Sur les terrains subalpins et le wildflysch entre Bulle et Montreux. Bulletin de la Société Vaudoise des Sciences Naturelles 362, 151-183.

WEISS, H. 1949. Stratigraphie und Mikrofauna des Klippenmalm. PhD thesis.

WEISSERT, H.J., AND BERNOULLI, D. 1985. A transform margin in the Mesozoic Tethys: evidence from the Swiss Alps. Geologische Rundschau 74, 665-679.

WICHT, J.M. 1984. Les flysch de la nappe de la Simme dans les Préalpes romandes. PhD, n° 877 thesis.

WILCOX, R.E., HARDING, T.P., SEELY, D.R. 1973. Basic Wrench Tectonics. American Association of Petroleum Geologists Bulletin 57, 74-96.

WINKLER, W. 1984. Palaeocurrents and petrography of the Gurnigel-Schlieren Flysch: a basin analysis. Sedimentary Geology 40, 169-189.

WISSING, S.B., AND PFIFFNER, O.A. 2002. Structure of the eastern Klippen nappe (BE, FR): Implications for its Alpine tectonic evolution. Eclogae geologicae Helvetiae 95, 381-398.

ZOBACK, M.L. 1992. First- and second-order patterns of stress in the lithosphere: the World Stress Map project. Journal of Geophysical Research B, solid earth and planets 97, 11703-11728.

*****

7 - Appendices

1 Data

1.1 Detailed Paleostress Results

Every one of the 51 outcrops locality is described by its accurate location (coordinates) which represents often a mean value of several smaller measurement areas taken together. The number of measurements corresponds to the initial number of fault-slip data collected at an outcrop in a particular. S0 signifies the orientation and the inclination of the bedding, but in a vastly folded area it represents an average value expressing the trending direction. First analysis of the fault-slip data deals with the raw data containing the entire data set without separation into subsets and expresses its evalutions by the Angelier-, P-t and Right Dihedra diagram calculated by the program TectonicsFP developed by Reiter and Acs (1996 - 2002). Data separation into subsets, tensor calculations based on the Right Dihedra method and the additional rotational optimisation was carried out by the WinTensor program generated by Delvaux (2006). Only data that can be attributed to a partucular subset are displayed.

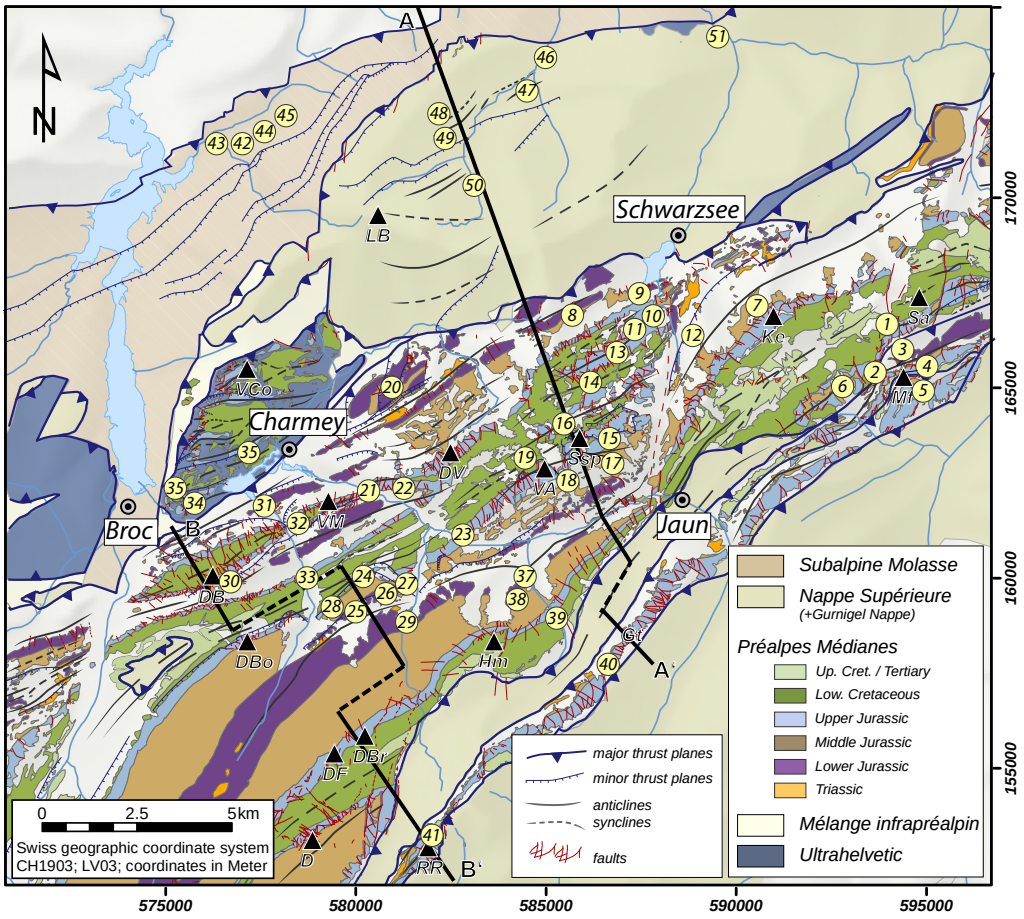

1 Schafarnisch *Préalpes Médianes Plastiques*

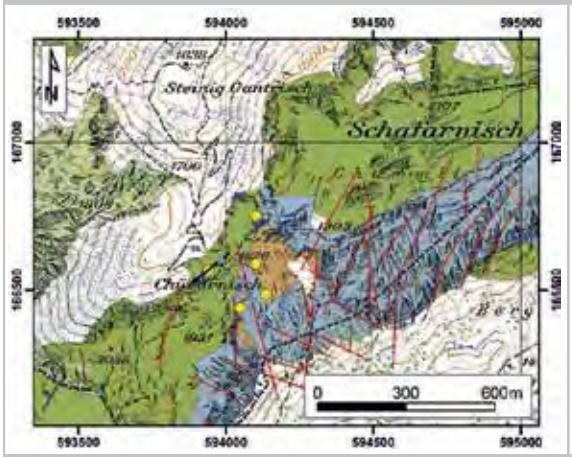

Outcrop description:

(593869/ 166818 1700m)

Lower Cretaceous small-scale folds, with a general dip direction towards NW, fold axis is trending in NE direction. Outcrop conditions were of minor quality often along the path or below the rock faces; slickenfibres were rare, for this reason the fault-slip measurements were distributed over a larger area (500m). Crosscutting veins and stylolites are frequent and allow defining a chronology of the different stress states.

N = 21 *Lower Cretaceous* *bedding = 349/25*

ANGELIER

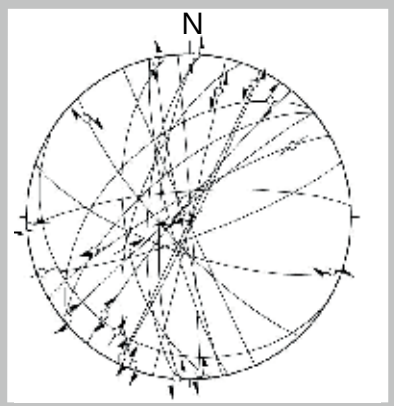

P-T

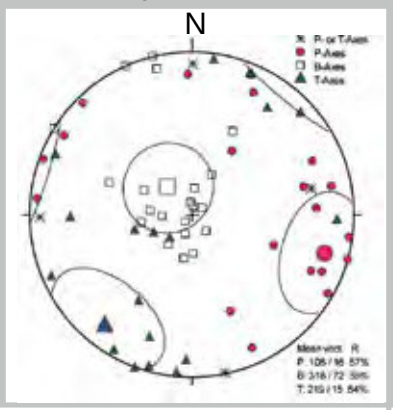

RIGHT DIHEDRA

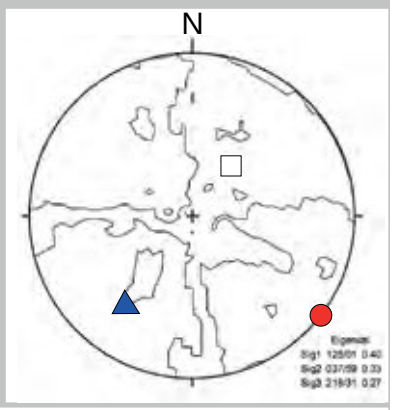

TENSOR

N = 8

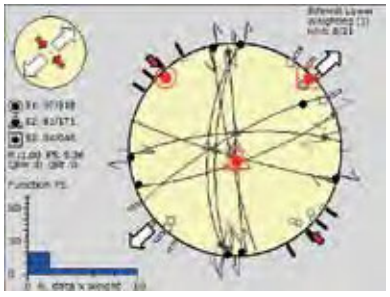

N = 7

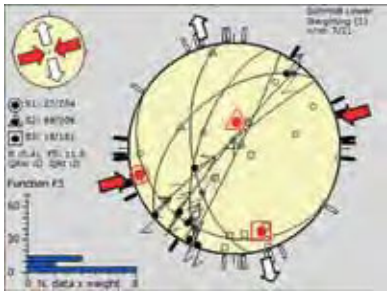

VEINS

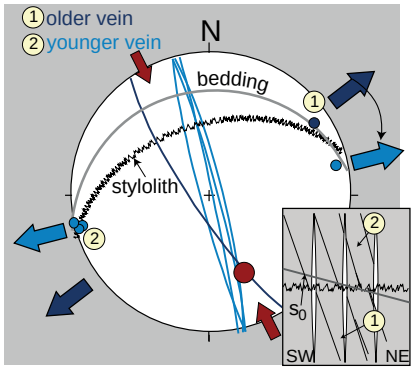

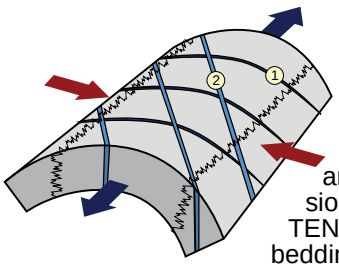

Stress field description

In the Schafarnisch area, two stress regimes are distinguished both show strike-slip stress-states with a dominating exten-sional deviatoric stress axes. The stress regime with the compres-sional stress axis oriented to-wards NW-SE occurs more frequently than the one with the compres-sional stress axis towards ESE-WNW. The relation-ship of cross-cutting veins and the presence of stylolites allow the following chro-nology: NW-SE oriented veins are older whereas NNW-SSE oriented veins are younger. Stylolites agree with a NNW-SSE trending compres-sion in the youngest stage. Pole-to-plane projections of the older vein array and the stylolites ac-cord with the exten-sional deviatoric stress axis of the first TENSOR plot. However, the pole to the bedding projection of the younger vein family does not coincide with the extensional direction of the second plot and has therefore to be related to another not represented stress regime.

2 **Trimlegabel** *Préalpes Médianes Heiti imbricate*

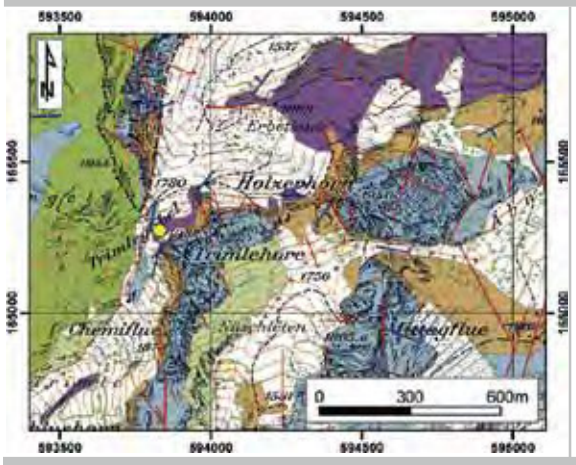

Outcrop description:

593829/ 165271 1800m

The Trimlegabel outcrop lies in the Heiti imbricate near the major thrust plane separating this tectonic imbricate from the Préalpes Médianes Plastiques. The data come from a restricted area with well-developed slickenfibres. Despite the vicinity to the major thrust zone, the area is overall affected by large sinistral strike-slip faults oriented N-S.

N = 13 *Middle Jurassic* *bedding = 313/ 76*

ANGELIER

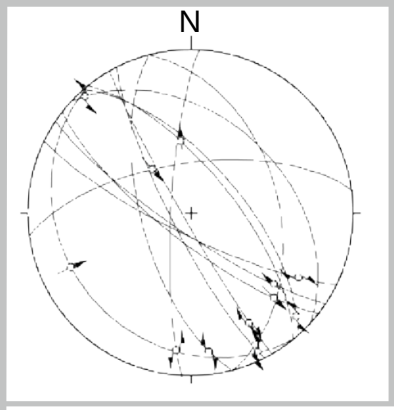

P-T

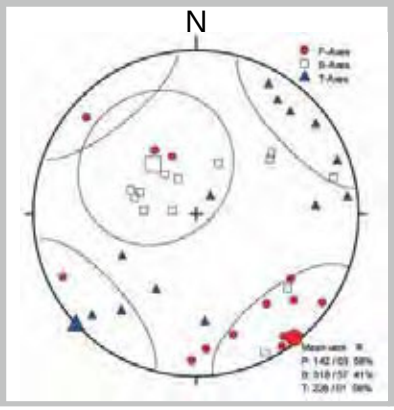

RIGHT DIHEDRA

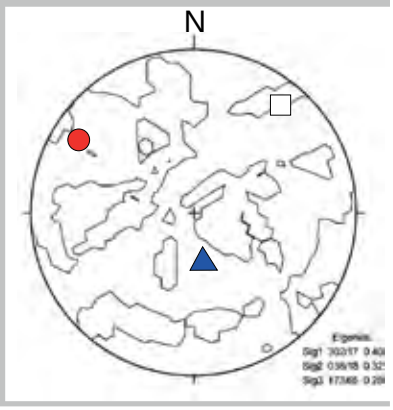

TENSOR

N = 6

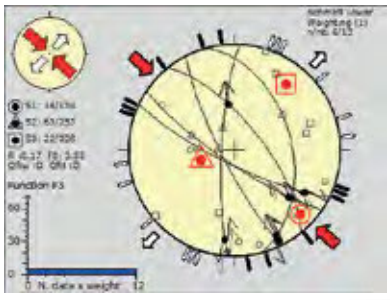

Stress field description

Throughout data separation processes, more than half of the data were rejected. The remaining data show a strike-slip stress regime that corresponds with field observations showing large-scale strike-slip faults dominating the overall structural context.

3 Erbetlaub *Préalpes Médianes Heiti imbricate*

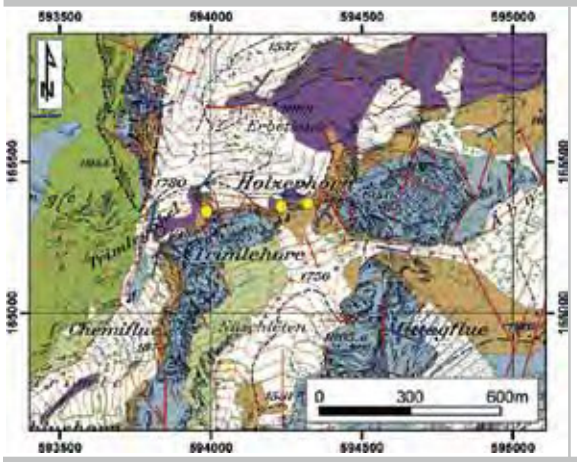

Outcrop description:

594'264/ 165'383 1800m

Large-scale normal faults are dominating the zone between the Holzer- and the Trimlehorn, in such a way that between the two mountain tops - consisting of massif limestones of the Upper Jurassic - lays a zone of Middle Jurassic rock limited by important normal faults. The dataset was collected directly at the base of the rock face in a restricted area. Weathering of the Middle Jurassic rocks and the orientation of the rock face towards north diminished the quality of the outcrop.

N = 15 *Middle Jurassic* *bedding = 160/ 22*

ANGELIER

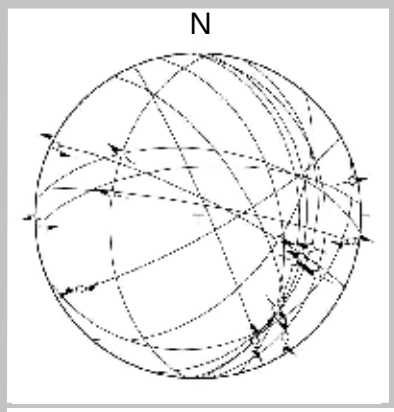

P-T

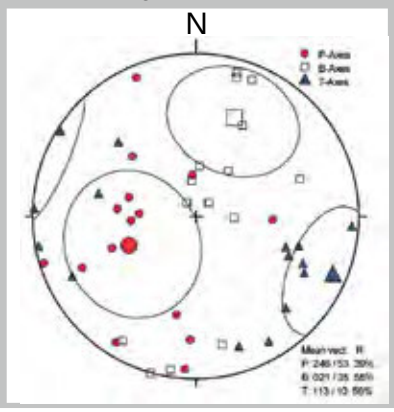

RIGHT DIHEDRA

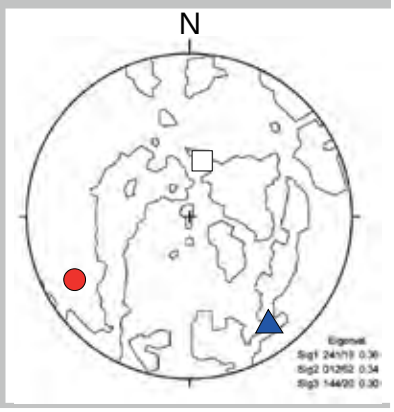

TENSOR

N = 7

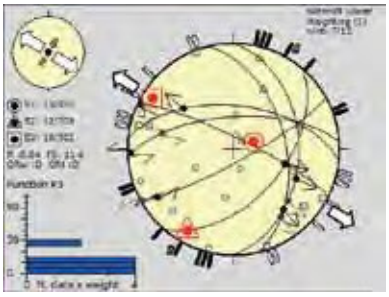

Stress field description

The dominating extensional regime already visible in the field is also reflected in the resulting paleostress evaluation as indicated by a major extensional stress state with the extensional deviatoric stress axis pointing towards NW, respectively SE. Only 55% of the total fault-slip data are remaining after data sorting. The illustration represents the P-T diagrams of the Trimlegabel and the Holzerhorn area and show nicely the influence of a strike-slip system for the Trimlegabel and an extensional system for the Holzerhorn.

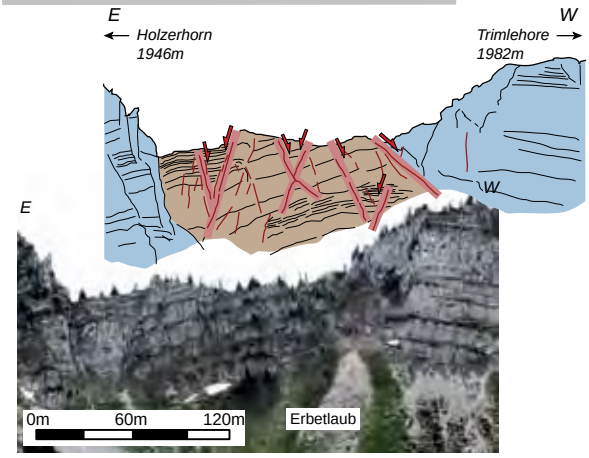

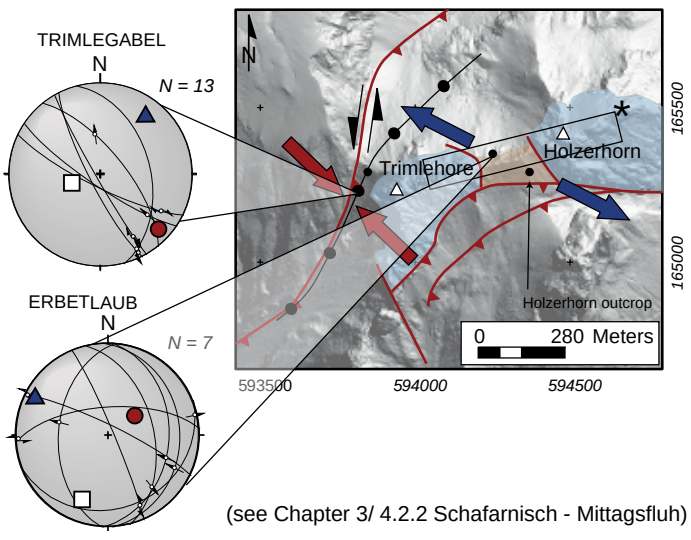

(see Chapter 3/ 4.2.2 Schafarnisch - Mittagsfluh)

4 Holzerhorn *Préalpes Médianes Heiti imbricate*

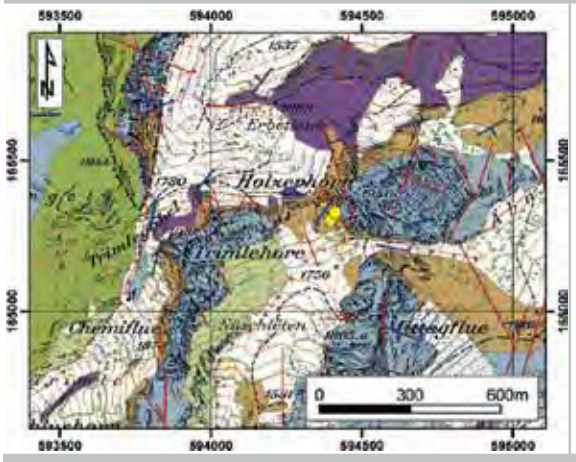

Outcrop description:

594337/ 165264 1810m

The fault-slip data were collected on top of the Middle Jurassic rock face of the previous location (Holzerhorn 3). NNW-SSE striking faults sinistral faults are widespread; veins show the same direction and agree with the with a strike-slip stress regime.
Normal faults striking NW-SE, clearly visible in the field but poorly represented in the dataset due to the lack of slickenfibres.

N = 15 *Middle Jurassic* *bedding = 132/ 43*

ANGELIER

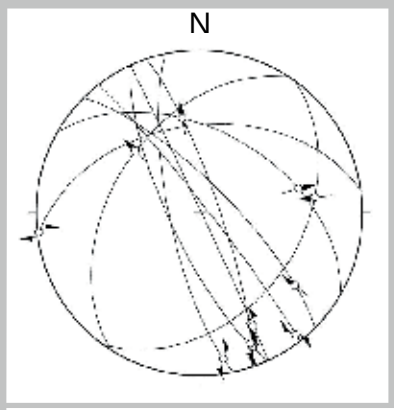

P-T

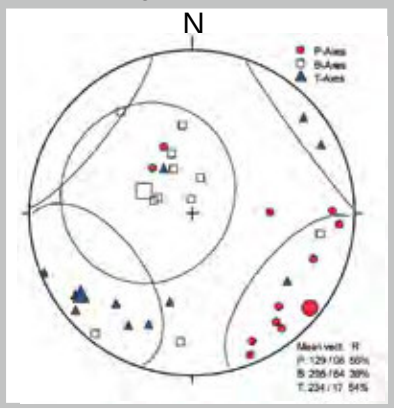

RIGHT DIHEDRA

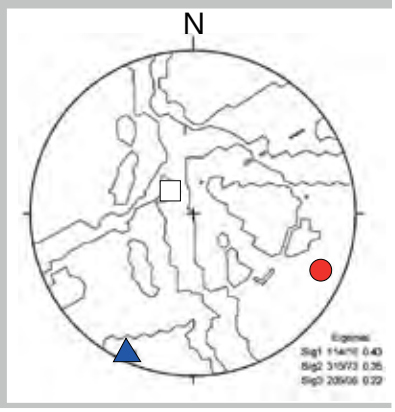

TENSOR

N = 6

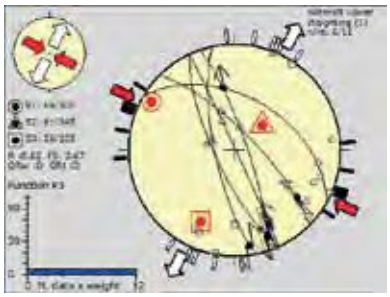

Stress field description

Not far from the previous outcrop, a strike-slip stress regime is prevailing, as we observe in the re-sulting plot of the paleostress analysis. The extensional stress axis is oriented in direction NNE-SSW, which coincide with the overall extension axes of vein measurements. At one outcrop, two sets of slickenfibres allow the distinction between two faulting

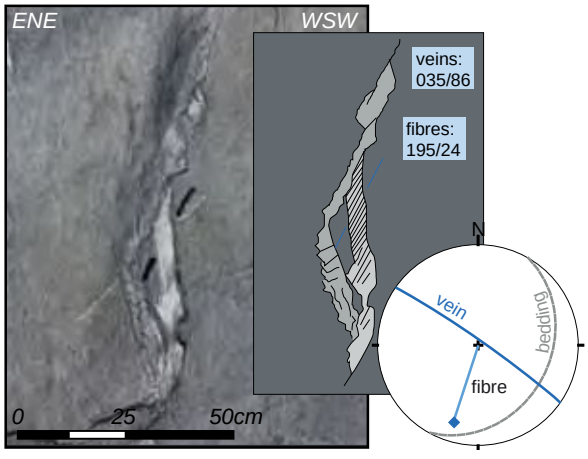

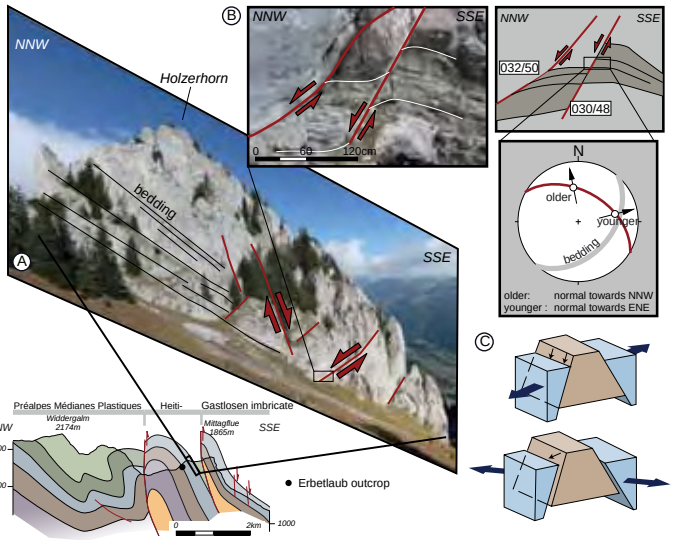

(see Chapter 3/ 4.2.2 Schafarnisch - Mittagsfluh)

5 **Mittagsfluh Egg** *Préalpes Médianes Gastlosen imbricate*

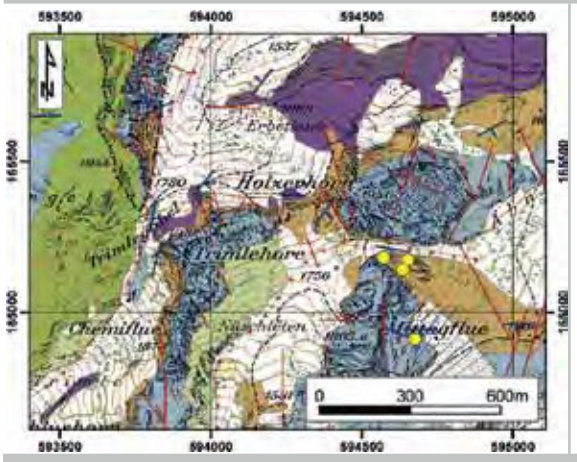

Outcrop description:

594680/ 164905 1480m

The measurements were collected along the face north of the Mittagflue; slickenfibres and veins were rare. The SE face of the Mittagflue is affected by an important rock fall; the fractures of the lower part of its detachment zone show a dominating distribution of NNW-SSE oriented fracture planes.

N = 14 *Middle Jurassic* *bedding = 186/ 66*

ANGELIER

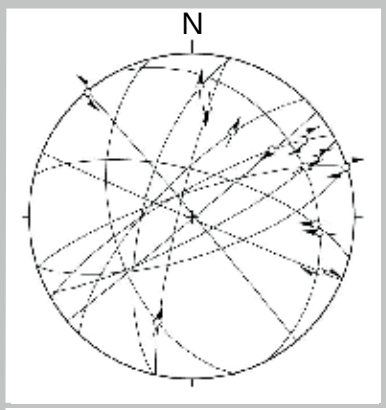

P-T

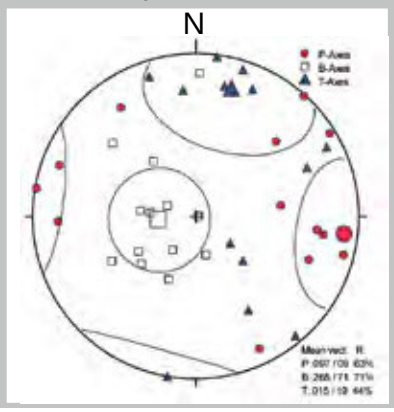

RIGHT DIHEDRA

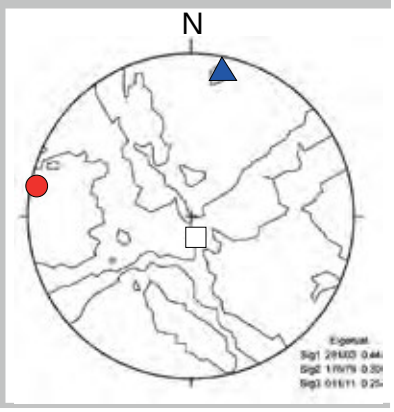

TENSOR

N = 6

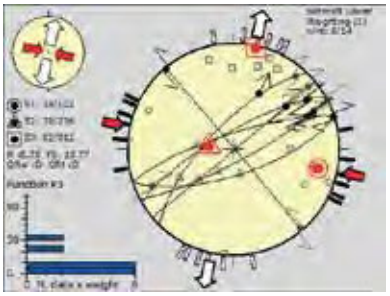

fracture orientation rock fall

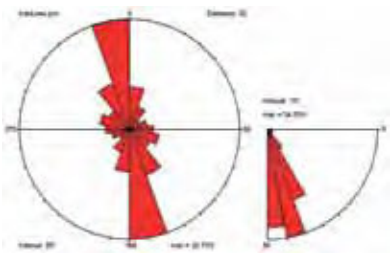

Stress field description

Stress field description:
The obtained stress field belongs to a strike-slip stress regime with the compressional stress axis oriented WNW-ESE. The dominating fracture direction above the detachment zone of a vast rock fall is NNW-SSE. With a sinistral strike-slip movement, they would fit into the observed strike-slip system.

6 Walop *Préalpes Médianes Plastiques*

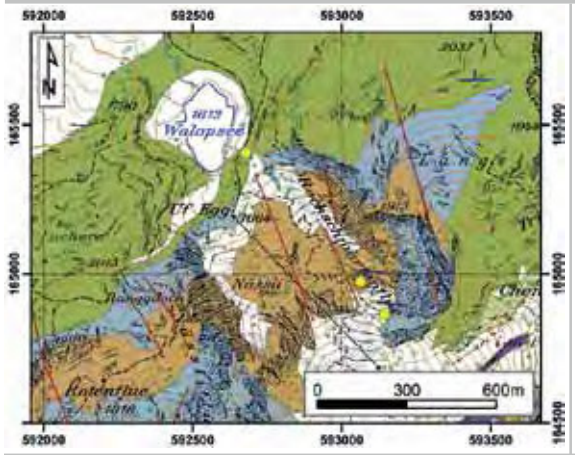

Outcrop description:

592977/ 164960 1430m

Measurements were taken in two different areas, both along the path up to the lake Walop, one in the Middle Jurassic and the other in the Lower Jurassic rocks. Both outcrops showed a great number of slickenfibres, but they were limited to a few blocks. Veins were rare.

N = 28 *Lower Cretaceous/ Middle Jurassic* *bedding = 180/ 55*

ANGELIER

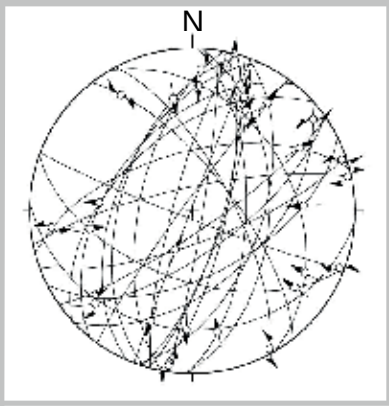

P-T

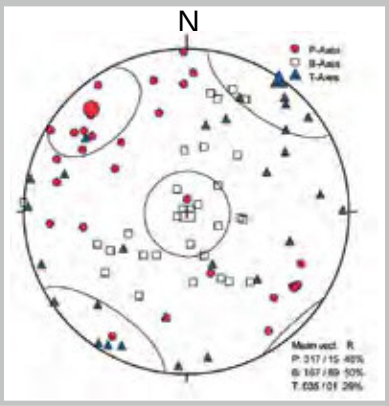

RIGHT DIHEDRA

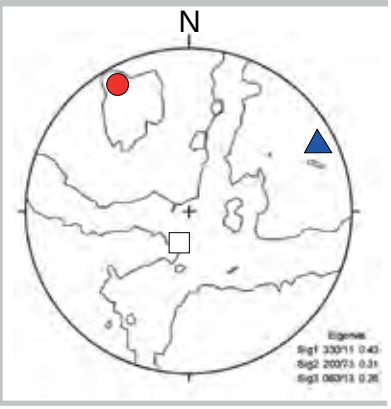

TENSOR

N = 13

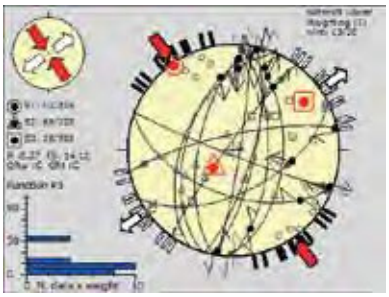

N = 6

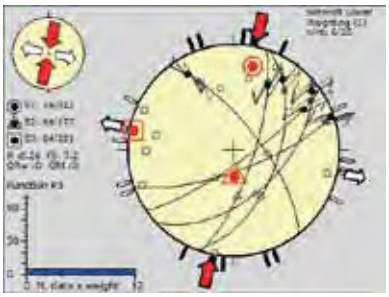

Stress field description

Throughout the process of data separation, two different stress regimes were detected in the Walop area. The prevailing strike-slip regime with a NW-SE directed compressional axes obtained a “C” in quality ranking. A secondary strike-slip stress regime was identified with the compressional stress axis oriented towards NNE-SSW.

7 Kaiseregg *Préalpes Médianes Plastiques*

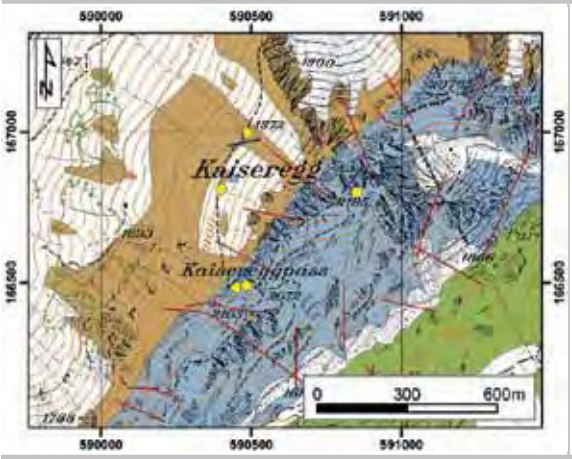

Outcrop description:

590482/ 166485 2010m

The Upper Jurassic limestones expose a whole set of fractures with well-developed slickenfibres, especially along the path to the Kaiseregg, which is recently cut into the rock, so the erosion did not damage the calcite fibres.

N = 32 *Upper Jurassic* *bedding = 137/ 64*

ANGELIER

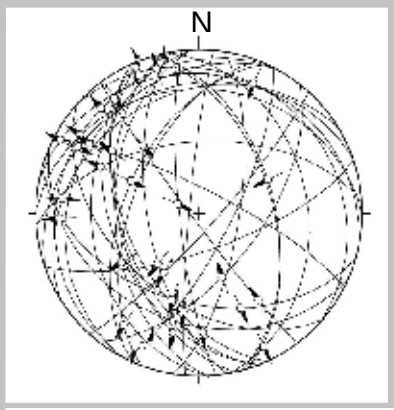

P-T

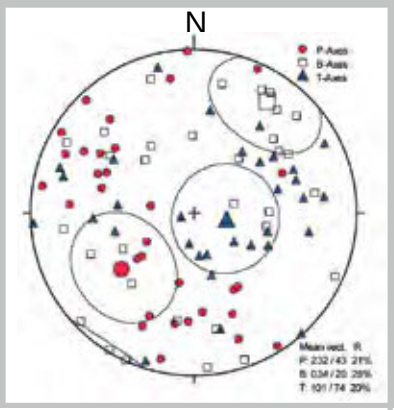

RIGHT DIHEDRA

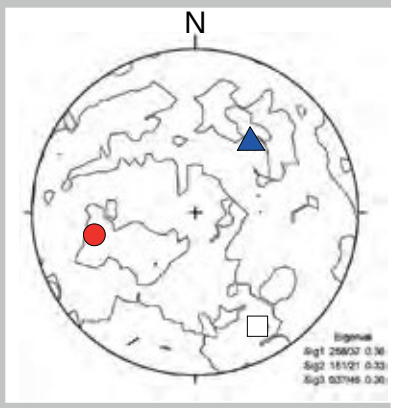

TENSOR

N = 11

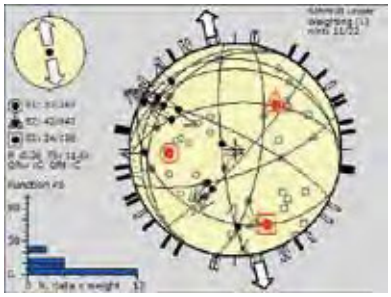

N = 7

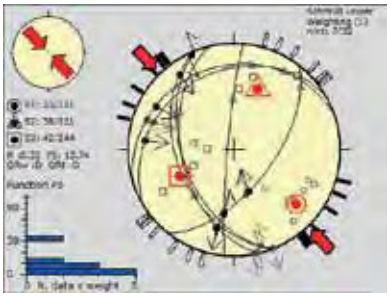

Stress field description

Two different stress systems are identified whereof the prevailing stress regime is extensional with its extensional stress axis trending towards NNW-SSE, and the secondary stress regime is strike-slip with a more pronounced compressional axis pointing towards NW-SE. The illustrated fault plane with slickenfibres on it and en-echelon veins works under the first stress regime.

VEINS AND SLICKENFIBRES

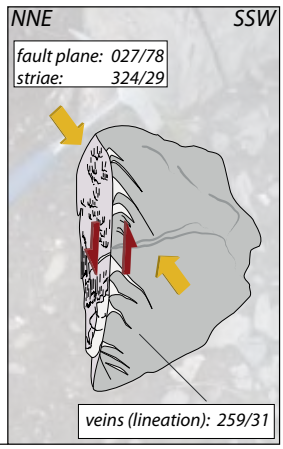

8 **Unter Recardet** *Préalpes Médianes Plastiques*

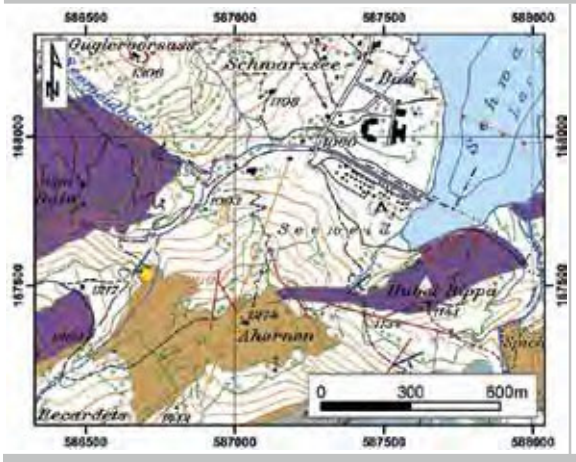

Outcrop description:

586708/ 167540 1200m

The road up to Unter Recardet exposes in a bend a Middle Jurassic limestone outcrop where the measurement of several slickenfibres was possible but it was only restricted to this place. Several calcite fibres were of lower quality due to weathering.

N = 11 *Middle Jurassic* *bedding = 124/ 69*

ANGELIER

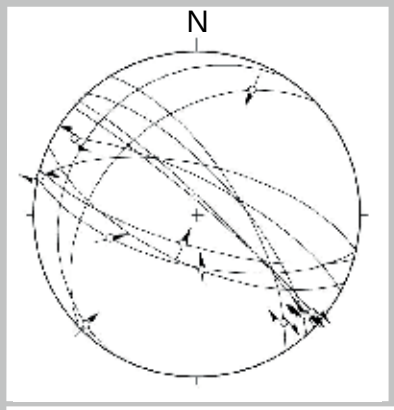

P-T

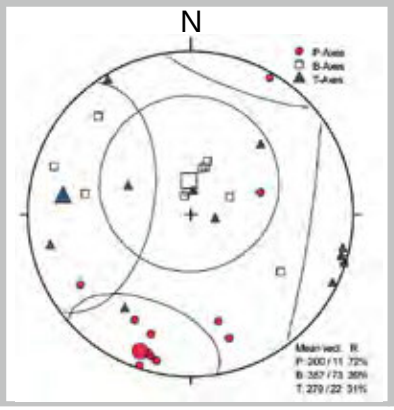

RIGHT DIHEDRA

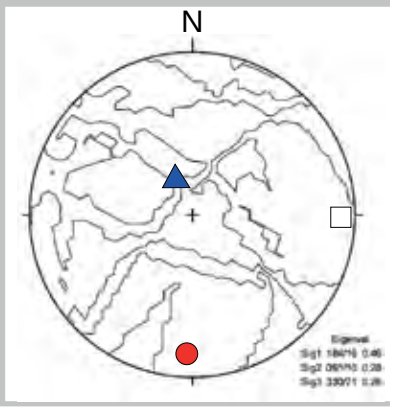

TENSOR

N = 9

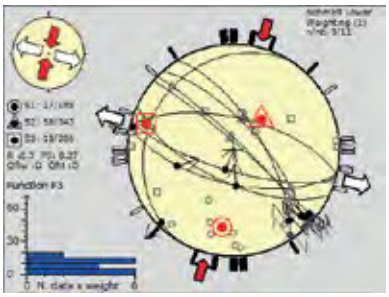

Stress field description

Eliminating three strike-slip data, the resulting strike-slip stress regime with the compressional stress axis orientated towards NNE-SSW shows a rather homogeneous stress field.

9 **Hubel Rippa** *Préalpes Médianes Plastiques*

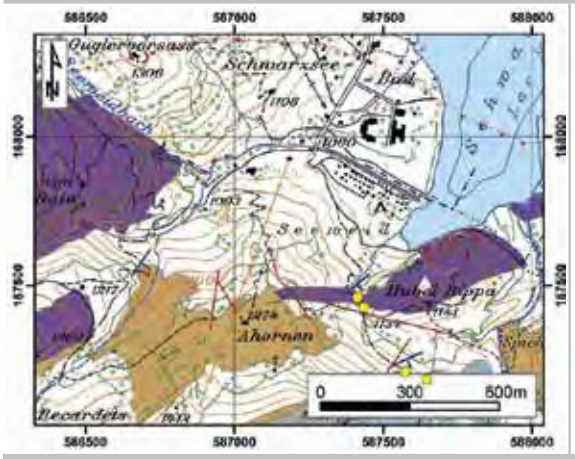

Outcrop description:

587435/ 167436 1130m

The fault-slip measurements were taken in vicinity to a major NW-SE trending dextral fault. The outcrop is limited to several blocks outcropping along the pathway up to the Breccaschlund. The Lower Jurassic marly limestones expose slickenfibres of average quality.

N = 12 *Lower Jurassic* *bedding = 134/ 70*

ANGELIER

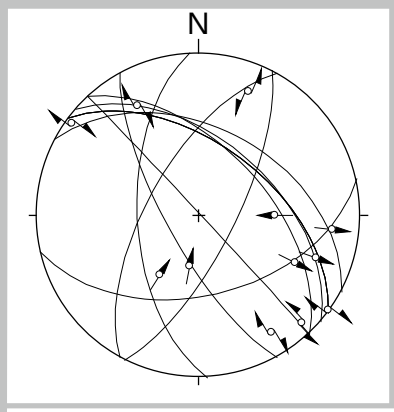

P-T

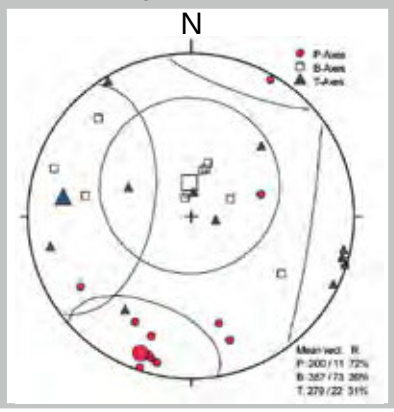

RIGHT DIHEDRA

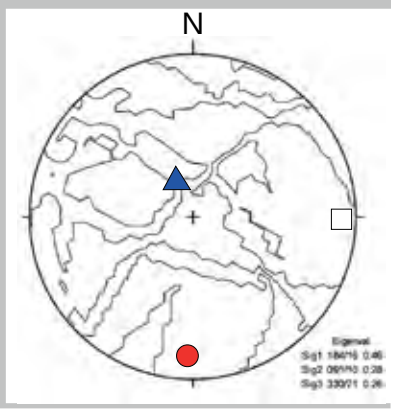

TENSOR

N = 8

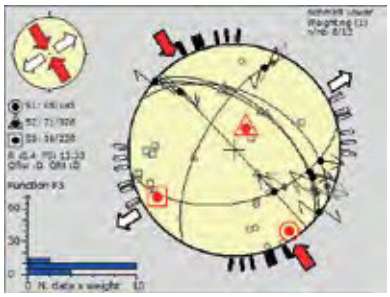

Stress field description

The influence of a large-scale NW-SE oriented dextral strike-slip fault is well represented by the TENSOR plot showing a strike-slip stress regime, the compressional stress axes oriented towards NNW-SSE.

10 **Welschi Rippa** *Préalpes Médianes Plastiques*

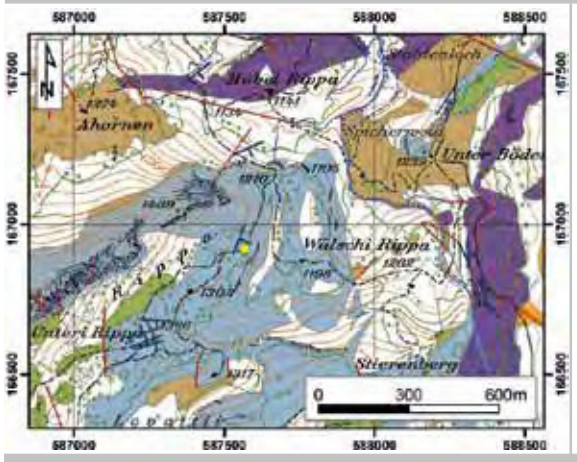

Outcrop description:

587623/ 167180 1210m

Upper Jurassic limestones are outcropping over a several meters along the path heading to the Breccaschlund. Highly fractured rocks expose a large variety of different fault-slip orientations.

N = 19 Upper Jurassic bedding = 156/ 41

ANGELIER

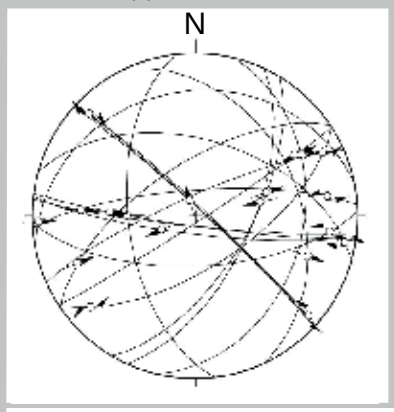

P-T

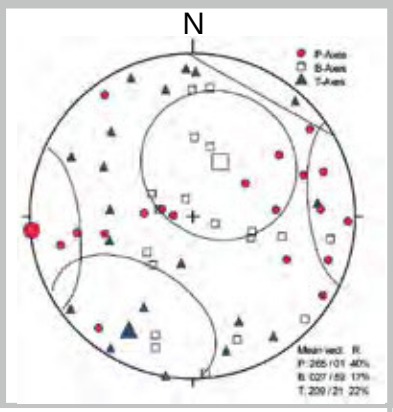

RIGHT DIHEDRA

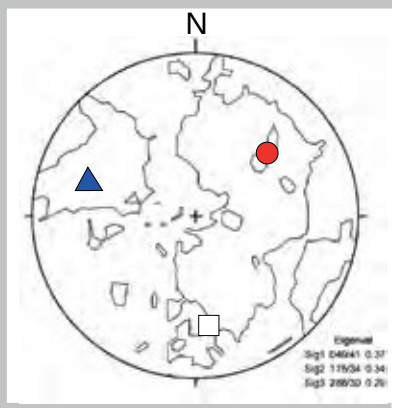

TENSOR

N = 9

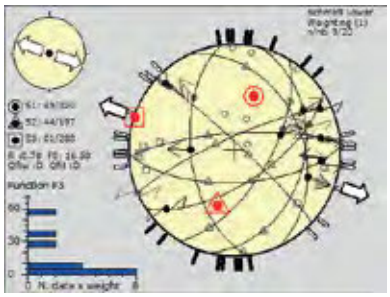

N = 6

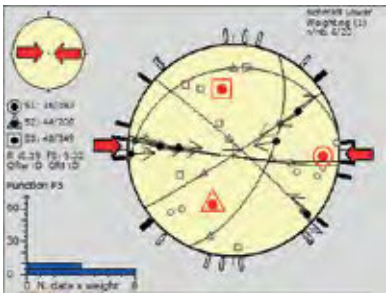

Stress field description

The resulting TENSOR plots show either an extensional or a compressional stress field with the extensional stress axis trending towards WNW-SES, respectively the compressional stress axis towards W-E. Most probably, these two stress regimes are both related to the folding structure.

11 ***Underi Rippa*** *Préalpes Médianes Plastiques*

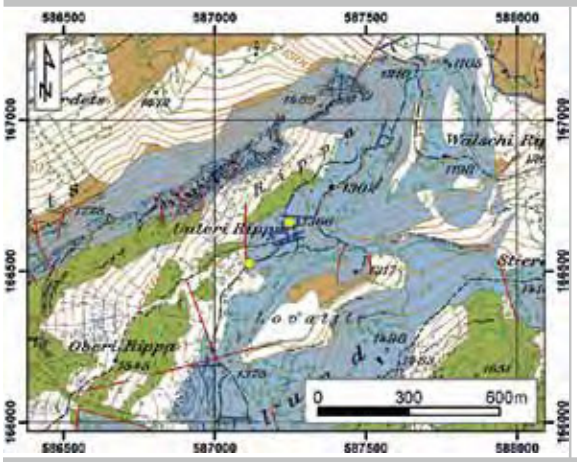

Outcrop description:

587256/ 166659 1366m

Upper Jurassic limestones with small-scale folds expose several fractures containing well-developed slickenfibres and veins, which could be attributed to two different deformation events: older veins oriented ENE-WSW with an overall extension axis towards NNW-SSE is crosscut by broader veins in NNW-SSE direction, with an overall extension axis to the ENE-WSW. The second event coincides with the extensional direction proposed by the pale-ostress evaluation.

N = 19 Upper Jurassic bedding = 341/ 80

ANGELIER

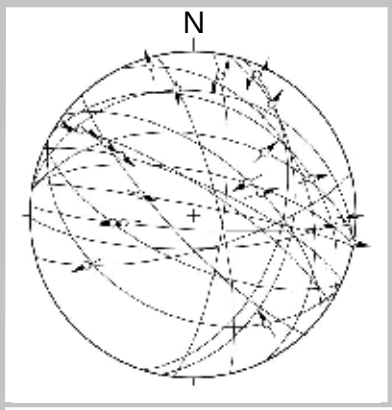

P-T

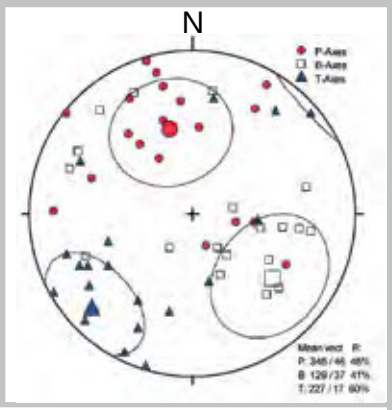

RIGHT DIHEDRA

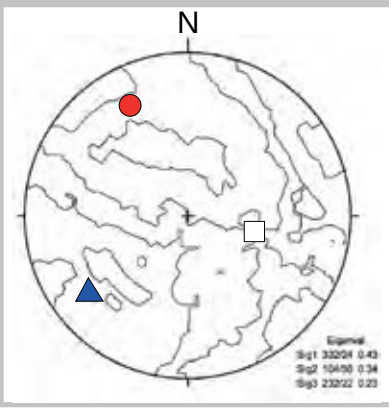

TENSOR

N = 9

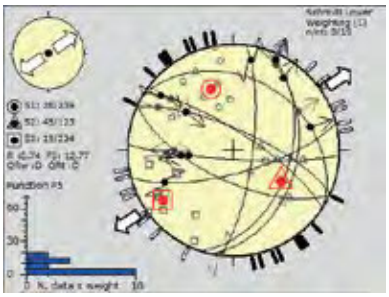

VEINS

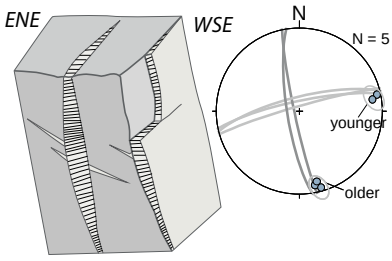

Stress field description

The resulting extensional stress regime shows an extensional stress axis towards NE-SW. Vein observation witness the same ENE-WSW extensional axes of younger veins crosscutting older veins oriented ENE-WSE. These older extension towards SSE-NNW is not represented in our paleostress results. The dominant extensional stress regime is probably related to the folding.

12 Mitzlere *Préalpes Médianes Plastiques*

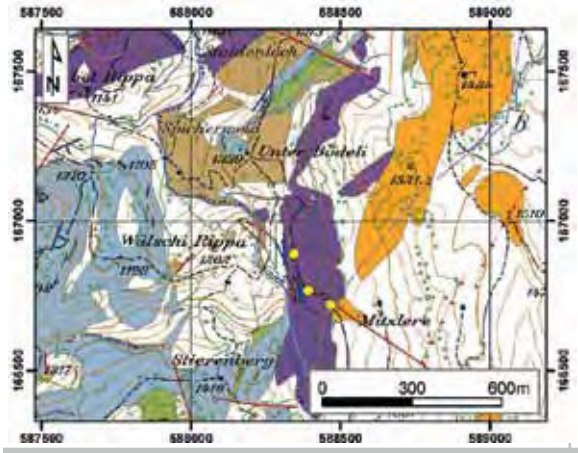

Outcrop description:

578922/ 166637 1300m

The outcrop reaches a length of more than 400m of Lower Jurassic Limestones along the wayside heading towards the Euschels pass. The orientation of the faults is mostly NNW-SSE but indicates both sinistral and dextral sense of shear. Furthermore, a large-scale fault oriented NNW-SSE lays in direct vicinity. Due to the opposite sense of shear two different paleostress subsets have to be created.

N = 35 Lower Jurassic *bedding = 064/23*

ANGELIER

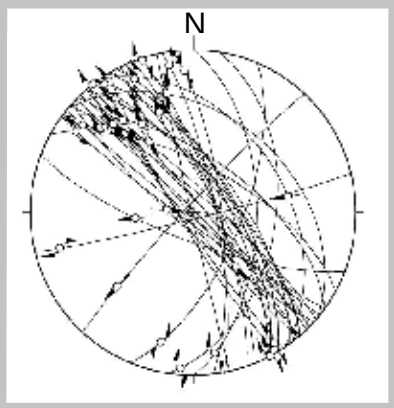

P-T

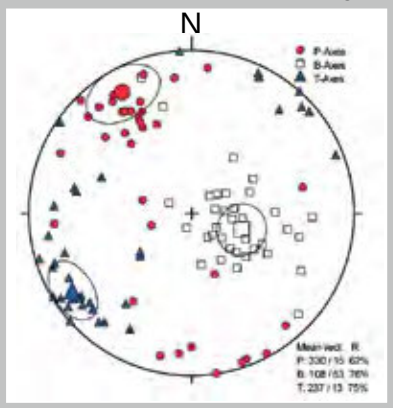

RIGHT DIHEDRA

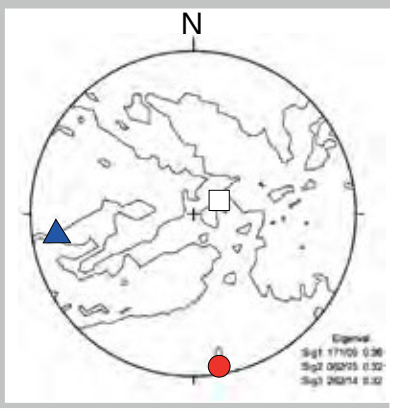

TENSOR

N = 10

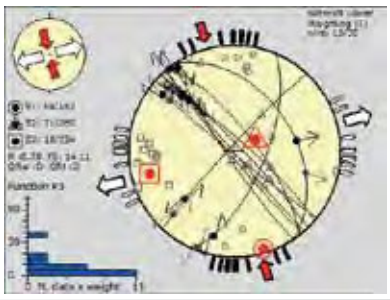

N = 12

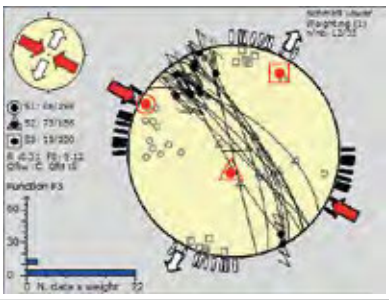

Stress field description

As the movement on the predominant fault direction is either sinistral or dextral, they have to belong to two different stress regimes. Both are strike-slip systems, whereas in the first TENSOR plot the compressional axis is oriented NNW-SSE; and in the second TENSOR plot the compressional axis trends towards NW-SE.

13 **Brecca** *Préalpes Médianes Plastiques*

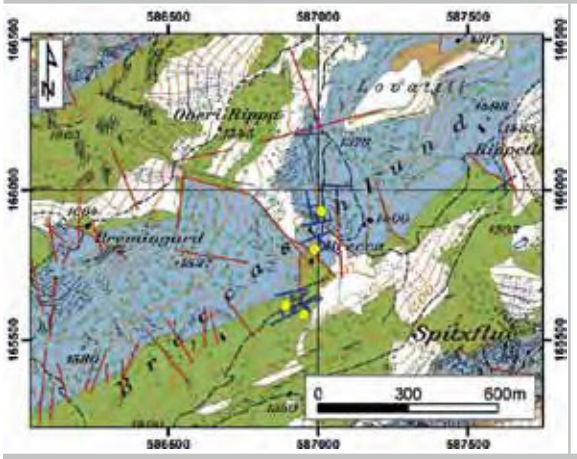

Outcrop description:

587013/ 165933 1320m

Lower Cretaceous small-scale folds characterise this outcrop along the path. Veins and calcite fibres are well developed. Most of the fractures are oriented parallel to the fold axes.

N = 25 Lower Cretaceous *bedding = 159/ 33*

ANGELIER

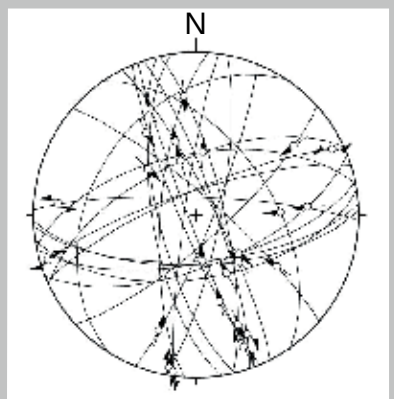

P-T

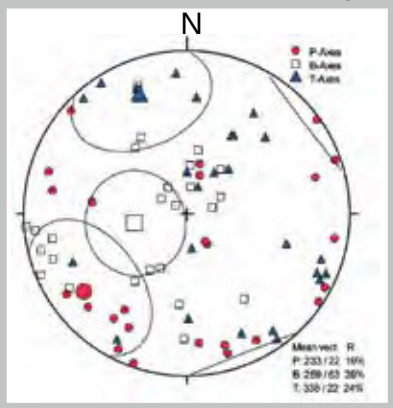

RIGHT DIHEDRA

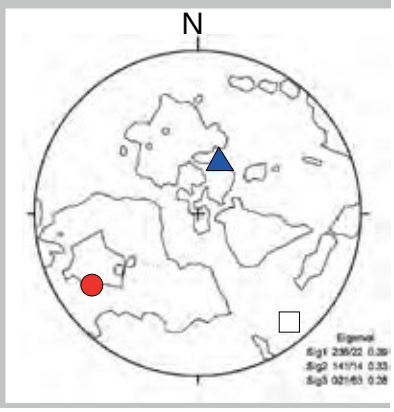

TENSOR

N = 9

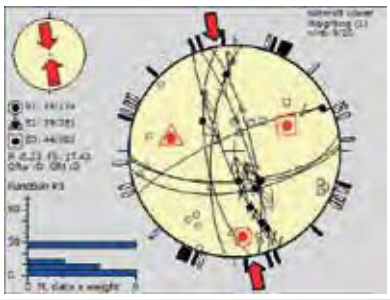

N = 7

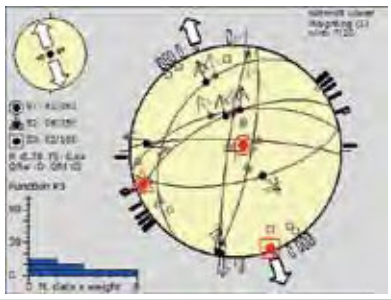

Stress field description

Both resulting stress regimes are based on rather a small amount of data and are therefore rated as “D” in the quality ranking. The stress regimes are either pure compressive or pure extensive. Its compressional stress axis is oriented NNW-SSE for the first stress regime and the extensional stress axes trends towards NNW-SSE for the extensional regime. Probably, the two stress regimes are linked together to the folding structure.

14 ***Cerniets/ Combi*** *Préalpes Médianes Plastiques*

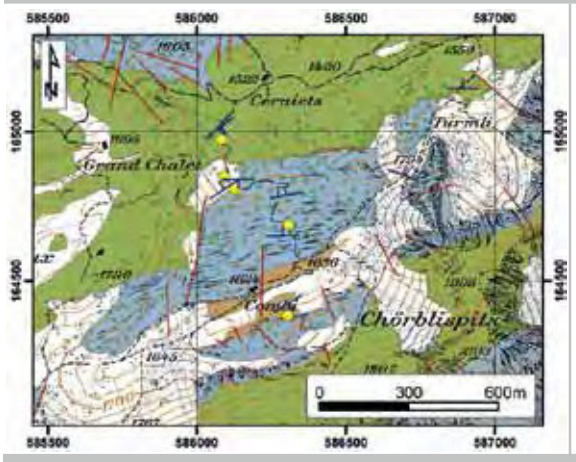

Outcrop description:

586708/ 167540 1200m

The road up to Unter Recardet exposes in a bend a Middle Jurassic limestone outcrop where the measurement of several slickenfibres was possible but it was only restricted to this place. Several calcite fibres were of lower quality due to weathering.

N = 29 Lower Cretaceous *bedding = 326/ 76*

ANGELIER

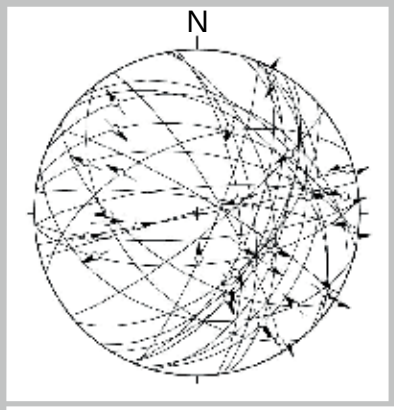

P-T

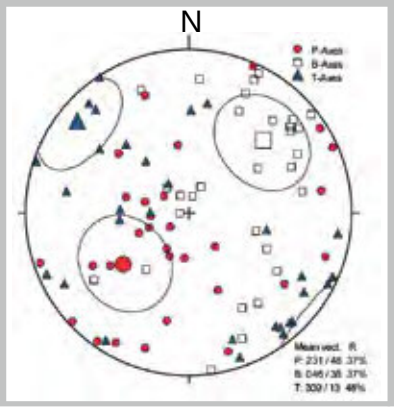

RIGHT DIHEDRA

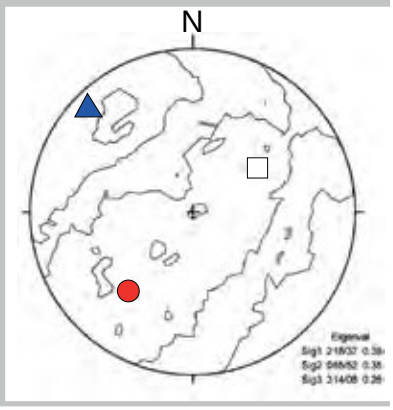

TENSOR

N = 10

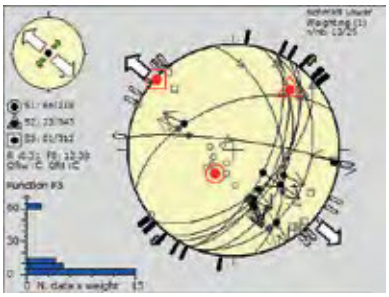

Stress field description

The data sorting process eliminated a large number of fault-slip date, so that the remaining data are represented in a extensional stress regime with the extensional stress axis oriented towards NW-SE.

15 ***Combi/ Alpigen*** *Préalpes Médianes Plastiques*

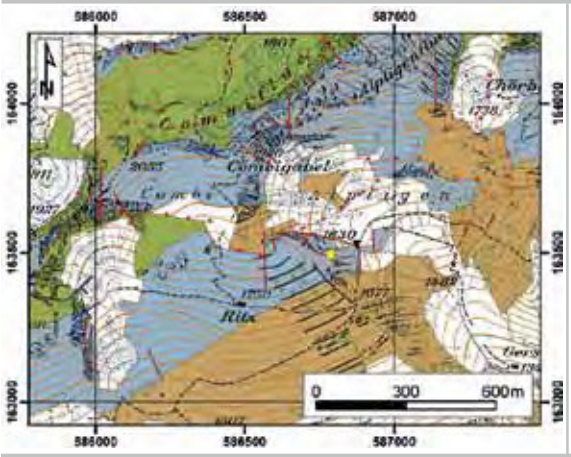

Outcrop description:

586701/ 163568 1630m

Fault-slip measurements were reproduced after the diploma thesis of Stefan Fuchs (2003), he points out that mainly sinistral strike-slip faults are domi-nating this outcrop.

N = 13 Upper Jurassic *bedding = 331/ 85*

ANGELIER

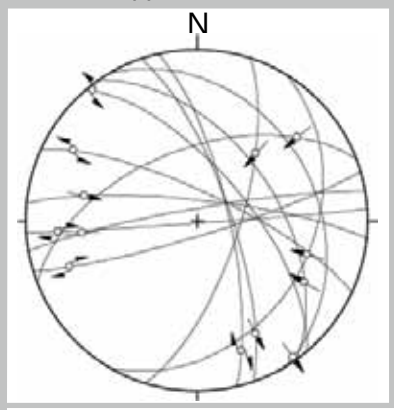

P-T

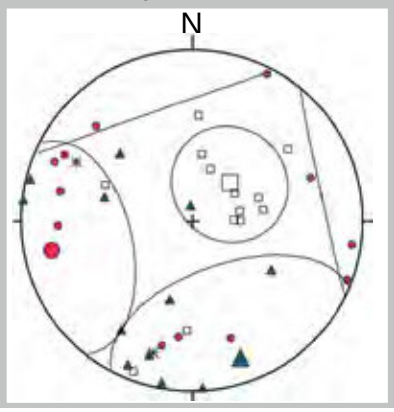

RIGHT DIHEDRA

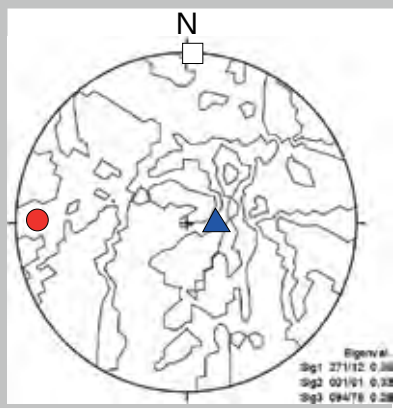

TENSOR

N = 7

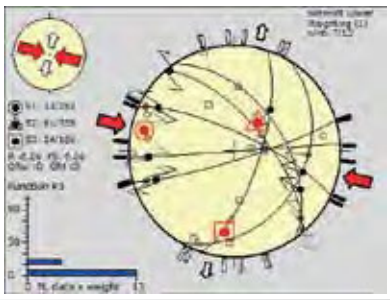

Stress field description

After separation of the initial fault-slip data set, a strike-slip data set remained with the compressional stress axis oriented WNW-SES. The quality of the data set is rather low and considering the plots containing the entire data set, another stress regime sticks out: a strike-slip regime with the compressional stress axis trending toward NE-SW.

16 ***Pass Schopfenspitz*** *Préalpes Médianes Plastiques*

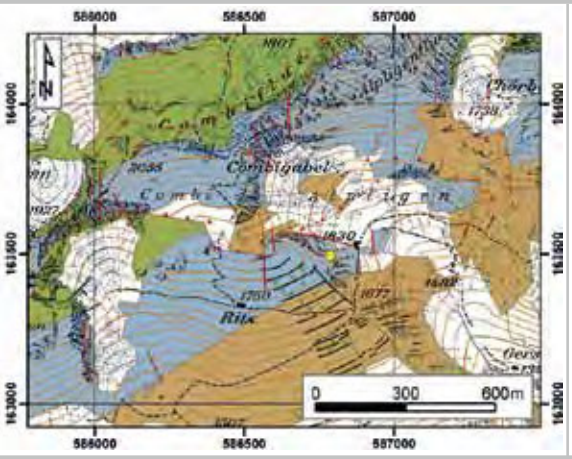

Outcrop description:

585482/ 163639 2012m

Fault-slip measurements were reproduced after the diploma thesis of Stefan Fuchs (2003). The fracture orientation is rather various but show besides reverse and normal faults some dextral strike-slip faults, oriented NW-SE.

N = 16 Upper Jurassic *bedding = 328/ 31*

ANGELIER

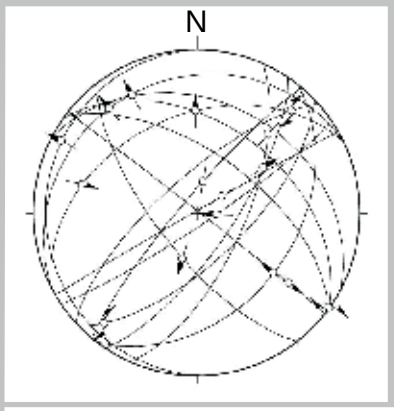

P-T

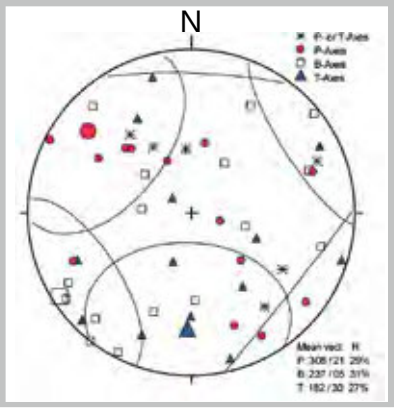

RIGHT DIHEDRA

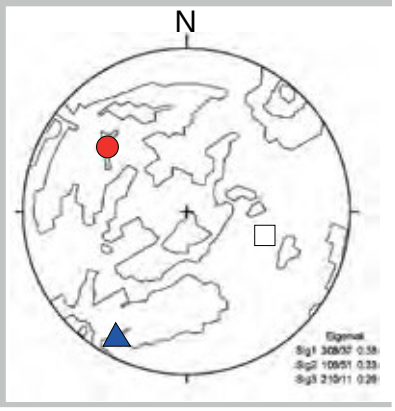

TENSOR

N = 7

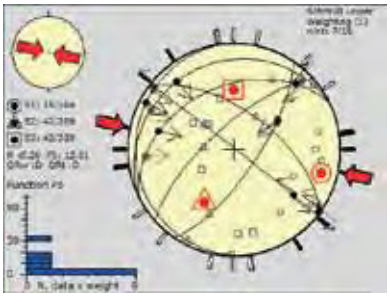

Stress field description

The resulting stress regime is highly influenced by the presence of the important Schopfenspitz thrust and shows therefore a compres-sional stress regime with a compressional stress axis oriented WNW-SES.

17 Jansegg — *Préalpes Médianes Plastiques*

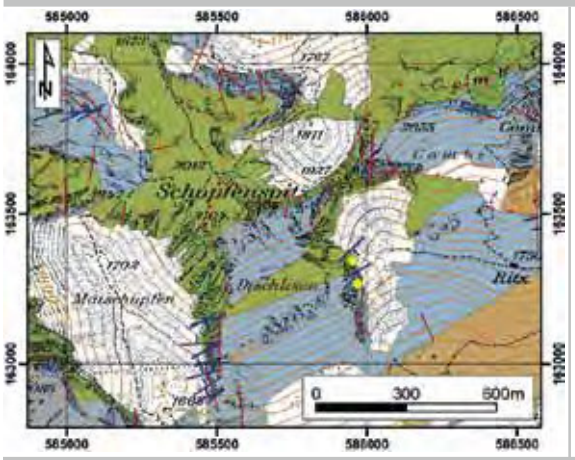

Outcrop description:

585973/ 163252 1750m

Fault-slip measurements were reproduced after the diploma thesis of Stefan Fuchs (2003). The fault planes are mostly oriented in a NE-SW direction and show a normal slip-component, despite of the overall compressional context of the Schopfenspitz fault.

N = 12 Upper Jurassic *bedding = 139/ 85*

ANGELIER

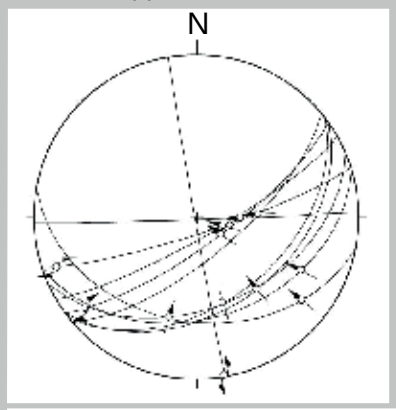

P-T

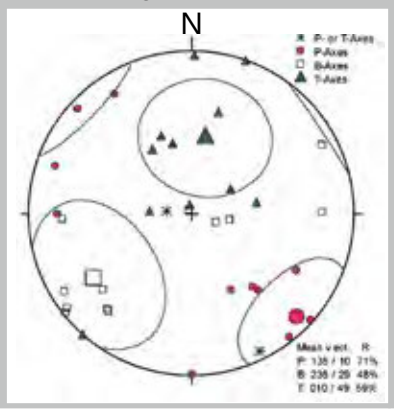

RIGHT DIHEDRA

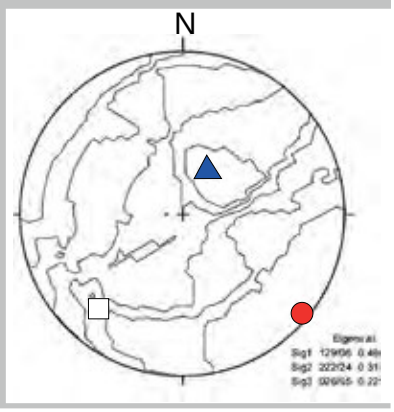

TENSOR

N = 7

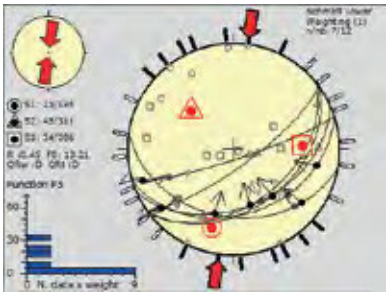

Stress field description

Like the previous outcrop, the Jansegg outcrop is highly influenced by the presence of the Schopfenspitz thrust and shows for that reason a compressional strike-slip system oriented N-S. Considering the plots of non-selected strike-slip data an overall compressional axis towards NW-SE can be observed.

18 Maischüpfen *Préalpes Médianes Plastiques*

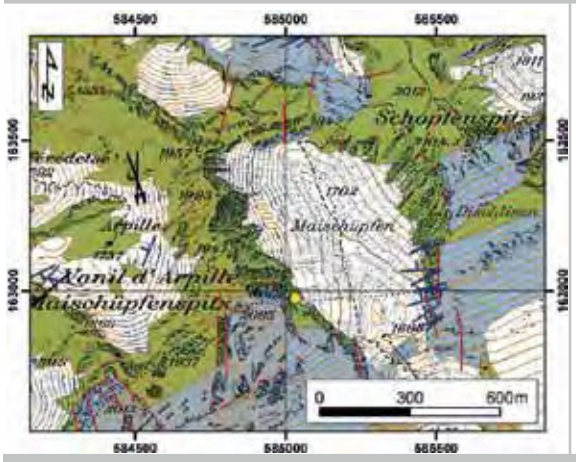

Outcrop description:

585325/ 162630 1750m

Fault-slip measurements were reproduced after the diploma thesis of Stefan Fuchs (2003). Fractures show a NW-SE orientation with reverse slip-movement, which can be related to the Schopfenspitz, thrust.

N = 20 Upper Jurassic *bedding = 248/ 85*

ANGELIER

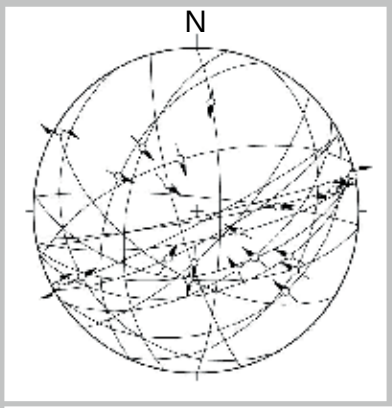

P-T

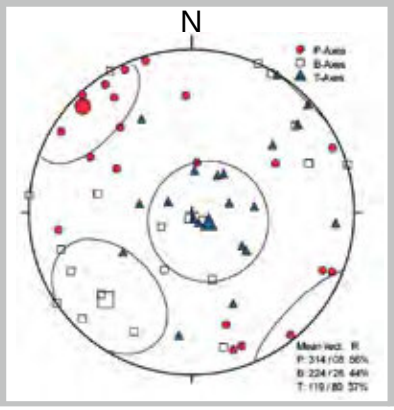

RIGHT DIHEDRA

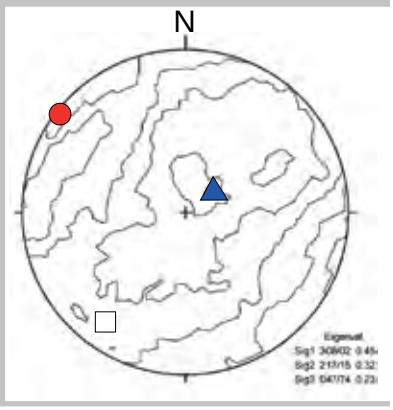

TENSOR

N = 10

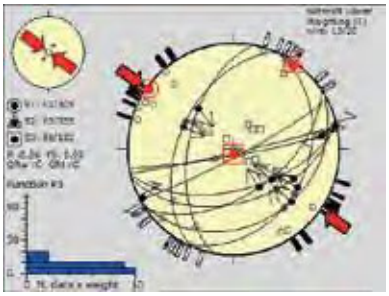

Stress field description

Again, the stress regime of the Maischüpfen area is affected by the vicinity of the important Schopfenspitz thrust. The compressional stress regime is orientated towards NW-SE and agrees with the non-selected dataset.

19 **Arpille** *Préalpes Médianes Plastiques*

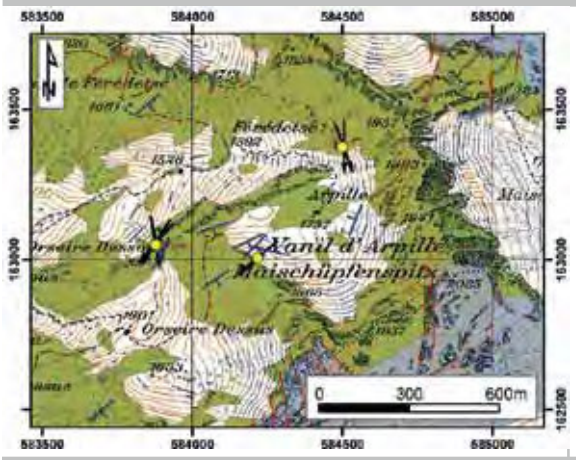

Outcrop description:

584504/ 163378 1750m

Small-scale folds dominate the outcrop area, which extends over a larger area containing several smaller outcrops. Fractures are mostly oriented NE-SW and show both a sinistral and a dextral strike-slip movement. The Lower Cretaceous lime-stones are strongly folded and show several vein sets often without any clear chronological indica-tion, except at one place where vertical NE-SE oriented veins cross-cut nearly horizontal ones.

N = 27 *Lower Cretaceous* *bedding = 304/ 51*

ANGELIER

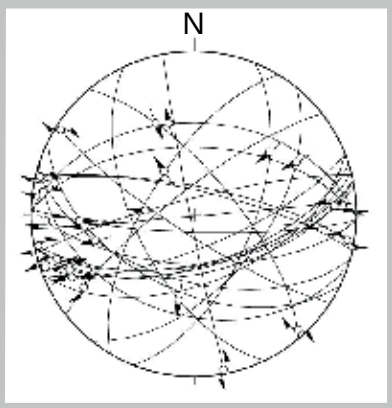

P-T

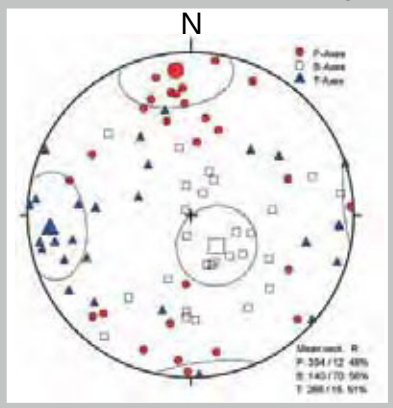

RIGHT DIHEDRA

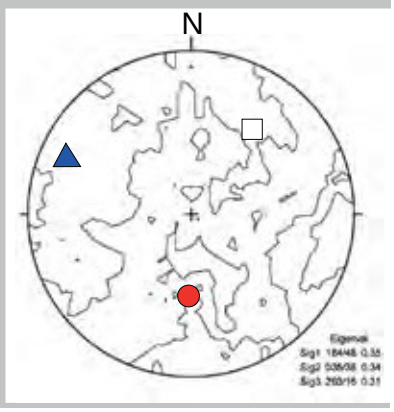

TENSOR

N = 10

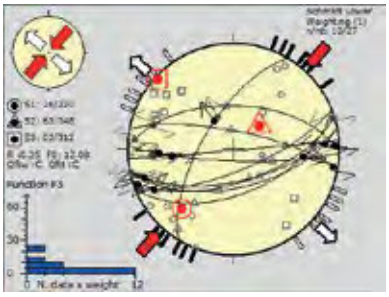

N = 8

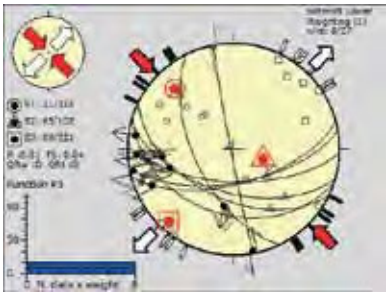

Veins

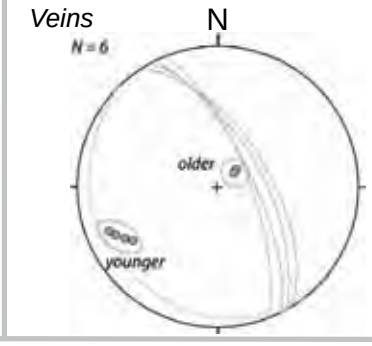

Stress field description

Throughout the process of data separation, two different stress regimes were detected in the Walop area. The prevailing strike-slip regime with a NW-SE directed compressional axes obtained a “C” in quality ranking. A secondary strike-slip stress regime was iden-tified with the compressional stress axis oriented towards NNE-SSW.

20 Arsajoux *Préalpes Médianes Plastiques*

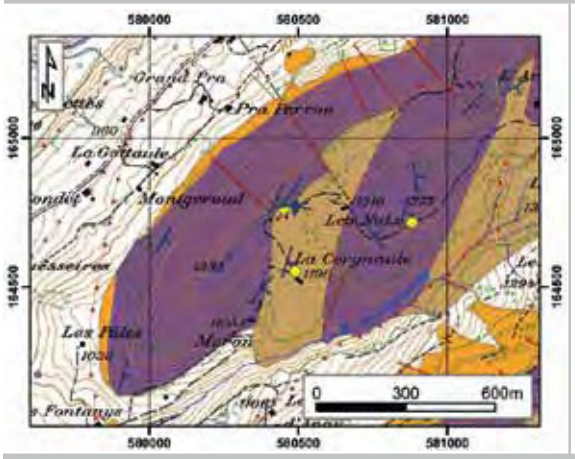

Outcrop description:

584504/ 163378 1750m

The Arsajoux plot takes three more restricted measure localities together. The overall structure of the Arsajoux area is affected by three larger thrusts forming limited imbricates thrusting towards WSW. Most of the fractures show strike-slip faults.

N = 21 *Lower Cretaceous* *bedding = 109/ 40*

ANGELIER

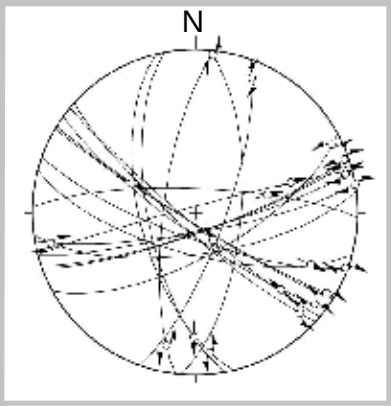

P-T

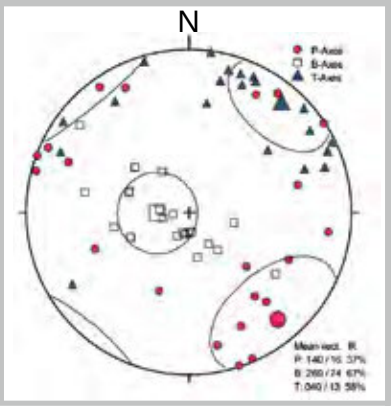

RIGHT DIHEDRA

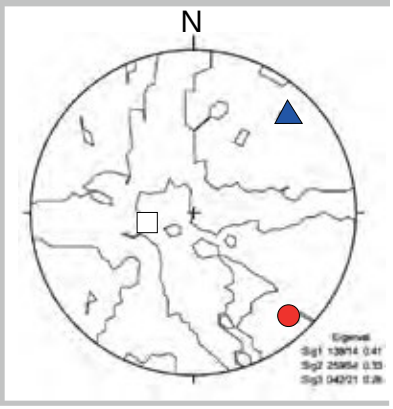

TENSOR

N = 13

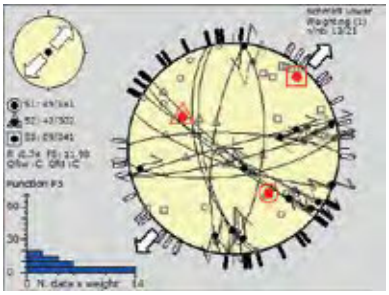

N = 6

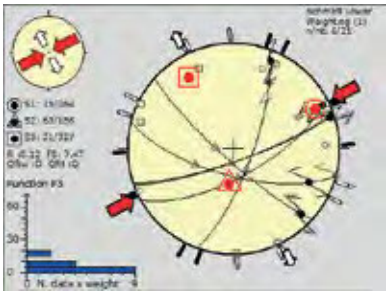

Stress field description

The oblique orientation of the Arsajoux thrust slices have effects on the orientation of the stress field that is predominantly an oblique strike-slip system with an extensional stress axis oriented NE-SW. A secondary strike-slip regime exists with a NE-SW orientation of the compressional stress axis.

21 **Carrière Tzintre** *Préalpes Médianes Plastiques*

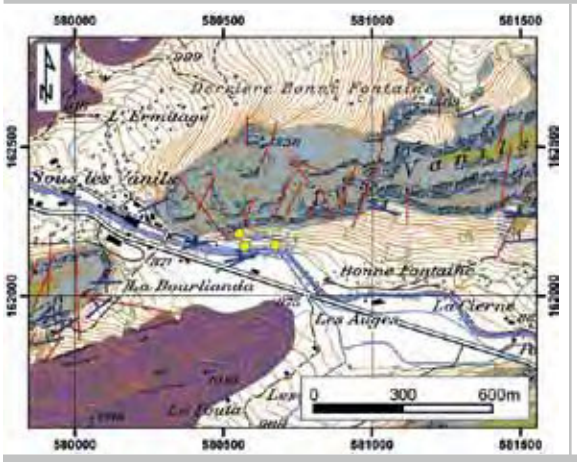

Outcrop description:

580552/ 162203 880m

The Tzintre quarry gives one of the best insights into the complexity of the fracturing of the Préalpes Médianes. The quality of the outcrop is high as excavation work is still going on. Most of the larger scale faults show several sets of slick-enfibres on them, expressing a reactivation of these faults with different movement directions. The dominant fracture orientations are NE-SW and N-S. Shear bands and veins are frequent. Their cross-cutting relationships show a younger extensional direction towards NE-SW and an older one towards NW-SE.

N = 89 *Middle Jurassic* *bedding = 334/ 44*

ANGELIER

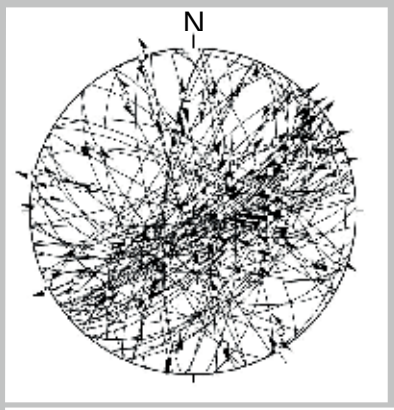

P-T

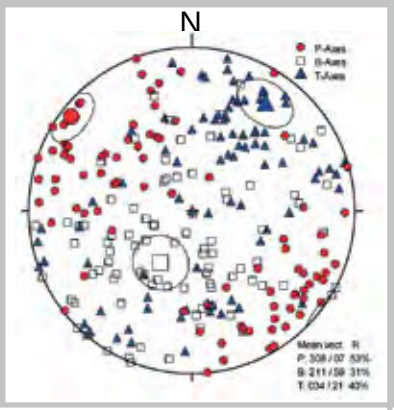

RIGHT DIHEDRA

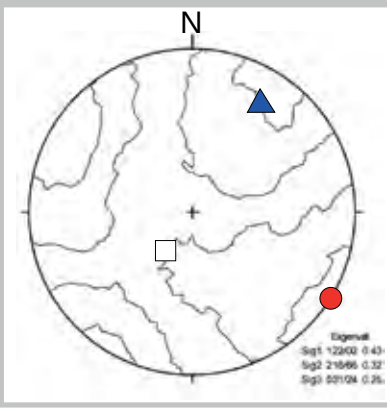

TENSOR

N = 29

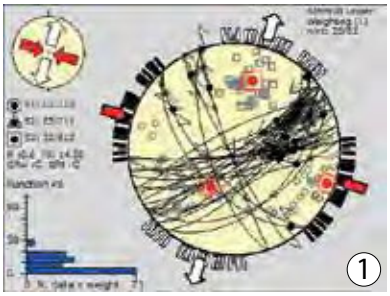

N = 17

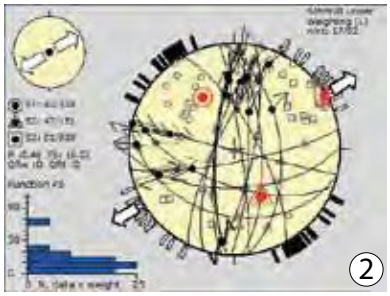

Veins

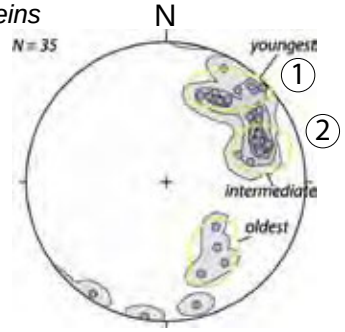

Stress field description

The predominant dextral strike-slip fault striking NE-SW operate under a strike-slip stress regime with its com-pressional stress axis oriented WNW-SES. A secondary, more oblique strike-slip fault regime with a dominating extensional component can be differentiated. Vein intersections expose the following chronology: The youngest veins show an overall extensional direction towards NNE-SSW and can probably be related to the first stress regime. The intermediate veins with an overall extensional ENE-SWS direction coincide nicely with the extensional stress of the secondary plot. The oldest veins show an extensional direction towards NW-SE and cannot be related to one of the resulting TENSOR plots, but considering the P-T plot containing the entire fault-slip data sets some faults with the same extensional stress axes can be observed.

22 Les Vanils *Préalpes Médianes Plastiques*

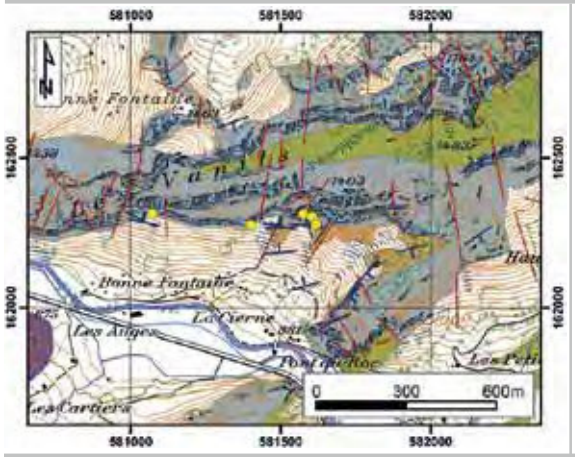

Outcrop description:

581072/ 162311 1030m

Just a few hundred meters farther to the E of the previous outcrop, the quality of the measurements decreases because of the lack of fresh outcrops. Most of the fracture planes are weathered and therefore without any calcite fibres. The majority of the fractures are oriented more or less perpendicu-lar to the fold axis.

N = 17 Upper Jurassic bedding = 358/ 47

ANGELIER

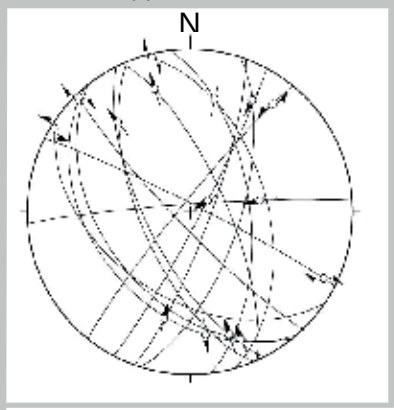

P-T

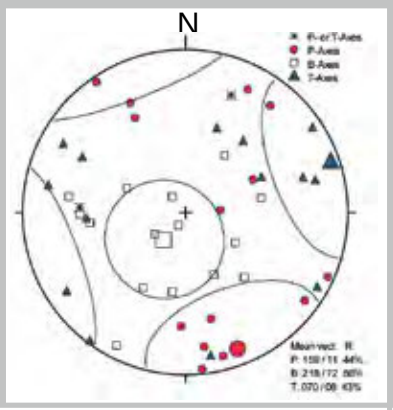

RIGHT DIHEDRA

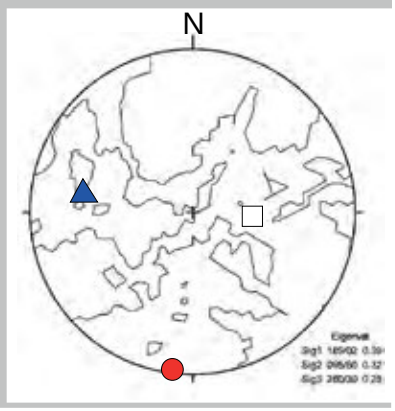

TENSOR

N = 11

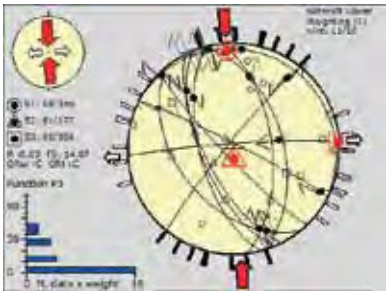

N = 6

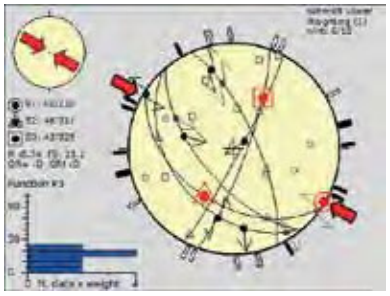

Stress field description

The dominant stress system is a strike-slip stress regime with the compressional axes oriented NNW-SSE. A compressional stress regime oriented NW-SE acts only as a minor stress system.

23 ***Le Brésil*** *Préalpes Médianes Plastiques*

Outcrop description:

582773/ 161049 900m

A second quarry gives us another high quality out-crop. Stylolites, veins were found frequently, whereas slickenfibres were less abundant than in the Tzintre quarry. Unless one large fault plane with its broad fault zone, the general structures seem to be less complex than in the previous quarry. The dominating fault direction is N-S with an either dextral or sinistral strike-slip movement, which agrees with the orientation of the large faults. The occurrence of veins and stylolites allow defining a chronology of structural events.

N = 31 *Upper Jurassic* *bedding = 334/ 74*

ANGELIER

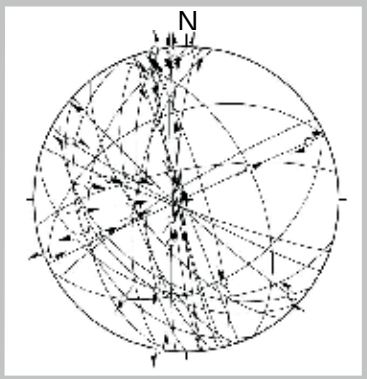

P-T

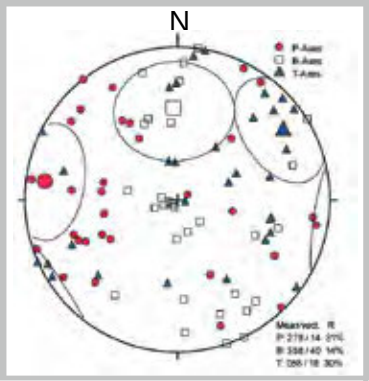

RIGHT DIHEDRA

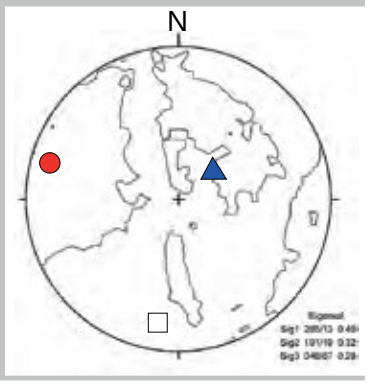

TENSOR

N = 9

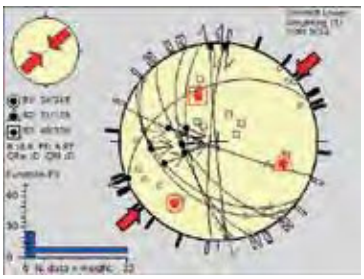

N = 9

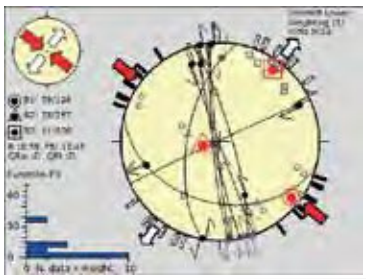

VEINS AND SLICKENFIBRES

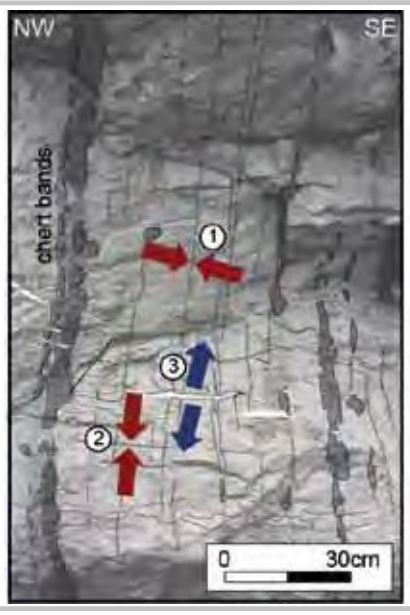

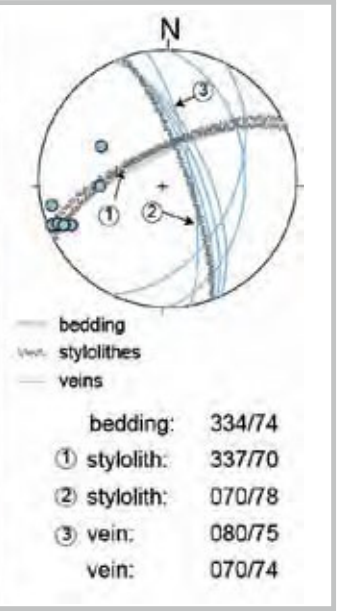

Stress field description

At the Brésli quarry two stress regimes are defined: a strike-slip regime with a NW-SE oriented compressional axis and a purely compressional stress regime ori-ented towards NE-SW. Veins and Stylolites expose the following succession of events:
1) stylolites parallel to the bedding due to the compaction of the sedimentary layers; 2) vertical compression forming horizontal stylolites, 3) extensional veins with an extension direction towards NE-SW. Following the chronology deduced by intersecting veins, the strike-slip stress regime should be younger than the purely compressional.

24 **Gros Haut Crêt** *Préalpes Médianes Plastiques*

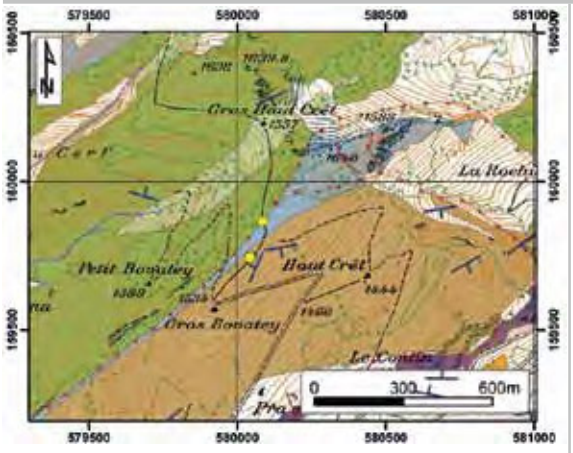

Outcrop description:

580084/ 159863 1560m

The outcrop is located in vicinity to important thrust faults striking in NE-SW direction. Several fractures represent this thrusting movement as seen in the second stereographic projection. The normal movement on some of the fault planes is mostly related to overturned thrust planes. For this reason, the first plot should be interpreted with caution

N = 20 Lower Cretaceous *bedding = 161/ 80*

ANGELIER

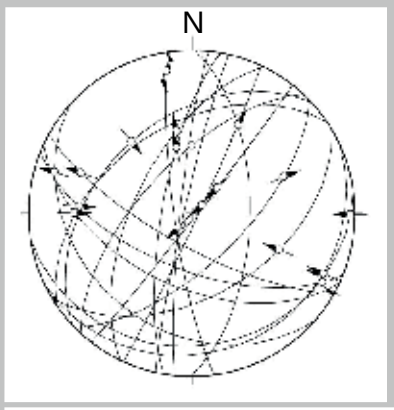

P-T

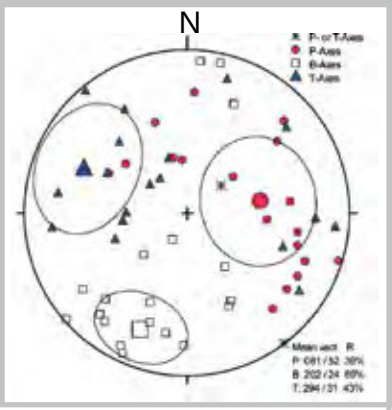

RIGHT DIHEDRA

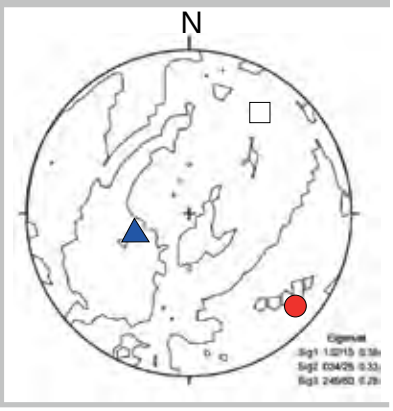

TENSOR

N = 9

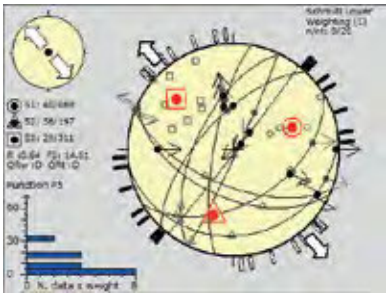

N = 8

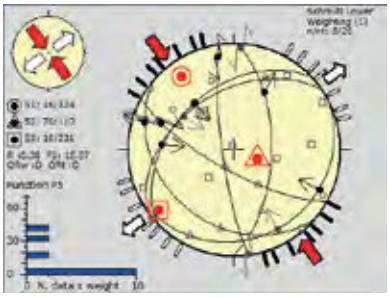

Stress field description

Paleostress analysis show that the Gros Haut Crêt area is affect-ed by an oblique extensional strike-slip system with the extensional stress axis trending towards NW-SE and a strike-slip system with the com-pressional stress axis oriented in NW-SE direction.

25 Long Sia *Préalpes Médianes Plastiques*

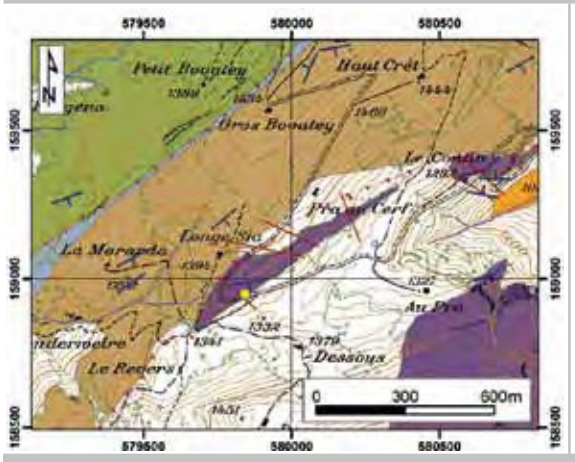

Outcrop description:

579841/ 158955 1390m

The outcrop along the road up to Gros Haut Crêt exposes in a curve a rather long outcrop of Lower Jurassic marly limestones which are highly fractured and show nicely developed slickenfibres. Most of the fractures are oriented towards NE-SW, parallel to the fold axis.

N = 14 Lower Cretaceous *bedding = 140/ 85*

ANGELIER

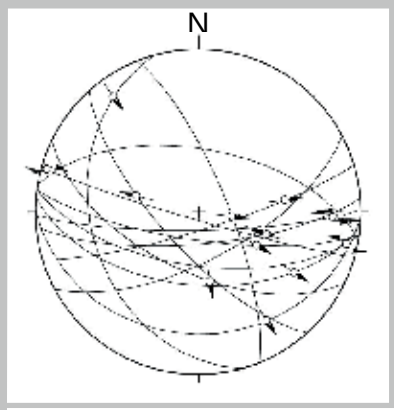

P-T

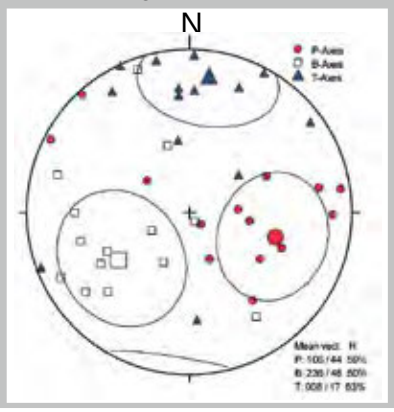

RIGHT DIHEDRA

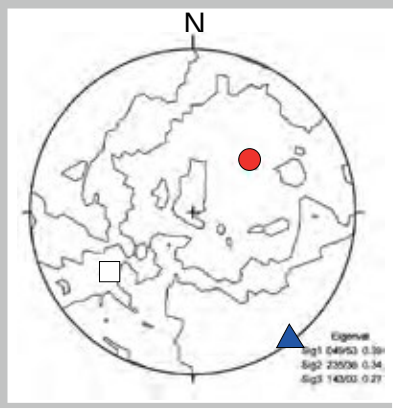

TENSOR

N = 9

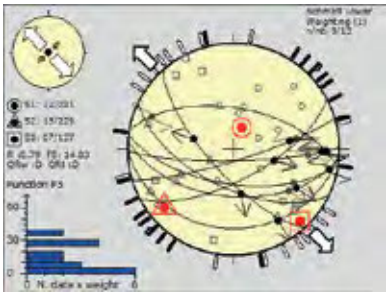

Stress field description

Data selection and evaluation revealed a purely extensional stress system with the extensional stress axis oriented towards NW-SE. This stress regime agrees with the surrounding stress results and is probably related to the folding as the extension direction perpendicular to the fold axis shows.

26 Le Contin *Préalpes Médianes Plastiques*

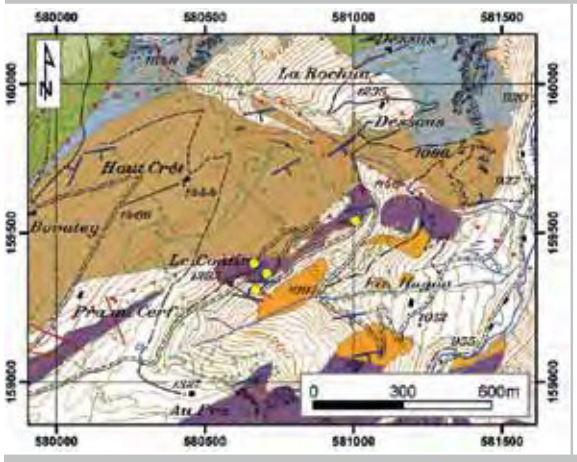

Outcrop description:

580719/ 159382 1250m

The plots gather two outcrops: one in Triassic rocks near the centre of the anticline and another in Lower Jurassic rocks. The fractures are highly influenced by the vicinity to the centre of the anticline. Therefore, the extensional axis in plot 1 is perpendicular to the fold axis. In addition, strike-slip faults are common, mostly oriented NNE-SSW with a sinistral shear sense. Veins are frequent but chaotically distributed.

N = 26 *Lower Jurassic/ Triassic* *bedding = 001/55*

ANGELIER

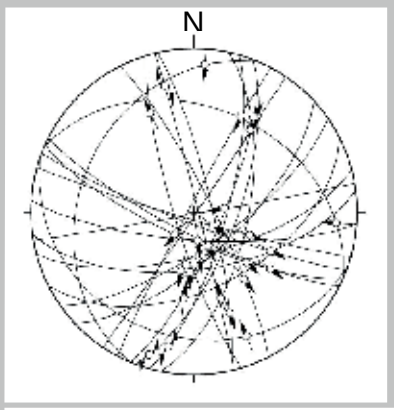

P-T

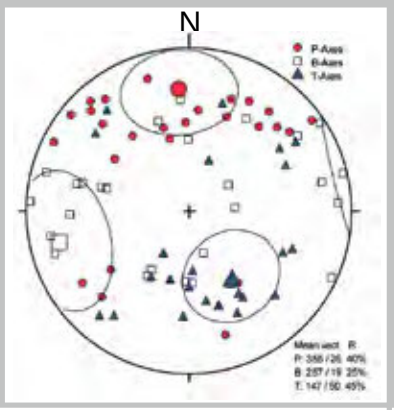

RIGHT DIHEDRA

TENSOR

N = 9

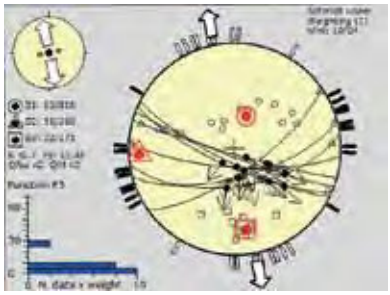

N = 8

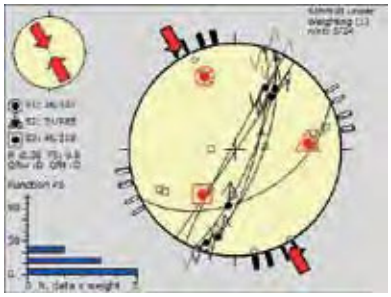

Stress field description

The vicinity to the core of the anticline influences highly the local stress regime. Either a purely extensional or a purely compressional regime are predominant in the Le Contin area, both oriented perpendicular to the fold axis in NW-SE direction.

27 La Rochua dessous 27 *Préalpes Médianes Plastiques*

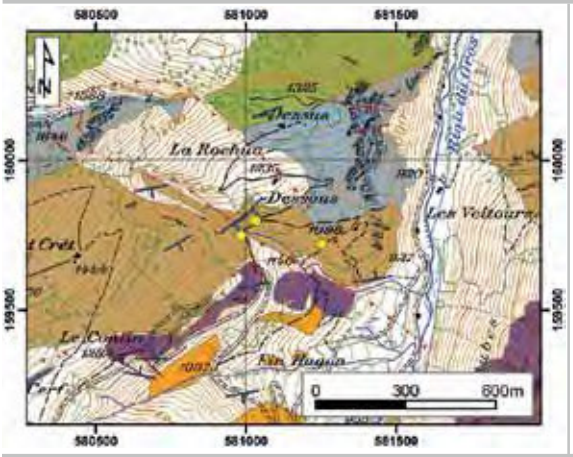

Outcrop description:

586708/ 167540 1200m

The road up to Unter Recardet exposes in a bend a Middle Jurassic limestone outcrop where the measurement of several slickenfibres was possible but it was only restricted to this place. Several calcite fibres were of lower quality due to weathering.

N =16 *Middle Jurassic* *bedding = 143/ 65*

ANGELIER

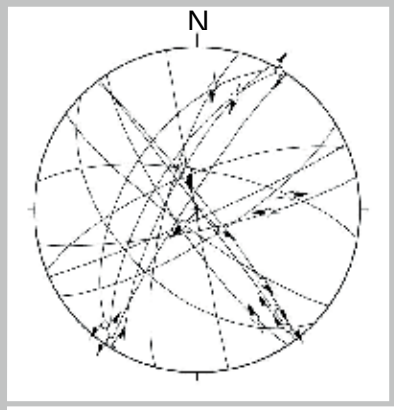

P-T

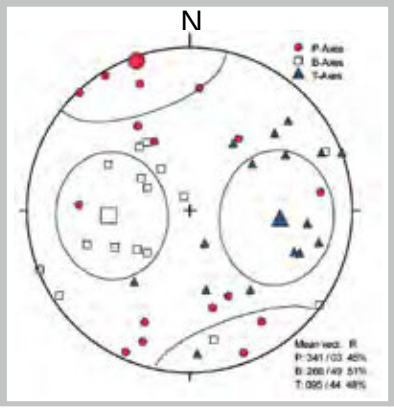

RIGHT DIHEDRA

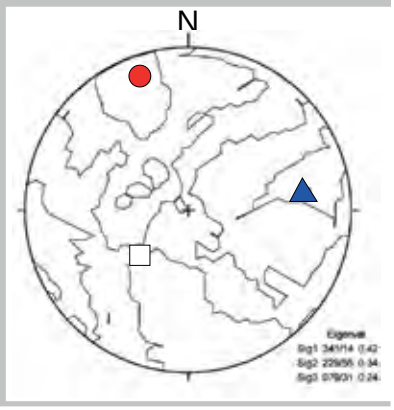

TENSOR

N = 10

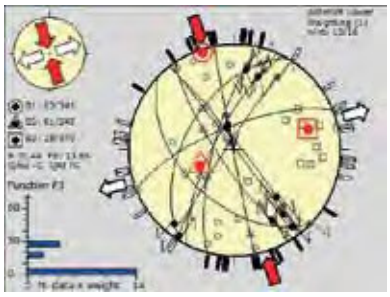

Stress field description

The general lateral ramp structure with a dextral strike-slip movement have an effect on the fault-slip dataset that represent a clear strike-slip system with a NW-SE oriented compressional stress axes.

28 La Morarda *Préalpes Médianes Plastiques*

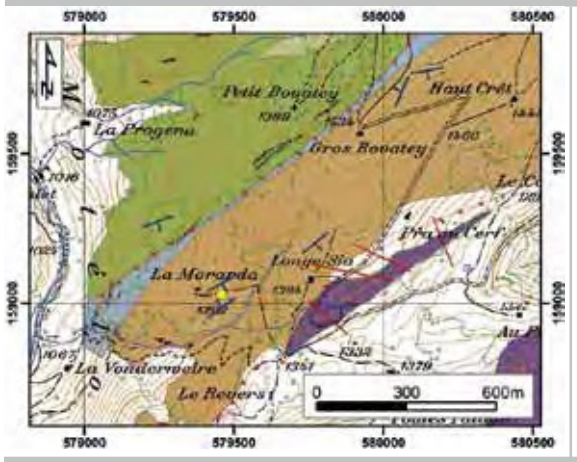

Outcrop description:

579453/ 159034 1300m

A rather chaotic accumulation of fractures was found at this Middle Jurassic outcrop at the way-side near the Morarda chalet. The quality of the slickenfibres is rather high, even with curved fibres at one place: they are oriented ENE-WSW and turn from an older reverse into a younger dextral strike-slip movement.

N = 22 *Middle Jurassic* *bedding = 324/ 86*

ANGELIER

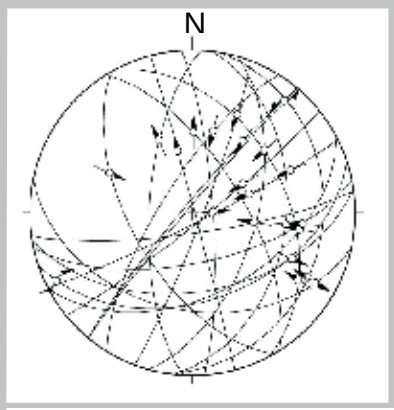

P-T

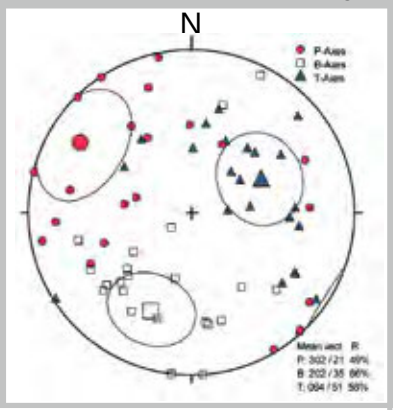

RIGHT DIHEDRA

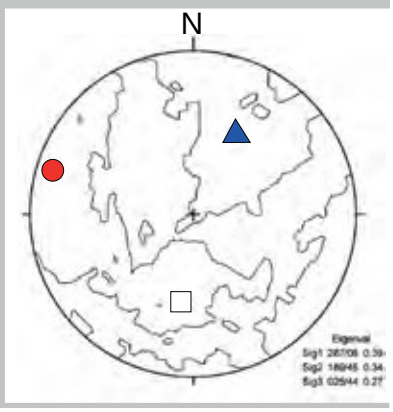

TENSOR

N = 10

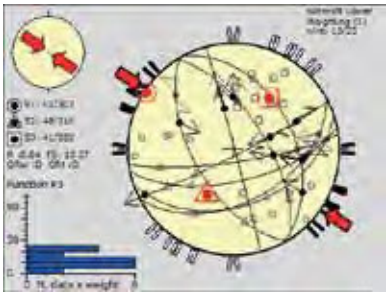

N = 6

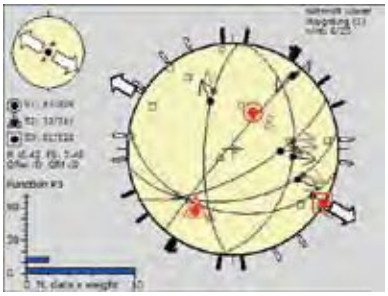

Stress field description

Paleostress analysis expose two different stress-slip regimes both most probably related to the folding process. Both, purely extensional and compressional show a NW-SE orientation for their most important stress axes.

29 ***Rouvenens devant*** *Préalpes Médianes Plastiques*

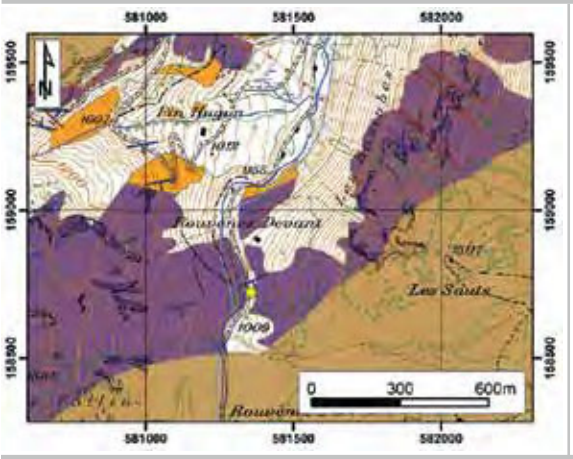

Outcrop description:

581354/ 158734 1000m

Along the road to Gros Mont, an outcrop of several meter length exposes fractures within Lower Jurassic limestones with slickenfibres of a rather good quality. Most of the fault planes are oriented in E-W direction and show a normal to oblique strike-slip movement with a dextral shear sense.

N = 22 *Lower Jurassic* *bedding = 159/65*

ANGELIER

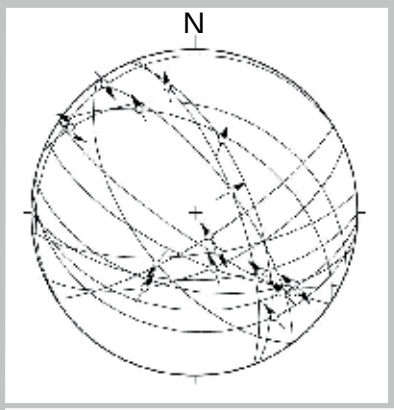

P-T

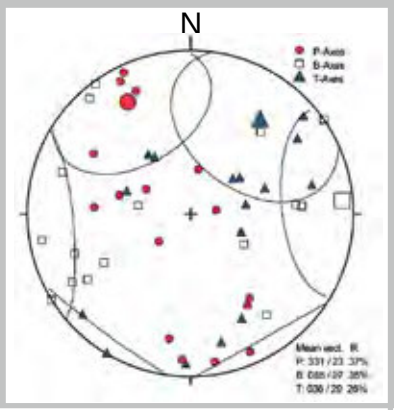

RIGHT DIHEDRA

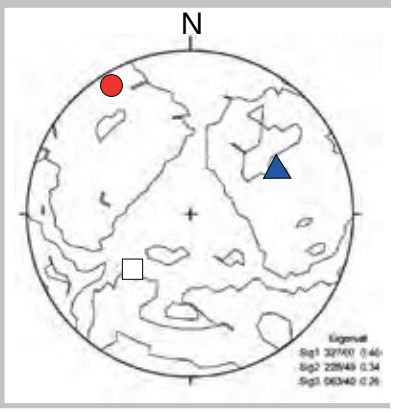

TENSOR

N = 10

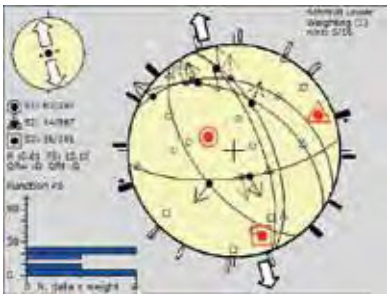

N = 6

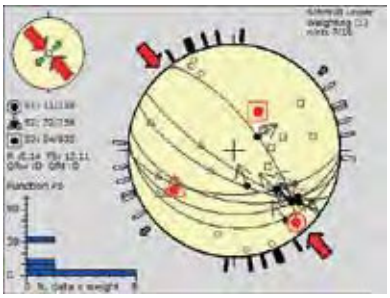

Stress field description

As already observed in the previous outcrops, the Rouvenens devant outcrop is governed by two stress regimes: a purely compressional stress regime with the compressional axis oriented towards NW-SE and an extensional stress regime with a NNW-SSE oriented extensional stress regime.

30 Dent de Broc — *Préalpes Médianes Plastiques*

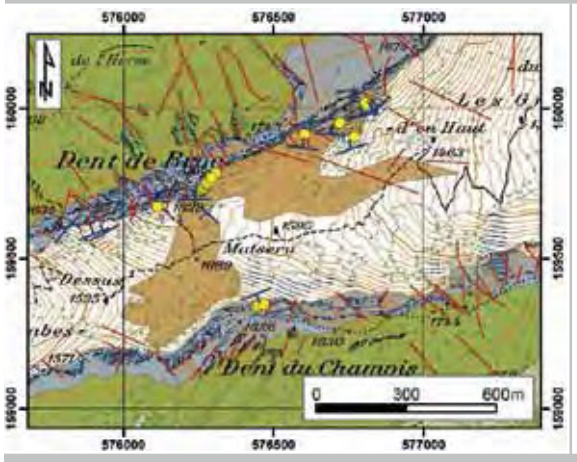

Outcrop description:

576280/ 159734 1710m

The Dent de Broc mountain range is highly frac-tured by large-scale normal faults, which are segmenting the entire synclinal fold structure. The outcrop lies on the north-eastern face of the Dent de Broc and contains mainly Middle and Upper Jurassic rocks. The data evaluation confirms a fold axis parallel extension as well as an extension perpen-dicular to the folding. Furthermore, vein orientations attest this extensional regime.

N = 21 *Middle/ Upper Jurassic* *bedding = 358/ 52*

ANGELIER

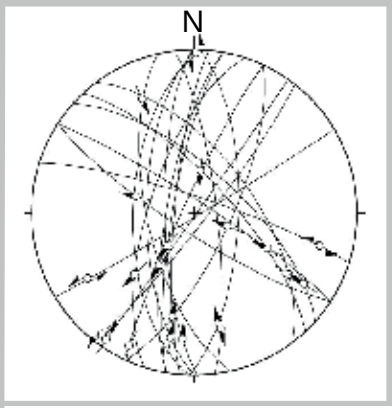

P-T

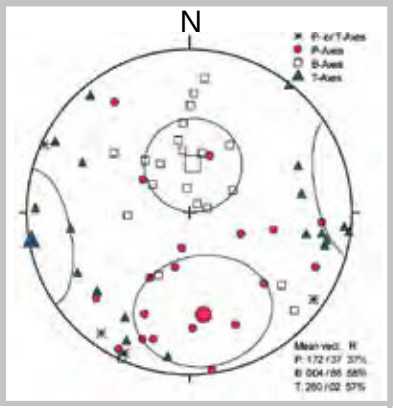

RIGHT DIHEDRA

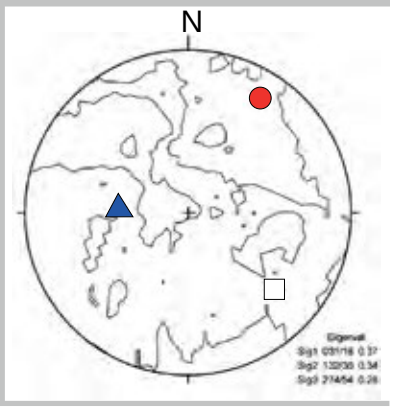

TENSOR

N = 6

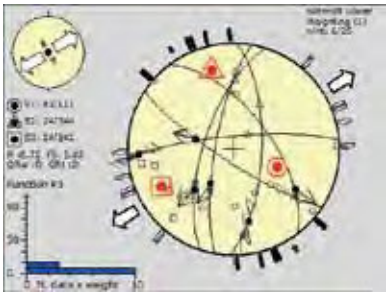

N = 7

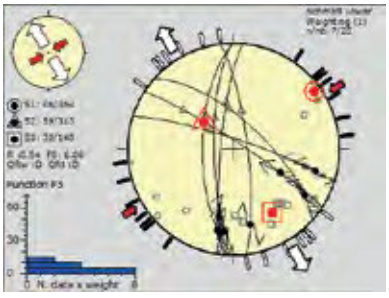

veins

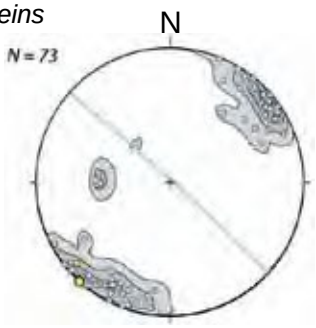

Stress field description

The Dent de Broc area is mainly dominated by an overall extensional stress regime, which is already ex-pressed in the morphology of the Dent de Broc mountain range. One of the stress regimes is oriented parallel to the fold axis with its extensional stress axis pointing towards NE-SW. The second stress system is a strike-slip stress regime with a much more pronounced extensional stress axis directing towards NW-SE. Vein observations proof a NE-SW oriented extension.

31 Petit Liençon — *Préalpes Médianes Plastiques*

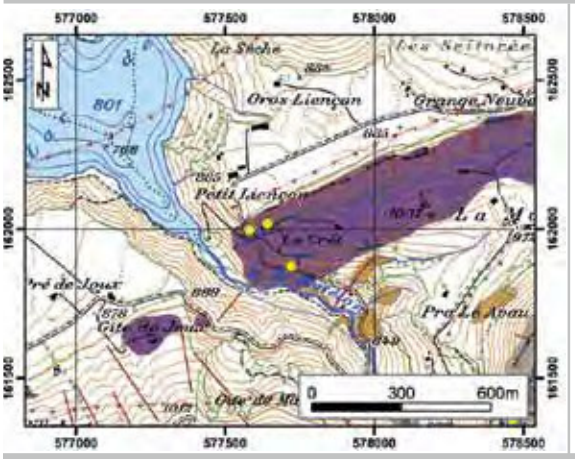

Outcrop description:

576339/ 159797 900m

A large outcrop lays along the road into the Mo-télon valley and exposes strongly fractured Lower Jurassic rocks with nicely preserved slickenfibres. The outcrop quality is high due to relatively fresh fracture planes because of road works.

N = 22 *Lower Jurassic* *bedding = 336/ 75*

ANGELIER

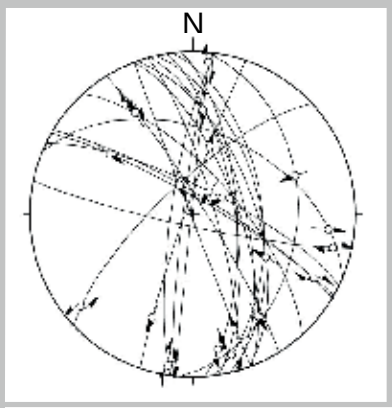

P-T

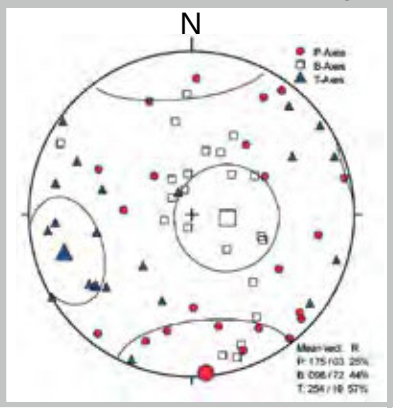

RIGHT DIHEDRA

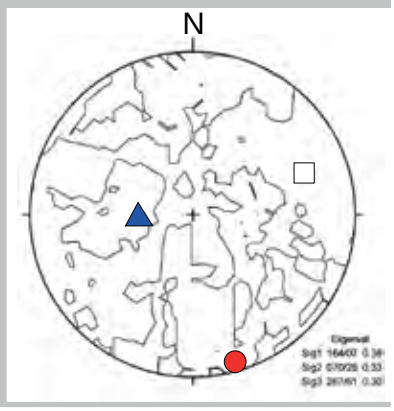

TENSOR

N = 10

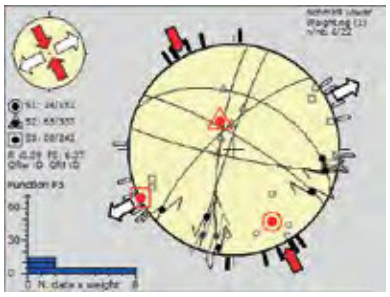

N = 6

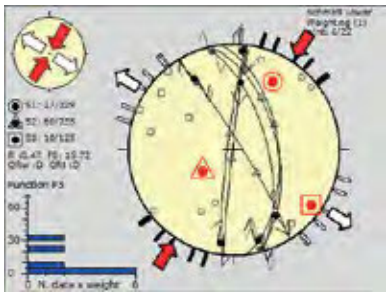

Stress field description

The Petit Liençon outcrop is influenced by an important thrust fault laying close by. This is nicely represented in the first TENSOR plot with a compressional stress system oriented towards NW-SE. Additionally, a strike-slip stress regime can be found with its compressional stress axes oriented NE-SW.

32 Vanil de la Monse — *Préalpes Médianes Plastiques*

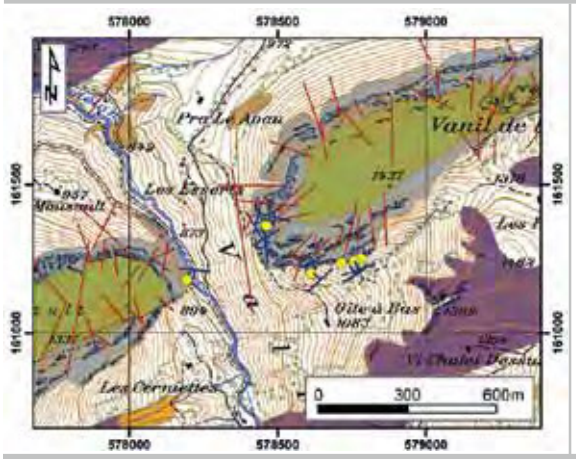

Outcrop description:

578190/ 161175 880m

The outcrops of the Vanil de la Monse and La Ruja where taken together as they are situated in more or less the same structural context. The observed fractures are oriented generally NW-SE and NNE-SSW and have either a dextral or a sinistral move-ment. The conditions of the fracture planes are mediocre due to weathering.

N = 19 *Upper Jurassic* *bedding = 318/ 81*

ANGELIER

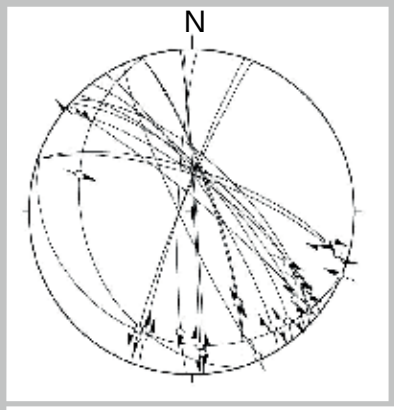

P-T

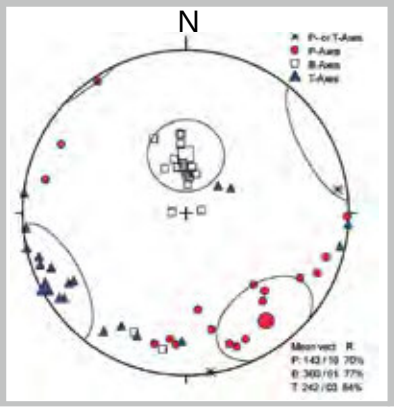

RIGHT DIHEDRA

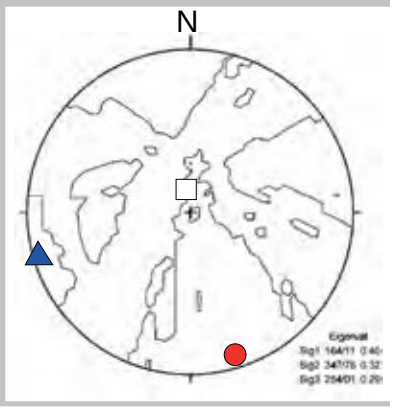

TENSOR

N = 10

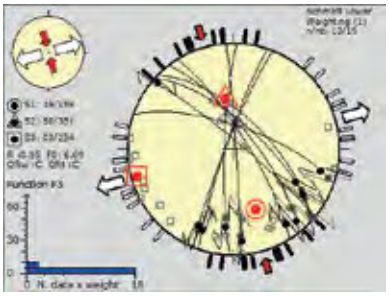

Stress field description

A strike-slip stress regime with a dominating extensional component is exposed at the Vanil de la Monse outcrop. The extensional stress axis is oriented in the same direction than the fold axis towards NE-SW.

33 ***Motélon*** *Préalpes Médianes Plastiques*

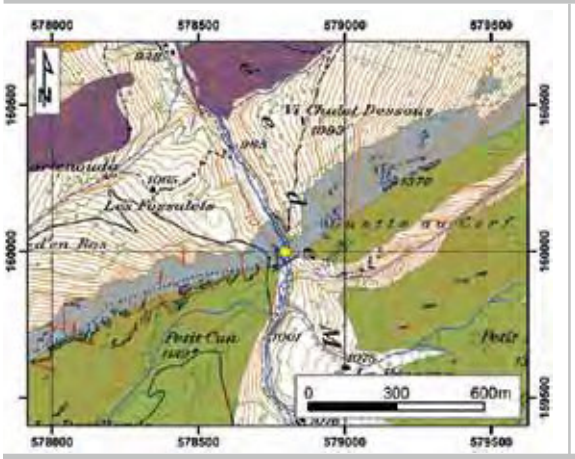

Outcrop description:

578783/ 159983 980m

The measured fractures were found at a restricted outcrop along the path going up to the Dent de Broc. Most of the fractures are oriented NNW-SSE and well-developed slick-enfibres are rare, because of the vegetation overgrowing the Upper Jurassic limestones.

N = 8 *Upper Jurassic* *bedding = 328/ 86*

ANGELIER

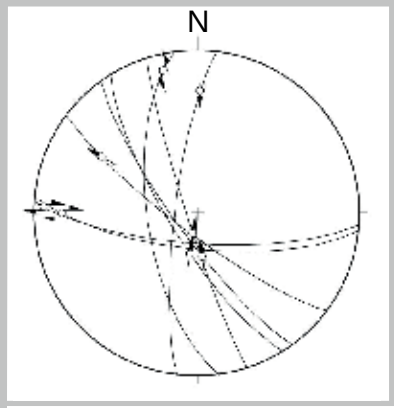

P-T

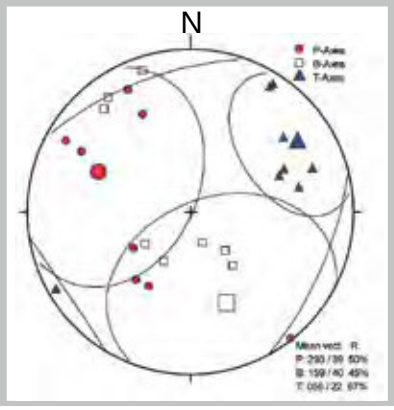

RIGHT DIHEDRA

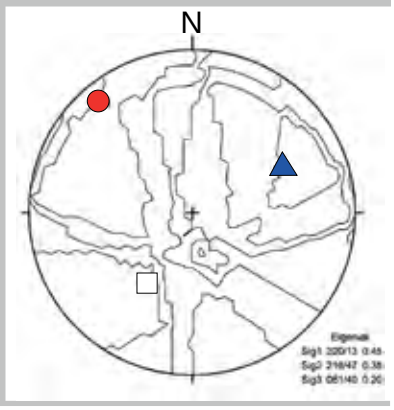

TENSOR

N = 6

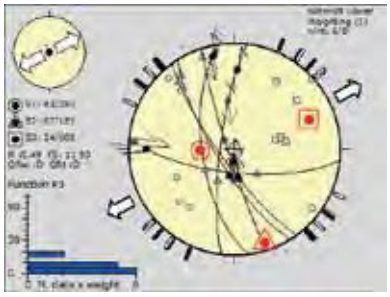

Stress field description

The few fault-slip data remaining represent an extensional stress regime oriented towards NE-SW, parallel to the fold axes direction.

34 **Gorge de la Jogne** *Préalpes Médianes Plastiques*

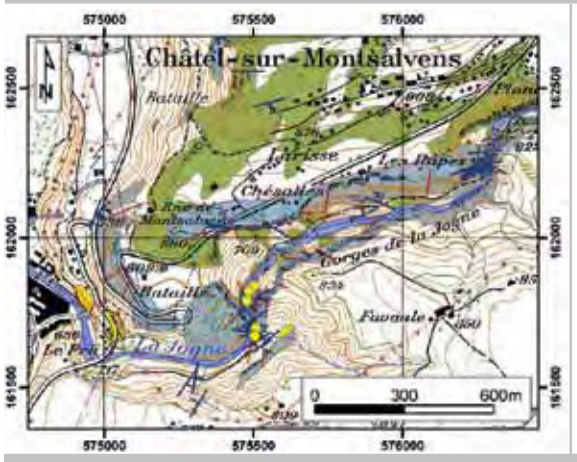

Outcrop description:

575498/ 161854 830m

The Ultrahelvetic Upper Limestones in the Gorge de la Jogne area are nicely exposed and allow measurements of well-developed slickenfibres. Crosscutting striae show older normal faults over-printed by younger strike-slip faults.

N = 36 Upper Jurassic *bedding = 320/ 85*

ANGELIER

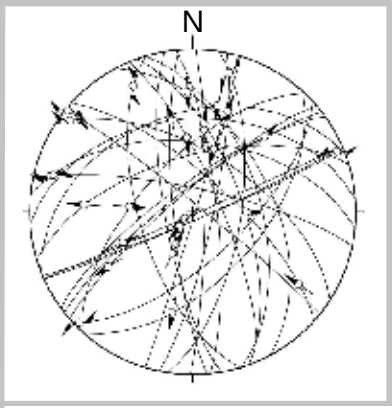

P-T

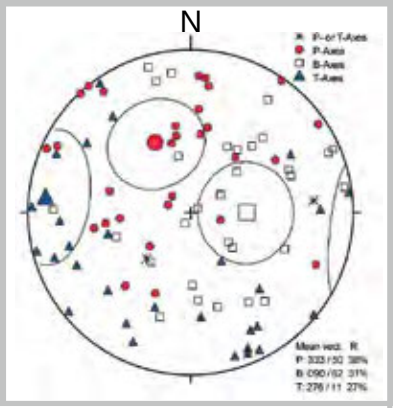

RIGHT DIHEDRA

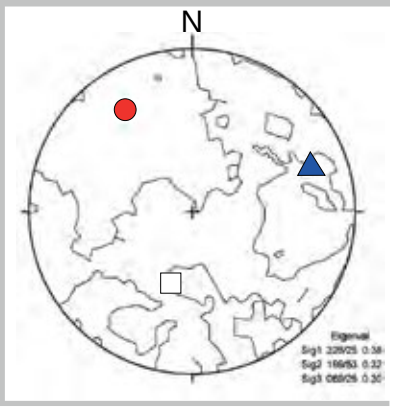

TENSOR

N = 11

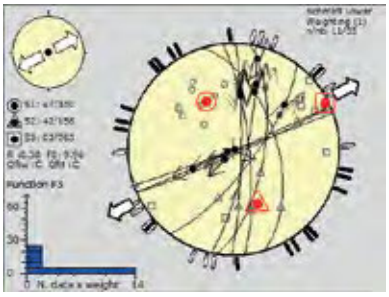

N = 9

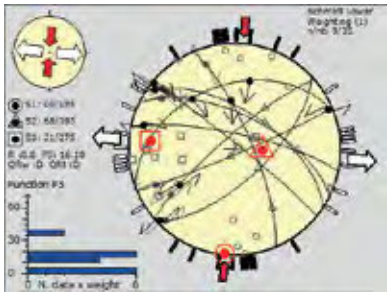

Stress field description

Throughout the data separation process several data were rejected, the remaining fault slip data reveal two stress regime. An extensional stress regime oriented towards NE-SW of a rather good quality (quality ranking “C”)= and a strike-slip stress regime with a N-S oriented compressional stress axis.

35 Châtel sur Montsalvens *Ultrahelvetic*

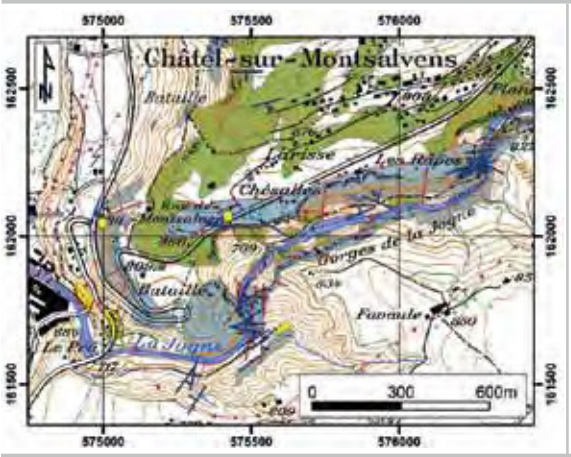

Outcrop description:

575418/ 162067 860m

The measurements of two restricted localities were evaluated together. The fracture orientation shows a predominant WNW-ESE orientation of strike-slip faults with well-preserved slickenfibres on them. One of the outcrops lies directly next to an im-portant thrust, which is striking WNW-ESE towards the same direction as most of the fractures with a dextral shear sense.

N = 24 *Upper Jurassic* *bedding = 340/ 39*

ANGELIER

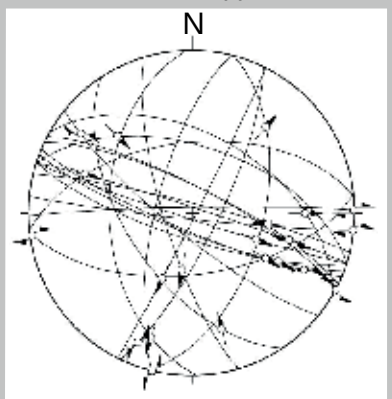

P-T

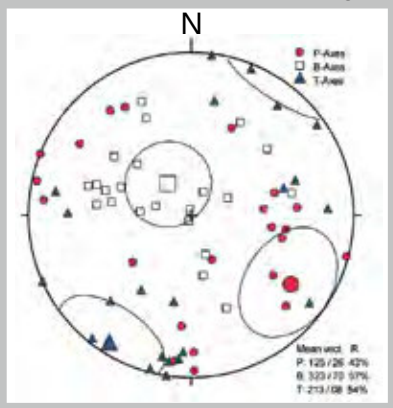

RIGHT DIHEDRA

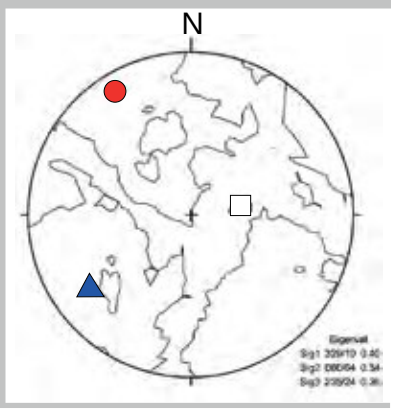

TENSOR

N = 12

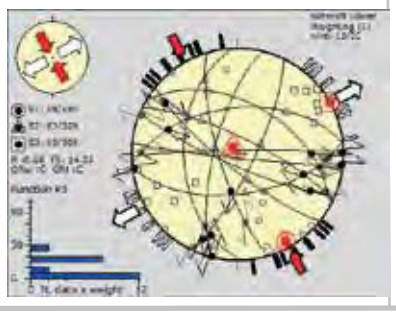

N = 8

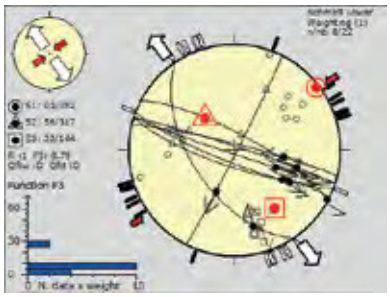

Stress field description

The Châtel sur Montsalvans area is governed by two strike-slip stress regime, the predominant one with the compressional stress axes oriented towards NNW-SSE, and a secondary one oriented NE-SW, with a more pronounced extensional component.

36 Cerniat — *Ultrahelvetic*

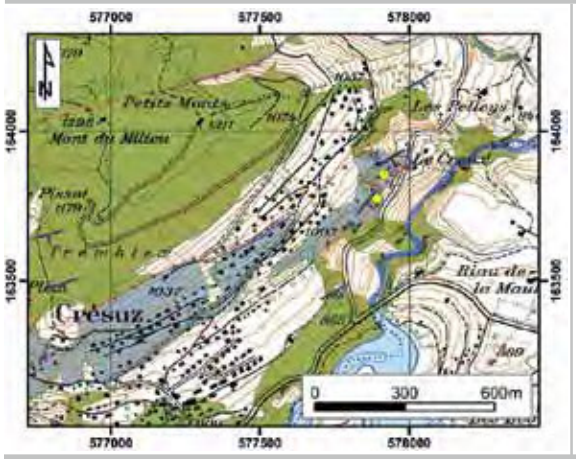

Outcrop description:

577913/ 163858 1020m

The measurements were taken in an ancient quarry. The outcrop orientation is situated bedding parallel so only a few fractures planes were exposed at the border of the quarry. The majority of the fractures show a dextral sense of shear but also normal faults are frequent.

N = 18 Upper Jurassic — *bedding = 148/ 69*

ANGELIER

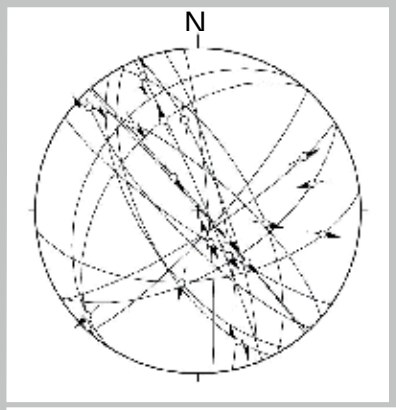

P-T

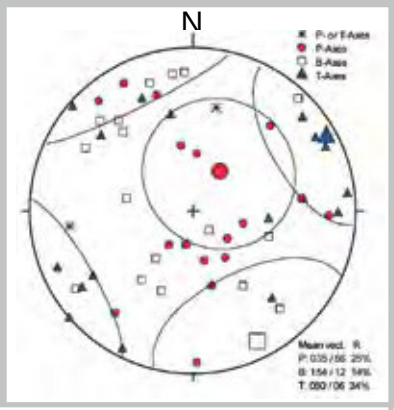

RIGHT DIHEDRA

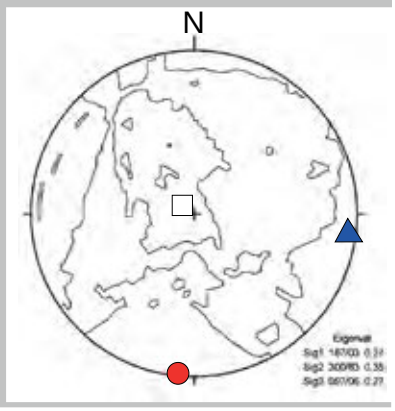

TENSOR

N = 8

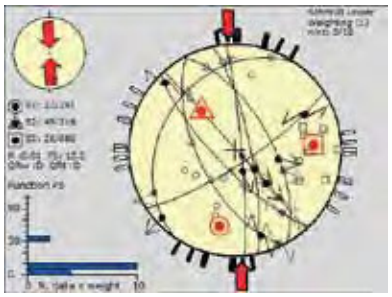

N = 7

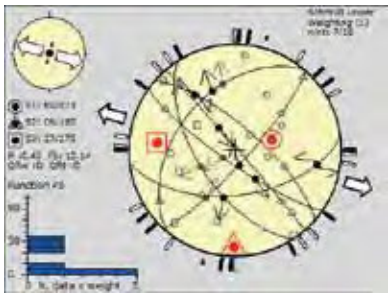

Stress field description

The vicinity of an important thrust fault influences the resulting stress evaluation as seen in the first TENSOR plot with a N-S oriented compressional regime. The second plot represents an exten-sional stress regime with and overall extension direction to-wards WNW-ESE.

37 ***Petit Mont Weidli*** *Préalpes Médianes Plastiques*

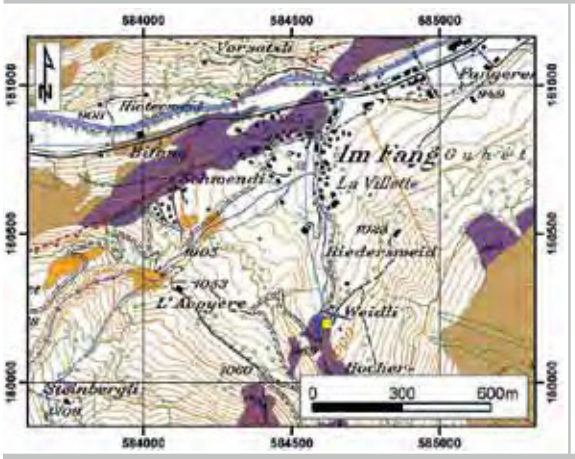

Outcrop description:

584609/ 160199 950m

Along the road up to the Petit Mont, several fractures were exposed in Lower Jurassic marly lime-stones. Despite the high amount of vegetation and the humidity at this outcrop, the slickenfibres were preserved rather well. Most of the fractures are either N-S oriented with a dextral shear sense or distributed with various orientations and a reverse movement direction.

N = 22 *Lower Jurassic* *bedding = 196/ 70*

ANGELIER

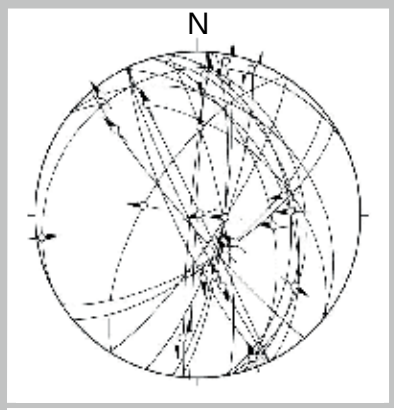

P-T

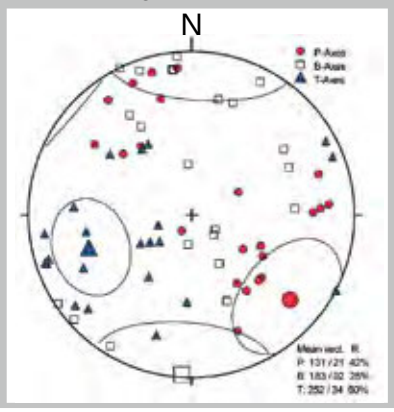

RIGHT DIHEDRA

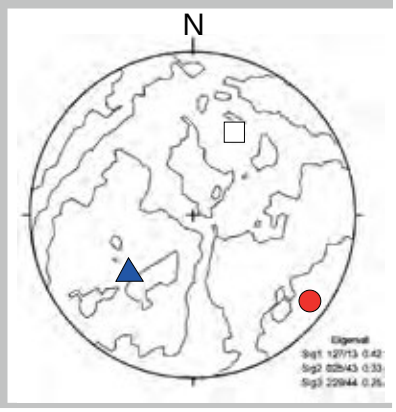

TENSOR

N = 10

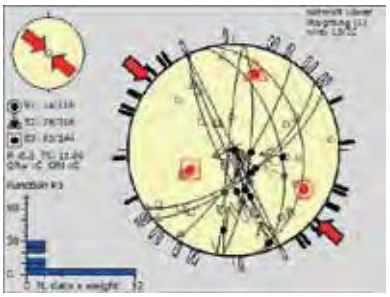

Stress field description

Throughout the data sorting process, more than half of the data were rejected. The remaining fault-slip data represent an compressional NW-SE oriented stress regime.

38 Petit Mont Ratzewald *Préalpes Médianes Plastiques*

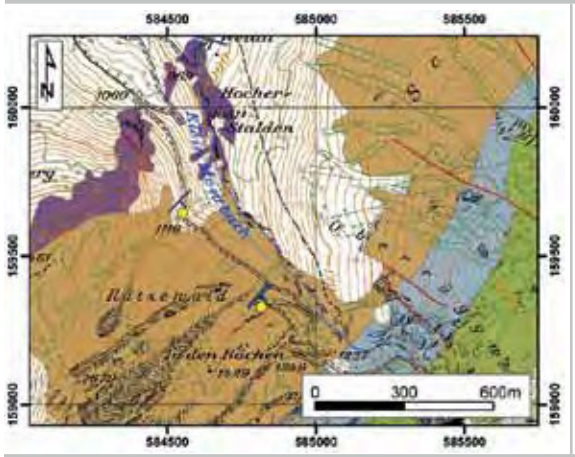

Outcrop description:

584799/ 159330 1120m

The outcrop is dominated by massive limestone bands interrupted with marly interlayers, which are affected by stronger deformation expressed by several shear bands. Veins are distributed all over the outcrop area. Generally, they show the follow-ing chronology: older horizontal veins are cut by younger vertical veins with a NW-SE orientation

ANGELIER

N = 33 Middle Jurassic

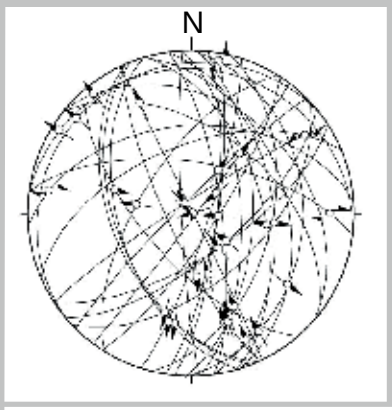

P-T

bedding = 127/ 84

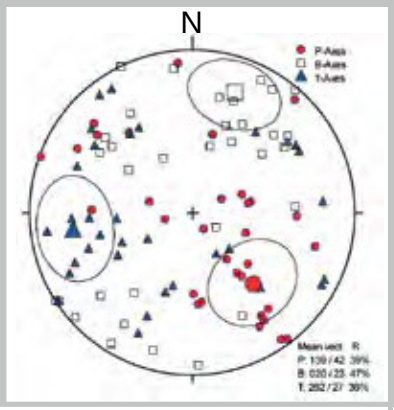

RIGHT DIHEDRA

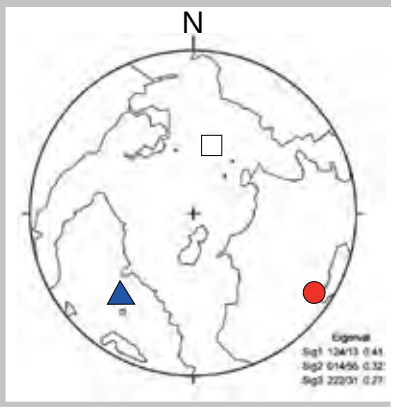

TENSOR

N = 10

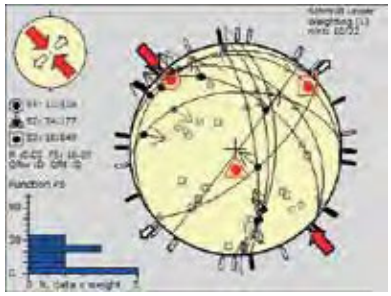

N = 9

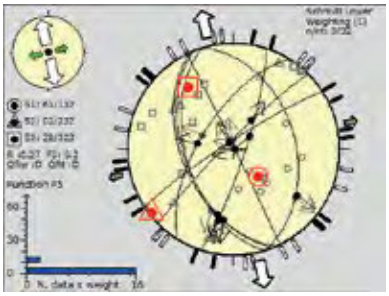

Veins

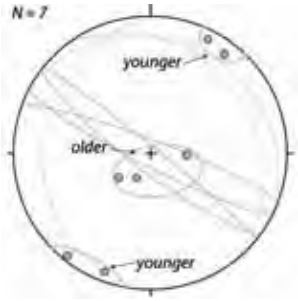

Stress field description

The dominating stress regime expresses a strike-slip system with a more pronounced NW-SE compressional component. The extensional stress axis coincides with the overall extension direction of the youngest vein family, which are nearly vertical and oriented NW-SE. A secondary stress regime is purely extensional in direction NNW-SSE. Vein measurements witness a vertical extension direction that could not be observed in the field-data, but is most probably related to the folding and the thrusting process of the Préalpes Médianes Plastiques.

39 ***Petit Mont Schänis*** *Préalpes Médianes Plastiques*

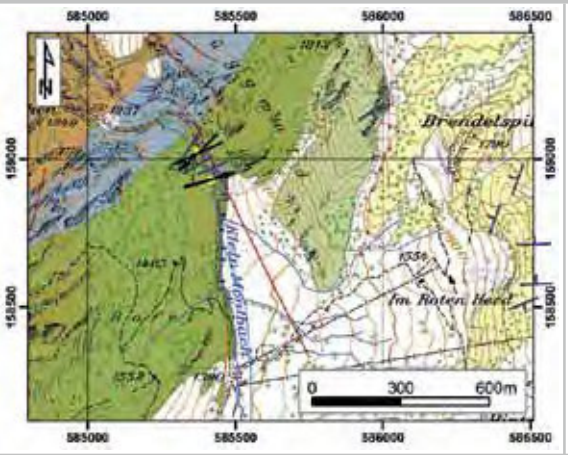

Outcrop description:

585379/ 159037 1330m

The outcrop along the road exposes the strongly folded Lower Cretaceous limestones. Fold axes of the small-scale folds trend generally towards NE-SW and are often cut by minor thrusts to compen-sate the compression. The meas-ured fractures are mainly oriented towards NW-SE and show a dextral strike-slip movement. Veins are frequent with younger NW-SE oriented veins crosscutting older horizontal veins.

N = 36 *Lower Cretaceous* *bedding = 152/ 41*

ANGELIER

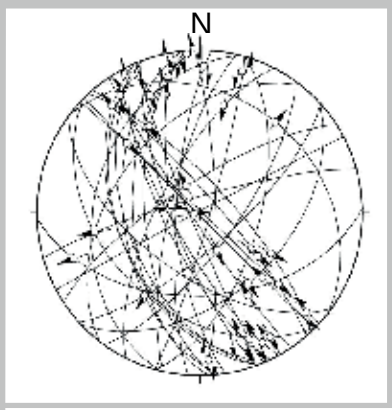

P-T

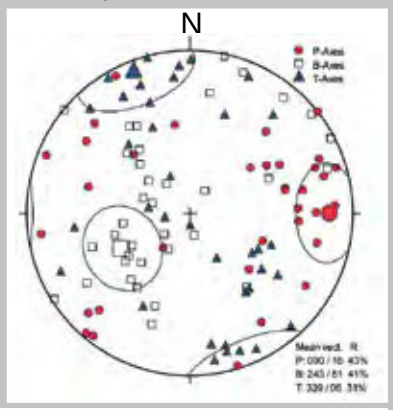

RIGHT DIHEDRA

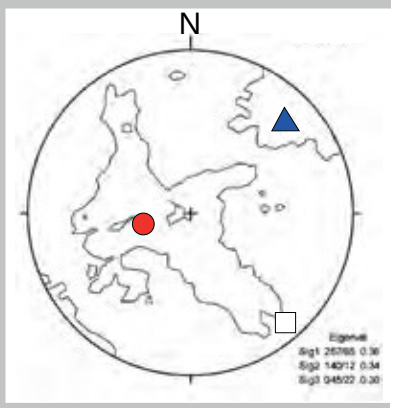

TENSOR

N = 16

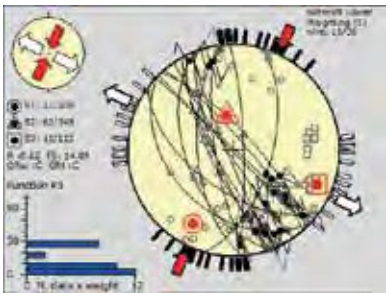

N = 8

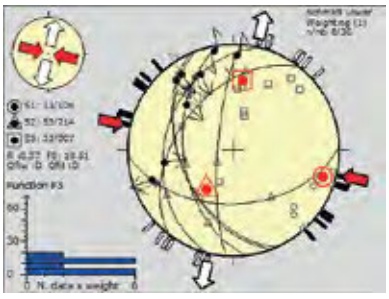

VEINS

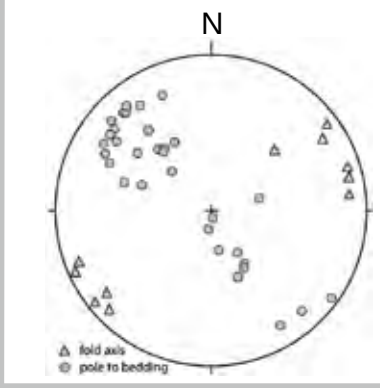

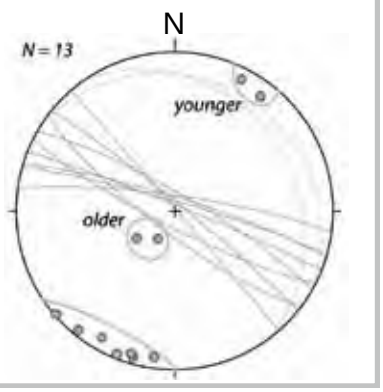

Stress field description

The heterogeneous fault-slip da-taset was subdivided into two different strike-slip stress regimes: major one with the compressional stress axis oriented towards NNE-SSW and the less abundant one with WNW-ESE trending compres-sional stress axis. The chronology observed by measuring veins showed the well-known youngest extensional event towards NNE-SSW, which would agree with the second stress regime.

40 Gastlosen — *Préalpes Médianes Gastlosen imbricate*

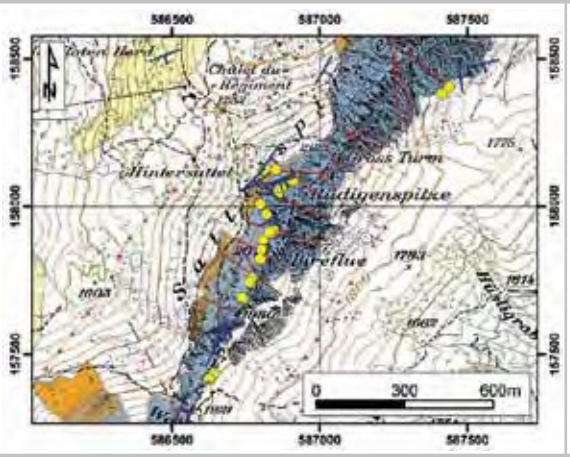

Outcrop description:

586810/ 158120 1820m

Along the steep cliff of the Gastlosen range, several fractures were measured. Most of them are oriented NNW-SSE and a little less frequently NW-SE with an either sinistral or dextral sense of shear. Most of the fractures planes have lost their shear sense indicator due to karstification of the surfaces, but some of them remained and show now a clear strike-slip regime. Veins were frequent, but did not show a clear chronology.

N = 22 Upper Jurassic — *bedding = 162/ 62*

ANGELIER

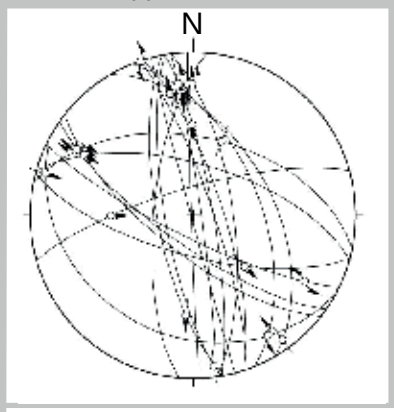

P-T

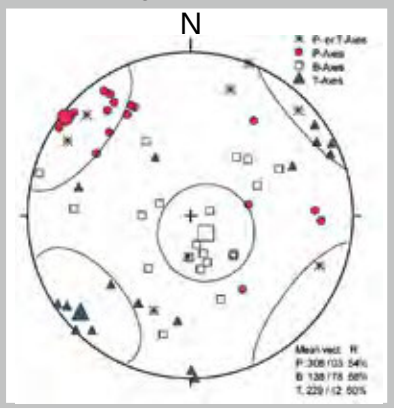

RIGHT DIHEDRA

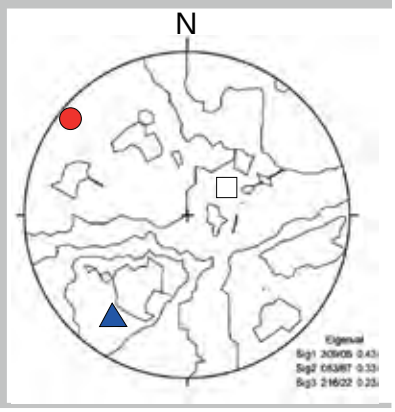

TENSOR

N = 14

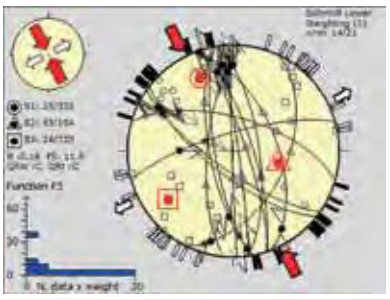

Stress field description

As already seen in the morphology, the Gastlosen range is highly influenced by large-scale strike-slip faults. Evaluating the fault-slip data-set reveals a strike-slip regime with its compressional stress axis oriented towards NW-SE and agrees therefore with the field observation.

41 **Rocher des Rayes** *Préalpes Médianes Gastlosen imbricate*

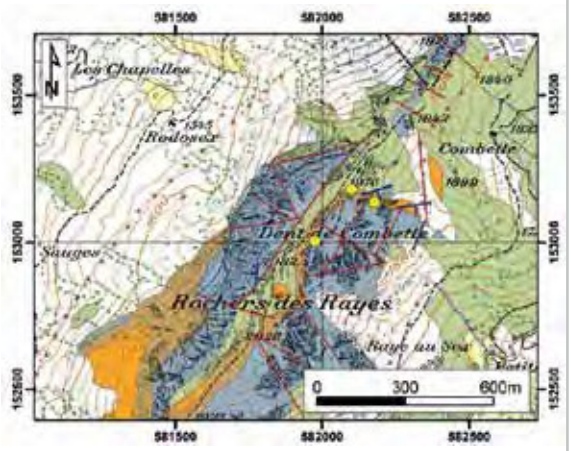

Outcrop description:

582099/ 153180 1910m

Several small-scale outcrops were taken together for this evaluation. Most of the measurements were collected in the Middle Jurassic limestones at the base of the rock face of the Dent de Combettes. The dominant fracture orientation is NNE-SSW and NW-SE with an either sinistral or dextral movement.

The general structure of this area is mostly dominated by large-scale thrust faults forming the Rocher de Rayes imbricate. Fault slip data show no evidence for thrusting, but shear bands along the cliff witness thrusting movement towards NW-SE. Furthermore, the Rocher des Rayes mountains are pre-fractured by large normal faults probably related to former paleofaults.

N = 20 Middle Jurassic bedding = 161/ 47

ANGELIER

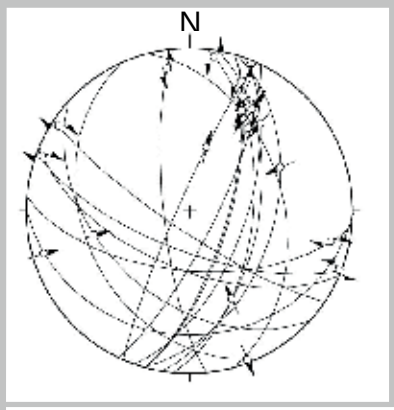

P-T

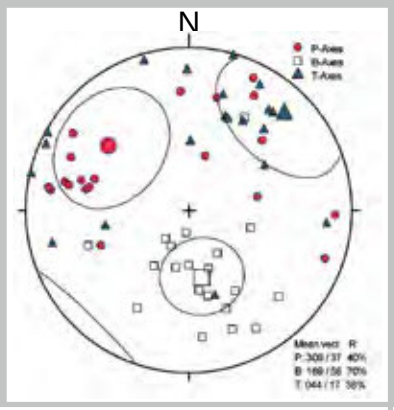

RIGHT DIHEDRA

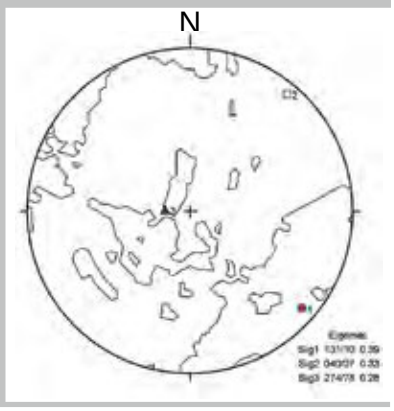

TENSOR

N = 7

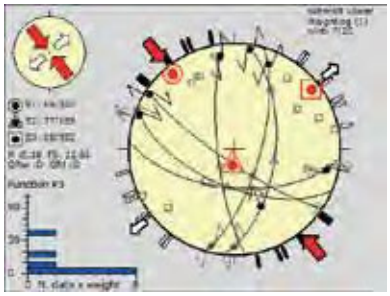

N = 8

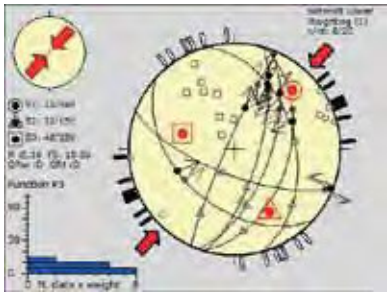

Stress field description

The Rocher des Rayes area is clearly affected by a strike-slip stress regime with its compressional axis oriented towards NW-SE. The secondary plot reveals also a compressional stress re-gime, which is surprisingly orient-ed towards NE-SW and not as expected towards NW-SE.

BRITTLE SHEAR BAND

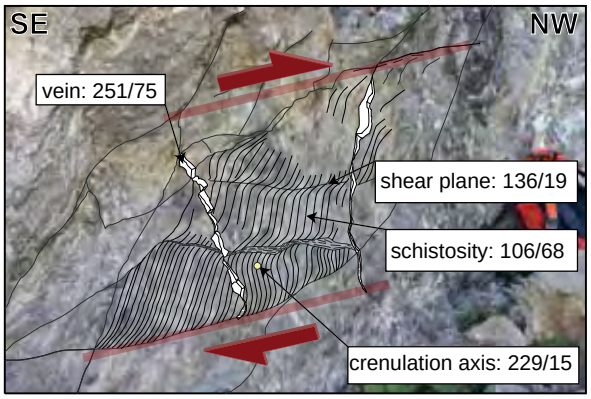

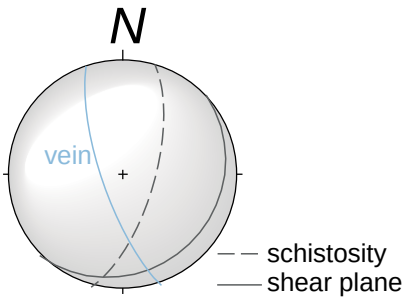

42 La Roche sur le Bey *Subalpine Molasse*

Outcrop description:

576900/ 171215 820m

The road up to the La Berra Ski region exposes a rather large outcrop of Subalpine Molasse. The quality of the calcite fibres in these sandstones is minor compared to the previous slickenfibres found in the préalpine limestones. Nevertheless, a considerable amount of data was collected due to the good outcrop conditions. NE-SW oriented reverse fault occur predominantly but also strike-slip faults appear frequently.

N = 29 Oligocene *bedding = 146/ 35*

ANGELIER

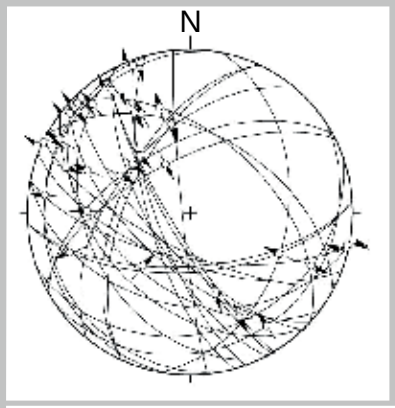

P-T

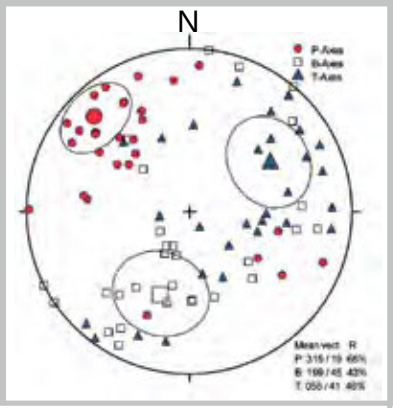

RIGHT DIHEDRA

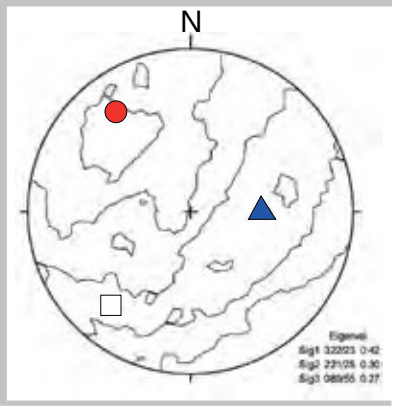

TENSOR

N = 12

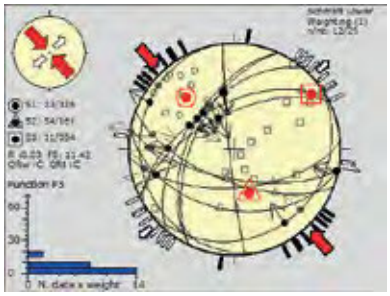

N = 7

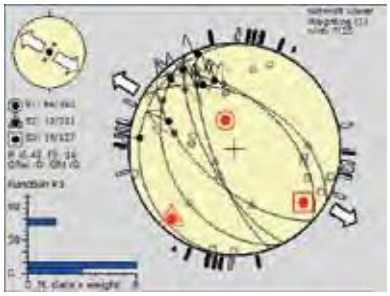

veins

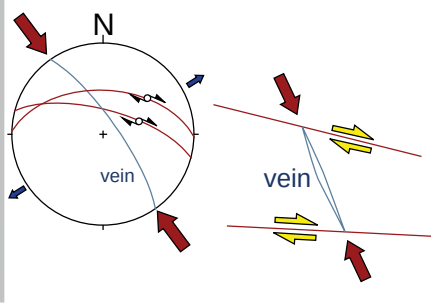

Stress field description

Despite showing a general NW-SE trend for the compressional stress axis, the entire dataset could be subdivided into two different stress regimes, a NW-SE orientated compressional strike-slip system, and a NW-SE orientated extensional stress regime.

43 ***Ruisseau du Stoutz*** *Subalpine Molasse*

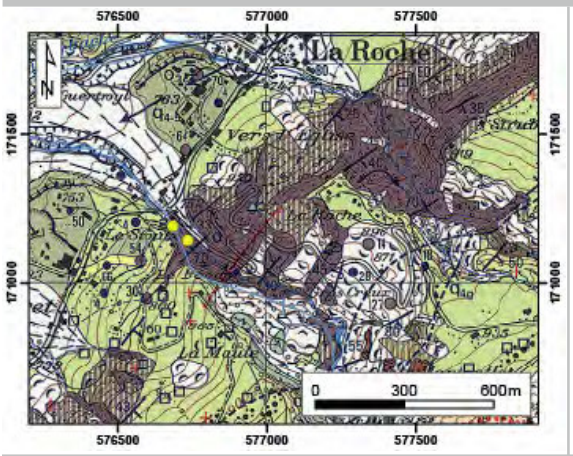

Outcrop description:

576727/ 171140 760m

Molasse sandstones were cropping out along the Stoutz brook and expose randomly distributed fractures with a prevailing N-S direction for sinistral strike-slip faults and a NE-SE orientation for reverse faults. Some of the measured slickenfibres are extremely well preserved and witness sometimes different movement events by a crosscutting relationship or curved calcite fibres.

N = 30 Oligocene *bedding = 149/ 51*

ANGELIER

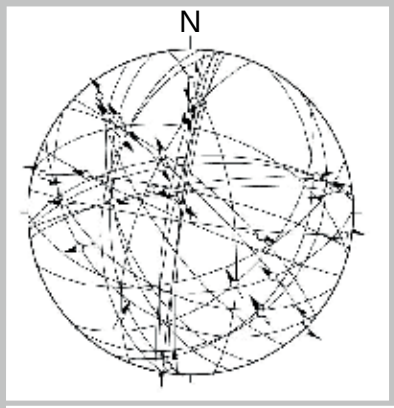

P-T

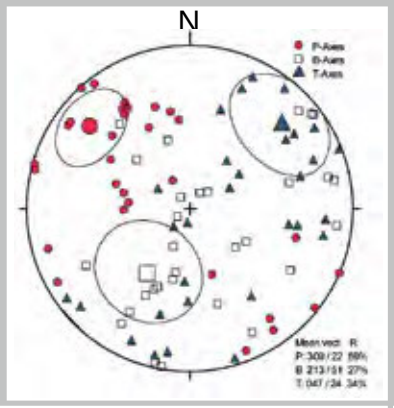

RIGHT DIHEDRA

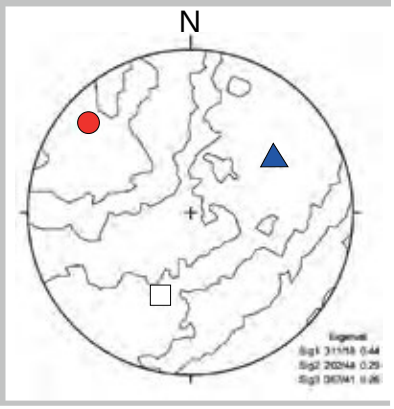

TENSOR

N = 11

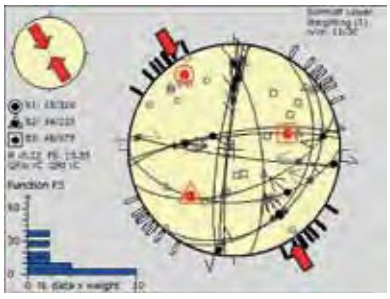

N = 7

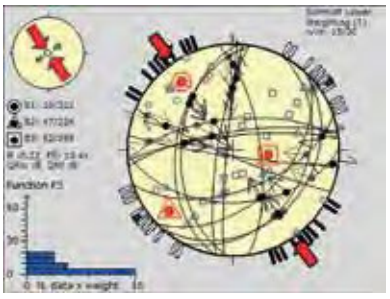

Stress field description

NE-SW oriented thrusts with a top to the NW moving direction, as well as NW-SE and WMW-ESE oriented strike-slip faults work under a NW-SE oriented stress regime. A secondary NNE-SSW oriented extensional stress regime can be ascribed to presence of normal faults in NE-SW direction. Superposing veins expose two deformational stages: an older oblique dextral (1) and younger oblique sinistral (2) one, fitting into the first, respectively into the second stress regime and showing therefore a possible chronology of the stress regimes: the secondary stress regime corresponds to an older, whereas the prevailing stress regime represents a younger deformational phase.

VEINS

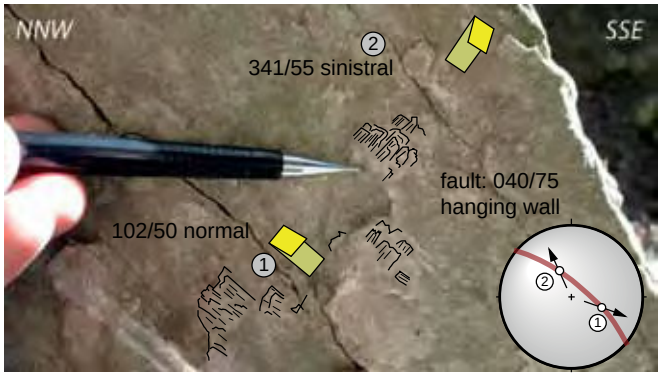

44 ***Ruisseau du Bey*** *Subalpine Molasse*

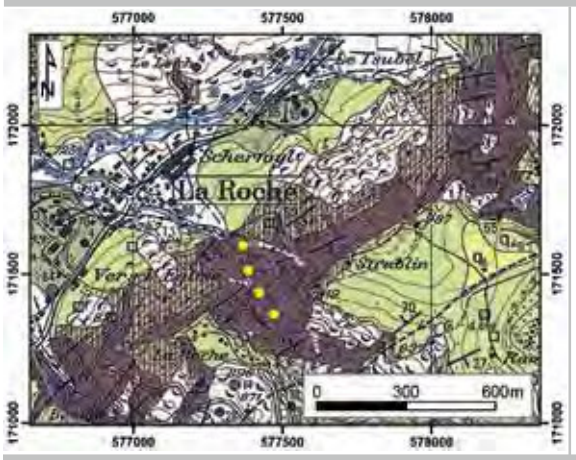

Outcrop description:

577355/ 171618 780m

The outcrop lays along the Bey brook and shows highly fractured Molassic sandstones with an overall trend in direction NE-SW for the reverse faults coinciding with the overall structural context of the Subalpine Molasse thrust slices. At this as well, curved veins affirm changes in de- formational history. The observed striae turn from a dextral strike-slip into a reverse movement.

N = 27 Oligocene *bedding = 149/ 44*

ANGELIER

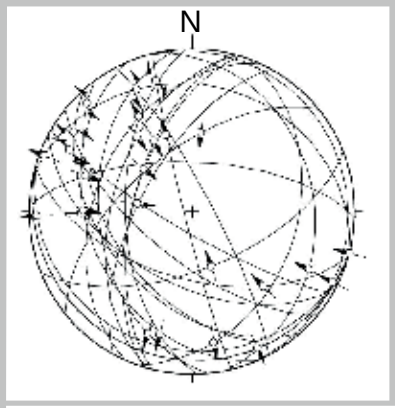

P-T

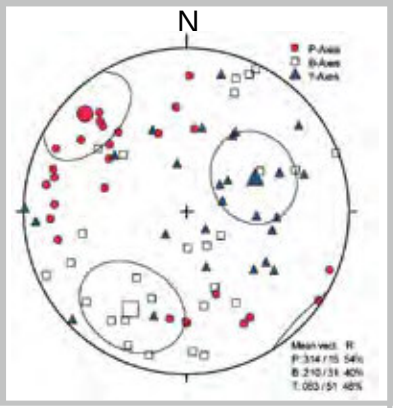

RIGHT DIHEDRA

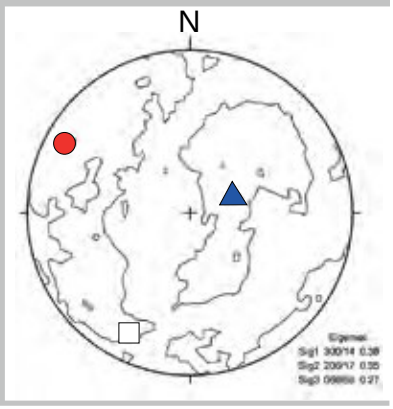

TENSOR

N = 12

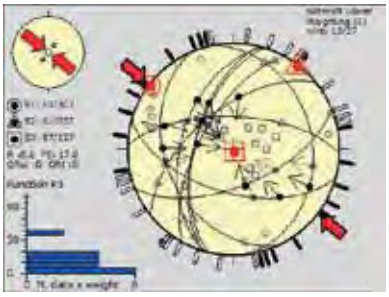

N = 8

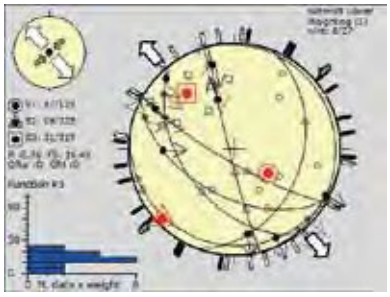

Stress field description

NW-SE oriented thrust faults show mostly a top to the SE movement, and only a few thrust display a NW oriented moving direction. These thrust faults were clearly generated under a NW-SE oriented compressional stress regime. Sinistral oblique strike-slip faults, as well as normal faults were attributed to a NW-SE orientated extensional stress regime.

45 ***Ruisseau du Hap*** *Subalpine Molasse*

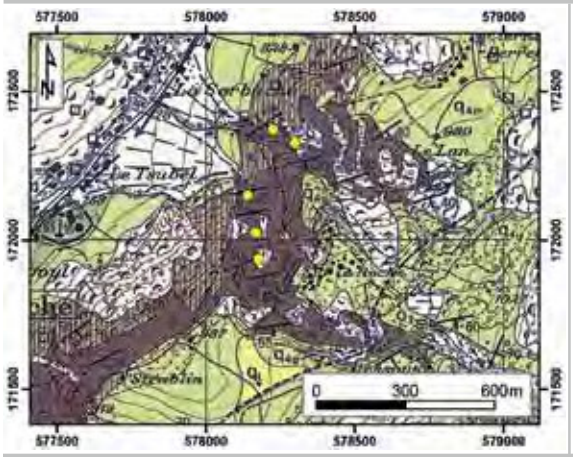

Outcrop description:

578246/ 172364 820m

The outcrop exposed by the Hap brook resembles the previous Subalpine Molasse outcrop, but it fractures with slicken-fibres are less frequent and the outcrop length is rather small. Sinistral strike-slip faults are most abundant at this outcrop.

N = 14 *Oligocene* *bedding = 108/ 54*

ANGELIER

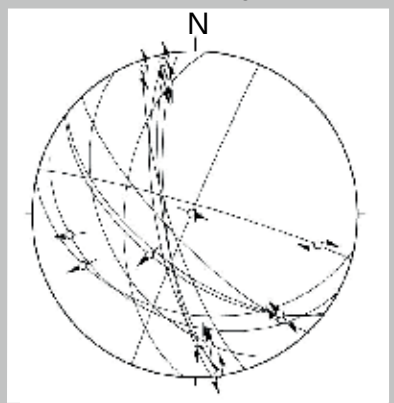

P-T

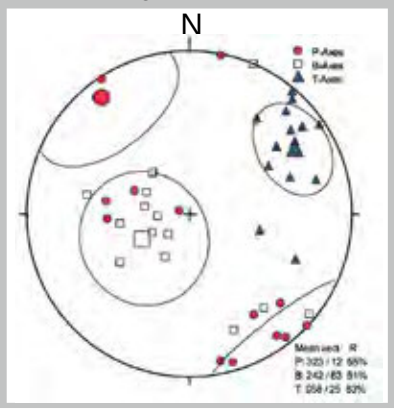

RIGHT DIHEDRA

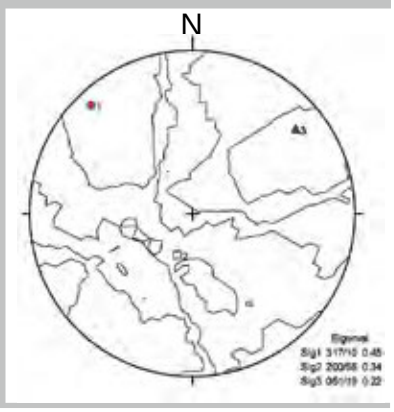

TENSOR

N = 9

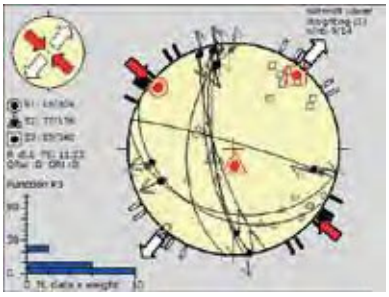

Stress field description

N-S oriented strike-slip faults, as well as NW-SE oriented oblique normal faults with a top to the SW movement were active under a strike-slip stress regime with a compressional component orientated in NW-SE direction.

46 Fall quarry — *Gurnigel Nappe*

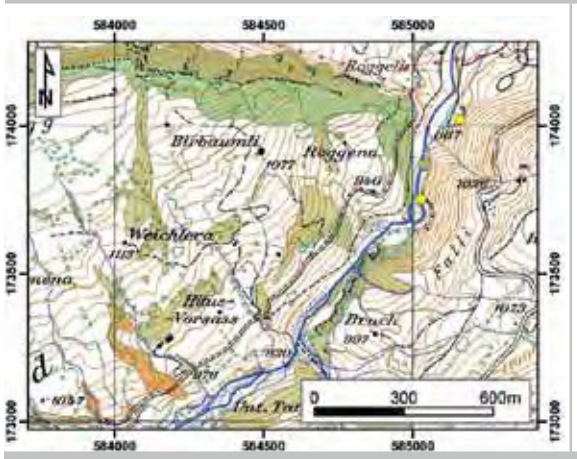

Outcrop description:

585030/ 173753 880m
Two abandoned quarry in the Gurnigel Flysch de-posits shows highly fractured sandstones with well-preserved slickenfibres on them. Most of the fractures show a strike-slip or a reverse movement direction which are generally limited to fault planes striking NE-SW.

N = 31 Paleocene *bedding = 168/ 08*

ANGELIER

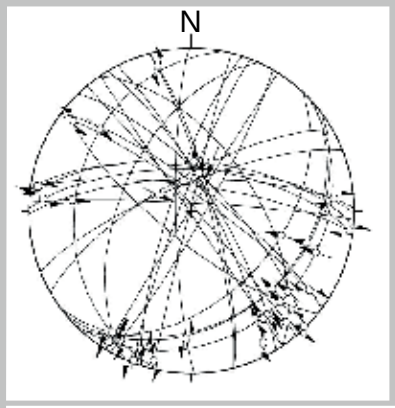

P-T

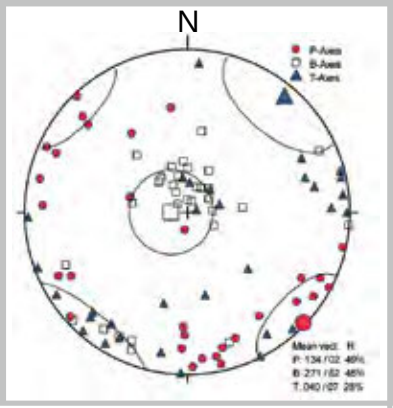

RIGHT DIHEDRA

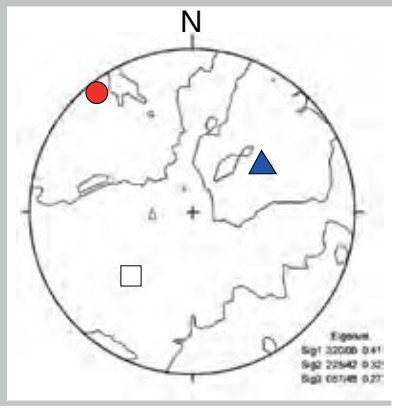

TENSOR

N = 15

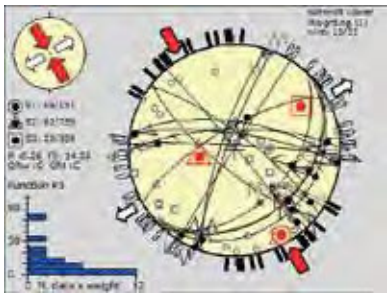

N = 9

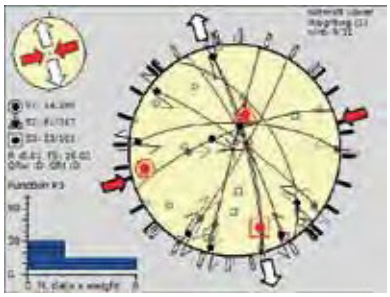

Stress field description

The Fall quarry is clearly affected by two strike-slip stress regime, whereas the prevailing one the compressional axis is oriented NW-SE and in the secondary ENE-WSW. NNE-SSW oriented sinistral and E-W oriented dextral faults, as well as NE-SW oriented faults with a top to the NW movement are active under the same stress regime. Only a few faults belong to the secondary stress regime, mostly NE-SW oriented dextral and NW-SE oriented sinistral strike-slip faults.

47 Tatüre quarry *Gurnigel Nappe*

Outcrop description:

584328/ 172805 1030m

The excavation work of the Tatüre quarry is still on-going. Therefore, measurements on freshly exposed fault planes expose high-quality slickenfibres. The general structure of the Tatüre outcrop is dominated by a medium-scale anticline, whose hinge line lies directly behind the out-cropping quarry. The majority of the fault planes and veins are oriented perpendicular to the fold axis but act with strike-slip movement. The observed veins show a conjugated relationship and agree with the orientation of the strike-slip fault system.

N = 61 Paleocene *bedding = 346/ 36*

ANGELIER

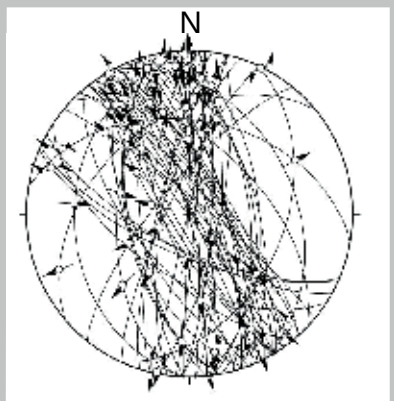

P-T

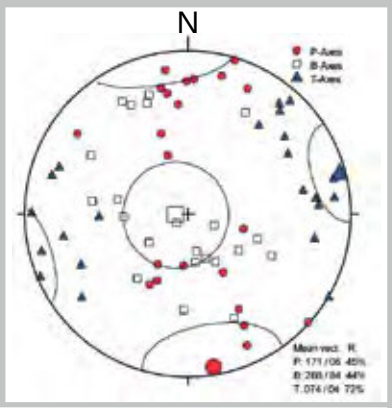

RIGHT DIHEDRA

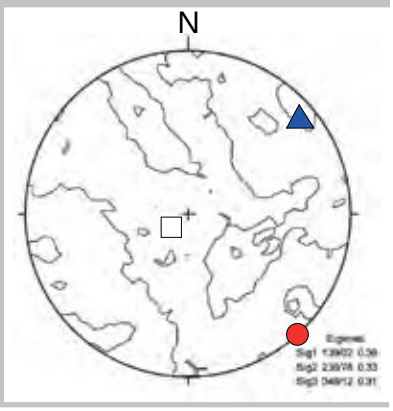

TENSOR

N = 23

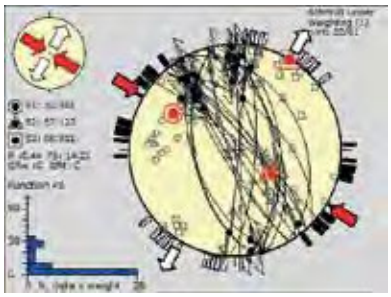

N = 16

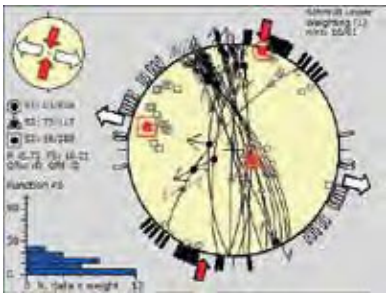

veins

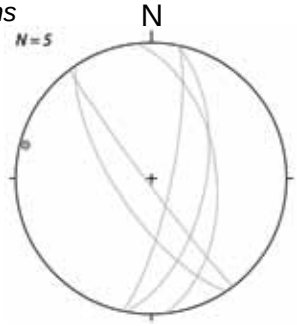

Stress field description

In the Tatüre quarry, two different strike-slip stress regimes were differentiated. Most of the fractures are oriented in NNW-SSE direction showing both, a sinistral, or a dextral shear-sense, which is probably related to a reactivation of the same fault planes within two different deformation phases. The NW-SE oriented sinistral strike-slip faults belong to the first stress regime that is generally prevailing in the Plasselbschlund area, whereas the NW-SE oriented dextral faults and NE-SW oriented normal faults belong to the secondary stress regime. The orientation of the veins is clearly related to the medium-scale fold of this outcrop.

48 Wüsterbach *Gurnigel Nappe*

Outcrop description:

582285/ 171946 1200m

The outcrop lies along the Wüsterbach river for several hundreds of meters. The Flysch deposits are regularly banded and bear a large amount of fractures, but only on a few fractures shear sense could be identified, where it was possible strike-slip faults were dominant, but also some NE-SW oriented thrust faults.

N = 13 Eocene *bedding = 167/ 36*

ANGELIER

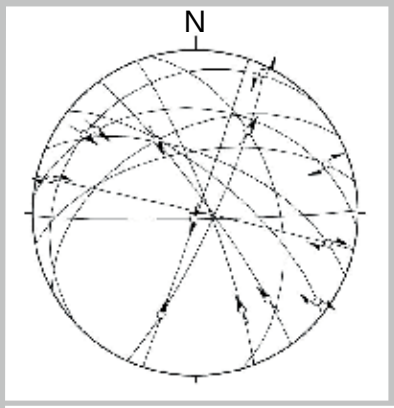

P-T

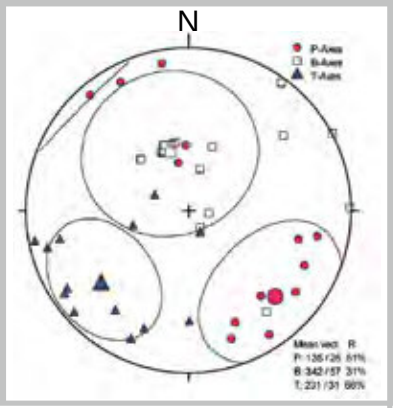

RIGHT DIHEDRA

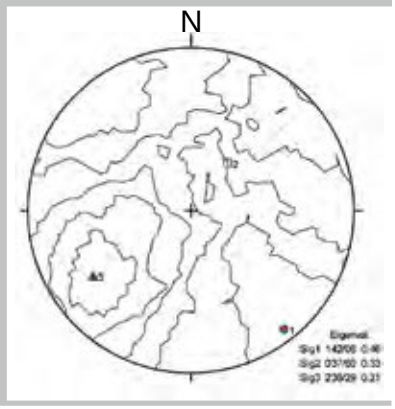

TENSOR

N = 8

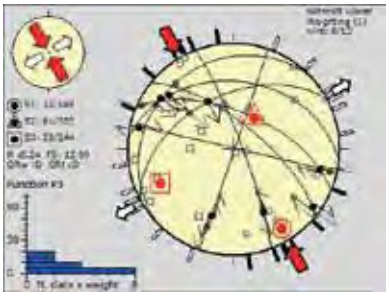

veins

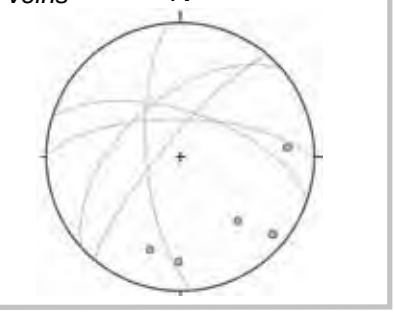

Stress field description

NE-SW oriented thrust faults, as well as WNW-ESE oriented dextral and NNE-SSW oriented sinistral faults were generated under a strike-slip stress regime with the compressional stress axis oriented NW-SE

49 ***Paradiesbach*** *Gurnigel Nappe*

Outcrop description:

582001/ 171563 1250m

The outcrop conditions are similar to the previous one along the Wüsterbach, than along the riverbed of the Paradiesbach the turbiditic flysch deposits are laminated and show some characteristic small-scale slumps which are highly fractured. Most of the small-scale fractures are oriented NE-SW with a dextral sense of shear. The outcrops are often limited to zones of higher river flow activity. The presence of veins is common.

N = 17 *Eocene* *bedding = 176/ 16*

ANGELIER

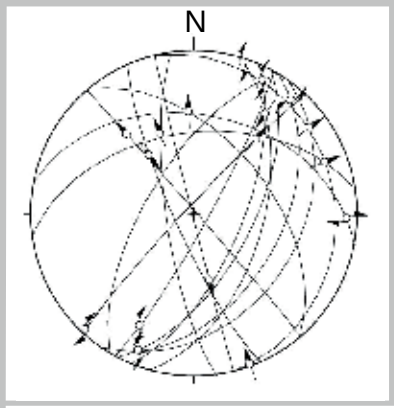

P-T

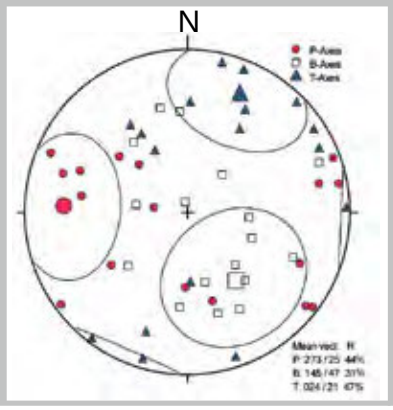

RIGHT DIHEDRA

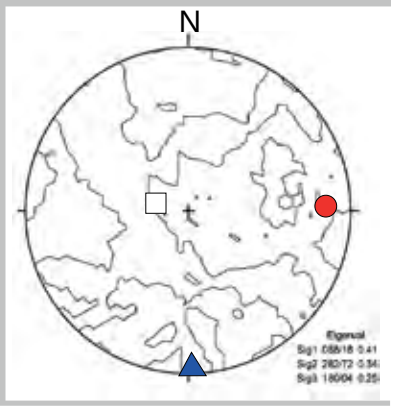

TENSOR

N = 8

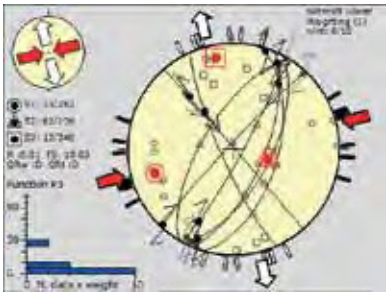

Stress field description

The resulting strike-slip stress regime shows a ENE-WSW oriented compressional axis that allows a dextral strike-slip movement of the prevailing NE-SW orientated strike-slip faults.

50 *Italienera* *Gurnigel Nappe*

Outcrop description:

583227/ 170207 1100m

Measurements were taken along the Gérine river, whose riverbed attains already a remarkable with but is above all filled with rather large blocks of stone. The fractures are randomly distributed but show well preserved sllickensides on their fault planes allowing a more detailed stress analysis. N-S trending, oblique dipping thrusts are common, whereas strike-slip faults are clearly less represented. Veins are frequent and older veins oriented NE-SW are clearly cut by younger veins oriented NW-SE.

N = 76 *Eocene* *bedding = 159/ 85*

ANGELIER

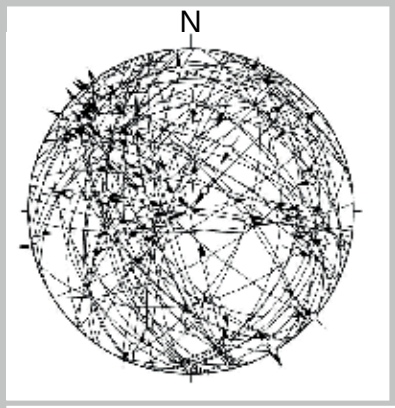

P-T

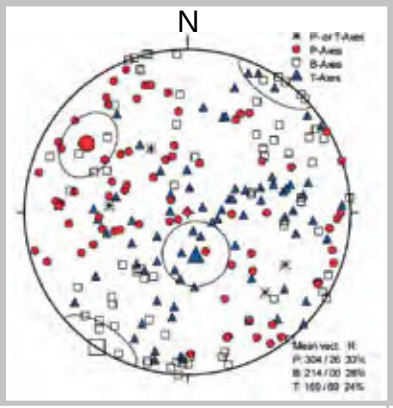

RIGHT DIHEDRA

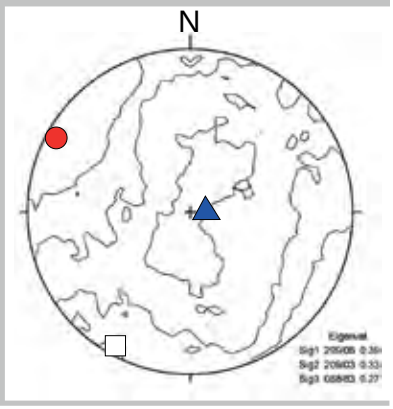

TENSOR

N = 23

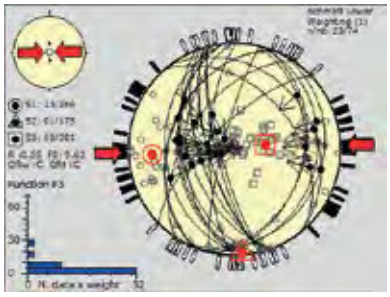

N = 12

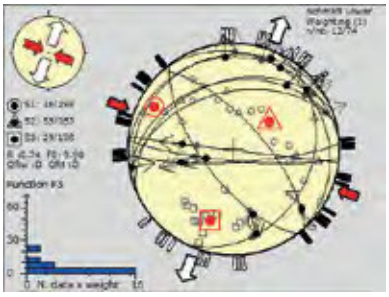

N = 13

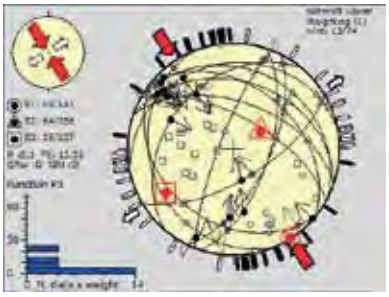

VEINS

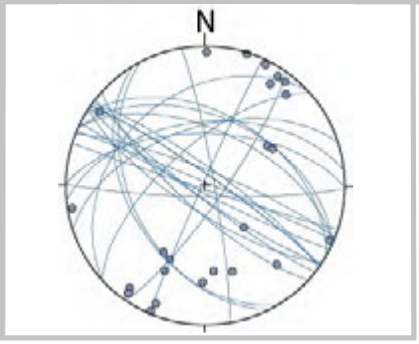

Stress field description

The separation of the entire dataset yields three different stress regimes at the Italienera outcrop. The presence of N-S oriented faults thrusting either top to the E or top to the WSW were generated under a E-W orientated compressional stress regime. The prevailing presence of the first stress regime suggests a recent thrusting activity. Two secondary strike-slip stress regime represent the more regional stress regime, whereas W-E oriented normal faults were generated under the second and NE-SW oriented normal faults under the third stress regime.

51 Zollhaus — *Gurnigel Nappe*

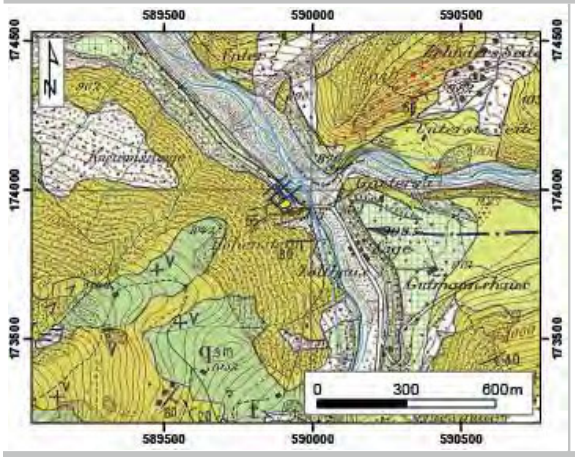

Outcrop description:

589895/ 173959 880m

The abandoned Zollhaus quarry exposes still rather fresh surfaces of fault plane, but on most of the fault planes slickenfibres were missing. Whether a slip direction could be determined, they were mostly strike-slip.

N = 16 *Eocene* *bedding = 140/ 55*

ANGELIER

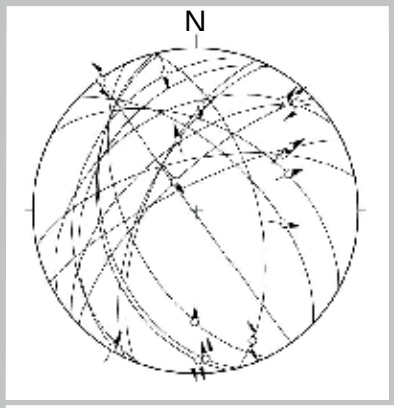

P-T

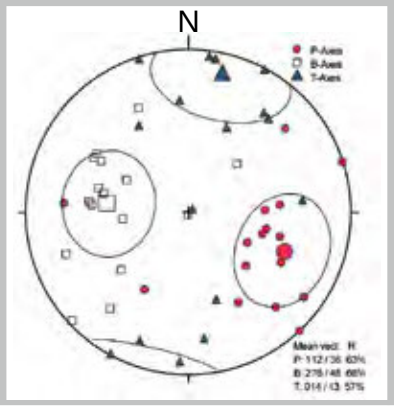

RIGHT DIHEDRA

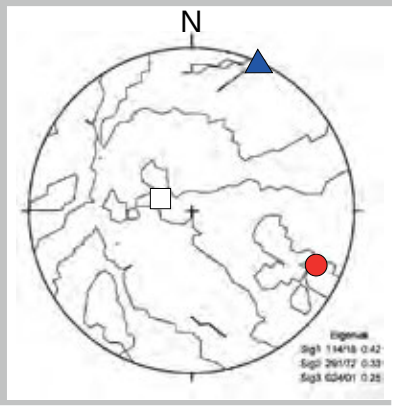

TENSOR

N = 7

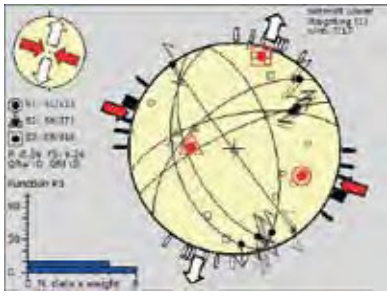

Stress field description

NNW-SSE oriented sinistral strike-slip faults, as well as some ENE-WSW oriented dextral strike-slip faults were active under a NW-SE oriented strike-slip stress regime.

2 3D Modelling

2.1 Procedures, Comments and Tips

The reconstruction of the 3D-model was sometimes time-consuming and nerve-racking; therefore, a few important steps are listed here concerning the modelling process from the data import at the beginning to the model export, the post-treatment, and the visualisation at the end. This chapter addresses future users of the 3DGeomodeller program to facilitate the modelling processes.

2.1.1 Importing DTM

Right at the beginning, after the definition of the modelling extent, the topography in terms of a DTM can be added to the model box. However, the DTM usually available appear as ASCII-file format, corresponding to a matrix of elevation data in X and Y direction, requiring a transformation into a .SEMI-file format, disposing of an X, Y and Z column and an informational first line. For this conversion, the Reformattor Toolbox program developed by Maxelon (2004). Additionally, the Reformattor Toolbox program allows a downsizing of the DTM resolution, since a resolution of 1m - as available for the Canton Fribourg - is by far too precise for the 3Dmodelling. For the general 3Dmodel of the préalpine nappe structure a precision of 107m in E-W direction and 88m in N-S direction was sufficient, whereas for the detailed 3D models a resolution of 30m was chosen.

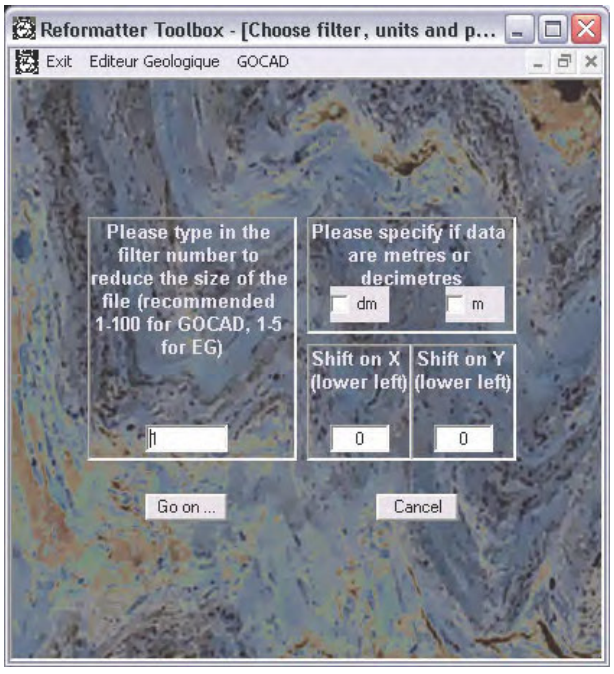

Fig. 7.1: main window of the Reformattor Toolbox program (MAXELON, 2004) that allows converting the .ascii-files into .semi-files as required by the 3DGeoModeller program.

2.1.2 Stratigraphic series

The stratigraphic pile allows introducing a chronology within the different formations, without tectonic activity, the oldest units are located at the bottom, whereas the youngest units can be found on top. Subparallel stratigraphic layers are regrouped as a « stratigraphic series ». In the 3D model of the Préalpes Romandes, the individual nappes were handled as individual formations. Whereas in the four detailed 3D models within the Préalpes Médianes, the stratigraphic layers ranging from the Lower Jurassic (Liassic) to the Upper Cretaceous (Couches Rouges) were grouped as one series. For each series, a distinct potential field was interpolated. For modelling reasons, different geological blocs were defined consisting of the same geological series. Thereby, it was possible to interpolate the continuation of geological formations on both sides of important faults (such as thrust faults) where the inclination of the structures varies considerably. Without regrouping, 3DGeoModeller had difficulties to combine the continuation of the structures on both sides of the thrust. In this way, each segment in between two thrust planes was handled individually with a distinct potential field. The delimiting thrust planes were defined as Triassic formation with an erosional base allowing modelling the detachment horizon and at the same time filling in the folding structures of the series above.

Furthermore, the 3DGeoModeller software requires the definition of the reference line (contact), which can be either the “top” contact or the “bottom” contact of a stratigraphic layer. The choice of a “bottom” reference appears to be more logical for the application of erosive layers to simulate thrust faults.

A brief overview of the stratigraphic series of the four different detailed models is given in the following subchapters.

Dent de Broc

Three major thrust planes affect the Dent de Broc modelling area subdividing the model in three major packages delimited by the base of the Triassic layers (Fig. 7.2A). To simulate the thrust planes, the contact of the Triassic layers is defined as “erosive”. The packages DDB1, DDB2, and DDB3 are following the upper contact of the Triassic layers and their contacts are therefore defined as “onlapping”. Within the stratigraphic pile applied for the 3Dmodelling, a triple repetition can be recognised.

Gros Haut Crêt

In the Gros Haut Crêt area two main thrust, both located at the Triassic base and two minor thrusts,

acting as thrust splays, are distinguished (Fig. 7.2B). The minor thrusts are located at the base of the Dogger, therefore they are defined as erosional series while the Malm 3 layer is characterised as onlapping series to take into account the real dipping of the stratigraphic layer. The modelling area was spitted into 2 main structural packages (GHC1 and GHC4) while Dogger 2, 3 and Malm 3 are only minor packages with incomplete stratigraphic series.

Schopfenspitz

Within the Schopfenspitz area, only two major packages have to be defined delimiting a sector SE (Ssp1) and a sector NW (Ssp2) of the important Schopfenspitz thrust fault (Fig. 7.2C). The second package (Ssp 2) is affected by several thrust that are discontinuous throughout the entire model. For this reason, they have to be defined as faults with a certain extent in the model. Different structural packages only make sense in the klippen part, as these thrust defines a distinct limit between these units, whereas the other faults are affecting the stratigraphic layers just locally and diminish laterally.

Schafarnisch - Mittagflue

The Schafarnisch - Mittagflue area is characterised by the transition from the Préalpes Médianes Plastiques (PMP) to the intermediate zone in between the PMP and the Préalpes Médianes Rigides marked by two imbricates: the Heiti (HI) and the Gastlosen (GI) imbricate (Fig. 7.2D). To simplify the modelling process, the PMP and the two imbricates were handled as three independent packages. As in the previous 3D models, the thrusts were interpolated as Triassic layers with an erosive base. The Nappe Supérieure thrusting the Préalpes Médianes was determined as the highest stratigraphic unit.

2.1.3 Import maps and cross-sections

As most of the data were collected from geological maps and cross-sections, the import of this information into the 3D model is essential. Maps and cross-sections were adapted to the 3D model by defining anchor points with known coordinates and heights. Subsequently, the cross-sections were placed into the 3D model, where a correspondence between the topographic line within the model and the one drawn in the inserted cross-section. This is noted here, because several of the older or interpretative cross-sections are often not precise enough to be localised at an exact position. This was mainly observed in the Préalpes Romandes model, where a large amount of geological cross-sections was introduced. However, as this model focus on the less detailed structures of the préalpine nappes, this impact was so significant and did not affect the accuracy of the model considerably. The only inconveniences were imprecisions concerning the orientation of the cross-sections, since already a minor deviation of the azimuth shows important consequences on the inclination of the structural units.

Subsequently, the digitalisation of the limits of the different formations was realised directly based on the 2D input of maps and cross-section. Once digitised, the contact points were attributed to their corresponding formation. Together with at least one orientation data per stratigraphic series, a first 3D model was calculated. Hereby, we can easily notice where the model requires further data input to better define the 3D structures. These additional data are mainly based on field measurement and on conceptual interpretations. They were inserted as additional cross-sections into the model at areas where the model is under-defined or where throughout the 3D modelling process obvious errors occur. Especially, around faults the limits of the formations on both sides need to be defined accurately to clearly indicate the offset of the fault.

The whole trick is to find the ideal amount of data input required for the 3D interpolation: enough contact points to obtain an accurate 3D model, but not too many to overload the model, which has negative effects on the model calculation process.

2.1.4 3D model calculation

Since during the 3D model construction, the data were mostly handled in 2D, both on maps and on cross-sections, it is important to verify their 3D representation of the calculated units. For this process, a rather low resolution is sufficient to detect potential modelling errors. Thereby, the calculation time can be reduced and the probability of a crash of the 3DGeoModeller program can be reduced.

However, for the final export of the entire 3D model, a rather high resolution of the modelling grid is required to represent clearly the intersection of the geological structures with the topography, as well as to recognise important topographic features in the 3D model. The choice of the model resolution remains a compromise solution between the maximal memory capacities of the program and the precision of the topography. For the Préalpes Romandes a resolution of 220m and for the detailed 3D models a resolution of 30m was attained. Depending on the size of the model, the amount of calculated shapes ranges from 1’500’000 to 5’550’000 shapes, which corresponds to a relatively long calculation time between 4 and 8 hours. For this reason, it is even more irritating that often right at the end of the 3D model calculation an

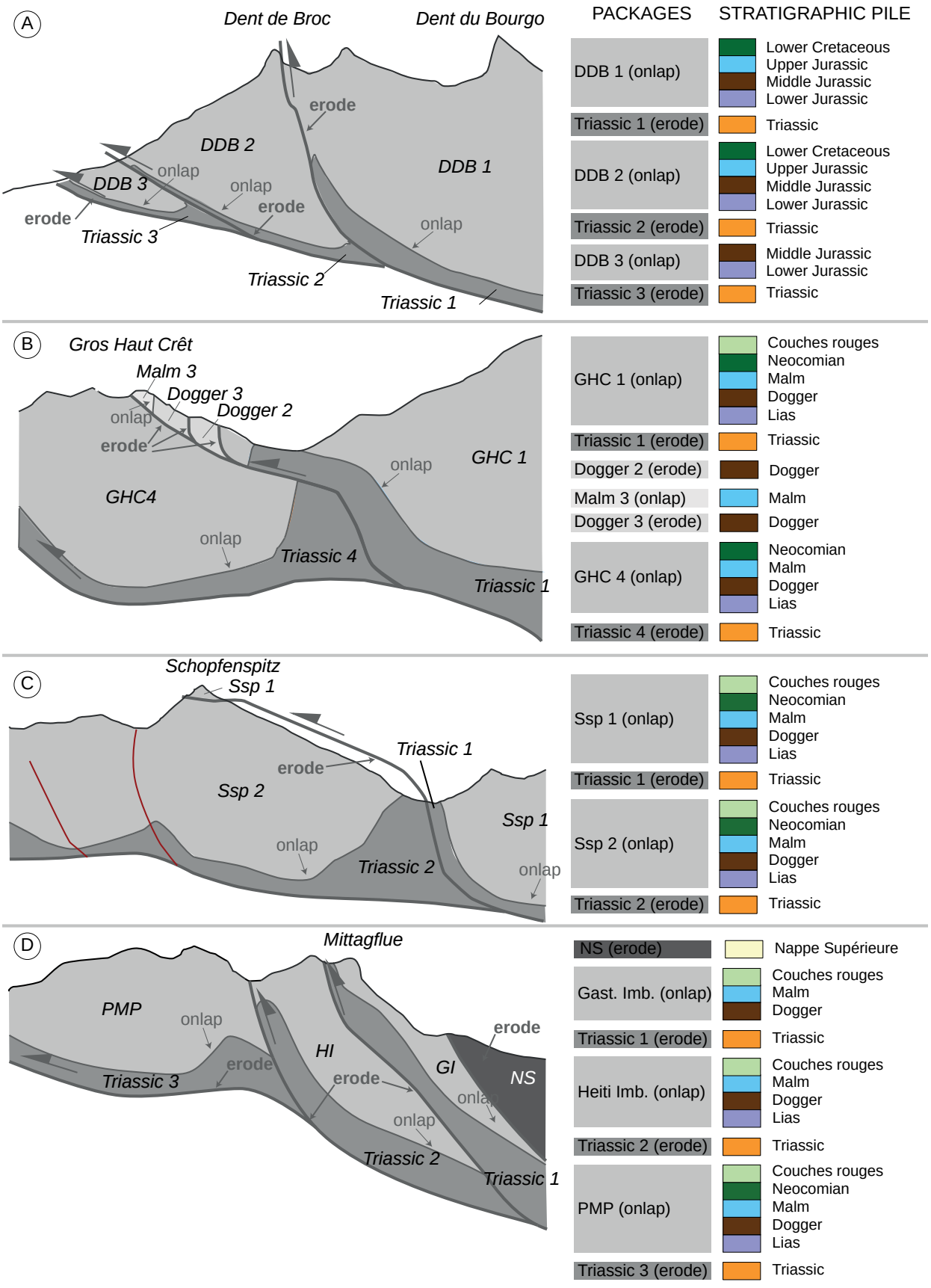

Fig. 7.2: Illustration explaining the stratigraphic pile of the four detailed 3D models. Cross-section shows the different packages and the relationship of the different stratigraphic contacts (erosive or onlapping). Abbreviations in A) DDB = Dent de Broc; B) GHC = Gros Haut Crêt ; C) Ssp = Schopfenspitz and D) PMP = Préalpes Médianes Plastiques, HI = Heiti Imbricate, GI = Gastlosen Imbricate and NS = Nappe Supérieure.

error report indicates a crash of the program and with that the loss of the entire calculations.

Without changing the resolution parameters, about one of four calculation attempts was successful. By this trial and error approach, it appeared as helpful to toggle off the "Draw shapes after building" button

Moreover, it seemed to be another bug of the 3DGeoModeller program that the insertion of the favoured resolution is not accepted the first time, but requires a certain persistence to be filled in.

Another issue of the 3DGeoModeller program is that it is not compatible to hyper-threading processes, as it is common for computer programs focussed on computers with a multi-core system. Hyper-threading technology helps to improve the parallelisation of computation of multiple tasks at once. Thereby, the available processor cores share the workload between them to benefit from the efficiency of all the individual processors. As 3DGeoModeller does not support hyper-threading, it only uses one processor and does therefore not exploit the full potential of a powerful computer with several processors. However, it is possible to open and run 3DGeomodeller several times in parallel, so that one program fully uses one processor. To increase the efficiency of one processor it is useful to deactivate the hyper-threading function of the computer to get the maximal capacity out of a processor.

2.1.5 Export 3D model

After the calculation of the 3D model by the use of the 3DGeoModeller program, it is important to export this interpolation into another program to improve its visualisation or to allow further analyses. Different export file formats are provided by 3DGeoModeller, whereof the "TSurf" (.ts) file format, an ASCII file format, proves to be very useful. This format is supported by other programs, such as GoCAD and can easily be converted into a ".wrl" file format, which is compatible with a large number of programs, such as NX unigraphics 7.5, a powerful 3D engineering program (Siemens, 2011). This graphical export method generates exclusively the contact surfaces instead of the entire volume between the contacts – the 3Dmodel becomes "lighter" and therefore easier to handle. One disadvantage of this export method is that, interfering contact surfaces at out-thinning layers provoke errors such as vacant and redundant facets in the triangular mesh. For that reason, the mesh of the exported model surfaces requires a cleaning of the model impurities by the use of MeshLab v1.3.0 (CIGNONI, 2011).

2.1.6 Post-processing

By the use of MIRARCO ParaViewGeo 1.4.14 program (), it was possible to get an overview of the model and over each stratigraphic unit, as each formation is defined in a proper file. Despite the availability of several filter functions, we used this program mainly to transform the "TSurf" file format into a ".vrlm", respectively by overwriting the ".vrml" into a ".wrl" file format. In this way, it was possible to open the individual 3D formations in MeshLab v1.3.0 to clean the models impurities (see Fig. 7.3).

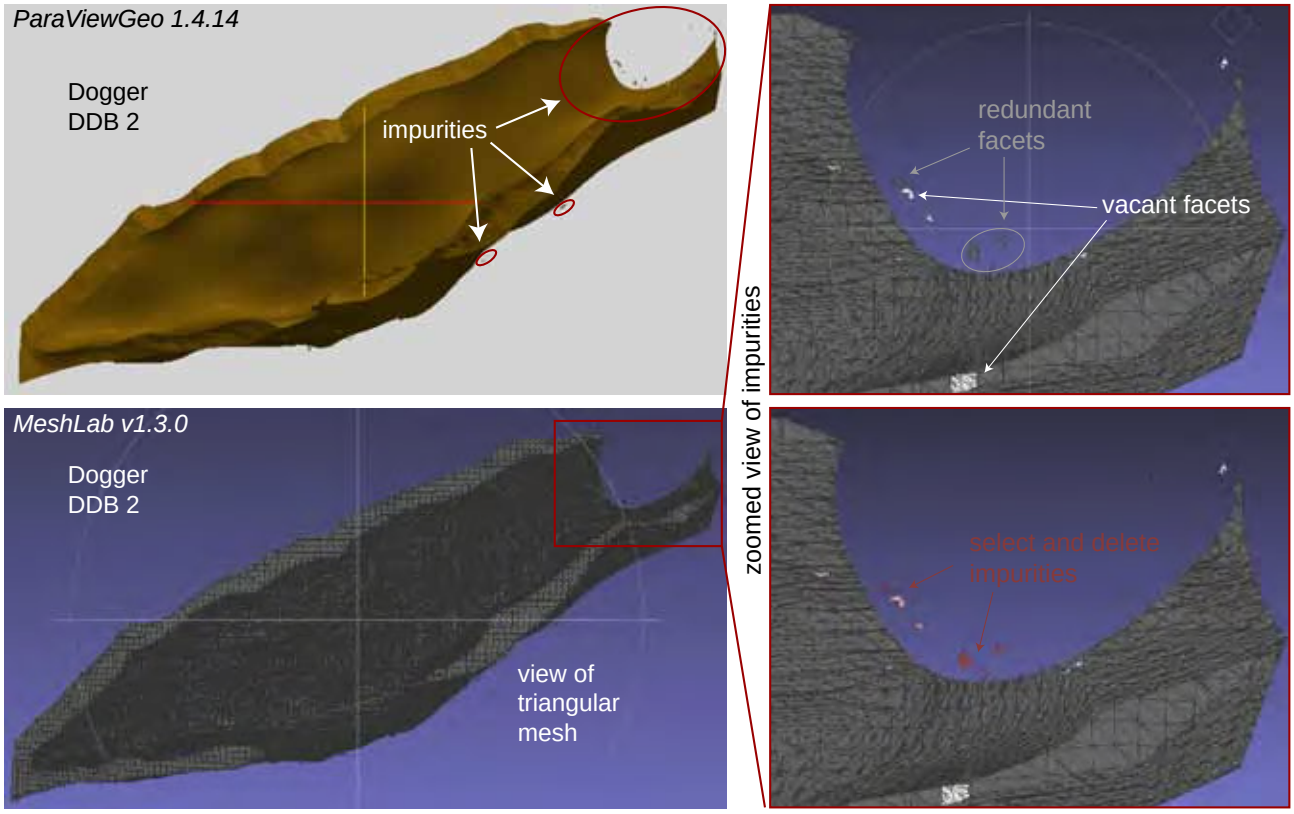

Fig. 7.3: Illustration of the Dogger layer of the Dent de Broc syncline within the Dent de Broc 3D model is represented in the ParaViewGeo program (upper left) and the MeshLab program (lower left) with focus on the impurities. Zoom into a zone of impurities within the triangular mesh displaying vacant and redundant facets (upper right) that can be selected and deleted by the use of the Meshéab program.

CURRICULUM VITAE

EVA MATZENAUER

Date and place of birth: 10.12.1981 in St.Gallen (Switzerland)

EDUCATION

July 2007 - date	PhD thesis in structural geology at the University of Fribourg, Department of Geosciences *Title: "Structural evolution of the Préalpes Klippen in the Canton of Fribourg (CH)"* Supervisor: Dr Jon Mosar
October 2005 - July 2007	Master in Earth Science at the University of Fribourg, Department of Geosciences Title: *"Spannungsanalyse der Mittelland Molasse des Kantons Freiburg anhand von Deformationserscheinungen an Geröllen und Bruchbildungen" ("Stress analysis of the Plateau Molasse of the Canton Fribourg based on deformed, pitted pebbles and fracture arrangement")* Supervisor: Dr Jon Mosar
October 2002 - 2005	Bachelor in Geography at the University of Fribourg, Department of Geosciences
September 2001 - May 2002	Language stays in London (Cambridge Certificate in Advanced English) and Vichy (F)
August 1998 - 2001	Grammerschool, Kantonsschule St- Gallen, Matura Typus B

WORK EXPERIENCE

July 2007 - date	Scientific lecturer at the University of Fribourg, Department of Geosciences *Practical course of „Regional Geology" (1 and 2): geological maps and cross-sections* *Several mapping field camps in Salanfe, Chasseral, Gastlosen*
April - November 2009	Geological guide: geological educational trail Gastlosen, FR, CH Translation of the geological guidebook and website from French to German: „Geologischer Pfad Gastlosen" by Luc Braillard and Daniel Rebetez
2007 – 2010	Several technical translations from French to German

July/August 2007 & 2008	Summer holiday program: paleontological excursions for children in collaboration with Jean-Pierre Berger and Gruyère Escapade
October 2005 – June 2007	Tutor in the practical course „Regional Geology“ (1 and 2): geological maps and cross-sections Mapping field camps: Chasseron, Montbovon

Courses and Further Education

March 2011	Move Workshop, swisstopo
September 2009	Workshop: “3D geometrical modelling for geological interpretation and mapping (Program: 3DGeoModeller)”
February - June 2008	course: “Rock mechanics, ENAC, EPFL Lausanne”
April 2008	course: “Les techniques d’exploration des hydrocarbures”

Conference Contributions and Excursions

8th Swiss Geoscience Meeting, Fribourg 2010

Thrusting and faulting in the Préalpes Médianes (talk)

Matzenauer E., Mosar J.

Northern Alpine foreland deformation in western Switzerland: New insights from field and seismic data of the Plateau Molasse

Ibele T., Matzenauer E., Mosar J.

The Fribourg Structure and Fribourg Zone: an Active fault system or The Rösti Graben - Geologic evidence!

Mosar J., Meier B., Sommaruga A., Abednego M., Eichenberger U., Ibele T, Matzenauer E., Sprecher , Ch., Vouillamoz N.

Alpine Workshop Cogne, Italy, 2009

Tectonics and Neotectonics in the Prealpes and Molasse Basin of Western Switzerland. Part 2 Paleostress (poster)

Matzenauer E., Ibele T., Mosar J.

Tectonics and Neotectonics in the Prealpes and Molasse Basin of Western Switzerland. Part 1 structural geology (poster)

Ibele T., Matzenauer E., Mosar J.

Past and Present Tectonics of the western Alpine Molasse Basin between Jura and Prealpes Klippen

Jon Mosar, Tobias Ibele, Fribourg, Eva Matzenauer

Taiwan-Switzerland Workshop on: Source to Sink Relationships and Petroleum Occurrences in Foreland Basin Systems, 2009

6th Swiss Geoscience Meeting, Lugano 2008

Brittle tectonics in the Subalpine Molasse and in the Préalpes Klippen (Poster)

Matzenauer E., Ibele T., Mosar J

Brittle tectonics in the Swiss Molasse Basin (Poster)
Ibele T., Matzenauer E., Mosar J.

Skills

MS office applications:	Microsoft Office Word, Excel, PowerPoint
Graphic applications:	Adobe CS: Photoshop, Illustrator, InDesign
Technical applications:	ArcGIS, 3DGeomodeller, Tectonic FP, WinTensor, T-Tecto
German:	Mother tongue
English:	Proficient user (CAE) (C1); written and oral
French:	Proficient user (C2); written and oral (lectures and conversation language during my studies)